SYNTHESIS AND STRUCTURE OF MANGANESE AND RUTHENIUM COMPLEXES DERIVED FROM SOME ADIPOYL DIHYDRAZONES

ABSTRACT

SUBMITTED IN PARTIAL FULFILLMENT OF THE REQUIREMENT OF THE DEGREE OF DOCTOR OF PHILOSOPHY IN CHEMISTRY

BY

DEBAJANI BASUMATARY

DEPARTMENT OF CHEMISTRY

SCHOOL OF PHYSICAL SCIENCES

NORTH-EASTERN HILL UNIVERSITY

SHILLONG

2008

ABSTRACT

Chapter-I

Introduction and Literature Survey

This chapter presents a brief account of the importance of the monometallic complexes of the metal ions manganese and ruthenium selected in the present study in various fields such as biological, homogeneous catalysis and synthesis of solid state phases of industrial and technological importance.

This is followed by description of various characteristic coordination modes of the dihydrazones.

At the end, it also deals with the relevant literature on transition and non-transition metal complexes of dihydrazones derived from condensation of aryl, aroyl, pyridoyl dihydrazones and thiocarbohydrazides with variety of aldehydes and ketones as well as on dihydrazones derived from condensation of dialdehydes and diketones with monoacylhydrazines, pyridoylhydrazines, thiosemicarbozide and related ligands. An effort has been made to survey literature on all these ligands up-to date.

Chapter-II

Experimental

In this chapter the experimental details regarding the preparations of adipoyldihydrazine, disalicylaldehyde adipoyldihydrazone and bis(2-hydroxy-1-naphthaldehyde)adipoyldihydrazone have been described. Procedure for elemental analysis, physico-chemical techniques and instruments used are also described.

Chapter-III

Synthesis, Characterization and Structural Assessment of Monometallic Manganese(II) Complexes derived from Polyfunctional Adipoyldihydrazones

This chapter deals with the preparation, characterization and structural assessment of fourteen monometallic manganese(II) complexes derived from polyfunctional disalicylaldehyde adipoyldihydrazone ($slahH_4$) and bis(2-hydroxy-1-naphthaldehyde)adipoyldihydrazone ($npahH_4$) ligands.

In the beginning, a brief account of literature in respect of coordination behaviour of ligands related to adipoyldihydrazone such as monoacylhydrazines, monoaroyldihydrazines and their hydrazones, acyldihydrazines, aroyldihydrazines, pyridoyldihydrazines, simple dihydrazones and dihydrazones containing hydroxy groups, is discussed.

The monometallic manganese(II) complexes of the compositions $[Mn^{II}(slahH_2)(H_2O)_2]$ (1), $[Mn^{II}(npahH_2)]$ (8), $[Mn^{II}(slahH_2)(A)_2].nH_2O$ (where A = py(pyridine, 2); 2-pic(2-picoline, 3); 3-pic(3-picoline 4); 4-pic(4-picoline, 5), (n = 0, 1)), $[Mn^{II}(npahH_2)(A)_2]$ (where A = py(pyridine, 9); 2-pic(2-picoline, 10); 3-nic(3-picoline, 11); 4-pic(4-picoline, 12), (n = 0, 1)),$[Mn^{II}(slahH_2)(NN)]$ (where NN = bpy(2, 2' bipyridine, 6), phen(1, 10-phenanthroline, 7)) and $[Mn^{II}(npahH_2)(NN)]$ (where NN = bpy(2, 2' bipyridine, 13) and phen(1, 10-phenanthroline, 14)) were isolated.

The complexes (1) to (7) are dull or light brown in colour while complexes (8) to (14) are yellowish brown in colour. All of the complexes are air-stable and decompose above 300 °C without melting.

The mass spectral signal at m/z value equal to 536 of the complex (8) indicates its monomeric nature.

The molar conductance values in the range 1.5-3.7 ohm^{-1} cm^2 $mole^{-1}$ for these complexes are attributed to their non-electrolytic nature in DMSO solution.

The μ_{eff} value for the complex (8) is 1.12 B.M which indicates that the complex is in the low-spin state. This value is much less than the values reported for the Mn(II) complexes in the low-spin state. This indicates considerable interaction between metal ions in the structural unit of the complex in the solid state.

On the other hand, the μ_{eff} values for remaining complexes fall in the range 5.79-6.02 B.M. These values lie well within the range reported for Mn(II) complexes in the high-spin state ($t_{2g}^3 e_g^2$, S = 5/2).

The essential features of the ligand bands in the electronic spectra of the complexes suggest that the ligands are bonded to the metal centre in the same conformation as in the uncoordinated state.

In addition to the intra-ligand bands, the complexes of $npahH_4$ possess one additional absorption bands in the region 448-600 nm, respectively in their electronic spectra. These bands can be assigned to the charge transfer transitions from phenolate/naphtholate oxygen atom to the metal centre.

The EPR spectrum of the complex (8) in the polycrystalline state shows an isotropic spectrum with g = 2.019. The width of the signal at g = 2.019 is about 330 G which indicates spin-exchange between manganese(II) centres in the solid state which is consistent with very low μ_{eff} value of the complex. The width of the signal in the g = 2.019 region is increased to about 500 G in DMSO solution. This rules out the possibility of the presence of any exchange interaction between the metal centres in DMSO solution.

The central resonance in this complex shows splitting into five components with average nitrogen superhyperfine splitting constant A_N equal to 12 G indicating coordination of two nitrogen atoms to the manganese metal centre.

The remaining complexes show EPR spectral features characteristic of Mn(II) in high spin state. The isotropic g-values lie in the region 1.994-2.050.

The uncoordinated ligands show a strong band at 1679 and 1666 cm^{-1} which are assigned to νC=O stretching vibration. The band at 1679 cm^{-1} in free $slahH_4$ disappears in the IR spectra of the complexes (1) to (5) indicating that the ligand $slahH_4$ coordinate to the metal centre in enol form. On the other hand, these bands appear in the region 1640-1680 cm^{-1} in the remaining complexes. This indicates coordination of the ligands to the metal centre in keto form. However, the νC=O band is shifted either to lower frequency by about 10-26 cm^{-1} as in the complexes (6) to (10) and (13), (14) or remains almost unshifted in position as in the complexes (11) and (12). Such a feature associated with νC=O band in the IR spectra of the complexes rule out the possibility of coordination of >C=O group to the metal centre because the >C=O group absorbs almost in the same region in these complexes in which uncoordinated >C=O groups have been reported to absorb in dihydrazone metal complexes as has been confirmed by X-ray crystallography. The lower shift of νC=O band has been attributed to involvement of >C=O groups in the strong intermolecular H-bonding with secondary NH group in the complexes. The bands observed at 1620 and 1630, 1573 cm^{-1} in free dihydrazones are attributed to νC=N stretching vibrations. These bands, on an average, shift to lower frequency by 2-15 cm^{-1} in the complexes indicating coordination of >C=N group to the metal centre.

In the dihydrazones, a strong band appears at 1275 cm^{-1} in $slahH_4$ and a medium intensity band at 1281 cm^{-1} in $npahH_4$, respectively. These bands are assigned to β(C-O)(phenolic/naphtholic). In the complexes (1) to (7) derived from $slahH_4$, this band,

on an average, undergoes shift to lower position by 5 to12 cm^{-1} while in the complexes (8) to (14) derived from $npahH_4$, this bands shifts to higher frequency by 2 to 20 cm^{-1}. Such a feature associated with β(C-O) band in these complexes suggests involvement of phenolic/naphtholic C-O group in coordination. The shift of β(C-O)(phenolic) to lower position in the complexes (1) to (7) may be related to flow of π-electron density of aromatic ring to metal centre through azomethine group while the shift of β(C-O)(naphtholic) band to higher frequency in the complexes (8) to (14) suggest that the π-electron density of aromatic ring in these complexes flow to metal centre through naphtholate oxygen atom. The complex (1) shows a distinct band at 635 cm^{-1} which is attributed to arise from rocking mode of coordinated water molecules to the metal centre. The free pyridine bases absorb at around ~604 cm^{-1} due to in-plane ring deformation mode. In the complexes (2), (4) to (7) and (9) to (14), a new medium to weak band is observed in the region 657-696 cm^{-1}. This band has been assigned to arise due to in-plane ring deformation mode of coordinated pyridine bases.

The complexes have been characterized by cyclic voltammetry also.

At the end, the tentative structures for the complexes have been proposed.

Chapter-IV

Synthesis and Characterization of Monometallic Manganese(IV) complexes of Bis(2-hydroxy-1-naphthaldehyde)adipoyldihydrazone

The present chapter describes the synthesis and characterization of Mn(IV) complexes derived from bis(2-hydroxy-1-naphthaldehyde)adipoyldihydrazone ($npahH_4$).

The complexes of the compositions $[Mn^{IV}(npah)(A)_2].nH_2O$ and $[Mn^{IV}(npah)(NN)]$ (where A = H_2O, (15); py, (16); 2-pic, (17); 3-pic, (18); 4-pic,

(19); NN = bpy, (20); phen, (21), (n = 0, 1)) were isolated.

All of the complexes are shining black. They are air stable. All of the complexes decompose above 300 °C without melting. The complexes are insoluble in water and common organic solvents such as ether and benzene. The complexes are sparingly soluble in methanol, acetonitrile and dichloromethane. They are completely soluble in DMSO and DMF.

The complex (17) was characterized by FAB mass spectra as representative sample to assess the molecular complexity of the complexes. The mass spectrum of the complex (17) shows a signal at m/z value 536, which most probably, results from the formation of $[Mn(npah)]^+$ species. Such a feature of the mass spectrum of the complex shows its monomeric nature.

The molar conductance values for the complexes in DMSO indicate that they are all non-electrolytic in nature.

The magnetic moment values for the complexes lie in the range 3.83-4.39 B.M. The μ_{eff} values suggest the presence of Mn(IV) centres in the complexes.

The electronic spectra of all the complexes recorded in DMSO show red shift of ligand bands that gives a good evidence of chelation of dihydrazone to the metal centre. The magnitude of shift of ligand bands indicates strong bonding between the ligand and the metal. The ligand bands show almost similar feature in the complexes as in case of manganese(II) complexes in Chapter III and in the uncoordinated ligand indicating that the conformation of the ligand in the complexes remains almost the same as that in the uncoordinated state. In addition to the ligand bands, the complexes show a cluster of three bands in the region 400-470 nm. A band in this region is assigned to $^4T_{2g} \leftarrow {}^4A_{2g}$ transition. One band in this region is assigned to ligand band at 363 nm. But it is difficult to pin point which of the bands arises from ligand band

The complexes (16) and (18) showed featureless EPR spectra in the solid state as

the solid state and in the solution state. The former resonance is of greater intensity in the solid state but for glassy state, the resonances are almost of the same intensity. For the complexes (20) and (21), $g_{\perp} \sim 5.0$ and $g_{\parallel} \sim 2.0$ with the signal at former g-value being of low intensity is observed in both crystalline and glassy state. The EPR signal at $g \cong 2$ shows ^{55}Mn hyperfine splitting constant is equal to 80 G in complexes (20) and (21) which is closer to the values observed for Mn(IV) than that for Mn(II).

The complexes (16) – (18) showed featureless EPR spectra in the solid state as well as in the solution state at R.T and liquid nitrogen temperature. Hence, the complexes (15) and (19) to (21) only have been analyzed by EPR spectroscopy. All of these complexes exhibit highly anisotropic EPR spectra in polycrystalline state as well as in the glassy state.

The EPR spectra reveals that the ligand provides effective electronic environment for the metal that is highly distorted in the ground state in the complexes (15) and (19) but only slightly distorted in the ground state in the complexes (20) and (21). The distortion is sensitive to geometrical orientation of the donor atoms. The effective environment of Mn(IV) lie close to ideally pseudo-octahedral environment.

The essentially contrasting EPR spectra of the complexes (15) and (19) as compared to those of the complexes (20) and (21) has been related to coordination of the nitrogen donor atoms from co-ligands bipyridine and 1, 10-phenanthroline in the complexes (20) and (21) which occupy *cis*-position around the metal atoms by virtue of their geometry while the donor atoms from co-ligands in the complexes (15) and (19) occupy *trans*-positions.

The dihydrazone is coordinated to the metal centre in enol form in all of the complexes. The νC=N bands observed at 1630 and 1593 cm^{-1} in free dihydrazone shift to lower frequency, on an average by 3-11 cm^{-1}. This indicates coordination of azomethine nitrogen atoms to the metal centre. The νC=N bands appear as a couple

of bands in metal complexes. The existences of two bands of almost same intensity similar to that in the uncoordinated dihydrazone suggest that the ligand retains same conformation in the complexes as in the uncoordinated state. The free dihydrazone shows a medium intensity band at 1281 cm^{-1} attributed to β(C-O) vibrations. This band shifts to higher frequency by 1-18 cm^{-1} in all of the complexes indicating coordination of naphtholic C-O group to the metal centre in the complexes. The complexes (17) to (19) and (21) also show a weak band in the region 650-660 cm^{-1} which is assigned to arise due to in-plane ring deformation modes of pyridine bases indicating their coordination to the metal ion.

The bands observed in the region 265 to 280 cm^{-1} as weak bands in the complexes (16) to (19) and (21) are assigned to ν(M-N) band from coordinated pyridine or substituted pyridine bases. The non-ligand band appearing in the region 510-526 cm^{-1} is tentatively assigned to νM-O(naphtholate).

These complexes have also been characterized by cyclic voltammetry.

The tentative structures for the complexes have been proposed at the end.

Chapter-V

Synthesis and Characterization of Monometallic Ruthenium(II) Complexes of Disalicylaldehyde adipoyldihydrazone and Bis(2-hydroxy-1-naphthaldehyde) adipoyldihydrazone

The introductory part dwells briefly on the rationality for selecting ruthenium in the present study. Subsequently, it describes the importance of ruthenium complexes in various fields like photochemistry, photocatalyis, biology and electrochemistry. The chapter describes following complexes

(1) $[Ru^{II}(slahH_4)(H_2O)_2]Cl_2$ (22)

(2) $[Ru^{II}(slahH_4)(A)_2]Cl_2$ [A = py, (23); 2-pic, (24); 3-pic, (25); 4-pic, (26)]

(3) $[Ru^{II}(slahH_4)(bpy)]Cl_2$ (27)

(4) $[Ru^{II}(slahH_4)(phen)]Cl_2$ (28)

(5) $[Ru^{II}(npahH_4)(A)_2]Cl_2$ [A = H_2O, (29); py, (30); 2-pic, (31); 3-pic, (32); 4-pic, (33)]

(6) $[Ru^{II}(npahH_4)(bpy)]Cl_2$ (34)

(7) $[Ru^{II}(npahH_4)(phen)]Cl_2$ (35)

The complexes have been prepared by four general methods.

All of the complexes are amorphous in nature. Their colour ranges from brown, grey to dull green. All of these complexes melt in the temperature range 210-240 °C and are stable for some period of time. They then decompose and change their colours and become brown. When the complexes are dissolved in DMF, they yield a mixture of colours. All of these complexes are insoluble in water and other common organic solvents such as ethanol, methanol, acetone, CCl_4, $CHCl_3$, ether and benzene. However, they are partially soluble in acetonitrile and completely so in DMSO and DMF.

The molar conductance values for the complexes suggest that they are non-electrolyte in DMSO. All of the complexes are diamagnetic indicating presence of ruthenium in the +2 oxidation state consistent with low spin d^6 configuration of the metal centre.

In addition to ligand bands the complexes show either one or two moderate –to-strong bands in the 540-690 nm region. The band in the region 614 -690 nm has been assigned to the spin–allowed $^1A_{1g} \rightarrow {}^1T_{1g}$ transition while the band in the region 545-604 nm to $^1A_{1g} \rightarrow {}^1T_{2g}$ transition. Further, the complexes show a strong band in the region 429-470 nm. The molar extinction

coefficient for this band lies in the region 678-3500 $dm^3mol^{-1}cm^{-1}$. Such a high intensity of this band indicates that it owes its origin to the charge transfer, most probably from metal-to-ligand.

The complexes (25), (27), (29), (32) and (34) were characterized by ^1H NMR spectroscopy. Two proton doublet observed in the regions δ 11.20-12.665 ppm and δ 10.18-11.26 ppm downfield of TMS have been assigned to δOH and δNH protons while those in the region δ 8.20-9.15 ppm to δ-CH=N protons, respectively. The multiplets appearing in the region δ 6.90-8.42 ppm have been assigned to phenyl/naphthyl protons. The dihydrazones show doublets in the region δ 2.11-2.58 ppm which are assigned to methylene protons $(-CH_2-)_4$.

δOH proton signals remain almost unshifted on complexation. This indicates that the phenolic/naphtholic –OH groups are not deprotonated even on complexation.

Signals observed in the region δ10.18-11.26 ppm and δ 8.26-9.15 ppm also retain essentially similar position in the complexes which rules out the possibility of coordination of secondary NH nitrogen atom or azomethine group to the metal centre. It appears that the effect of coordination on downfield shifting of the δ-CH=N proton signal is almost the same as that of H-bonding i.e. the non-shift of δ-CH=N-signals may be related to the difference of bonded species to the azomethine group i.e. >CH=N....H to >CH=N→M. It is worth mentioning that δOH and δ-CH=N- signals appear in the form of two signals in all of the complexes. This may be related to coordination of dihydrazone to the metal centre in anti-cis configuration.

The complexes (25) and (32) show an intense signal at δ 2.54 and 2.50 ppm due to methyl protons of 3-picoline molecules. Features associated with 2-pyridyl protons of pyridine, 3-picoline, and 4-picoline confirm flow of electron density from ring nitrogen atoms of these donor molecules. The naphthyl protons multiplet appears

in the region δ 7.11-8.42 ppm. The complexes (29), (32) and (34) have been characterized by ^{13}C NMR spectroscopy as well which confirm the findings of ^{1}H NMR spectroscopy.

IR spectral evidences confirm the findings obtained from ^{1}H NMR and ^{13}C NMR spectra.

Electron transfer reaction some of the complexes have been studied by cyclic voltammetry.

Chapter-VI

Synthesis and Characterization of Heterobimetallic Complexes of Manganese and Ruthenium Derived From Disalicylaldehyde adipoyldihydrazone and Bis(2-hydroxy-1-naphthaldehyde)-adipoyldihydrazone

The introductory part of the chapter dwells briefly on the importance of monometallic and heterobimetallic complexes in various fields like metalloenzymes, homogeneous catalysis and synthesis of solid state phase of industrial and technological importance followed by brief literature on heterobimetallic complexes in general and on manganese and ruthenium complexes in particular.

Heterobimetallic complexes of the compositions $[Mn^{IV}Ru^{II}(slah)(A)_3Cl]Cl.nH_2O$ (where A = H_2O, (36); py, (37); 2-pic, (38); 3-pic, (39); 4-pic, (40), (n = 0, 3)) and $[Mn^{IV}Ru^{II}(npah)(A)_3Cl]Cl.nH_2O$ (where A = H_2O, (41); py, (42); 2-pic, (43); 3-pic, (44); 4-pic, (45), n = 0, 3)) were isolated.

The complexes vary in colour from yellow, brown, dull green, muddy brown, brownish green to dark green. The complexes are partially soluble in acetonitrile, CH_2Cl_2 and insoluble in methanol, ethanol, CCl_4, $CHCl_3$, ether, benzene etc. All of them are freely soluble in DMSO and DMF. All of the complexes decompose above

300 °C. The molar conductance values for the complexes (36) to (45) at 10^{-3} M dilution in DMSO solution lie in the region 35.5–29.7 ohm^{-1} cm^2 mol^{-1}. The molar conductance values for the complexes suggest their 1:1 electrolytic nature.

The magnetic moments for all of the complexes in the present study fall in the region 3.02–4.12 B.M. These values are close to the spin–only value for a d^3 Mn(IV) system i.e. it exhibits a magnetic moment for monomanganese(IV) derivatives corresponding to uncoupled S = 3/2 system. Such a magnetic behaviour of these complexes suggest the presence of Mn(IV) and Ru(II) in these complexes.

The complexes (36) to (40) and (43) show more number of bands than those present in the free ligands due to splitting of ligand bands which is the result of heterobimetallic complex formation. These bands have been attributed to arise due to $n\rightarrow\pi^*$ and $\pi\rightarrow\pi^*$ transitions located on the ligands. In addition to the ligand bands, the complexes show additional bands in the region 439-732 nm. The band of lowest energy observed in the visible region for the complexes (38) and (40) to (45) between 548-732 nm region is assigned to d-d transition mainly localized on Mn(IV) centre but it is also expected to have contribution from $Ru(d\pi)–\pi^*(L)$ transition as these bands have appreciably high molar extinction coefficient values.

The EPR spectral features of the complexes are characteristic of the presence of Mn(IV) and Ru(II) in the complexes. This is evident from the fact that the spectra of the complexes show a strong signal at $g \cong 2$ and another weak signal at $g \cong 4$. The complexes do not show any new signal in the 0–4000 G range which could be assigned to arise due to Ru(III).

The essential features of the IR bands in the region 3000-3600 cm^{-1} indicate the involvement of phenolic –OH/naphtholic –OH group in bonding via deprotonation. The ligand is coordinated to the metal centre in the enol form. The IR structural features of these complexes suggest that the water molecules are not coordinated to

the metal centre in the complexes (38) to (40) and (44). In all these complexes a strong band appears in the region 1600-1613 cm^{-1} attributed to >C=N-N=C< group that indicates condensation of $-NH_2$ group of hydrazide and >C=O group of salicylaldehyde/2-hydroxy-1-naphthaldehyde. The position of this band lies in the region where azomethine nitrogen has been suggested to coordinate to the metal centre in hydrazone complexes. The higher shift of ν(C-O) band in the complexes suggests bonding through phenolate/naphtholate oxygen to the metal centre and reflects strength of (M-O) phenolate/naphtholate band.

All the complexes show a weak to medium intensity non-ligand band in the region 815-857 cm^{-1} which is characteristic of tetraatomic species 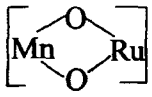

which results from the involvement of phenolate/naphtholate oxygen atom in bridge formation. The band in the region 241–244 cm^{-1} is assigned to νM-N (M = Mn, Ru) stretching frequency due to coordination of pyridyl ring nitrogen atom to the metal centre.

Weak to medium intensity band is observed in the region at 302-307 cm^{-1} in the complexes which is assigned to ν(Ru-Cl).

The electron-transfer reactions of the complexes have been studied with the help of cyclic voltammetry.

SYNTHESIS AND STRUCTURE OF MANGANESE AND RUTHENIUM COMPLEXES DERIVED FROM SOME ADIPOYL DIHYDRAZONES

THESIS

SUBMITTED IN PARTIAL FULFILLMENT OF THE REQUIREMENT OF THE DEGREE OF DOCTOR OF PHILOSOPHY IN CHEMISTRY

BY

DEBAJANI BASUMATARY

DEPARTMENT OF CHEMISTRY

SCHOOL OF PHYSICAL SCIENCES

NORTH-EASTERN HILL UNIVERSITY

SHILLONG

2008

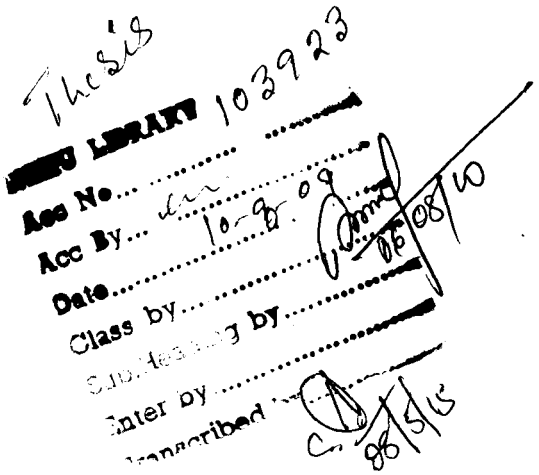

Dedicated to my beloved parents

DECLARATION

I, Debajani Basumatary, hereby declare that the subject matter of this thesis is the record of work done by me, that the contents of this thesis did not form the basis of the award of any previous degree to me or to any body else to the best of my knowledge. I have not submitted the thesis for my research degree in any other University or any Institution. This is being submitted to the North-Eastern Hill University, Shillong for the degree of Doctor of Philosophy in Chemistry.

Debajani Basumatary

Place: Shillong
Date: 24th June 2008

(DEBAJANI BASUMATARY)
Candidate

DEPARTMENT OF CHEMISTRY

NORTH-EASTERN HILL UNIVERSITY, NEHU PERMANENT CAMPUS, UMSHING SHILLONG 793022 (INDIA)

CERTIFICATE

This is to certify that the research work presented in the thesis entitled "Synthesis and Structure of Manganese and Ruthenium complexes Derived from some Adipoyl dihydrazones" is carried out by Ms Debajani Basumatary under my supervision in the Department of Chemistry, School of Physical Sciences, North-Eastern Hill University, Shillong. The work embodied in the thesis does not form the basis for the award of any previous, diploma, fellowship or any other similar title and that it represents entirely an independent work on the part of the candidate.

Prof. R. A. Lal
Supervisor
Department of Chemistry
North-Eastern Hill University
Shillong-793022

Prof. R. H. D Lyngdoh
Head
Department of Chemistry
North-Eastern Hill University
Shillong-793022

Date: 24/6/2008
Place Shillong

R. A. Lal

Tel :+91 364272616; **Fax**: 91 3642550486(work)
Email: ralal@rediffmail.com

ACKNOWLEDGEMENT

The author wishes to express her most sincere gratitude and indebtedness to her supervisor Prof. R. A. Lal, Department of Chemistry, North-Eastern Hill University, Shillong-793022, Meghalaya for his guidance, valuable suggestions and discussions during the tenure of this work. His generous attitude has immensely helped her to do this research work and complete it successfully.

The author desires to express her gratitude to the former and present Head, Dept. of Chemistry, North-Eastern Hill University, Shillong, Prof. R. K. Poddar and Prof. R. H. D. Lynghdoh for providing all the necessary laboratory facilities. Further, author is thankful to the Dean of Physical Sciences, Prof. K. Ismail and other Faculty members of the Department of Chemistry, North-Eastern Hill University, for their cooperation during the progress of this work.

The author desires to convey her sincere gratitude to Dr. A. Lemtur, Department of Chemistry, North-Eastern Hill University, Shillong, for his constant help and guidance in cyclic voltammetric studies. The author also thanks Prof. B. Myrboh and Dr. E. K. Rymmai for their suggestions and help.

The author is thankful to other staff members of Chemistry Department, for their constant help. She is thankful to SAIF (NEHU), Shillong; IIT, Mumbai; CDRI, Lucknow; IIT, Guwahati; IACS, Jadavpur for carrying out spectral studies and elemental analyses.

She is thankful to Council of Scientific and Industrial Research, New Delhi for the award of Senior Research Fellowship.

The author conveys her thanks to her friends and all well wishers for their help, support, valuable suggestions, encouragement and cooperation at various stages of her work.

The author wishes to express her deepest sense of gratitude to her beloved father, mother, brothers and sisters for their immense love, care, affection, inspiration and support throughout her academic life.

Date: 24th June 2008

Debajani Basumatary
(DEBAJANI BASUMATARY)
Department of Chemistry
North-Eastern Hill University
Shillong-793022
Meghalaya

PREFACE

Studies on synthesis, physico-chemical characterization and structural assessment on complexes of Mn(II, IV) and Ru(II) derived from polyfunctional nitrogen and oxygen donor ligands and their incorporating some coligands is the focal theme of the work described in the present thesis. The entire matter of the thesis is distributed over six chapters (**Chapter I-VI**) and **Annexure-I**. Each chapter is virtually complete in itself. The description of the results of work undertaken for the present research work are presented in **Chapter-III** through to **Chapter-VI**. These **Chapters (III-VI)** include a short **Introduction** justifying the specific objective of the work followed by a section on **Experimental** describing the synthesis and then **Results and Discussion** and finally the tentative structures of the complexes.

The first chapter (**Chapter-I**) dealing with Introduction provides a background pertaining to the work described in the thesis. The significance, interest and scope of some polyfunctional Schiff bases have been portrayed in this chapter with citations from contemporary literature. Diversity of structures, synthetic procedures and characterization of coordination compounds have found particular attention in this chapter.

Chapter-II, includes the details of instruments used, synthetic methods of preparation of principal ligands and analytical methods for solid-state characterization of the complexes.

Chapter-III of this thesis is concerned with synthesis, characterization and assessment of the structures of Mn(II) complexes of Disalicylaldehyde adipoyldihydrazone and Bis(2-hydroxy-1-naphthaldehyde)adipoyldihydrazone incorporating pyridine, 2-picoline, 3-picoline, 4-picoline, 2, 2' bipyridine and 1, 10-phenanthroline as coligands. The complexes reported here are of the type

$[Mn^{II}(slahH_2)(H_2O)_2]$ **(1)**, $[Mn^{II}(slahH_2)(py)_2].H_2O$ **(2)**, $[Mn^{II}(slahH_2)(2\text{-pic})_2].H_2O$ **(3)**, $[Mn^{II}(slahH_2)(3\text{-pic})_2].H_2O$ **(4)**, $[Mn^{II}(slahH_2)(4\text{-pic})_2].H_2O$ **(5)**, $[Mn^{II}(slahH_2)(bpy)]$ **(6)**, $[Mn^{II}(slahH_2)(phen)]$ **(7)**, $[Mn^{II}(npahH_2)]$ **(8)**, $[Mn^{II}(npahH_2)(py)_2]$ **(9)**, $[Mn^{II}(npahH_2)(2\text{-pic})_2]$ **(10)**, $[Mn^{II}(npahH_2)(3\text{-pic})_2]$ **(11)**, $[Mn^{II}(npahH_2)(4\text{-pic})_2]$ **(12)**, $[Mn^{II}(npahH_2)(bpy)]$ **(13)**, $[Mn^{II}(npahH_2)(phen)]$ **(14)**.

Synthesis, characterization, electrochemical studies and structural assessment of Bis(2-hydroxy-1-naphthaldehyde)adipoyldihydrazone complexes of manganese(IV) with coligands forms the subject matter of **Chapter-IV**. The complexes mentioned here are $[Mn^{IV}(npah)(H_2O)_2]$ **(15)**, $[Mn^{IV}(npah)(py)_2].H_2O$ **(16)**, $[Mn^{IV}(npah)(2\text{-pic})_2]$ **(17)**, $[Mn^{IV}(npah)(3\text{-pic})_2].H_2O$ **(18)**, $[Mn^{IV}(npah)(4\text{-pic})_2].H_2O$ **(19)**, $[Mn^{IV}(npah)(bpy)]$ **(20)** and $[Mn^{IV}(npah)(phen)]$ **(21)**.

Chapter-V of this thesis presents an account of synthesis, characterization, electrochemical studies and structural assessment of ruthenium(II) complexes of Disalicylaldehyde adipoyldihydrazone and Bis(2-hydroxy-1-naphthaldehyde)-adipoyldihydrazone with the coligands pyridine, 2-, 3-, 4-picoline, 2, 2' bipyridine and 1, 10-phenanthroline. The reported complexes are of the type $[Ru^{II}(slahH_4)(H_2O)_2]Cl_2$ **(22)**, $[Ru^{II}(slahH_4)(py)_2]Cl_2$ **(23)**, $[Ru^{II}(slahH_4)(2\text{-pic})_2]Cl_2$ **(24)**,$[Ru^{II}(slahH_4)(3\text{-pic})_2]Cl_2$**(25)**, $[Ru^{II}(slahH_4)(4\text{-pic})_2]Cl_2$ **(26)**, $[Ru^{II}(slahH_4)(bpy)]Cl_2$ **(27)**, $[Ru^{II}(slahH_4)(phen)]Cl_2$ **(28)**, $[Ru^{II}(npahH_4)(H_2O)_2]Cl_2$ **(29)**, $[Ru^{II}(npahH_4)(py)_2]Cl_2$, **(30)**, $[Ru^{II}(npahH_4)(2\text{-pic})_2]Cl_2$ **(31)**, $[Ru^{II}(npahH_4)(3\text{-pic})_2]Cl_2$ **(32)**, $[Ru^{II}(npahH_4)(4\text{-pic})_2]Cl_2$ **(33)**, $[Ru^{II}(npahH_4)(bpy)]Cl_2$ **(34)**, $[Ru^{II}(npahH_4)(phen)]Cl_2$ **(35)**.

The final chapter **Chapter-VI** deals with synthesis, characterization, electrochemical studies and structural assessment of $[Mn^{IV}Ru^{II}(slah)(H_2O)_3Cl]Cl$ **(36)**, $[Mn^{IV}Ru^{II}(slah)(py)_3Cl]Cl$ **(37)**, $[Mn^{IV}Ru^{II}(slah)(2\text{-pic})_3Cl]Cl.3H_2O$ **(38)**, $[Mn^{IV}Ru^{II}(slah)(3\text{-pic})_3Cl]Cl.3H_2O$ **(39)**, $[Mn^{IV}Ru^{II}(slah)(4\text{-pic})_3Cl]Cl.3H_2O$ **(40)**,

$[Mn^{IV}Ru^{II}(npah)(H_2O)_3Cl]Cl$ **(41)**, $[Mn^{IV}Ru^{II}(npah)(py)_3Cl]Cl$ **(42)**, $[Mn^{IV}Ru^{II}(npah)(2\text{-}pic)_3Cl]Cl$ **(43)**, $[Mn^{IV}Ru^{II}(npah)(3\text{-}pic)_3Cl]Cl.3H_2O$ **(44)**, $[Mn^{IV}Ru^{II}(npah)(4\text{-}pic)_3Cl]Cl$ **(45)**. Room temperature magnetic moment and EPR spectral data are consistent with the system comprising of Mn(IV) and Ru(II) with no interaction between metal centres in the complexes

A **summary** describing the research highlights and **references** have been given at the end. Part of the work described in **Chapter-III** and **IV** have been communicated for publication and rest are being compiled for publication.

CONTENTS

CHAPTER-I

INTRODUCTION AND LITERATURE SURVEY

INTRODUCTION

The present thesis is an embodiment of the development of heterobimetallic chemistry of manganese and ruthenium. Hence, it appears pertinent to mention the importance of manganese and ruthenium in general and to describe the characteristic features of bonding properties of dihydrazones and then literature survey on dihydrazones metal complexes.

Manganese is an essential cofactor of green plant photosynthesis in photosystem II for the oxidation of water to dioxygen. Another important role of manganese is as the active catalytic centre in mitochondrial and several bacterial superoxide dismutases [1]. Manganese also plays a central role in an azide sensitive catalase [2]. Besides this, it occurs in some enzymes. Some multinuclear enzymes like arginase also require manganese to show their biological activity [3].

The role of manganese in our natural ecosystem is far more important. Manganese is known to be a key player of water-oxidation, a process that occurs during the natural photosynthesis [4]. Plants use an extensive array of photopigments in photosystem-II, 4 manganese ions, calcium and chloride. In photosystem-II, the water oxidizing enzyme uses water as an electron source. Therefore, it provides an unlimited source of electron to the entire biosphere.

The key player in water oxidation is a triad composed of a multimer of chlorophyll, (named P_{680}), a redox-active aminoacid (named tyrosine) and a Mn cluster composed of 4 Mn ions of high valence (the oxygen evolving complex, OEC). In the PSII, the tetramanganese complex serves as an electron donor.

Upon the absorption of photon, P_{680} is excited and loses an electron leading to formation of P^{+}_{680}. This is the first step of the conversion of light into chemical energy. P^{+}_{680} is transformed reversibly into the original photosynthesizer P_{680} by receiving an electron from the tetramanganese complex. Further it has been established that O_2 evolution continues even when some of the manganese atoms are replaced with other divalent metal ions which restore electron transportation in PSII [5].

Our entire ecosystem is dependent on this process for the harvesting of the solar energy. Solar energy emerges as one of the most promising source for future sustainable production of fuel and electricity. The concept of natural photosynthesis can be used to build an artificial system which can harvest solar energy. This system should convert solar energy into fuel, such as hydrogen which could be stored in a chemical form. However, at present no system is known which operates on the principle of the photosynthesis of green plants. Fundamental research work is clearly required in this area. In nature, the solar energy is converted into chemical energy with water as electron source. The efficiency in the crucial steps is remarkably high. The construction of artificial system that exactly mimics these reactions remains a great challenge to chemists. If a successful mimetic system could be made, much would be learnt at the fundamental level. Furthermore and potentially very importantly, we would have new tools to better exploit solar energy for the generation of fuels and electricity.

Ruthenium exhibits a wide range of oxidation states in its compounds and complexes stabilized by a wide variety of co-ordinating ligands. These varying oxidation states control the chemistry of the metal. Ruthenium-Schiff base complexes, particularly those containing oxygen and nitrogen as donor atoms, are found to be very efficient catalysts in oxidation reactions. High

valent polypyridyl ruthenium oxo-complexes have been found to be stoichiometric or catalytic oxidants.

Thus, the complexes of ruthenium have been widely explored because of their potential in electron transfer reactions [6] and excited state redox properties that renders their potential application in areas as diverse as solar energy conversion [7], artificial photosynthesis and test theories of photophysics.

Further, because of photophysical and photochemical properties of ruthenium complexes, it has been suggested that they might find applications in many fields, like use as semiconductors in solar energy conversion [8].

Ruthenium complexes have attracted much attention not only because of their favourable photophysical and photochemical properties but also because of their potential ability as molecular switches [9] in photodynamics, chemotherapy and for charge transport through DNA [10, 11]. The luminescent properties [12] of ruthenium complexes have rendered their applications as bioanalytical species [13]. The rational design of Ru(II) complexes containing a biotin moiety have been characterized recently as a new class of species.

Bimetallic ruthenium complexes present, perhaps, the best functional model for the chemistry associated with the manganese proteins. In this scheme, a ruthenium(III) dimer undergoes oxidation by either chemical or electrochemical means to produce dioxygen from two coordinated water molecules. During this process, the ruthenium atoms cycle reversibly between d^5 and d^3 configurations. The same is, probably true of the photosynthetic manganese centres. The ruthenium complex draws particularly more attention because it presents the oxidative portion of the popular $[Ru(bpy)_3]^{2+}$ sensitized photosystem [14]. The significance of ruthenium complex is that they can form the core of new

polymetallic systems that may have applications in excited state energy and electron transfer reactions [15].

If some complex systems containing manganese and photosensitizer ruthenium could be prepared, this may undergo an intermolecular electron transfer in the presence of an electron acceptor, in solution from photoexcited state of Ru^{II} to an acceptor followed by an intermolecular electron transfer from coordinated Mn complexes. This will lead to regeneration of the Ru^{II} and oxidation of Mn centre in the complex. The manganese centre then may receive electron from coordinated water molecules leading to its oxidation to molecular dioxygen and production of H^+ ions which could be restored in the chemical form.

In view of the above stated importance of manganese and ruthenium and absence of work on ruthenium complexes derived from dihydrazones, present study has been undertaken, as a part of the training programme. Further, as the monometallic complexes serve as precursor in the synthesis of heterobimetallic complexes, it was imperative to synthesize and characterize them as well. Accordingly, the study of monometallic and heterobimetallic manganese and ruthenium complexes of the polyfunctional dihydrazones has been undertaken and the present thesis embodies the results of such an investigation.

The study could develop into a very wide field. The present investigation is restricted to only manganese and ruthenium and specific dihydrazones, disalicylaldehyde adipoydihydrazone ($slahH_4$) and bis(2-hydroxy-1-naphthaldehyde)adipoyldihydrazone ($npahH_4$).

The reactions have been carried out in neutral and alkaline methanol media at room temperature, higher temperature or under reflux. A number of monometallic complexes of manganese and ruthenium from $slahH_4$ and $npahH_4$ have been synthesized under different experimental conditions. The compositions of the complexes have been established based on data obtained

from analytical studies. The structural assessment of the complexes have been carried out on the basis of molar conductance, magnetic moment data, EPR, electronic, infrared and ^{1}H NMR spectroscopic studies. Electrochemical studies of some complexes have also been done. These results are presented in chapter III to VI.

A chapter-wise summary of the work and references have also been given at the end.

DESCRIPTION OF LIGANDS

The ligands disalicylaldehyde adipoyldihydrazone ($slahH_4$) and bis(2-hydroxy-1-naphthaldehyde)adipoyldihydrazone ($npahH_4$) selected in the present study have been derived from condensation of adipoyldihydrazine with salicylaldehyde and 2-hydroxy-1-naphthaldehyde. These contain four methylene flanked by keto groups in addition to other functional groups like amide, azomethine and phenol functions, each in duplicate. All of the donor atoms because of their symmetrical character have equal probability of taking part in coordination. The ligands can react with the metal ions in keto, keto–enol and enol forms respectively.

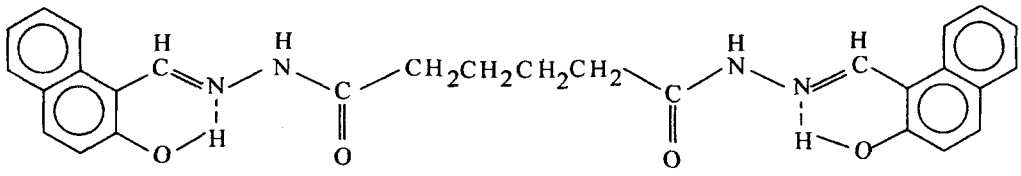

Thus because of the presence of as many as eight bonding sites, its ability to exhibit keto-enol tautomerism in the complexes and its ability to offer chemically flexible ligand framework due to free rotation of the two hydrazone groupings about C-C single bond, it can bound to metal ions in several different ways as under:

i) It may function as a neutral bidentate ligand coordinating either through two carbonyl oxygen atoms (I) or the two secondary amine nitrogen atoms (II), OH groups remaining hydrogen bonded in the complexes.

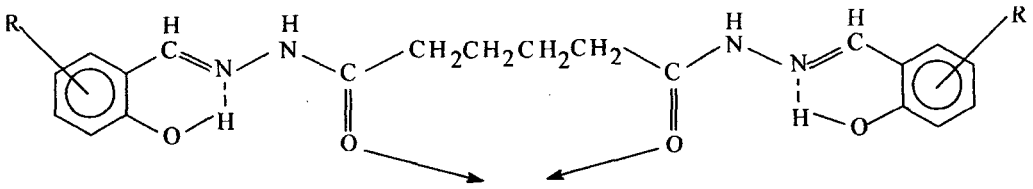

(I)

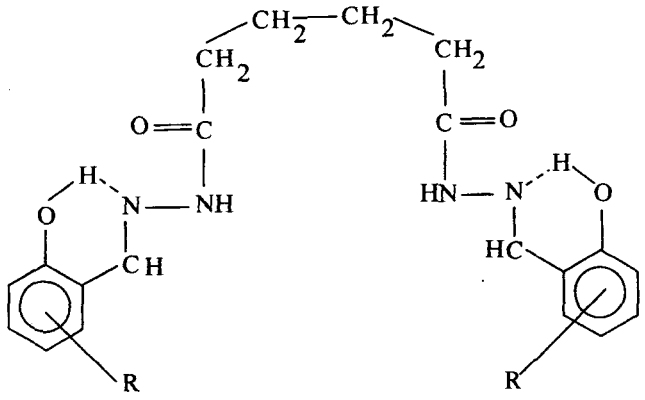

(II)

(ii) It may function as monobasic tridentate ligand coordinating through one hydroxyl oxygen, one azine group nitrogen and one >C=O group oxygen atom (III) while the other half portion of the molecule remaining unbonded.

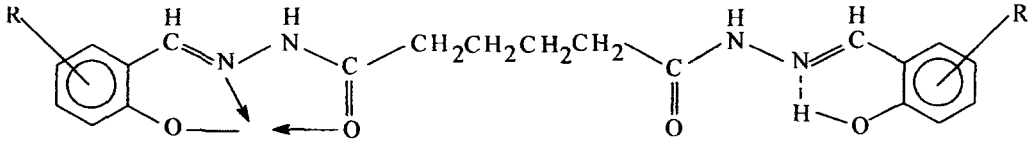

(III)

(iii) It may function as a dibasic tetradentate ligand coordinating through the two hydroxyl oxygen atoms and the azine group nitrogen atoms (IV), the two carbonyl atoms remaining unbonded.

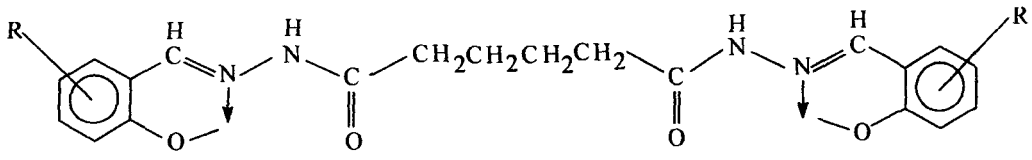

(IV)

(iv) It may act as a dibasic hexadentate ligand bonding to the same metal ion through two hydroxyl oxygen, two azine nitrogen and two carbonyl oxygen atoms (V).

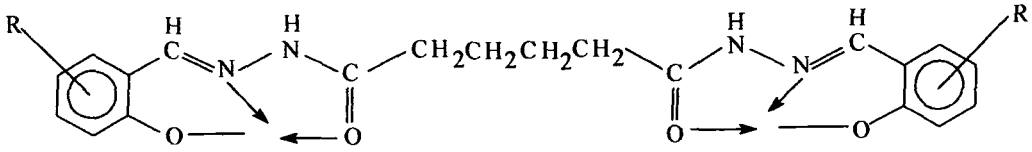

(V)

(v) It may function as a dibasic octadentate ligand bonding to the same metal ion through all the available bonding sites (VI) but such a probability is ruled out on account of the simultaneous coordination of the secondary amine nitrogen and carbonyl oxygen to the same metal or even different metal atoms due to the steric considerations and inductive effect.

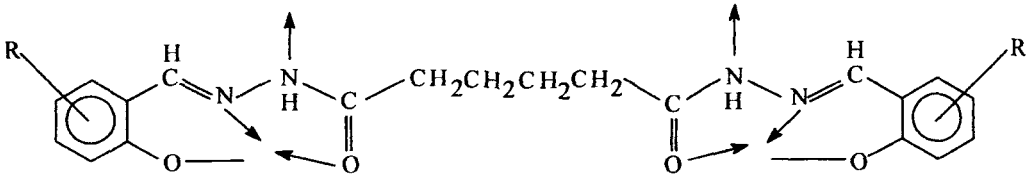

(VI)

(vi) When the ligand undergoes enolization as shown below it may afford newer bonding possibilities. In this form it can act as dibasic tridentate (VII), dibasic tetradentate (VIII), dibasic pentadentate (IX) and tetrabasic hexadentate (X) ligand bonding to the same or different metal ions. In the enolized form it can also act as a binucleating or polynucleating ligand.

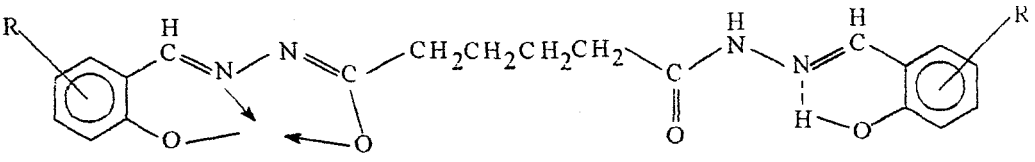

(VII)

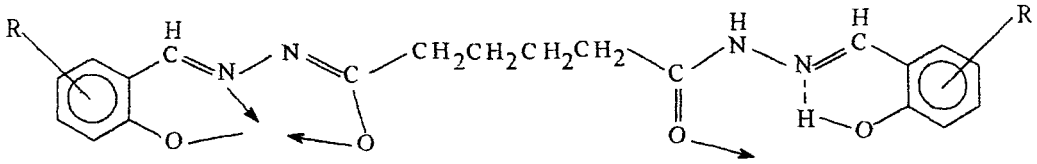

(VIII)

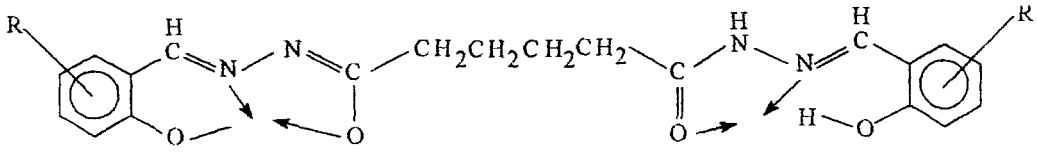

(IX)

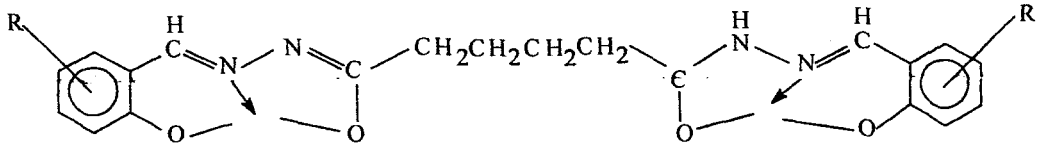

(X)

(vii) It may also coordinate to the metal ion in *keto-enol* (XI) and enol (XII) forms involving active methylene proton in enolization.

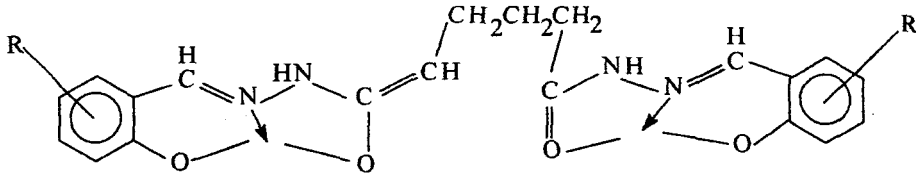

(XI)

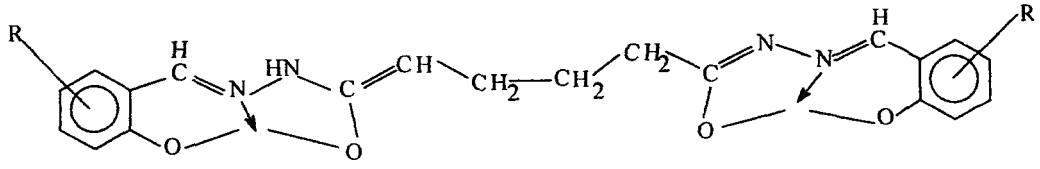

(XII)

(viii) It may function as a tetrabasic octadentate ligand bonding to the same metal ion through all the available bonding sites (XII), but such a probability is also ruled out on account of the reason cited above at (v).

The dihydrazone can exist in the metal complexes either in the *staggered*-configuration (XIII) or *cis*-configuration. In *cis*-configuration, the dihydrazone can adopt either *syn-cis* configuration (XIV) or *anti-cis* configuration (XV).

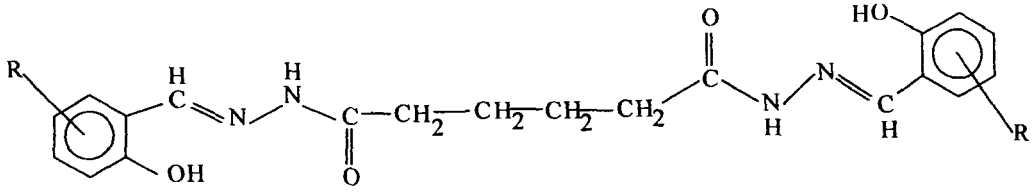

(XIII)

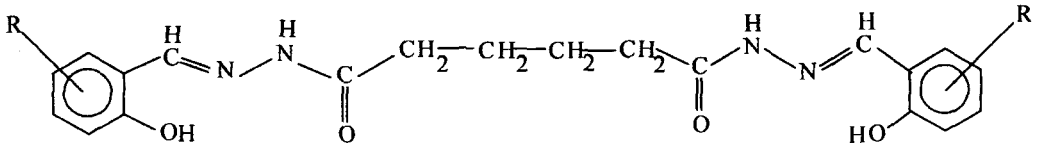

(XIV)

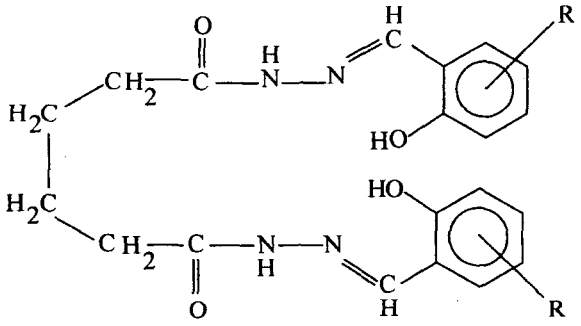

(XV)

All these possibilities can actually be realized in practice if the nature of the metal salt, mole ratio of the metal ion and the ligand, the nature of the counter cation and anion, reaction medium, pH and temperature are varied.

LITERATURE SURVEY

Hydrazine is a potential ligand which functions in metal complexes as monodentate, bidentate chelating and bridging ligand. The coordination behaviour of hydrazine is modified by substitution of one of the hydrogen in hydrazine by an acyl group, which provides additional bonding sites of carbonyl oxygen atoms, the resulting -CONH- group is capable of existing in keto-enol equilibrium. In such monoacyl hydrazines, the bridging character of hydrazine is lost and the studies have revealed that such derivatives act as bidentate ligands coordinating through carbonyl oxygen and $-NH_2$ groups.

Further, condensation of N-acyl hydrazines with aldehyde and ketones give acyl-hydrazones (Schiff bases). In such ligands basicity of nitrogen atoms in hydrazine residue is considerably reduced by substitution on either side. A variety of such hydrazones can be prepared in which the number of bonding sites can be increased as desired by changing acyl groups. Condensation of acylhydrazines with an o-hydroxy aromatic aldehyde and ketones enhances chelating tendencies of the acylhydrazones. The Schiff bases derived from monoacyl and aroylhydrazines with hydroxyaldehydes and ketones form 1:1 and 1:2 (metal:ligand) complexes can function either as a monobasic bidentate [16], monobasic tridentate [17] in keto form [17, 18] or dibasic tridentate in enol form [19, 20] and yield dimeric or polymeric chelates in which they coordinate to metal ion through >C=O and >C=N groups besides bonding through -OH group. Closely related to monoacyl, aroyl-, and pyridoyl-, hydrazones are acyl-, aroyl- and pyridoyl, dihydrazones containing same donor group but each in duplicate, which increases their bonding potentialities. In such dihydrazones, the two hydrazone parts may be linked to one another either directly or by methylene chains of varying length or phenyl or pyridyl groups.

The dihydrazones can be obtained from condensation of acyl-, aroyl- and pyridoyl- dihydrazines [$R(CONHNH_2)_2$; R = O, $-(CH_2)_n$, $-C_6H_4<$, $C_5H_3N<$] with o-hydroxy aromatic aldehydes and ketones. Another category of the dihydrazones can be obtained from condensation of dialdehydes [$R(CR^1O)_2$, R = O, $-(CH_2)_n$, $-C_5H_3N<$, R^1 = alkyl groups] with mono acyl-, aroyl-, pyridoyl- and quinaldinoyl- hydrazines. Accordingly, the literature survey is presented under the following two major sections.

A) Complexes of dihydrazones derived from condensation of acyl-, aroyl-, and pyridoyl- dihydrazones with simple and o-hydroxy aromatic aldehydes and ketones.

B) Complexes of dihydrazones derived from condensation of dialdehydes with monoacyl-, aroyl-, pyridoyl- and quinaldinoyl-hydrazines.

Sacconi [21] has isolated a series of diamagnetic nickel(II) complexes of dihydrazones obtained from condensation of aliphatic dicarboxylic acid dihydrazides with salicylaldehyde, 2-hydroxy-1-naphthaldehyde, o-aminobenzaldehyde and o-hydroxyacetophenone. He showed that the hydrazones react in the *enol* form with $Ni(OAc)_2$ in aqueous alcoholic ammonia as bis tridentate complexing agents.

Aggarwal and Singh [22] isolated complexes of the compositions $[VO(LH_2)]SO_4$, $[VO(LH_2)]Cl_2$, $[VO(LH_2)py]SO_4$ and $M(LH_2)Cl_2$ (where M = Zn(II), Cu(II), Ni(II) and Co(II) from reaction of vanadyl sulphate and chloride and metal(II) chloride with bis(acetone)oxaloyldihydrazone, bis(acetone)malonoyldihydrazone and bis(acetone)succinoyldihydrazone in alcoholic medium. The complexes $[VO(LH_2)]SO_4$, $[VO(LH_2)]Cl_4$ were proposed to have square pyramidal stereochemistry while the remaining complexes were proposed to have octahedral stereochemistry.

Iskander and coworkers [23] isolated the metal(II) complexes of the composition $M(LH_3)X.nH_2O$, $M_2(LH_2)X_2.nH_2O$, $M(LH_2).nH_2O$ and $M(LH_2).nH_2O$ (where M = Cu(II), Ni (II), and Co(II); X= Cl, Br, I) from reaction of the metal (II) salts with dihydrazones (LH_2) derived from condensation of salicylaldehyde with acyldihydrazines containing methylene backbone varying from (1) to (5) under different experimental conditions. They assigned a pseudo-octahedral stereochemistry for the nickel(II) complexes $[Ni(LH_3)X].nH_2O$ (X= Cl, Br, I) and $[Ni_2(LH_2)Cl_2].2H_2O$ on the basis of magnetic moment data and spectral studies. The latter complexes change to penta-coordinated state on dehydration. However, five coordinate structure was proposed for the nickel(II) complexes $[Ni(LH_2)].nH_2O$ as against a distorted octahedral structure for the corresponding cobalt(II) analogues. On the otherhand, Kapoor and coworkers [24] suggested that the nickel(II) complexes $[Ni(LH_2)].nH_2O$ have octahedral stereochemistry. Anomalous magnetic behaviour of the nickel complexes $[Ni(L)].nH_2O$ (μ_{eff} values lying in the range 1.65-1.70 B.M) is ascribed to arise due to the presence of two magnetically non-equivalent sites in the same unit cell. All the cobalt(II) complexes are proposed to have octahedral stereochemistry. The copper complexes $[Cu(LH_3)X].nH_2O$ and $[Cu_2(LH_2).X_2].nH_2O$ are proposed to have square pyramidal stereochemistry. The low magnetic moment values than spin-only values attributed to superexchange interactions through the oxygen bridges.

Narang and Lal [25] have described complexes of disalicylaldiminesuccinamide (H_2L) and N, N-Bis(o-hydroxyacetophenone-imine)succinamide (H_2J) of the types ML, MJ′, M(HL)Cl, M(HJ)Cl and $M'(HL)_2$ (where M = Cu(II), Ni(II) or Co(II) and M′ = Ni(II) or Co(II)). The complexes are proposed to have either octahedral stereochemistry or square planar stereochemistry.

Narang and Lal [26] have reported mono and binuclear zinc(II) complexes Zn(HL)Cl and $Zn_2(L-2H)$ derived from multidentate acyldihydrazone ligands (H_2L). The reaction medium, zinc salts and ligand geometry are shown to influence the composition and stereochemistry of the complexes. The zinc centres were proposed to have octahedral as well as tetrahedral stereochemistry.

Polymeric metal (II) complexes [27] of the type M_2L, derived from dihydrazones obtained from condensation of oxaloyldihydrazide, succinoyldihydrazide and phthaloyldihydrazide with salicylaldehyde or o-hydroxyacetophenone have been described by the above authors. The anomalously low magnetic moments of some complexes are related to M-M interactions via oxo-bridge structure.

Narang and Lal [28] have prepared and characterized the metal(II) complexes $M(H_2J)$, $M(H_2K)$, $M(H_3J)Cl$, $M(H_3K)Cl$; M_2J, M_2K and $M_2(HK)(CH_3COO)$ (where M = Cu(II), Ni(II) and Co(II) derived from di(salicylaldimine)malonamide (H_4K) and the zinc(II) complexes $Zn(H_2L)$ and $Zn_2(L)$ from a number of multidentate acyldihydrazones (H_4L).

Narang and coworkers [29] synthesized new series of polymeric cobalt(II) complexes of the type $Co_2(L).nH_2O$ from reaction of metal(II) acetate and dihydrazone (LH_4) where LH_4 is bis(o-hydroxyacetophenone)-oxaloyldihydrazone or bis(salicylaldehyde)oxaloyldihydrazone, bis(o-hydroxyacetophenone)succinoyldihydrazone in the ratio 4:1 (metal:ligand) in ethanol under reflux. The complexes have been proposed to possess polymeric structure with strong Co-Co interactions with planar dispositions of donor atoms around metal centres.

Sahni and coworkers [30] synthesized and characterized complexes of the type $[M(LH_2)]X_3$ (where M = Cr(III), Mn(III), Fe(III) or Co(III); X = Cl, NO_3 or

(OAc)) from reaction of metal(III) salt with N, N-dibenzylidene dipicoline acid hydrazone (LH_2) in ethanol medium. The ligand acts as a pentadentate unit having coordination sites at pyridine nitrogen, amide oxygens and hydrazinic nitrogens or azomethine nitrogens. In this context, it is important to mention that these authors [31] have also claimed that dipicolinic acid dihydrazine behaves as pentadentate ligand. On the other hand, Dutta and Sarkar [32] have argued in favour of neutral tridentate behaviour of this ligand in which it can function either as a (NNN) or as (ONO) donor.

Kapoor and coworkers [33] have studied reaction of vanadyl chloride and dipicolinic acid dihydrazone in presence of acetylacetone or other β-diketones in ethanol and acetic acid. They isolated brown solid complexes of macrocyclic ligand bis(β-diketone)dipicolinoyldihydrazones. On the otherhand, they isolated a non-macrocyclic pyrazole derivative when reaction of vanadyl chloride was carried out with the preformed bis(β-diketone)dipicolinic acid dihydrazone. Similar products [34] were also isolated in case of zirconium(IV).

Teotia and Rana [35] synthesized complexes $[M(L)(H_2O)_2]$ (M = Cu(II), Ni(II) and Co(II) of the above macrocyclic ligands by treating a methanol solution containing acetylacetone and 2, 6-dipicolinic acid hydrazide and the appropriate metal chloride. The IR spectra indicated condensation of both the oxygen atoms of acetylacetone with NH groups of dihydrazine. The electronic spectral bands agree reasonably well with five coordinate geometry.

Kapoor and coworkers [36] synthesized a number of metal(II) and metal(III) complexes from the reaction of metal(II) and metal(III) salts with dihydrazones obtained from condensation of salicylaldehyde with oxaloyldihydrazone, malonoyldihydrazine and succinoyldihydrazine under different experimental conditions. The trivalent metal ions are found to yield complexes having compositions $[M_2LX_2].nH_2O$ and $[M_2(LH_2)X_4)].nH_2O$ (M =

Cr(III), Fe(III) and Mn(III); X= Cl, NO_3, OAc, OH) while the bivalent metal ions were found to form complexes having compositions $[M(LH_2)]$ and $[ML(H_2O)_4]$ (M = Mn(II) and Fe(II)). The dihydrazones are suggested to function as dibasic and tetrabasic hexadentate binucleating ligands. In Mn(III) complexes were characterized by Mossbauer spectroscopy as well.

Narang and Yadav [37] studied reaction of aluminum(III) salts with several dihydrazone ligands in aqueous medium at controlled pH and characterized the resulting complexes by infrared spectroscopy. The complexes are suggested to be polymeric with dihydrazones coordinated in the keto form.

Narang and Dubey [38] have described Zn(II), Cu(II), Ni(II) and Co(II) complexes of solid polymers derived from glyoxal and organic acid dihydrazides. They have discussed the structure of the complexes in the light of magnetic moment, electronic and IR spectral studies.

Yacouta and coworkers [39] studied the complexation behaviour of uranyl ion with various dihydrazides and their dihydrazones obtained from condensation of simple o-hydroxyaromatic aldehydes and ketones with dihydrazides. They isolated several monometallic and bimetallic uranyl complexes and characterized them by various physico-chemical data and spectroscopic studies. They also studied effect of excess acetate ion on complex formation.

Lal and coworkers [40] have prepared several homotrinuclear complexes having general formula $[M_3LCl_2(H_2O)_3]$ (where M = Mn(II), Co(II) or Ni(II) from bis(acetophenone)-2, 6-dipicolinoyldihydrazone (LH_4) in alcoholic medium by adjusting pH to ~8 by KOH. The complexes show μ_{eff} values much less than those expected for the high-spin metal ions possibly due to metal-metal interaction and antiferromagnetic exchange. The complexes are proposed to have mixed six-coordinate octahedral and five coordinate square

pyramidal stereochemistry.

Narang and Singh [41] have synthesized polymeric complexes $M(L-2H).nH_2O$ (where M = Fe(II), Mn(II), Co(II), Ni(II), Cu(II), Zn(II), Cd(II) and Hg(II); L = A, B) from bis(2-hydroxy-1-naphthaldehyde)-oxaloyldihydrazone (A) and bis(2-hydroxy-1-naphthaldehyde)-malonoyldihydrazone (B) by solid-solution reaction. All of the complexes were suggested to have distorted octahedral stereochemistry.

Lal and coworkers [42] studied reaction of uranyl acetate with the above dihydrazones (H_4L) in aqueous–alcoholic media and isolated complexes of the type $(UO_2)_2L.6H_2O$. The dihydrazones coordinate to the metal centre in enol form. They have studied the effect of complexation on the coupling of >C=O vibrations, in enolized form and of ligand coordination to the uranyl ion as a function of the number of methylene group by comparing the asymmetric stretching vibrations of the uranyl ion in various complexes recorded under identical conditions.

Lal and Das [43] studied reaction of uranyl nitrate and acetate with dihydrazones (H_4L) (where H_4L = disalicylaldehyde-oxaloyldihydrazone (H_2L), -malonoyldihydrazone (H_4B), -succinoyldihydrazone (H_4C), -glutoyl-dihydrazone (H_4D), -adipoyldihydrazone (H_4E) and phthaloyldihydrazone (H_4F) in 3:1 molar ratio in alcoholic medium. The complexes $[(UO_2)_2(H_2L)(NO_3)_2(H_2O)_4].2H_2O$ and $[(UO_2)_2(H_2L)(CH_3COO)_2-(C_2H_5OH)_2].C_2H_2OH$ have been isolated and characterized.

Lal and coworkers [44] synthesized copper(II) complexes $Cu_2(L).nH_2O$ and dioxouranium(VI) complexes $[(UO_2)_2(H_2L)(C_2O_4)]_n.2nH_2O$ of the above dihydrazones. The $C_2O_4^{2-}$ group is suggested to coordinate to the uranium centre retaining its D_{2h} symmetry.

Lal [45] synthesized a series of uranyl complexes of the composition

$[UO_2(LH_3)_2].nH_2O$ from above reaction of uranyl nitrate with salicylaldehyde and acyl- and aroyl-dihydrazines in 1: 4: 2 molar ratio ratio in ethanol medium.

Lal and coworkers [46] studied reactions of disalicylaldehyde adipoyldihydrazone with uranyl nitrate and uranyl acetate in aqueous and ethanol media under different experimental conditions. The complexes of the compositions $[UO_2(H_2L)(H_2O)]_n$, $[UO_2(H_2L)_2]_n.3nH_2O$, $[UO_2(H_2L)(CH_3COO)]_n.3nH_2O$, $[UO_2Zn(L)(H_2O)]_n.2nH_2O$, $[(UO_2)_2(H_2L)(C_2O_4)]_n.2nH_2O$, $[(UO_2)_2(L)(py)_2(H_2O)_4]$, $[(UO_2)_2(HL)(OAc)(H_2O)_3]_n.nH_2O$, $[(UO_2)_3(L)(CH_3COO)_2(H_2O)_2]_n.2H_2O$, $[(UO_2)_2(L)(py)_2(H_2O)_2]_n.xnH_2O$ (where py = pyridine or α-, β-, γ- picoline; x = 0, 1) have been isolated and characterized. In these complexes the ligand functions as a bridging monobasic tetradentate, dibasic hexadentate and tetrabasic hexadentate ligand and exhibits keto-enol tautomerism.

Lal and coworkers [47] have described dioxouranium(VI) and zinc(II) complexes $[M(H_2L)(H_2O)_2]_n.2nH_2O$ (where M = UO_2^{2+}, Zn^{2+}) of bis(o-hydroxynaphthaldehyde)oxaloyldihydrazone (H_2L). Dioxouranium(VI) complex is proposed to be eight coordinate involving coordination of dihydrazone in the enolic form with *cis*-configuration while the zinc complex is proposed to be octahedral involving coordinated dihydrazone in enolic form in the *staggered*-configuration. The naphtholic -OH groups are shown to be non-coordinated. They have, further, synthesized dioxouranium(VI) complexes $[UO_2(H_2L)]_n.2nH_2O$ and $[(UO_2)_2(L)(H_2O)_6]_n$ [48] from reaction of uranyl nitrate with preformed bis(o-hydroxynaphthaldehyde)oxaloyldihydrazone in a 3:1 molar ratio in aqueous and ethanol media, respectively, under reflux. Based on the splitting of the δ-NH- signal in monometallic complex and δ-CH=N signal in both the complexes into quartet as compared to the singlet in free

dihydrazone, the complexes are proposed to exist in chair conformation with the *anti-cis*-configuration of dihydrazone involving eight coordinated uranium atoms, respectively.

The complexes $Na_4[(UO_2)_4(L)_2(OAc)_4(H_2O)_4].4H_2O$ and $Na_4[(UO_2)_4(L)_2F_4(H_2O)_4]$ [49] obtained from the same ligand have also been described by them.

Patil and Kulkarni [50] and others [51] obtained complexes of the type $[UO_2L].nH_2O$ from *interaction of uranyl acetate and disalicylaldehyde* thiocarbohydrazone (H_2L) and established their structure by ^1H NMR and IR spectroscopic studies.

Kapoor and coworkers [52] studied reactions of malonoyldihydrazine and phthaloyldihydrazine with β-diketones in the presence of dioxouranium(VI) cation which appears to function as a metal template. This facilitates condensation of dihydrazide with diketones giving macrocyclic ligands which coordinate to the metal centre leading to the formation of several dioxouranium(VI) complexes. The formation of a macrocyclic ring was confirmed from infrared spectroscopic studies. However, when dioxouranium(VI) nitrates is treated with the condensation product of phthaloyldihydrazine and acetophenone, an entirely different pyrazole derivative is formed.

Sahoo and coworkers [53] have synthesized several first series transition metal complexes from several dihydrazones. The complexes were characterized by elemental analysis, physico-chemical data and spectral studies.

Pandey [54] reported a number of organometallic complexes derived from pyridoyldihydrazones. In this study, he showed from IR spectral data that dihydrazones coordinate to the metal centre in keto form through both >C=O and >C=N groups.

Mahale and Havanur [55] studied dioxomolybdenum(VI) complexes of the composition $[(MoO_2)_2(L)(py)_2]$ synthesized from dihydrazones (H_4L) obtained from condensation of several acyl-dihydrazines and substituted salicylaldehydes.

Panda and coworkers [56] synthesized heterobimetallic complexes $[MNiM(BTDO)_2X_2(H_2O)_4].nH_2O$ (where M = Ni(II), Co(II) and Cu(II); X = Cl, NO_3; n = 0 or 0.5 and BTDO = 1, 8-Bis(2-oxophenyl)-2, 3, 6, 7-tetraza-4, 5-dimethyl-1, 3, 5, 7-octatetraene) from the precursor nickel complex nickel [bis(diacetyldihydrazone)]. The metal centres have been proposed to have octahedral stereochemistry.

Gopinathan and coworkers [57] have shown that the Schiff base, $(HOC_6H_4CH{=}NNCO)_2CH_2(H_4L)$ derived from the condensation of salicylaldehyde and malonoyldihydrazine reacts with organotin chlorides to yield binuclear complexes of the type $R_2Sn(L)SnR_2$, where R = CH_3-, C_2H_5-, C_4H_9-, C_6H_5-, $CH_3CO_2CH_2CH_2$ and $C_6H_5CH_2$. The complexes have been characterized and the structures assigned on the basis of their elemental analyses, IR, ^1H, ^{13}C, ^{119}Sn NMR spectra and X-ray crystallographic data. They studied the structure of the complex $[(C_2H_5)_2Sn]_2(OC_4H_4CH{=}NNCO)_2CH_2$ by X-ray crystallography. The crystal belongs to monoclinic space group 12/a.

Sacconi [58] studied reactions of biacetyl-bis(benzoylhydrazone) with nickel(II) acetate in alcohol in the presence of concentrated ammonia and isolated orange coloured biacetyl-bis(benzoylhydrazonato)nickel(II) complex and studied its reaction with pyridine [59]. The formation constant of complexes formed between biacetyl-bis(bezoylhydrazonato)nickel(II) and various alkyl amines [60] have been studied. Complexes of lead(II), lead(IV) and tin(IV) of the types [Pb(L)], $[Ph_2Pb(L)]$, $[Sn(L)_2]$, [phSn(L)Cl] and $[ph_2Sn(L)]$ have been obtained by mixing methanol solutions of the appropriate metal salts and the

ligands [61].

Pelizzi and coworkers [62] have studied reaction of copper(II) chloride dihydrate with 2, 6-diacetylpyridine-bis(picoloylhydrazone) (LH_2) in refluxing ethanol yielding dark green crystal of $Cu_2(L)Cl_2.H_2O$. IR spectral data indicate coordination of all the three pyridine nitrogens. The ligands behave as an octadentate bridging (NONNNNNN) donor. The authors have established the square pyramidal structure of the complex unequivocally by X-ray crystallography. The environment about one Cu(II) is made up of basal plane consisting of a chloride, two nitrogen atoms from the ligand (LH_2), an oxygen atom from second adjacent ligand molecule and another nitrogen atom from the same adjacent ligand molecule taking up the axial position. The environment around the second Cu(II) is made up of four nitrogen atoms from the first ligand molecule, while a chloride ion takes up apical site. Some authors [63] have isolated another series of complexes of the type $M(LH_2)Cl_2.nH_2O$ (M = Mn(II), Co(II), Ni(II) and Cu (II)), by mixing chloroform solution of LH_2 and ethanolic solution of the metal chlorides in 1:1 molar ratio. Another Mn(II) compound $MnL.9H_2O$ was obtained by adding, dropwise, a dilute NaOH solution to a warm ethanol–water solution containing LH_2 and $MnCl_2.4H_2O$ in (1:1) molar ratio until pH~ 8.0. The compounds were characterized by magnetic moment data, electronic and IR spectroscopic studies.

The complex $Mn(LH_2)Cl_2.5H_2O$ was shown to have pentagonal bipyramidal stereochemistry by X-ray crystallography [64]. On the basis of similarity of IR spectra of Cu(II), Ni(II) and Zn(II) complexes with that of Mn(II) complexes, a similar pentagonal bipyramidal stereochemistry was proposed for them also with ligand acting as a ONNNO donor and chloride or water molecules occupying apical positions. The complex $MnL.9H_2O$ was also characterized by X-ray crystallography and shown to have pentagonal

bipyramidal stereochemistry.

Curtis and coworkers [65] and others [66] studied Cu(II) and Ni(II) complexes of acetylacetonebis(picolinoylhydrazone) and acetylacetonebis-(isonicotinoylhydrazone). They carried out X-ray structural analysis of copper(II) complex of acetylacetonebis(isonicotinoylhydrazone) obtained from reaction of metal(II) salt, isonicotinoylhydrazine and acetylacetone and confirmed the square pyramidal stereochemistry.

Giordano and coworkers [67] isolated cobalt(II) and nickel(II) complexes of compositions $[Co(LH_2)(H_2O)(NO_3)].NO_3$ and $[Ni(LH_2)(H_2O)_2](NO_3)_2.2H_2O$ from reaction of metal nitrates with 2, 6-diacetylpyridinebis(benzoylhydrazone) (LH_2) in 95% ethanol. The X-ray crystallographic study confirmed that the metal atoms are in pentagonal bypiramidal arrangement in the structural unit of the complexes.

Palenik and coworkers [68] isolated lanthanum complexes of composition $[La(LH_2)(H_2O)_3]$ from reaction of lanthanum nitrate and ligand in ethanol at 55 °C in the presence of water. The complex was characterized by infrared spectroscopy and X-ray crystallographic studies. They showed lanthanum to be eleven coordinated in these complexes. A decahedral arrangement of the donor atoms of the ligand is proposed around the lanthanum atom in the complexes.

Paolucci and coworkers [69] prepared a series of dioxouranium(VI) complexes of 2, 6-diacetylpyridinebis(4-methoxybenzoylhydrazone) (H_2dapmb). The neutral compound of the composition $[UO_2(dapmb)]$ was formed in two different crystalline forms α and β, depending upon the experimental conditions. The geometries of the two forms of $[UO_2(dapmb)]$ are very similar, the only significant difference being the difference in the conformation of carbon atoms in a methoxy group. Seven fold coordination of uranium (VI) was established with the five donor nitrogen atoms in the equatorial plane.

Pelizzi and coworkers [70] isolated tin(IV) complexes of the composition [$Snpr_2(LH_2)$] from reaction of n-propyltinchloride in anhydrous acetone under nitrogen atmosphere with boiling suspension of 2, 6-diacylpyridinebis(salicylhydrazone) (LH_2) in dry methanol. The X-ray crystal structure study has established that tin atoms is seven coordinated in the complex with pentagonal bipyramidal arrangement of ligands atoms. The -OH groups remain uncoordinated.

Teotia and coworkers [71] have studied reaction of metal(II) salts [M = Cu(II) and Ni(II)], with picolinoyl/isonicotinoyl-hydrazine in presence of acetylacetone. They isolated complexes of the compositions [M(LH)X] (M = Ni(II), Cu(II); X = Cl, Br, NO_3 and NCS, LH_2 = acetylacetonebis(picolinoylhydrazone) or acetylacetonebis(isonicotinoylhydrazone). All the complexes have been established to have square pyramidal stereochemistry. Complexes [$M(LH)X_2$] (X = Cl, Br, NO_3, NCS for M = Cu(II); X = OAc, Cl, Br, NCS for Mn(III) and OH for Co(III) were also prepared similarly [72] by them. The complexes have been suggested to have six-coordinated tetragonal structure.

Paolucci and coworkers [73] synthesized several complexes of 2, 6-diformylphenol bis(benzoylhydrazone) and its substituted derivatives with the bivalent metal ions (M = Co(II), Ni(II), Cu(II) and Zn(II) and established their molecular structure by various physico-chemical techniques.

Dutta and coworker [74] isolated complex of the composition [VO(L)] from reaction of $VO(acac)_2$ with acetylacetonebis(benozoylhydrazone) (LH_2) in acetone. The same ligand on reaction with CoX_2 (X = Cl, Br) in anhydrous medium yielded blue coloured tetrahedral polymeric complexes [$Co(LH_2)X_2$] [75]. However, in the presence of water, bromide salt yields pink coloured pseudo-octahedral [$Co(LH_2)Br_2(H_2O_2]$ complex. The dihydrazone

reacts with nickel(II) chloride in rectified spirit and yields diamagnetic, orange, yellow complex [Ni(L)] [76]. However, reaction with anhydrous $NiCl_2$ in warm anhydrous methanol gives a paramagnetic complex $[Ni(LH_2)Cl_2]$ having *trans*-dichloro pseudo-octahedral structure. When this complex is exposed to moist atmosphere and over KOH, the partial dechlorination occurs giving the complex [Ni(LH)Cl]. The complex is proposed to have five coordinate structure. They also isolated complex [Zn(L)], $[Cd(L).2H_2O]$ and [Pb(L)] from the interaction of appropriate metal acetate with the ligand in ethanol.

Snow and coworkers [77] studied the reaction of bis(acetylacetonato)-oxovanadium(IV) with benzoylhydrazine in dry methanol under dry nitrogen. They isolated bis(acetylacetonebenzoylhydrazonato)vanadium(IV). A trigonal prismatic geometry was verified for this complex.

Dutta and coworkers [78] showed that the reaction of $VO(acac)_2$ with benzoylhydrazine and related ligands in methanol, ethanol and methyl acetate yielded violet or almost black coloured bis(acetylacetonebenzoyl-hydrazonato)vanadium(IV) whereas reaction in acetone and ethyl methyl ketone yielded (acetylacetonebenzoylhydrazonato)oxovanadium(IV). While in the former complex, the abstraction of oxo-group has been suggested to occur, in the latter complex is retained.

Lanthanide complexes [79] of the type $[Ln(L)(OH)(H_2O)]$ (Ln = La(III), Pr(III), Nd(III), Sm(III), Gd(III), Ho(III), Er(III) have been obtained in situ by refluxing biacetylbenzoylhydrazine and appropriate metal chloride in ethanol in the presence of a regulated quantity of NH_4OH. The ligand acts as a quadridentate ONNO donor in its enol form.

Pelizzi and coworkers [80] have isolated a new series of metal(II) complexes of type $[M(LH_2)(H_2O)Cl]$ (M = Co(II), Ni(II), Mn(II), Cu(II) and

Zn(II) by mixing LH_2 and metal(II) chloride in ethanol in 1:1 molar ratio. With metal(II) acetates, the compounds of the type [ML] are obtained. The ligand reacts with metal centres in keto form in complexes $[M(LH_2)(OH_2)Cl]Cl$ and enol form in complexes [ML]. Some of the complexes are characterized by X-ray crystallographic method as well. The complexes are shown to have pentagonal bipyramidal stereochemistry.

Dutta and coworkers [81] have studied the reaction of $MoO_2(acac)_2$ with benzoylhydrazine and related ligands in different solvents. They isolated the complex (benzoylhydrazine)(benzoylhydrazido)(acetylacetonato)molybdenum (VI) in dry methanol while in ordinary methanol, the complex (acetylacetonato)(cis-dioxo)molybdenum(VI)-μ-diol-(benzoylhydrazinato)(cis-dioxo)molybdenum(VI) dihydrate was isolated. They have shown that in dry methanol acetylacetone and hydrazines condense to give Schiff base complexes whereas no Schiff base formation occurs in ordinary methanol.

The Schiff bases derived from acetylacetone and 2-picolinoylhydrazide or isonicotinoylhydrazide are similar to one another and gave complexes of the type $[UO_2L]Cl$ (where LH = Schiff base) with UO_2Cl_2. However, in 2-picolinoylhydrazone complex, the Schiff base coordinates through both azomethine nitrogen atom and pyridine nitrogen atoms while in the case of isonicotinoylhydrazone complex, the Schiff base coordinates through azomethine nitrogen atom and carbonyl oxygen atom [82] .

On the basis of IR and conductivity data Dey et al [83] have reported the formation of $[UO_2(LH_2)](NO_3)_2]$ (where LH_2 represents 1, 2-dimethylbis(4-methoxybenzoylhydrazone)). Similarly, they have reported the formation of $[UO_2(LH_2)(NH_3)]NO_3$ on acidification of $[UO_2L]$ with HNO_3. Ligands are proposed to coordinate to the metal centres in keto as well as enol forms. Interaction of these complexes with neutral mono and bidentate ligands lead to the

formation of $[UO_2L(A)_2]$ and $[UO_2L(AA)]$ (where, A = pyridine, picolines, methylamine, aniline, $OPph_3$; AA = en, ph, phen), respectively .

Marangoni and coworkers [84] synthesized mercury(II) complex with 2, 6-diacetylpyridinebis(2-pyridoylhydrazone). They carried out X-ray structural analysis of the complex and confirmed its pentagonal bipyramidal stereochemistry.

Pelizzi and coworkers [85] synthesized nickel(II) complex $[\{Ni(H_2apsh)(OH_2)\}_2Cl_2].2dmf.5H_2O$ and cobalt(II) and copper(II) complexes, viz., $[Co(H_2dpsah)(OH_2)_2]Cl.4H_2O$ of 2, 6-diacetylpyridinebis[2-semicarbazono)-propionylhydrazone] (H_4apsh) and 2, 6-diacetylpyridinebis[2-semicarbazono)-acetophenoylhydrazone] (H_2dapsh), respectively. In the nickel complex, the four atoms of semicarbazone system are not involved in coordination while in the cobalt complex, semicarbazone system does not participate in coordination. They established structure of the complexes by IR spectroscopy and X-ray crystallography.

Pelizzi and coworkers [86] studied the structure of a tetranuclear copper(II) complex $[Cu_2(dappc)(OH_3)]_2[Cu_2(dappc)(OH_2)_2$- $(ClO_4]_2.(ClO_4)_6.2H_2O$ (I) and $[Cu_2(dapip)Br]_2$ (II) derived from the polyfunctional ligand 2, 6-diacetylpyridinebis-(2-pyridinecarbonylhydrazone) (H_2dappc) and 2, 6-diacetylpyridinebis(2-(2-pyridine-carbonylhydrazone)(phenylacetohydrazone) (H_4dapip), respectively. The structure of compound (I) is built up of complex cations of formula $[Cu_2(dappc)(OH_2)_3]_2^{4+}$ and $[Cu_2(dappc)(OH_2)_2ClO_4]^{2+}$, ClO_4^- anions and uncoordinated H_2O molecule while that of the compound (II) consists of neutral unit of formula $[Cu_2(dapip)Br]_2$ and solvating H_2O molecules. In both compounds two metal atoms are present for one hydrazone and the ligand is bideprotonated in complex (I) and trideprotonated in complex (II).

A monoperoxo complex of Schiff base (H_5C_6=N-NHC(S).$SCH_2C_6H_5)_2(LH_2)$,

has been reported by Tarafder et al. [87]. The complex $[UO_2(O_2)L]$ was prepared by treating uranyl nitrate with the Schiff base dissolved in a solution of KOH in 30 % H_2O_2. The Schiff base behaves as dibasic NNSS tetradentate ligand, while peroxo group is bonded to the metal centre as bidentate chelating ligand.

Toshev and coworkers [88] reported the dioxouranium complex of diacetylbis(thiobenzoylhydrazone) in which uranium has a distorted pentagonal bipyramidal structure with the uranyl oxygen atoms at the axial positions.

Pelizzi and coworkers [89] synthesized copper complex of di-2-pyridyl ketone(phenylsemicarbazone)acetylhydrazone (H_2pash) and studied their structure by X-ray crystallography. They showed that the copper complex $[Cu_2(psah)Cl].H_2O$ consists of pair of structurally distinct metal centres with different environments bound to the heptadentate hydrazone ligand and held together by a -N-N- bridge.

Katti and coworkers [90] synthesized a number of palladium(II) complexes from a series of phosphorous hydrazide and hydrazones. The complexes were characterized by elemental analysis. The structural assessment was carried out by NMR and IR spectroscopic studies. The structure of one complex was established by X-ray crystallography as well.

Lukyanenko and coworkers [91] have determined complex stability of Na^+, K^+, Rb^+ and Cs^+ ions with bis(benzo-15-crown-5) with acylhydrazide fragments in the linking chain in 95 % aqueous methanol. In all cases, the formation of 1:1 complex was observed. They studied biscrown ethers form more stable complexes than benzo-15-crown-5. The stability of biscrown ether complexes is substantially determined by the length of the linking chain. Biscrown ether with a glutaric acid residue in the linking chain exhibits striking potassium selectivity. High selectivity and stability of the

complexes are due to the increase of their sandwich structure rigidity resulting from the formation of H-bonds between acylhydrazide fragments.

Ji and coworkers [92] studied several dinuclear yttrium(III) and lanthanide(III) picrate complexes derived from acetylferrocenepyridine-2, 6-diformylhydrazone having the stoichiometric formula $Ln_2L_2pic_6.n(1\text{-}C_3H_7OH).m\ H_2O$ (pic = picrate anion, Ln = Y, La, Pr, Nd, Sm, Eu, Gd, Tb, Dy, Ho, n = 2, m = 4; Ln = Er, Tm, Yb, n = 0, m = 2). These complexes were characterized by EPR, IR, UV, ^1H NMR spectra and molar conductance data. It was found that the ligand coordinates in keto form to the lanthanide ions. All the complexes described in the present study are 1:6 electrolyte in methanol.

Xiaozeng and coworkers [93] synthesized binuclear zinc(II) complex $[Zn_2L(OAc)_2].EtOH$, from binucleating ligand 2, 6-diformylpyridine N-oxide bis(benzoylhydrazone) (L) via template reaction in alcohol. They characterized the complex by X-ray cryatallographic studies.

Pelizzi and coworkers [94] synthesized six complexes of copper(II), nickel(II) and Iron(II) from a chiral ligand 2, 6-diacetylpyridinebis[DL-hydroxy(phenyl)acetic]hydrazone (H_4dapm) and characterized them by spectroscopic studies. They established the structure of the nickel complex $[Ni(H_4damp)(H_2dapm)].13H_2O$ by X-ray diffraction methods. The complex crystallized in the monoclinic space group C2/c. With the help of ^1H NMR spectroscopic studies, the existence of ligand in three forms *i.e.*, meso DL and two enantiomeric DD and LL was established. The ^1H NMR spectrum of the complex $[Ni(H_4damp)(H_2dapm)].13H_2O$ showed the presence of two inequivalent ligand molecules i.e., one in meso form and the other in DD or LL form.

Rana and coworkers [95] synthesized several manganese(II), iron(II),

cobalt(II), nickel(II) and copper(II) complexes of 2, 6-diacetylpyridine (benzylacetone)hydrazone (H_2L). The complexes have been shown to have composition $[M(H_2L)X_2]$ (where M = Mn, Fe, Co, Ni and Cu; X = Cl, NO_3, SCN) and have been characterized by molar conductance, magnetic moment data, infrared and electronic spectroscopy.

Paolucci and coworkers [96] studied the interaction of potentially binucleating ligand 2, 6-diacetylpyridine(1-phthalazinylhydrazone) (H_2dapz), containing only nitrogen donor atoms, with nickel(II) copper(II) and zinc(II) salts. They showed that depending on the nature of the counter ions, Ni(II) and Cu(II) ions, selectively, enter in one of the two compartments present in the ligand. They isolated five series of mononuclear complexes [dapzM], $[H_2dapzMCl_2]$, [HdapzMCl], $[(H_2dapz)_2M][ClO_4]_2$, $[HdapzM][ClO_4]$, from reactions of metals acetates, metal chlorides and metal perchlorates respectively and the ligand. The complexes were characterized by analytical techniques and spectroscopic methods. Crystal structure analysis on the bisdeprotonated complex $[dapzNi]_2$ shows that the compound is dimeric with the metal ions octahedrally coordinated into the upper compartment and the pyridine nitrogens bridging the two nickel atoms.

Maurya and coworkers [97] synthesized binuclear dioxotungsten (VI) complexes of the type $[(WO_2)_2L]$, where L is a flexibly bridged hexadentate tetra anionic Schiff base derived from condensation of methylene or dithiobissalicylaldehyde with isonicotinoylhydazine, bezoylhydrazine, p-nitrobenzoylhydrazine and furoylhydrazine are reported. The IR and NMR spectral data suggests an oligomeric structure for these complexes in which each tungsten atom achieves a pseudo-octahedral structure via W=O→W bridging.

Lal and coworkers [98] synthesized the bimetallic manganese (II, III) and dioxouranium(VI) complexes $[Mn_4(H_2L)_2(OAc)_4].4H_2O$, $[Mn_4(L)_2(H_2O)_8].4H_2O$,

$K_4[Mn_4(L)_2F_6(H_2O)].2H_2O$, $[UO_2(H_2O)_4]_2[Mn_4(L)_2(OAc)_4].4H_2O$ and $K_4[UO_2Mn_3(L)_2F_5(H_2O)_3]$ from bis(2-hydroxy-1-naphthaldehyde)oxaloyl-dihydrazone (H_4L). The complexes have been characterized by physical and spectral data. IR spectral data indicate that the dihydrazone coordinates to the metal centres in keto as well as enol forms in the *anti-cis*-configuration in all of the complexes.

Lal and Adhikari [99] synthesized the hexamer compound $[(MoO_2)_2(L)H_2O].2H_2O$ from the reaction of $MoO_2(acac)_2$ with bis(2-hydroxy-1-naphthaldehyde)oxaloyldihydrazone (H_4L) in ethanol-acetonitrile in 3:1 molar ratio under reflux. The *anti-cis*-configuration of the dihydrazone moieties leads to the chair conformation of the complex.

Lal and coworkers [100] isolated the homobimetallic complex $[(MoO_2)_2(L)].4H_2O$ (1) from bis(2-hydroxy-1-naphthaldehyde)oxaloyl-dihydrazone (H_4L) in the solid state. It reacts with Lewis bases pyridine and 3-picoline to form the complexes $[\{\mu_2\text{-}O)MoO_2\}MoO_2(H_2L)].2D.4H_2O$ (where D = pyridine (py, 2); 3-picoline (3-pic, 3)) and with proton bases salicyloylhydrazine ($sylshH_3$) and isonicotinoylhydrazine ($inhH_3$) to yield the Mo(V) compounds $[Mo_2(L)(sylsh)_2].5H_2O$ (4) and $[Mo_2(L)(inh)_2(H_2O)_2].5H_2O$ (5), respectively. The complexes have been characterized by elemental analyses, molecular weight determinations, molar conductance, magnetic moment, EPR, electronic, infrared and ^1H NMR spectral studies. The complexes (4) and (5) are paramagnetic to the extent of 3.02 and 3.16 B.M. respectively.

Lal and coworkers [101] have synthesized the complexes of the type $[(UO_2)_4(L)_2(H_2O)_8].4H_2O$ (1), $K_4[(UO_2)_4(L)_2(OAc)_4(H_2O)_4].4H_2O$ (2) and $K_4[(UO_2)_4(L)_2F_4(H_2O)_4]$ (3) from bis(o-hydroxynaphthaldehyde)oxaloyl-dihydrazone (H_4L) and characterized by elemental analysis, molecular weight determination, molar conductance data and electronic, IR and ^1H NMR

spectroscopic studies.

Lal and Kumar [102] have synthesized an unstable monomeric yellow complex of type $[(MoO_2)_2(CHsalmlhH_4)(H_2O)_2].H_2O$ {complex (A)} from the reaction between bis(acetylacetonato)dioxomolybdenum(VI) and disalicylaldehyde malonoyldihydrazone ($CH_2salmlhH_4$) in ethanol. This is transformed into an intermediate complex $[(MoO_2)(CHsalmlhH)(H_2O)]_2.4H_2O$ {complex (AB)} after sometime. Ultimately a stable brown isomer complex $[(MoO_2)_2(CH_2salmh)(H_2O)].4H_2O$ {complex (B)} is obtained. All the products have been characterized by various physico-chemical techniques and IR and ^1H NMR spectroscopic studies.

Lal and coworkers [103] isolated the complexes of the composition $[UO_2(H_3salligh)(OAc)].3H_2O$ and $[UO_2Zn(salligh)(H_2O_2].2H_2O$ where $H_4salligh$ refers to disalicylaldehyde oxaloyldihydrazone ($H_4saloxlh$), malonoyldihydrazone ($H_4salmlh$), succinoyldihydrazone ($H_4salsuch$), glutaroyldihydrazone ($H_4salguth$) and phthaloyldihydrazone ($H_4salphth$). The complexes have been characterized by molar conductance and spectral data.

Lal and coworkers [104] have synthesized the complexes $Na_4[(UO_2)_4(L)_2(OAc)_4(H_2O)_4].4H_2O$ (1) and $Na_4[(UO_2)_4(L)_2F_4(H_2O)_4]$ (2) from bis(o-hydroxynaphthaldehyde)oxalodihydrazone (H_4L) and characterized by elemental analysis, molar conductance, electronic, IR and ^1H NMR spectroscopic studies. On the basis of these studies, it is suggested that the fluoro complex exists in chair conformation in which coordination of both azomethine nitrogen atoms of the dihydrazone in *cis*-configuration to the same metal centre leads to coupling between azomethine protons. In acetato complex, the coordination of two hydrazone parts of the dihydrazone even in *cis*-configuration to different metal centres eliminates the possibility of coupling between azomethine protons and thus, its existence in chair conformation.

Lal and coworkers [105] have synthesized the monometallic complexes of the type $[Zn_2(H_4L)_2(SO_4)_2]$, $[Zn_2(H_2L)_2(H_2O)_2]$, $K_2[Zn_2(H_2L)_2F_2]$ and the heterobimetallic complexes of the type $[(UO_2)_2Zn_2(L)_2(H_2O)_6]$, $K_4[(UO_2)_2Zn_2(L)_2F_4(H_2O)_2]$, $[Cu_2Zn_2(L)_2(H_2O)_4]$ and $K_4[Cu_2Zn_2(L)_2F_4(H_2O)_2]$ and characterized by analytical, molar conductance, magnetic moment data, and electronic, EPR, IR and ^1H NMR spectroscopic studies. All of the complexes have been proposed to be dimer on the basis of molecular weight determinations. Monometallic complexes have been shown to contain the coordinated dihydrazone in *syn-cis*-configuration while the heterobimetallic complexes have been shown to contain the coordinated dihydrazone in the *anti-cis* configuration.

Fenton and coworkers [106] prepared green coloured nitrato complex of copper $Cu_3(HL)(NO_3)_2.2CH_3OH.2H_2O$ from reaction of cupric nitrate with bis(salicylhydrazone) derived from the diethyl ester of iminodiacetic acid in methanol-chloroform solution. They also prepared dark green perchlorato complex $[Cu_3(HL)(ClO_4)_2]$ from reaction of $Cu(ClO_4)_2.6H_2O$ with the title ligand in absolute ethanol. The compound crystallized from DMSO solution was found to have the composition of $[Cu_6(HL)_2(dmso)_5(EtOH)(H_2O)_2].(ClO_4)_4.2H_2O$. The structure of the perchlorato complex established that a coordination polymer has formed in which the repeat unit was based on six copper(II) atoms with an alternating mononuclear-dinuclear motive with the help of X-ray crystallography. All of the copper atoms were found to have the square pyramidal structure.

Lal and coworkers [107] synthesized homobimetallic and heterobimetallic complexes $[Zn_4(LH_2)_2(OAc)_4].2H_2O$ (1), $[Zn_4(L)_2(H_2O)_4].4H_2O$ (2), $M_4[Zn_4(L)_2F_4(H_2O)_4]$ (where M = K for (3) and Na for (4), $[UO_2(H_2O)_4]_2[Zn_4(L)_2(OAc)_4].2H_2O$ (5), $M_4[UO_2Zn_3(L)_2F_4(H_2O)_4].4H_2O$ (where M = K for (6) and Na for (7)) from bis(2-hydroxy-1-naphthaldehyde)-oxaloyldihydrazone (LH_4). The structural assessment of the complexes was done

by molecular weight determinations, molar conductance data, electronic, IR and ^{1}H NMR spectral data. In the complexes, the dihydrazones has been suggested to coordinate to the metal centre in *anti-cis*-configuration in the keto as well as in enol forms

Lal and coworkers [108] synthesized and characterized manganese(IV) and manganese(II) complexes $[Mn^{IV}(L)(H_2O)_2]$ (1) and $[Mn(II)(LH_2)(A_2)]$ (where A = H_2O (2), pyridine (py, 3), 3-picoline (3-pic, 4) and 4-picoline (4-pic, 5) from bis(2-hydroxy-1-naphthaldehyde)malonoyldihydrazone. The complex (1) has μ_B value equal 4.02 B.M which is in good agreement with the moments of the characterized manganese(IV) complexes. For the remaining complexes, the μ_β value falls in the range 5.90-5.85 B.M, a region characteristic of Mn(II) complexes. The electronic spectra of the complexes show LMCT bands in the visible region and UV-visible border region. The Mn^{IV} complex (1) shows two resonances, a strong one near $g \cong 2.0$ and a weak one near $g \cong 4.9$ in its EPR spectrum. The ^{55}Mn hyperfine coupling constant for $g \cong 2.0$ signal is equal to 78 G which is closer to the values observed for Mn(IV) than for Mn(II). The EPR spectral features for the remaining complexes are characteristic for Mn(II). In all of the complexes, the dihydrazone is suggested to coordinate to the metal centres in enol form.

Lal and coworkers [109] prepared manganese(IV) complexes $[Mn^{IV}(L)(A)_2].2H_2O$ (where LH_4 = bis(2-hydroxy-1-napthaldehyde)oxaloyl-dihydrazone and A = H_2O (1), pyridine (py, 2), 2-picoline (2-pic, 3), 3-picoline (3-pic, 4), 4-picoline (4-pic, 5) in ethanol by the template method directly from manganese(II) acetate, oxaloyldihydrazone (H_2oxh) and 2-hydroxy-1-napthaldehyde. All of the complexes have μ_β values in the range 3.96-4.08 B.M. which are in good agreement with manganese(IV) complexes. Electronic spectra of the complexes are dominated by ligand-to-metal charge

transfer (LMCT) transitions. In the polycrystalline phase at LNT, two resonances at $g \cong 2.0$ (strong) and $g \cong 4.9$ (weak) are observed. In the magnetically dilute glassy state, the ^{55}Mn hyperfine structure is well resolved for the resonance near $g \cong 2.0$. Between every pair of the six hyperfine line of the $g \cong 2.0$ resonance, there is a pair of relatively weak forbidden transition. The ^{55}Mn hyperfine coupling constant for the $g \cong 2.0$ signal is 78 G. The dihydrazone is coordinated to the metal centre in keto form through deprotonated secondary amine nitrogen atom and deprotonated naptholate oxygen atoms in atoms in *anti-cis*-configuration.

Monometallic copper(II) complex $[Cu(LH_2)(H_2O)_2]$ (1) and heterobimetallic complexes $[MCu(L)(H_2O)_3]$ (where M = UO_2 (2) and Zn (4) and $[MCu(L)(H_2O)_4]$ (where M = MoO_2(3), Ni(5), Co(6) and Mn(7)) and homobimetallic copper(II) complex $[Cu_2(L)(H_2O)_4].2H_2O$ (8) have been isolated and characterized by Lal and coworkers [110] by analytical, molecular weight, magnetic moment, electrical conductance, electronic, IR and EPR spectral data. IR spectral evidences indicate that dihydrazone coordinates to the metal centres in enol forms. The monometallic copper(II) complex (1) and the heterobimetallic complexes UO_2Cu (2) and MoO_2Cu (3) and Zn-Cu (4) are normal paramagnetic indicating absence of metal–metal interaction in the structural unit of the complexes while the remaining heterobimetallic complexes Ni-Cu (5), Co-Cu (6) and Mn-Cu (7) have much less μ_{eff} values than those required for 3, 4 and unpaired electrons indicating considerable metal-metal interactions. The monometallic copper(II) complex (1) shows an anisotropic EPR spectrum at LNT (77K). The parallel and perpendicular features are resolved. The essential feature of the spectrum are consistent with octahedral stereochemistry. The EPR spectral feature of homobimetallic copper(II) complex (8) suggest square pyramidal stereochemistry of the complex. The heterobimetallic complexes

have also been characterized by EPR spectral studies. The EPR spectral data indicate that either there is no interaction or very weak interaction between metal centres in the structural unit of the heterobimetallic complexes. The complexes have been characterized by electronic and IR spectral data also. Copper has distorted octahedral geometry in monometallic complexes and heterobimetallic complexes. Uranium has pentagonal bipyramidal stereochemistry while zinc has square pyramidal stereochemistry.

The monometallic uranium(VI) complex $[UO_2(CH_2LH_2)(H_2O)]$ has been synthesized by Lal and coworkers [112] from bis(2-hydroxy-1-naphthaldehyde)-malonoyldihydrazone (CH_2LH_4) in ethanol. The reaction of this complex with bis(acetylacetonate)dioxomolybdenum(VI) and metal acetates (M = Zn, Cu, Ni, Co, and Mn) in (1:1) molar ratio in ethanol (methanol in the case of copper) under reflux yields heterobimetallic complexes $[MUO_2(CH_2L)(H_2O)_2]$ (M = Zn and Cu) and $[MUO_2(CH_2L)(H_2O)_3]$ (M = MoO_2, Ni, Co and Mn), respectively. The complexes have been characterized by analytical, molecular weight, molar conductance, magnetic moment data and spectral studies. In all the complexes, the dihydrazones coordinates to the metal centres in an *anti-cis* configuration.

The complexes $[(UO_2)(CH_2L)(H_2O)_4].4H_2O$ (1), $[M_4(CH_2L)_2(H_2O)_4].4H_2O$ (M = Zn(2) and Cu(3)), $(M')_2[(UO_2F)_2(CH_2L)(H_2O)_2]$ [M = K(4), Na(6)], $M'[(UO_2)_2(CH_2L)(OAc)(H_2O)_2]$ [M = K(5), Na(7)], $K_4[(MF)_2(CH_2L)_2].4H_2O$ [M = Zn(8) and Cu (9)] have been synthesized by Lal and coworkers [113] from reaction of appropriate metal salts with bis(2-hydroxy-1-naphthaldehyde)-adipoyldihydrazone (CH_2LH_4) in different experimental conditions in ethanol/methanol media. The complexes have been characterized by elemental analyses, molecular weight, molar conductance, magnetic moment and EPR data. The structural assessments of the complexes have been carried out on the basis of electronic, infrared, ^1H NMR and ^{13}C NMR spectral studies.

Gang etal [114] synthesized the lanthanide chelates $Na_2[Ln(C_{34}H_{28}N_8O_8)Cl].nH_2O$ from malonoyl dihydrazone salicylaldehyde and characterized them by elemental analysis, IR, UV, molar conductance and TGA. They showed that the ligand coordinates to the central metal ion with one hydrazone unit in the keto form with one chloride ion in the coordination sphere. These chelates are 1:2 electrolyte in DMF and are more thermostable than the ligand due to the formation of chelate rings.

Bolger and coworkers [115] synthesized a series of dihydrazone and substituted dihydrazone derivatives of biacetyl and of hydrazone and phenylhydrazone derivatives of 2-acetylpyridine like biacetyl di(phenylhydrazone) (1a), biacetyl di[methyl(phenyl)hydrazone] (1b), biacetyl di(o-tolylhydrazone) (1c), biacetyl di(dimethylhydrazone) (1d), biacetyl dihydrazone (1e), biacetyl di(benzaldehyde azine) (1f), 2-acetylpyridine phenylhydrazone (1g) or 2-acetylpyridine hydrazone or 2-acetylpyridine hydrazone (1h). Subsequently, they studied the reactions of these dihydrazones with $[Ru(bpy)_2Cl_2]$ (where bpy = bipyridine) and isolated the complexes of the composition $[Ru(bpy)(L\text{-}L)](PF_6)_2$ where L-L represents dihydrazone. The structures of all complexes were determined using IR, UV-vis, NMR and microanalysis. The proton NMR spectra of the complexes derived from dihydrazones (1a-1c) showed an unusual dependence on probe temperature with broadened aromatic resonances. The signals sharpened at both high and low temperature in the complexes derived from dihydrazone 1b and 1c. Emission was observed for the complexes with two hydrazones and 1g and 1h containing only one hydrazone moiety. The molecular structure of 1a was determined and it was shown that a hydrazone phenyl group lies over each of the bipyridyl rings.

Khan and coworkers [116] synthesized a new class of tetraiminetetraamide macrocylcic (Ph_4[20]tetraene, N_8O_4, and Ph_6[20]tetraene,

N_8O_4) complexes through the metal ion controlled reaction of 1, 2-diphenylethane-1, 2-dione dihydrazone (DPEDDH) with succinic acid $[ML_1X_2]$ or phthalic acid $[ML_2X_2]$ [M = Mn, Co, Ni, Cu or Zn; X = Cl or NO_3]. They elucidated the structures of the complexe on the basis of IR, ^1H NMR, EPR and electronic spectral data and conductance as well as magnetic properties. An octahedral geometry was assigned for all the complexes involving coordination of all imine nitrogens.

Labib and coworkers [117] synthesized a series of polyacylhydrazones by condensing diacetyl with oxalic, malonic, succinic, glutaric and adipic dihydrazides and characterized them by conventional spectroscopic studies. The complexes of the compositions $\{[Cu_2(L)(AcO)_2(OH)(H_2O)_2].yH_2O\}_n$, $\{[Cu(L)(AcO)(HO)(H_2O)].yH_2O\}_n$, $\{[Ni_2(L)(AcO)_2(HO)_2].yH_2O\}_n$ and $\{[Ni(L)(AcO)(HO)].yH_2O\}_n$, were isolated where L refers to the neutral dihydrazone unit. Magnetic susceptibility measurements in the 4.2 – 300 K range indicated significant antiferromagnetic coupling between the Cu^{II} centres in the metallopolymers. The results indicate the presence of two polymer chains crosslinked by bis-μ-acetatocopper(II) bridges. Based on IR, spectral and magnetic measurements tentative structures of the Cu^{II} and Ni^{II} metallopolymers were proposed. The dihydrazone units in these polymers were found to be coordinated to the metal(II) via the azomethine nitrozen(s) whereas the amide group was found to be uncoordinated. Each Cu^{II} is penta coordinated in a distorted square pyramidal environment and bridged by one acetate group. A hydroxide ion is also coordinated to the Cu^{II} centre. The fifth coordination site is occupied by water molecule. In the nickel(II) metallopolymers, the metal ions were in a tetrahedral environment and were coordinated to azomethine nitrogen, two bridged acetate oxygens and to the hydroxide ion.

Larin and coworkers [118] synthesized the dinuclear copper(II) complexes

with 2-hydroxypropiophenone, 2-hydroxy-5-methyl and 5-chloro-2-hydroxy-acetophenone, acylhydrazones (H_4L) having the compositions [$Cu_2L.mPy$], where the L ligand contains the polymethylene chain with different lengths from two to five units. The crystal and molecular structures of the 2-hydroxy propiophenone adipoyldihydrazone complex [$Cu_2L.4Py$]Py were established by X-ray diffraction analysis. Each copper(II) atom was found to have the tetragonal pyramidal geometry. The EPR spectra of solutions of the complexes derived from acyldihydrazones of succinic, glutaric and adipic acids contain seven HFS lines with the constant ~ 40.10^{-4} cm^{-1}. Such a value of HFS constant indicated that the two copper atoms are coupled to one another as a result of the spin–spin exchange interaction between unpaired electrons. An increase in the polymethylene chain length to five units prevents exchange interactions. The EPR spectrum of the complex with pimelic acid dihydrazone contains a signal of four HFS lines with A_{Cu} = $73.4.10^{-4}$ cm^{-1}, which is typical of mononuclear copper(II) complexes.

Andelkovic and coworkers [119] synthesized Zn(II), Pd(II) and Pt(II) complexes with 2′-[1-(2-pyridinyl)ethylidene]oxamohydrazide (Hapsox). The Zn(II) complexes was found to contain two coordinated apsox ligands to Zn(II) while Pd(II) and Pt(II) complexes were found to contain one coordinated apsox ligand to the metal centres. In each case, the polydentate ligand was coordinated via pyridine and hydrazone introgens and α-oxyazine oxygen. An octahedral geometry around Zn(II) and a square planar geometry around Pd(II) and Pt(II) were established. The structure determination was performed by IR, ^1H NMR and ^{13}C NMR spectroscopy. The structure of Zn(II) complex was established unequivocally by X-ray diffraction analysis.

Para et al [120] synthesized dialdehyde starch dihydrazone from reaction of dialdehyde starch (32 %) from periodate oxidized potato starch with hydrazine DASHZ. The dihydrazone (DASHZ) coordinated to Ca, Cd, Co(II), Cu(II),

Fe(II), Mg, Mn(II), Ni(II), Pb(II) and Zn ions. The nitrogen atoms of the C=N moiety in dihydrazone as well as the oxygen atom of the pyranose ring of starch moiety were the coordination sites. Metal ions were chelated to a different extent while Cu(II) could coordinate with three moles of DASH while Mn(II) could coordinate with 50 moles of the DASHZ units. The ligand DASHZ and the metal complexes decomposed, thermally in four steps but the rates of decomposition of the ligand and chelates in relevant steps were different. Mg complex has a very high rate of decomposition while complexes of other metals have low rates of decomposition.

Zhao and coworkers [121] synthesized polynuclear manganese(II), cobalt(II)/(III), iron(II)/(III) and nickel(II) complexes of a group of flexilble polydentate dihydrazone ligands, based on pyridine -2, 6-dipicolinic (A), oxalic (B) and malonic (C) subunits. They reported the structural details for the linear dinuclear complexes $[Ni_2(2poap)_2(H_2O)_2](NO_3)_4.2CH_3OH.2.5H_2O$ (1), $[Mn_2(pttp)(NO_3)_2(CH_3OH)_2(H_2O)_2](NO_3)_2].H_2O$ (2) and $[Mn_2(mapttp)_2(NO_3)_2$-$(H_2O)_2](NO_3)_2.10H_2O$ (3), a square tetranuclear complex $[Co_4(pttp)_4]Br_6.9H_2O$ (4), a tetranuclear tetrahedral complex $[Ni_4(pttp)_6](BF_4)6F_2].14H_2O$ (7) and a mixed spin state tetranuclear Ni(II) complex $[(2pyoap)_2Ni_4(CH_3OH)_4].1.5CH_3COH$ (10), with a diamond-like arrangement of metal ions. The paramagnetic metal centres are well separated in each case, leading to weak antiferromagnetic coupling or non-existent spin exchange.

Tirosh and coworkers [122] synthesized cadmium complex $[Cd(C_4H_{10}N_4)_3](ClO_4)_2$ from reaction of $Cd(ClO_4)_2.H_2O$ with biacetyl dihydrazone in methanol. They established the crystal structure of the compound at ca. 110 K with the help X-ray crystallography. The cation was found to be located on a $\bar{3}$ axis. The complexes were characterized by an approximate octahedral geometry, with each of the ligands occupying two coordination sites around the metal.

Carcelli and coworkers [123] synthesized a series of lanthanides (III) complexes with two potentially hexadentate ligands containing a rigid phenanthroline moiety and two flexible hydrazonic arms with different donor atom sets (NNN'N'OO and NNN'N'N''N'') respectively. These hydrazones are (diformylphenanthroline)bis(benzoyl)hydrazone (H_2L), (2, 9-diformyl phenanthroline)bis(2-pyridyl)hydrazone (HL_2). They prepared complexes of H_2L^1 with La, Eu, Gd and Tb and characterized them fully. They presented the X-ray crystal structure of the complex $[Eu(HL^1)(CH_3COO)_2].5H_2O$. The stability constants of the equilibria regarding synthesis of the complexes were determined by UV spectrophotometric titrations in DMSO at 25 °C. They also synthesized nitrate complexes of H_2L^2 with La, Eu, Gd and Tb. The X-ray crystal structures of the complexes $[La(H_2L^2)(NO_3)_2(H_2O)](NO_3)$, $[Eu(H_2L^2)(NO_3)_2](NO_3)$ and $[Tb(H_2L^2)(NO_3)_2](NO_3)$ were also established.

Salen [124] synthesized a series of new acyldihydrazones, H_2L^n from condensation of ethylpyruvate with oxalic, malonic, succinic, glutaric and adipic acid dihydrazides. They synthesized copper(II) complexes $[Cu_2(L^{1n})H_2O].xH_2O$ where L^{1n} refers to the quadruply deprotonated pyruvic acid dihydrazone ligand and n refers to the number of carbon atoms of the aliphatic spacer between the two acylhydrazone units. The isolated complexes were characterized by elemental analyses, infrared spectra, mass spectra as well as variable temperature magnetic susceptibility measurements. Magnetic susceptibility measurements in the 4.2 - 298 K range indicated significant antiferromagnetic coupling between Copper(II) centres and suggested association of the coordinated copper(II) units Cu(ONO) via oxazine oxygen bridges. This led to a polymeric structure where the dimeric units are connected together with aliphatic spacer. From the best fit values of the mole fraction of paramagnetic uncoupled copper(II) centres (ρ), the degree of association in these polynuclear copper (II) complexes was estimated.

Elengoz et al [125] synthesized zinc(II) complex tris(biacetyl- dihydrazone–k^2 N, N' zinc(II)bis(perchlorate), $[Zn(C_4H_{10}N_4)_3](ClO_4)_2$ and determined its crystal structure at 110 K. The metal-organic cation is located on a $\bar{3}$ axis and is characterized by an approximate octahedral geometry in which each of the ligands occupies two coordination sites around the metal. The compound crystallizes in the trigonal space group $P\bar{3}c1$ with two units of the $[Zn(C_4H_{10}N_4)_3]^{2+}$ cationic complex and four ClO_4^- anions in the unit cell. The zinc(II) atom is located on a $\bar{3}$ axis, while the perchlorate anion is located on a threefold rotation axis. The cation is characterized by perfect $\bar{3}$ symmetry, in which three chelating ligands occupy the octahedral coordination sites of the zinc metal ions. The imine N atoms of the ligand provide the coordination sites to the central metal ion.

The conformation about the central C-C bond of the ligand is *cis* with the two C=N bonds being nearly coplanar, to direct the two imine coordination sites towards the metal centre. The N-Zn-N bond angle involving two coordinating N-atoms of a given ligand is 74.33 (11)°. In the free form of the ligands, the N-N=C-C=N-N backbone adopts a planar *anti*-conformation [126].

From the survey of literature presented above, it is evident that although mono and bimetallic complexes of various types of dihydrazones have been synthesized and characterized, in some detail, those derived from dihydrazones containing methylene function and bulky fragments in their molecular skeleton have scarcely been studied. Further the heterobimetallic complexes of such dihydrazones are almost non-existent. In view of limited investigations on metal complexes of dihydrazones containing methylene function and bulky fragments in their molecular skeleton, the present project has been undertaken. It is quite possible to extend and develop such a study, with the help of variety of metal ions into a major field, but because of time factor, it has been

restricted to monometallic and heterobimetallic complexes of disalicylaldehyde adipoyldihydrazone ($slahH_4$) and bis(2-hydroxy-1-naphthaldehyde)-adipoyldihydrazone ($npahH_4$) with manganese and ruthenium metal ions.

CHAPTER-II

Particulars of Instruments/Equipments used, Synthetic Procedure of Ligands and Details of Analytical Methods for Characterization of Complexes

Experimental

This chapter deals with experimental details regarding synthesis of ligands, method of analysis, physico-chemical techniques and the instruments employed for studying the ligands as well as the complexes. The details about preparation of complexes are given in the respective chapters.

Materials

The metal salts $Mn(OAc)_2.4H_2O$, $RuCl_3.3H_2O$, diethyl adipate $[(CH_2)_4(COOEt)_2]$, hydrazine hydrate $(N_2H_4.H_2O)$, salicylaldehyde $[C_6H_4(OH)CHO]$ and 2-hydroxy-1-naphthaldehyde $[C_{10}H_6(OH)CHO]$ and KOH were E-Merck or equivalent grade reagents.

The organic solvents viz methanol, ethanol, benzene, acetone, acetonitrile, dimethyl sulphoxide (DMSO) and dimethyl formamide (DMF) were purified by standard literature procedures.

Preparation of ligands

The ligand disalicylaldehyde adipoyldihydrazone ($slahH_4$) and bis(2-hydroxy-1-naphthaldehyde)adipoyldihydrazone ($npahH_4$) were prepared in two steps. In the first step, adipoyldihydrazine (DH_2) was prepared by reacting diethyl adipate with hydrazine hydrate in 1: 2 molar ratio. In the second step, adipoyldihydrazine thus obtained was allowed to react with salicylaldehyde or 2-hydroxy-1-naphthaldehyde in 1:2 molar ratio in ethanol which yielded the ligands.

(i) Preparation of adipoyldihydrazine $[(CH_2)_4(CONHNH_2)_2]$

Adipoyldihydrazine (DH_2) was prepared by reaction of diethyl adipate

(1.00 g, 4.94 mM) and hydrazine hydrate (0.55 g, 10.89 mM) in 1: 2 molar ratio under reflux for 30 mins in ethanol (20 mL). The product was recrystallized from dilute ethanol.

$$(CH_2)_4(CO_2Et)_2 + 2N_2H_4 \xrightarrow{H_2O} (CH_2)_4(CON_2H_3)_2 + 2EtOH + 2H_2O$$

(ii) **Preparation of disalicylaldehyde adipoyldihydrazone ($slahH_4$) and bis(2-hydroxy-1-naphthaldehyde)adipoyldihydrazone ($npahH_4$)**

In order to prepare disalicylaldehyde adipoyldihydrazone ($slahH_4$) and bis(2-hydroxy-1-naphthaldehyde)adipoyldihydrazone ($npahH_4$), adipoyl- hydrazine (1.00 g, 5.75 mM) in dilute ethanol (20 mL) was allowed to react with salicylaldehyde (1.40 g, 11.48 mM) in ethanol (20 mL) or with 2-hydroxy-1-naphthaldehyde (2.18 g, 12.65 mM) in 1:2 molar ratio over hot plate at 70 °C with constant gentle stirring for about 30-45 mins. The white precipitate of disalicylaldehyde adipoyldihydrazone ($slahH_4$) (A) and light yellow precipitate of bis(2-hydroxy-1-naphthaldehyde)adipoyldihydrazone ($npahH_4$) (B) thus obtained were purified by repeated washings with hot ethanol and dried over $CaCl_2$.

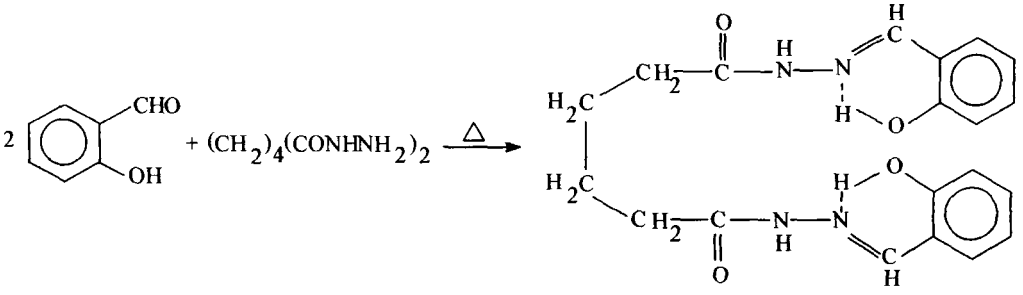

(A)

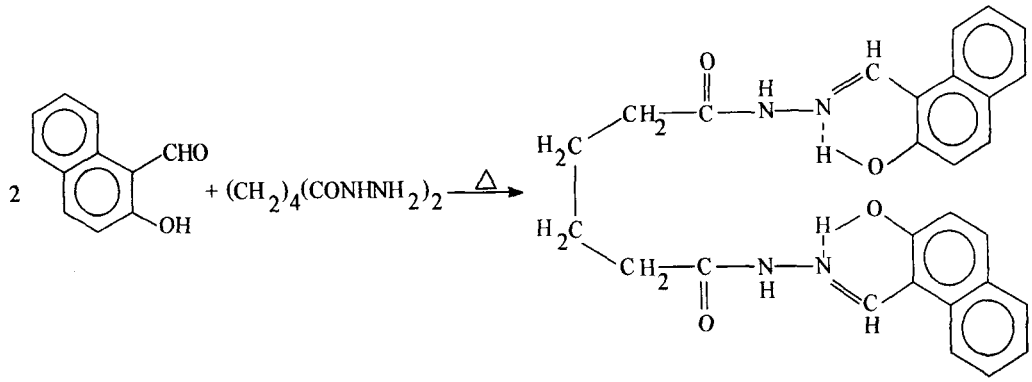

(B)

The carbon, hydrogen and nitrogen analysis and m.ps for the ligands have been presented in **Table 2.**

Analysis of C, H, N, Metal and Anions present in the Complexes and determination of Co-ligands

C, H and N were estimated microanalytically on Perkin-Elmer 2400, Series-II instrument. Water, pyridine, 2-picoline, 3-picoline and 4-picoline molecules were determined by heating the samples in an electric oven at 110 or 180 and 220 °C, respectively and determining the weight loss. Water molecules were determined by passing the vapour through a trap containing anhydrous $CuSO_4$ which turned blue while pyridine molecules were determined by passing the vapours through a test tube containing $CHCl_3$ and NaOH solution which turned red [127]. Metals [128, 129] and chlorine [128] were determined by following standard literature procedures.

Estimation of metals

For estimation of metals, 0.40 g of the complex was accurately weighed and taken in a 100 mL beaker. To this, 30 mL water was added and shaken well. To this resulting suspension, 1 mL concentrated H_2SO_4 and 0.50 mL concentrated HNO_3 were added. The solution was evaporated upto dryness. This process was repeated 5 to 6 times. The residue was extracted with 1 mL of concentrated HCl and again evaporated to dryness. The final content was diluted to 200 mL with distilled water.

The estimation was done by following the standard literature procedures [128, 129].

Estimation of Chlorine

Accurately weighed 0.20 g of chloro complex was digested with 0.50 g of NaOH for about 2 h. The solution so obtained was filtered and the filtrate was treated with nitric acid. Any undissolved material was rejected by filtration. To this solution, 0.10 N $AgNO_3$ solution was added keeping it slight excess. The precipitate so obtained was allowed to settle for 2 h in dark. White precipitate of AgCl was filtered through a gooch crucible and dried to a constant weight at 110 °C.

Physico-Chemical Measurement

Room temperature magnetic susceptibility measurements were carried out on Sherwood Scientific Magnetic Susceptibility Balance. Experimental magnetic susceptibility values have been corrected for diamagnetism by the procedures given by Figgis and Lewis [130] and Earnshaw [131]. The molar conductance of the complexes at 10^{-3} M dilution in DMSO solution were measured on a Direct Reading Conductivitymetre-304 with a dip-type conductivity cell at room temperature. Infrared spectra were recorded on Bomen DA-8FT-IR spectrophotometer in the range 4000-450 cm^{-1} in KBr discs and in the range 600-150 cm^{-1} in CsI discs on Thermo Nicolett, Model No. Magna-550. The electronic spectra were recorded on a Perkin Elmer Lambda 25 UV/Vis Spectrophotometer and Beckman DU 650 spectrometer using DMSO solution. The electron paramagnetic resonance (EPR) spectra of the complexes in powdered as well as solution state were recorded at X-band frequency on varian E-112E–Line Century series ESR spectrometer using TCNg (g = 2.0027) as an internal field marker. The FAB mass spectra of the complexes were recorded on a JEOLSX 102/DA-6000 mass spectrometer/Data system using Argon/Xenon (6 KV, 10 mA) as FAB gas. Nitrobenzyl alcohol (NBA) was used as the matrix. The ^{1}H and ^{13}C NMR spectra were recorded on Varian 400 MHz NMR spectrophotometer, model no. Mercury plus 400 NMR

spectrophotometer in DMSO-d_6 using TMS as an internal standard. Cyclic voltammetric measurements of the compound in DMSO (10^{-3} M) was done using CH Instruments Electrochemical Analyzer under nitrogen atmosphere. The electrolytic cell comprises of 3-electrodes. The working electrode was a glassy–carbon disk from BAS and the reference electrode was an aqueous SCE or Ag/AgCl separated from the sample solution by a salt bridge. 0.1 M TBAP was used as the supporting electrolyte.

Table 2: Melting Point and C, H, N Analysis of Ligands

Ligand	Formula	M.P. (° C)	Analysis: found (Calcd) %		
			C	H	N
1. Adipoyldihydrazine (DH_2)	$C_6H_{14}N_4O_2$	190	41.41 (41.38)	8.07 (8.05)	31.28 (32.18)
2. Disalicylaldehyde adipoyldihydrazone ($slahH_4$)	$C_{20}H_{22}N_4O_4$	>300	65.91 (66.30)	5.97 (6.08)	15.37 (15.47)
3. Bis(2-hydroxy-1-naphthaldehyde) adipoyldihydrazone ($npahH_4$)	$C_{28}H_{26}N_4O_4$	>300	69.50 (69.71)	5.30 (5.40)	11.70 (11.62)

CHAPTER-III

Synthesis, Characterization and Structural Assessment of Monometallic Manganese(II) Complexes derived from Polyfunctional Adipoyldihydrazones

Introduction

An examination of molecular model of adipoyl dihydrazone indicates that the ligands are related to monoacylhydrazines, aroylhydrazines and their derivatives. Hence, it is relevant to briefly mention the type of complexes formed by them and examine their bonding mode.

The monoacylhydrazines and monoaroylhydrazines, $RCONHNH_2$ (R = alkyl and aroyl) form 1:1, 1:2, 1:3 (metal:ligand) complexes with metal ions [132-135, 17]. They coordinate to metal ions in keto form (I) [16] or in enol form (II) [136] functioning as a neutral bidentate ligand or monobasic bidentate ligand.

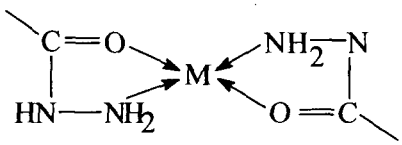

(I)

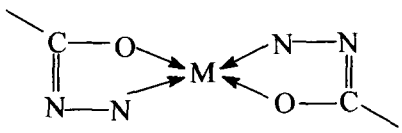

(II)

The Schiff bases (III) derived from monoacyl and aroylhydrazines and hydroxy aldehydes and ketones form 1:1 and 1:2 (metal:ligand) complexes and function either as a monobasic bidentate (IV) [137], monobasic tridentate (V) [17] in keto form [17, 18] or dibasic tridentate (VI) in enol from [19, 20, 190] and yield dimeric or polymeric chelates in which they coordinate to metal ions from >C=O and >C=N groups besides bonding through –OH group.

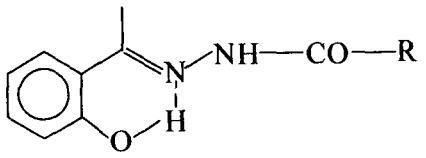

(III)

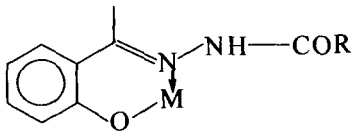

(IV)

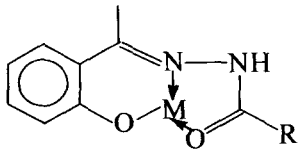

(V)

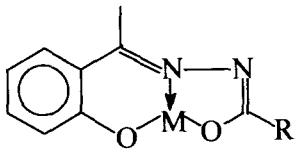

(VI)

Dutta and Sengupta [138] and Sahni et al [139] reported that acyl and aroyldihydrazines [138, 139] derived from aliphatic dicarboxylic acids, containing two -$CONHNH_2$ groups coordinate as a neutral bidentate ligand through two imino nitrogens (>NH) although the potentially strong donor functions like >C=O and $-NH_2$ are present. It has been suggested that strong intramolecular hydrogen bonding in them as shown below (VII), probably makes them unavailable for coordination.

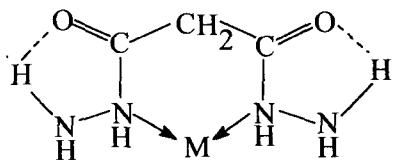

(VII)

However, when methylene or phenyl functions are substituted by pyridyl functions in dihydrazines, the resulting picolinoyl dihydrazine co-ordinates to the metal centre as a neutral pentadentate ligand through pyridyl nitrogen, two >C=O and two $-NH_2$ groups [140]. It appears that this ligand, because of the presence of pyridyl nitrogen atom, makes >C=O and NH_2 groups reactive.

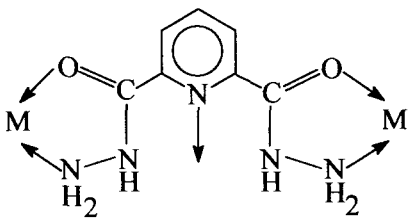

(VIII)

Further, Maki and coworkers [141] synthesized dioxouranium (VI) complexes of some dicarbonyl acid dihydrazones in ethanol medium in presence or absence of NaOAc. The dihydrazones were found to co-ordinate in a tetradentate fashion in the enol form except adipic acid hydrazide which co-ordinated in the keto form. The existence of dihydroxo bridges for the complexes isolated in the presence of NaOAc or basic medium (N_2H_4) was also established.

When the terminal $-NH_2$ groups are condensed with aldehyde and ketones, the resulting Schiff bases in which the above type of hydrogen bonding (VII) is likely to disappear possess >C=O and >C=N groups instead of >C=O and NH_2 groups in dihydrazides.

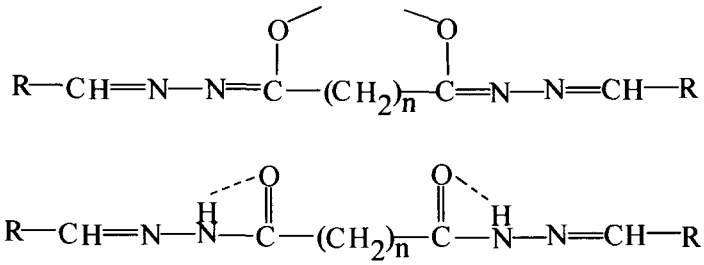

(IX)

Aggarwal and coworkers [142] reported first series transition metal complexes of 1:1 (metal:ligand) neutral and cationic complexes of such dihydrazones. In their study they have shown that the dihydrazones behave either as a neutral tetradentate ligand or dibasic tetradentate ligand coordinating through carbonyl oxygen and azomethine nitrogen atoms.

Further, if the aldehydes and ketones are aromatic compounds containing an orthohydroxy group, the resulting Schiff bases (X) have –OH groups in addition to >C=O and >C=N groups. In such Schiff bases the possibility of existence of newer hydrogen bonding in solid state as shown in (X) can't be ruled out.

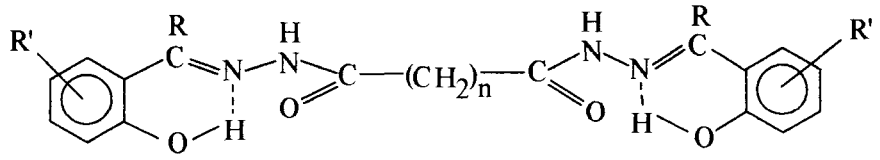

(X)

Such Schiff bases existing in keto–enol form offer several alternate bonding sites and can act as potential multidentate coordinating or chelating ligands resulting in the formation of complexes having different stoichiometries under different experimental conditions. The molecular model of the dihydrazones indicate their flexible nature in the space due to which they are able to offer planar as well as tetrahedral set of donor atoms depending upon the preferred stereochemical disposition of the metal valences, nature of R-groups and the nature of the bonds formed in the coordination process. The various donor sites in the ligand can bond either to the same metal atom or to the different metal atoms leading to a monomeric or polymeric structure of the complexes [180]. However, polymerization may also arise due to oxo-bridged [143, 144] structure.

The ligands disalicylaldehyde adipoyldihydrazone ($slahH_4$) and bis(2-hydroxy-1-naphthaldehyde)adipoyldihydrazone ($npahH_4$) selected in the present study have been derived from condensation of adipoyl dihydrazine with salicylaldehyde and 2-hydroxy-1-naphthaldehyde, respectively. They contain four methylene functions flanked by keto groups in addition to other functional groups like amide, azomethine and phenol functions, each in duplicate. The ligands may exist in diketo form, keto-enol form and dienol form, respectively, and are among examples of few ligands which offer chemically flexible ligand framework because of free rotation of the two

hydrazone groupings about C-C single bond and its potential to offer any set of donor atoms depending upon the preferred stereochemical disposition of the metal valences and the nature of the bonds formed in coordination process, in contrast to aroyl and pyridoyl–dihydrazones in which the central phenyl and pyridyl rings between the two hydrazone groupings impose planarity on them. Evidently, the ligands can assume monobasic, dibasic, tribasic, tetrabasic or even pentabasic character in forming metal complexes either in *staggered* configuration or *syn–cis* configuration or *anti-cis* configuration.

A survey of literature has disclosed that few complexes of the first row transition metal ions, with the dihydrazones derived from condensation of salicylaldehyde and related o-hydroxyaromatic aldehydes and ketones with malonoyldihydrazine and other acyldihydrazines, aroyldihydrazines and pyridoyl-dihydrazines have been reported [108]. But to the best of our knowledge, not even a single complex of Mn(II) derived from adipoyl dihydrazones has been reported.

In view of the significant role played by manganese in the conversion of solar energy into chemical energy in the form of reduced organic compounds and importance of monometallic complexes in the synthesis of heterobimetallic complexes and absence of work on metal complexes of title dihydrazones, the monometallic manganese (II) complexes have been synthesized in methanol and are described in the present chapter. The composition of the isolated complexes has been judged mainly from the elemental analysis, thermoanalytical data and mass spectral data. The structures of manganese (II) complexes have been discussed in the light of molar conductance, magnetic moment, electronic, infrared spectroscopic and EPR studies. The electron transfer reactions of the complexes have also been studied with the help of cyclic voltammetry.

Experimental

Preparation of the complexes

The complexes were prepared by the following general methods.

Preparation of $[Mn^{II}(slahH_2)(H_2O)_2]$ (1)

$Mn(OAc)_2.4H_2O$ (1.00 g, 4.08 mM) in methanol (20 mL) was added to a suspension of disalicylaldehyde adipoyldihydrazone ($slahH_4$) (1.60 g, 4.20 mM) in 20 mL methanol and stirred for 10 mins at 60 °C. The above homogenous suspension was stirred vigorously for another half an hour which precipitated, a yellow compound. The compound was filtered, washed with hot methanol, and air dried (Yield: 71%).

Preparation of $[Mn^{II}(slahH_2)(A)_2].nH_2O$ and $[Mn^{II}(slahH_2)(NN)]$ (where A = pyridine (py, 2); 2-picoline (2-pic, 3); 3-picoline (3-pic, 4) and 4-picoline (4-pic, 5) and NN = 2, 2' bipyridine (bpy, 6) and 1, 10-phenanthroline (phen, 7); (n = 0, 1))

These compounds were prepared by following essentially the above procedure by adding pyridine bases to the reaction mixture obtained by mixing $Mn(OAc)_2.4H_2O$ solution (1.00 g, 4.08 mM) in methanol (20 mL) and $slahH_4$ (1.60 g, 4.20 mM) in methanol (20 mL), maintaining M:L:pyridine molar ratio at 1:1:10 (Yield: 60%, (2); 57 % (3), (4); 55 % (5)).

The complexes (6) and (7) were also prepared similarly by adding bipyridine/1,10–phenanthroline to the reaction mixture instead of pyridine/2-picoline/3-picoline/4-picoline and maintaining M:L:NN molar ratio at 1:1:2 (Yield: 51 % (6); 48% (7)).

Preparation of $[Mn^{II}(npahH_2)]$ (8)

$Mn(OAc)_2.4H_2O$ (1.00 g, 4.08 mM) in methanol (20 mL) was added to a solution of bis(2-hydroxy-1-naphthaldehyde)adipoyldihydrazone ($npahH_4$) (1.97g, 4.06 mM) in 20 mL methanol accompanied by stirring at 60 °C for 10 mins. The homogenous suspension was stirred vigorously for another half an hour, a yellow-brownish compound was obtained. The compound was filtered, washed with hot methanol and

air dried (Yield: 76%).

Preparation of $[Mn^{II}(npahH_2)(A)_2]$ and $[Mn^{II}(npahH_2)(NN)]$ (where A = pyridine (py, 9); 2-picoline (2-pic, 10); 3-picoline (3-pic, 11) and 4-picoline (4-pic, 12) and NN = 2, 2' bipyridine (bpy, 13) and 1, 10-phenanthroline (phen, 14))

$Mn(OAc)_2.4H_2O$ (1.00 g, 4.08 mM) in 20 mL methanol was added to a homogeneous suspension of ligand $npahH_4$ in 20 mL methanol and stirred vigorously for 10 mins at 60 °C. To this, the pyridine bases in 20 mL methanol were added maintaining M:L:pyridine molar ratio at 1:1:10 and the whole suspension was vigorously stirred for 45 mins again at 60 °C. The compounds were isolated by filtration, washed with hot methanol and air dried (Yield: 60 % (9), (10) (Yield: 57 % (11)-(14)).

Further, the complexes (13) and (14) were also prepared similarly by adding bipyridine/1,10–phenanthroline to the above hot reaction mixture instead of pyridine/2-picoline/3-picoline/4-picoline and maintaining M:L:**NN** molar ratio at 1:1:2 (Yield: 51% (13) and (14)).

Results and Discussion

Disalicylaldehyde adipoyldihydrazone ($slahH_4$) and bis(2-hydroxy-1-naphthaldehyde adipoyldihydrazone ($npahH_4$) are polyfunctional ligands containing amide, azomethine and phenol/naphthol functions, each in duplicate. They have been derived from condensation of adipoyldihydrazine with salicylaldehyde and 2-hydroxy-1-naphthaldehyde, respectively. In these ligands, two hydrazone groupings are joined to each other through four methylene functions. Because of the presence of as many as eight bonding sites, the ligands can bond to metal ions in several different ways: as a monobasic bidentate ligand coordinating through one hydroxyl oxygen and one azine group nitrogen or as a monobasic tridentate or as dibasic tridentate ligand coordinating through one hydroxyl oxygen, one azine group nitrogen and one C=O group while the other half of the molecule remains unbonded; as a neutral bidentate ligand coordinating

either through the carbonyl oxygens or the two secondary amine nitrogen atoms with the OH groups remaining intact hydrogen bonded in the complexes; as a dibasic tetradentate ligand coordinating through the two hydroxyl oxygen and the two azine group nitrogen atoms; and as dibasic hexadentate ligands bonding to the same metal ion through the two hydroxyl oxygens, two azine group nitrogens and two carbonyl oxygens in the keto form. Further, these ligands may undergo enolization affording newer bonding possibilities leading to the formation of the binuclear or polynuclear complexes. All the above possibilities can be actually realized in practice if the metal salt, concentration of metal ion and ligand, reaction medium, pH and temperature are varied.

In order to isolate the manganese complexes, manganese (II) acetate was allowed to react with dihydrazone in 1:1 molar ratio either as such or in the presence of KOH. Pyridine bases were also added at appropriate stages to isolate the products. It is interesting to note that Mn(II) is oxidized to Mn(IV) in the presence of KOH. Thus the two methods of preparation yielded manganese complexes in +2 and +4 oxidation state. The manganese (II) complexes constitute the subject matter of the present chapter while the manganese (IV) complexes constitute the subject matter of the next chapter.

The colour, decomposition point, analytical, magnetic moment and molar conductance data for the complexes are set out in **Table 3.1**. The compositions of the complexes have been deduced based on the data obtained from elemental analyses and mass spectral data.

$$slahH_4 + Mn^{II}(OAc)_2.4H_2O \xrightarrow[(1:1)]{methanol} [Mn^{II}(slahH_2)(H_2O)_2]\ (1) + 2CH_3COOH + 4H_2O$$

$$slahH_4 + Mn^{II}(OAc)_2.4H_2O + A \xrightarrow[(1:1:10)]{methanol} [Mn^{II}(slahH_2)(A)_2].H_2O + 2CH_3COOH + 4H_2O$$

(where A= py, (2); 2-pic, (3); 3-pic, (4); 4-pic, (5))

$$slahH_4 + Mn^{II}(OAc)_2.4H_2O + NN \xrightarrow[(1:1:2)]{methanol} [Mn^{II}(slahH_2)(NN)] + 2CH_3COOH + 4H_2O$$

(where NN = bpy, (6); phen, (7))

$$npahH_4 + Mn^{II}(OAc)_2.4H_2O \xrightarrow[(1:1)]{methanol} [Mn^{II}(npahH_2)]\ (8) + 2CH_3COOH + 4H_2O$$

$$npahH_4 + Mn^{II}(OAc)_2.4H_2O + A \xrightarrow[(1:1:10)]{methanol} [Mn^{II}(npahH_2)(A)_2] + 2CH_3COOH + 4H_2O$$

(where A = py, (9); 2-pic, (10); 3-pic, (11); 4-pic, (12))

$$npahH_4 + Mn^{II}(OAc)_2.4H_2O + NN \xrightarrow[(1:1:2)]{methanol} [Mn^{II}(npahH_2)(NN)] + 2CH_3COOH + 4H_2O$$

(where NN = bpy, (13); phen, (14))

The $slahH_4$ complexes are all either dull brown or light brown, while $npahH_4$ complexes are all yellowish brown in colour. They are air stable. All these complexes decompose without melting above 300 °C. This indicates that in these complexes, the metal-ligand bonds have comparatively higher ionic character. All of these complexes are insoluble in water and other common organic solvents but they dissolve freely in coordinating solvents like DMSO and DMF.

Complex (8) does not show weight loss either at 110 °C or at 180 °C ruling out the possibility of presence of water molecules either in the lattice structure or in the first coordination sphere around metal ion. While complex (1) shows weight loss at 180 °C indicating the presence of water molecules in the first coordination sphere around metal ion.

On the otherhand, the complexes (2) to (7) and (9) to (14) show weight loss at 220 °C corresponding to two pyridine/2-, 3- and 4-picoline or one bipyridine/ phenanthroline molecules. The expulsion of these donor molecules at such a high temperature indicates that they are coordinated to the metal centre.

Mass Spectra

The complexes (8) and (10) have been characterized by FAB mass spectra as representative sample to assess their molecular complexity. The FAB mass spectra of the complexes (8) and (10) in m-nitrobenzyl alcohol matrix are shown in **Figs. 3.1.1** and **3.1.2**. The spectra of both the complexes show a signal at m/z value 536 which, most probably, results from the formation of $[Mn(npahH_2)]^+$ species. The species $[Mn(npahH_2)]^+$ in complex (8) results from the breakdown of the polymeric structure. On the otherhand, the peak at m/z value 536 in complex (10), most probably, results from the loss of two 2-picoline molecules. The existence of these species in these complexes at m/z value 536 indicates that the complexes are quite stable in monomeric form. Both the complexes show a peak at m/z value 483 which might be attributed to arise from the protonated ligand $[npahH_5]^+$ which results from the loss of manganese atoms in complex (8) and two 2-picoline molecules and one manganese atom in complex (10). Further, the complex (10) shows two prominent peaks at m/z value, 678 which is attributed to $[Mn(npahH_2\text{-}C_3H_6)(2\text{-}picH_2^+)]$. The existence of these species in the mass spectra of these complexes indicates their monomeric nature.

Molar Conductance

The molar conductance values for the complexes were recorded in DMSO. The

The molar conductance values for the complexes lie in the range 1.5–3.7 ohm^{-1} cm^2 $mole^{-1}$.

The molar conductance values for the complexes of different electrolyte types depend on the nature of the solvent [145]. Some of the Λ_M ranges reported for 10^{-3} M dilution of the complexes of different electrolyte types in aqeous and non-aqeuous solvents are given in the following **Table 3.2**.

Table 3.2 Molar Conductance Ranges for 10^{-3} M Solution of the Complexes of Different Electrolyte Types in Aqeuous and Non-aqeuous Solvents

Solvent	Electrolyte Type(ohm^{-1} cm^2 mol^{-1})			
	1:1	2:1	3:1	4:1
Water	95	225-270	380-452	above 520
Nitromethane	75-95	150-180	220-260	above 320
Nitrobenzene	20-30	50-60	70-82	90-100
Acetone	100-140	160-200	270-?	360-?
Acetonitrile	120-160	220-300	340-420	500-?
DMF	65-90	130-170	200-240	300-?
Methanol	80-115	160-220	290-350	450-?
Ethanol	35-45	70-90	120-?	160-?
DMSO	35-70	-	109-?	-

A comparison of the molar conductance data in DMSO for the complexes in present study with the value in **Table 3.2** indicates that all of the complexes have molar conductance values less than the expected value required for 1:1 electrolyte. The molar conductance values for the complexes may be attributed to their non-electrolytic nature in this solvent.

Magnetic Moment

The magnetic moment values for the complexes have been given in **Table 3.1.** The manganese(II) complex (8) has μ_B value equal to 1.12 B.M. while the remaining manganese(II) complexes have μ_B value in the range 5.79–6.02 B.M region. The μ_B value for the complex (8) suggests that it is a low-spin complex while the other complexes are high-spin.

The value of 1.12 B.M. falls outside the range reported for Mn(II) complexes in the low–spin state (t_2g^5, S = 1/2).

Very few low-spin complexes of di- and tri- valent manganese are currently known. Thus, manganese(II) complexes with cyano ligands [146, 147], phospine ligands [148] and oxine ligands [149, 150] have been reported. Although the complex (8) should show μ_B value corresponding to one unpaired electron, considering orbital contribution, the μ_B value exhibited by the complex (8) should fall around ca 2.18 B.M. [151].

The experimentally observed μ_B value of 1.12 B.M is much less than that expected on no-interaction basis between metal ions. Such a lowering in μ_B value indicates spin-spin coupling in the solid state between unpaired electrons belonging to different Mn(II) centres in the structural unit of the complexes.

A decrease in the magnetic moment value of the complex (8) can occur due to direct overlap of metal orbitals of one structural unit with metal orbitals of other structural unit. Alternatively, the decrease in the μ_B value of this complex can occur due to superexchange via overlap of the metal orbital with the orbitals of the bridging oxygen atoms of naphtholate group [152].

The μ_B values for the remaining complexes lying in the region 5.79 - 6.02 B.M. fall within the range reported for Mn(II) complexes in the high–spin state ($t_{2g}^3 eg^2$, S = 5/2). The μ_B values rule out the possibility of any spin-spin coupling in the solid state between unpaired electrons belonging to different Mn(II) centres in the structural unit of the complexes.

Electronic Spectra

The electronic spectral bands for dihydrazones and their metal complexes along with their molar extinction coefficients have been listed in **Table 3.3**. The electronic spectra for the ligands and the complexes nos. (4), (6), (8), (10), (12) and (14) have been shown in **Figs. 3.2.1** to **3.2.8**.

The free ligand slahH_4 shows two bands at 284 (4308) and 320 (2808) nm while npahH_4 shows three bands at 290 (2041), 335 (2300), 363 (1852) nm. The bands at 284 and 290 nm are assigned to intraligand π - π^* transitions while the bands in the region 313 - 363 nm are assigned to n-π^* transitions.

The bands in the region 313-363 nm are characteristic of salicylaldimine/napthaldimine part of the ligand as has been reported in several monoacyl hydrazones [153]. It is important to mention that the first ligand band in slahH_4 and the last two bands in npahH_4 are split into two components each in the complexes. The position of the bands as well as the molar extinction coefficients for the split bands are the average value for the split components. The splitting of the ligand bands in the ligands suggest that the two hydrazone fractions are not in the same plane. This, alternatively, suggests that the free dihydrazones exist in *anti-cis* configuration as concluded from IR spectroscopic studies.

The first ligand band in slahH_4 complexes (1) and (6) undergo blue shift by 8 nm while red shift by 2-6 cm^{-1} in the remaining slahH_4 complexes. The slahH_4 band observed at 320 nm due to salicylaldimine fraction shifts to longer wavelength by 2-10 nm. This shows the effect of complexation.

The spectra of $npahH_4$ complexes (8) to (14) possesses a new strong absorption bands in the region 256-263 nm while no such band is observed in the $slahH_4$ complexes (1) to (7). This band is assigned to some naphthaldimine band which appears below 250 nm in the electronic spectrum of free ligand on complexation, this band shows red shift and appears in the region 256-263 nm. The ligand band at 290 nm shows a red shift of about 25-30 nm and appears in the region 315-320 nm while that at 313 nm shows red shift of about 30-52 nm appearing in the region 330-365 nm. Such a high red shift of ligand bands in the complexes indicates strong bonding between metal and ligand. The spectra of $npahH_4$ complexes posseses one additional band in the region 448-600 nm. This band appears to have contribution from ligand band at 363 nm which is, most probably, red shifted in complexes as well as from charge transfer bands arising from charge transfer from naphtholate oxygen atom to metal centre [154]. The essential features associated with the electronic spectra of the complexes suggest bonding of the ligands to the metal centre.

The ligand bands in the electronic spectra of the complexes have almost the same splitting patterns as in the uncoordinated ligands. This suggests that the conformation of the ligands in the complexes remains essentially the same as in those of the free ligands i.e. the ligands are coordinated to the metal in *anti-cis* configuration.

The d-d transition in the Mn (II) complexes are very weak because they are both spin as well as laporte forbidden. Hence, these bands generally, do not appear in the visible region [155] of the electronic spectra of the complexes.

EPR Spectra

All of the complexes have been characterized by EPR spectroscopy. The EPR magnetic parameters for the complexes have been set out in **Table 3.3**. The EPR spectra of the complexes (1) to (4) and (8) have been shown in **Figs. 3.3.1 to 3.3.5** as representative samples.

The EPR spectrum of the complex (8) in the crystalline powder form shows an

isotropic signal with g = 2.019. The width of the signal at g = 2.019 is about 330 G which indicates spin exchange [156] between manganese(II) centres in the solid state which is consistent with very low μ_B value of the complex (**Figs. 3.3.5 (a)** and **(b)**). Although the essential features of the EPR spectrum of the complex in solution remain the same as in the polycrystalline state, yet the width of the signal in the g = 2.019 region is dramatically increased to about 500 G. This rules out the possibility of the presence of any exchange interaction in DMSO solution. This may be due to breaking of polymeric structure resulted from coordination of highly donor solvent DMSO molecules to the metal centre.

In DMSO solution, the complex (8) shows ^{55}Mn hyperfine splitting. The ^{55}Mn hyperfine splitting constant in this complex in DMSO solution is equal to 100 G. In the low-spin manganese(II) complexes, 'A_{Mn}' values span the range 75-100 G, the 90-100 G domain being more frequented [148]. The 'A_{Mn}' values of 100 G lies in the range reported for the low-spin manganese Mn(II) complexes without metal–metal interaction. The central resonance in this complex shows splitting into five components with average nitrogen superhyperfine splitting constant A_N equal to 12 G indicating coordination of two nitrogen atom to the manganese metal centre [158].

By studying the temperature dependence of EPR signal intensity, it is possible to determine the sign and possibly estimate the size of the electronic coupling between the manganese ions. The **Figs. 3.3.3 (b)** and **(c)** illustrate the relative change in the spectra observed on lowering the temperature from ambient to LNT. The spectra were recorded under conditions where microwave power saturation did not occur so that the intensities are representative of the state populations. The qualitative result which is seen from the figures is that the intensity centered at g ≅ 2.00 near 3200 G is reduced.

On the otherhand, the EPR spectra of the complexes (1) to (7) derived from

slahH_4 and the complexes (9) to (14) derived from npahH_4 in the solid state are essentially similar to one another at LNT and show an isotropic signal with g-value in the region 1.994-2.050. This shows that all of the complexes have similar stereochemistry. No other signal is observed in the 8000 G span as would have been expected for non–cubic Mn(II) complexes with an appreciable zero field splitting. On the otherhand, in the DMSO solution at RT, six line spectrum is obtained with ^{55}Mn hyperfine splitting constant falling in the range 94-104 G. This ^{55}Mn hyperfine splitting constant is characteristic of Mn(II) complexes rather than for Mn(IV) complexes. The overall intensity of the split component of the signal due to ^{55}Mn hyperfine splitting at LNT is weak as compared to that at RT. This might be attributed to the effect of strong coordination of DMSO molecules to the metal centre.

The total width of the central isotropic resonance in the case of the complexes (2) to (7) falls in the region 470-520 G at X-band. Such an isotropic resonance has been related to the absence of any exchange narrowing phenomenon, where Mn(II) ions are not coupled to any other ion [159].

Infrared Spectra

Some structurally significant IR bands for free dihydrazones and the monometallic complexes have been set out in **Table 3.4**. The I.R spectra of free dihydrazones and the complexes (1), (2), (8) and (14) have been shown in **Figs. 3.4.1-3.4.6**.

The spectra of the ligands are very much complicated due to overlapping of the bands arising from several groups occurring in the same region. However, some typical bands have been selected for the location of bonding sites of the ligand. The solution spectrum of the ligand could not be investigated due to its insolubility in most of the common organic solvents. Hence, it has not been possible to eliminate the effect of intermolecular hydrogen bonding by comparing the solid state spectra of the complexes with the solution spectra of the parent ligands.

An examination of the IR spectra of dihydrazones and their complexes suggests that the ligand slahH_4 is present in enol-form in the complexes (1) to (5) while both the ligands are present in keto form in the remaining complexes.

OH and NH Stretching Frequency

The uncoordinated dihydrazones show a medium to strong broad band in the region 3300-3600 cm^{-1} and two strong, relatively, more intense bands in the region 3000-3224 cm^{-1}. While the first medium to strong band is assigned to νOH of salicylaldehydato/naphthaldehydato part of the dihydrazones, those in the region 3000-3224 cm^{-1} are assigned to arise from secondary NH group. The IR spectra of the complexes (1) to (5) show a medium to strong broad band in the region 3000-3600 cm^{-1}, with their centres lying in the region 3431-3449 cm^{-1}. This is attributed to arise from stretching vibration, either due to lattice or coordinated water molecules or may be due to phenolic/naphtholic –OH group from the dihydrazones. Although from the shape and position of νOH band, no inference can be drawn regarding the nature of water molecules, yet a band present at 635 cm^{-1} in the complex (1) assigned to ρ_r mode of coordinated water molecules suggest unambiguously that atleast some water molecules are coordinated. On the otherhand, the complexes (2) to (5) do not show any new band in the region 618-652 cm^{-1} which may be assigned to ρ_r mode of coordinated water molecules. This indicates the absence of coordinated water molecules in the complexes (2) to (5). When the complexes (2) to (5) are heated, they show loss of weight at 110 °C which suggests the possibility of the presence of water molecules in their lattice structure. However, the complex (1) shows loss of weight at 180 °C corresponding to two water molecules indicating their presence in the first coordination sphere around the metal centre. Further, these complexes do not show any band in the region 3000-3300 cm^{-1} which may be assigned to secondary NH group. Such a feature associated with the IR spectra of these complexes in this region suggests destruction of NH group of the ligand as a result of enolization on complexation. In view of such IR

spectral features of these complexes, it is suggested that the strong broad band in the region 3000–3600 cm^{-1} is either due to νOH vibration of water molecules absorbed by KBr during pellet preparation or due to νOH vibration of enolic group. Moreover, these complexes show medium band in the region 2500-2900 cm^{-1}. The origin of this band in the complexes indicates presence of a new kind of H-bonding in the complexes resulted from involvement of enolic –OH group in intramolecular H-bonding.

The IR spectra of the remaining complexes in the region 3000-3600 cm^{-1} are only slightly modified on complexation. The essential IR spectral features of the complexes remain the same as those of the uncoordinated dihydrazones suggesting that the dihydrazones coordinate to the metal centre in keto-form and retain [160] the same conformation as existing in uncoordinated state. The νNH vibrations observed in the region 3000-3224 cm^{-1} in the uncoordinated dihydrazone either remain almost unshifted in positions (complexes (6) and (7)) or are shifted to lower frequency by about 4-54 cm^{-1} in the remaining complexes. From such a lower shift of νNH vibrations, we have refrained from drawing any conclusion regarding involvement of secondary NH group in bonding or otherwise because of the complex nature of the bond in this region in the complexes. However, it may be related to the presence of stronger intramolecular hydrogen bonding between secondary NH hydrogen and >C=O group of the ligand in the coordinated state.

Amide Frequency

The uncoordinated ligands show a strong band at 1679 and 1666 cm^{-1} which are assigned to stretching vibration of >C=O group. This band splits either into two bands as in the complexes (6) and (7) or it appears as a single band in the complexes (8) to (14). The νC=O band remains either almost unshifted in position as in the complexes (11) and (12). Almost unaltered position of νC=O band rules out the possibility of coordination of >C=O group to the metal centre. On the otherhand, in the complexes (6) to (10) and (13), (14), the νC=O band shifts to lower frequency by 10-46 cm^{-1} and

appears in the region 1640-1680 cm^{-1}. Such a lower shift of νC=O band in these complexes cannot be related to coordination of >C=O to the metal centre because >C=O groups absorb almost in the same region in those complexes in which the uncoordinated >C=O groups have been reported to absorb in the metal complexes of dihydrazones by X-ray crystallography. The lower shift of νC=O band is attributed to involvement of >C=O groups in the strong intramolecular H-bonding with secondary NH group in the complexes. This is also corroborated from the shift of νNH band to lower frequency in these complexes by 4-54 cm^{-1}. On the otherhand, the νC=O band disappears in the complexes (1) to (5) indicating destruction of amide structure and coordination of dihydrazone to the metal centre in the enol form.

>C=N Stretching Vibrations

The ligand $slahH_4$ shows a single strong band at 1620 cm^{-1} while $npahH_4$ shows a doublet centred at 1612 cm^{-1}. This band is assigned to arise from stretching vibrations of >C=N group [161]. νC=N stretching vibration occurs in the range 1665-1635 cm^{-1} in Schiff bases derived from condensation of hydrazide with aliphatic aldehyde and ketones whereas in the range 1630-1610 cm^{-1} in those derived from aromatic aldehydes and ketones [161]. The bands observed in the above region in hydrazide and dihydrazide Sciff bases and their transition and non-transition metal complexes have been used by us [46, 100] and others [132, 133, 136] for the interpretation of the IR spectra of the complexes of hydrazide schiff bases.

In the present study, the dihydrazone ligands $slahH_4$ and $npahH_4$ show bands in the region 1593-1630 cm^{-1}. These band have been assigned to stretching vibration of >C=N group. This band shifts to lower position by 9-15 cm^{-1} in the complexes derived from $slahH_4$ while by 2 to 4 cm^{-1} in the complexes derived from $npahH_4$ indicating coordination of dihydrazones through the azomethine nitrogen atoms to the metal centre.

The dihydrazones derived from condensation of salicylaldehyde, 2-hydroxy-1-

naphthaldehyde and ketones with acyl, aroyl and pyridoyl dihydrazones are polyfunctional ligands and can coordinate to the metal centre in a *staggered* configuration, *anti-cis* configuration and *syn–cis* configuration either in keto, keto-enol or enol forms, respectively. They are capable of yielding mononuclear and polynuclear complexes involving ligand bridging as well as oxo-bridging [163]. If the dihydrazones coordinate in a *staggered*–configuration or *syn–cis* configuration to the different metals, there is no possibility of any steric crowding in the molecule. However, when the dihydrazones co-ordinate to the metal centre in *anti-cis* configuration, the two hydrazone parts would co-ordinate to the same metal centre. This would introduce steric crowding in the molecule. In this configuration, the two phenolate oxygen atoms and two azomethine nitrogen atoms co-ordinate to one and the same metal centre while carbonyl oxygen atoms may or may not co-ordinate to the second metal centre depending upon whether the complex is bimetallic or monometallic. Because of steric crowding, one hydrazone part would attain an axial position while the other part would remain in the equatorial plane. Consequently, groups in the axial position would absorb at lower frequency as compared to their equatorial counterparts and the absorption bands corresponding to them in the IR spectra of the complexes would appear at different frequencies. Due to richness of spectra, because of various bands arising from different groups which absorb in the overlapping regions, it has not been possible to assign bands to equatorial and axial counter parts of different groups. However, the νC=N band which is free from interference by any other group in the IR spectra of the complexes appears as a couplet in the IR spectra of the complexes (8) to (14) derived from $npahH_4$. The band in the region 1615-1622 cm^{-1} is assigned to equatorial >C=N group while the band in the region 1590-1600 cm^{-1} is assigned to axial >C=N group. On the otherhand, in the IR spectra of the complexes (1) to (7), derived from $slahH_4$, both νC=N band merge into one another giving rise to a single band only. It appears that the νC=N band

appear either as a shoulder to the first band or the energy difference between two >C=N groups is so less that they appear very close to each other leading their merger into one another. At the same time, this also suggests that there is less steric crowding in these metal complexes as compared to those derived from dihydrazones containing bulky groups. Further, it has not been possible to identify the axial and equatorial counter parts of the other groups like amide II, (C-O)(phenolate) and (M-O)phenolic because of the complex nature of the IR spectra in the respective regions.

Amide II + ν(C-O)(phenolate/naphtholate) Bands

The free dihydrazones show strong to weak intensity bands at 1560 and 1530 cm^{-1} respectively. The band is assigned to have composite character due to mixed contribution of the amide II and νCO(phenolic/naphtholic) [164]. The complexes (1) to (4) show a medium to strong band in the region 1535-1541 cm^{-1}. Such a negative shift of this band as compared to that in the free ligand slahH_4 shows the involvement of phenolic –OH group in bonding via deprotonation. This is also confirmed by the occurrence of intense non-ligand band in the region 580-592 cm^{-1} due ν(M-O)(phenolate) [165]. As these complexes (1) to (5) do not show the band due to amide I group, in their IR spectra, the band in the region 1535-1541 cm^{-1} also appears to have contribution due to stretching vibration of NCO^- group produced as a result of destruction of 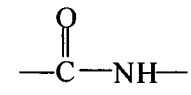 group as a consequence of enolization. In the remaining complexes, the amide II + ν(CO)(phenolic/ naphtholic) band either remains unshifted or shifts to higher position by 8-22 cm^{-1}. This rules out the posibility of coordination of >C=O group to the metal centre. However, the position of this band still falls in the region in which phenolic/naphtholic –OH groups are bonded to the metal centre via deprotonation.

β(C-O)(phenolate/naphtholate) band

In the dihydrazones, a strong to medium intensity band occurs at 1275 and 1281

cm^{-1}, respectively. This band is similar in nature as observed in other ligands containing phenol group. Hence, this band is assigned to β(C-O)(phenolic/naphtholic) [166]. This band undergoes splitting into two bands in the IR spectra of the complexes (4), (6) and (7) which appears to be the effect of bonding of phenolic C-O group to the metal centre. In the complexes (1) to (7) derived from slahH_4, this band on an average undergoes shift to lower position by 5-12 cm^{-1} while in the complexes (8) to (14) derived from npahH_4, this band shifts to higher position by 2-20 cm^{-1}. Such a feature associated with β(C-O) band in these complexes suggests involvement of phenolic/naphtholic C-O group in coordination. The shift of β(C-O)(phenolic) to lower position in the complexes (1) to (7) may be related to flow of π-electron density of aromatic ring to metal centre through azomethine group while the shift of β(C-O)(naphtholic) to higher position in the complexes (8) to (14) suggests that the π-electron density of aromatic ring in these complexes flow to metal centre through naphtholate oxygen atoms.

N-N and C-N Stretching Vibrations

The region below 1200 cm^{-1} is not well defined for hydrazine derivatives and contain bands due to νN-N, C-H bending vibration and ν(OH). Though, due to several vibrational modes, the region is quite complicated, the N-N stretching frequency occurring in the region 1050-800 cm^{-1} in the hydrazine derivatives has been identified and its shift has been found useful in understanding the involvement of nitrogen atoms in coordination. νN-N has been shown to increase from 885 cm^{-1} in N_2H_4 [167] to 973 cm^{-1} in $N_2H_5^+$ [168] and 1024 cm^{-1} in $N_2H_6^{2+}$ [169] due to protonation which is akin to involvement of lone pairs of electrons on nitrogen atoms in coordination to metal ions. Onyszchuk [170] and Sacconi [171] have observed νN-N near the above quoted frequencies in the complexes containing unidentate and bidentate hydrazine, respectively. But the above ranges in no way can be taken as specific for co-ordination of one or two nitrogen atoms in substituted hydrazine

complexes. Futher, it appears in the 1014-986 cm^{-1} region in metal complexes of monosubstituted hydrazines of the type NH_2-NH-Y [172]. But in metal complexes of N-N diacylhydrazines, νN-N has been observed in 1049-970 cm^{-1} region [173].

Eliminating the bands due to C-H in-plane deformation in the 1050-900 cm^{-1} region, medium to weak intensity bands at 1036 and 1030 cm^{-1} in the present ligands have been assigned to νN-N. The νN-N band remains either almost unshifted in position as in the complex (7) or shifts to higher position in the remaining complexes by 2-65 cm^{-1}. Such a feature associated with this band in the metal complexes indicates coordination of only one hydrazine nitrogen atom in coordination.

Water Bands

The antisymmetric and symmetric OH stretching modes of lattice water appears in the region 3500-3000 cm^{-1} while the H-O-H bending modes appears in 1630-1610 cm^{-1} region. The coordinated water molecules also show the above modes in the complexes in addition to absorption bands between 900-750 cm^{-1}.

In the complexes (1) to (5), water molecules are lost at 110 °C without change in colour. Hence, these water molecules are suggested to be present in the lattice structure of the complexes [174]. The broad band appearing in the region 3432-3449 cm^{-1} in the complexes (2) to (5) are assigned to antisymmetric and symmetric stretching vibrations of lattice water molecules while the band in the above region in the complexes (1) is assigned to coordinated water molecule. The complex (1) shows weight loss corresponding to two water molecules at 180 °C accompanied by change in colour, hence, these water molecules are considered to be present in the first coordination sphere around the metal centre [175]. On the basis of theoretical calculations, Sartori and coworkers [176] have suggested the rocking and wagging stretching vibrations of coordinated water to appear at 900-768 cm^{-1}, respectively. However, these frequencies are sensitive to the strength of coordinate bonds as well to hydrogen bonding in crystals. A distinct band appearing in 635 cm^{-1} in the complex

(1) arises due to rocking mode of coordinated water molecules to the metal centre.

Pyridine or Substituted Pyridine Co-ordination

The free pyridine bases absorb at around ~604 cm^{-1} due to in-plane ring deformation mode [177]. In the complex (2) to (7) and (9) to (14), a new medium to weak band is observed at 657-696 cm^{-1}. This band is assigned to arise due to in-plane ring deformation mode of pyridine bases indicating their coordination to the metal centre.

Low Frequency Region 600-620 cm^{-1}

Infrared spectra of the organic molecules containing aromatic rings, show bands due to the out-of-plane ring [16] deformation and out –of–plane C-H bending modes [160] and deformation vibrations of the carbonyl group [179] in low frequency region. The dihydrazones absorb at 603(w) and 577(m) cm^{-1}. These bands occur at almost the same frequencies in the infrared spectra of metal complexes or slightly shifted. However, a few new bands arise which may be assigned to metal–ligand vibrations.

From a stereochemical consideration of the ligand, it may be expected that a maximum of four kinds of metal ligand vibrations may arise viz νM-O(phenolic/naphtholic), νM-O (M-O-C and M←O=Cl) and νM-N in the complexes. A survey of literature related with metal-phenolate [180], metal enolate (M←O=Cl and M-O-C-) [181] and νM-N indicates that νM-O occurs in the range 600-500 cm^{-1} in metal complexes of N-salicylidene [182] and in the range 570-540 cm^{-1} in metal complexes of N-salicylidene glycine, but the range 250-220 cm^{-1} has been reported for ν(M-O) due to coordinated glycine part. The actual position of ν(M-O) depends upon the nature of the metal ion [180] and the ligand bonded to metal centre. On the otherhand, literature records the M-O stretching frequency in the metal acetylacetonates [183] occurs in the region 500-400 cm^{-1}. Fujiter et al [184] suggested the ν(M-O) in potassium salts of oxalate complexes of zinc(II), copper(II) and

cobalt(II) in the 446-416 cm^{-1} region. On the otherhand, the ν(M-N) stretching frequency has been found to occur in the region 440-325 cm^{-1} [185] in MCl_2^- hydrazine complexes. Two ν(M-N) ranges 560-490 cm^{-1} and 480-400 cm^{-1} have been proposed in case of metal-N-alkylsalicylaldimine complexes [182]. In various metal–ammonia [186], metal-imidazole [187], metal-pyridine [188] complexes, the ν(M-N) has been found to occur in the 420-350 cm^{-1} region.

In some cases, the assignments have been confirmed from isotopic substitution studies as well [189]. Thus from literature records, it can be said that the various metal–ligand stretching frequency regions are overlapping with one another.

The present ligands are the combination of adipic acid, hydrazine and salicylaldimine/naphthaldimine parts. In metal acetylacetonates and oxalates, νM-O is observed in the 470-420 cm^{-1} and 446-419 cm^{-1} regions, respectively, while in metal-salicylaldimines, the νM-O is observed in the 600-490 cm^{-1} region. The ν(M-N) in salicylaldimine complexes has been found in the 550-490 cm^{-1} and 470-390 cm^{-1} regions, respectively. But ν(M-N) in the hydrazine complexes has been proposed to occur in the 440-306 cm^{-1} region. Keeping all assignments in view, the various νM-O(phenolate/naphtholate) and νM-O(carbonyl) bands have been assigned in the metal complexes in the present study. Ligand bands have been excluded and the new bands appearing in the 580-600 cm^{-1} region have been assigned to νM-O(phenolate/naphtholate). The complexes do not show any new band in the region 500-400 cm^{-1} which may be assigned to νM-O(carbonyl) which rules out the possibility of coordination of carbonyl oxygen atom to the metal centre either as such or in the enol form.

We have refrained from making an assignment regarding M-N stretching frequency in the complexes which appear to occur below 400 cm^{-1} a range in which absorption due to lattice vibrations of KBr obscure any vibrations.

Cyclic Voltammetry

The cyclic voltammogram of a 2 mM solution of the complexes in DMSO solution due to their insolubility in CH_3CN with 0.1 M TBAP as a supporting electrolyte were run at several scan rates. The data have been set out in **Table 3.5** at a scan rate of 100 mV/s. The cyclic voltammograms of the dihydrazones ($L'H_4$ = $slahH_4$ and $npahH_4$ = LH_4) and the complexes (1) to (5), (7), (9), (12) and (13) are shown in **Figs. 3.5.1-3.5.11.**

The potentials of the complexes were scanned upto +2.00 to −2.00 V. The complexes showed no redox activity either in the range +1.60 to +2.00 or −1.60 to −2.00 V range. This is true regardless of the scanning direction i.e. whether starting point is 0.00 or 2.00 V. This shows that the oxidation of the complexes is not occurring up to the potentials from 1.60 to 2.00 or from −1.60 to −2.00 V. Potentials more positive than +1.20 V in view of the excessive current avoided. It should be mentioned that the supporting electrolyte TBAP in DMSO did not show any redox activity in the potential range studied. However, the ligands $slahH_4$ and $npahH_4$ are electroactive and show one oxidative wave at +0.35 V and 0.00 V respectively, which are associated with the reductive waves at +0.20 and −0.15 V, respectively. Further, the ligand $npahH_4$ shows an additional irreversible oxidative wave at +0.35 V.

When the voltammogram of the complex $[Mn^{II}(slahH_2)(H_2O)_2]$ (1) is recorded at a scan rate of 100 mV/s, an oxidative wave at +0.05 V and a reductive wave at −0.25 V is observed. Another reductive wave at +0.20 V is also observed in the complex corresponding to which a very weak inflexion is observed at +0.30 V. It is worth noting that the oxidative wave at +0.05 V is very strong and broad which shows that it is more than one electron process. It appears that it contains wave due to ligand oxidation as well. When the scan rate is enhanced to 300 mV/s, the CV feature still is not clear in the oxidative region. However, at a scan rate of 500 mV/s, the oxidative wave is split and a new oxidative wave is visible at +0.45 V in addition to the one at +0.20 V. At this scan rates, the first oxidative wave appears at +0.20 V in

addition to the second oxidative wave at +0.45 V while the reductive waves at −0.25 V and +0.20 V remain constant in position. The oxidative wave at +0.45 V and reductive wave at +0.20 V are assigned to ligand centred redox processes because they are very close to the oxidative and reductive waves in the free ligand. The remaining oxidative wave at +0.20 V and reductive wave at −0.25 V (oxidative wave at +0.05 V and reductive wave at −0.20 V at a scan rate of 100 mV/s) are assigned to metal-centred redox process. The redox processes corresponding to these reactions may be shown as below

$$[Mn^{II}(L'H_2)] + e \rightleftharpoons [Mn^{II}(L'H_2^{-})]^{-1}$$

$$[Mn^{II}(L'H_2^{-})]^{-1} \rightleftharpoons [Mn^{I}(L'H_2)]^{-1}$$

The cyclic voltammogarm of the complex (1) are shown in **Figs. 3.5.3 (a), (b)** and **(c)** at scan rates of 100, 300 and 500 mV/s, respectively.

The essential features of CV of pyridine complex (2) remain same as that of the complex (1) with the difference that the potentials become more negative at scan rate of 100 mV/s. The complex (2) shows an oxidative wave at +0.32 V while the corresponding reductive wave appears at −0.25 V. It is worthwhile to mention that the same wave is merged with ligand centred wave in the complex (1). The shift of the oxidative and reductive waves to more negative potentials indicate that the complex acquires negative character when pyridine becomes coordinated to the metal centre. The redox processes, may similarly be assigned in this case also. The essential features of voltammogram of the complex remain the same as in the case of complex (1) at the various scan rates.

On the otherhand, the complex $[Mn^{II}(slahH_2)(2\text{-pic})_2].H_2O$ (3) shows substantially different feature as compared to those of the complexes (1) and (2). At a scan rate of 100 mV/s, oxidative waves are observed at positive potentials of

+0.35 and +1.01 V in the backward scan. The reductive waves in the complex appear at −0.84 and +0.05 V respectively. The reduction peak at +0.05 V may be assigned to the redox couple

$$[Mn^{II}(L'H_2)] + e \rightleftharpoons [Mn^{I}(L'H_2)]^{-1}$$

The Mn^{+} species then remains stable over a long period of time until a low potential of -0.84 V is attained. At this potential, the Mn^{I} centre is reduced to Mn^{0}. In the return scan, the Mn^{0} state in the complex is again quite stable. It oxidizes only at a potential of +0.35 V to Mn^{I} which then further oxidizes to Mn^{II} at a potential of +1.01 V. Thus these potentials are assigned to Mn^{II}/Mn^{I} and Mn^{I}/Mn^{0} redox couple respectively. When the scan rate is increased, the essential features of CV remains the same. But, at the scan rate of 500 mV/s, the reduction wave at −0.84 V and oxidative wave at +1.01 V dissappear which means that Mn^{I} is not reduced to Mn^{0} at this scan rate. Only one reversible redox couple is observed at Epa = +0.10 and Epc = +0.04 V with $E_{1/2}$ = +0.07 V. This reversible wave is assigned to the redox couple $Mn^{II}(L'H_2)/Mn^{I}(L'H_2)$. This complex does not show any redox couple which could be assigned to ligand centred redox reaction.

The complexes (4) and (5) (**Figs. 3.5.6** and **3.5.7**) show essentially similar feature in their cyclic voltammogram. Both the complexes, (4) and (5) show a single broad reductive wave centred at −0.90 V and −0.70 V in the forward scan at a scan rate of 100 mV/s, respectively. In the return scan, two distinct oxidative peaks are observed at −0.35 V and +0.25 V (complex (4)) and at −0.35 V and +0.20 V (complex (5)), respectively. At a scan rate of 200 mV/s, the reductive wave at −0.90 V in the complex (4) is split into two waves at −0.70 and −0.91 V while that at −0.70 V in the complex (5) is split into two waves at −0.55 V and −0.84 V respectively. The corresponding oxidative waves appear at +0.17 V and −0.28 V (complex (4)) and at +0.32 V and −0.15 V (complex (5)), respectively at this scan rate. As these waves are sensitive to

the nature of the coordinated co-ligands, they are supposed to arise from metal centred redox reactions. The reductive waves at −0.90 V and −0.70 V in the two complexes at a scan rate of 100 mV/s are assigned to arise from Mn^{II}-Mn^{I} and Mn^{I}-Mn^{0} reduction processes which are superimposed upon each other.

The complex $[Mn^{II}(slahH_2)(bpy)]$ (6) shows a strong oxidative peak at +0.45 V while a weak reductive peak at +0.18 V at 100 mV/s. The oxidative peak at +0.45 V appears to arise from multielectron step. This peak may be assigned to electron transfer reactions centred on principal ligand $slahH_4$ as well as on metal. When the scan rate is increased to 200 mV/s, again only one oxidative peak appears at +0.63 V. The original reductive peak appears at positive potentials of +0.10 V while an additional reductive peak appears at +0.81 V. Out of the two reductive peaks, the one at +0.10 V is assigned to metal centred electron transfer reactions while the one at +0.81 V may be assigned to bipyridine centred electron transfer reaction. The electrode processes may be written as

$$[Mn^{II}(slahH_2)(bpy)] + e \rightleftharpoons [Mn^{II}(slahH_2)(bpy^{-})]^{-1}$$

$$[Mn^{II}(slahH_2)(bpy^{-})]^{-1} \rightleftharpoons [Mn^{I}(slahH_2)(bpy)]^{-1}$$

The essential features of the cyclic voltammograms remain almost the same even at higher scan rates although the metal-centred redox processes shift to more negative values. It is imperative to mention that the redox processes shift towards positive potential at scan rate of 200 mV/s, while at still higher scan rate, the redox processes shift to more negative values.

Complex (8) shows a weak reductive wave at +0.18 V corresponding to which there is a weak oxidative wave at +0.28 V. Another strong reductive wave is observed at −0.78 V. However, the corresponding oxidative wave at −0.25 V is weak. The first weakly resolved redox couple is attributed to Mn^{II}/Mn^{I} couple and the redox reaction for this couple is given as

$$[Mn^{II}(npahH_2)] + e \rightleftharpoons [Mn^{I}(npahH_2)]^{-1}$$

The second redox process is attributed to ligand-centred electron transfer process.

In complex (9), at 100 mV/s, the reductive waves are clearly resolved and appear at +0.06 and −0.10 V while the corresponding oxidation waves appear merged into one another. A broad oxidative wave centred at +0.27 V contains the oxidative wave for the reduction processes $Mn^{II} \rightarrow Mn^{I}$ and $Mn^{I} \rightarrow Mn^{0}$. It appears that the oxidative peaks corresponding to these electrode processes are merged into one another. However, at lower scan rates of 5-10 mV/s, these reductive waves at +0.16 and −0.07 V appear weakly resolved with the corresponding oxidative waves at +0.27 and +0.18 V, respectively. The redox processes corresponding to first redox wave (oxid. wave: +0.27 V; red. wave: +0.16 V) and second redox wave (oxid. wave: +0.18 V; red. wave: −0.07 V) are assigned as below

$$[Mn^{II}(npahH_2)(py)_2] + e \rightleftharpoons [Mn^{I}(npahH_2)(py)_2]^{-1} \quad (I)$$

$$[Mn^{I}(npahH_2)(py)_2]^{-1} + e \rightleftharpoons [Mn^{0}(npahH_2)(py)_2]^{-2} \quad (II)$$

At a scan rate of 100 mV/s, the complexes (13) and (14) show broad waves. The broad reductive and oxidative waves are centred at +0.13 and +0.35 V, respectively in complex (13) while they are centred at 0.00 and +0.38 V, respectively in complex (14). However, when the scan rates are lowered to 5-10 mV/s, two well resolved metal-centred oxidation and reduction peaks are observed. At 5 mV/s complex (13), shows two oxidative waves at +0.27 and +0.16 V, corresponding to which the reductive waves appears at +0.02 and −0.07 V, respectively. The metal-centred redox processes involved, may be assigned as follows

$$[Mn^{II}(npahH_2)(bpy)] + e \rightleftharpoons [Mn^{I}(npahH_2)(bpy)]^{-1} \quad (I)$$

$$[Mn^{I}(npahH_2)(bpy)]^{-1} + e \rightleftharpoons [Mn^{0}(npahH_2)(bpy)]^{-2} \quad (II)$$

The redox processes are quasireversible with ΔE = 250 and 230 mV. For complex (14), at 5 mV/s the same processes occur and the oxidative waves appear at +0.30 and −0.30 V. Corresponding to these waves, the reductive waves appear at 0.00 and -0.40 V with ΔE = 300 mV and 100 mV for the first and second redox processes, respectively.

The complex (11) shows two reductive waves at −0.01 and −0.55 V in the forward scan. The first reductive process is metal centred while the second process is attributed to arise due to electron transfer reactions centred on the ligand. The reduction of the metal centre from $Mn^{II} \longrightarrow Mn^{I}$ occurs at −0.01 V. The reductive wave at −0.55 V is ligand-centred. In the reverse scan the reduced species get oxidized at +0.29 and −0.30 V, respectively.

The electrode processes are shown below

$$[Mn^{II}(npahH_2)(3\text{-}pic)_2] + e \rightleftharpoons [Mn^{I}(npahH_2)(3\text{-}pic)_2]^{-1} \quad (I)$$

$$[Mn^{I}(npahH_2)(3\text{-}pic)_2]^{-1} + e \rightleftharpoons [Mn^{I}(npahH_2)^{-}(3\text{-}pic)_2]^{-2} \quad (II)$$

Complex (12), at a scan rate of 100 mV/s shows two weakly resolved reductive waves at +0.16 V and −0.26. The corresponding oxidative peaks appear at +0.40 and 0.00 V, respectively. These are assigned to metal centred redox processes as shown below

$$[Mn^{II}(npahH_2)(4\text{-}pic)_2] + e \rightleftharpoons [Mn^{I}(npahH_2)(4\text{-}pic)_2]^{-1} \quad (I)$$

$$[Mn^{I}(npahH_2)(4\text{-}pic)_2]^{-1} + e \rightleftharpoons [Mn^{0}(npahH_2)(4\text{-}pic)_2]^{-2} \quad (II)$$

At lower scan rates of 10 and 50 mV/s in this complex, single broad oxidative and reductive waves are observed. These waves are centred at +0.20 V (reductive wave) and +0.25 V (oxidative wave) at 10 mV/s and at +0.30 V (reductive wave) and +0.40 V (oxidative wave) at 50 mV/s. At a higher scan rate of 200 mV/s in this complex, one weak reductive wave is observed at +0.05 V, corresponding to which a weak oxidative wave at +0.40 V is observed. Another strong reductive wave is observed at -0.95 V, corresponding to which is a strong oxidative wave at 0.00 V. The second

redox process is irreversible and is ligand centred.

The complex (10) shows an almost featureless CV.

Conclusion

Mn^{II} complexes derived from dihydrazone ligands have been synthesized, characterized and described in this chapter. On the basis of various physico-chemical and spectral studies, it has been concluded that the ligands disalicylaldehyde adipoyldihydrazone ($slahH_4$) and bis(2-hydroxy-1-naphthaldehyde)adipoyldihydrazone ($npahH_4$) coordinate as a dibasic tetradentate ligand through azomethine nitrogen and phenolate/naphtholate oxygen to the metal centre in all of the complexes. The various donor sites bond to the same Mn centre leading to a monomer structure of the complexes. The ligand disalicylaldehyde adipoyldihydrazone ($slahH_4$) coordinates to the metal centre in enol form in the complexes (1) to (5) and in the keto form in the remaining complexes (6) and (7). On the otherhand, the ligand bis(2-hydroxy-1-naphthaldehyde)adipoyldihydrazone coordinates to the metal centre in the *anti-cis* configuration in all of the complexes. This configuration arises due to coordination of both the azomethine nitrogen atoms and phenolate/naphtholate oxygen atoms of the same dihydrazone molecule to the same metal centre. This introduces steric crowding in the molecule. As a result one dihydrazone arm remains in the equatorial plane while the other hydrazone arm attains axial position. In this configuration, axial azomethine protons absorb at lower frequency as compared to equatorial azomethine protons which absorb at higher frequency in the IR spectra. It is suggested that the disalicylaldehyde adipoyldihydrazone also coordinates to the metal centre in *anti-cis* configuration. It appears that in the complexes (1) to (7) derived from $slahH_4$, ν>C=N bands merge into one another giving a single band only. The νC=N band occurs either as a shoulder to the first band or the energy difference between two >C=N group is so

less that they appear very close to each other leading between two their merger into one another. At the same time, this also suggests that there is less steric crowding in metal complexes derived from disalicylaldehyde adipoyldihydrazone as compared to those derived from bis(2-hydroxy-1-naphthaldehyde)adipoyldihydrazone containing bulky naphthyl groups. The donor atoms of the dihydrazones are suggested to be arranged in the equatorial plane around the metal centre while its axial positions are occupied by co-ligands i.e. H_2O/pyridine/2-picoline/3-picoline/4-picoline in the complexes (1) to (5) and (8) to (12). The nitrogen atoms of the bidentate bases (2, 2'-bipyridine and 1, 10-phenanthroline) occupy the *cis* positions in the complexes (6), (7), (13) and (14). The two equatorial positions around the metal centre are occupied by distorted azomethine nitrogen atoms while the axial positions are occupied in the complexes (6), (7) (13) and (14) by azomethine nitrogen atoms while the axial positions are occupied by phenolate/naphtholate oxygen atoms. All the monometallic manganese (II) complexes are proposed to have high-spin distorted octahedral stereochemistry except the complex (8) which is suggested to have low-spin square planar stereochemistry [111] involving significantly metal-metal interaction.

The electron transfer reactions of the complexes have been investigated with the help of cyclic voltammetry.

On the basis of results obtained from various physico-chemical and spectral studies, the structures of the complexes have been proposed as shown in **Figs. 3.6.1-3.6.5**.

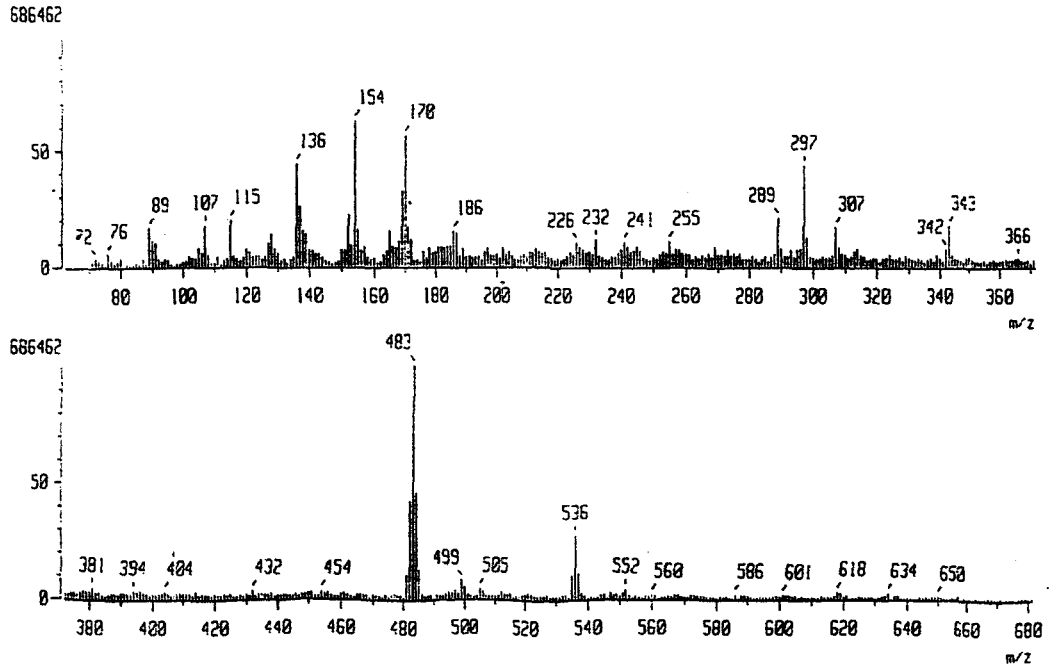

Fig. 3.1.1 Mass spectrum of complex $[Mn^{II}(npahH_2)]$ **(8)**

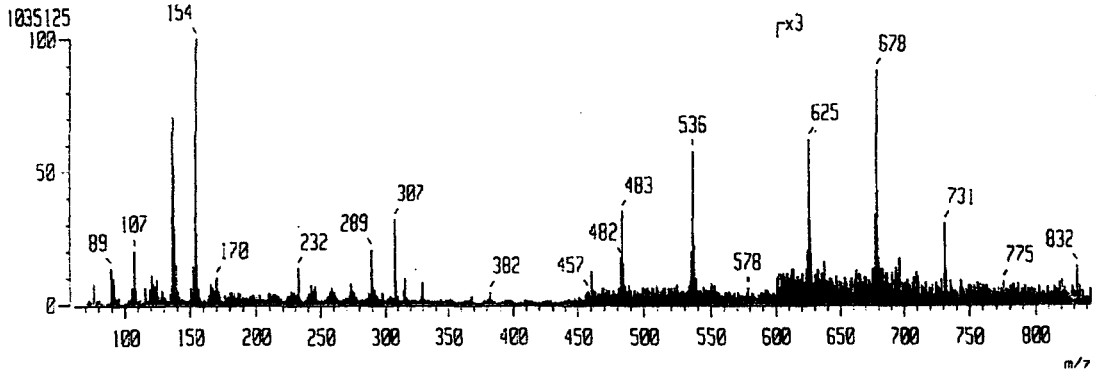

Fig. 3.1.2 Mass spectrum of complex $[Mn^{II}(npahH_2)(2\text{-pic})_2]$ **(10)**

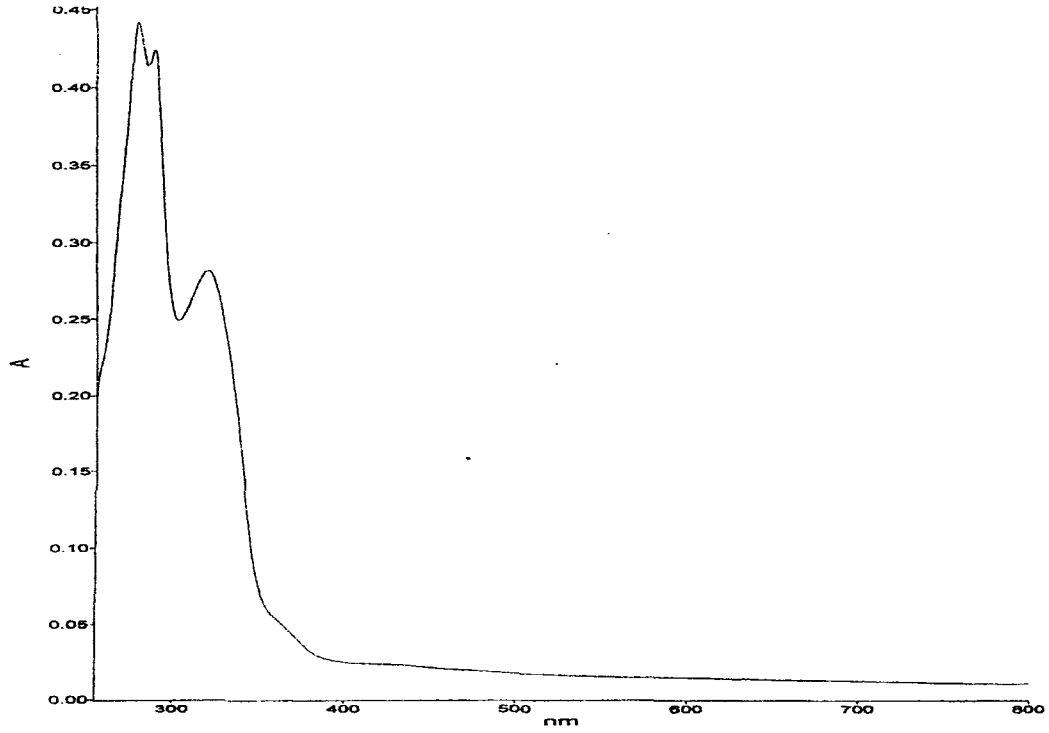

Fig. 3.2.1 Electronic spectrum of Ligand Disalicylaldehyde adipoyldihydrazone ($slahH_4$)

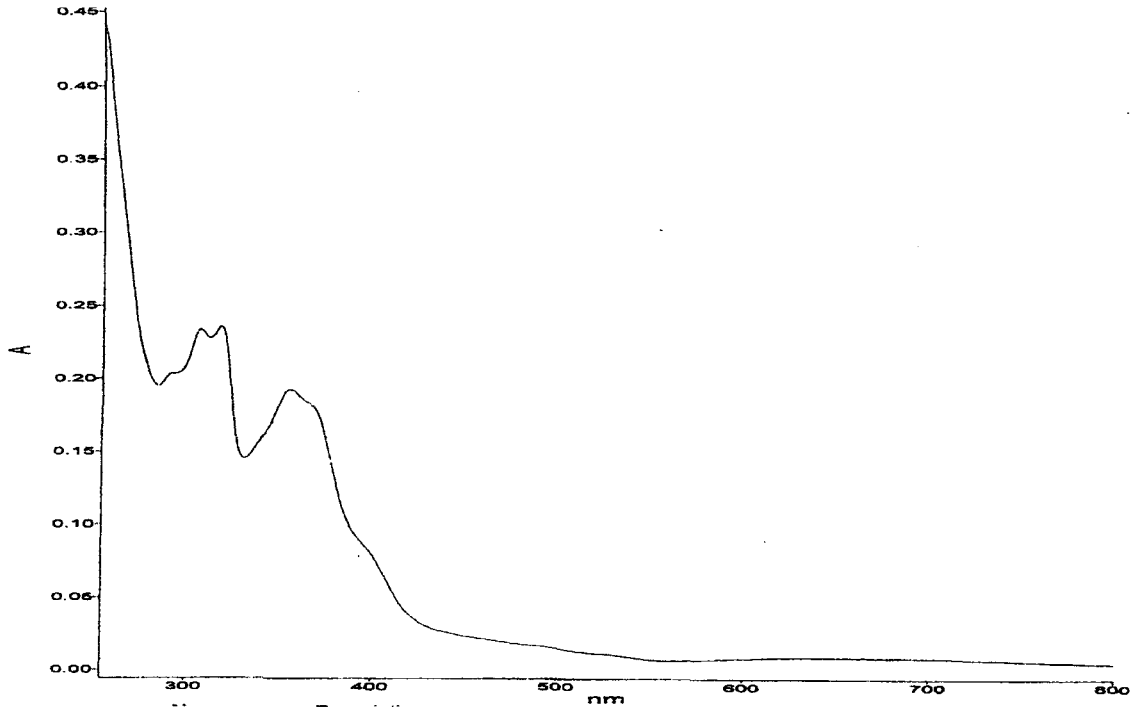

Fig. 3.2.2 Electronic spectrum of Ligand Bis(2-hydroxy-1-naphthaldehyde)adipoyldihydrazone (*npah*H_4)

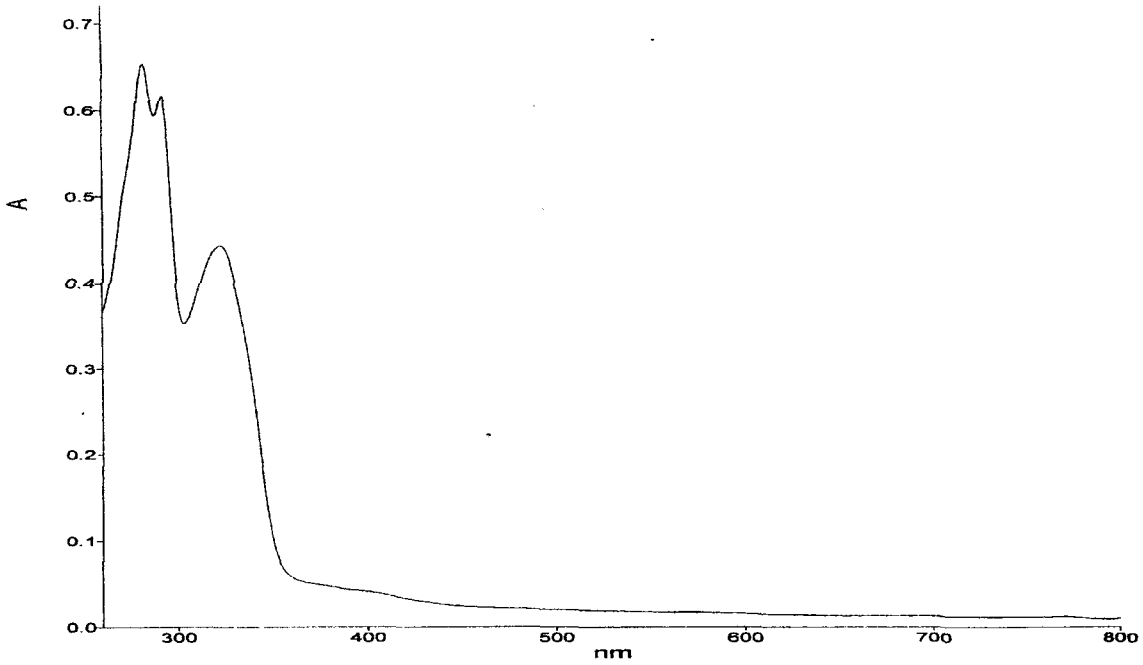

Fig. 3.2.3 Electronic spectrum of complex $[Mn^{II}(slahH_2)(3\text{-}pic)_2].H_2O$ **(4)**

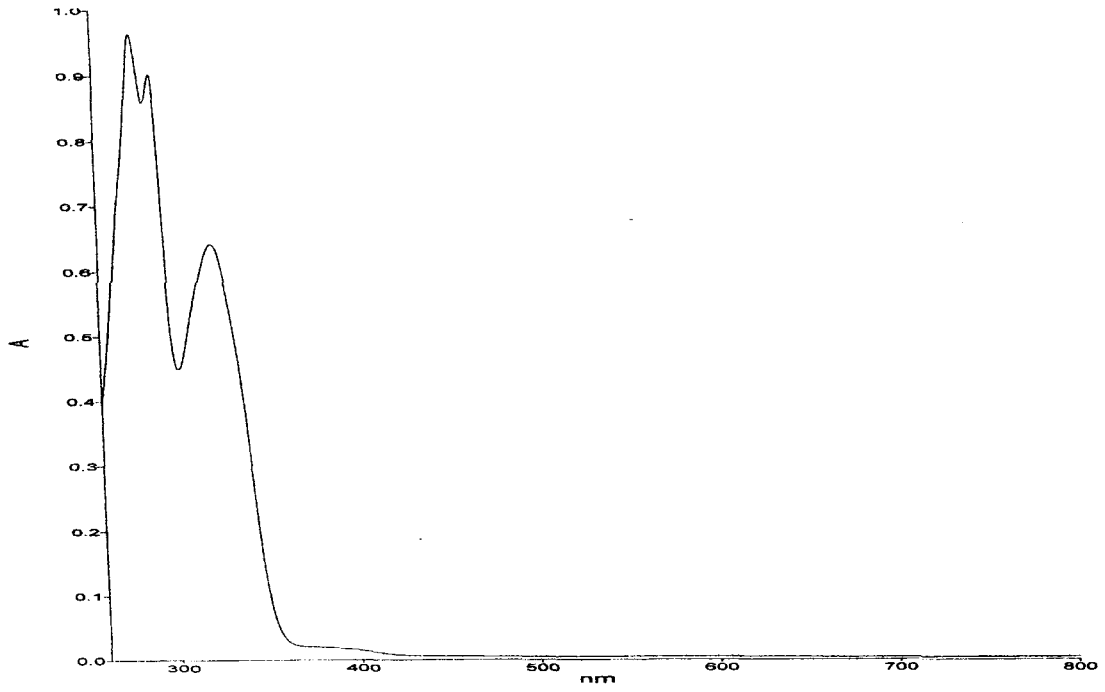

Fig. 3.2.4 Electronic spectrum of complex $[Mn^{II}(slahH_2)(bpy)]$ **(6)**

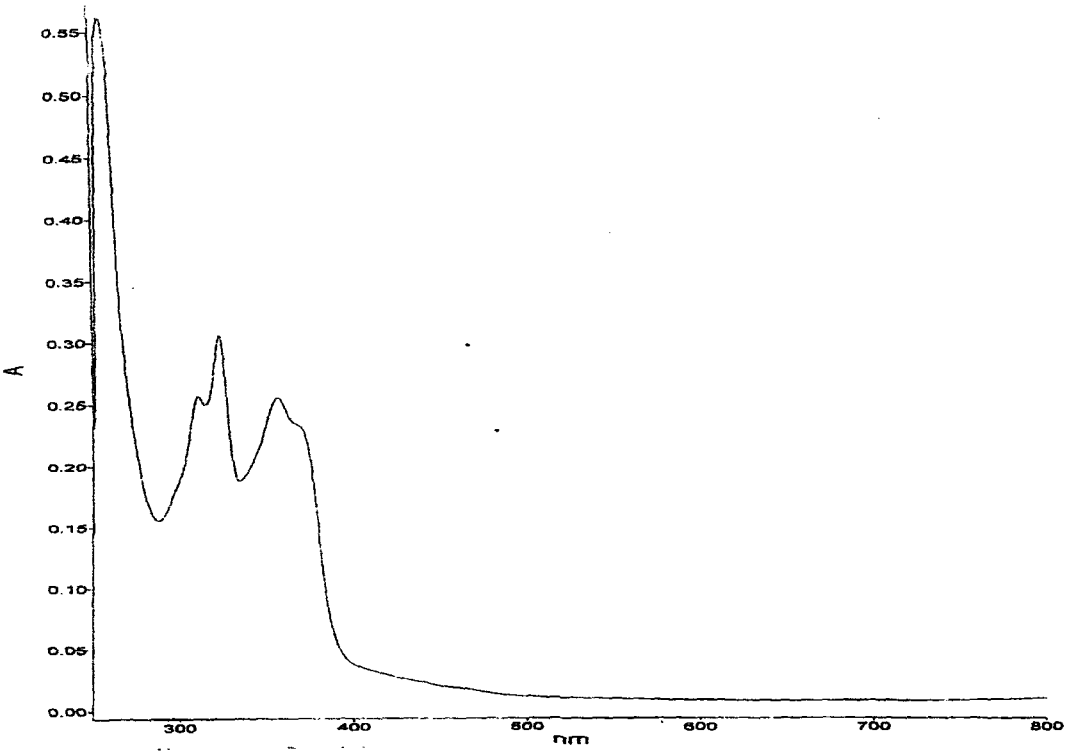

Fig. 3.2.5 (a) Electronic spectrum of complex $[Mn^{II}(npahH_2)]$ **(8)**

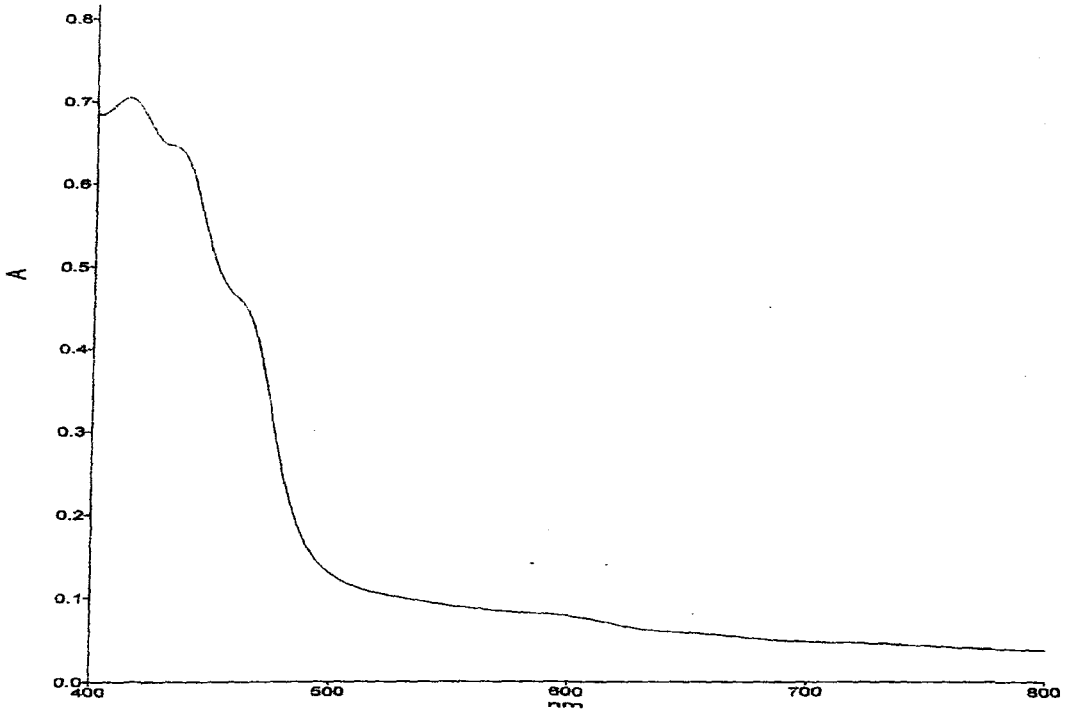

Fig. 3.2.5 (b) Electronic spectrum of complex $[Mn^{II}(npahH_2)]$ **(8)**

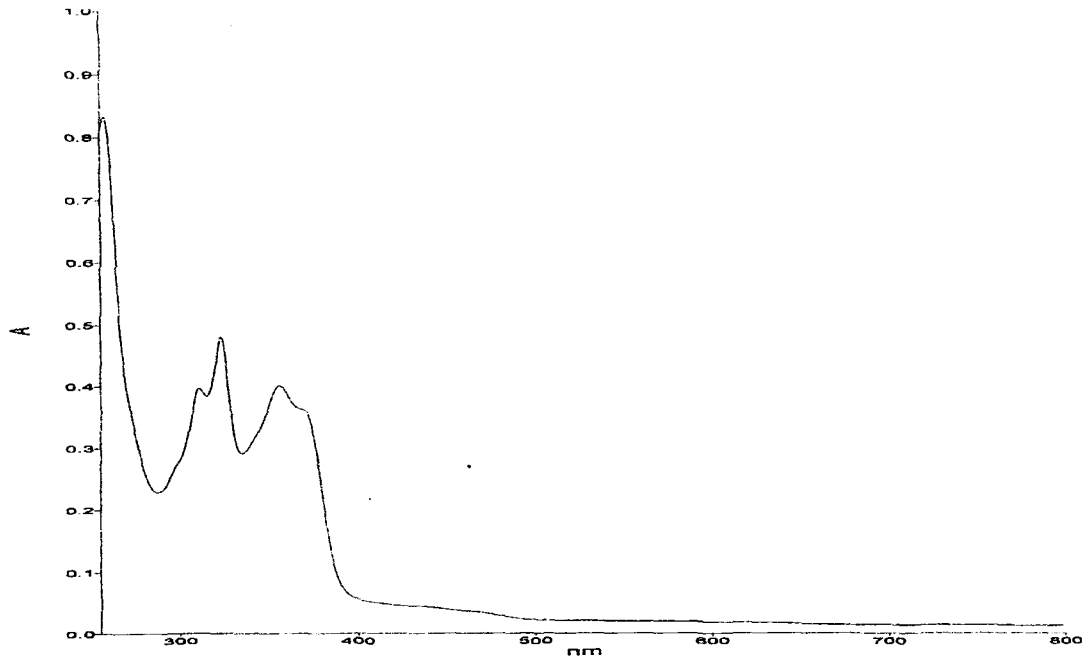

Fig. 3.2.6 Electronic spectrum of complex $[Mn^{II}(npahH_2)(2\text{-pic})_2]$ **(10)**

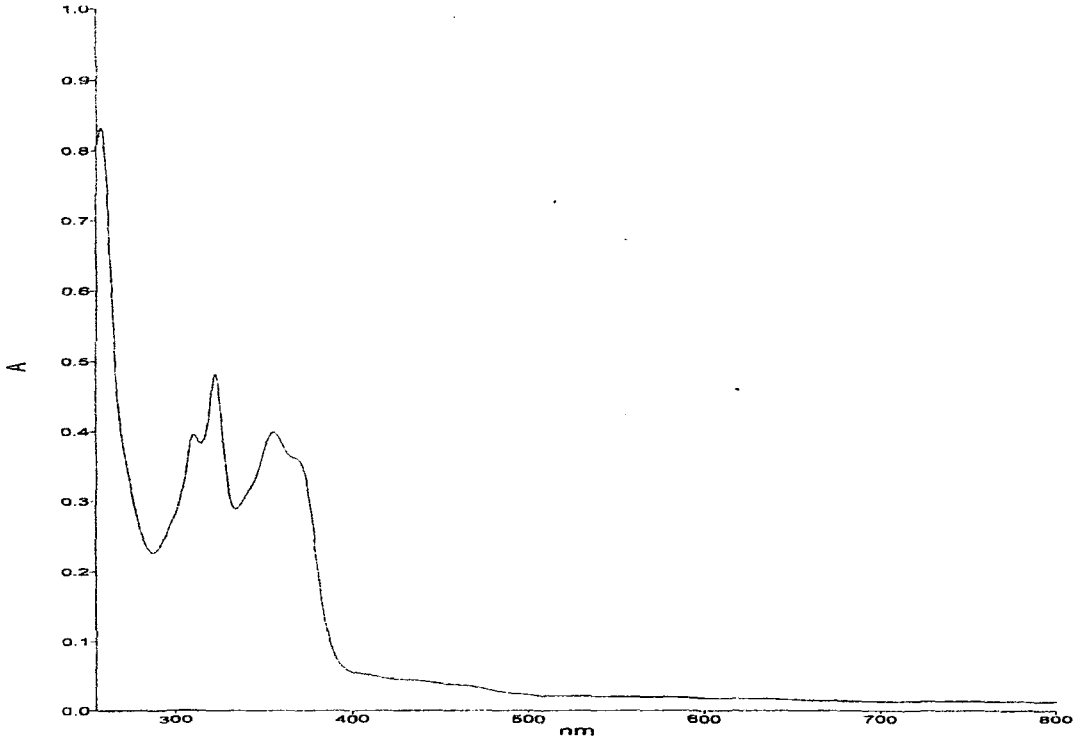

Fig. 3.2.7 Electronic spectrum of complex $[Mn^{II}(npahH_2)(4\text{-pic})_2]$ **(12)**

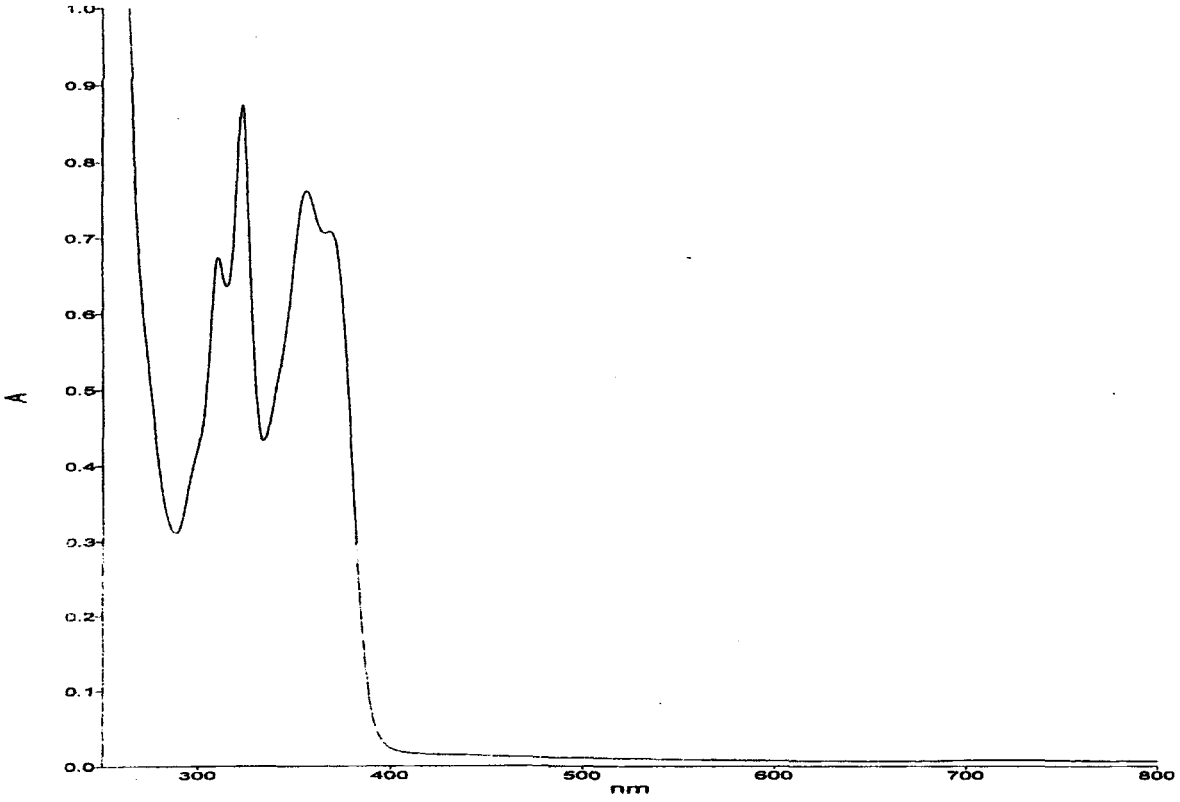

Fig. 3.2.8 (a) Electronic spectrum of complex $[Mn^{II}(npahH_2)(phen)]$ **(14)**

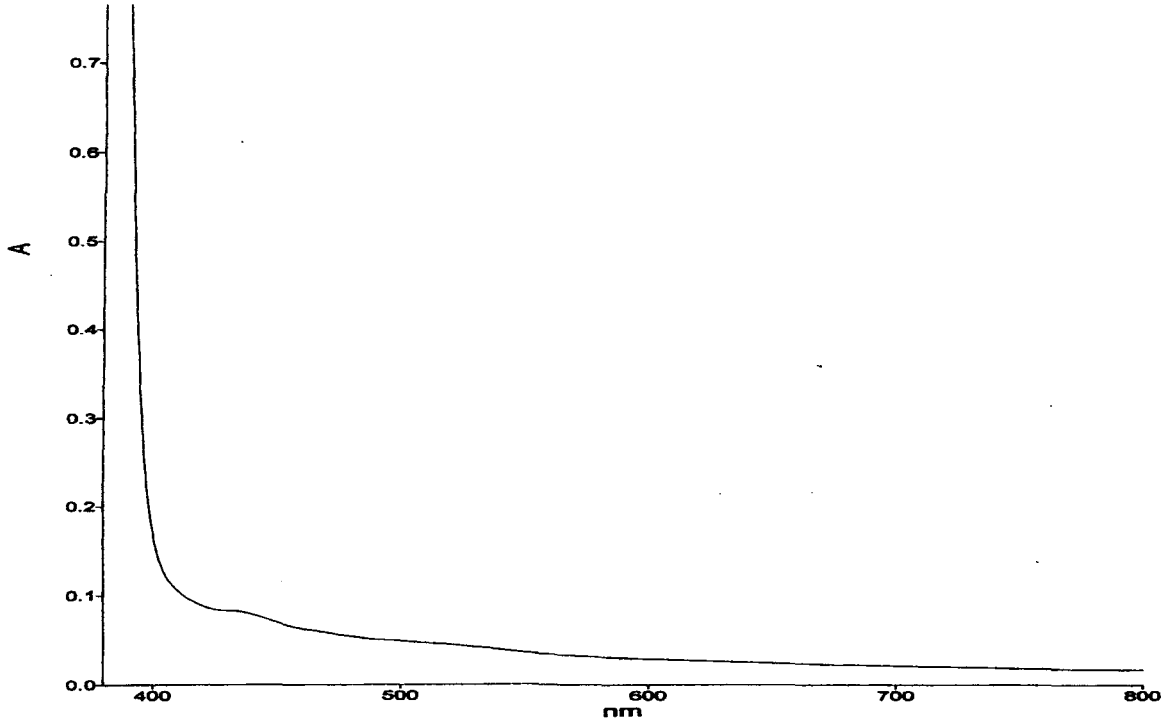

Fig. 3.2.8 (b) Electronic spectrum of complex $[Mn^{II}(npahH_2)(phen)]$ **(14)**

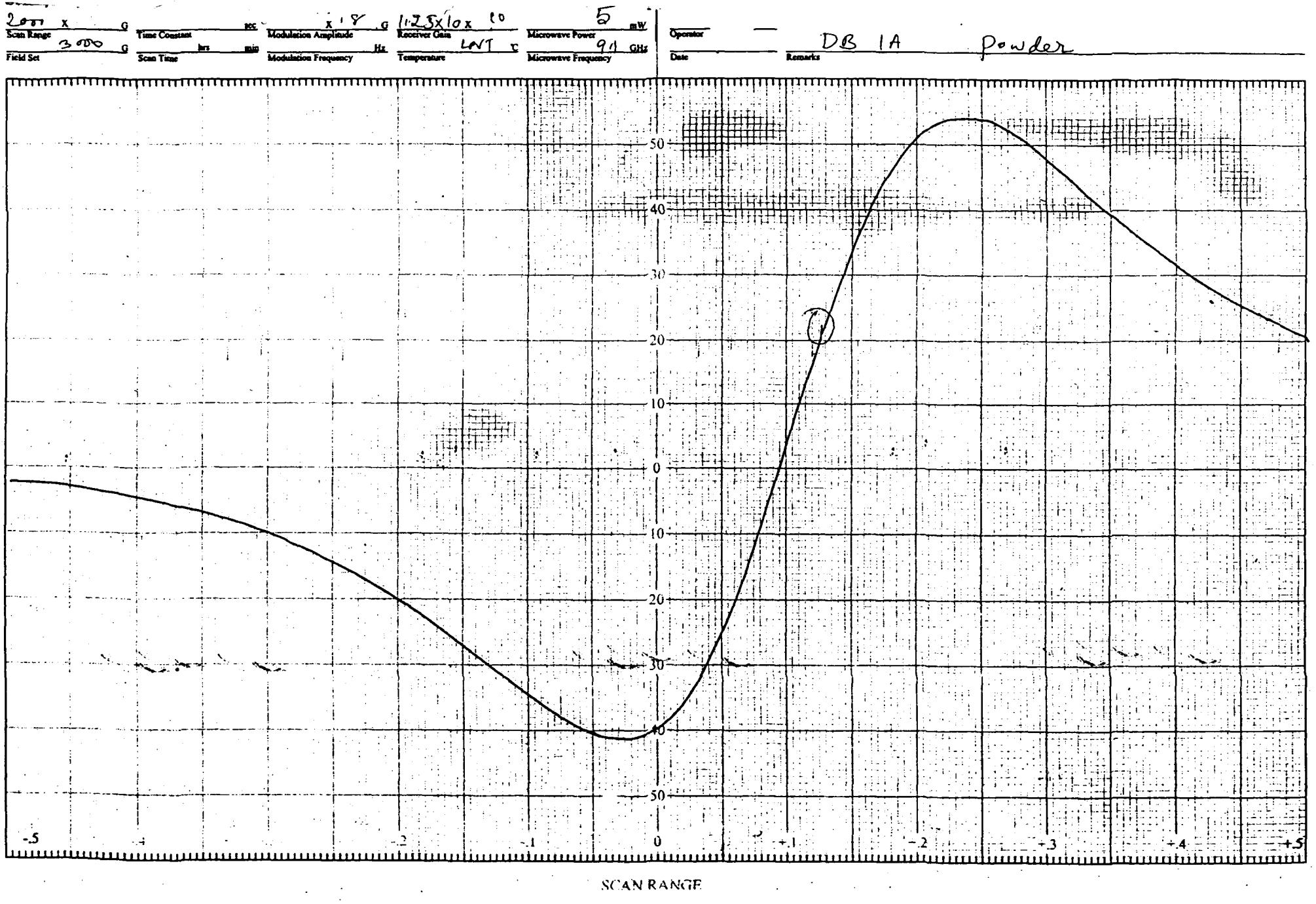

Fig. 3.3.1 EPR powder spectrum of complex $[Mn^{II}(slahH_2)(H_2O)_2]$ **(1)** at Temperature: LNT, Frequency: 9.1 GHz, Scan range: 2000 G and Field Set: 3000 G

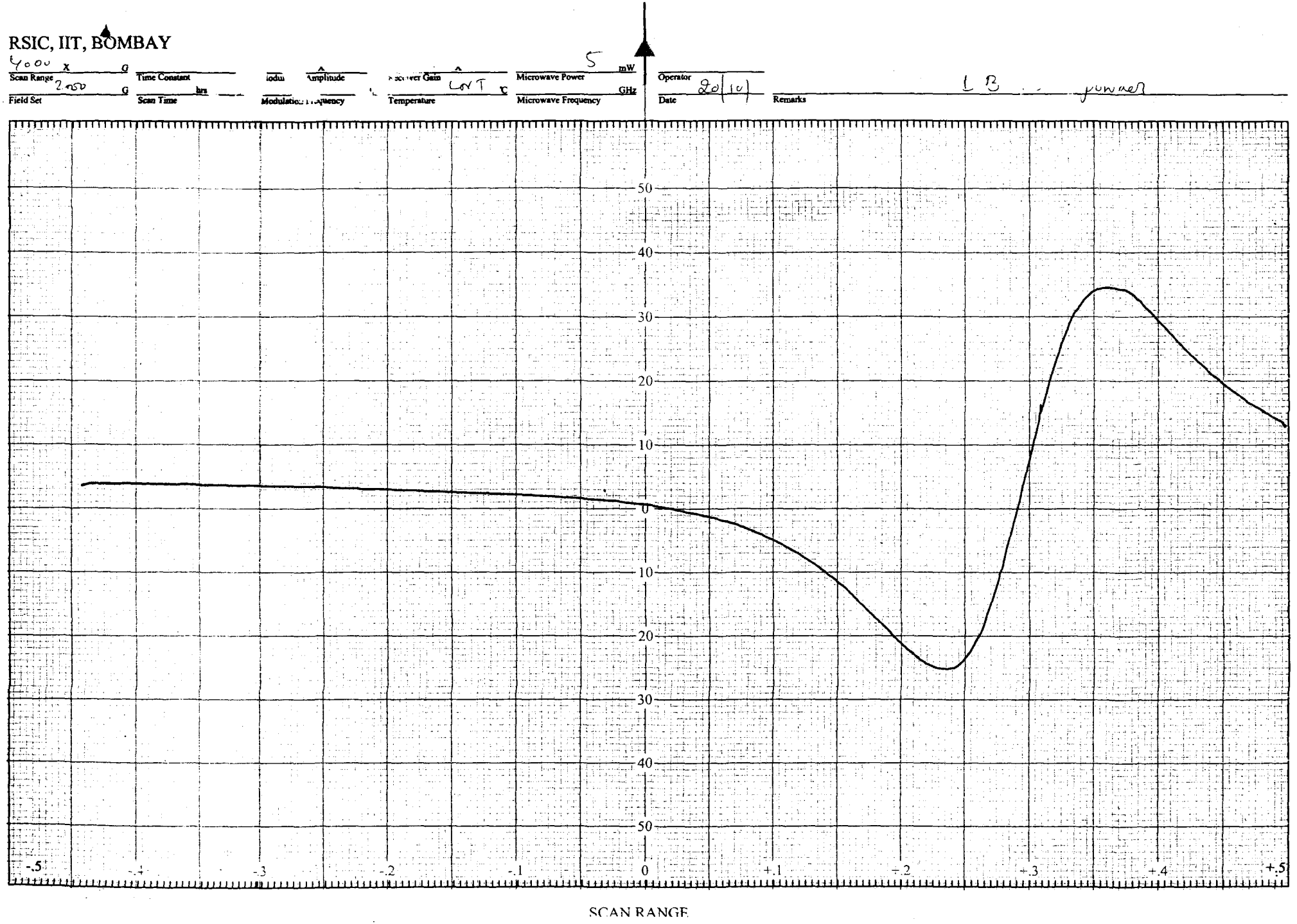

Fig. 3.3.2 (a) EPR powder spectrum of complex $[Mn^{II}(slahH_2)(py)_2].H_2O$ **(2)** at Temperature: LNT, Frequency: 9.1 GHz, Scan range: 4000 G and Field Set: 2000 G

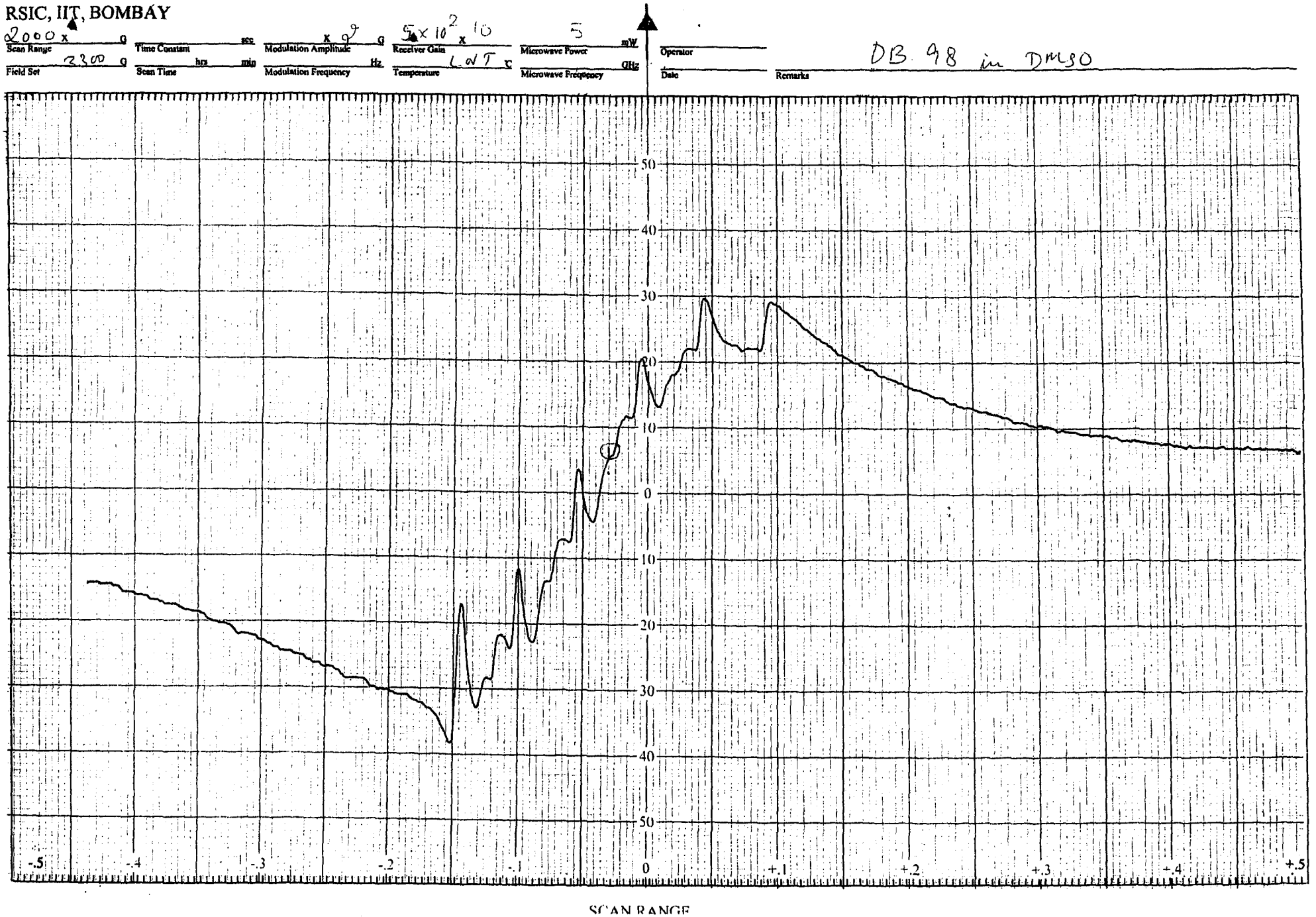

Fig. 3.3.2 (b) EPR spectrum of complex $[Mn^{II}(slahH_2)(py)_2].H_2O$ **(2)** in DMSO at Temperature: LNT, Frequency: 9.1 GHz, Scan range: 2000 G and Field Set: 3300 G

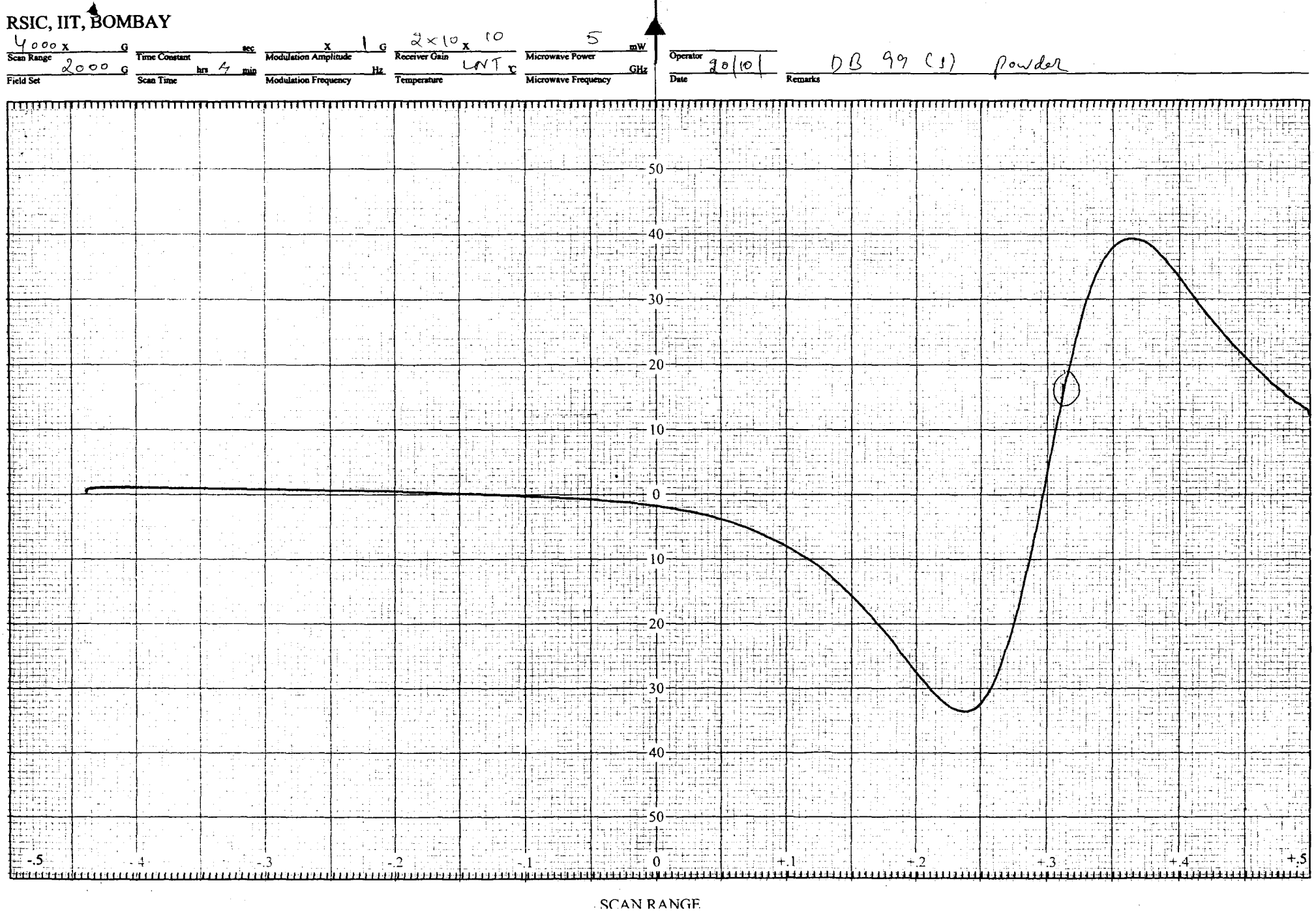

Fig. 3.3.3 (a) EPR powder spectrum of complex $[Mn^{II}(slahH_2)(2\text{-pic})_2].H_2O$ **(3)** at Temperature: LNT, Frequency: 9.1 GHz, Scan range: 4000 G and Field Set: 2000 G

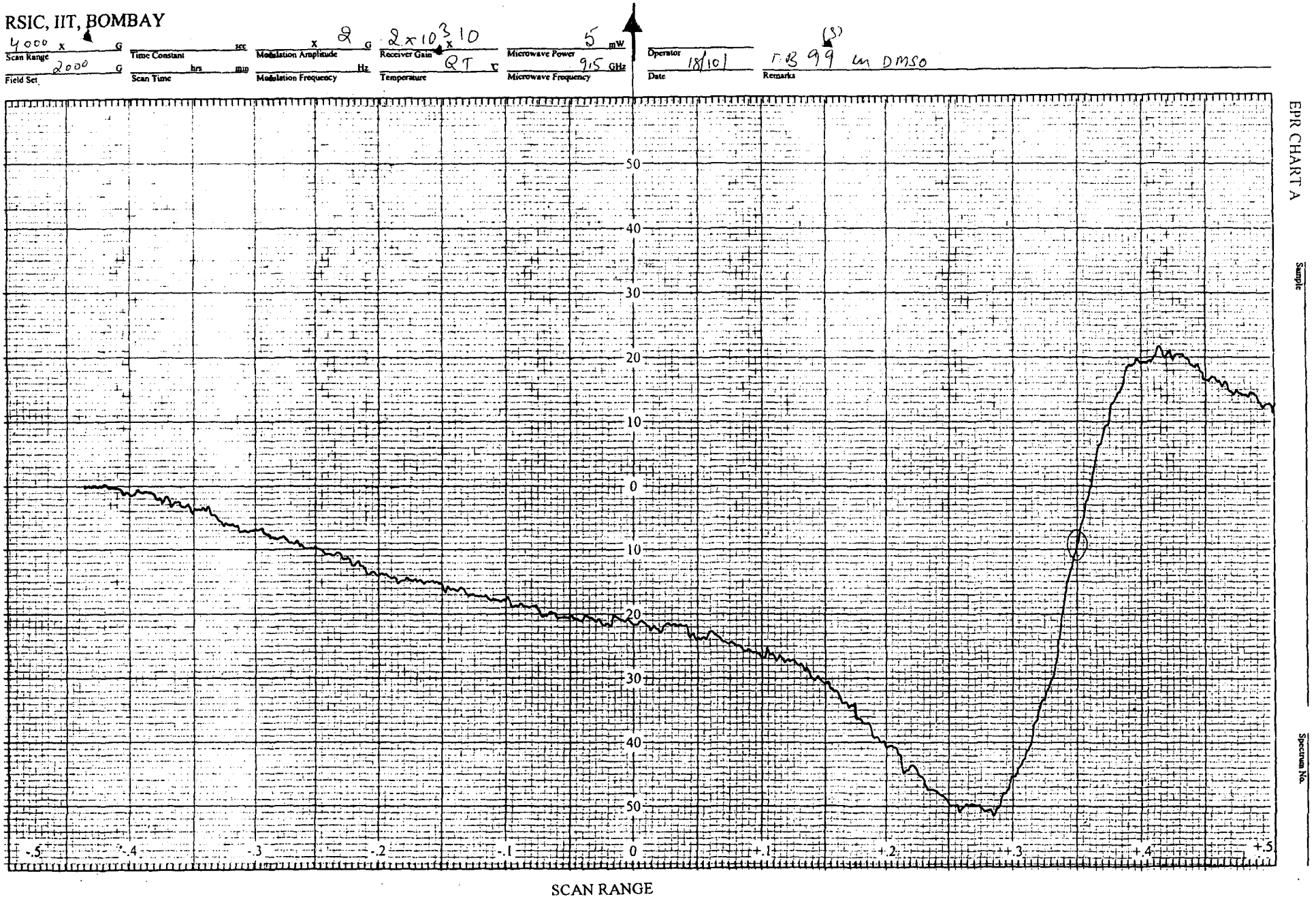

Fig. 3.3.3 (b) EPR spectrum of complex $[Mn^{II}(slahH_2)(2\text{-pic})_2].H_2O$ **(3)** in DMSO solution at Temperature: RT, Frequency: 9.1 GHz, Scan range: 4000 G and Field Set: 2000 G

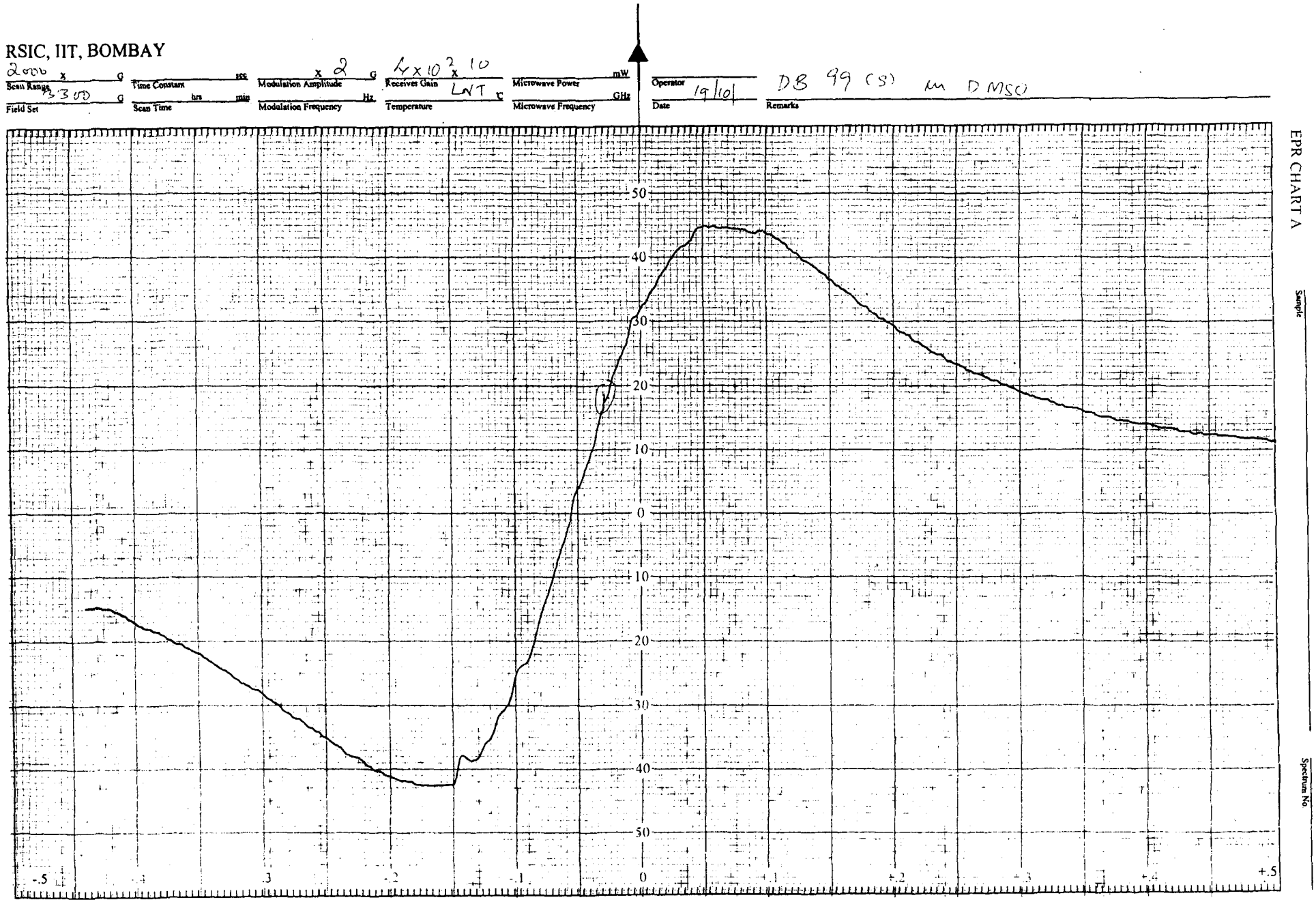

Fig. 3.3.3 (c) EPR spectrum of complex $[Mn^{II}(slahH_2)(2\text{-pic})_2].H_2O$ **(3)** in DMSO solution at Temperature: LNT, Frequency: 9.1 GHz, Scan range: 2000 G and Field Set: 3300 G

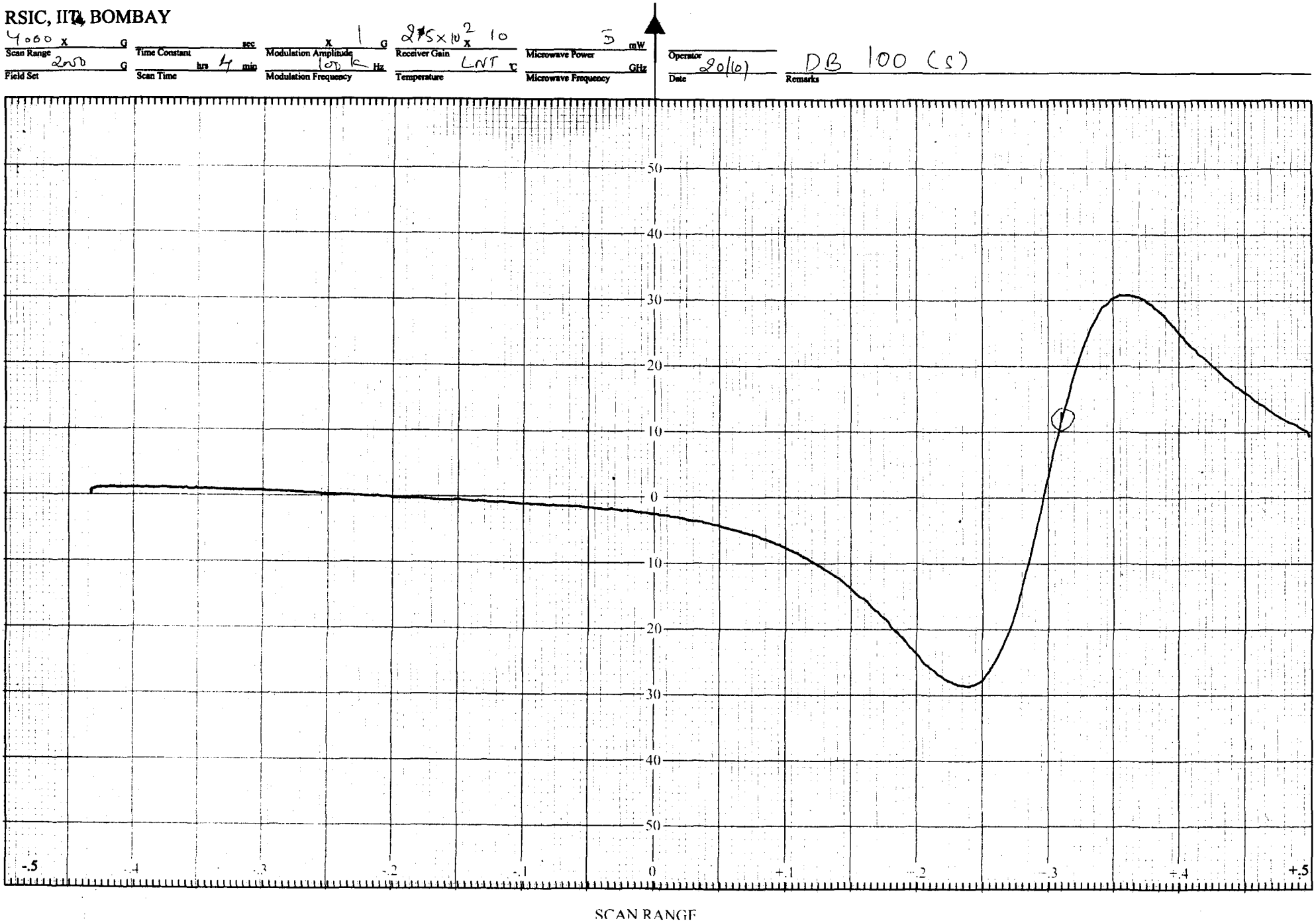

Fig. 3.3.4 (a) EPR powder spectrum of complex $[Mn^{II}(slahH_2)(3\text{-pic})_2].H_2O$ **(4)** at Temperature: LNT, Frequency: 9.1 GHz, Scan range: 4000 G and Field Set: 2000 G

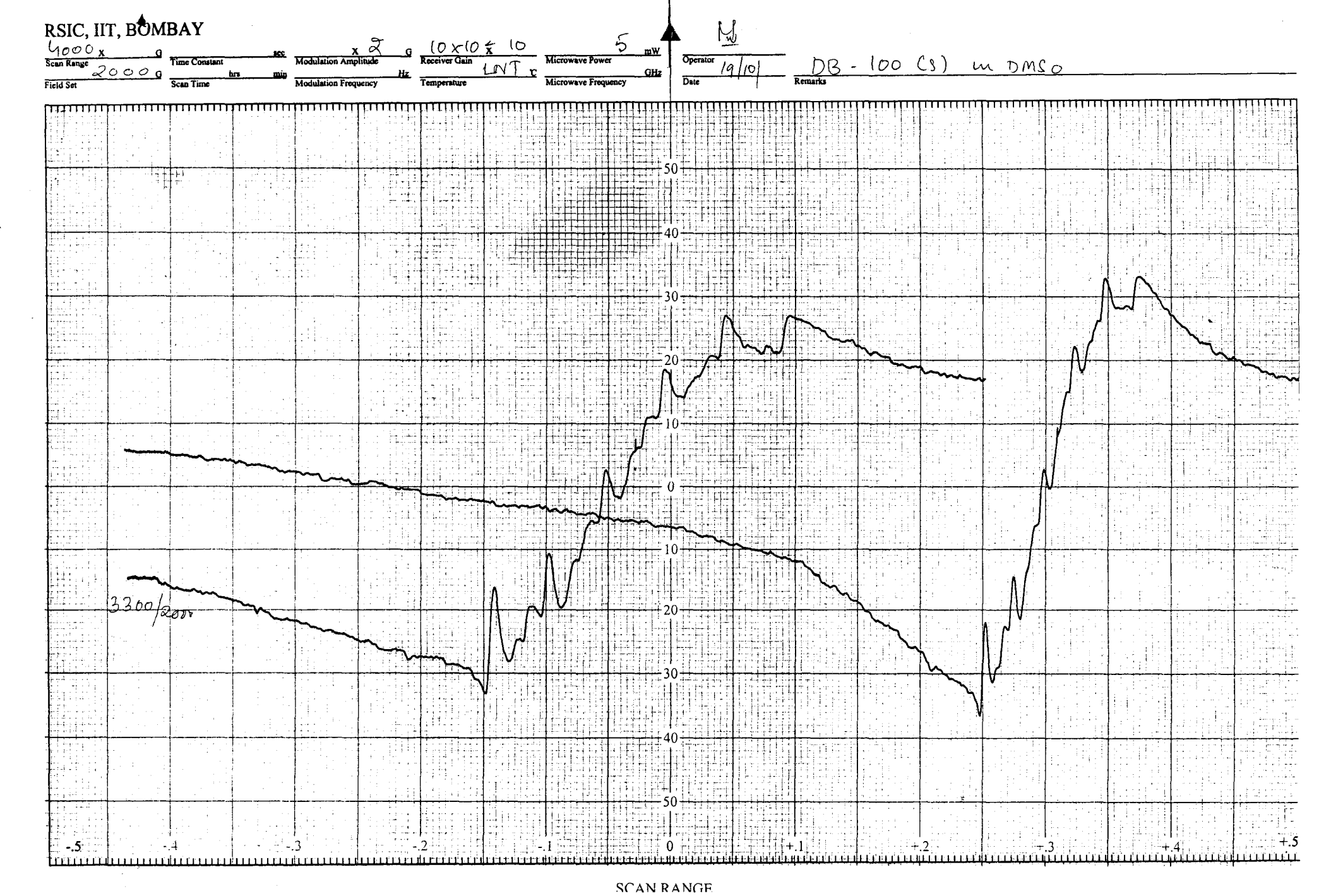

Fig. 3.3.4 (b). EPR spectrum of complex $[Mn^{II}(slahH_2)(3\text{-pic})_2].H_2O$ **(4)** in DMSO at Temperature: LNT, Frequency: 9.1 GHz, Scan range: 4000 G and Field Set: 2000 G

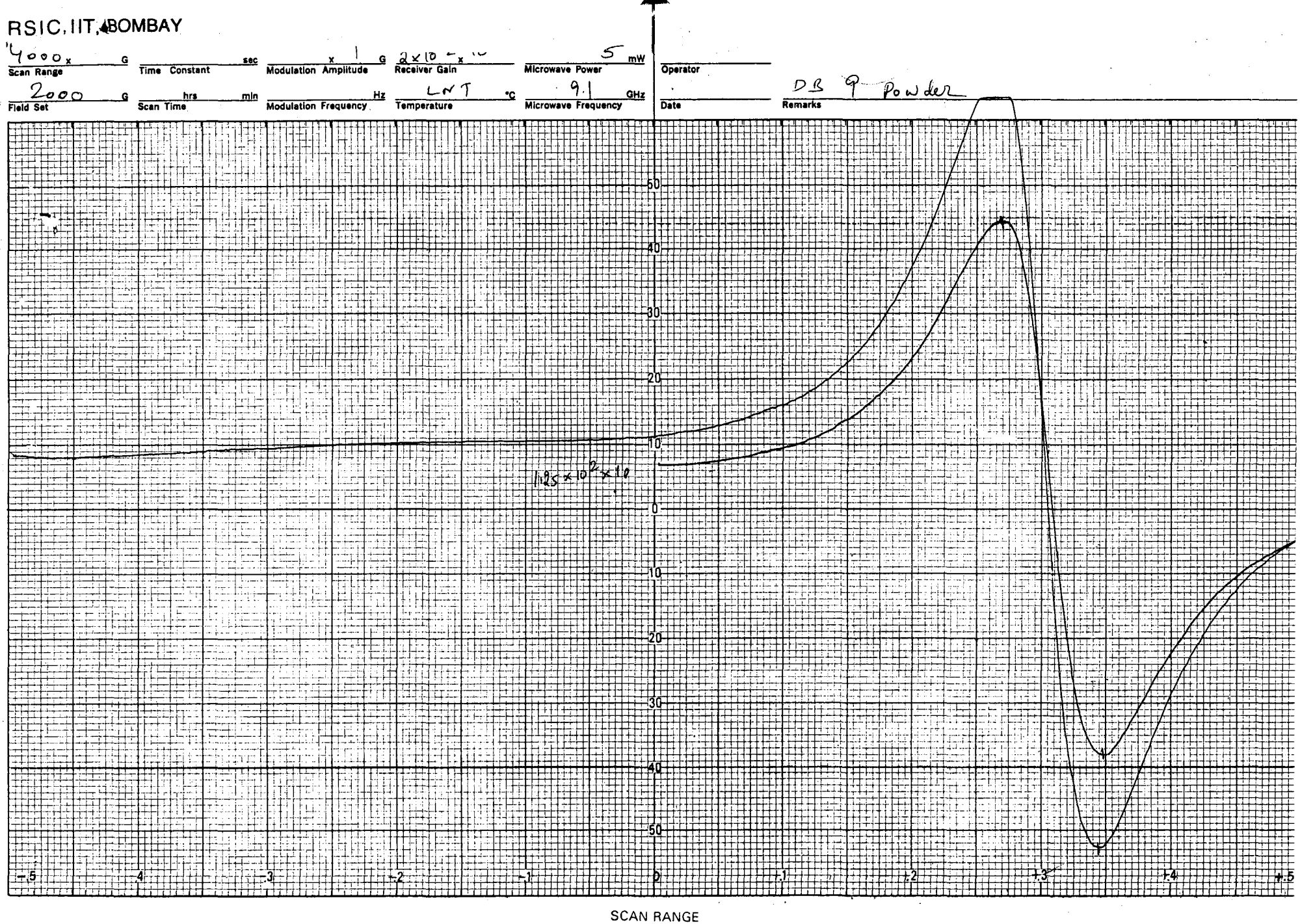

Fig. 3.3.5 (a) EPR powder spectrum of complex $[Mn^{II}(npahH_2)]$ **(8)** at Temperature: LNT, Frequency: 9.1 GHz, Scan range: 4000 G and Field Set: 2000 G

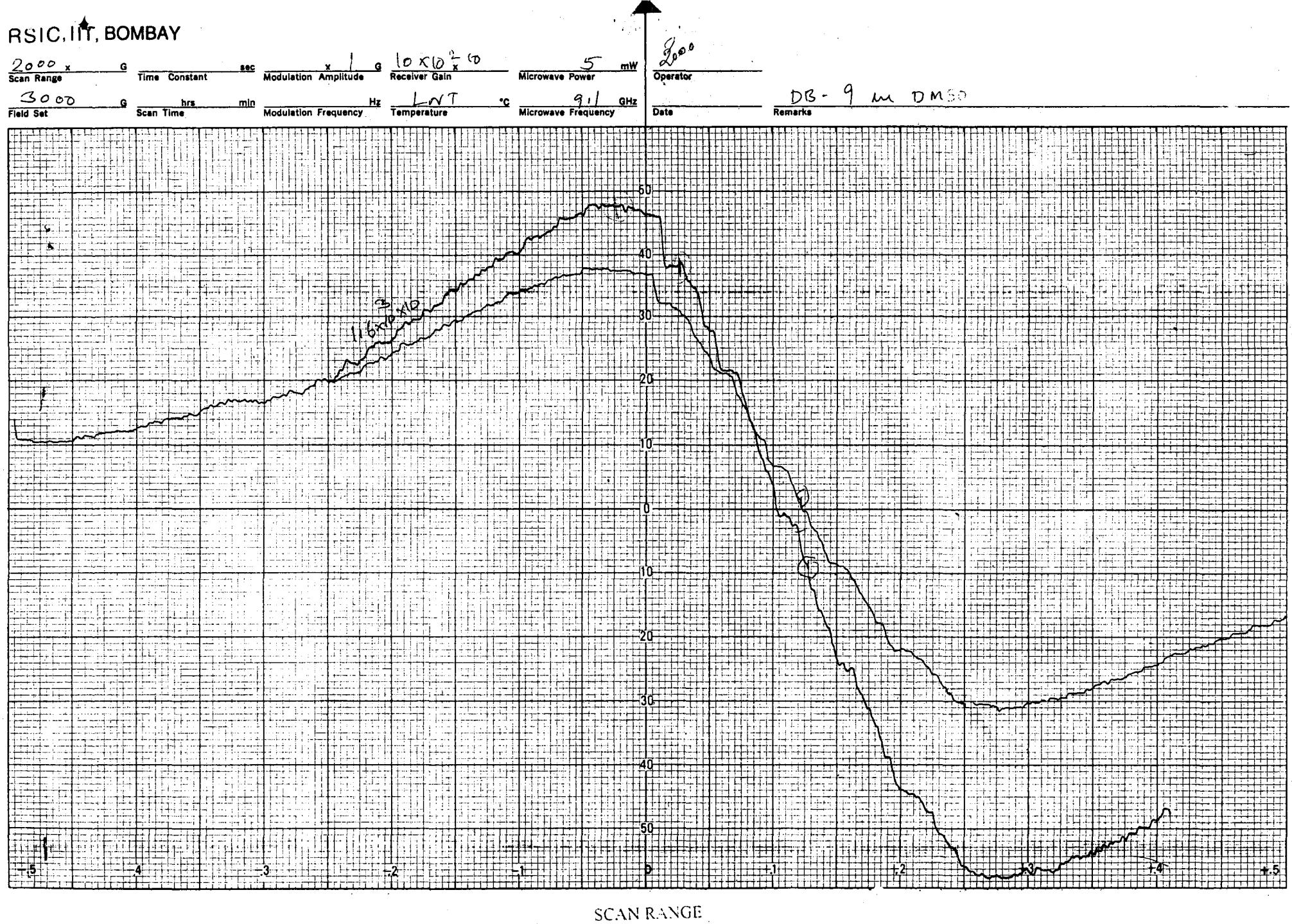

Fig. 3.3.5 (b) EPR spectrum of complex $[Mn^{II}(npahH_2)]$ **(8)** in DMSO at Temperature: LNT, Frequency: 9.1 GHz, Scan range: 2000 G and Field Set: 3000 G

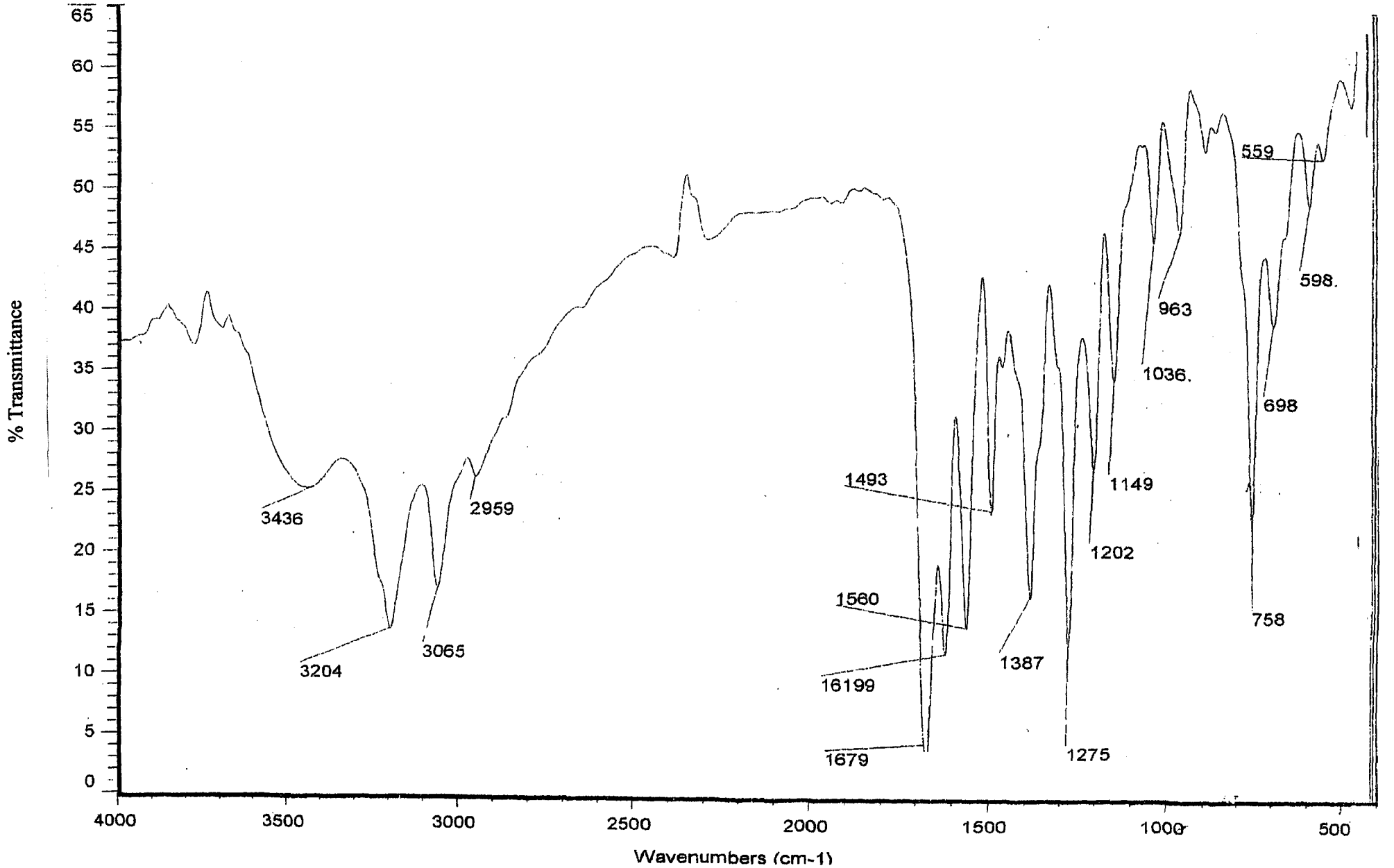

Fig. 3.4.1 (a) IR spectrum of Ligand Disalicylaldehyde adipoyldihydrazone ($slahH_4$) in KBr

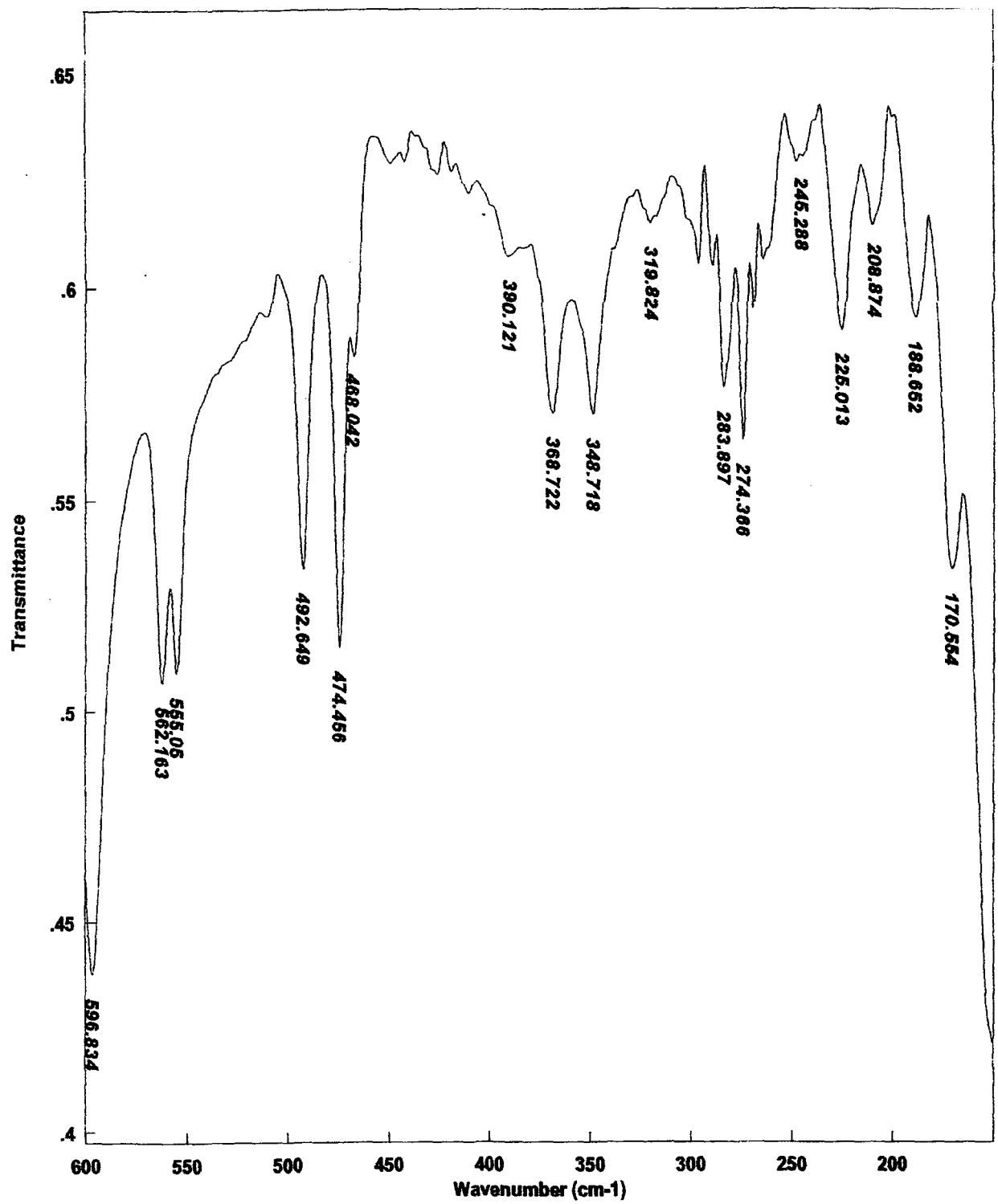

Fig. 3.4.1 (b) IR spectrum of Ligand Disalicylaldehyde adipoyldihydrazone ($slahH_4$) in CsI

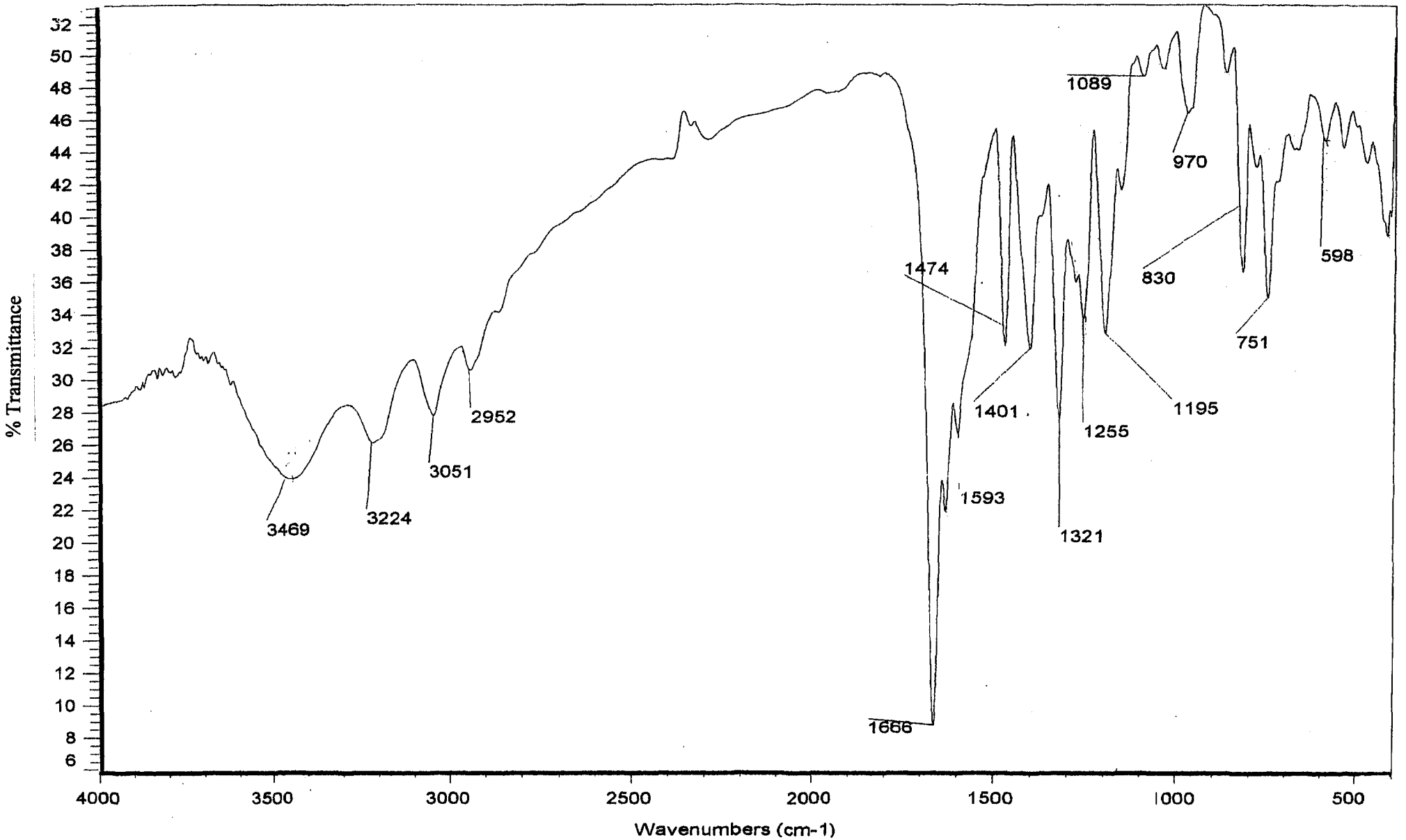

Fig. 3.4.2 (a) IR spectrum of Ligand Bis(2-hydroxy-1-naphthaldehyde)adipoyldihydrazone ($npahH_4$) in KBr

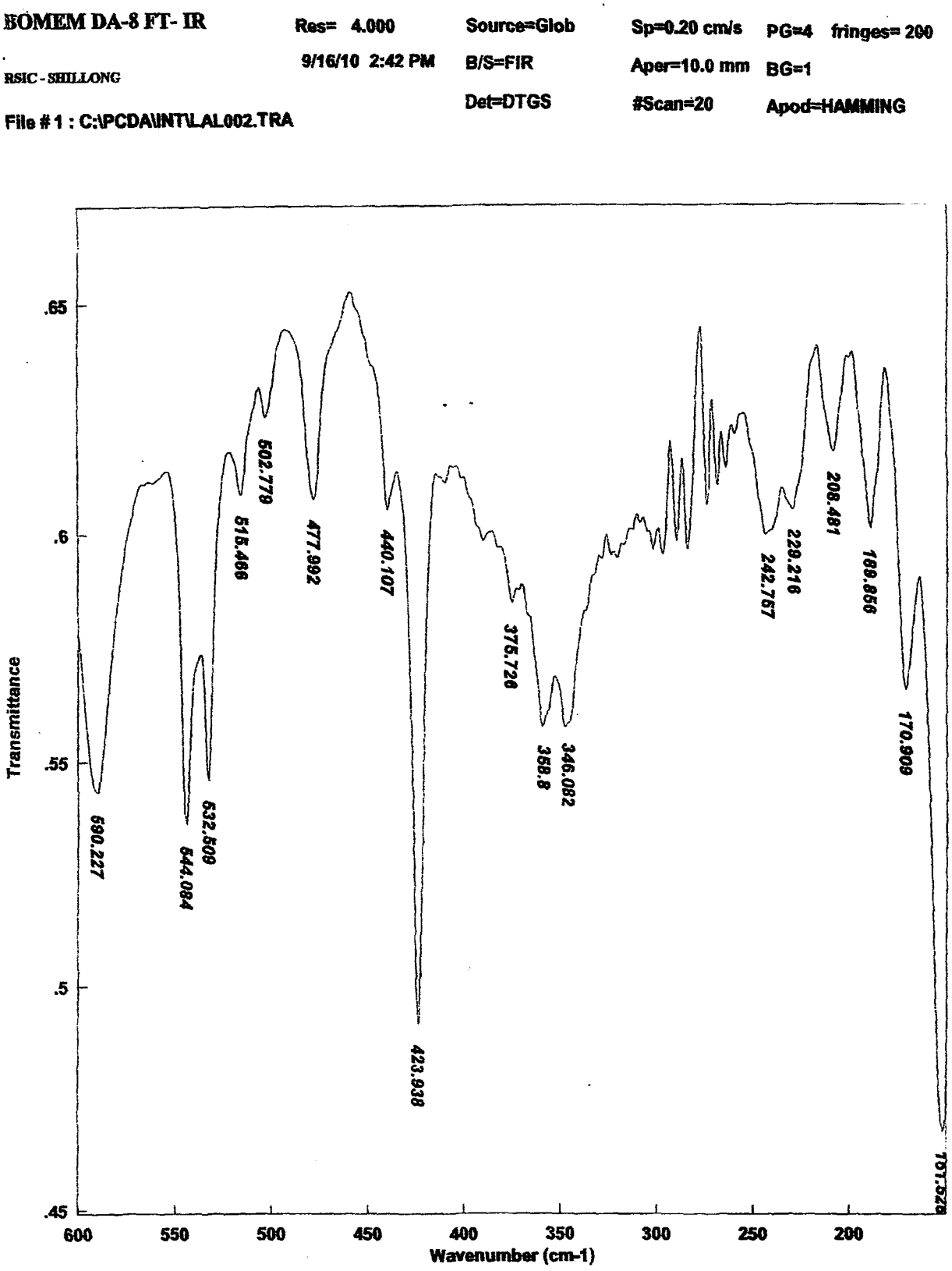

Fig. 3.4.2 (b) IR spectrum of Ligand Bis(2-hydroxy-1-naphthaldehyde)adipoyldihydrazone ($npahH_4$) in CsI

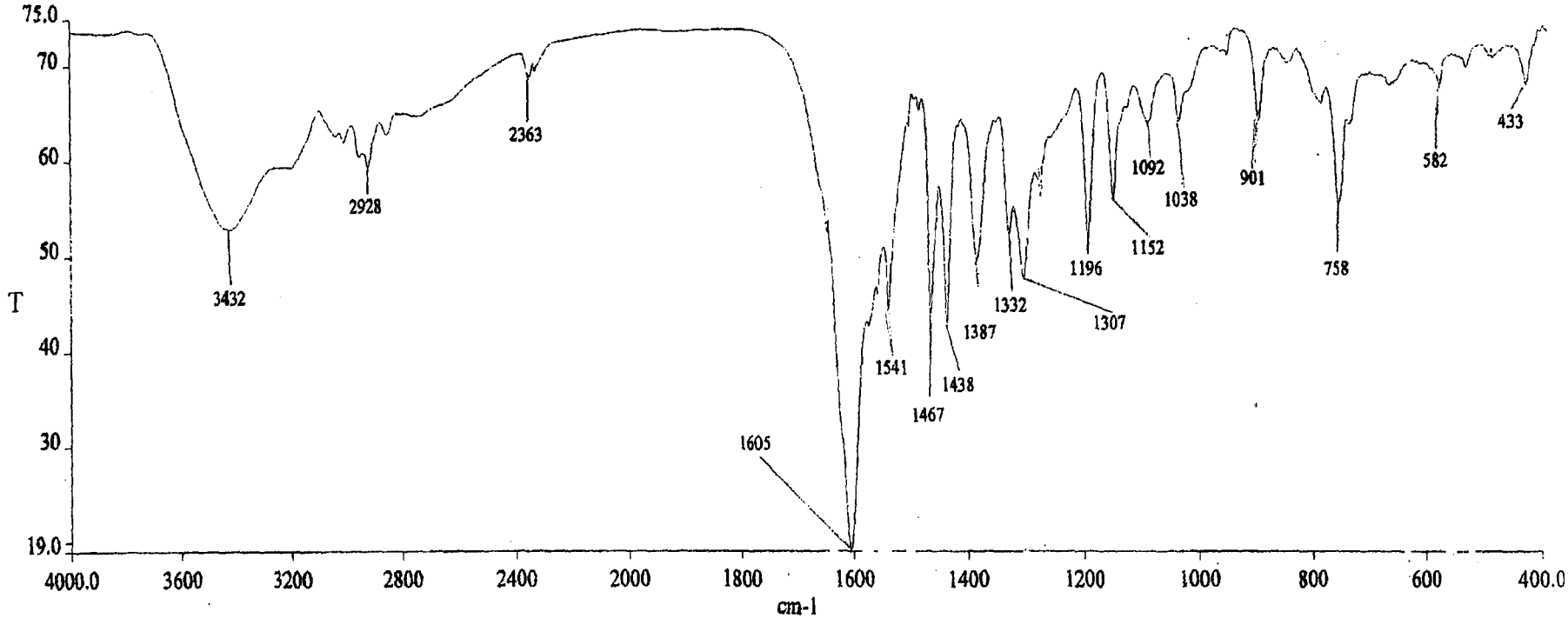

Fig. 3.4.3 IR spectrum of complex $[Mn^{II}(slahH_2)(H_2O)_2]$ **(1)** in KBr

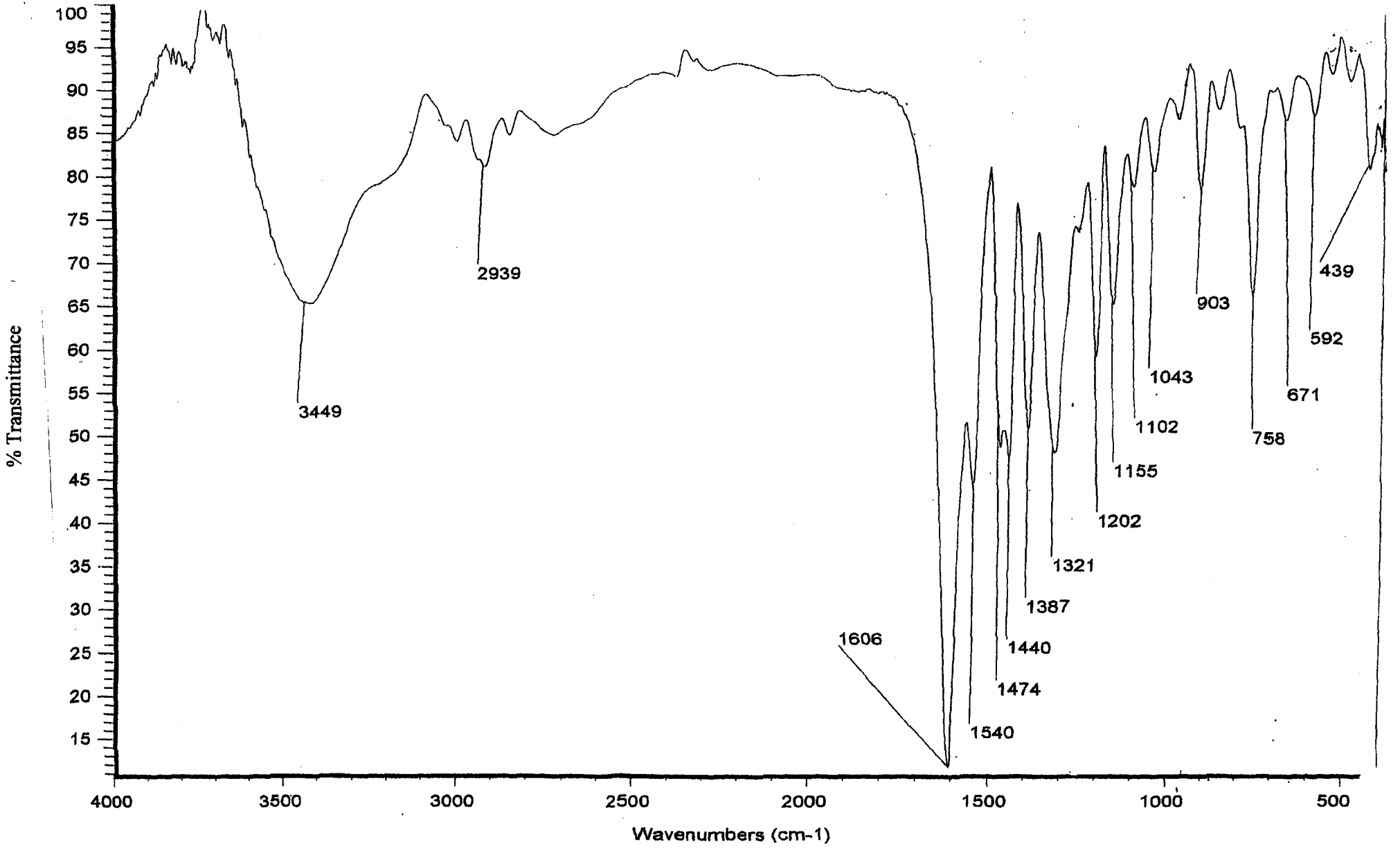

Fig. 3.4.4 IR spectrum of complex $[Mn^{II}(slahH_2)(py)_2].H_2O$ **(2)** in KBr

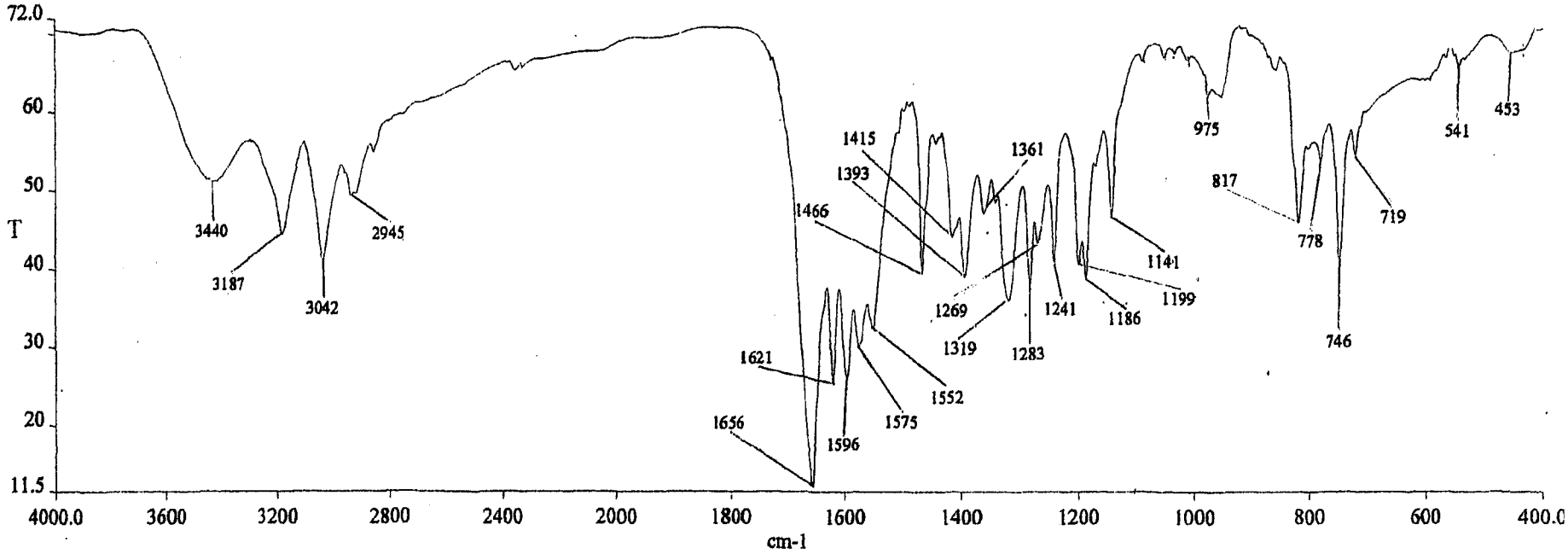

Fig. 3.4.5 IR spectrum of complex $[Mn^{II}(npahH_2)]$ **(8)** in KBr

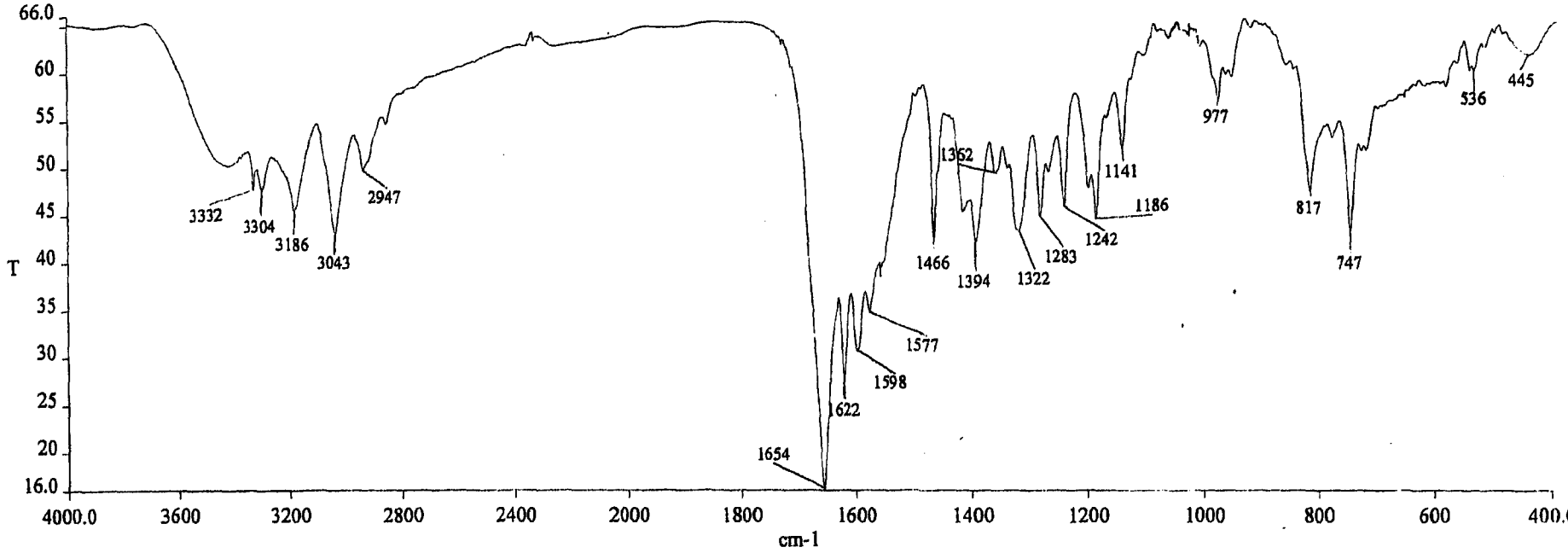

Fig. 3.4.6 IR spectrum of complex $[Mn^{II}(npahH_2)(phen)]$ **(14)** in KBr

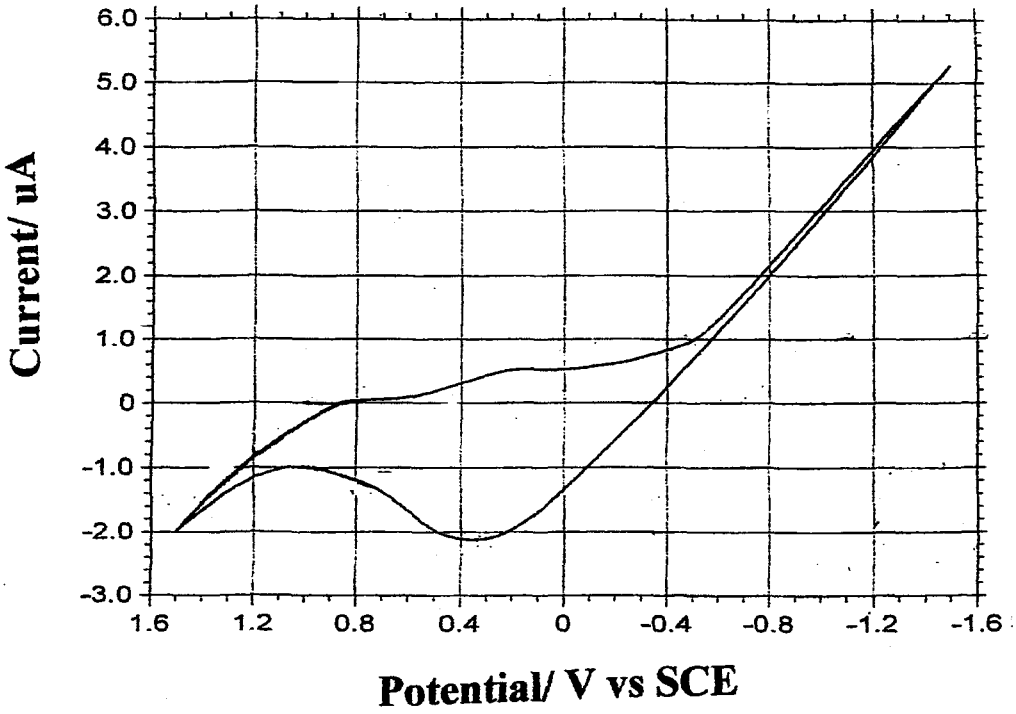

Fig. 3.5.1 Cyclic voltammogram of Ligand Disalicylaldehyde adipoyldihydrazone ($slahH_4$)

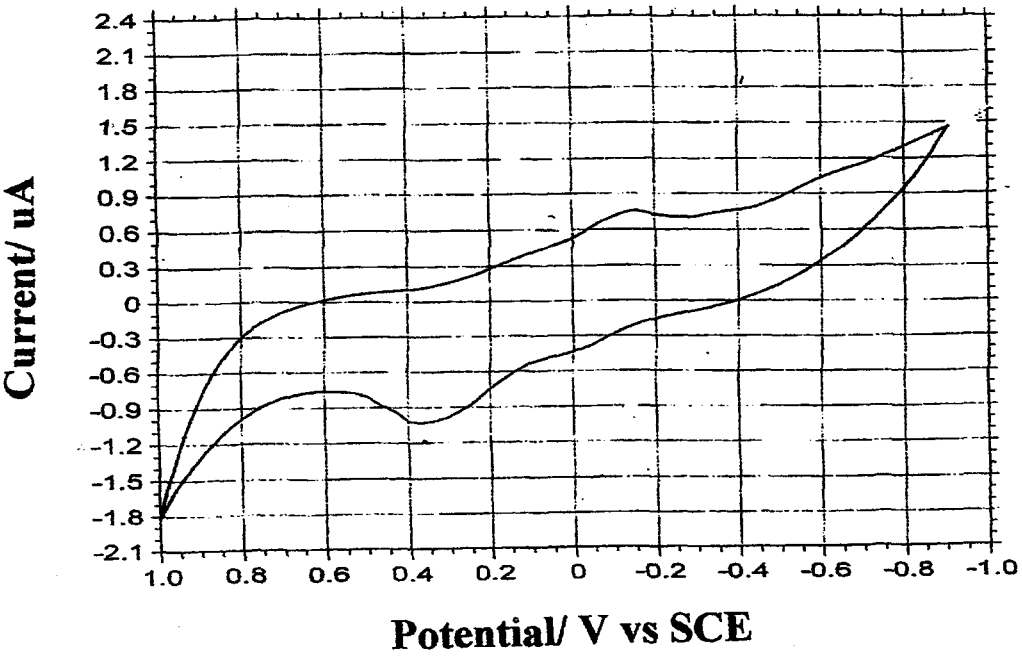

Fig. 3.5.2 Cyclic voltammogram of Ligand Bis(2-hydroxy-1-naphthaldehyde)-adipoldihydrazone ($napahH_4$)

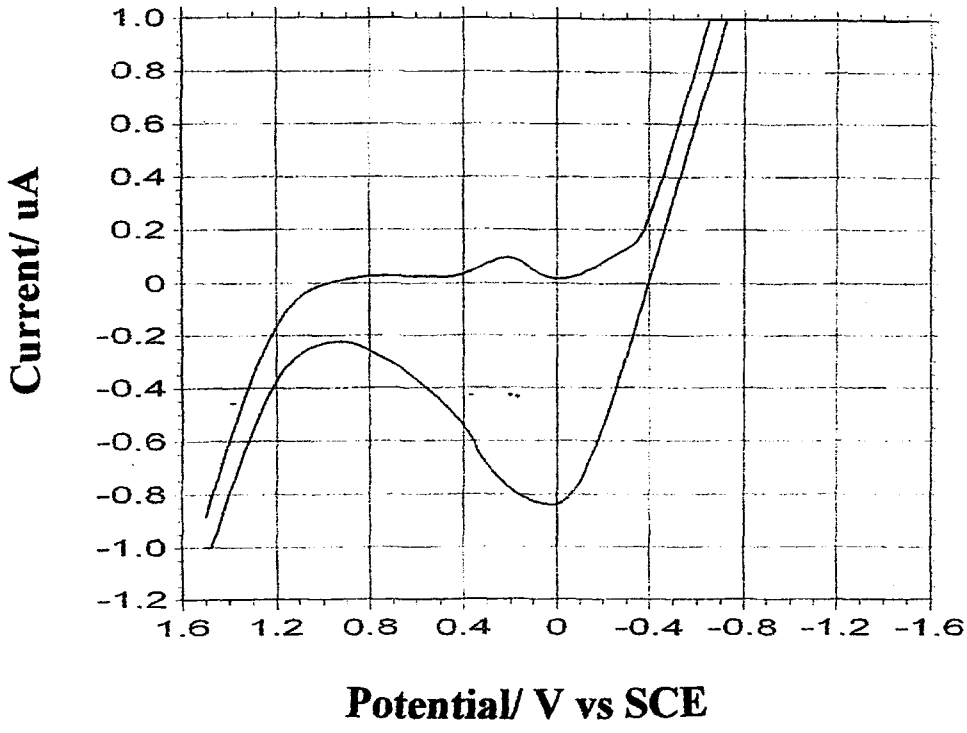
Current/ uA
1.0
0.8
0.6
0.4
0.2
0
-0.2
-0.4
-0.6
-0.8
-1.0
-1.2
1.6 1.2 0.8 0.4 0 -0.4 -0.8 -1.2 -1.6
Potential/ V vs SCE

(a)

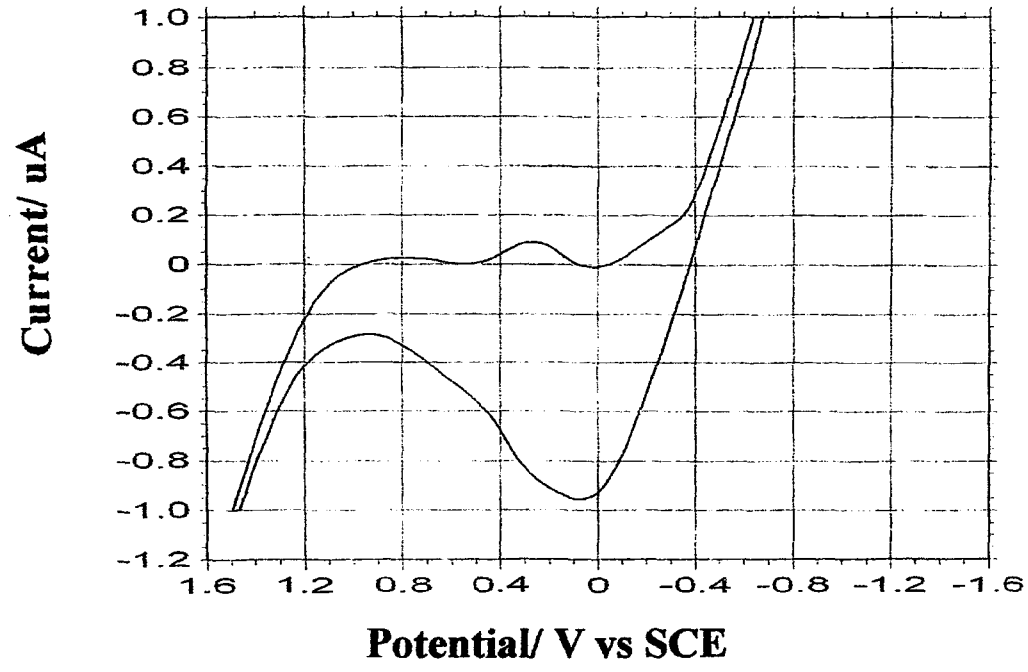
Current/ uA
1.0
0.8
0.6
0.4
0.2
0
-0.2
-0.4
-0.6
-0.8
-1.0
-1.2
1.6 1.2 0.8 0.4 0 -0.4 -0.8 -1.2 -1.6
Potential/ V vs SCE

(b)

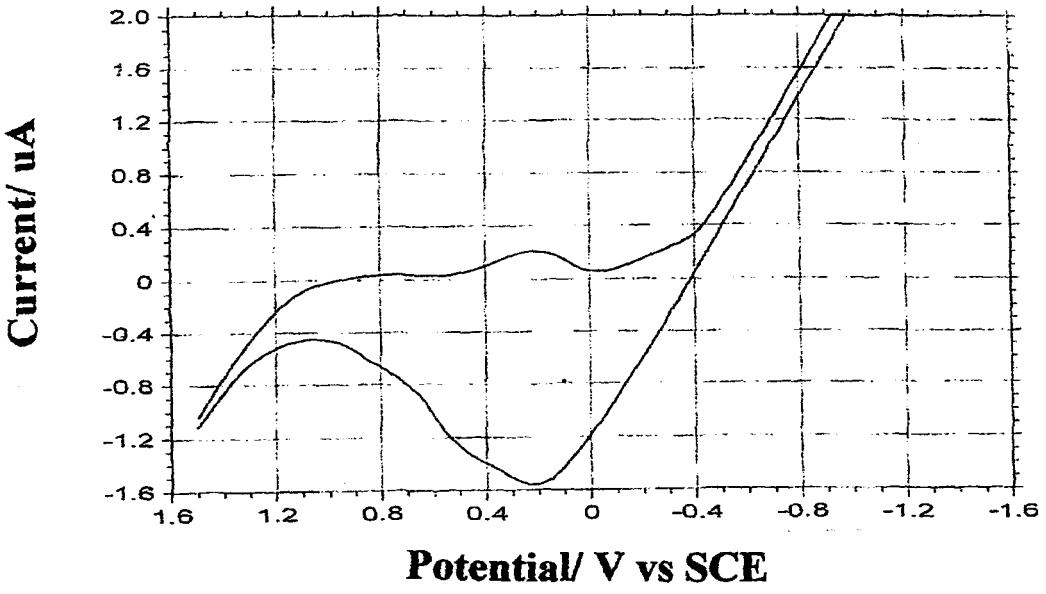

(c)

Fig. 3.5.3 (a), (b) and (c) Cyclic voltammograms of complex $[Mn^{II}(slahH_2)(H_2O)_2]$ **(1)** at scan rates **(a)** 100 mV/s **(b)** 300 mV/s **(c)** 500 mV/s

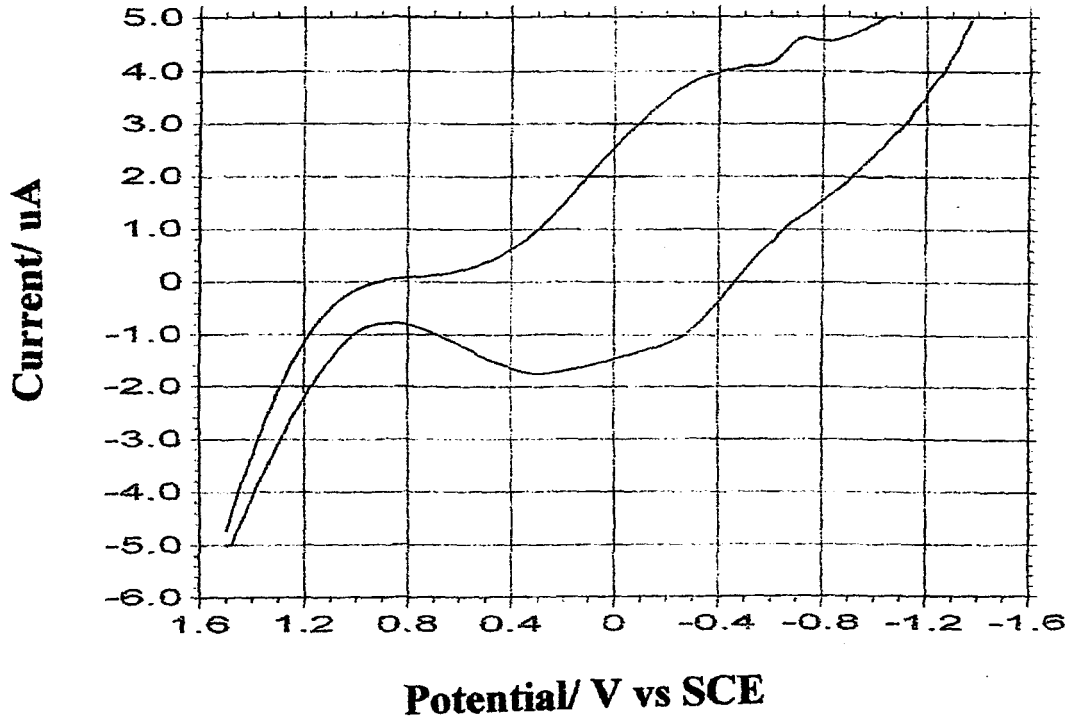

Fig. 3.5.4 Cyclic voltammogram of complex $[Mn^{II}(slahH_2)(py)_2].H_2O$ **(2)** at scan rate 100 mV/s

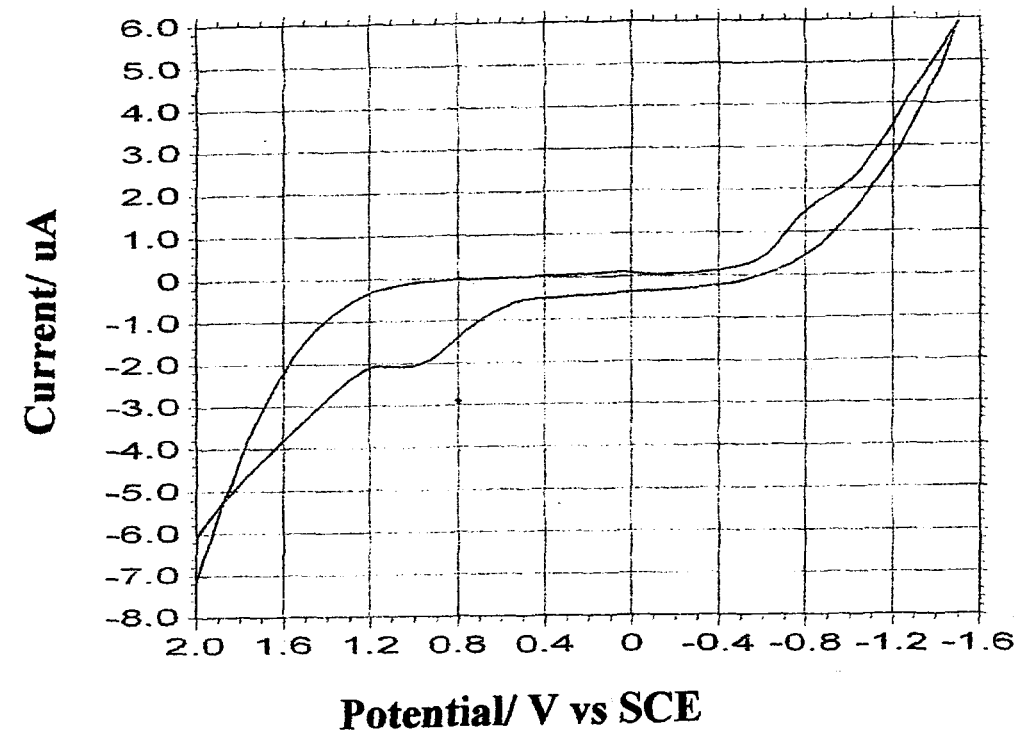
Current/ uA
6.0
5.0
4.0
3.0
2.0
1.0
0
-1.0
-2.0
-3.0
-4.0
-5.0
-6.0
-7.0
-8.0
2.0 1.6 1.2 0.8 0.4 0 -0.4 -0.8 -1.2 -1.6
Potential/ V vs SCE

(a)

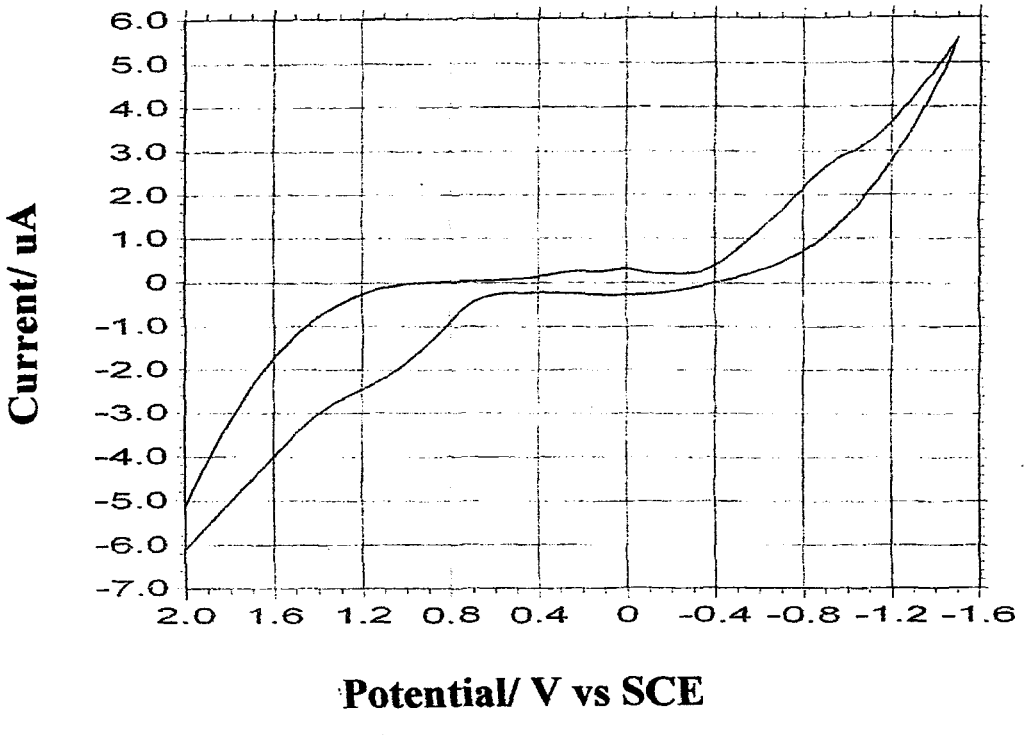
Current/ uA
6.0
5.0
4.0
3.0
2.0
1.0
0
-1.0
-2.0
-3.0
-4.0
-5.0
-6.0
-7.0
2.0 1.6 1.2 0.8 0.4 0 -0.4 -0.8 -1.2 -1.6
Potential/ V vs SCE

(b)

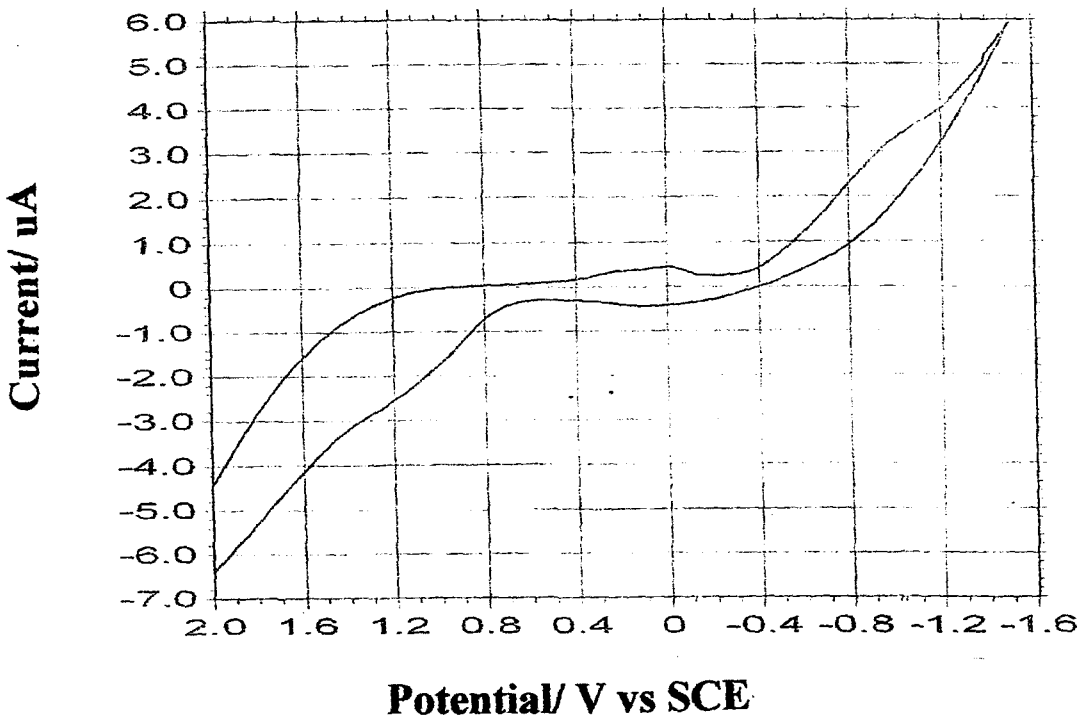
Current/ uA
6.0
5.0
4.0
3.0
2.0
1.0
0
-1.0
-2.0
-3.0
-4.0
-5.0
-6.0
-7.0
2.0 1.6 1.2 0.8 0.4 0 -0.4 -0.8 -1.2 -1.6
Potential/ V vs SCE

(c)

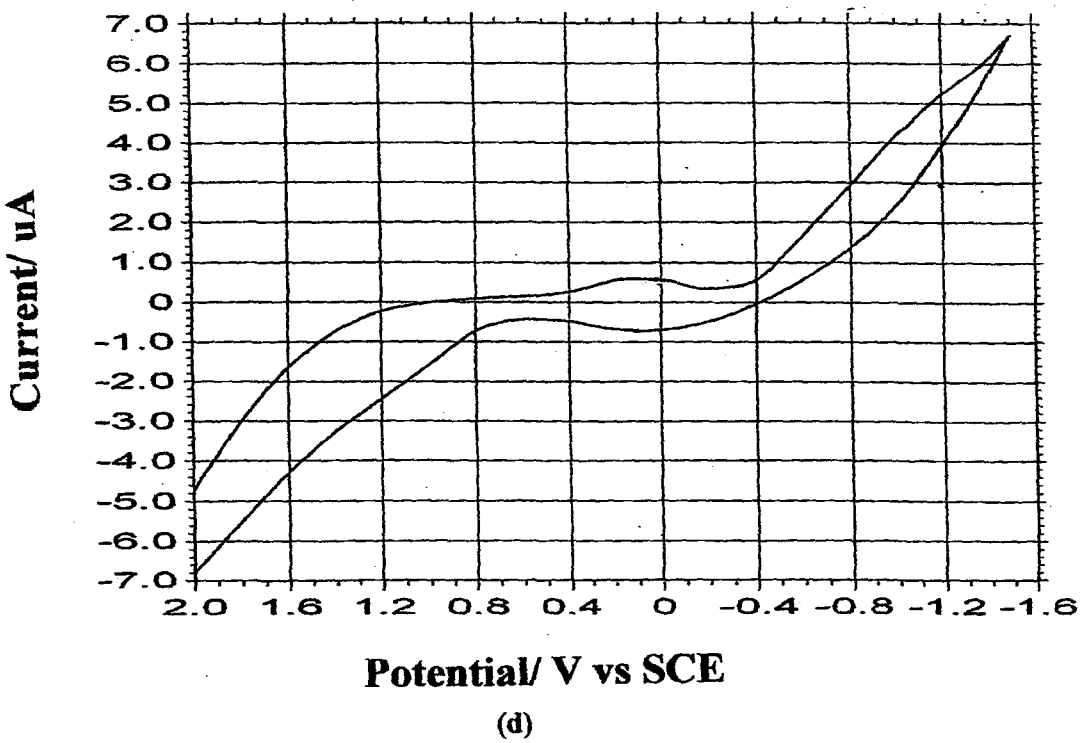
Current/ uA
7.0
6.0
5.0
4.0
3.0
2.0
1.0
0
-1.0
-2.0
-3.0
-4.0
-5.0
-6.0
-7.0
2.0 1.6 1.2 0.8 0.4 0 -0.4 -0.8 -1.2 -1.6
Potential/ V vs SCE

(d)

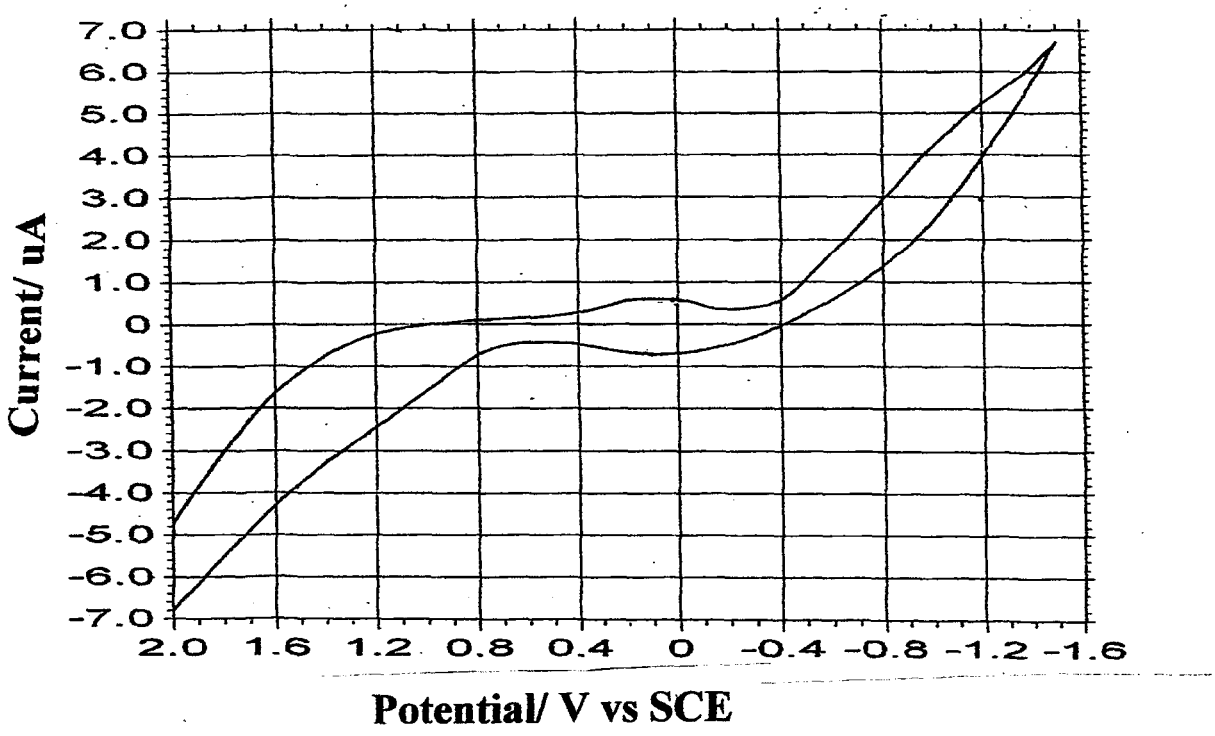

(e)

Fig 3.5.5 (a), (b), (c), (d) and (e) Cyclic voltammograms of complex $[Mn^{II}(slahH_2)(2\text{-pic})_2].H_2O$ **(3)** at scan rates **(a)** 100 mV/s **(b)** 200 mV/s **(c)** 300 mV/s **(d)** 400 mV/s **(e)** 500 mV/s

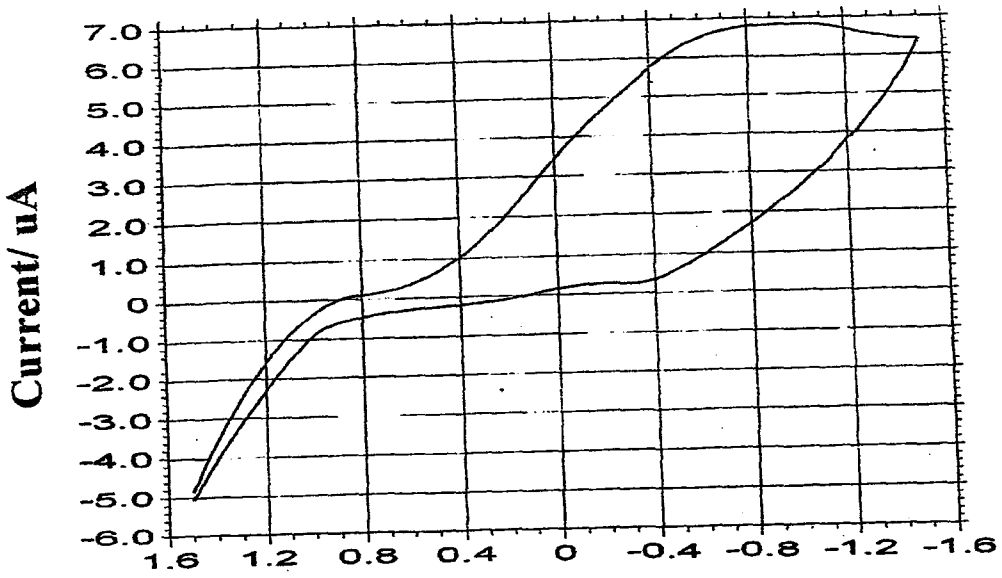

(a)

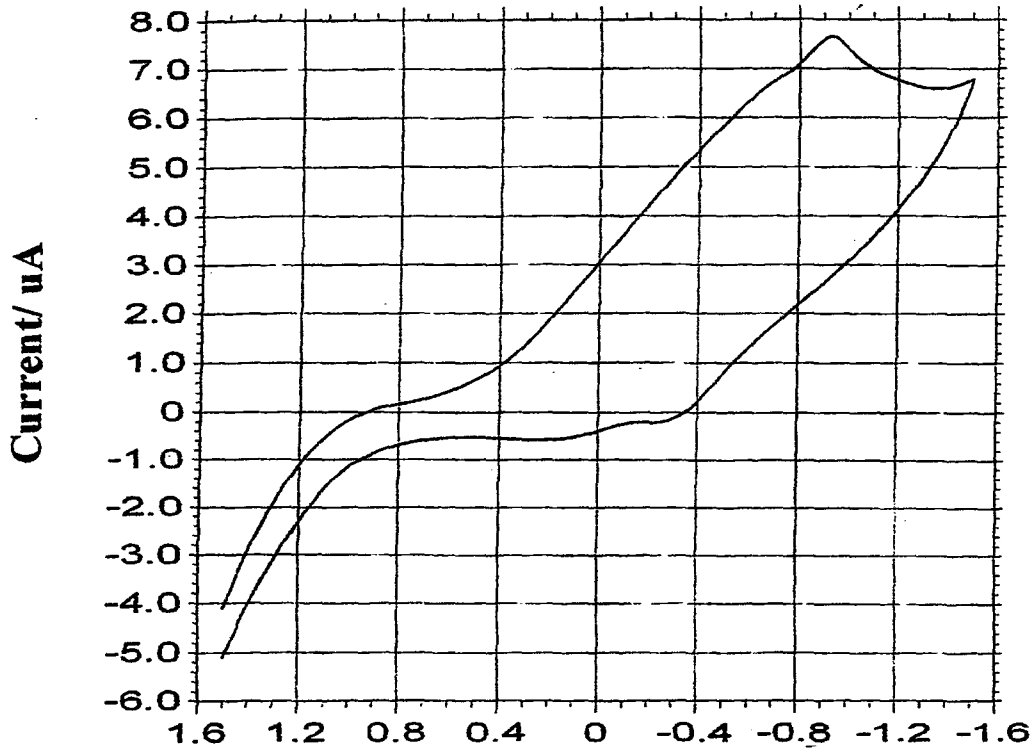

(b)

Fig. 3.5.6 (a) and (b) Cyclic voltammograms of complex $[Mn^{II}(slahH_2)(3\text{-pic})_2].H_2O$ **(4)** at scan rates **(a)** 100 mV/s **(b)** 200 mV/s

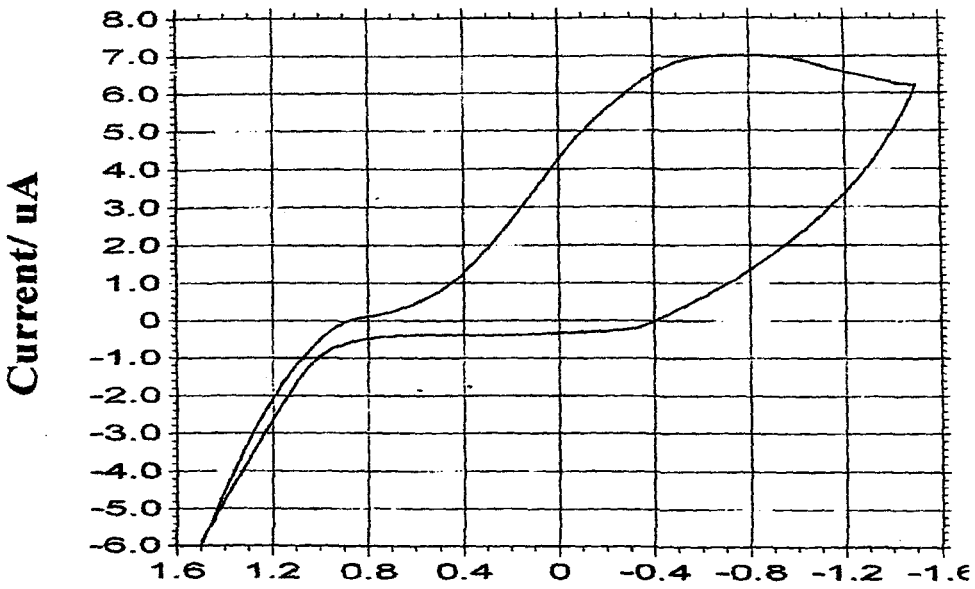

(a)

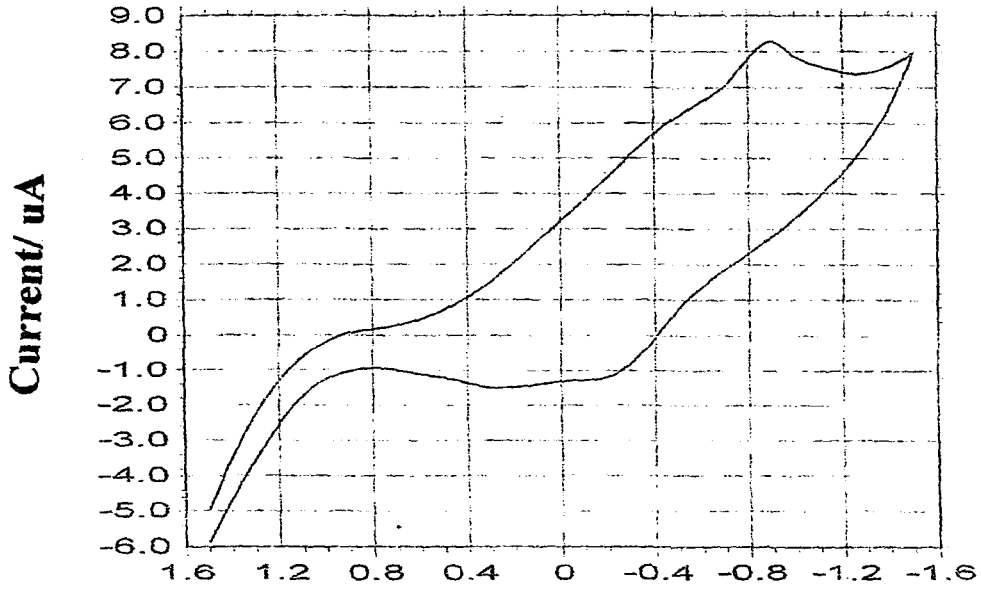

(b)

Fig. 3.5.7 (a) and (b) Cyclic voltammograms of complex $[Mn^{II}(slahH_2)(4\text{-pic})_2].H_2O$ **(5)** at scan rates **(a)** 100 mV/s **(b)** 200 mV/s

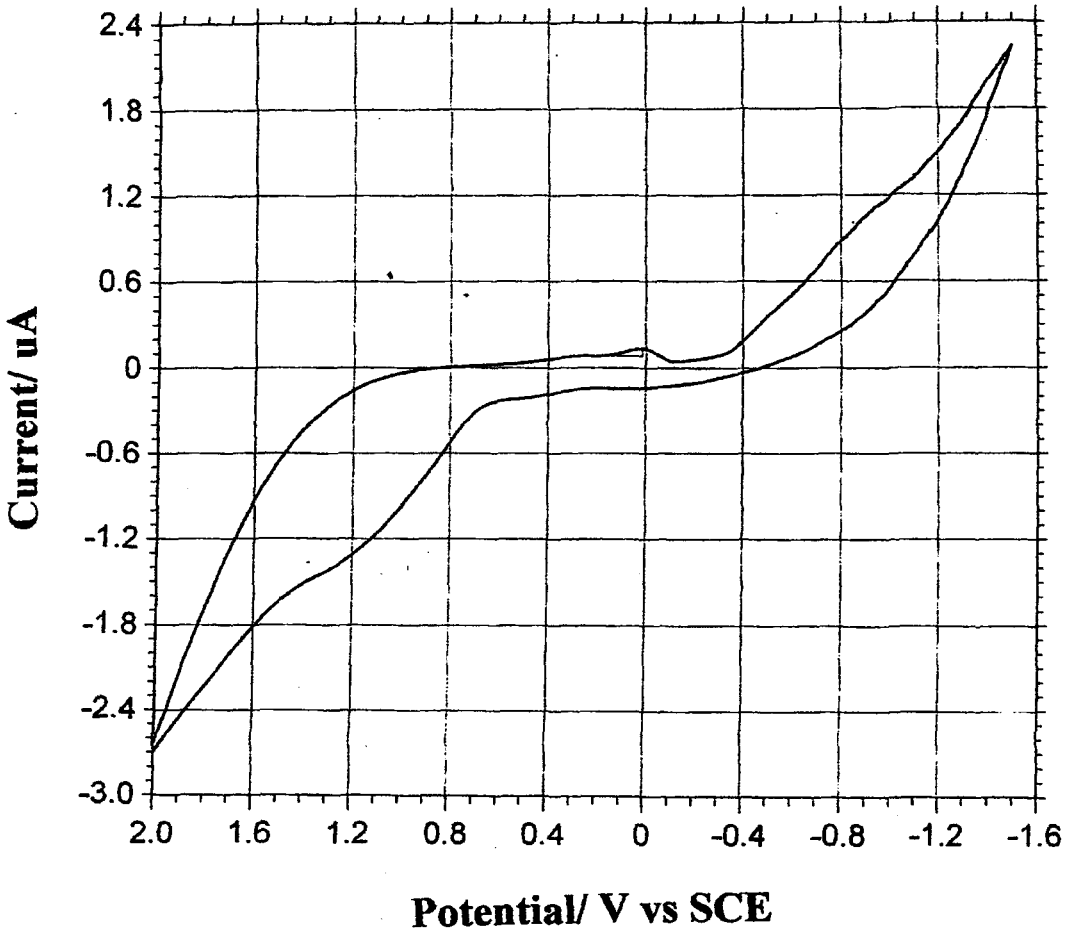

Fig. 3.5.8 Cyclic voltammogram of complex $[Mn^{II}(slahH_2)(phen)]$ (7)

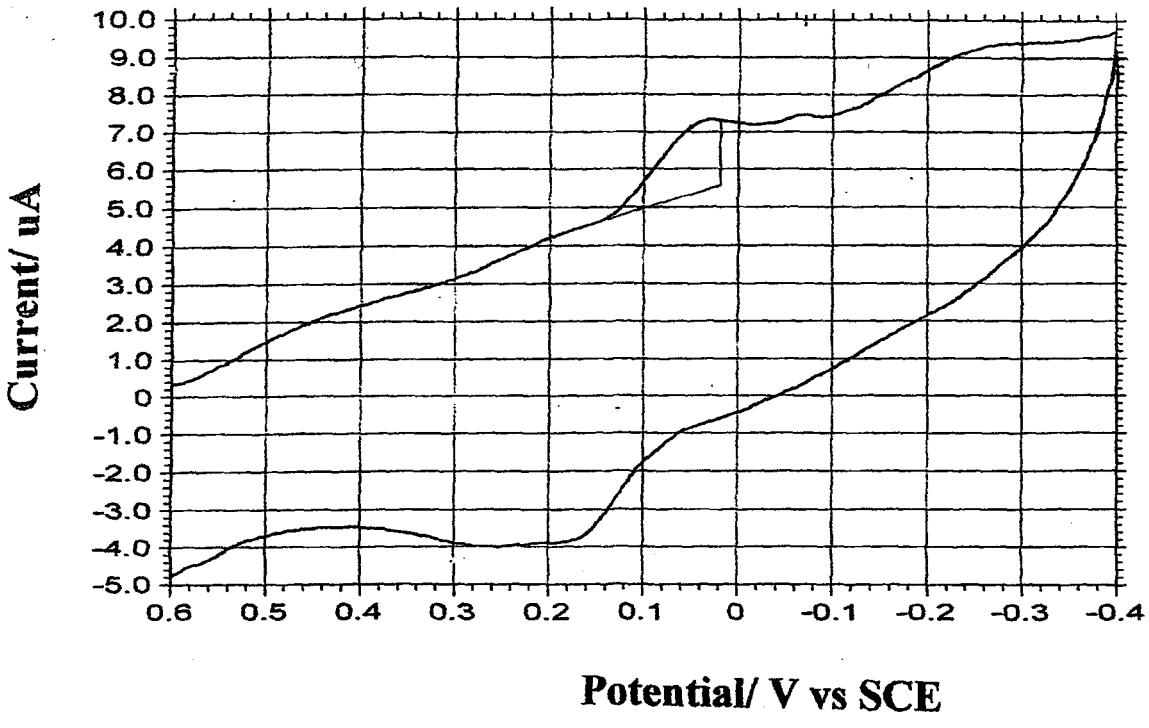

(a)

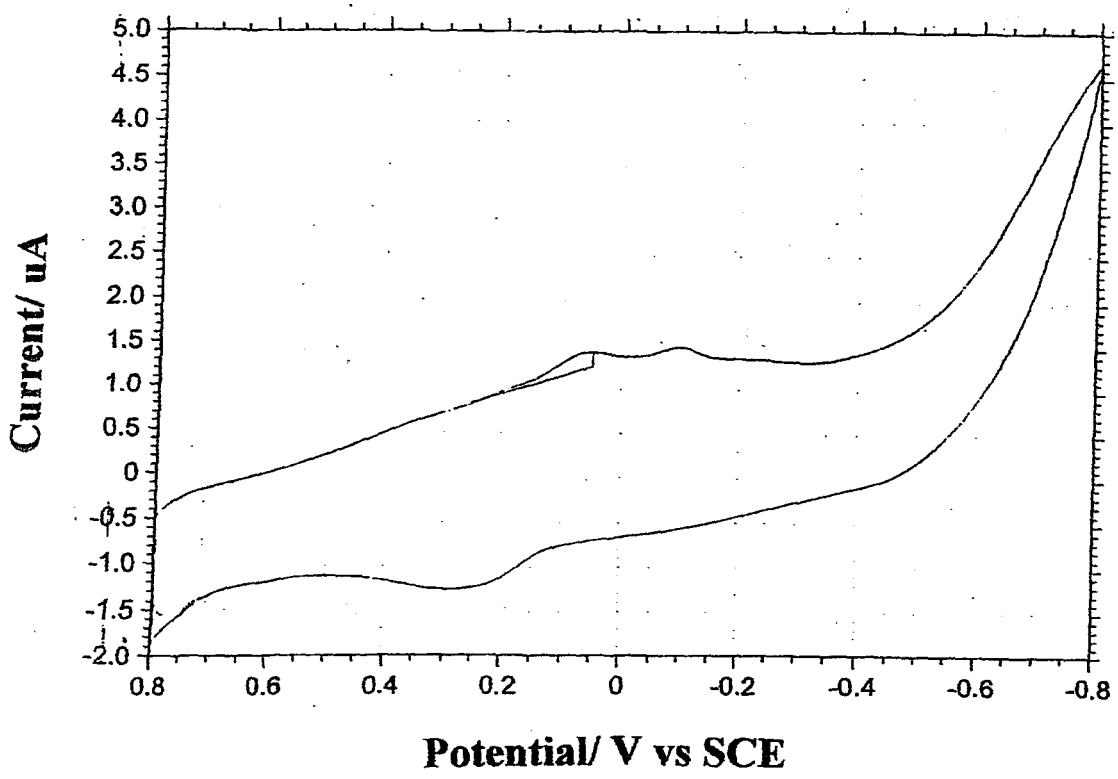

(b)

Fig. 3.5. 9 **(a)** and **(b)** Cyclic voltammograms of complex $[Mn^{II}(npahH_2)(py)_2]$ **(9)** at scan rates **(a)** 5 mV/s **(b)** 100 mV/s

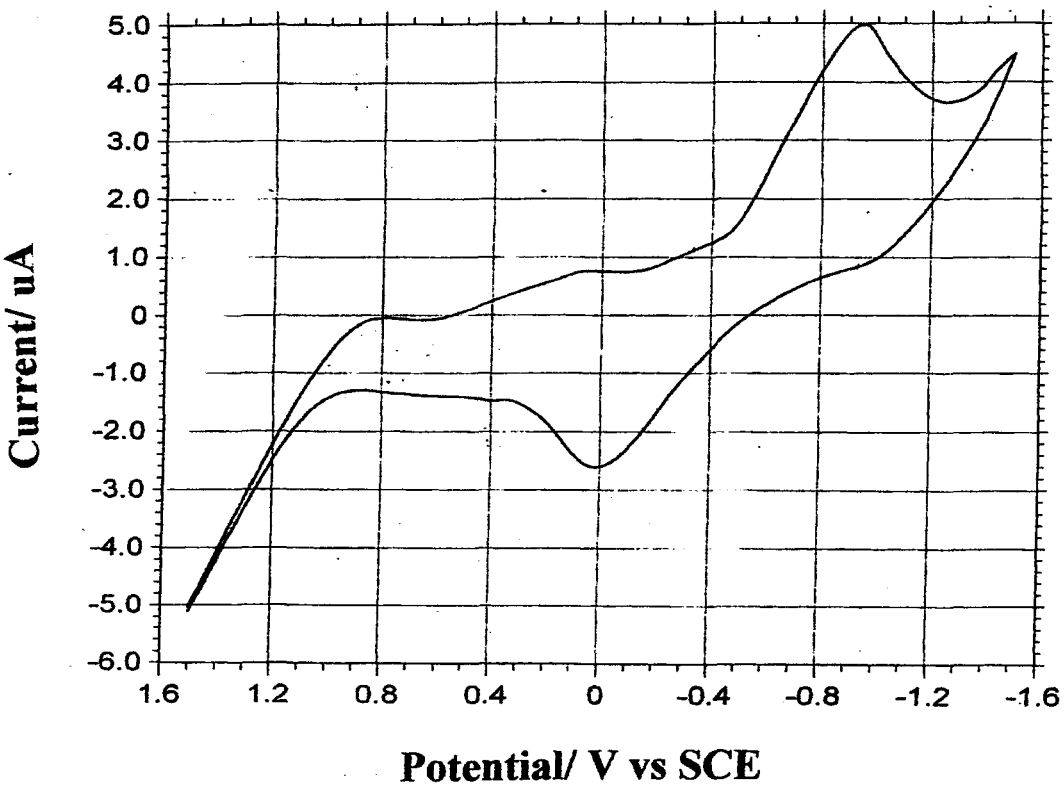

Fig. 3.5.10 Cyclic voltammogram of complex $[Mn^{II}(npahH_2)(4\text{-pic})_2]$ **(12)** at scan rate 100 mV/s

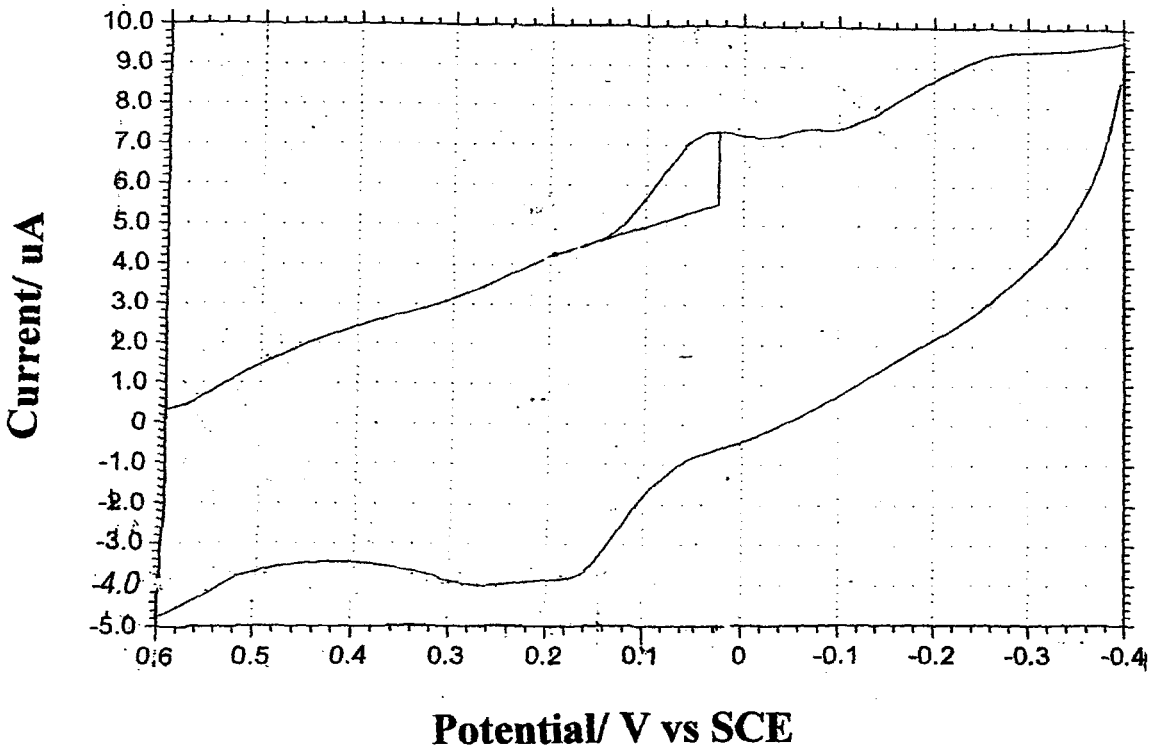

(a)

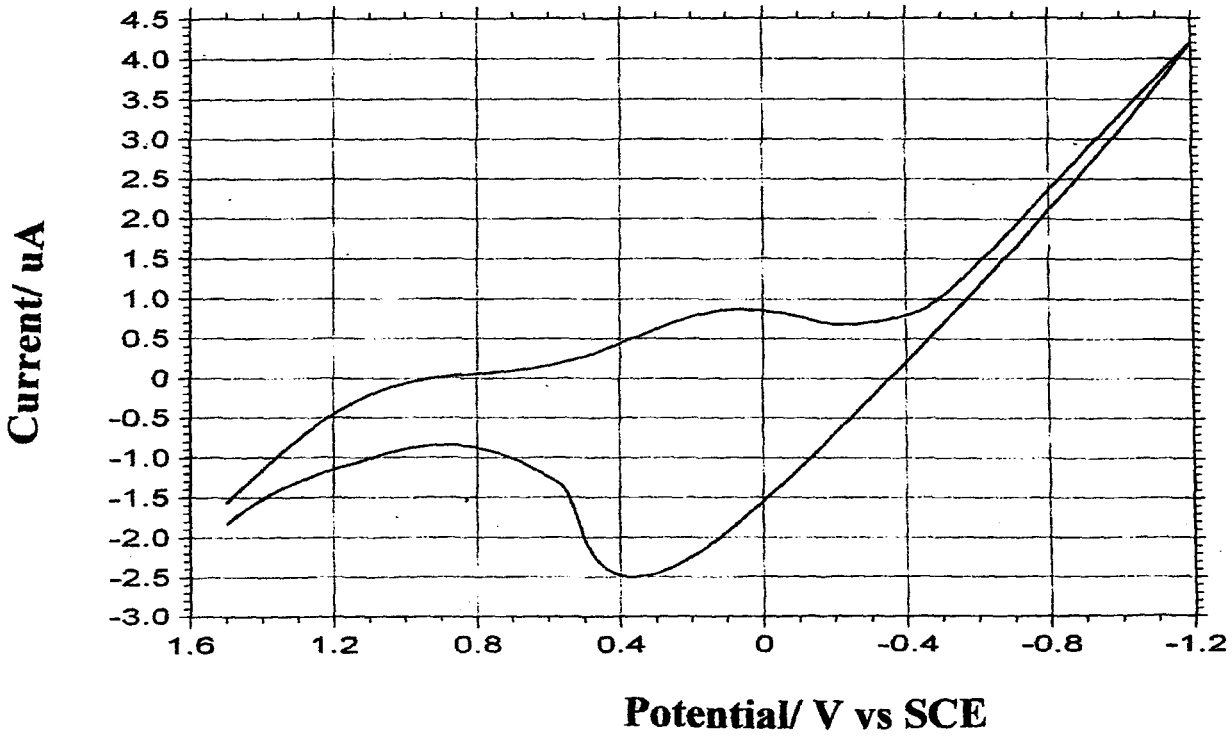

(b)

Fig. 3.5.11 **(a)** and **(b)** Cyclic voltammograms of complex $[Mn^{II}(npahH_2)(bpy)]$ **(13)** at scan rates **(a)** 5 mV/s **(b)** 100 mV/s

Table 3.1: *Colour, Decomposition Point*, Analytical, Magnetic Moment and Molar Conductance Data for Complexes of Disalicylaldehyde adipoyldihydrazone ($slahH_4$) and Bis(2-hydroxy-1-naphthaldehyde)adipoyldihydrazone ($npahH_4$)

Sl. No	Complex	Colour	D.P (°C)	Analysis: Found(Calcd)%				μ_B (B.M)	Molar Conductance Λ_m (ohm^{-1} cm^2 mol^{-1})
				Mn	C	H	N		
1.	$[Mn^{II}(slahH_2)(H_2O)_2]$	Light-brown	>300	11.650 (11.677)	50.952 (50.955)	5.101 (5.096)	11.873 (11.890)	5.87	1.5
2.	$[Mn^{II}(slahH_2)(py)_2].H_2O$	Light-brown	>300	8.895 (9.002)	58.941 (58.919)	5.234 (5.237)	13.740 (13.748)	6.02	1.5
3.	$[Mn^{II}(slahH_2)(2\text{-}pic)_2].H_2O$	Dull-brown	>300	8.631 (8.634)	60.191 (60.283)	5.350 (5.338)	12.781 (13.187)	5.86	2.8
4.	$[Mn^{II}(slahH_2)(3\text{-}pic)_2].H_2O$	Dull-brown	>300	8.613 (8.634)	60.298 (60.283)	5.401 (5.338)	13.143 (13.187)	5.79	1.7
5.	$[Mn^{II}(slahH_2)(4\text{-}pic)_2].H_2O$	Dull-brown	>300	8.615 (8.634)	60.131 (60.283)	5.511 (5.338)	13.131 (13.187)	5.89	2.5
6.	$[Mn^{II}(slahH_2)(bpy)]$	Light-brown	>300	9.679 (9.769)	63.403 (63.943)	4.870 (4.973)	9.951 (9.947)	5.95	1.9
7.	$[Mn^{II}(slahH_2)(phen)]$	Dull-brown	>300	9.291 (9.338)	65.144 (65.195)	5.151 (5.093)	9.391 (9.508)	5.98	2.2

8. $[Mn^{II}(npahH_2)]$	Yellowish-brown	>300	10.305 (10.280)	62.831 (62.804)	4.452 (4.486)	10.432 (10.467)	1.12	1.5
9. $[Mn^{II}(npahH_2)(py)_2]$	Yellowish-brown	>300	8.915 (7.937)	66.122 (65.801)	5.001 (4.706)	12.134 (12.121)	5.91	3.2
10. $[Mn^{II}(npahH_2)(2\text{-}pic)_2]$	Yellowish-brown	>300	7.650 (7.628)	66.523 (66.571)	5.232 (5.270)	11.649 (11.650)	5.83	2.8
11. $[Mn^{II}(npahH_2)(3\text{-}pic)_2]$	Yellowish-brown	>300	7.650 (7.638)	66.581 (66.571)	5.241 (5.270)	11.641 (11.650)	5.89	3.7
12. $[Mn^{II}(npahH_2)(4\text{-}pic)_2]$	Yellowish-brown	>300	7.642 (7.638)	66.580 (66.571)	5.231 (5.270)	11.632 (11.650)	5.96	1.6
13. $[Mn^{II}(npahH_2)(bpy)]$	Yellowish-brown	>300	7.982 (8.296)	68.735 (68.778)	4.821 (4.827)	8.451 (8.446)	5.87	3.3
14. $[Mn^{II}(npahH_2)(phen)]$	Yellowish-brown	>300	7.821 (7.983)	69.654 (69.666)	4.951 (4.935)	8.101 (8.128)	5.95	2.5

Table 3.3: Important Electronic Spectral Bands and EPR data for Manganese (II) Complexes of Disalicylaldehyde adipoyldihydrazone and Bis(2-hydroxy-1-naphthaldehyde)adipoyldihydrazone

Sl. No	Ligand/Complex	λ_{max}(nm)[ε_{max} dm^3 mol^{-1} cm^{-1}) for conc 10^{-2}M soln			Temp	solid/ soln	g-value	A_{Mn} (G)
	$slahH_4$	284(4308)	320(2808)					
	$npahH_4$	290(2041)	313(2300)	363(1852)				
1.	$[Mn^{II}(slahH_2)(H_2O)_2]$	276 (7670)	324(3450)		LNT LNT RT	SOLID DMSO DMSO	2.019 2.007 1.924	- 96 -
2.	$[Mn^{II}(slahH_2)(py)_2].H_2O$	290(9450)	325(3600)		LNT LNT RT	SOLID DMSO DMSO	2.045 2.019 1.935	- 96 96
3.	$[Mn^{II}(slahH_2)(2\text{-}pic)_2]. H_2O$	287(8670)	330(4055)		LNT LNT RT	SOLID DMSO DMSO	2.032 2.038 1.924	- 96 -
4.	$[Mn^{II}(slahH_2)(3\text{-}pic)_2].H_2O$	287(6313)	322 (4423)		LNT LNT RT	SOLID DMSO DMSO	2.032 2.045 1.924	- 94 94
5.	$[Mn^{II}(slahH_2)(4\text{-}pic)_2]. H_2O$	290 (9270)	328(4950)		LNT LNT RT	SOLID DMSO DMSO	2.044 2.050 1.950	- 94 92
6.	$[Mn^{II}(slahH_2)(bpy)]$	276(9266)	323(6420)		LNT LNT RT	SOLID DMSO DMSO	2.045 2.032 -	- - -
7.	$[Mn^{II}(slahH_2)(phen)]$	286(8790)	330(5680)		LNT LNT RT	SOLID DMSO DMSO	2.045 2.032 -	- - -

8. $[Mn^{II}(npahH_2)]$	257(5735)	315(2890)	364(2460)	600(790)	LNT LNT	SOLID DMSO	2.019 2.007	- 100
9. $[Mn^{II}(npahH_2)(py)_2]$	355 (6160)	483(4860)			LNT LNT RT	SOLID DMSO DMSO	2.019 2.036 2.226	- 100 96
10. $[Mn^{II}(npahH_2)(2\text{-}pic)_2]$	256 (8340)	316(4362)	365(3705)	448(2475)	LNT LNT RT	SOLID DMSO DMSO	2.038 2.019 1.944	- 94 94
11. $[Mn^{II}(npahH_2)(3\text{-}pic)_2]$	256(8340)	316(4362)	364(3753)	450(394)	LNT LNT RT	SOLID DMSO DMSO	2.038 2.019 1.804	- 94 94
12. $[Mn^{II}(npahH_2)(4\text{-}pic)_2]$	263(8270)	317(4194)	363(3532)	450(198)	LNT LNT RT	SOLID DMSO DMSO	2.032 2.006 1.840	- 94 94
13. $[Mn^{II}(npahH_2)(bpy)]$	260(5760)	320(4570)	364(8080)	455(706)	LNT LNT RT	SOLID DMSO DMSO	2.036 1.994 1.838	- - 98
14. $[Mn^{II}(npahH_2)(phen)]$	315(7637)	363(7320)	450(160)		LNT LNT RT	SOLID DMSO DMSO	2.032 2.010 1.890	- - 100

Table 3.4: Structurally Significant Infrared Spectral Bands of Disalicylaldehyde adipoyldihydrazone ($slahH_4$) and Bis(2-hydroxy -1-naphthaldehyde)adipoyldihydrazone ($npahH_4$) and their Monometallic Manganese (II) Complexes

Sl. No	Ligand/Complex	ν(OH) +ν(NH)	ν(C=O)	ν(C=N)	Amide(II) + ν(CO) phenolic/ naphtholic)	β(C-O) (phenolic/ naphtholic)	ν(N-N)	ν(M-O) phenolic/ naphtholic	ν(M-N) py/bpy/phen vibration in plane
	$slahH_4$	3300-3600(sbr) 3445(m) 3436(m) 3204(s) 3065(sbr)	1679(s)	1620(s)	1560(s)	1275(s)	1036(m)		
	$npahH_4$	3300-3600(sbr) 3469(sbr) 3430(sbr) 3224(s) 3051(sbr)	1666(s)	1630(s) 1593(m)	1530(w)	1281(m)	1030(w)		
1.	$[Mn^{II}(slahH_2)(H_2O)_2]$	3000-3600(sbr) 3432(s)	-	1605(s)	1541(s)	1270(w)	1038(w)	582(m)	-
2.	$[Mn^{II}(slahH_2)(py)_2].H_2O$	3000-3600(sbr) 3449(s)	-	1606(s)	1540(s)	1270(w)	1043(m)	592(m)	671(m)
3.	$[Mn^{II}(slahH_2)(2\text{-}pic)_2].H_2O$	3000-3600(sbr) 3430(s)	-	1605(s)	1535(msh)	1260(w)	1050 (w)	580(w)	-
4.	$[Mn^{II}(slahH_2)(3\text{-}pic)_2].H_2O$	3000-3600(sbr) 3432(s)	-	1605(vs)	1541(s)	1277(m 1250(m)	1038(m)	581(m)	660(m)
5.	$[Mn^{II}(slahH_2)(4\text{-}pic)_2].H_2O$	3000-3600(sbr) 3431(s)	-	1605(vs)	-	1270(m)	1050(w)	580(mbr)	680(w)
6.	$[Mn^{II}(slahH_2)(bpy)]$	3445(s) 3202(s) 3068(s)	1667(s) 1680(m)	1611(s)	1559(m)	1277(s) 1250(msh)	1050(w)	580(w)	680(w)
7.	$[Mn^{II}(slahH_2)(phen)]$	3430(s) 3202(s) 3067(s)	1667(m) 1675(s)	1607(s)	1560(s)	1277(w) 1250(msh)	1035(m)	582(w)	696(w)

8.	**$[Mn^{II}(npahH_2)]$**	3440(mbr) 3187(m) 3042(m)	1656(s)	1621(s) 1596(s)	1552(m)	1283(m)	1080(w)	600(wbr)	-
9.	**$[Mn^{II}(npahH_2)(py)_2]$**	3430(sbr) 3180(mbr) 3000(m)	1650(s)	1615(s) 1600(s)	1540(s)	1310(w)	1080(w)	600(wbr)	690(m)
10.	**$[Mn^{II}(npahH_2)(2\text{-}pic)_2]$**	3398(wbr) 3200(wbr) 3000(w)	1640(sbr)	1620(vs) 1600(vs)	1539(s)	1280(w)	1080(w)	600(wbr)	657(m)
11.	**$[Mn^{II}(npahH_2)(3\text{-}pic)_2]$**	3402(wbr) 3170(w) 3000(w)	1664(s)	1620(vs) 1600(vs)	1539(s)	1301(w)	1070(w)	600(wbr)	680(wbr)
12.	**$[Mn^{II}(npahH_2)(4\text{-}pic)_2]$**	3427 (sbr) 3170(mbr) 3038(m)	1664(mbr)	1620(vs) 1600(vs)	1539(vs)	1301(w)	1093(w)	600(wbr)	649(w)
13.	**$[Mn^{II}(npahH_2)(bpy)]$**	3425(mbr) 3186(w) 3047(w)	1654(s)	1620(s) 1599(s)	1540(m)	1300(w)	1095(w)	600(wbr)	660(wbr)
14.	**. $[Mn^{II}(npahH_2)(phen)]$**	3410(mbr) 3332(w) 3304(w) 3186(m) 3043(m)	1654(m)	1622(s) 1598(m)	1538(m)	1283(m)	1084(w)	-	660(wbr)

Table 3.5: The Electrochemical Parameters for the Dihydrazones and their Monometallic Manganese(II) Complexes (Pot vs SCE)

Sl. No.	Ligand/ Complex	Epa/V	Epc/ V
	$slahH_4$	+0.35	+0.20
	$npahH_4$	0.00 +0.35	-0.15 -
1.	$[Mn^{II}(slahH_2)(H_2O)_2]$	+0.30 +0.05	+0.20 -0.25
2.	$[Mn^{II}(slahH_2)(py)_2].H_2O$	+0.32 -0.39	-0.25 -0.70
3.	$[Mn^{II}(slahH_2)(2\text{-}pic)_2].H_2O$	+1.01 +0.35	+0.05 -0.84
4.	$[Mn^{II}(slahH_2)(3\text{-}pic)_2].H_2O$	+0.25 -0.35	-0.90 (broad)
5.	$[Mn^{II}(slahH_2)(4\text{-}pic)_2].H_2O$	+0.20 -0.35	-0.70 (broad)
6.	$[Mn^{II}(slahH_2)(bpy)]$	+0.45 (broad)	-0.18
7.	$[Mn^{II}(slahH_2)(phen)]$	+0.45 -	+0.26 +0.02
8.	$[Mn^{II}(npahH_2)]$	+0.28 -0.25	+0.18 -0.78
9.	$[Mn^{II}(npahH_2)(py)_2]$	+0.27 (broad)	+0.06 -0.10
11.	$[Mn^{II}(npahH_2)(3\text{-}pic)_2]$	-0.29 -0.30	-0.01 -0.55
12.	$[Mn^{II}(npahH_2)(4\text{-}pic)_2]$	+0.40 0.00	+0.16 -0.26
13.	$[Mn^{II}(npahH_2)(bpy)]$	+0.35	+0.13
14.	$[Mn^{II}(npahH_2)(phen)]$	+0.38	0.00

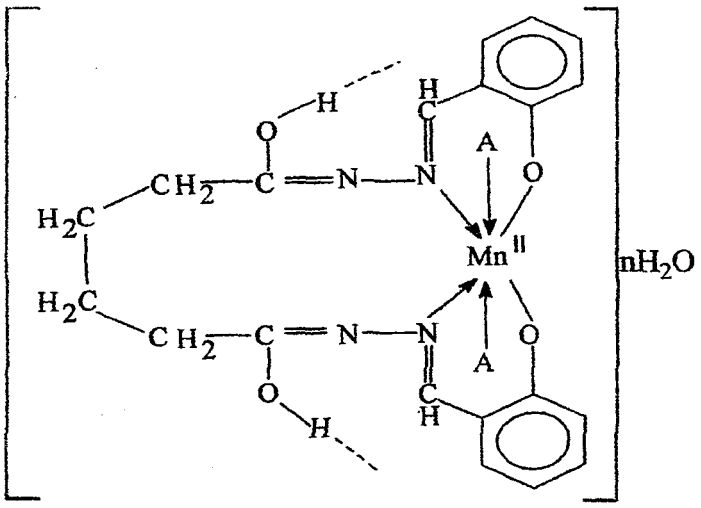

Fig. 3.6.1 Suggested structure of complex $[Mn^{II}(slahH_2)(A_2)].nH_2O$ (where A= H_2O, **(1)**; py, **(2)**; 2-pic, **(3)**; 3-pic, **(4)** and 4-pic, **(5)**; n = 0, 1)

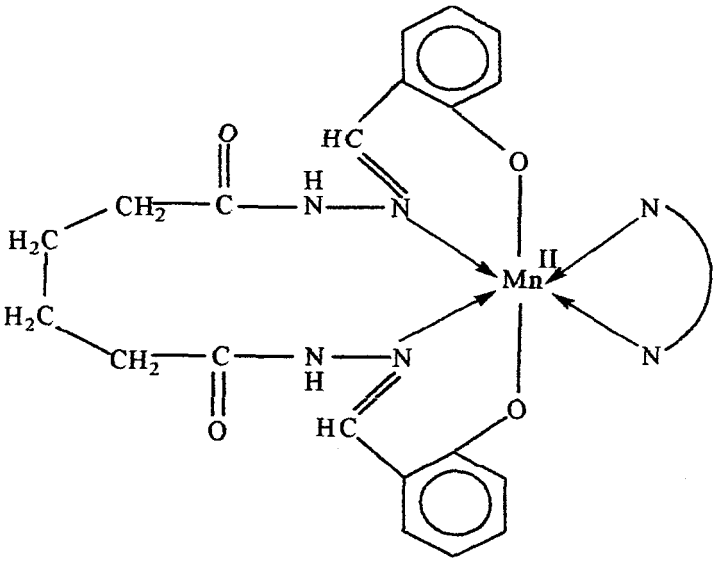

Fig. 3.6.2 Suggested structure of complex $[Mn^{II}(slahH_2)(\widehat{NN})]$ (where $\widehat{NN}$ = bpy, **(6)** and phen, **(7)**)

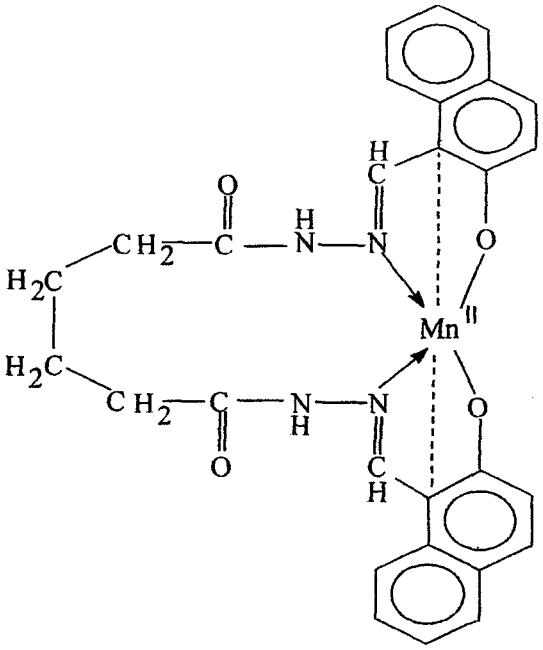

Fig. 3.6.3 Suggested structure of complex $[Mn^{II}(npahH_2)]$ **(8)**

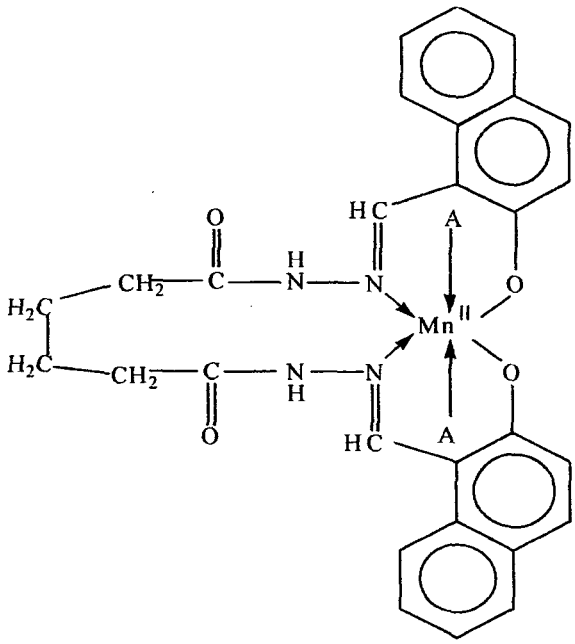

Fig. 3.6.4 Suggested structure of complex $[Mn^{II}(npahH_2)(A_2)]$ (where A= py, **(9)**; 2-pic, **(10)**; 3-pic, **(11)** and 4-pic, **(12)**)

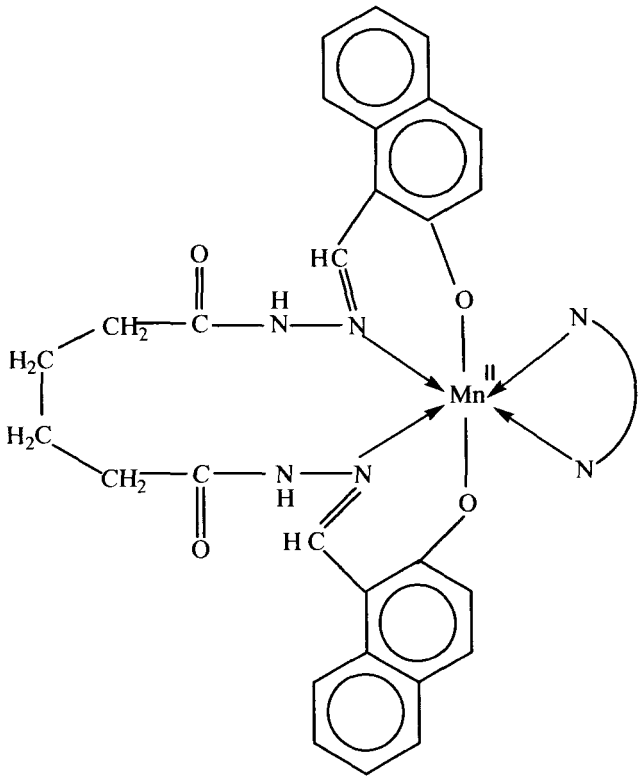

Fig. 3.6.5 Suggested structure of complex $[Mn^{II}(npahH_2)(\overset{\frown}{NN})]$ (where $\overset{\frown}{NN}$ = bpy, **(13)** and phen, **(14)**)

CHAPTER-IV

Synthesis and Characterization of Monometallic Manganese (IV) complexes of Bis(2-hydroxy-1-naphthaldehyde)adipoyldihydrazone

Introduction

The previous chapter describes the synthesis and characterization of manganese(II) complexes derived from polyfunctional dihydrazone ligands disalicylaldehyde adipoyldihydrazone ($slahH_4$) and bis(2-hydroxy-1-naphthaldehyde)adipoyldihydrazone ($npahH_4$). It was observed that the reactions of preformed ligands with $Mn(OAc)_2.4H_2O$ in methanol formed manganese(II) complexes only. Although manganese occurs in some of the enzymes as Mn(II) yet in some other biological systems, it occurs in higher oxidation states such as Mn(III) and Mn(IV) like oxygen evolving complex (OEC) [191, 192] and as Mn(III) in manganese superoxide dismutase [193]. Futher, manganese is found in a variety of enzymes as mononuclear [194], binuclear [195] or multinuclear [196] clusters. Heteronuclear manganese clusters at the heart of PSII has been observed by a structural characterization at 3.8 A° resolution. In this dangler model, one manganese ion is distinct from the other three. Further, higher oxidation state manganese complexes serve as oxidizing agent, catalyst [197] and electro-catalysts [198] for the oxidation of compounds such as alcohols, ethers and water. Thus, a number of reports [178] have appeared involving use of manganese(III) and manganese(IV) complexes as oxidizing agents. The involvement of higher oxidation state oxo-bridged manganese dinuclear complexes in aliphatic and aromatic C-H activation and oxygen insertion reactions (mono-oxygenase) have been reported [199]. This has attracted attention to trinuclear, binuclear and mononuclear complexes of manganese in higher oxidation state

as structural and functional models for enzymes as well as for variety of catalytic reactions.

Schiff base and oxo-bridged manganese complexes have been of particular interest because they seem to mimic the coordination environment of Mn in PSII which does not contain a porphyrinic system and is thought to be made up of O and N-atoms. An interesting feature associated with the ligands containing phenolate/naphtholate donor atoms is their good-donor ability to stabilize higher oxidation states with highly covalent (phenolate/naptholate) bonds and their tendency to form phenyl radical. Dihydrazones derived from condensation of acyldihydrazones, aroyldihydrazones and pyridoyldihydrazones with o-hydroxy aromatic aldehydes and ketones are potential polyfunctional ligands possessing as many as eight and nine bonding sites such as phenolic/naphtholic-OH, azomethine, secondary –NH and carbonyl oxygen in duplicate and pyridyl nitrogen in their molecular skeleton in duplicate. They are capable of giving rise to mononuclear and polynuclear complexes. The present ligand contains two hydrazone groupings joined together through a series of four intervening methylene groups. Further, it contains bulky naphthyl fragment in its molecular skeleton. The compounds containing bulky fragment in their molecular skeleton are capable of giving rise to complexes possessing discrete molecularity.

In view of the significant role played by manganese in the biological systems and above importance of manganese compounds in higher oxidation states and importance of monometallic complexes in the synthesis of bimetallic complexes and meagre amount of work on complexes of the title dihydrazones with the metal ions in higher oxidation state, we have set an aim of synthesizing monometallic manganese(IV) complexes from preformed title dihydrazones. As we were interested in manganese complexes in higher oxidation state, we preferred to carry out reactions

in alkaline media. Accordingly, the reaction of manganese(II) acetate with preformed dihydrazones were carried out in alkaline methanolic media either as such or in the presence of pyridine bases and the products isolated form the subject matter of the present chapter. The compositions of the isolated complexes have been judged mainly from elemental analysis, and mass spectral data. The structures of manganese(IV) complexes have been discussed in the light of molar conductance, magnetic moment, electronic, infrared spectroscopic and EPR data. Electron transfer reactions of the complexes have also been studied with the help of cyclic voltammetric studies as well.

Preparation of the complexes

The complexes were prepared by following general methods.

(1) Preparation of $[Mn^{IV}(npah)(H_2O)_2]$ (15)

A methanol solution (20 mL) of $Mn(OAc)_2.4H_2O$ (0.51 g, 2.08 mM) was added to a suspension of dihydrazone ($npahH_4$) (1.00 g, 2.07 mM) in methanol (20 mL), accompanied by vigorous stirring for 10 mins at 50 °C. To the resulting yellow solution, KOH (0.47 g, 8.21 mM) in methanol (20 mL) was added accompanied by gentle stirring. The resulting solution was stirred for another half an hour. The solution was then kept for two days, which precipitated black coloured compound. This was suction filtered, washed with methanol and air-dried (Yield: 60 %).

(2) Preparation of $[Mn^{IV}(npah)(A)_2].nH_2O$ and $[Mn^{IV}(npah)(NN)]$ (where A = (py, 16); 2-picoline (2-pic, 17); 3-picoline (3-pic, 18); 4-picoline (4-pic, 19); NN = 2, 2'-bipyridine (bpy, 20); 1-10 phenanthroline (phen, 21); (n = 0, 1))

These compounds were also prepared by following essentially the above method by adding pyridine bases to the reaction mixture obtained by mixing $Mn(OAc)_2.H_2O$ and $npahH_4$ maintaining $Mn(OAc)_2.4H_2O$: $npahH_4$: KOH ratio of

1:1:4:10 in case of pyridine bases (Yield: 70 % (16), (17); 67 % (18), 58 % (19)) and 1:1:4:3 ratio in case of 2, 2'- bipyridine base and 1, 10-phenanthroline (Yield: 50 %, (20); 48 %, (21)).

Results and Discussion

The complexes described in the present chapter together with their colour, decomposition point and molar conductance data are set out in **Table 4.1** while the analytical and magnetic moment data are set out in **Table 4.2**. The compositions of the complexes have been deduced based on the data obtained from elemental analysis and mass spectra.

In the present chapter, we were interested in isolating and characterizing the manganese complexes in higher oxidation state using both the ligands disalicylaldehyde adipoyldihydrazone ($slahH_4$) and bis(2-hydroxy-1-naphthaldehyde)adipoyldihydrazone ($npahH_4$). Accordingly, manganese(II) acetate tetrahydrate was allowed to react with the dihydrazones in 1:1 molar ratio in the presence of KOH either as such or in the presence of pyridine bases. The reactions yielded Mn(IV) complexes in case of $npahH_4$ but the corresponding reactions with $slahH_4$ yielded complex polynuclear species which we could not characterize by conventional methods. An effort was done to crystallize the complexes in various solvent systems under different experimental conditions to establish their molecularity and structure by X-ray crystallography. Both saturated and dilute solutions of the complexes in various solvent systems such as DMSO, DMF, DMSO-CH_3CN, DMSO-CH_2Cl_2, DMF-CH_2Cl_2, each were kept for half, one and two months at ambient temperature to grow crystals. Furthermore, the solutions were gently evaporated at 40, 50 and 60 °C in hot air to promote crystal growth. Solvent diffusion methods were also used to grow crystals. Unfortunately, in all our efforts, amorphous compounds only precipitated which prevented analysis of the complexes by X-ray

crystallography. Consequently, the species obtained from these reactions in case of slahH_4 were rejected. Hence, the present chapter describes the synthesis and characterization of Mn(IV) complexes derived from npahH_4 only.

The complexes of the compositions $[Mn^{IV}(npah)(A)_2].nH_2O$ and $[Mn^{IV}(npah)(NN)]$ (where A= H_2O (15); py, (16); 2-pic (17); 3-pic, (18); 4-pic, (19); NN = bpy, (20); phen, (21); (n = 0, 1)) were isolated and have been described in the present chapter.

The formation of the complexes may be represented by the following equations

$$npahH_4 + Mn^{II}(OAc)_2.4H_2O \xrightarrow[(1:1:4)]{\text{methanol, KOH}} [Mn^{IV}(npah)(H_2O)_2]\ (15) + 2CH_3COOH + 4H_2O$$

$$npahH_4 + Mn^{II}(OAc)_2.4H_2O + A \xrightarrow[(1:1:4:10)]{\text{methanol, KOH}} [Mn^{IV}(npah)(A)_2].nH_2O + 2CH_3COOH + 4H_2O$$

(where A = py, (16); 2-pic, (17); 3-pic, (18); 4-pic, (19), (n = 0, 1))

$$npahH_4 + Mn^{II}(OAc)_2.4H_2O + NN \xrightarrow[(1:1:4:3)]{\text{methanol, KOH}} [Mn^{IV}(npah)(NN)] + 2CH_3COOH + H_2O$$

(where NN = bpy, (20); phen, (21))

All of the complexes are shining black. They are air stable. All of the complexes decompose above 300 °C without melting. This indicates that in these complexes, the metal-ligand bonds have comparatively higher ionic character.

The complexes are insoluble in water and common organic solvents such as ether and benzene. The complexes are sparingly soluble in methanol, acetonitrile and dichloromethane. They are completely soluble in DMSO and DMF. Complexes (16), (18) and (19) show weight loss corresponding to one water molecule at 110 °C suggesting their presence in lattice structure while the complex (15) shows weight loss corresponding to two water molecules at 180 °C indicating that they are coordinated to the metal centre. On the otherhand, the complexes (16) to (19) show

weight loss at 220 °C corresponding to two pyridine/2-picoline/3-picoline/4-picoline molecules while the complexes (20) and (21) show weight loss corresponding to one bipyridine and one 1, 10 phenanthroline molecules, respectively. The expulsion of these molecules at such high temperature indicates that they are coordinated to the metal centre.

Mass Spectra

The complex (17) was characterized by FAB mass spectroscopy as representative sample to assess the molecular complexity of the complexes. The FAB mass spectrum of the complex (17) in m-nitrobenzyl alcohol matrix is shown in **Fig. 4.1.1**. The spectrum of the complex shows a signal at m/z value 536, which most probably, results from the formation of $[Mn(npah)]^+$ species. The species $[Mn(npah)]^+$ in the complex results from the loss of both the 2-picoline molecules. Such a feature of the mass spectrum of the complex shows its monomeric nature.

Molar Conductance

The molar conductance values for the complexes were recorded in dimethyl sulphoxide solution at 10^{-3} M dilution. The complexes have molar conductance values in the range 1.9-3.7 $ohm^{-1} cm^2 mol^{-1}$ in DMSO. These values indicate that they are all non-electrolyte in this medium.

Magnetic Moment

The μ_B values for the complexes isolated in the present study have been given in **Table 4.2**.

The μ_B values for the complexes lie in the range 3.83-4.39 B.M. These values are consistent with manganese(IV) complexes adopting a d^3 high–spin electronic configuration [200, 108]. The μ_B values rule out the possibility of any spin-spin coupling in the solid state between unpaired electrons belonging to different Mn(IV) centres in the structural unit of the complexes.

Electronic Spectra

The important electronic spectral bands for dihydrazone ligand ($npahH_4$) and monometallic complexes isolated in the present study along with their molar extinction coefficients have been given in **Table 4.3**. The electronic spectra for complexes (15), (16), (18) and (19) have been shown in **Figs. 4.2.1-4.2.4**.

The electronic spectra of the ligand and all of the complexes were recorded in DMSO. The free ligand shows absorption bands at 290(2041), 313(2800) and 363(1852).

In octahedral Mn(IV) complexes, three spin allowed d-d transitions are expected. The position of the absorption band for $[MnF_6]$ is shown below [201].

$$450\ nm\ {}^4T_{2g} \longleftarrow {}^4A_{2g}$$

$$360nm\ {}^4T_{1g}(F) \longleftarrow {}^4A_{2g}$$

$${}^4T_{1g}(P) \longleftarrow {}^4A_{2g}$$

The third band arising from to ${}^4T_{1g}(P) \longleftarrow {}^4A_{2g}$ transition is obscured either by strong charge transfer band or by strong ligand band.

The ligand bands at 290 and 313 nm in the free ligand are shifted by 20-25, and 45-55 nm respectively in the spectra of the complexes. Such a high red shift of ligand bands in the spectra of the complexes indicates strong bonding between metal and ligand. The ligand band at 363 nm shows even more red shift of about 70-107 nm and interferes with any d-d band occurring in the region 433-470 nm. The ligand bands show almost similar feature in the complexes again as seen in case of manganese (II) complexes in Chapter-III and the uncoordinated ligands indicating that the conformation of the ligand in the complexes remains almost same as that in the uncoordinated state.

In addition to the ligand bands, the complexes invariably show a cluster of three bands in the region 400-470 nm. The position given in **Table 4.3** is the average of the position of the three bands in the complexes.

Sawyer and coworkers [202] and Percoraro etal [203] reported a band in the 545-575 nm region in mononuclear tris(glucarato), tris(gluconato) and tris(sorbitolato)manganese (IV) complexes and manganese(IV) complexes of 1-hydrox-y-2-(salicylideneamino)ethane and related hydroxyl ligand with molar extinction coefficients in 1508-2380 dm^3 mol^{-3} cm^{-1} region. They assigned this band to d-d transition. The higher value of molar extinction coefficients was attributed to the presence of adjacent charge transfer band which contributed to its intensity.

Cooper and coworkers [204] reported an intense band at ~585 nm with molar extinction coefficient equal to ~4500 dm^3 mol^{-1} cm^{-1} in manganese(IV) complexes derived from catecholate ligands. They assigned this band to a catechol → Mn(IV) LMCT band on the basis of its high molar extinction. Okawa and coworkers [205] reported a band at ~650 nm with molar extinction coefficient in 2090-3020 dm^3 mol^{-1} cm^{-1} region in manganese(IV) complexes derived from 2-substituted (salicylideneamino)phenol. They assigned this band to charge transfer transition from phenolic oxygen to manganese(IV) ion.

In the present study, the complexes show a cluster of three bands in the region 400-470 nm. The molar extinction coefficient of this band lies in the region 458-3280 cm^{-1}. These values are much less than the values reported for bands arising from transfer of charge from ligand to metal in the manganese(IV) complexes [205]. Further, these bands appear at almost the same wavelength as assigned to $^4T_{2g} \leftarrow {}^4A_{2g}$ transition of the ligand–field bands reported for manganese(IV) complexes [206]. Hence, this band is assigned to arise from $^4T_{2g} \leftarrow {}^4A_{2g}$ transition. However, slightly higher values of molar extinction coefficients of the bands than that expected from d-d bands in the manganese(IV) complexes may be attributed to arise from contribution due to LMCT bands, most probably, from naphtholate oxygen atoms to the metal centre. One of the bands in the region 400-470 nm arises may be assigned to ligand band at 363 cm^{-1}. However, it is difficult to pin-point which of the bands arises from ligand band.

Electron Paramagnetic Resonance

EPR spectra of the manganese(IV) complexes (15) to (21) have been recorded in the solid state as well as in the solution state at cryogenic temperature both. The EPR spectra of the complexes (15), (19) in the solid state and (20) in the solid state and the solution state at LNT have been shown in **Figs. 4.3.1- 4.3.3.**

The magnetic parameters for the complexes have been set out in **Table 4.3** alongwith the electronic spectral data.

The complexes (16), (17) and (18) showed featureless spectra in the solid state as well as in the solution state at R.T and cryogenic temperature. Hence, the complexes (15) and (19) to (21) only have been analyzed by EPR spectroscopy. All of these complexes exhibit highly anisotropic EPR spectra in polycrystalline state as well as in the glassy state at LNT.

The complexes (15) and (19) show two resonances with $g_{\perp} \cong 4$ and $g_{\parallel} \cong 2$ both in the solid state and in the solution state. The former resonance is of greater intensity in the solid state but for glassy state, the resonances are almost of the same intensity.

For the complexes (20) and (21), $g_{\perp} \sim 5.0$ and $g_{\parallel} \sim 2.0$ with the signal at former g-value being of low intensity is observed in both crystalline and glassy state. For both these complexes, the polycrystalline phase and magnetically dilute glassy state spectra are also well resolved. Specially the hyperfine coupling of (S = 3/2) of ^{55}Mn nucleus is well resolved in the glassy state [207, 208] for these complexes with six clean hyperfine lines at $g \cong 2$ signal suggesting that they retain the same structures in solution as in the solid state. But the EPR spectra are broad in polycrystalline state and are similar in features for both the complexes (20) and (21).

The weak transition g = 5 in these complexes probably corresponds to spin forbidden $\Delta m = 3$ transition. The assymmetric appearance of the low field signal and weaker broad resonance at $g \cong 5$ with a stronger signal at $g \cong 2$ reveal anisotropy with axial distortion.

The EPR signal at $g \cong 2$ shows ^{55}Mn hyperfine splitting constant is equal to 80 G in complexes (20) and (21). In a MnO matrix, the Mn(IV) hyperfine coupling constant of 77 G has been reported while for Mn(II), the value is 87 G.

In a crystal field of strict octahedral symmetry, a d^3 ion has $^4A_{2g}$ ground state leading to an isotropic resonance at $g \cong 2.0$ [209].

Distortion and spin–orbit coupling split the ground state quartet into two Krammer doublet separated by $2(D^2 + E^2)$ where D and E are respectively axial and rhombic zero field splitting parameter [210]. The complexity of an EPR spectra of a d^3 ion in an axial field (E/D = 0) is dependent on the magnitude of a zero field splitting parameter [211, 212]. Two limiting cases are when the value of axial zero field splitting parameter, 2D is either much larger than or much smaller than hν (0.31 cm^{-1} X-band frequencies). In the first case, when 2D is much larger than hν, the feature at low field is strong, the $g \cong 2$ component is weak. This is the observation for tris(catacholato)manganese(IV) [213] and tris(sorbitolato)manganese(IV) complexes [214]. In the second case when D is small, the $g \cong 2$ component should dominate with relatively weak signals in the low field region. This is observed for tris(thio-hydroxamato)manganese(IV) [215] and thiocarbamato complexes [216].

The EPR spectra of the Mn(IV) complexes (15) and (19) do not fit either the axial limits. Instead they exhibit marked rhombic electronic distortion. On the otherhand, for the complexes (20) and (21), the spectra fully corresponds to a Mn(IV) ion in octahedral field with axial distortion $2D \ll h\nu$.

The EPR spectra reveals that the ligand provides effective electronic environment for the metal that is highly distorted in the ground state in the complexes (15) and (19) but only slightly distorted in the ground state in the complexes (20) and (21). The distortion is sensitive to geometrical orientation of the donor atoms. The effective environment of Mn(IV) lies close to ideally pseudoctahedral environment.

The EPR spectral features of the complex (15) in the solution state at LNT remain essentially the same as that in the solid state, but that of the complex (19) is entirely changed on dissolution in DMSO. This may be attributed to replacement of water and 4-picoline molecules by solvent molecules in the DMSO solution. While water and DMSO provide the same donor atom (oxygen) in bonding to the metal centre which leads to almost unchanged EPR spectra of the complex (15) in the solution state as compared to that in the solid state. The replacement of 4-picoline molecules by DMSO molecules in complex (19) significantly changes the coordinating environment around the metal ion which changes the spectral features significantly. On the otherhand, the features of the EPR spectra of the complexes (20) and (21) remain same essentially in the solid state as well as in the DMSO solution. This indicates that the highly coordinating solvent molecules do not replace the coordinated co-ligands, bipyridine and 1, 10-phenanthroline from the complex in the solution and the complexes retain the same structure in the DMSO solution as in the solid state. The essentially contrasting EPR spectra of the complexes (15) and (19) as compared to those of the complexes (20) and (21) suggests that the nitrogen donor atoms from co-ligands bipyridine and 1, 10-phenanthroline in the complexes (20) and (21) occupy cis-position around the metal atoms by virtue of their geometry while the donor atoms from co-ligands in the complexes (15) and (19) occupy trans-positions.

Infrared spectra

Some structurally significant IR bands for free dihydrazones and monometallic complexes have been set out in **Table 4.4**. The IR spectra of free dihydrazones and complexes (15), (16), (17), (20) and (21) have been shown in **Figs. 4.4.1** to **4.4.5**, respectively.

A comparison of the IR spectral features of the complexes with that of the free ligand suggests that of the dihydrazone is coordinated to the metal centre in

enol form in all of the complexes.

OH and NH Stretching Frequency

The IR spectra of the complexes (15) to (21) show a strong broad band in the region 3000-3600 cm^{-1} with their centres lying in the region 3429-3492 cm^{-1}. The complexes do not show any band in this region which may be attributed to stretching vibration of secondary NH group of the ligands. This suggests destruction of NH groups of the ligand as a result of enolization on complexation. This fact is corroborated by the observation that these complexes do not show amide-I band. It is suggested that the band in this region arises due to water molecules either as a part of lattice of the complexes or as a part of the first coordination sphere or due to water molecules absorbed by KBr during pellet preparation which is moisture sensitive.

In order to decide upon whether the bands in this region arise due to H_2O molecules or due to moisture absorbed by KBr pellets, the compounds were heated at 110 °C and 180 °C respectively. The ensuing vapour was passed through a trap containing anhydrous $CuSO_4$. Except for the complexes (15), (16), (18) and (19), other complexes did not show weight loss either at 110 °C or 180 °C ruling out the possibility of the presence of lattice or coordinated water molecules. Complex (15) showed weight loss corresponding to two water molecules at 180 °C. The vapours turned anhydrous $CuSO_4$, blue. This confirmed that they originate from water molecules. This suggests that the complex (15) contains water molecules in its coordination sphere. On the otherhand, the complexes (16), (18) and (19) show weight loss corresponding to one water molecule at 110 °C only but no weight loss is observed at 180 °C. This shows that the complexes contain one water molecule in lattice structure but no water molecule in the first coordination sphere around the metal centre.

Amide Frequency

The uncoordinated ligand shows a strong band at 1666 cm^{-1} assignable to >C=O

group stretching vibrations. This band disappears in the complexes indicating the collapse of amide structure and coordination of the ligand in enol form.

>C=N Stretching Vibrations

The present ligand shows strong to medium intensity bands at 1630 and 1593 cm^{-1}. These bands are assignable to stretching vibration of azomethine groups [58, 215, 217]. On an average, these bands shift to lower frequency by 3-11 cm^{-1}. This indicates coordination of azomethine nitrogen atom to the metal centres. The existence of two bands of almost same intensity similar to that in the uncoordinated dihydrazone suggests that the ligand retains same conformation in the complexes as in the uncoordinated state. The appearance of two bands in the region 1586-1621 cm^{-1} in the complexes suggest that the two azomethine groups are inequivalent. This inequivalency of the two >C=N groups suggest that the two azomethine nitrogen-to-metal bonds are of unequal strength. Such inequivalency in the strength of the M←N bonds may be related to coordination of dihydrazone to the metal centre in the *anti-cis* conformation. In this configuration, one hydrazone part remains in axial position while the other hydrazone part remains in the equatorial position [218]. The axial band absorbs at lower frequency as compared to equatorial counterpart.

Amide II and νC-O(naphtholate) Bands

The free dihydrazone shows a weak band at 1530 cm^{-1}. This band arises due to mixed contributions of the amide-II and ν(C-O)(naphtholate) [219]. In the IR spectra of the complexes, this band is replaced by a strong band in the region 1503-1560 cm^{-1} which is assigned to stretching vibration of newly created NCO^- groups created as a result of enolization of the ligand.

β(C-O)(naphtholate) Band

In the dihydrazone a medium intensity band occurs at 1281 cm^{-1}. This band is similar in nature as observed in other ligands containing phenol group. Hence, this band is assigned to β(C-O)(naphtholic) [42]. This band shifts to higher frequency

by 1-18 cm^{-1} in all of the complexes. The shift of β(C-O)(naphtholic) band to higher positon suggests that the π-electron density of aromatic ring flows to metal centre through naphtholate oxygen atom.

N-N Stretching Vibration

Eliminating the bands due to C-H in-plane deformation in the 1050-900 cm^{-1} region, weak band at 1030 cm^{-1} in the present ligand have been assigned to νN-N. The νN-N band remains almost unshifted in position in all the complexes. This may be related to coordination of only one hydrazine nitrogen atom in coordination.

Pyridine or substituted Pyridine Coordination

The free pyridine bases absorb at around ~604 cm^{-1} due to in-plane-ring deformation mode [53, 177]. In the complex (17) to (19), a new medium to weak band is observed in the region 600-660 cm^{-1}. This band is assigned to arise due to in-plane ring deformation mode of pyridine bases indicating their coordination to the metal centre. The complex (21) also shows a weak band at ~660 cm^{-1} which is assigned to arise due to in-plane ring deformation modes of 1, 10-phenanthroline indicating the coordination to the metal ion.

Water Bands

The strong broad band appearing in the region 3000–3600 cm^{-1} in the complexes (15), (16), (18) and (19) may be assigned to antisymmetric and symmetric stretching vibrations of water molecules.

Lattice water absorbs in the region 1630-1610 cm^{-1} due (H-O-H) bending modes. The stretching and bending modes of lattice water overlap with >C=N stretching modes in these complexes, so they cannot be distinguished with certainty while coordinated water besides showing above modes, absorbs between 900-650 cm^{-1}. However, complex (15) shows weight loss corresponding to two water molecules at 180 °C suggesting the presence of coordinated water. On the otherhand, the

complexes (16), (18) and (19) show weight loss corresponding to one water molecule at 110 °C. This indicates that the complexes (16), (18) and (19) possesses one water molecule in their lattice structure.

Low Frequency Region Below 600 cm^{-1}

The region below 600 cm^{-1} is very complicated and several weak bands in addition to that observed in ligand are observed in the present complexes.

Infrared red spectra of the ligands containing aromatic rings in low frequency region, show bands due to the out–of–plane ring deformation [178] and out-of-plane C-H bending modes [49] and deformation vibrations of the carbonyl group [50] Ligand $npahH_4$ absorbs at 590 (s), 544(s), 533(s), 478 (w), 440 (w), 424 (s), 359 (m), 346 (m), 243 (w), 229 (w), 208 (w), 189 (w) and 171 (m). These bands occur at almost the same frequencies in the infrared spectra of metal complexes or slightly shifted. However, a few new bands which arise in the complexes may be assigned to metal-ligand vibrations.

From a stereochemical consideration of the ligand, it may be expected that a maximum of four kinds of metal-ligand vibrations may arise viz νM-O(naphtholic), νM-O(M-O-C(and M←O=C() and νM-N in the complexes. Further, the low frequency region is supposed to contain the metal ligands due to coordinated coligands water/pyridine/substituted pyridine/bipyridine/1-10 phenanthroline.

From literature records it can be said that the various metal-ligand stretching frequency region are overlapping with one another. The present ligand is the combination of adipic acid, hydrazine and naphthaldimine parts. In metal complexes, νM-O(naphtholate) is observed in the region 510-526 cm^{-1} as weak to strong bands. The ν(M-N) in the complexes has been found in 430-435 cm^{-1} as strong or weak bands. These bands occurs due to the ν(M-N) group from the azomethine part.

The bands observed in the region 265-280 cm^{-1} as weak bands in the complexes (16) to (21) are assigned to ν(M-N) band from coordinated pyridine or pyridine

bases/bipyridine/1,10 phenanthroline. The complexes do not show any new band in the region 500-400 cm^{-1} which may be assigned to ν(M-O) band due to coordinated carbonyl group either as such or in the enol form. The rules out the possibility of coordination of carbonyl oxygen atom to the metal centre.

Cyclic Voltammetry

The cyclic voltammograms of 2 mM solution of the complexes in DMSO medium with 0.1 M TBAP as supporting electrolyte were run at a scan rate 100 mV/s are shown in **Figs. 4.5.2-4.5.4** for the dihydrazone and complexes (15), (19) and (20). Satisfactory cyclic voltammograms were obtained.

The free ligand exhibits a single quasi-reversible redox couple at a potential of +0.27 V ($E_{1/2}$) (ΔE = 90 mV) against Ag/AgCl electrode.

The complex (15) shows reductive wave at -0.18 V and -1.00 V, respectively, the corresponding oxidative waves appear at -0.06 V and -0.65 V. The peak current corresponding to the redox process (Epa = -0.65 and Epc = 1.00 V) is more than double the peak current at (Epa = -0.06 V and -0.18 V). A completely reversible, Nertian one-electron transfer will have an Ep value independent of scan rate, ΔE value of 58 mV and a ratio 1.00 for cathodic to anodic peak current [220, 222]. The free ligand $npahH_4$ exhibits a single quasi-reversible redox couple at a potential of +0.27 V ($E_{1/2}$) (ΔE = 90 mV) against Ag/AgCl electrode. Hence, the observed waves of the complex at (Epa = -0.06 V and -0.18 V) is considered to be centred on the coordinated dihydrazone. Apart from the waves due to ligand centre, the other waves may be assigned to redox process centred on the metal. Accordingly, the reductive wave at -1.00 V and oxidative wave at -0.65 V might arise due to metal-centred electron transfer. This redox couple may be assigned to result from one electron transfer process and the electrode processes may be assigned to proceed as follows

$$[Mn^{IV}(L)(H_2O)_2] \underset{}{\overset{e}{\rightleftharpoons}} [Mn^{IV}(L^{-})(H_2O)_2]^{-1} \overset{e}{\rightleftharpoons} [Mn^{III}(L^{-})(H_2O)_2]^{2-}$$

On the otherhand, the complexes (16) to (18) show three oxidative and three reductive waves each. The observed oxidations of the complexes within the range -0.01 V to -0.06 V are very close to the wave observed at +0.27 V in the free ligand. Hence, this oxidation is considered to arise due to coordinated dihydrazone. Apart from the wave due to ligand centred electron–transfer reactions, the other waves may be attributed to arise due to metal centred electron transfer reactions. The appearance of two metal centred redox waves is a direct consequence of coordination of pyridine/substituted pyridines to the metal centre which function both as σ-donor as well as π-acceptor. When these co-ligands are coordinated to the metal centre they donate electron to the metal centre through σ-bond and accept electrons from the metal donated by the principal dihydrazone ligand $npahH_4$. As a result, the electron density on the metal is considerably reduced as the metal transfers its electrons in steps. Consequently, the waves due to various electron transfer reactions are visible. Both the metal-centred redox couples in the complexes are visible. Both these redox couples in the complexes are quasi-reversible as judged from the separation between the cathodic and anodic peaks. Thus, all the three waves observed in the complexes may be assigned to the various redox processes as shown below (from positive site)

$$[Mn^{IV}(L)(A)_2] \underset{\longleftarrow}{\overset{e}{\longrightarrow}} [Mn^{III}(L)(A)_2]^{-1} \underset{\longleftarrow}{\overset{e}{\longrightarrow}} [Mn^{III}(L^{-})(A)_2]^{-2} \underset{\longleftarrow}{\overset{e}{\longrightarrow}} [Mn^{II}(L^{-})(A)_2]^{-3}$$

Mn^{IV}/Mn^{III} potentials for the present complexes lie almost in the same region in which the redox potentials have been reported for many manganese (IV) complexes derived from 2-(salicylideneimino) phenols [205]. Hence, it is obvious that the high oxidation state of manganese is significantly stabilized by the present ligand.

It may be noted that the separation of the most peaks for the manganese complexes are more than 200 mV which is much higher than that for an

uncomplicated one electron redox process (0.06 V). The high peak separation, most probably, originates from a slow heterogeneous electron exchange rate rather than from intervening homogeneous reactions [223].

Armstrong [229] reported a very high quasi-reversible redox potential of 1.35 V for a Mn^{IV}/Mn^{III} couple in a Mn^{IV} complex prepared from pyrazolyl based ligand. Okawa [223] synthesized a series of Mn^{IV} complexes derived from amide based ligands and reported their potential in the range -0.70 to -0.36 V (for Epc) and –1.08 to -0.83 V (for Epa). Chakraborty and Chandra [230] synthesized two Mn(IV) complexes of some hexadentate ligands incorporating amide-amine phenolate functions in their back-bone. They characterized the complexes by CV and reported redox potential around +0.01 to -0.07 V. Koo and Lei [231] synthesized Mn(IV) complexes from tridentate ligands comprising of mixed hard-soft donors. They reported redox potentials in he range -0.107 to -0.259 V for Mn^{IV}/Mn^{III} couple while redox potentials in the range -0.617 to -0.732 V for Mn^{III}/Mn^{II} couple.

A necessary criterion for the decision of model systems for the water oxidation reaction PSII is that they must have redox potential more or atleast positive than as the minimum of 0.6 V vs NHE required to oxidize water to dioxygen at pH 7 in the biomembrane [232, 227, 228]. The manganese complexes (16) and (17) with their oxidation potentials at +0.70 and +0.65 V against Ag/AgCl may thus be an appealing model system to simulate the water oxidizing complex of WOC of PSII in plant photosynthesis [233].

The complex (19) shows only two waves with oxidative waves at -0.24 and +0.15 V and the corresponding reductive waves -0.48 and +0.02 V, respectively unlike complexes (16) to (18) each of which shows three redox couples. **Table 4.5** shows that there is a regular decrease in reduction potential in going from pyridine to 2-picoline to 3-picoline to 4-picoline complexes for the Mn^{IV}/Mn^{III} couple and a regular increase in oxidation potential for Mn^{III}/Mn^{II} couple. This is due to increasing drainage of electron

density towards the metal centre in going from pyridine to 2-picoline to 3-picoline to 4-picoline complexes (Mn^{IV}/ Mn^{III}). It appears that the metal Mn^{IV}/Mn^{III} couple in the complex (19) has merged with the ligand centred metal waves at +0.085 V (quasireversible).

The cyclic voltammetric profile for bipyridine complex (20) has been shown in **Fig. 4.5.4.** The complex (20) does not show any redox wave in the range -0.30 V to +1.5 V which suggests that in this complex there is no electron transfer reactions centred on the principal dihydrazone ligand. This complex shows a one–electron reversible wave at -0.85 V (ΔE = 60 mV) and a quasi-reversible wave at -0.64 V (ΔE = 80 mV). Hence, these redox couples are assigned to arise due to metal-centred electron transfer reactions. The one-electron reversible wave at -0.85 V (ΔE = 60 mV) and the quasireversible wave at -0.64 V (ΔE = 80 mV) are assigned to Mn^{IV}/Mn^{III} and Mn^{III}/ Mn^{II} couples, respectively. An irreversible wave at -0.96 V is observed in the complex which may be attributed to the electron transfer reaction centred on bipyridine molecule.

The complex $[Mn^{IV}(npah)(phen)]$ (21) shows redox quasi-reversible waves at +0.97 and -0.275 V, respectively. These redox waves may be assigned to Mn^{IV}/Mn^{III} and Mn^{III}/Mn^{II} couples, respectively. The complex further shows an irreversible wave at +0.25 V in the forward scan which is not visible in the return scan. It appears that some transient species is produced in the forward scan which is not stable for a longer time and reverts back to original species. This irreversible wave may be assigned to reduction of phenanthroline molecule in the complex.

The redox process may be assigned as follows

$$[Mn^{IV}(L)(phen)] \underset{}{\overset{e}{\rightleftharpoons}} [Mn^{III}(L)(phen)]^{-1} \overset{e}{\rightleftharpoons} [Mn^{III}(L)(phen^{\cdot-})]^{-2} \rightleftharpoons$$

$$[Mn^{II}(L)(phen)]^{-2}$$

Thus the irreversible wave at +0.25 V might be assigned to transient species $[Mn^{III}(L)(phen^{-})]$.

It is again imperative to mention that the present complex again shows very high quasi-reversible redox behaviour at +0.97 V, a value which is near to the high positive redox potential of the complex synthesized by Armstrong from pyrazolyl based ligands. Hence, this complex might be anticipated to be an ideal candidate to simulate the water oxidizing complex of WOC of PSII.

Conclusion

In this chapter, manganese (IV) complexes only derived from dihydrazone ($npahH_4$) have been discussed. The complexes derived from ligand $slahH_4$ were found to have very complicated stoichiometry which needed their characterizatuion by X-ray crystallography. However, our inability to grow crystals of the complexes prevented us from their crystallographic analysis. Hence, the complexes derived from $slahH_4$ were rejected.

The dihydrazone $npahH_4$ coordinates to the metal centre in enol form through azomethine nitrogen and naphtholate oxygen atoms to the manganese (IV) centre. The dihydrazone donor atoms are arranged around the manganese centres in the equatorial plane while the axial positions are occupied by the co-ligands H_2O/ pyridine/2-picoline/3-picoline/4-picoline in the complexes (15) to (19). The nitrogen atoms of the bidentate bases are arranged in the *cis*-position in the complexes (20) and (21). In these complexes, it is suggested that azomethine nitrogen atoms are in equatorial position while naphtholate oxygens are in the axial positions. The remaining two equatorial positions are occupied by bidentate bpy/phen ligands. The enolate oxygen atoms in these complexes remain uncoordinated. The ligand $npahH_4$ is suggested to be coordinated to the metal centre in the *anti-cis* configuration in all of the complexes. This configuration arises due to coordination of both azomethine nitrogen and the naphtholate oxygen atoms of the same dihydrazone molecules to the same metal centre

which introduces steric crowding in the molecule. As a result one hydrazone arm remains in the equatorial plane while the other hydrazone arm attains axial positions. In this configuration, axial azomethine group absorbs at lower frequency as compared to equatorial azomethine protons which absorb at higher frequency in the IR spectra. The complexes are proposed to have distorted octahedral stereochemistry.

The complexes have been characterized by cyclic voltammetry. The metal centres have been shown to cycle among the $Mn^{IV} \rightarrow Mn^{III} \rightarrow Mn^{II}$ oxidation states.

On the basis of results obtained from various physico-chemical and spectral studies, the structures of the complexes have been proposed as shown in **Figs. 4.6.1-4.6.2**.

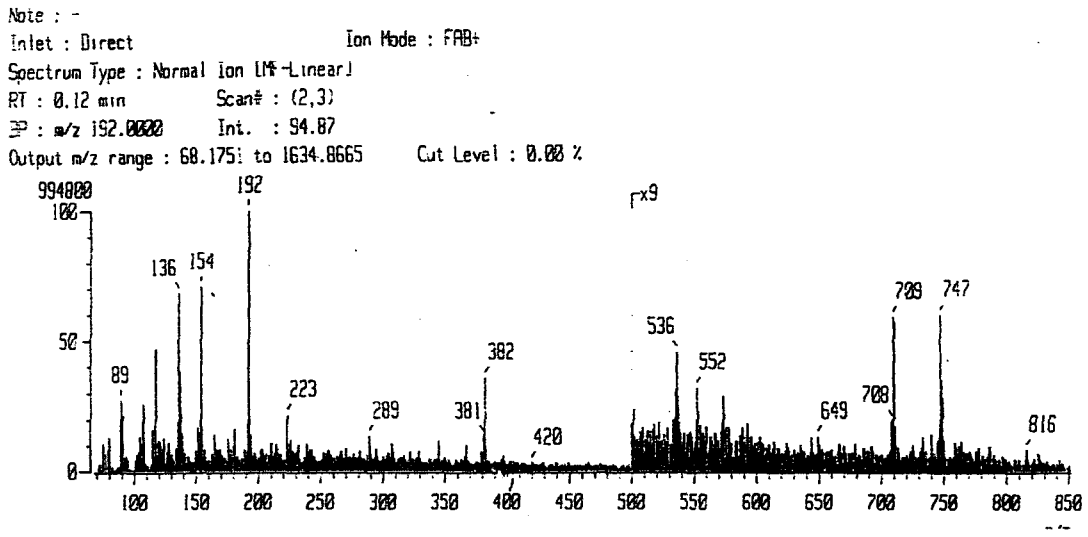

Fig. 4.1.1 Mass spectrum of complex $[Mn^{IV}(npah)(2\text{-pic})_2]$ (17)

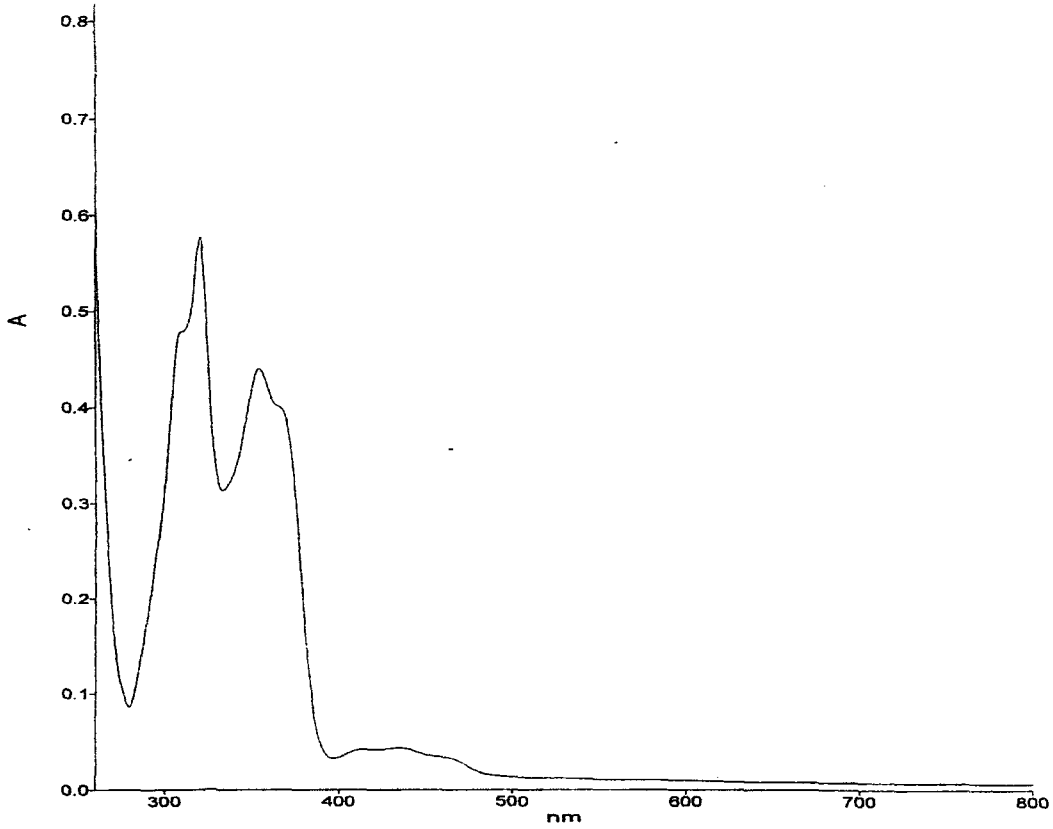

Fig. 4.2.1 Electronic spectrum for complex $[Mn^{IV}(npah)(H_2O)_2]$ **(15)**

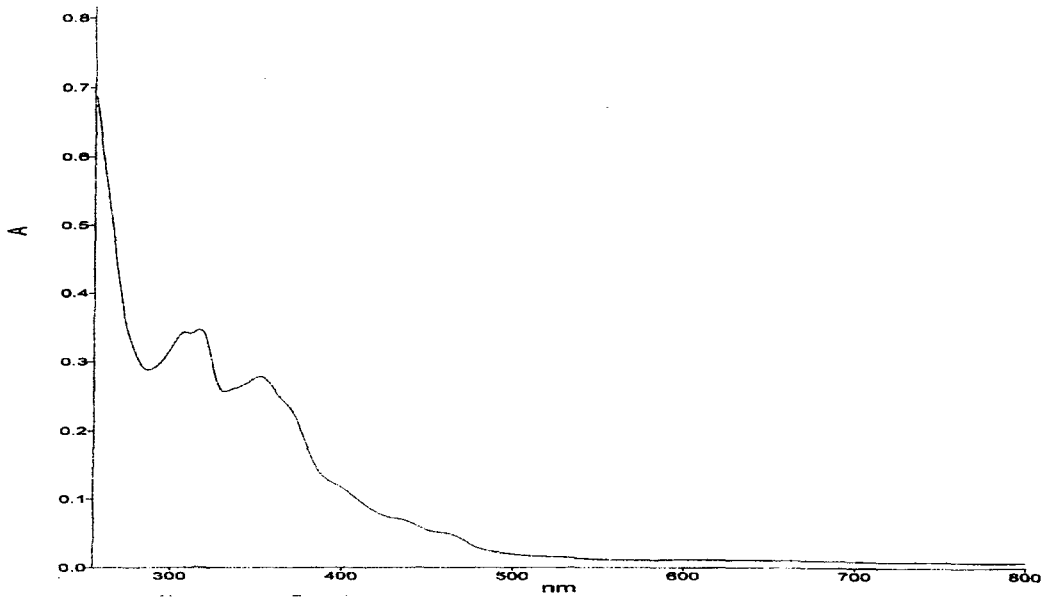

Fig. 4.2.2 Electronic spectrum of complex $[Mn^{IV}(npah)(py)_2].H_2O$ **(16)**

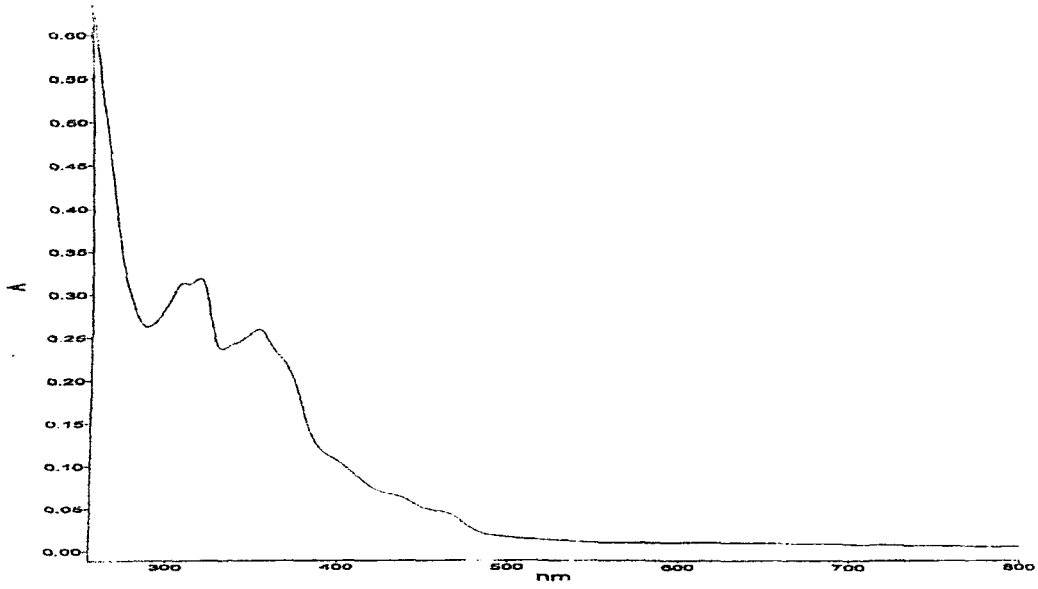

Fig. 4.2.3 Electronic spectrum of complex $[Mn^{IV}(npah)(3\text{-}pic)_2].H_2O$ **(18)**

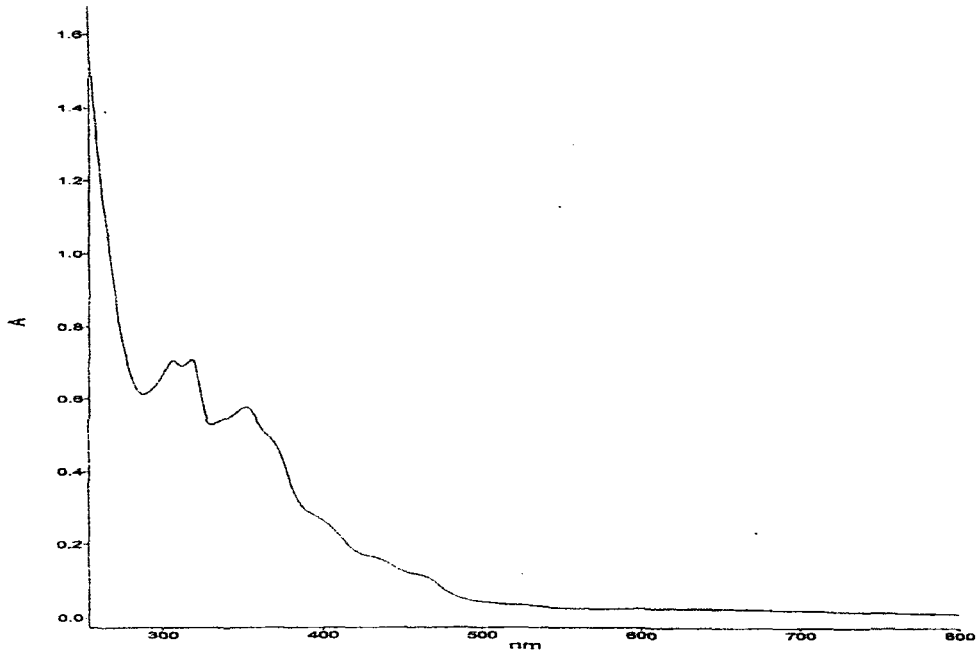

Fig. 4.2.4 Electronic spectrum of complex $[Mn^{IV}(npah)(4\text{-}pic)_2].H_2O$ **(19)**

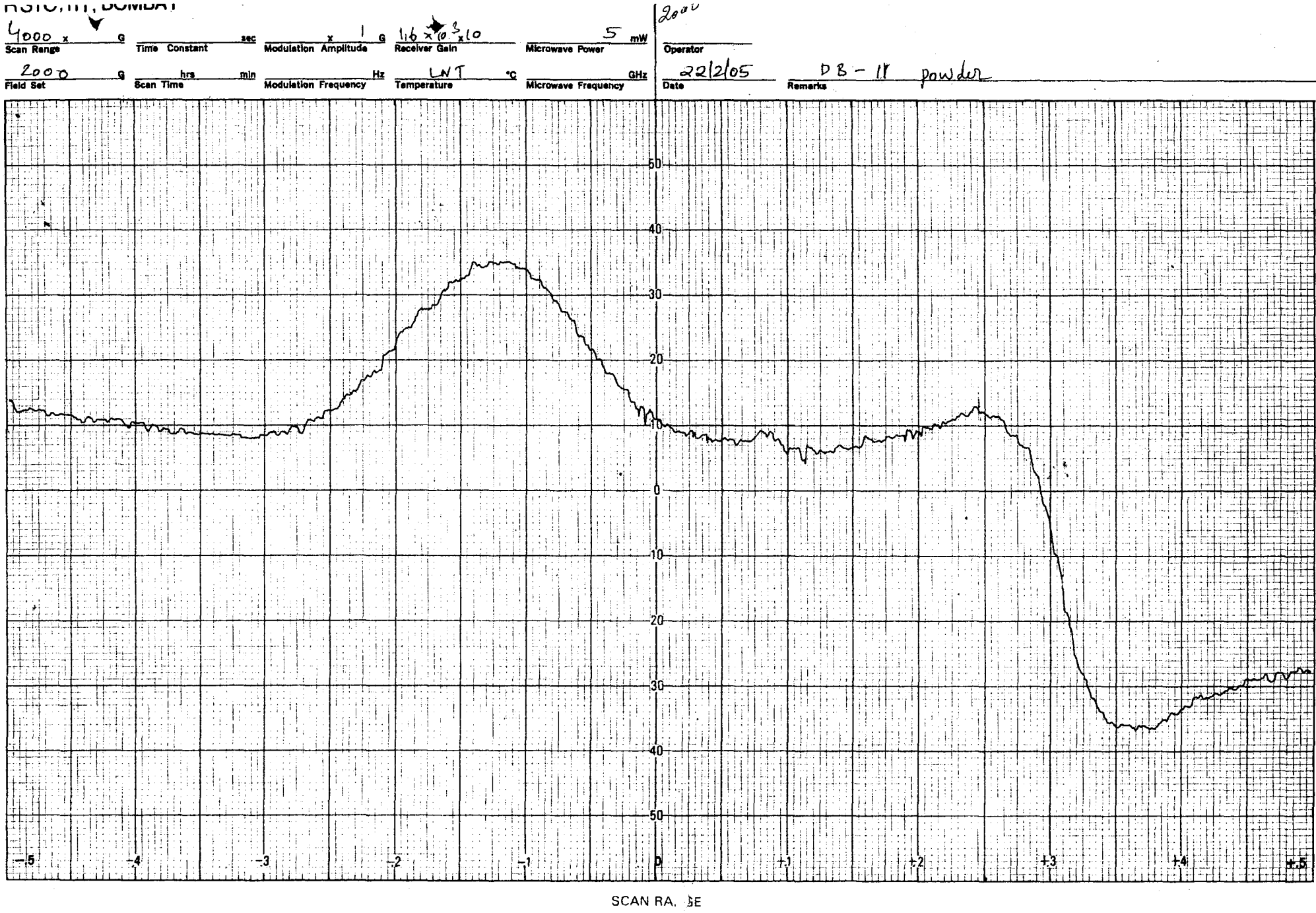

Fig. 4.3.1 EPR powder spectrum of complex $[Mn^{IV}(npah)(H_2O)_2]$ **(15)** at Temperature: LNT, Frequency : 9.1 GHz, Scan range: 4000 G and Field Set: 2000 G

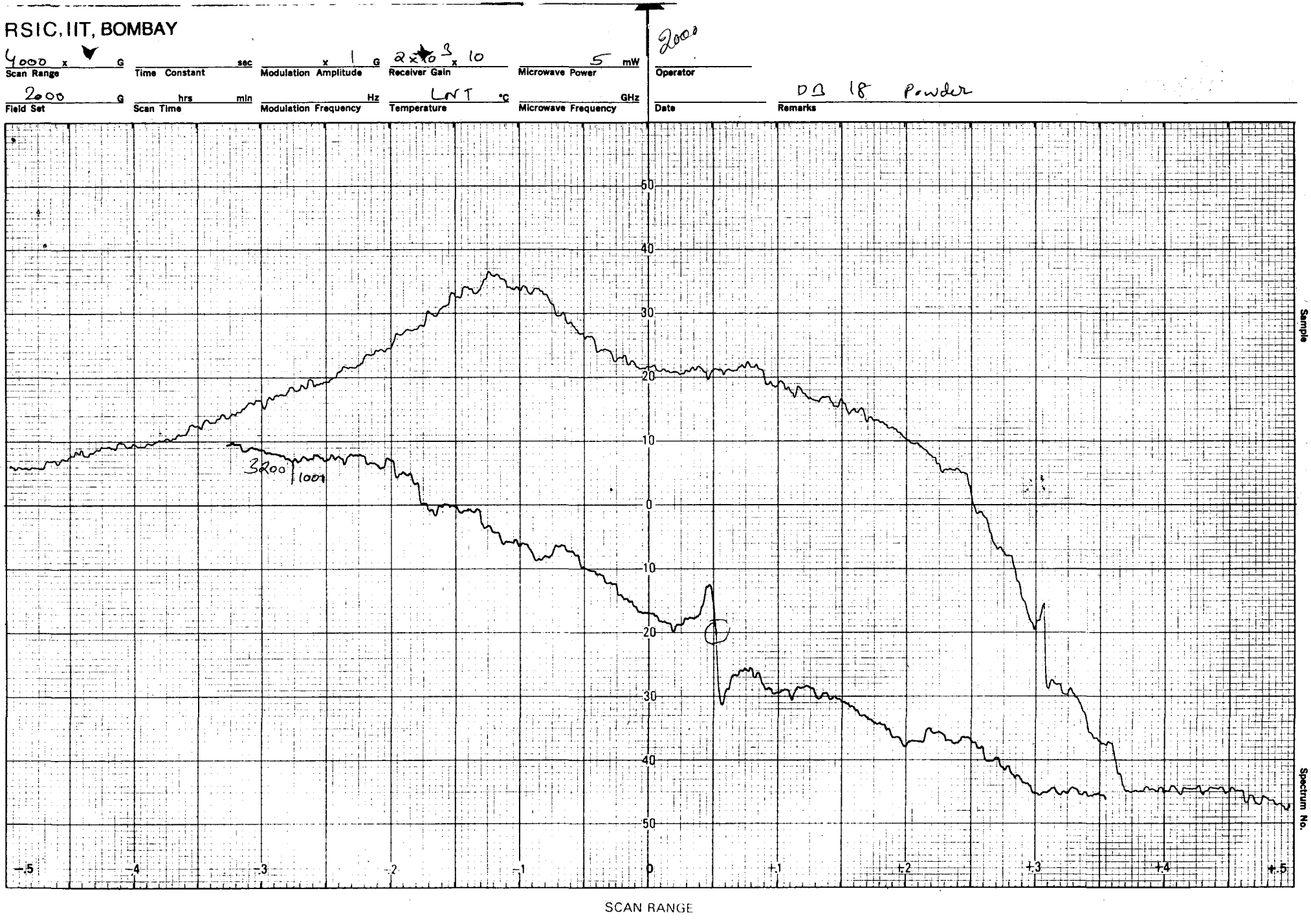

Fig. 4.3.2 EPR powder spectrum of complex $[Mn^{IV}(npah)(4\text{-pic})_2].H_2O$ **(19)** at Temperature: LNT, Frequency: 9.1 GHz, Scan range: 4000 G and Field Set: 2000 G

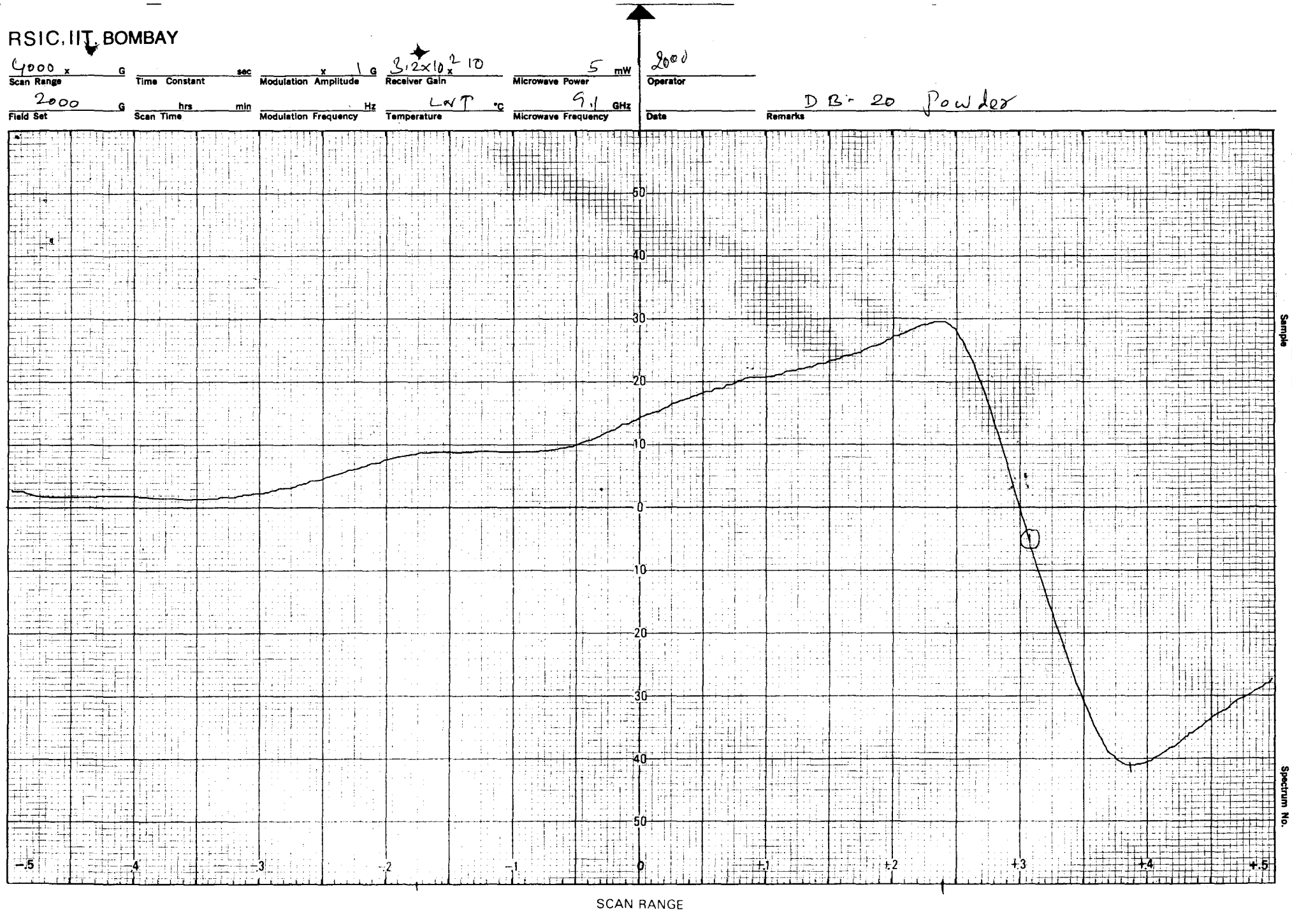

Fig. 4.3.3 (a) EPR powder spectrum of complex [Mn^{IV}(npah)(bpy)] **(20)** at Temperature: LNT, Frequency: 9.1 GHz, Scan range: 4000 G and Field Set: 2000 G

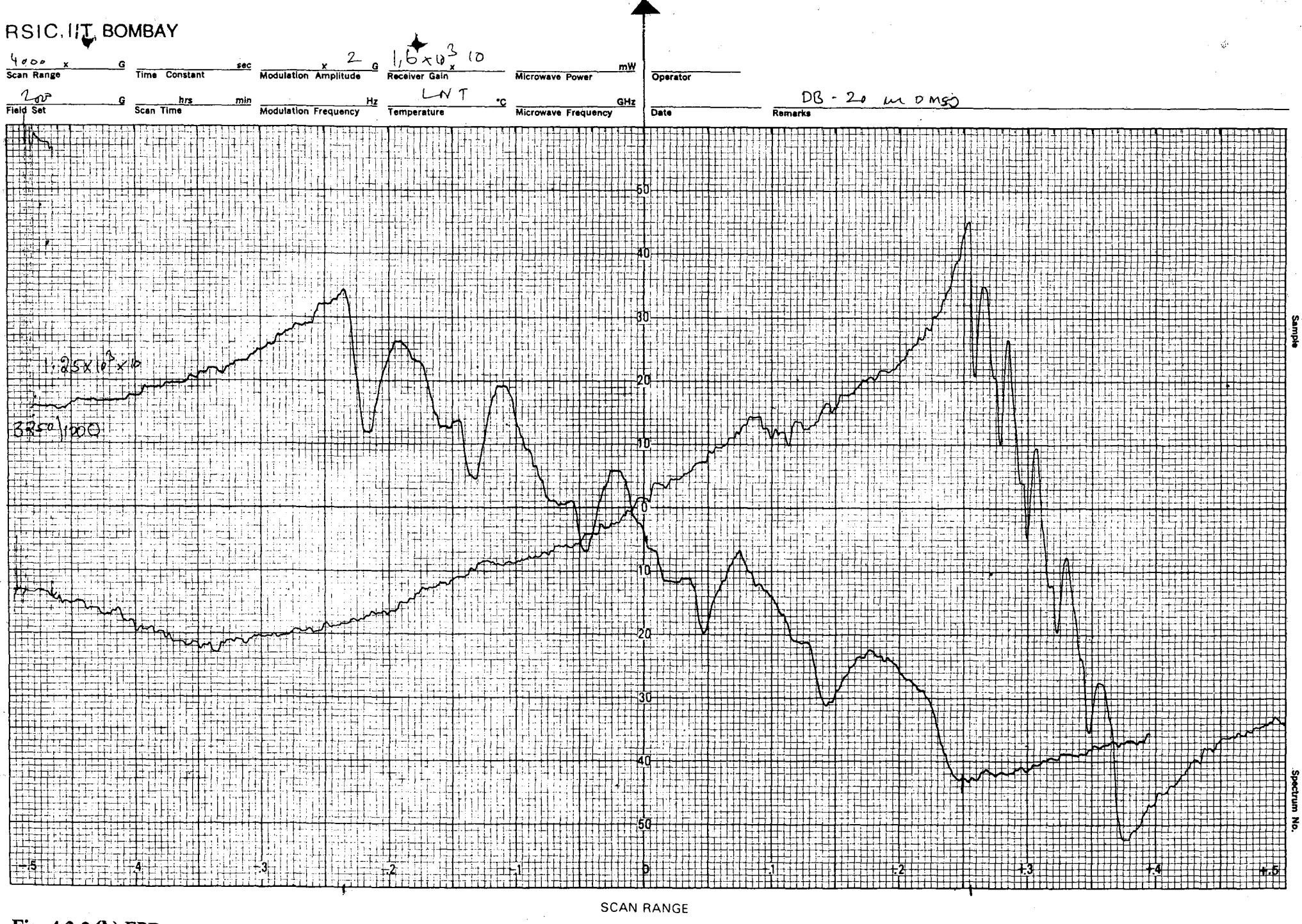

Fig. 4.3.3 (b) EPR spectrum of complex $[Mn^{IV}(npah)(bpy)]$ **(20)** in DMSO solution at Temperature: LNT, Frequency: 9.1 GHz, Scan range: 4000 G and Field Set: 2000 G

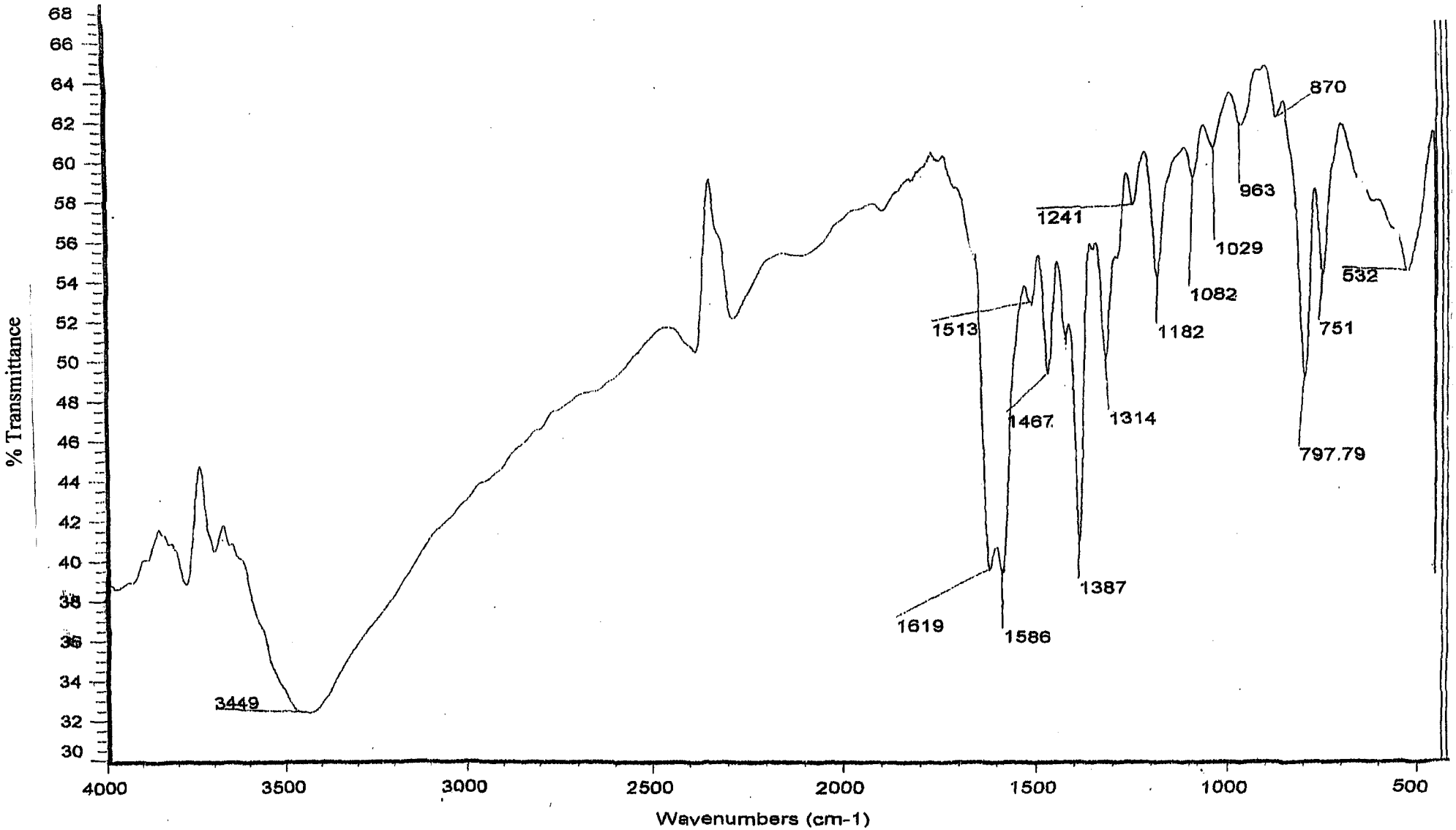

Fig. 4.4.1 (a) IR spectrum of complex $[Mn^{IV}(npah)(H_2O)_2]$ **(15)** in KBr

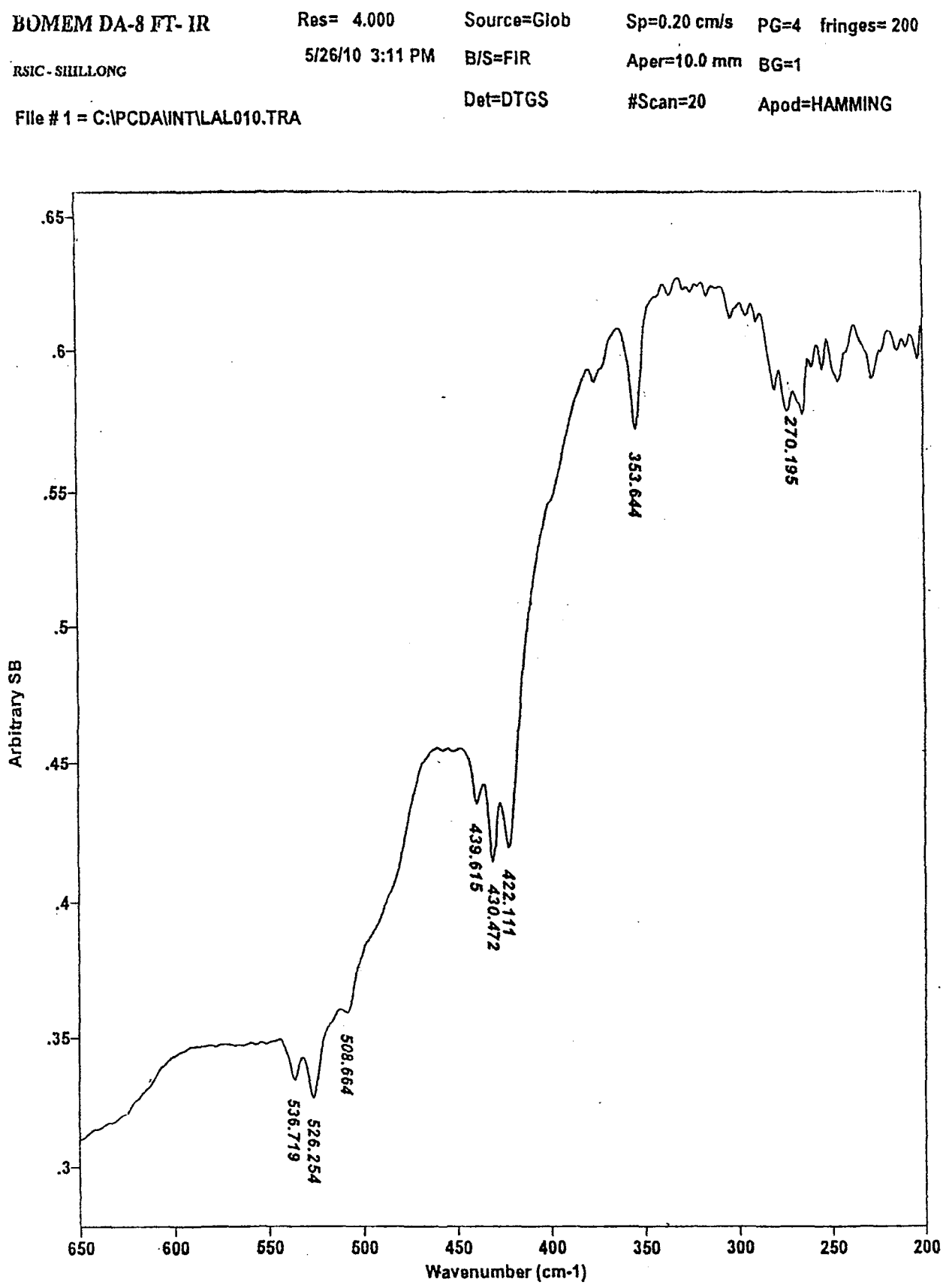

Fig. 4.4.1 (b) IR spectrum of complex $[Mn^{IV}(npah)(H_2O)_2]$ **(15)** in CsI

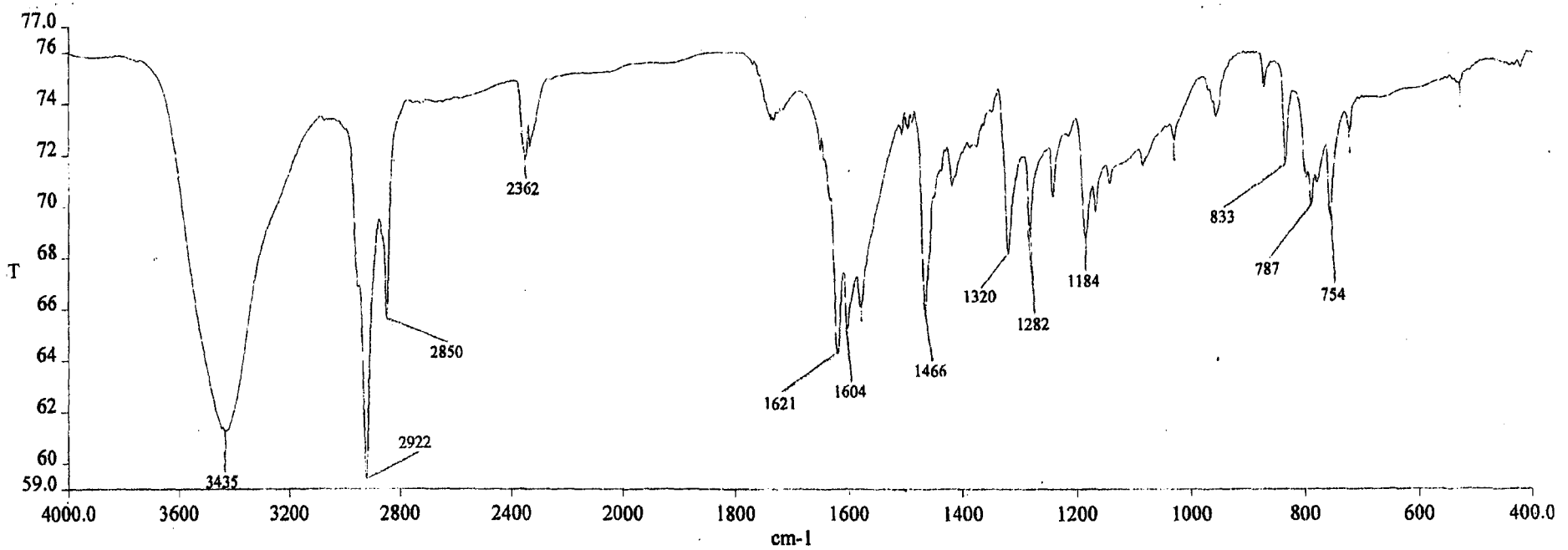

Fig. 4.4.2 IR spectrum of complex $[Mn^{IV}(npah)(py)_2].H_2O$ **(16)** in KBr

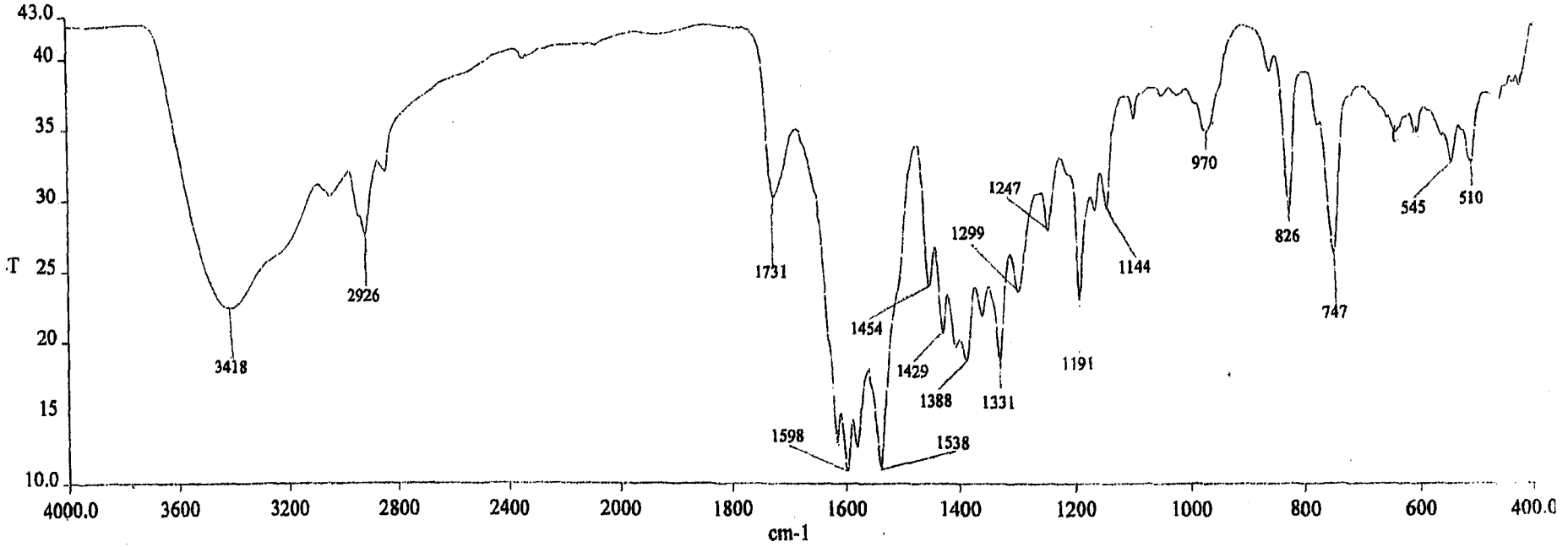

Fig. 4.4.3 (a) IR spectrum of complex $[Mn^{IV}(npah)(2\text{-pic})_2]$ **(17)** in KBr

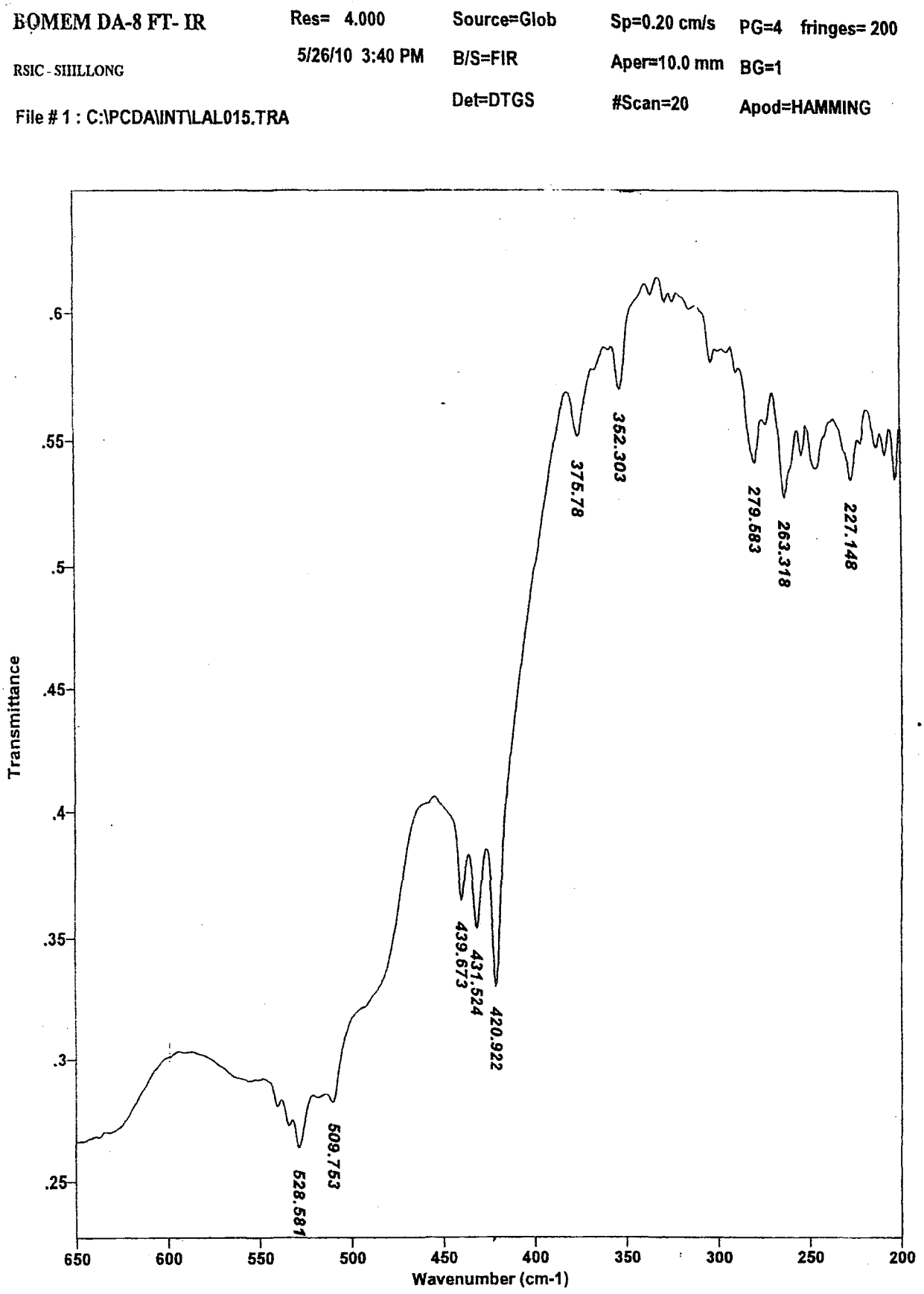

Fig. 4.4.3 (b) IR spectrum of complex $[Mn^{IV}(npah)(2\text{-pic})_2]$ **(17)** in CsI

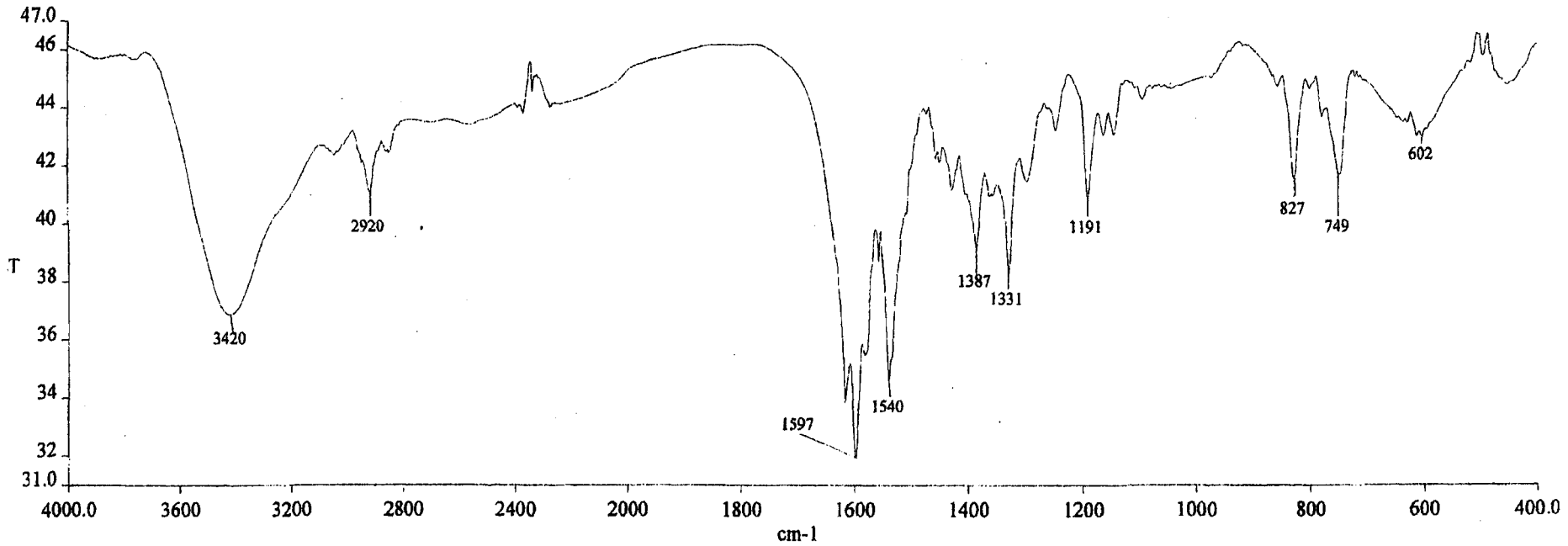

Fig. 4.4.4 IR spectrum of $[Mn^{IV}(npah)(bpy)]$ **(20)** in KBr

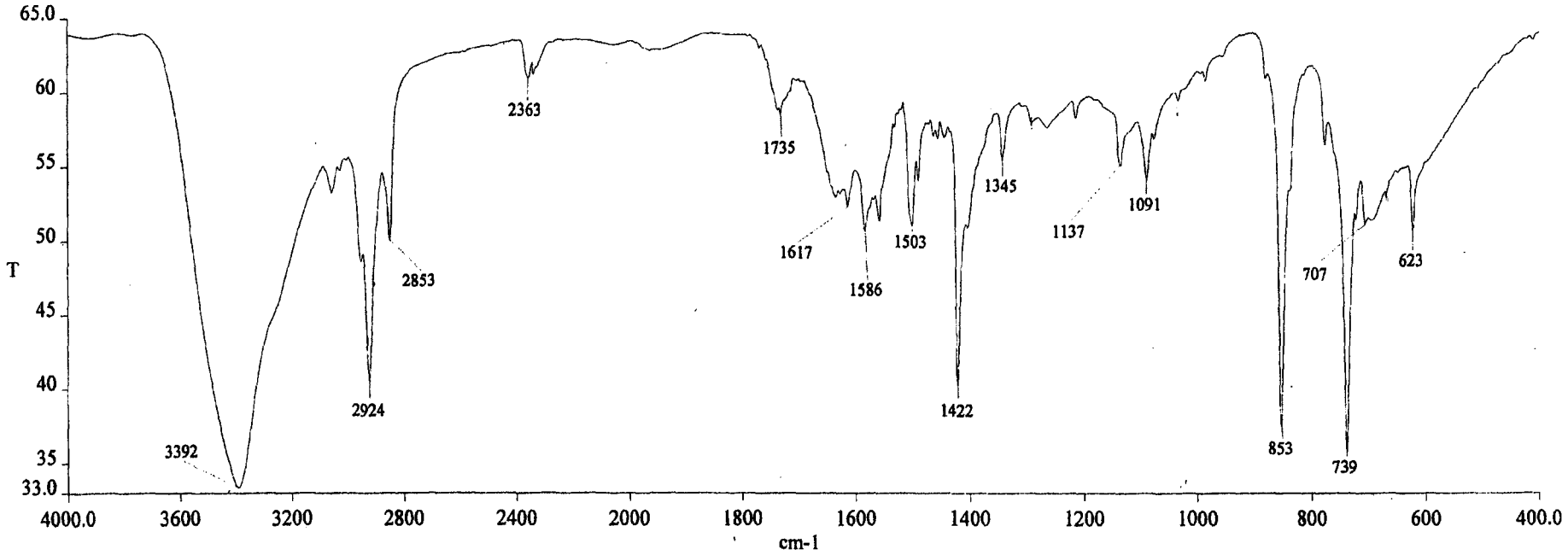

Fig. 4.4.5 IR spectrum of $[Mn^{IV}(npah)(phen)]$ **(21)** in KBr

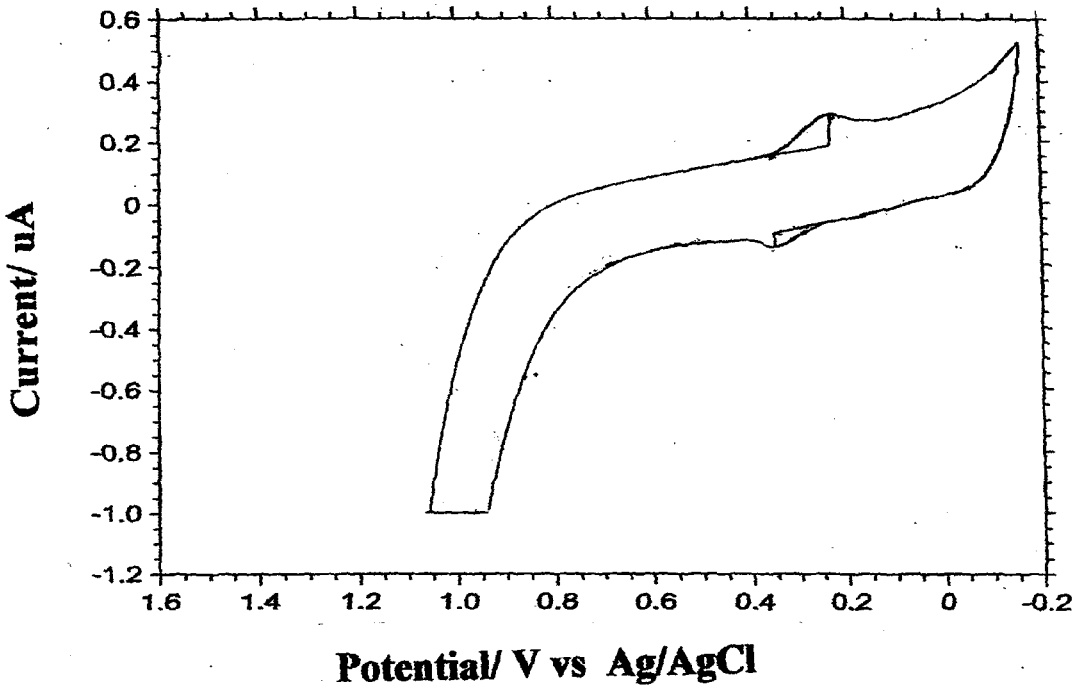

Fig. 4.5.1 Cyclic voltammogram of ligand Bis(2-hydroxy-1-naphthaldehyde)adipoyldihydrazone ($npahH_4$)

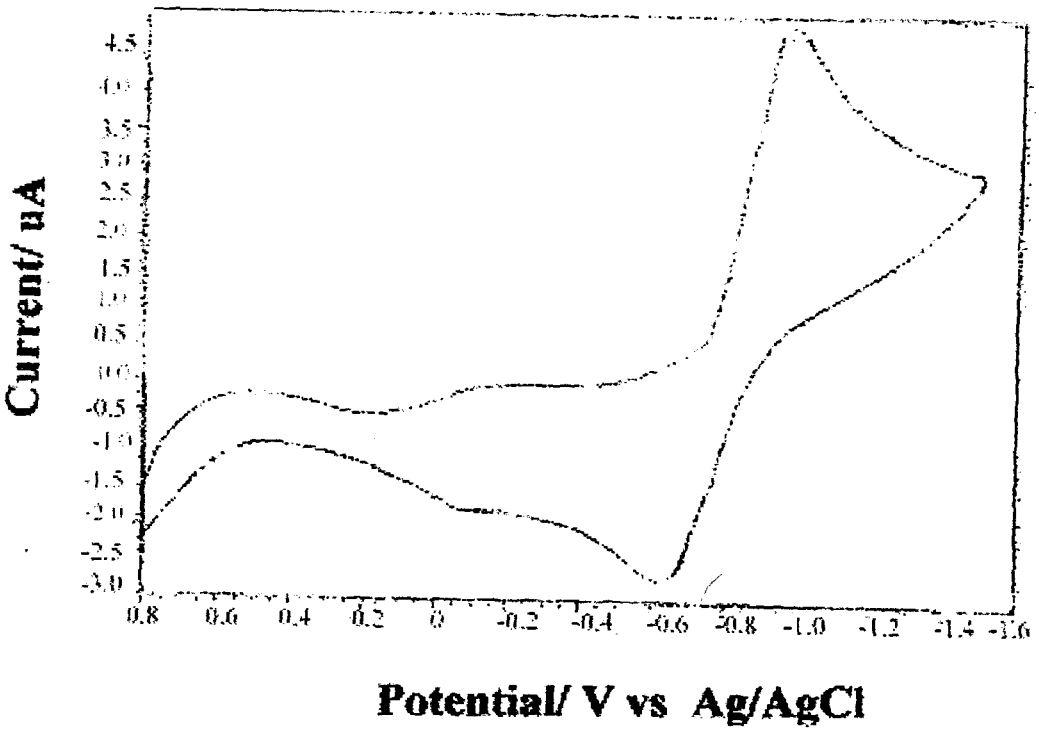

Fig. 4.5.2 Cyclic voltammogram of complex $[Mn^{IV}(npah)(H_2O)_2]$ **(15)**

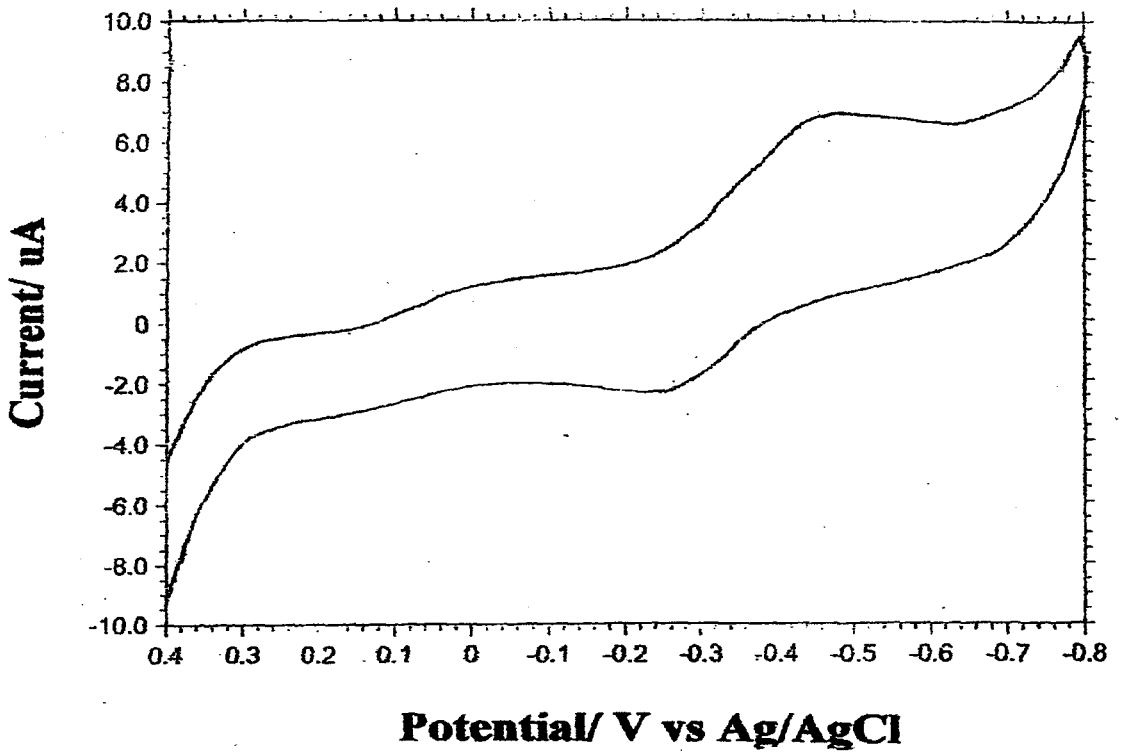

Fig. 4.5.3 Cyclic voltammogram of complex $[Mn^{IV}(npah)(4\text{-}pic)_2].H_2O$ **(19)**

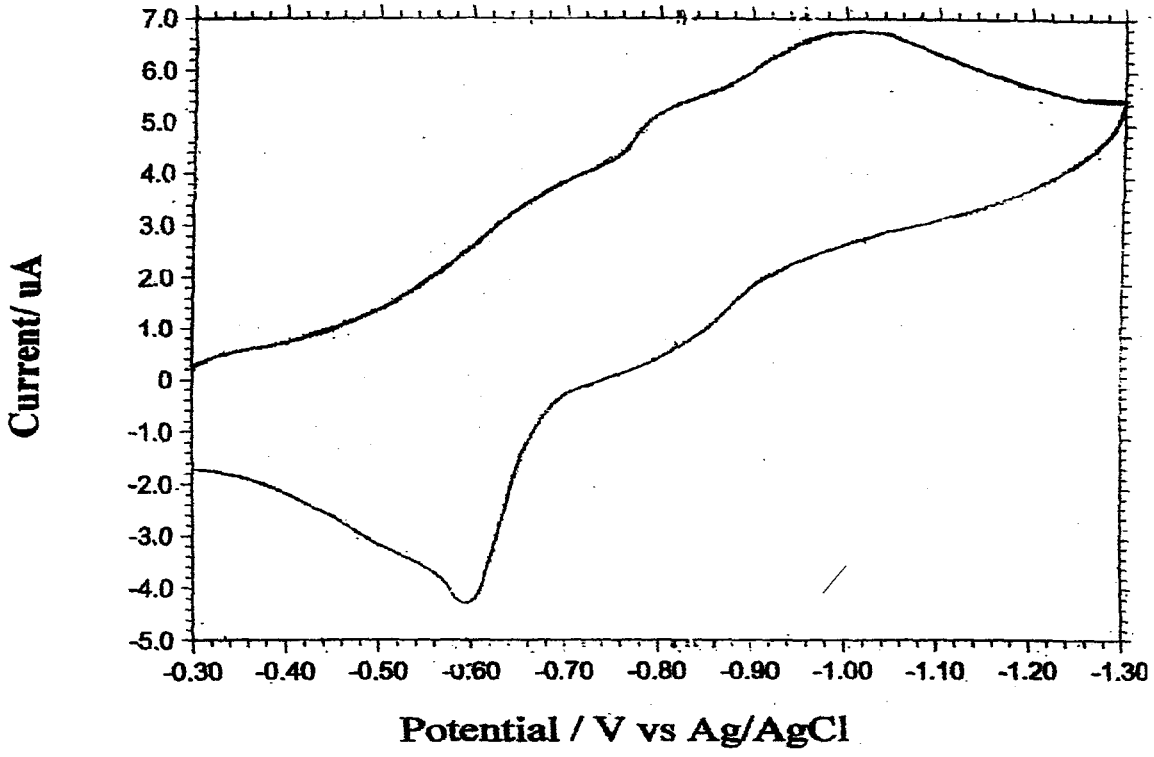

Fig. 4.5.4 Cyclic voltammogram of complex $[Mn^{IV}(npah)(bpy)]$ **(20)**

Table 4.1: Colour , Decomposition Point and Molar Conductance of Monometallic Manganese Complexes Derived from Bis(2- hydroxyl-1-naphthaldehyde)adipoyldihydrazone ($npahH_4$)

Sl. No	Complex	Colour	Decomposition Point (°C)	Molar Conductance (Λ_m) ($ohm^{-1}\ cm^2\ mol^{-1}$)
15.	$[Mn^{IV}(npah)(H_2O)_2]$	Shining black	>300	2.1
16.	$[Mn^{IV}(npah)(py)_2].H_2O$	Shining black	>300	2.5
17.	$[Mn^{IV}(npah)(2\text{-}pic)_2]$	Shining black	>300	3.7
18.	$[Mn^{IV}(npah)(3\text{-}pic)_2].H_2O$	Shining black	>300	1.9
19.	$[Mn^{IV}(npah)(4\text{-}pic)_2].H_2O$	Shining black	>300	2.2
20.	$[Mn^{IV}(npah)(bpy)]$	Shining black	>300	3.5
21.	$[Mn^{IV}(npah)(phen)]$	Shining black	>300	2.8

Table 4.2: Analytical and Magnetic Moment Data for Complexes of Bis(2-hydroxy-1-**naphthaldehyde)adipoyldihydrazone** ($npahH_4$)

Sl.No	Complex	Analysis: Found(Calcd)%				μ_B (B.M)
		Mn	C	H	N	
15.	$[Mn^{IV}(npah)(H_2O)_2]$	10.112 (9.735)	56.822 (57.345)	6.012 (6.018)	9.520 (9.412)	3.83
16	$[Mn^{IV}(npah)(py)_2].H_2O$	8.213 (7.937)	65.930 (65.801)	4.729 (4.906)	12.125 (12.120)	4.18
17.	$[Mn^{IV}(npah)(2\text{-}pic)_2]$	7.600 (7.607)	66.382 (66.390)	5.529 (5.533)	11.791 (11.618)	3.85
18.	$[Mn^{IV}(npah)(3\text{-}pic)_2].H_2O$	7.470 (7.422)	65.175 (64.780)	5.384 (5.398)	11.184 (11.336)	4.10
19.	$[Mn^{IV}(npah)(4\text{-}pic)_2].H_2O$	7.471 (7.422)	64.630 (64.780)	5.410 (5.398)	11.386 (11.336)	4.11
20.	$[Mn^{IV}(npah)(bpy)]$	8.020 (7.960)	66.011 (65.991)	4.514 (4.631)	11.950 (12.156)	4.02
21.	$[Mn^{IV}(npah)(phen)]$	7.614 (7.692)	67.100 (67.133)	4.412 (4.476)	11.712 (11.748)	4.39

Table 4.3: Important Electronic Spectral Bands and EPR data for Manganese(IV) Complexes of Bis(2-hydroxy-1-naphthaldehyde)adipoyldihydrazone ($npahH_4$)

Sl. No Ligand/Complex	λ_{max}(nm)(ϵ_{max} dm^3 mol^{-1} cm^{-1}) for conc 10^{-2} M soln			Temp	solid/ soln	g ⊥	g‖	A_{Mn} (G)
$npahH_4$	290(2041)	313(2800)	363(1852)					
15. $[Mn^{IV}(npah)(H_2O)_2]$	313(5302)	368(4210)	433(458)	LNT LNT	SOLID DMSO	4.335 4.064	2.008 1.947	- -
16. $[Mn^{IV}(npah)(py)_2].H_2O$	310(3379)	360(2700)	437(650)	-	-	-	-	
17. $[Mn^{IV}(npah)(2\text{-}pic)_2]$	310 (3100)	362(2500)	430(630)	-	-	-	-	
18. $[Mn^{IV}(npah)(3\text{-}pic)_2].H_2O$	310(3187)	358(2583)	437(667)	-	-	-	-	
19. $[Mn^{IV}(npah)(4\text{-}pic)_2].H_2O$	315(7070)	357(5785)	436(1714)	LNT LNT	SOLID DMSO	4.335 4.335	2.007 2.032	- -
20. $[Mn^{IV}(npah)(bpy)]$	310(2800)	356(2300)	470(3200)	LNT LNT	SOLID DMSO	4.780 4.223	2.036 2.007	- 80
21. $[Mn^{IV}(npah)(phen)]$	305(3671)	360(2000)	465(1000)	LNT LNT	SOLID DMSO	5.00 5.00	1.988 2.058	- 80

Table 4.4: Structurally Significant Infrared Spectral Bands of Bis(2-hydroxy-1-naphthaldehyde)adipoyldihydrazone ($npahH_4$) and its Monometallic Manganese(IV) Complexes

Sl. No	Ligand/Complex	ν(OH)+ν(NH)	ν(C=O)	ν(C=N)	Amide(II)) + ν(C-O) naphtholic	β(C-O) naphtholic	ν(N-N)	ν(M-N) in-plane ring deformation	ν(M-O) naphtholic	ν(M-N) azomethine	ν(M-N)py
	$npahH_4$	3300-3600(sbr) 3469(s) 3430(sbr) 3224(s) 3051(sbr)	1666(s)	1630(s) 1593(m)	1530(w)	1281(m)	1030(w)				
15.	$[Mn^{IV}(npah)(H_2O)_2]$	3000-600(sbr) 3449(s)	-	1619(s) 1586(s)	1513(s)	1285(w)	1029(m)	-	526(s)	431(w)	-
16.	$[Mn^{IV}(npah)(py)_2].H_2O$	3200-3600(sbr) 3435(s)	-	1621(s) 1604(s)	1515(s)	1282(m)	1029(m)	-	524(w)	433(w)	277(w)
17.	$[Mn^{IV}(npah)(2\text{-}pic)_2]$	3000-3600(sbr) 3418(s)	-	1620(s) 1598(vs)	1538(s)	1299(w)	1029(m)	660(w)	510(m)	431(w)	279(w)
18.	$[Mn^{IV}(npah)(3\text{-}pic)_2].H_2O$	3000-3600(sbr) 3500(s)	-	1600(s)	1560(s)	1290(s)	1029(wbr)	660(mbr)	525(s)	435(w)	280(w)
19.	$[Mn^{IV}(npah)(4\text{-}pic)_2].H_2O$	3000-3600(sbr) 3389(s)	-	1615(s) 1599(vs)	-	1295(s)	1029(m)	650(w)	510(w)	430(s)	274(w)
20.	$[Mn^{IV}(npah)(bpy)]$	3000-3600(sbr) 3420(s)	-	1620(s) 1597(s)	1540(s)	-	1029(w)	-	510(w)	435(s)	-
21.	$[Mn^{IV}(npah)(phen)]$	3000-3600(sbr) 3392(s)	-	1617(m) 1586(m)	1503(s)	1280(w)	1029(w)	660(w)	520(w)	430(s)	265(w)

Table 4.5: The Electrochemical Parameters for the Dihydrazone and their Monometallic Manganese (IV) Complexes (Pot vs Ag/AgCl)

Sl. No.	Ligand/Complex	Epa/V	Epc/V	ΔEp(mV)
	$npahH_4$	+0.32	+0.23	90
15.	$[Mn^{IV}(npah)(H_2O)_2]$	-0.06 -0.65	-0.18 -1.00	120 350
16.	$[Mn^{IV}(npah)(py)_2].H_2O$	+0.70 0.00 -0.50	+0.21 -0.30 -1.20	490 300 700
17.	$[Mn^{IV}(npah)(2\text{-}pic)_2]$	+0.65 0.00 -0.58	+0.20 -0.40 -0.95	450 400 370
18.	$[Mn^{IV}(npah)(3\text{-}pic)_2].H_2O$	+0.25 -0.04 -0.55	+0.13 -0.10 -0.70	120 60 150
19.	$[Mn^{IV}(npah)(4\text{-}pic)_2].H_2O$	+0.15 -0.24	-0.02 -0.48	130 240
20.	$[Mn^{IV}(npah)(bpy)]$	-0.60 -0.82 -	-0.68 -0.88 -0.96	80 60 -
21.	$[Mn^{IV}(npah)(phen)]$	+1.10 - -0.20	+0.84 +0.25 -0.35	260 - 150

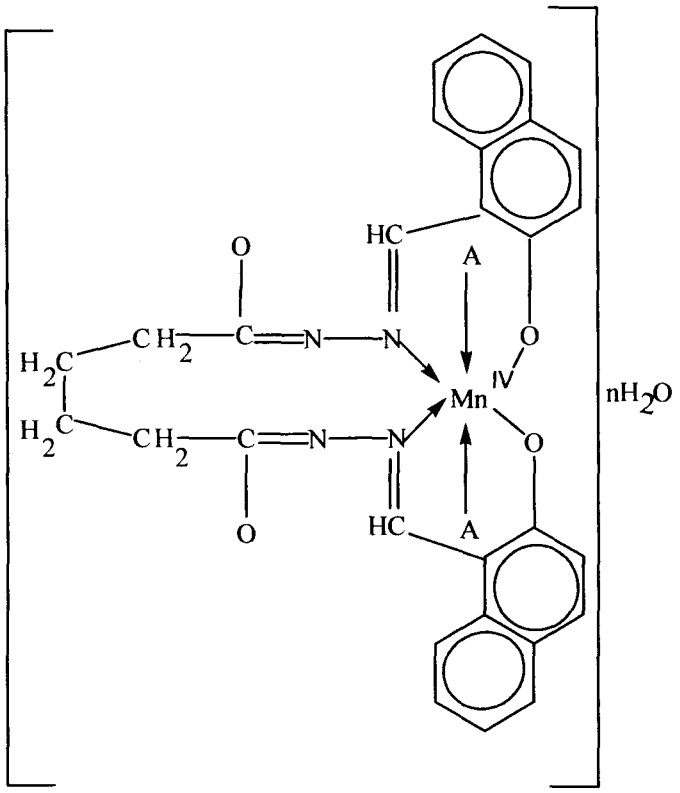

Fig 4.6.1: Suggested structure of complex $[Mn^{IV}(npah)(A_2)].nH_2O$ (where A = H_2O, **(15)**; py, **(16)**; 2-pic, **(17)**; 3-pic, **(18)** and 4-pic, **(19)**; n = 0, 1)

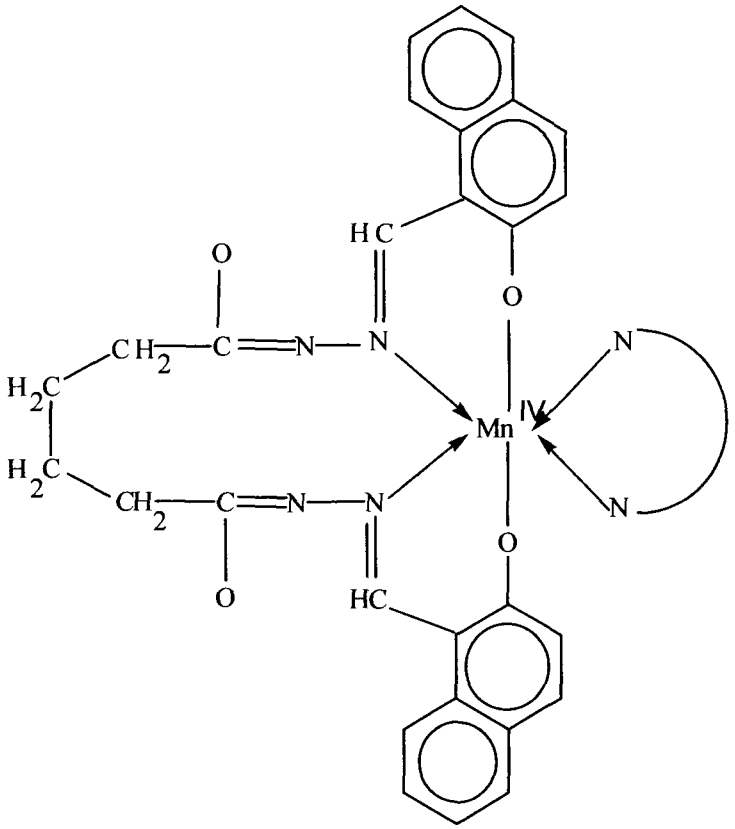

Fig. 4.6.2 Suggested structure of complex $[Mn^{IV}(npah)(\overset{\frown}{NN})]$ (where $\overset{\frown}{NN}$ =bpy, **(20)**; phen, **(21)**)

CHAPTER-V

Synthesis and Characterization of Monometallic Ruthenium (II) Complexes of Disalicylaldehyde adipoyldihydrazone and Bis(2-hydroxy-1-naphthaldehyde)adipoyldihydrazone

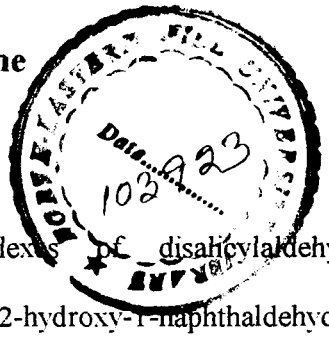

Introduction

The third chapter reports Mn(II) complexes of disalicylaldehyde adipoyldihydrazone ($slahH_4$) and bis(2-hydroxy-1-naphthaldehyde)-adipoyldihydrazone ($npahH_4$) while the fourth chapter reports Mn(IV) complexes derived from $npahH_4$ ligand only. It was observed in the third chapter that when $slahH_4$ and $npahH_4$ were allowed to react with Mn(II) acetate in methanol medium, Mn(II) complexes only precipitated while the same reaction in presence of KOH yielded Mn(IV) complexes in case of $npahH_4$ only but in case of $slahH_4$ the complexes obtained were found to have complicated compositions. Hence, they were rejected because their structures could not be unequivocally established as they failed to crystallize. This shows that the two ligands show different behaviour under similar experimental conditions. The difference in the behaviour of the two ligands might be attributed to the difference in the nature of their salicylaldimine and naphthaldimine fragments as well as reaction medium.

In the present study, ruthenium is another metal ion which has been selected for the purpose of studying the complex chemistry of the title dihydrazones. Its selection for studying its complexes stems from the fact that heterobimetallic complexes containing both ruthenium and manganese constitute a very active area of research in contemporary inorganic chemistry because of their potential in conversion of solar energy into chemical energy similar to that of PSII. In general, ligands capable of accepting electron density are known to stabilize the +2 oxidation state of ruthenium;

conversely electron-donating ligands favour the +3 oxidation state of ruthenium [234, 235].

Ruthenium Chemistry as a whole is wide and is very versatile. Another reason for selecting it in the present study is because of its extensive role in photocatalysis [236-241], photochemistry catalysis [237, 238, 242, 243, 245, 246], biology [224, 225, 247, 248] and electrochemistry [249, 182].

Ruthenium has $4d^7 5s^1$ electron configuration. And so it has the widest scope of oxidation states (from -2 valent in $[Ru(CO)_4]^{2-}$ to octavalent in RuO_4) of all elements of the periodic table and various coordination geometries in each electron configuration. For instance, in the principal lower oxidation states of 0, II, and III, ruthenium complexes normally prefer trigonal bipyramidal and octahedral structure, respectively. Indeed, until 1980's the reported useful synthetic methods using ruthenium reagents and catalysts were limited to a few reactions which include oxidation with RuO_4 hydrogenation reaction [250, 251] and hydrogen transfer reaction [251]. As the coordination chemistry of ruthenium complexes has progressed, specific characters of ruthenium have been made clear [252].

Complexes of Ru(II) and Ru(III) containing both strong and weak donor ligand have a strong potential to act as catalysts in various homogeneous reactions. Further metal catalyzed reactions have made a great contribution to the recent growth of organic synthesis and a variety of synthetic methods have been reported using complexes in stoichiometric or catalytic amounts.

A significant body of research currently exploits the synthesis of photoactive ruthenium compounds for the study of their photochemical, photophysical and electrochemical properties. These investigations have attempted to design and construct new ligands and their corresponding ruthenium complexes capable of performing useful light-induced function [253]. In these studies of Ru complexes, a metal-to-ligand charge transfer (MLCT) state of Ru(II) moiety, (^{3}CT)Ru, is responsible for all its

photochemistry.

Thus, ruthenium chemistry demonstrates, a variety of useful characteristic which include low redox potential, high electron transfer, high coordination ability to heteroatom and unique reactivity of metallic species. Its chemistry can become diverse with its different oxidation states. For instance Ruthenium(II) ion having d^6 low–spin configuration is classified to be moderately soft acid based on the Hard and Soft Acid and Base (HSAB) theory [254] so it has an ability to donate the dπ electron to a coordinated π-acceptor. Thus, the coordination to Ru(II) is attributed not only to σ-donation but π-back donation from dπ orbital of Ru(II) to π* orbital of the ligand.

A survey of literature has disclosed that few ruthenium(II) complexes with monoacylhydrazones and monoaroylhydrazones have been reported [163], yet it has failed to locate any study on ruthenium complexes of the dihydrazones.

In view of the above importance of ruthenium complexes and absence of work on the ruthenium complexes of dihydrazones, we have synthesized ruthenium complexes of the disalicylaldehyde adipoyldihydrazones and bis(2-hydroxy-1-naphthldehyde)adipoyldihydrazone and characterized them by various physico-chemical and spectral techniques.

The stoichiometry of the complexes has been judged mainly from the elemental analysis and thermoanalytical data. The structure of the complexes has been discussed in the light of conductivity, magnetic moment, electronic, EPR, IR and ^{1}H NMR spectral studies.

Electron transfer properties of the monometallic ruthenium complexes have been studied using cyclic voltammetric technique and discussed in this chapter.

Preparation of the complexes

Activation of $RuCl_3.3H_2O$

Commercial grade ruthenium trichloride (1.00 g) was activated by dissolving in concentrated HCl (5 mL) and then evaporating the solution to dryness at

110 °C on a steam bath. The process was repeated three times.

(1) Preparation of $[Ru^{II}(slahH_4)(H_2O)_2]Cl_2$ (22)

Disalicylaldehyde adipoyldihydrazone ligand (1.00 g, 2.80 mM) in methanol (20 mL) was added to a solution of $RuCl_3.3H_2O$ (0.75 g, 2.90 mM) in methanol (20 mL) maintaining 1.2:1 molar ratio and stirred for 10 mins at 50 °C. This gave a homogeneous brown suspension. The resulting reaction mixture was refluxed for 1 h which yielded a black precipitate. The precipitate was filtered in the hot condition and washed with hot methanol several times and air-dried (Yield: 71 %).

(2) Preparation of $[Ru^{II}(slahH_4)(A)_2]Cl_2$ and $[Ru^{II}(slahH_4)(NN)]Cl_2$ (where A = py, (23); 2-pic, (24); 3-pic, (25); 4-pic (26) and NN = bpy, (27); phen, (28))

These compounds were obtained by following essentially the above procedure except, that the pyridine bases were added to the stirred brown homogeneous suspension of ligand and $RuCl_3.3H_2O$ in methanol (40 mL) maintaining $RuCl_3.3H_2O$:$slahH_4$:base molar ratio either at 1:1.2:10 (in case of pyridine base) or 1:1.2:3 (molar ratio in case of bidentate bases) obtained as above. Stirring was continued for another 10 mins and then the reaction mixture was refluxed for an hour which turned the solution to dark green yielding a dark coloured precipitate. The precipitate was isolated by filtering under hot condition and thoroughly washing with hot methanol and air drying (~Yield: 65 % (23); 60 % (24); 57 % (25), (26); 68 % (27), (28)).

(3) Preparation of $[Ru^{II}(npahH_4)(H_2O)_2]Cl_2$ (29)

To the ligand suspension of bis(2-hydroxy-1-naphthaldehyde)-adipoyldihydrazone (1.00 g, 2.07 mM) in methanol (20 mL), $RuCl_3.3H_2O$ (0.54 g, 2.00 mM) in methanol (20 mL) was added at 1.2:1 molar ratio and stirred for 10 mins at 50 °C which yielded a brown homogeneous suspension. This reaction mixture was allowed to reflux for an hour. After 10-15 mins reflux, the reaction mixtures turned dark green which precipitated a dull yellow precipitate. This precipitate was

isolated by filtering the reaction mixture under hot condition and washing with hot methanol several times and air drying (Yield: 55 %).

(4) **Preparation of $[Ru^{II}(npahH_4)(A)_2]Cl_2$ and $[Ru^{II}(npahH_4)(NN)]Cl_2$ (where A= py, (30); 2-pic, (31); 3-pic, (32); 4-pic, (33)] and NN = bpy, (34) and phen, (35))**

These compounds were obtained by following essentially the above procedure except by addition of the pyridine bases to the homogeneous suspension of ligand and $RuCl_3.3H_2O$ as obtained above maintaining $RuCl_3.3H_2O$: $npahH_4$: base molar ratio either at 1:1.2:10 (in case of pyridine bases) (Yield: 56 %) or 1:1.2:3 molar ratio (in case of bidentate bases) (Yield: 63 %(30), (31), (32); 67 % (33)).

Results and Discussion

The colour, decomposition point and molar conductance of the complexes are set out in **Table 5.1**. The analytical and magnetic moment data for the complexes have been presented in **Table 5.2**. The electronic spectral data for the complexes have been presented in **Table 5.3**. The compositions of the complexes have been deduced based on the data obtained from elemental analysis.

In order to isolate complexes, preformed dihydrazones were allowed to react with $RuCl_3.3H_2O$ in methanol in 1.2:1 molar ratio either as such or in the presence of excess (10 mol) of pyridine bases or bipyridine and 1, 10-phenanthroline bases (1.2:1:3) molar ratio under reflux. This precipitated black, grey, brownish grey, brown, yellowish brown and greyish green compounds. The complexes of the following compositions were isolated.

(1) $[Ru^{II}(slahH_4)(H_2O)_2]Cl_2$ (22)

(2) $[Ru^{II}(slahH_4)(A)_2]Cl_2$ (A = py, (23); 2-pic, (24); 3-pic, (25); 4-pic, (26))

(3) $[Ru^{II}(slahH_4)(bpy)]Cl_2$ (27)

(4) $[Ru^{II}(slahH_4)(phen)]Cl_2$ (28)

(5) $[Ru^{II}(npahH_4)(A)_2]Cl_2$ (A = H_2O, (29); py, (30); 2-pic, (31); 3- pic, (32); 4-pic, (33))

(6) $[Ru^{II}(npahH_4)(bpy)]Cl_2$ (34)

(7) $[Ru^{II}(npahH_4)(phen)]Cl_2$ (35)

It is interesting to note that the metal centre is reduced from +3 to +2 in all of the complexes. The formation of the complexes may be represented by the following equations.

$$Ru^{III}Cl_3.3H_2O + slahH_4 \xrightarrow[1:1.2]{methanol} [Ru^{II}(slahH_4)(H_2O)_2]Cl_2\ (22) + 3H_2O$$

$$Ru^{III}Cl_3.3H_2O + slahH_4 + A \xrightarrow[1:1.2:10]{methanol} [Ru^{II}(slahH_4)(A)_2]Cl_2\ (23) + 3H_2O$$

(A= py, (23); 2-pic, (24); 3-pic, (25); 4-pic,(26))

$$Ru^{III}Cl_3.3H_2O + slahH_4 + NN \xrightarrow[1:1.2:3]{methanol} [Ru^{II}(slahH_4)(NN)]Cl_2 + 3H_2O$$

(NN = bpy, (27); phen, (28))

$$Ru^{III}Cl_3.3H_2O + npahH_4 \xrightarrow[1:1.2]{methanol} [Ru^{II}(npahH_4)(H_2O)_2]Cl_2\ (29) + 3H_2O$$

$$Ru^{III}Cl_3.3H_2O + npahH_4 + A \xrightarrow[1:1.2:10]{methanol} Ru^{II}(npahH_4)(A)_2]Cl_2 + 3H_2O$$

(A = py, (30); 2-pic, (31); 3-pic, (32); 4-pic, (33))

$$Ru^{III}Cl_3.3H_2O + npahH_4 + NN \xrightarrow[1.2:1:3]{methanol} [Ru^{II}(npahH_4)(NN)]Cl_2 + 3H_2O$$

(NN = bpy, (34); phen, (35))

All of the complexes are amorphous in nature. All of these complexes melt in the temperature range 210-240 °C and are stable for about one year. Beyond this period, they decompose and change to different colours. When the complexes are dissolved in DMF, after one year they yield a mixture of colour. All of these complexes are insoluble in water and other common organic solvents such as

ethanol, methanol, acetone, CCl_4, $CHCl_3$, ether and benzene etc. However, they are partially soluble in acetonitrile and completely so in DMSO and DMF.

In order to establish the structure of the complexes unequivocally with the help of X-ray crystallography, an effort was done to crystallize the complexes in various solvent systems under different experimental conditions. Both saturated and dilute solutions of the complexes in various solvent systems such as DMSO, DMF, DMSO-CH_3CN, DMSO-CH_2Cl_2, each were kept half, one and two months at ambient temperature to grow crystals. Furthermore, the solutions were gently evaporated at 40, 50 and 60 °C in hot air oven to promote crystal growth. Efforts were also done to grow the crystals from the reaction mixtures by layering a solution of the metal salts with a solution containing the ligand (ligand in methanol). Again, the metal salt solution was mixed with ligand and layered with diethyl ether and the reaction mixture was put in a big beaker containing n-hexane. Unfortunately, in all our efforts, only amorphous compounds precipitated which prevented analysis of the complexes by X-ray crystallography.

None of the complexes showed loss of weight at 110 °C which ruled out the possibility of presence of water molecules in their lattice structure. However, the complexes (22) and (29) showed loss of weight at 180 °C corresponding to two water molecules suggesting that they are present in the first coordination sphere around the metal centre. On the other hand, the complexes (23) to (26) and (30) to (33) showed weight loss corresponding to two of pyridine/2-picoline/3-picoline/4-picoline molecules in the temperature range 220-240 °C.

On the other hand, the complexes (27), (28), (34) and (35) showed weight loss corresponding to either one of bipyridine or 1, 10-phenanthroline molecules in the above temperature ranges. The expulsion of these molecules at such as a high temperature indicates that they are coordinated to the metal centre.

The loss of neutral molecules at such a high temperature may indicate their presence in the coordination sphere around the metal centre but the classification of solvent molecules on the basis TGA alone as being held in the lattice or being coordinated to the metal centre needs utmost caution in view of the fact that loss of solvent molecules/donor molecules at considerably high temperature might occur due to hydrogen bond network in the solid state of the complexes that might permeate the lattice.

The detailed decomposition studies of the complexes (22), (23), (29) and (30) have been carried out in the temperature range 80 - 250 °C and the vapours evolved have been identified by passing through a trap containing anhydrous copper sulphate and a test tube containing solution of sodium hydroxide and chloroform and another test tube containing solution of I_2 and sodium hydroxide. All of the complexes are stable in the temperature range 80-120 °C ruling out the possibility of presence of water or methanol molecules in the lattice structure. However, the complexes did show weight loss in various temperature ranges. The weight loss of the complexes selected occurs in only one step. In the complexes (22) and (29), the weight loss occurs in the temperature range 140-160 °C while in the complexes (23) and (30), the weight loss occurs in the temperature range 220-230 °C.

The vapours evolved in the temperature range 140-160 °C in the complexes (22) and (29) turned anhydrous $CuSO_4$ blue confirming that they originate from water molecules. However, the vapours evolved in none of the complexes gave yellow precipitate with a solution of iodine and sodium hydroxide in any temperature range ruling out the possibility of presence of ethanol molecules in them. Further, in the complexes (23) and (30), the vapours evolved in the temperature range 200-230 °C turned the $CHCl_3$ and NaOH solution red. This confirms that they originate from pyridine.

The weight loss commences at 140 °C in the complexes (22) and (29) and is

completed to 160 °C which corresponds to two water molecule. The loss of two water molecules in the temperature range 100-120 °C indicates that it is held in the first coordination sphere around the metal centre. On the otherhand, the weight loss commences at 160 °C in the complexes (23) and (30) and is completed at 230 °C. The weight loss corresponds to two pyridine molecules in their complexes indicating their coordinated nature.

Molar Conductance

The molar conductance values for the complexes at 10^{-3} M dilution in DMSO solution lies in the 1.2-4.7 ohm^{-1} cm^2 mol^{-1} region. A comparison of the molar conductance data for the complexes with the reported values for 1:1 and 2:1 electrolyte type complexes suggests that these complexes are non-electrolyte in DMSO [145]. Although the molar conductance values for the complexes fall in the non-electrolytic region, yet the formulation of the complexes suggests that the chloride ions must be ionic. Such a formulation of the complexes owes the most rational alternative because the formulation of the complexes keeping chloride inside the coordination would have been more offensive as it would amount to coordination of the chloride to the metal centre which is not actually. The most plausible explanation someway for the non-electrolytic nature of the complexes might be offered by suggesting strong hydrogen–bonding between chloride and hydrogen in the structural unit of the complexes.

Magnetic Moment

All of the complexes possess zero magnetic moment value. This indicates that the presence of ruthenium in +2 oxidation state in the complexes consistent with low-spin d^6 configuration of the metal centre.

Electronic Spectra

The important electronic spectral bands for dihydrazone ligands and their monometallic complexes isolated in the present study alongwith their molar

extinction coefficient have been given in **Table 5.3.** The electronic spectra for the complexes (28) and (31) to (35) have been shown in **Figs. 5.1.1-5.1.6.**

All the ruthenium complexes are diamagnetic indicating the presence of ruthenium in the +2 oxidation state. Accordingly, all these complexes contain bivalent Ru(II). Thus the ligands slahH_4 and npahH_4 containing donor atoms capable of σ and π-donation can stabilize +2 oxidation state and give rise to charge transfer bands involving metal and the ligand.

The electronic spectra of all these complexes could be recorded in DMSO in the range 350-800 nm only due to instrumental limitation which was functional in the range 350-800 nm. The ligand bands observed at 320 and 363 nm in the slahH_4 and npahH_4 respectively showed red shift as well as splitting in the complexes. The ligand bands in the complexes appear in the region 355-423 nm. The red shift of the ligand bands and their splitting into more bands as compared to that in the ligands in the complexes indicate that the bonding between metal and ligand is considerably strong. All of the complexes show a strong non-ligand band appearing in the region 429-477 nm which is of very high intensity having molar extinction coefficient in the region 678-3500 $dm^3\ mol^{-1}\ cm^{-1}$. Such a high intensity of this band indicates that it owes its origin to the charge transfer, mostly probably, from metal-to-ligand.

All of the complexes except the complexes (25), (34) and (35) show a single moderate-to-strong intensity band in the region 540-690 nm. The complexes (25), (34) and (35) show two bands in the region 545-690 nm. The ground state of ruthenium(II) in an octahedral environment is A_1g arising from t_2g^6 configuration. The excited state corresponding to the $t_{2g}^5eg^1$ configuration are $^3T_{1g}$, $^3T_{2g}$, $^1T_{1g}$ and $^1T_{2g}$, Hence four bands corresponding to the transition $^1A_{1g} \rightarrow {}^3T_{1g}$, $^1A_{1g} \rightarrow {}^3T_{2g}$, $^1A_{1g} \rightarrow {}^1T_{1g}$ and $^1A_{1g} \rightarrow {}^1T_{2g}$ are possible in the order of increasing energy. The band in 614-690 nm region have been assigned to the spin allowed $^1A_{1g} \rightarrow {}^1T_{1g}$ transition

[255]. The other high intensity band in the region between 545-604 nm in the complexes (25), (34) and (35) may be assigned to $^1A_{1g} \rightarrow {}^1T_{2g}$ transition. The high intensity of this band might be attributed to have contribution from adjacent charge-transfer band.

^{1}H NMR Spectra

An effort was done to characterize the Ru(II) complexes by ^{1}H NMR spectroscopy to decide upon the conformation of coordinated dihydrazones in the complexes. Accordingly, the ^{1}H NMR and ^{13}C NMR spectra of the dihydrazones and the complexes (25), (27), (29), (32) and (34) were recorded as representative samples. Although these complexes gave resolved ^{1}H NMR spectra, yet only the complexes (29), (32) and (34) gave only resolved ^{13}C NMR spectra. The ^{1}H NMR spectra of the ligands and complexes (25), (27), (29), (32), (34) have been shown in **Figs. 5.2.1-5.2.7** and the chemical shift changes $\Delta\delta$(ppm) are set out in **Table 5.4.**

The ^{1}H NMR spectra of dihydrazones have been recorded in DMSO-d_6 as they are insoluble in CCl_4 and $CHCl_3$. The assignments of the signals has been made to various types of protons in the light of literature records.

Maki and coworkers [39] studied ^{1}H NMR spectra of a series of dihydrazones in DMSO-d_6. They assigned the broad signal in the region δ 11.13-11.72 ppm and 12.23 -12.85 ppm to δ NH and δ OH protons respectively. The signal in the region δ 8.40-8.80 ppm was assigned to azomethine protons whereas a multiplet in the region δ 7.10-8.10 ppm to phenyl protons by them.

Lal and coworkers [46] studied the ^{1}H NMR spectra of a series of disalicylaldehyde acyl and aroyl-dihydrazones in DMSO-d_6. They assigned the singlets in the region δ 11.72-11.13 ppm, δ 11.27-11.13 ppm, doublets in the region δ 8.31-8.90 and multiplets in the region δ 6.67-8.20 ppm to phenolic –OH, secondary –NH, azomethine and phenyl protons, respectively.

Dey and coworkers have synthesized salicylaldehyde 4-methoxybenzoylhydrazone [83] and have assigned signals at 11.40 ppm and 12.90 ppm to δ NH and δOH protons, respectively. Gopinathan and coworkers [57] recorded ^{1}H NMR spectra of disalicylaldehyde malonoyldihydrazone in DMSO-d_6. They assigned the signals at δ 11.33, 11.70 ppm to δOH protons of salicylaldimine part and the signals at δ 8.90, 10.95 ppm to δNH protons. They observed a singlet at δ 3.23 and a multiplet in the region δ 6.53-7.59 ppm and attributed them to methylene protons and aromatic protons, respectively.

Ji and coworkers [92] synthesized acetyl-ferrocenepyridine-2, 6-diformyl-hydrazone and characterized it by ^{1}H NMR spectroscopy. They assigned the signal at δ 4.2 ppm (doublet) and δ 4.7 ppm (triplet) to substituted cyclopentadienyl protons. The protons on the unsubstituted cyclopentadienyl rings, the methyl groups and the amide nitrogens were found to resonate at δ 4.2 ppm (10 H, singlet), δ 2.35 ppm (6H, singlet) and δ 10.37 ppm (2H, broad singlet), respectively. The pyridyl ring protons were observed at 5.81 ppm (1H, triplet) and δ 8.4 ppm (2H, doublet), respectively.

Two proton doublet observed in the region δ 11.20-12.665 ppm downfield of TMS have been assigned to δ OH protons. The signals observed in the region δ 10.18-11.26 ppm are assigned to δ NH protons while those in the region δ 8.20-9.15 ppm to δ-CH=N protons, respectively. The multiplets appearing in the region δ 6.90-8.42 ppm have been assigned to phenyl/naphthyl protons. The dihydrazones show doublets in the region δ 2.11-2.58 ppm which are assigned to methylene groups (-CH_2-).

The appearance of methylene protons [69, 256] in the form of two doublet suggests the presence of two types of methylene groups. One doublet is assigned to methylene group directly bonded to >C=O group while the other doublet is assigned to methylene groups not directly bonded to >C=O groups.

The two proton doublet observed in the region δ 11.20-12.66 ppm in free dihydrazones assigned to δOH protons remain almost unshifted on complexation. This indicates that the phenolic/naphtholic –OH groups are not deprotonated even on complexation. The almost unshifted positions of these signals indicate the electron density over the phenolic/naphtholic –OH protons remains the same. Alternatively, this indicates that the –OH group which is hydrogen bonded in free dihydrazone also remains almost in the same situation in the complexes. This may result, from involvement of phenolic/naphtholic –OH protons in new type of hydrogen bonding, most probably with chloride ion. The δOH signals in all of the complexes presently studied appear in the form of two signals and also remain unshifted in position as compared to those in the free dihydrazone. From such a position of δOH signals to that in the free dihydrazone, we refrained from drawing any conclusions regarding involvement of phenolic/naphtholic OH group in coordination to the metal centre. However, help of the low frequency IR spectra of the complexes in the low-frequency region was taken to decide whether the phenolic/naphtholic OH group is involved in the bonding or not. Thus the complexes (29) to (35) showed a non-ligand weak to medium intensity band in the region 530-580 nm which were assigned to ν(M-O)(naphtholic) indicating involvement of naphtholic –OH group in bonding to the metal centre. However the complexes (22) to (28) did not show any new non-ligand band in the above region which ruled out the possibility of coordination of phenolic –OH group to the metal centre. Signals observed in the region 10.18-11.26 ppm also retain essentially similar position in the complexes which rule out the possibility of coordination of secondary NH nitrogen atom to the metal centre. The two signals observed in the region δ 8.26-9.15 ppm in the dihydrazones also remain almost unshifted in positions in the complexes. The position of azomethine proton signal does not lead to the conclusive evidence that azomethine group is bonded to the metal

centre. Such a feature associated with the δCH=N proton signals in the complexes is infact is due to two opposite effects.

(i) The effect of coordination on δCH=N proton would cause a downfield shift.

(ii) The effect of breaking intramolecular H-bonding between >C=N and phenolic/naphtholic -OH groups would cause upfield shift of δCH=N proton signals.

If both these effects were equal, the position of δCH=N- proton signals would remain unchanged. It appears that the effect of coordination on downfield shifting of the δ-CH=N proton signal is almost the same as that of upfield shift due to H-bonding i.e the non-shift of δ-CH=N- signals may be related to the difference of bonded species to the azomethine group i.e >CH=N...H to >CH=N→M. The appearance of δOH and δ-CH=N- signals in the form of two signals in all of the complexes may be related to coordination of dihydrazone to the metal centre in the *anti-cis* configuration. In this configuration both the azomethine nitrogen atoms of the same dihydrazone molecules are bonded to the same metal centre. This introduces steric crowding in the molecule as a result of which one hydrazone part attains axial position while other remains in equatorial position. In this configuration, the axial azomethine protons absorb at lower field as compared to equatorial azomethine protons which absorb at higher field. The appearance of two signals only indicates the absence of coupling between axial and equatorial azomethine protons. The pattern of the azomethine proton signals is assymmetric in nature in the complexes. This is the consequence of interchange between the two types of azomethine groups as a result of nitrogen inversion around the metal centre [257].

Another important feature of ^{1}H NMR spectra of the complexes is the downfield shift shown by methylene protons which appear in the δ 2.20-2.58 ppm region although the possibility of interferences of these signals with the signals arising from

water absorbed by DMSO-d_6 cannot be ruled out. These signals shift downfield by 0.03-0.16 ppm.

All of these ^{1}H NMR spectral evidences in combination with IR spectral evidences indicate that probably N_2O_2 coordination chamber is occupied by metal in the complexes. The azomethine nitrogen atoms invariably constitute the coordination sites of N_2O_2 coordination chamber in all the complexes. The naphtholic oxygen atoms constitute the coordination sites in the complexes (29) to (35) while in the complexes (22) to (28), these are the carbonyl oxygen atoms which constitute coordination sites around the metal centre. This is also supported from the fact that the δNH signals in the complexes (29) to (35) derived from npahH_4 and δOH, δCH=N signals in all of the complexes appear in the form of two signals. Another point of interest is the methylene proton signals which again appear in the form of two resonances and have doublet character in the complexes. The npahH_4 complexes show a doublet at δ 1.66 ppm. This signal is invariably present in the ^{1}H NMR spectra of the complexes in the region δ 1.65-1.72 ppm. But we were unable to assign the origin of this signal in the ligand and its complexes.

The complexes (25) and (32) show an intense signal at 2.54 and 2.50 ppm. Although the signals at the same position are also present in the ^{1}H NMR spectra of the free dihydrazone, yet the signals in the complexes have more intensity than those in the free dihydrazone. Hence, these signals are assigned to have contribution due to the methyl protons of 3-picoline molecules present in the complexes in addition to the signal from the methylene protons of coordinated ligands.

Methyl proton signals appear at δ 2.32 ppm in free 3-picoline molecules [256, 258]. In metal complexes (25) and (32), these signals appear at δ 2.54 and 2.50 ppm respectively and thus downfield shifted by 0.22 ppm and 0.18 ppm, respectively. This downfield shift is the result of drainage of electron density from Ru(II) atom to ring

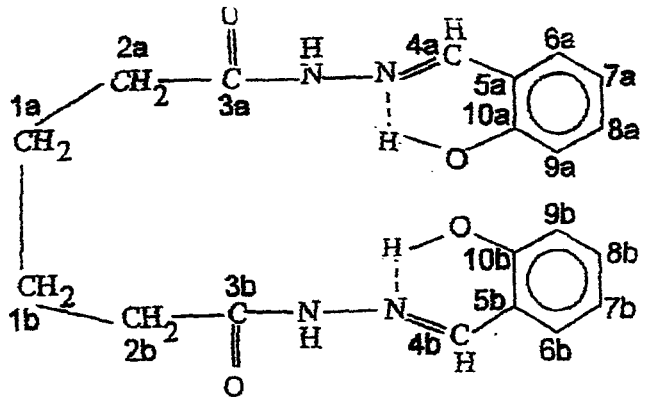

Fig. 5.5.1 Labelled structure of Ligand Disalicylaldehyde adipoyldihydrazone ($slahH_4$)

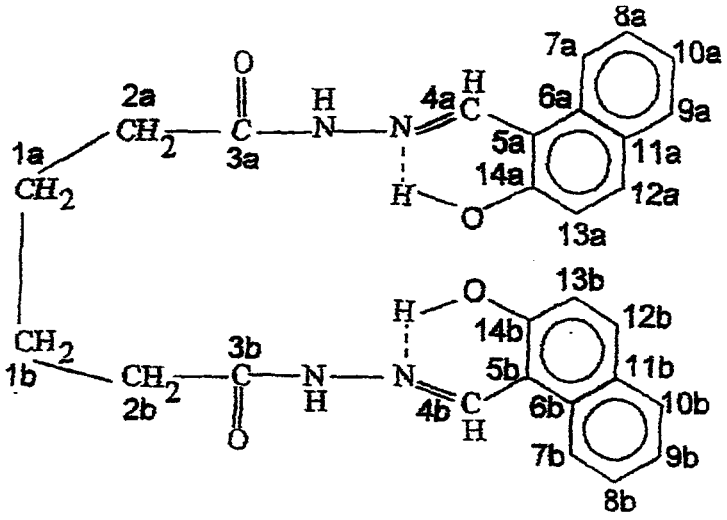

Fig. 5.5.2 Labelled structure of Ligand Bis(2-hydroxy-1-naphthaldehyde) adipoyldihydrazone ($npahH_4$)

nitrogen atom which increases the electron density on ring nitrogen atoms making it more electronegative than that in free pyridyl ring. Consequently, ring nitrogen atom withdraws electrons towards itself. Hence, the electron density on all carbon atom decreases which causes withdrawal of the electron from C-C bonds leading to downfield shift of methyl protons. Further, two signals are observed in the downfield region in the ^{1}H NMR spectra of the complexes which may be assigned to o-proton of 3-picoline molecules [259]. This indicates that the signals due to o-protons of 3-picoline are downfield shifted. Such features associated with the o-protons of 3-picoline confirms flow of electron density from ring nitrogen atoms of these donor molecules.

^{13}C NMR Spectra

The ruthenium complexes (29), (32) and (34) derived from $npahH_4$ have been characterized by ^{13}C NMR spectroscopy. The ^{13}C NMR spectra for $npahH_4$ and the complexes (29), (32) and (34) have been shown in **Figs. 5.2.8- 5.2.12**. The chemical shift δ(ppm from $SiMe_4$) and the chemical shift changes Δδ(ppm) accompanying the coordination of the ligand in the complexes are set out in the **Table 5.5**. The assignments for the ligand have been deduced taking into account the shift in the resonances of naphthyl ring carbon atoms caused by the substituents azomethine group and naphtholic –OH group. The numbering scheme for the carbon atoms in both ligands and complexes is the same as shown in **Figs. 5.5.1** and **5.5.2** the carbon atoms in the axial and equatorial positions have been designated by the letters 'a' and 'b', respectively.

As a result of coordination, some of the signals are shifted upfield whereas others are shifted downfield indicating coordination of the ligands to the metal centre. The number of signals observed in the complexes is almost same as those in the ligand. This suggests that the ligand retains the same conformation in the complexes as that in the uncoordinated state. The effect of metal ion on carbon resonances of

naphthyl ring shifts downfield the signals for C(6), C(8), C(9), C(10), C(12) and C(13) in the complex (29) by -0.04 to -0.89 ppm. The shift to downfield of the signal due to C(3) rules out the possibility of coordination of >C=O group to the metal ion.

The shift of C(3) signal downfield suggests decrease of electron density on this carbon atom. This indicates drainage of electron density from C(3) carbon atoms. The decrease in the electronegativity on C(3) carbon atom might be attributed to the nature of metal centre Ru(II) ion that has a d^6 configuration in which t_{2g} metal is completely filled. As a result, the metal functions as an electron rich metal. Hence, it functions as a better π-donor and worse σ-acceptor. Consequently, Ru(II) donates electron through π-back bonding to a greater extent to the ligand than it accepts electron through σ-band from the ligand. As a result, it donates electrons to azomethine nitrogen atoms which increases the electron concentration on a nitrogen atoms thereby. Hence, the N-atoms withdraw the electron density from the naphthyl ring carbon atoms. As a result, the naphthyl carbon atoms also show downfield shift except the carbon atoms C(4), C(11) and C(14).

It is, therefore, reasonable to expect that the C(14) and C(4) resonances will remain either unshifted or shift upfield since they are closer to the coordinated oxygen and nitrogen atoms. As a consequence, the signal for C(14) which in the free ligand were at 167.72 ppm could be either at 167.72 ppm or at lower position than this in the complexes. In the complex (29), a signal at 167.72 ppm is observed. Hence, this signal is assigned to C(14) carbon atoms in the complex. There is one more signal at δ 172.65 ppm which was assigned to C(3) carbon atoms of carbonyl group on the basis of its intensity. Although, the other signals could give still higher upfield shift but none of them could be assigned to C(14) carbon atoms because they correspond to remaining carbon atoms. On this basis, the signals in the region δ 156.50-157.51 ppm could only be assigned to the azomethine carbon atoms C(4) which in the free ligands were at δ 157.52 and 156.55 ppm giving a chemical shift

change of +0.06 in the complex indicating that the electron density on this C-atom is increased considerably in the complex. The signals in the region δ 142.15-144.62 ppm in the complex could be assigned to C(11) while those in the region 131.27-132.09 ppm to C(6) carbon atoms. These carbon atoms absorb at 144.62, 142.18 and 132.04, 131.30 ppm, respectively, in free dihydrazone giving chemical shift changes of the order of either 0.01 and -0.08 ppm, respectively. The signal in the region δ 118.01-118.61 ppm is assigned to C(5a) and C(5b) carbon atoms which in free ligand appeared at δ 118.60 and 118.05 ppm giving zero chemical shift change in complex (29). Such a feature associated with C(5a) and C(5b) resonances may be attributed to the combined effect of donation of electron density from azomethine nitrogen atom in the opposite direction. On the otherhand, in the complex (32) and (34), almost all carbon atoms show upfield shift as compared to their position in the uncoordinated dihydrazone except the carbon atoms C(11) and C(10) in complex (32) which show a downfield shift of about -0.01 and -0.2 ppm and the carbon atoms C(11) and C(7) in the complex (34) show a downfield shift of -0.02 and -0.19 ppm, respectively. Such an upfield shift of naphthyl ring carbon resonances may be attributed to coordination of 3-pic and bpy molecules in the complexes (32) and (34), respectively. These donor molecules donate electrons to Ru(II) atom, which by virtue of being a bad acceptor and good donor, transfer the electron density to nitrogen atom which after crossing a threshold is not able to retain the received electron density and then transfer the received electron density from 3-pic and bpy molecules to all carbon atoms in the molecule. As a result, almost all the carbon atoms in the complexed ligand molecules show an upfield shift.

In view of the above spectral features and discussions of the ^{13}C MR spectra of both the complexes (32) and (34), it is reasonable to suggest that the ligand and metal complexes have same symmetry and that the dihydrazone is coordinated to the metal centre in anti-cis configuration.

Some new signals have been observed in the ^{13}C NMR spectrum of the complex (32)(given in **Fig. 5.2.11**), which are present neither in the spectrum of free ligand nor in that complex (29). Hence, these signals are assigned to various carbon atoms of 3-picoline. In the free 3-picoline molecule, the signals due to C_2, C_3, C_4, C_5, C_6 and methyl carbon atoms appear at δ 150.1, 133.1, 136.4, 148.8 and 18.1 ppm while the corresponding signals in the complex appear at 146.48, 130.11, 136.82, 121.04, 146.48 ppm and 23.67 ppm [54]. A comparison of the free 3-picoline molecules suggests that they are all upfield shifted except the signals due to methyl group which is downfield shifted. Such an upfield shift of all carbon atoms in the picoline molecules in complex (32) suggests coordination of 3-picoline molecules to the metal centre through pyridyl ring nitrogen atom. This may be rationalized in terms of the fact that when lone pairs of electrons present on pyridyl N-atom is donated to the metal centre, the electronegativity of the pyridyl N-atoms decreases. As a result, the bonding pairs of electrons which were initially polarized toward nitrogen atom become polarized towards carbon atoms. This cause upfield shift of the signals due to them. It is worth noting that these signals are very weak and can be located only at the high resolution.

One more point that needs comments is that majority of the signals appear as pairs in free dihydrazone. Each resonance from a pair corresponds to the axial and equatorial carbon atoms. The ^{13}C NMR spectra of the complexes also show more number of signals than those in the free dihydrazone. The additional signals may be attributed to the effect of coordination of metal centre to the ligand molecule. Such feature of ^{13}C NMR spectra of the complexes support the *anti-cis* configuration of the ligand in free state as well as in the complexes as deduced from consideration of IR spectra and ^{1}H NMR spectra of the complexes.

Infrared Spectra

Due to complicated nature of spectra only a few bands have been selected in order to observe the effect of some structurally significant IR bands for free

dihydrazones and the monometallic ruthenium complexes have been set out in **Table 5.6**. The IR spectra of the complexes nos. (22), (23), (25), (27)-(30), (32), (34), have been shown in **Figs. 5.3.1-5.3.9**.

A comparison of the IR spectra of the complexes with those of the free ligands $slahH_4$ and $npahH_4$ suggests that the dihydrazones are coordinated to the metal centre in keto form in all of the complexes.

The uncoordinated ligands $slahH_4$ and $npahH_4$ show strong broad band centred at 3445 and 3469 cm^{-1}, respectively and two rather strong bands at 3204, 3065 and 3224, 3051 cm^{-1}, respectively. While the first strong broad band is assigned to νOH of o-hydroxybenzaldehyde/o-hydroxynaphthaldehyde part of the dihydrazone; those at 3204, 3065 and 3224 and 3051 cm^{-1} are assigned to arise from secondary NH group.

The IR spectra of the complexes show a strong broad band in the region 3350-3550 cm^{-1} with their centres lying in the region 3431-3496 cm^{-1}. The IR spectra of the complexes (22) and (29) are complicated in this region because of occurrence of bands due to stretching vibrations of secondary NH groups, and vibrations of coordinated water molecules and phenolic/naphtholic –OH groups. Further, complexity is added as the spectra of the complexes are recorded in KBr pellets which are moisture sensitive. Hence the bands in this region for the complexes (22) and (29) might have contribution from bands arising due to water molecules absorbed by KBr pellets as well. In order to decide upon whether the bands in this region arise due to H_2O molecules or due to moisture absorbed by KBr pellets, the compounds were heated as 110 °C and 180 °C, respectively. The ensuing vapour was passed through a trap containing anhydrous $CuSO_4$. Thus the complexes (22) and (29) showed weight loss of corresponding to the water molecules at 180 °C. These vapours turned anhydrous $CuSO_4$ blue which confirmed that they originate from two water molecules. This supports that the complexes (22) and (29) contain two water

molecules in the coordination sphere. This suggests that the bands appearing in the region 3350-3550 cm^{-1} in the complexes (22) and (29) have contribution from coordinated water molecules. On the otherhand, the remaining complexes shows no weight loss at 110 °C or 180 °C ruling out the possibility of the presence of lattice as well as coordinated water molecules. This indicates that in these complexes, the bands in the region 3350-3550 cm^{-1} arise due to moisture absorbed by KBr pellets. In all of the complexes, the νNH bands retain with slight modification in their positions. Sometimes, the νNH bands shift to higher frequency while other times to lower frequency. As the bands in the region 3000-3250 cm^{-1} do not show a relevant trend in their shift in the complexes, we have refrained from drawing any conclusion regarding involvement of -NH group in coordination or otherwise.

The νC=O stretching frequency appearing at 1679 cm^{-1} in the IR spectrum of slahH_4 undergoes shift to lower position by 7-33 cm^{-1} and appears in the region 1646-1679 cm^{-1} in the complexes (22) to (28). This shows that the >C=O group in these complexes is bonded to the metal centre. On the otherhand, the νC=O band in the IR spectra of the complexes (29) to (35) appears around 1666 cm^{-1}, a position which is almost similar to that in the uncoordinated dihydrazone npahH_4. Such a feature associated with these bands is related to non-coordination of the >C=O group to the metal centre.

The ligand slahH_4 shows one strong band at 1620 cm^{-1} while npahH_4 shows strong to medium intensity bands at 1630 and 1593 cm^{-1}. These bands are assigned to stretching vibration of azomethine groups. The average position of the νC=N bands shift to lower frequency by 2-47 cm^{-1} in the complexes nos. (22), (23), (24), (26), (28) and (32) to (35). This indicates coordination of azomethine nitrogen atom to the metal centre. On the otherhand, the νC=N stretching frequency either remains almost unshifted in position as in the complexes (25) and (27) or shifts to higher frequency by ~4 cm^{-1} as

in the complexes (29) and (31). Such a feature associated with ν>C=N band is due difference of bonded species (H^+ or M^{2+} or M^{3+}) to the >C=N group. This also indicates that the bonding between azomethine nitrogen atom and metal centre is weak. It is suggested that in the complexes (25), (27) and (29), (31) phenyl/naphthyl ring electron density flows to the metal centre through >C=N group increasing C-N bond order.

All of the complexes show two strong bands in the region 1576-1633 cm^{-1} corresponding to >C=N group except the complexes (24), (25) and (27) which show only one band in the region 1605-1619 cm^{-1}. The appearance of two νC=N stretching vibrations in the form of two bands in the IR spectra of the complexes indicates that the two >C=N- groups are inequivalent. This inequivalency of the two >C=N groups suggests that the two azomethine nitrogen-to-metal bonds are of unequal strength. Such an inequivalency in the strength of the M←N bonds may be related to coordination of dihydrazone to the metal centre in anti-cis configuration. In this configuration, one hydrazone part attains axial position while the other hydrazone part remains in the equatorial position [218]. It is suggested that in the complexes (24), (25) and (27) both the νC=N bands due to equatorial and axial >C=N groups merge into a single band.

The strong bands at 1275 (s) in slahH_4 and a medium intensity band at 1281 cm^{-1} in npahH_4 are observed in their IR spectra. These bands are similar in nature as observed in other ligands containing phenol group. Hence, these bands are assigned to β(C-O)(phenolic/naphtholic) [42]. In the complexes derived from slahH_4, this band either remains almost unaltered in position as in the complexes (22), (24), (25), (27) or shifts to higher frequency by 2 to 9 cm^{-1} as in the complexes (23), (26) and (28). Further, the intensity of this band in the complexes (22), (24), (25) and (27) remains unaltered as compared to that in the ligand slahH_4. These facts taken together rule out the possibility of coordination of phenolic –OH group to the metal centre.

On the otherhand, in the complexes derived from $npahH_4$, the band at 1281(m) undergoes shift to lower frequency by about 26-36 cm^{-1}. Such feature associated with β(C-O)(naphtholic) band indicates bonding through naphtholic oxygen atoms to the metal centre. In these complexes, there is no flow of naphthyl ring electron density to the metal centre through naphtholic oxygen atoms.

The region below 1200 cm^{-1} is not well defined for hydrazine derivatives and contains bands due to νN-N, CH bending vibrations and ν(OH) [250]. Though due to several vibrational modes the region is quite complicated νN-N stretching occuring in the range 1050-800 cm^{-1} has been identified and its shift has been found useful in understanding the involvement of nitrogen atoms in coordination. The νN-N stretching frequency has been shown to increase from 885 cm^{-1} in N_2H_4 [167] to 973 cm^{-1} $N_2H_5^+$ [168] and 1024 cm^{-1} in $N_2H_4^{2+}$ [169] due to protonation of one or both the nitrogen atoms. The protonation is akin to involvement of lone pairs of electrons on nitrogen atoms in coordination to metal ions. Onyszchuk [170] and Sacconi [171] have observed νN-N near the above quoted frequencies in the complexes containing unidentate and bidentate hydrazine respectively. But the above ranges in no way can be taken as specific for coordination of one or two nitrogen atoms in substituted hydrazine complexes. Further, it appears in the 1014-986 cm^{-1} region in metal complexes of monosubstituted hydrazine of the type NH_2-NH-Y [172]. But in metal complexes of N, N'-diacylhydrazine, νN-N has been observed in 1040-970 cm^{-1} region [173]. Eliminating the bands due to C-H in plane deformation in the 1050-900 cm^{-1} region, a medium to weak band at about 1036 cm^{-1} in $slahH_4$ and at 1030 cm^{-1} in $npahH_4$ has been assigned to νN-N. These bands either shift to higher frequency by about 4-20 cm^{-1} as in the complexes derived from $npahH_4$ or remains almost unshifted in position as in the complexes (25) and (27) derived from $slahH_4$ or shift to lower position by 2-6 cm^{-1} in the complexes (24), (26) and (28). Such a

feature associated with the νN-N in these complexes may safely be related to coordination of only one nitrogen atom of the >N-N< group of the ligand to the metal centre.

The ruthenium complexes (23) to (28) and (30) to (35) show a new very weak to medium intensity band in the region 1045-1095 cm^{-1}. This band is assigned to ring breathing mode of pyridine/2-picoline/3-picoline/4-picoline/bipyridine/1, 10-phenanthroline in the complexes. The presence of this band in the complexes indicates the coordination of pyridine/2-picoline/3-picoline/4-picoline/bipyridine/1, 10-phenanthroline molecules to the metal centre [244].

The complexes (23) to (26) and the complexes (30) to (33) also show weight loss corresponding to pyridine/ 2-picoline/ 3-picoline/ 4-picoline molecules while the complexes (27), (28), (34) and (35) show weight loss corresponding to one bipyridine/1,10-phenanthroline molecule at temperature 220 °C. The loss of these molecules at such a high temperature indicates that they are coordinated to the metal centre.

Low frequency IR Spectra

The region below 600 cm^{-1} is very complicated and several weak bands in addition to that observed in the ligand are observed in the resulting complexes. This is obviously due to the splitting of skeletal vibrations. From the infrared spectra discussed above in the complexes (22) to (28), the ligand $slahH_4$ binds to the metal centre through carbonyl oxygen and hydrazide nitrogen while in the complexes (29) to (35), the ligand $npahH_4$ coordinate to the metal centre through naphtholic oxygen and hydrazide nitrogen. The ν(M-O)(naphtholic) [180, 181, 265] may be expected to appear at higher frequency than ν(M-O)(carbonyl) [181, 226] because of difference in bond order. On examining the spectra of the ligands and its ruthenium complexes below 600 cm^{-1}, the new band appearing in the region 468-480 cm^{-1} is assigned to ν(M-O)(carbonyl) in the complexes (22) to (28). These

complexes do not show any new band in the region 500-600 cm^{-1} which could be assigned to ν(M-O)(phenolic). This rule out the possibility of coordination of phenolic oxygen atom to the metal centre. On the otherhand, the complexes (29) to (35) show a new band occurring in the region 500-600 cm^{-1} which is tentatively assigned to ν(M-O)(naphtholic). This suggests coordination of naphtholic oxygen atom to the metal centre. But these complexes do not show any new band in the region 450-500 cm^{-1} which could be assigned to ν(M-O)(carbonyl). This dismissed the possibility of coordination of carbonyl oxygen atom to the metal centre in these complexes.

The IR spectra of the complexes were recorded to decide whether the chloride is present in the coordination sphere or not, in the region 600-100 cm^{-1}. The spectra of the complexes (23), (29) and (34) are shown in the **Figs. 5.3.2(b), 5.3.6(b)** and **5.3.9(b)**. These complexes do not show any strong band in the region 300-400 cm^{-1} which could be assigned to νRu-Cl. These show that chlorine is not bonded to the metal centre in the complexes.

The free pyridine bases show absorption bands at around ~604 and ~405 cm^{-1} [177] due to in-plane and out-of-plane ring deformation modes respectively. These bands show considerable shift to higher frequency when pyridine bases are bonded to metal centre. The low frequency IR spectra of the complexes show new bands in the region 640-665 and 426-450 cm^{-1}, respectively. These bands are assigned to arise due to in-plane ring and out-of-plane ring deformation of pyridine bases. The presence of these bands in the low frequency region suggests coordination of pyridine bases to metal centre. A band observed in the region 275-290 cm^{-1} is assigned to ν(M-N) stretching vibration.

Cyclic Voltammetry

The majority of the ruthenium complexes (24) and (26) to (35) have been characterized by cyclic voltammetry. The cyclic voltammogram of a 2 mM

mM solution of the complexes in DMSO with 0.1 M TBAP as a supporting electrolyte were run at a scan rate of 100 mV/s. The voltammograms for the complexes (24) and (29) are shown in **Figs 5.4.1** and **5.4.2**, respectively. The data have been set out in **Table 5.7** at a scan rate of 100 mV/s.

The complexes show either one or two redox waves in the region -0.75 to +1.00 V at a scan rate of 100 mV/s.

The oxidative waves occurring in the region +0.25 to +0.38 V and reductive wave occurring in the region +0.05 to +0.30 V are assigned to electron transfer process centered on the ligand because they are close to the redox waves observed in free ligand. The remaining redox wave is assigned to the electron transfer reaction centred on the metal. The representative electrode reactions for these complexes are shown below:

$$[Ru^{II}(slahH_4)(A)_2]^{2+} \underset{}{\overset{e}{\rightleftharpoons}} [Ru^{I}(slahH_4)(A)_2]^{+} \overset{e}{\rightleftharpoons} [Ru^{I}(slahH_4^{-})(A)_2]$$

On the other hand, the complex (27) shows a reductive wave at -0.245 V and the corresponding oxidative wave at +0.01 V. These reductive and oxidative waves are assigned to electron transfer reactions centred on metal atom only. Thus this complex does not show redox process centred on the dihydrazone ligand. The electrode reaction for the complex is shown below:

$$[Ru^{II}(slahH_4)(bpy)]^{2+} \overset{e}{\rightleftharpoons} [Ru^{I}(slahH_4)(bpy)]^{+}$$

The complex $[Ru^{II}(npahH_4)(H_2O)_2]Cl_2$ (29) shows an oxidative wave at +0.38 V. The corresponding reductive wave appears at +0.05 V. In this case also, the difference ΔEp is around 330 mV making the redox process almost irreversible or quasireversible. This redox process is considered to be metal centred and is related to Ru^{II}/Ru^{I} redox couple. The cyclic voltammogram for the reduction of the complex is shown in **Fig. 5.4.2**.

Another oxidative wave appears at a potentiol of -0.18 V. The corresponding

reductive wave appears at -0.71 V. The difference ΔE, ΔE =ΔEox -ΔEred is around 530 mV which indicates that the redox process is irreversible. This redox couple is assigned to reduction of coordinated ligand.

The complex $[Ru^{II}(npahH_4)(2\text{-}pic)_2]Cl_2$ (31) shows two oxidative waves at +1.00 and -1.10 V while there is no reductive wave corresponding to the oxidative at -1.10 V, the oxidative wave at +1.00 V shows the corresponding reductive wave at -0.20 V. Thus the redox processes centred on complex are irreversible. The reductive wave at -0.20 V is assigned to arise due to reduction of Ru^{II} to Ru^{I} while the oxidative wave at +1.00 V is assigned to arise due oxidation of Ru^{I} to Ru^{II} centre. There is no reductive wave corresponding to the oxidative wave a -1.10 V making the process irreversible. It appears that this oxidative wave originates due to generation of some transient species which reverts to the original species

It is pertinent to mention that the complex $[Ru^{II}(npahH_4)(py)_2]Cl_2$ (30) shows a featureless CV at scan rate of 1100mV/s. However. it shows an oxidation wave at -0.20 V at a scan rate of 100 mV/s. A reductive peak appears at -0. 11V. The oxidation and reduction processes appear unrelated to one another. But when the scan rate is increased, the two processes becomes reversible process. With the increase of scan rate to 1000 mV/s, the separation between oxidative and reductive waves become as much as 350 mV. This complex shows no redox process centred on the coordinated ligand.

The CV of the complex $[Ru^{II}(npahH_4)(3\text{-}pic)_2]Cl_2$ (32) shows two oxidative wave at +0.15 and +0.48 V, respectively. The complex shows no reductive wave corresponding to oxidative wave at +0.15 V while a reductive wave at +0.15 V is observed corresponding to the oxidative wave at +0.48 V. The oxidative wave at +0.15 V is very strong which indicate that it arises from a multielectron transfer process. Most probably, it arises from two electron oxidation of coordinated ligand in the complex.

The oxidative wave at +0.48 V and reductive wave at +0.15 V are most probably metal centred. The separation between oxidative and reductive waves is 330 mV which shows almost irreversible in nature of the redox processes centred on the metal. This redox process is assigned to Ru^{II}/Ru^{I} couple in the complex.

The complex $[Ru^{II}(npahH_4)(4\text{-}pic)_2]Cl_2$ (33) shows almost similar feature as the complex (32) in its CV. Hence further discussion on CV of this complex is redundant.

The CV of the complex $[Ru^{II}(npahH_4)(bpy)]Cl_2$ (34) shows two oxidative waves at -0.30 and +0.35 V. This complex also shows two reductive waves at -0.70 and -0.12 V, respectively in contrast to other complexes. The additional reductive waves centred at -0.70 V is assigned to the electron transfer process centred on bpy ligand. The oxidative wave at -0.30 V is considered to be centred on the principal dihydrazone ligand due to its essential feature. The oxidative wave at +0.35 V and reductive wave at -0.12 V are considered to be related to metal centred processes. These waves are assigned to the Ru^{II}/Ru^{I} redox couple.

The complex (35) shows two oxidative waves at -0.10 and +0.50 V. There is a reductive wave at -0.30 V. The reductive wave at -0.30 is assigned correspond to oxidative wave at -0.10 V. The separation ΔEp between oxidative and reductive wave is 200 mV which suggests that the redox process is quasi-reversible.

Conclusion

This chapter describes ruthenium (II) complexes derived from dihydrazones $slahH_4$ and $npahH_4$. All of the complexes are monomeric. Both the dihydrazones coordinate to the metal centres as neutral tetradentate ligands. In all of the complexes, the dihydrazones coordinate in the keto form. In the complexes derived from $slahH_4$, the dihydrazone coordinate to the metal centre through carbonyl oxygen and azomethine nitrogen atoms while in the complexes derived from $npahH_4$, the dihydrazones coordinate to the metal centre through azomethine atoms and naphtholic –OH oxygen atoms. In the complexes (22) to (26), the equatorial positions are

occupied by carbonyl oxygen and azomethine nitrogen atoms while axial positions are occupied by monodentate ligands H_2O, py, 2-pic, 3-pic and 4-pic. In the complexes (27) and (28), the equatorial positions are occupied by carbonyl oxygen atoms and nitrogen atoms of the bidentate ligands bpy and phen while the axial positions of the complexes are occupied by azomethine nitrogen atoms. On the otherhand, the equatorial positions in the complexes (29) to (33) are occupied by azomethine nitrogen and naphtholic –OH groups while the monodentate ligands H_2O, py, 2-pic, 3-pic and 4-pic occupy axial positions. In the complexes (34) and (35), the equatorial positions are occupied by nitrogen atoms (two from azomethine nitrogen atoms and two from bidentate ligands bpy and phen) while axial positions are occupied by naphtholic –OH groups. In all of the complexes the chloride groups are present outside the coordination sphere in the H-bonded form involving phenolic/ naphtholic –OH group.

In all of the complexes, the dihydrazone ligands are bonded to the same metal centre in the anti-cis configuration. This introduces steric crowding in the molecules. As a result, one hydrazone arm is in the equatorial plane while the other occupies axial position.

Majority of the complexes have been characterized by cyclic voltammetry.

The complexes are suggested to have distorted octahedral stereochemistry around the metal centre.

On the basis of results obtained from various physico-chemical and spectral studies, the structures of the complexes have been proposed as shown in **Figs. 5.6.1-5.6.4**

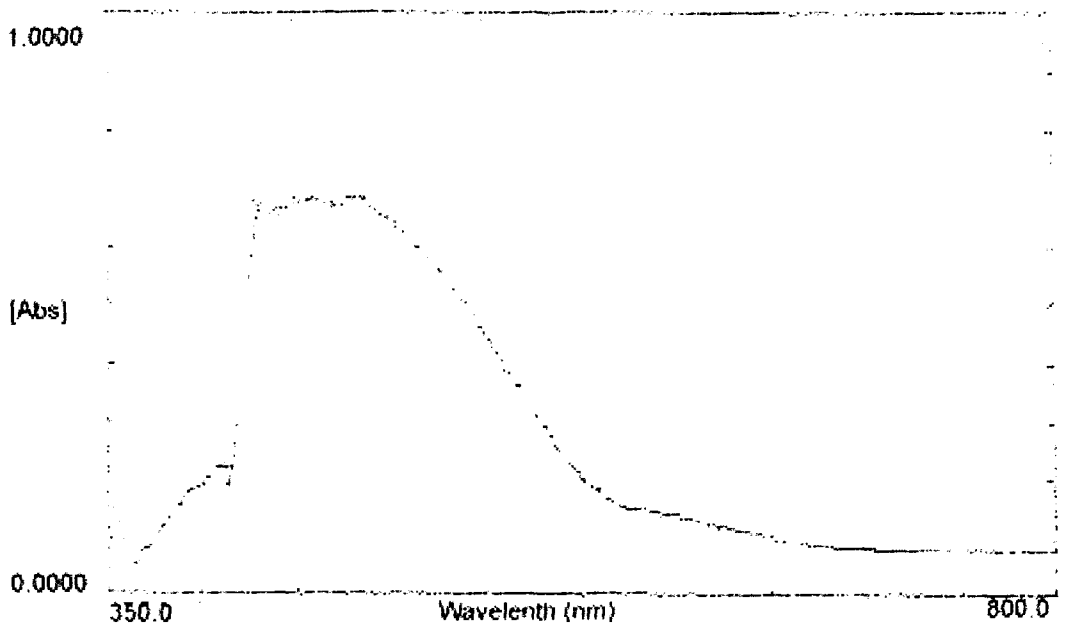

Fig. 5.1.1 Electronic spectrum of complex $[Ru^{II}(slahH_4)(phen)]Cl_2$ **(28)**

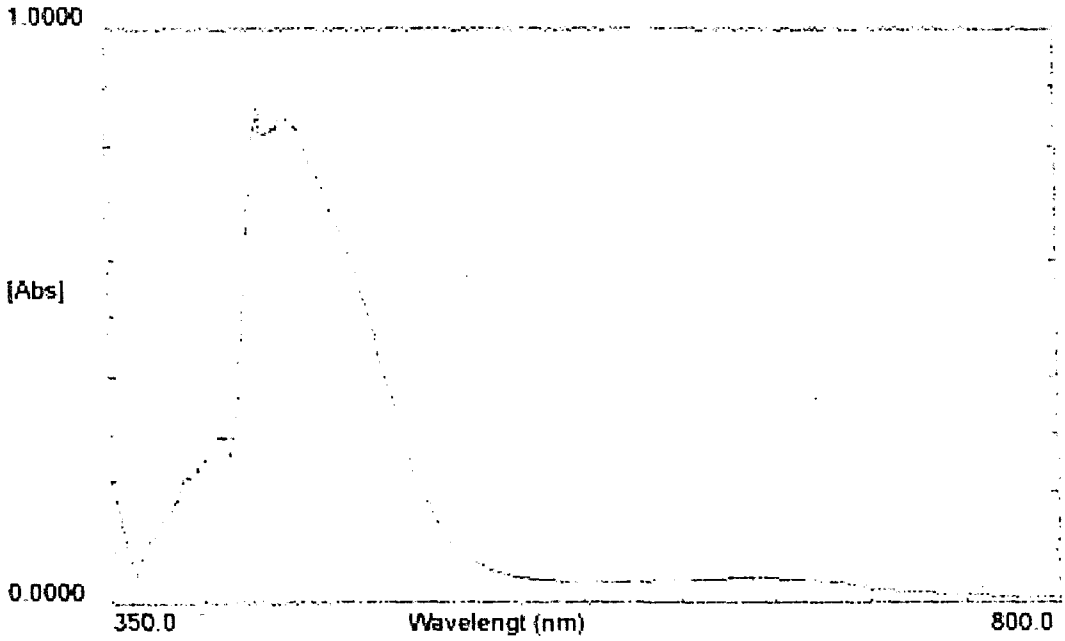

Fig. 5.1.2 Electronic spectrum of complex $[Ru^{II}(npahH_4)(2\text{-}pic)_2]Cl_2$ **(31)**

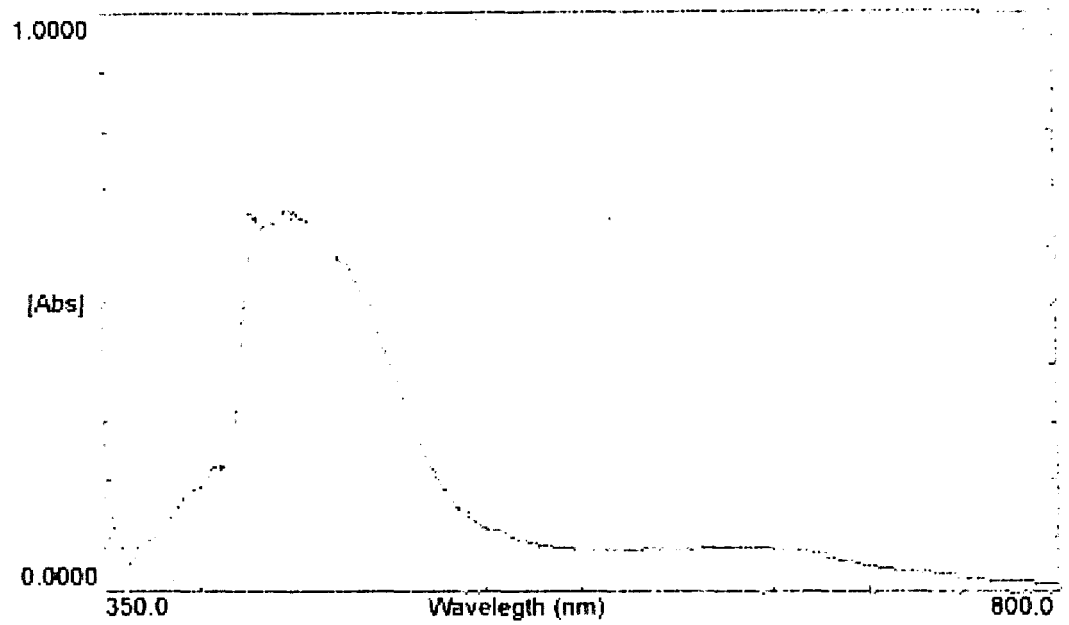

Fig. 5.1.3 Electronic spectrum of complex $[Ru^{II}(npahH_4)(3\text{-}pic)_2]Cl_2$ **(32)**

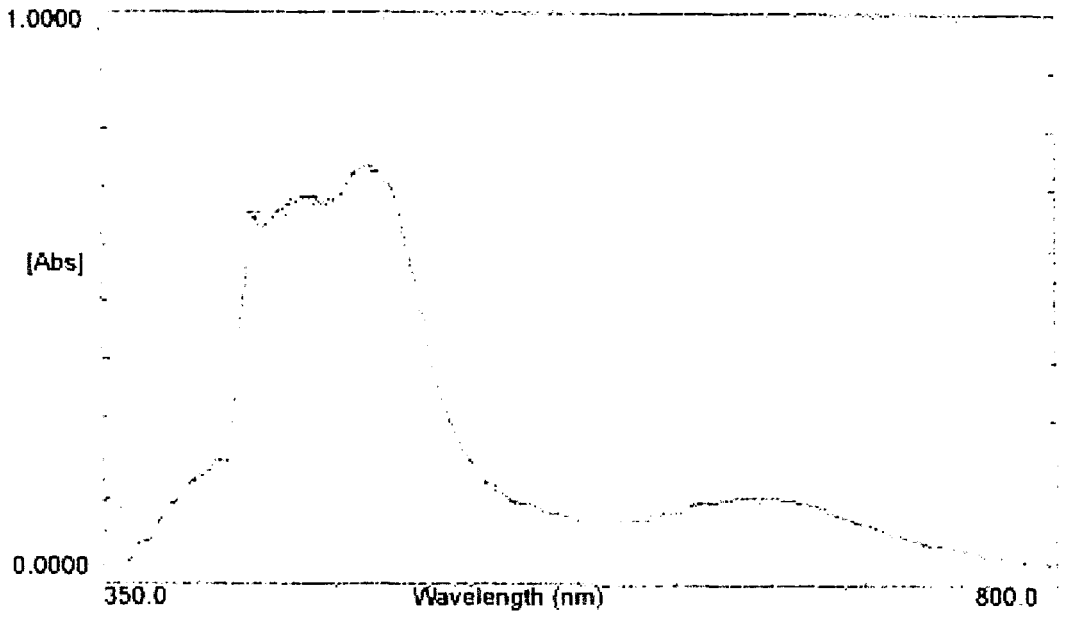

Fig. 5.1.4 Electronic spectrum of complex $[Ru^{II}(npahH_4)(4\text{-}pic)_2]Cl_2$ **(33)**

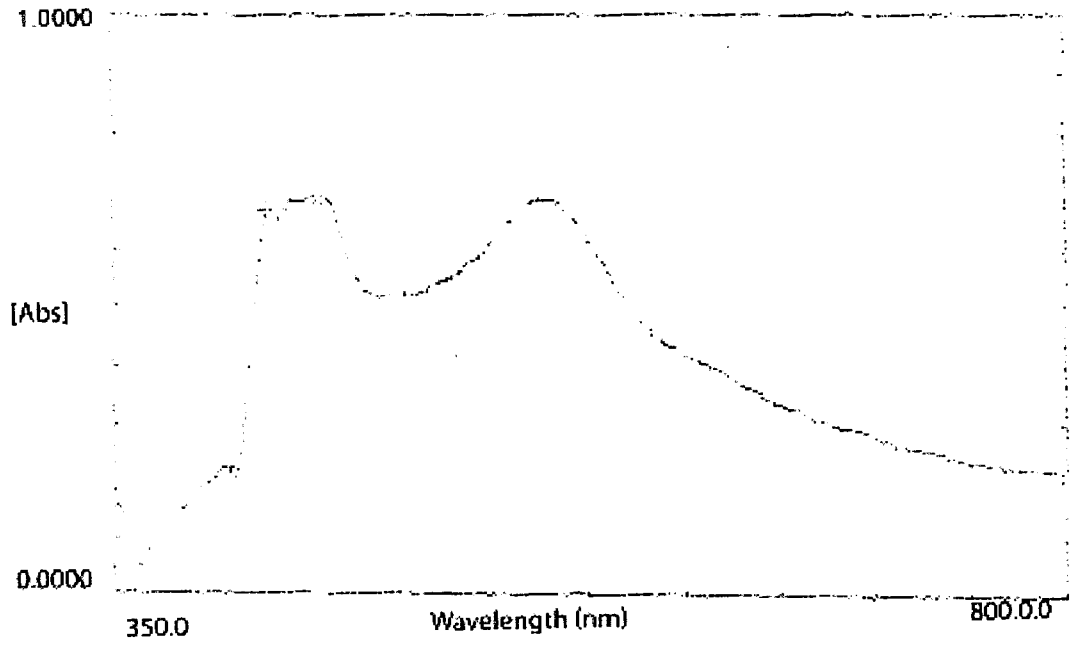

Fig. 5.1.5 Electronic spectrum of complex $[Ru^{II}(npahH_4)(bpy)]Cl_2$ **(34)**

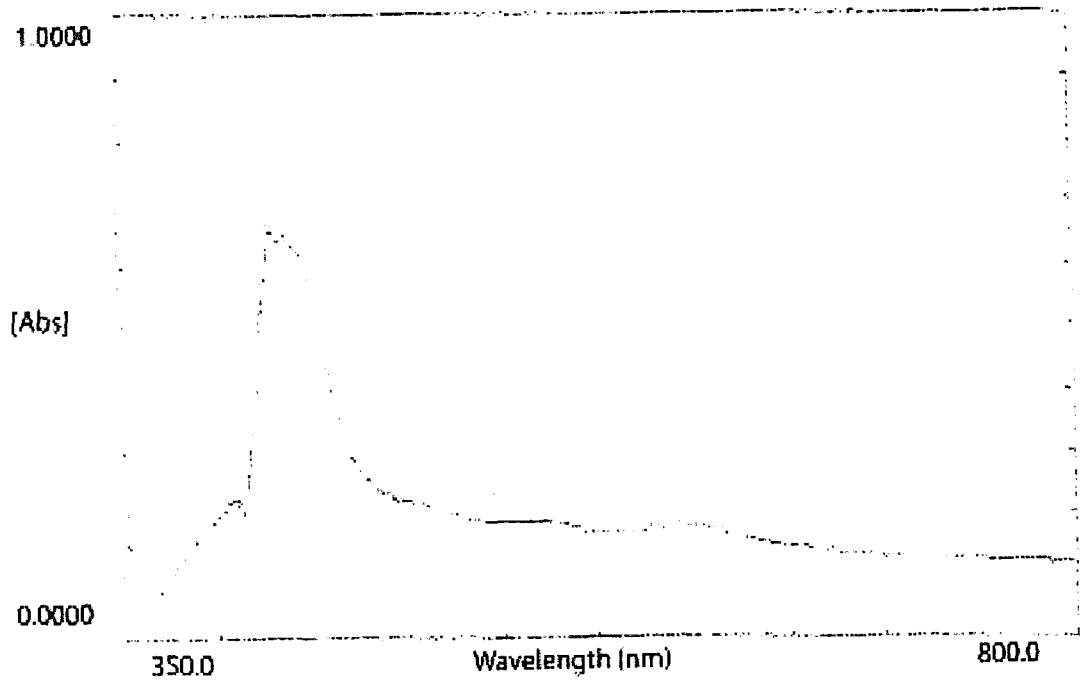

Fig. 5.1.6 Electronic spectrum of complex $[Ru^{II}(npahH_4)(phen)]Cl_2$ **(35)**

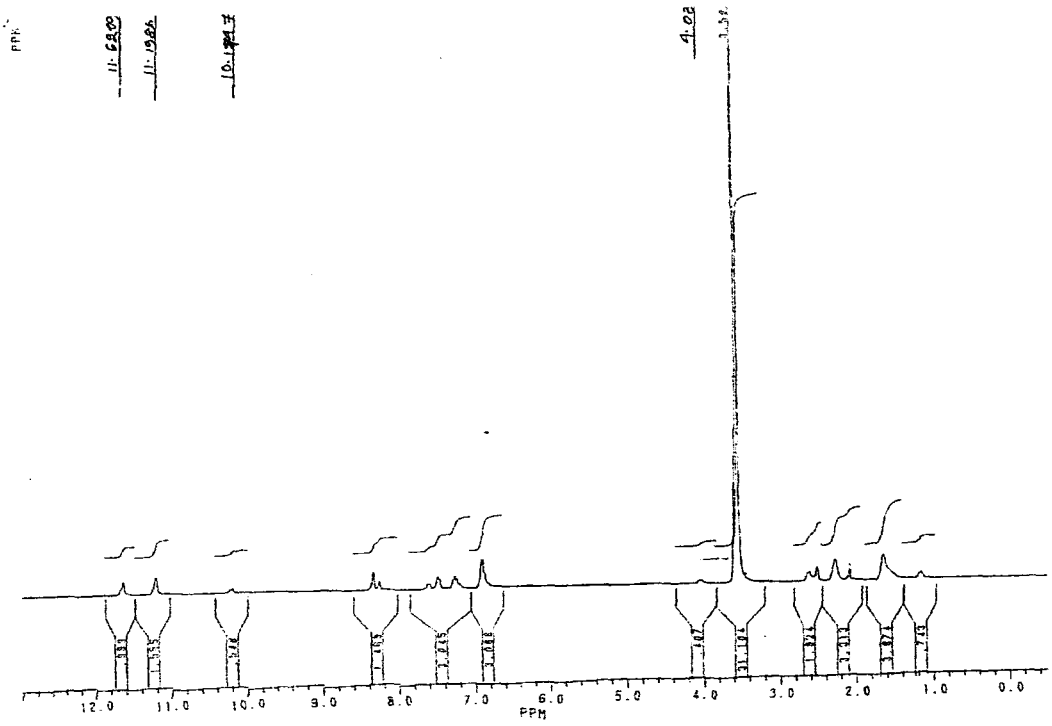

(a)

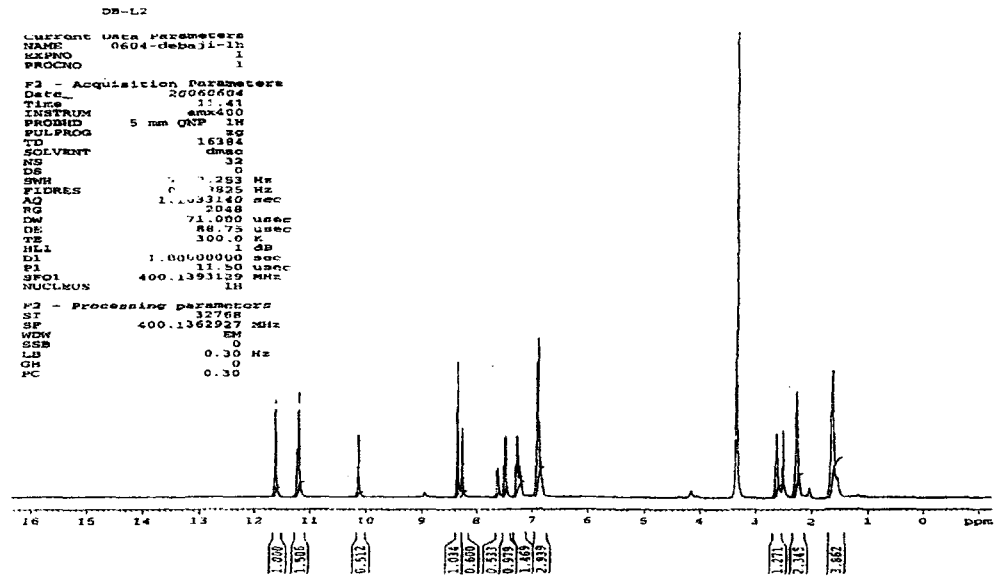

(b)

Fig. 5.2.1 (a) and (b) ^{1}H NMR spectrum of Ligand Disalicylaldehyde adipoyldihydrazone ($slahH_4$)

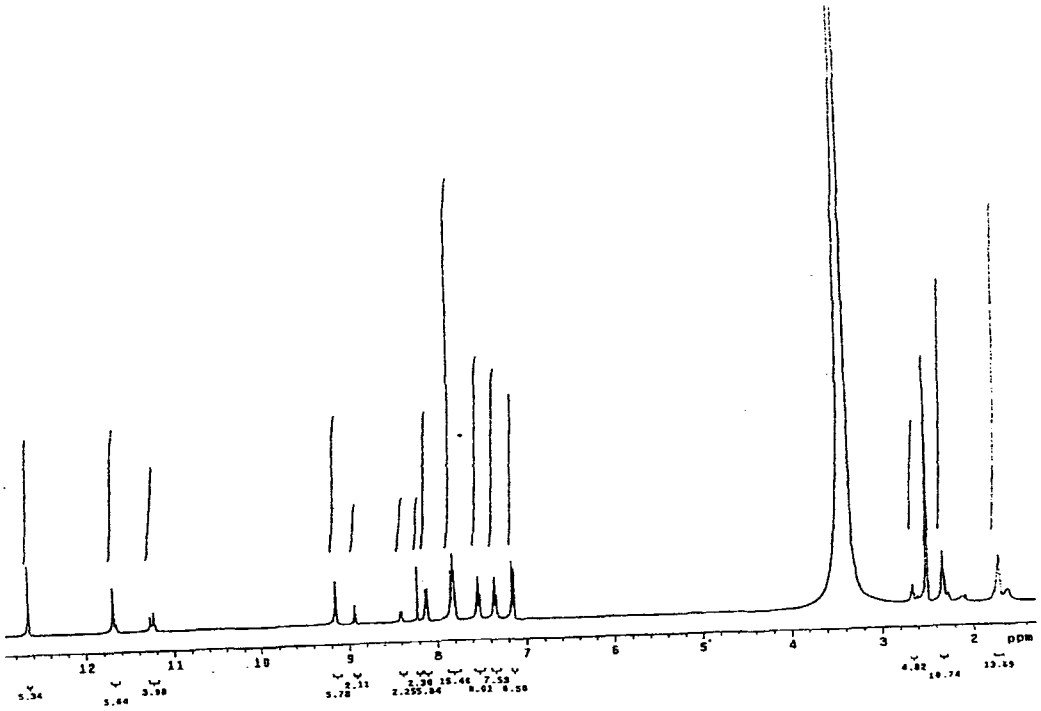

(a)

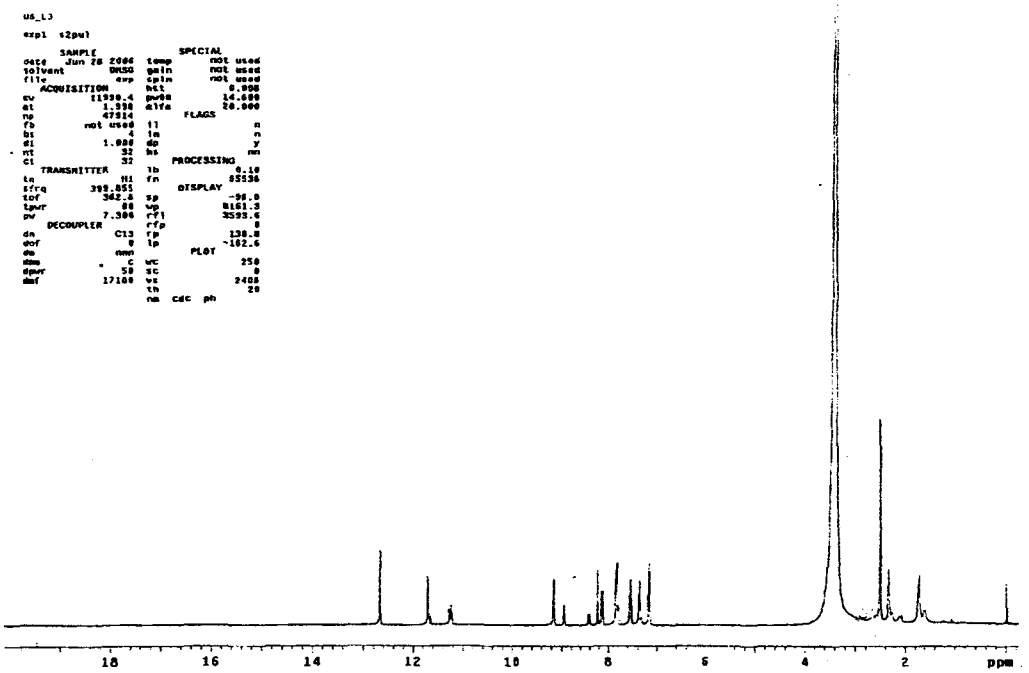

(b)

Fig. 5.2.2 (a) and **(b)** ^{1}H NMR spectrum of Ligand Bis(2-hydroxy-1-naphthaldehyde)adipoyldihydrazone ($npahH_4$)

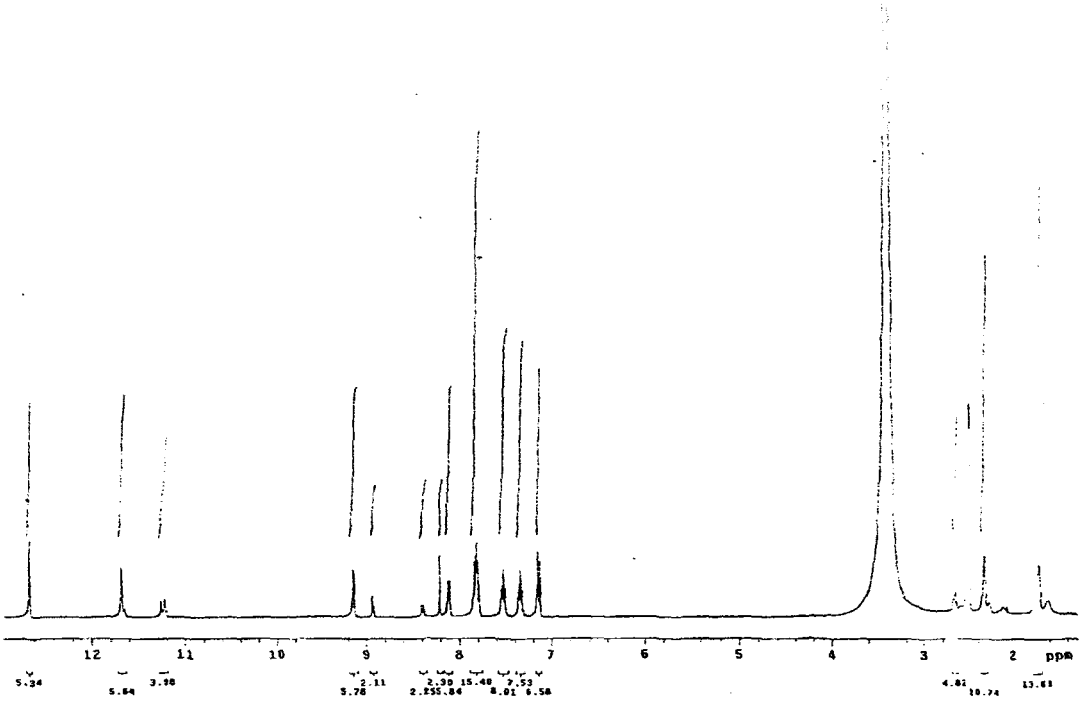

(c)

Fig. 5.2.2 (c) ^{1}H NMR spectrum of Ligand Bis(2-hydroxy-1-naphthaldehyde)adipoyldihydrazone ($npahH_4$)

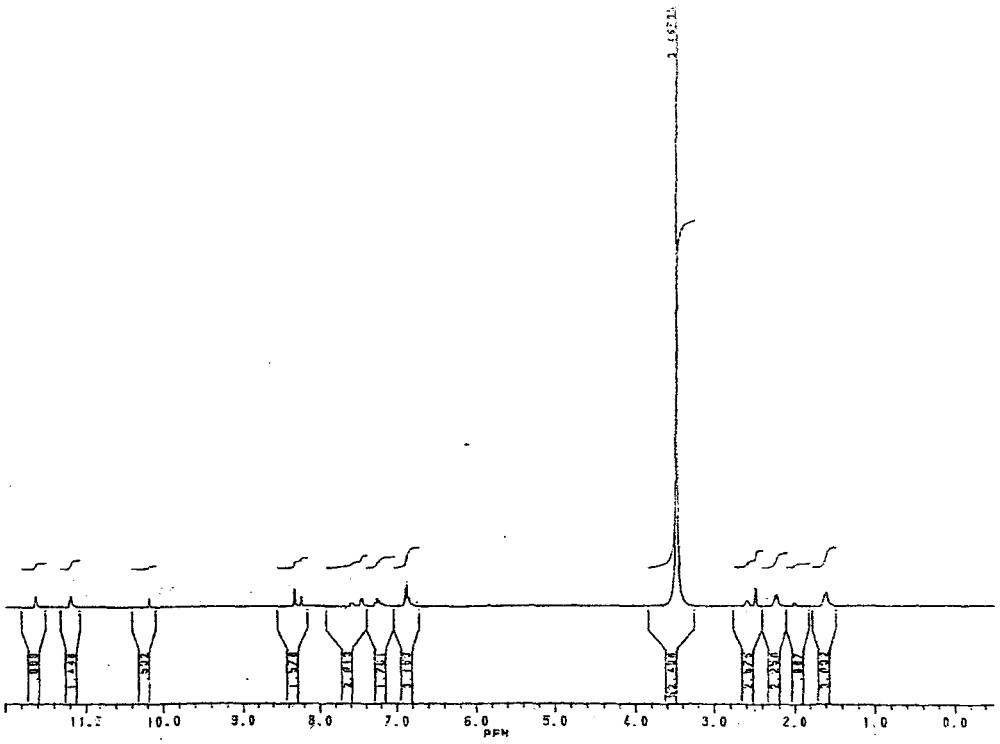

Fig. 5.2.3 ^{1}H NMR spectrum of complex $[Ru^{II}(slahH_4)(3\text{-pic})_2]Cl_2$ **(25)**

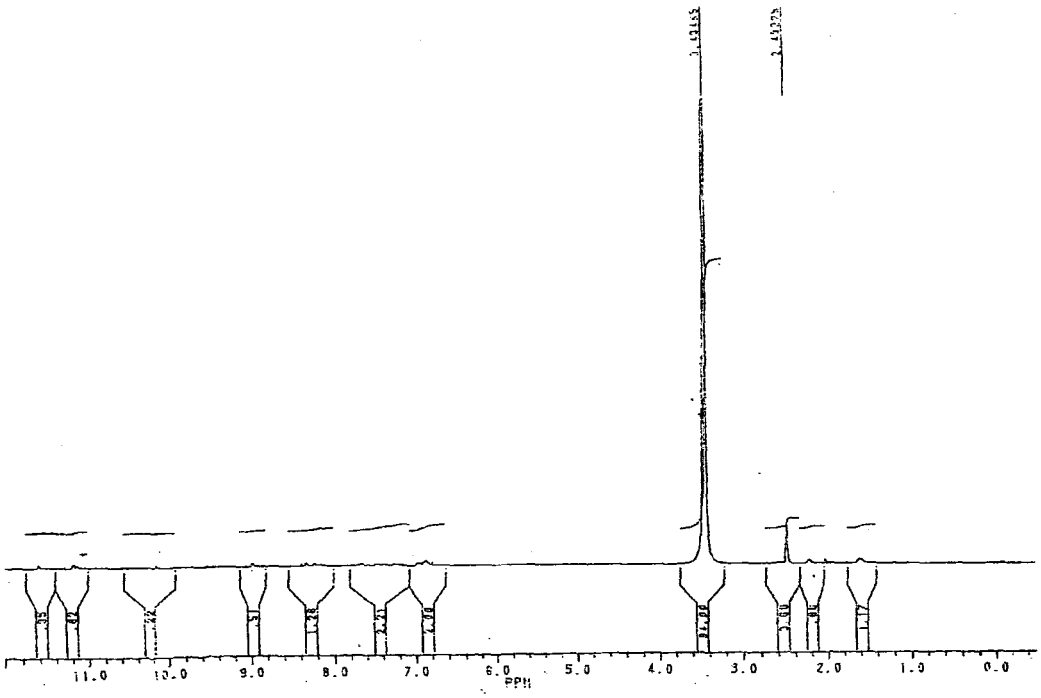

Fig. 5.2.4 ^{1}H NMR spectrum of complex $[Ru^{II}(slahH_4)(bpy)]Cl_2$ **(27)**

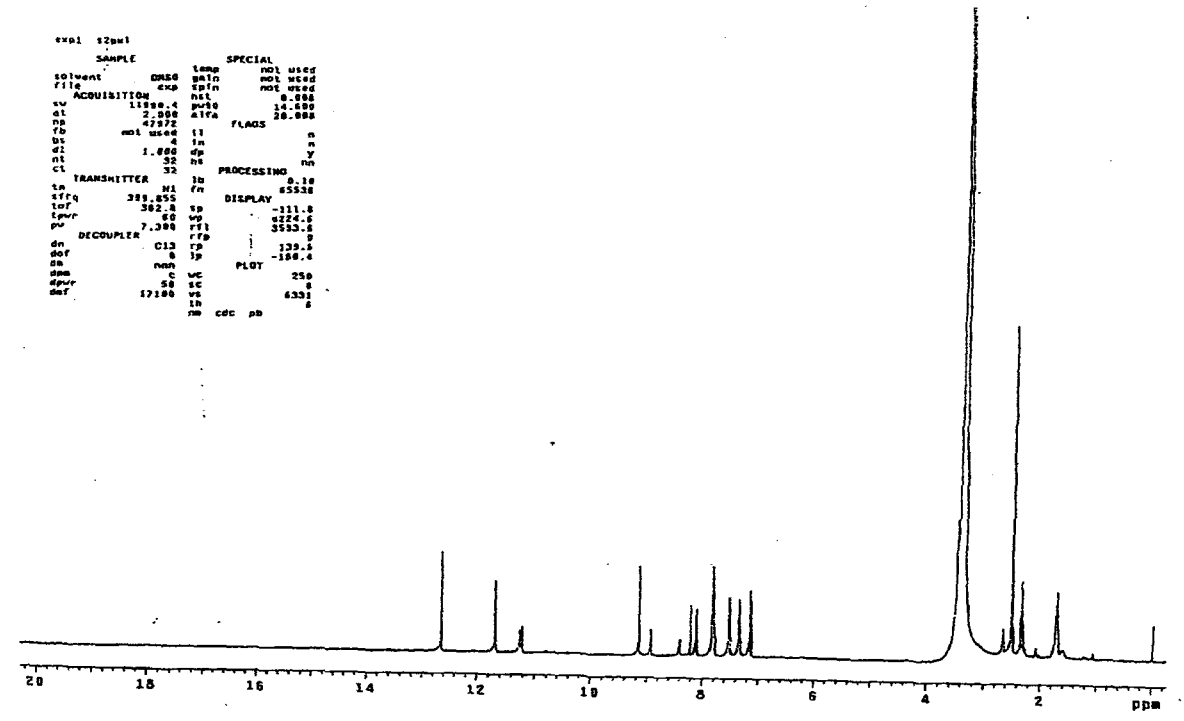

Fig. 5.2.5 ^{1}H NMR spectrum of complex $[Ru^{II}(npahH_4)(H_2O)_2]Cl_2$ **(29)**

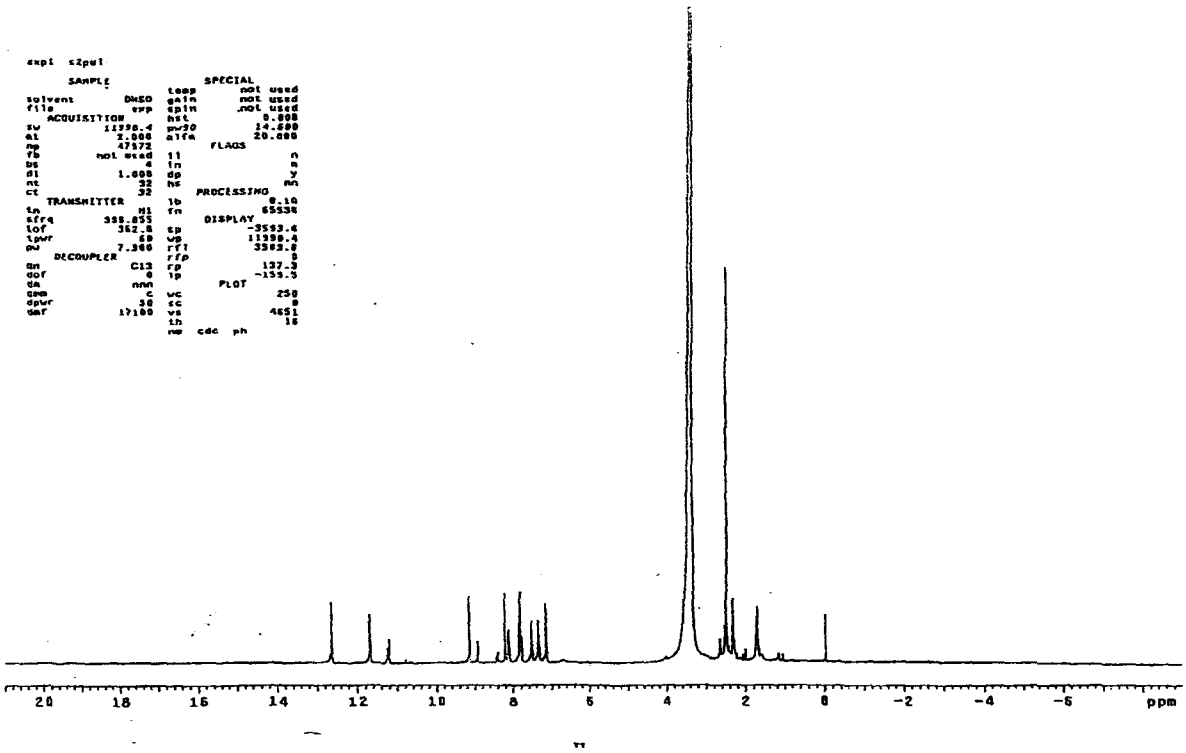

Fig. 5.2.6 ^{1}H NMR spectrum of complex $[Ru^{II}(npahH_4)(3\text{-pic})_2]Cl_2$ **(32)**

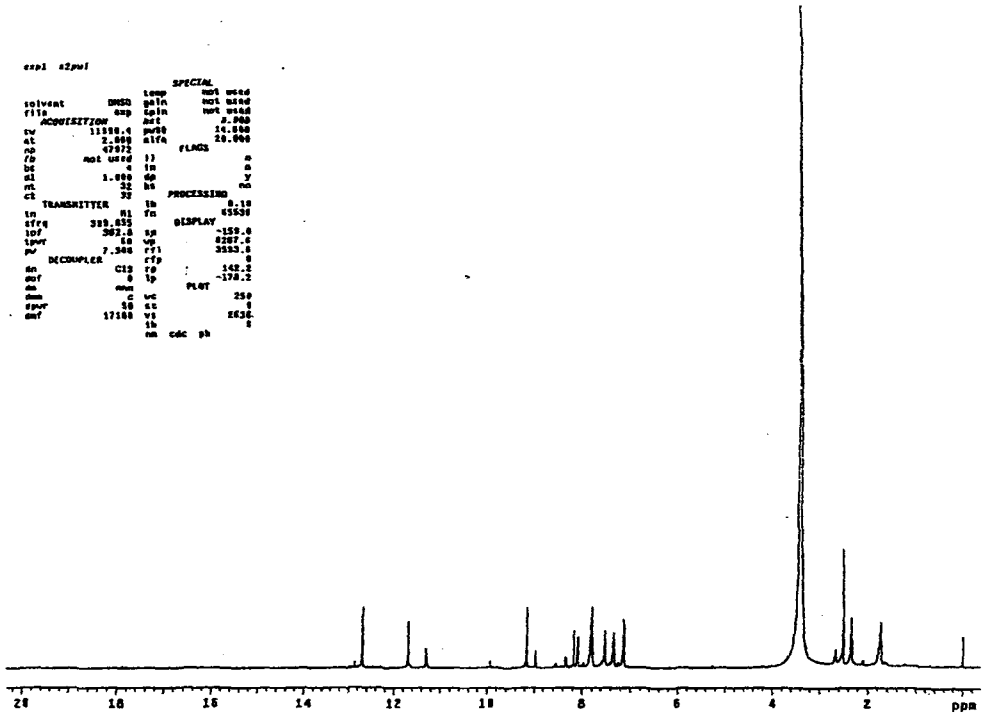

Fig. 5.2.7 ^{1}H NMR spectrum of $[Ru^{II}(npahH_4)(bpy)]Cl_2$ (34)

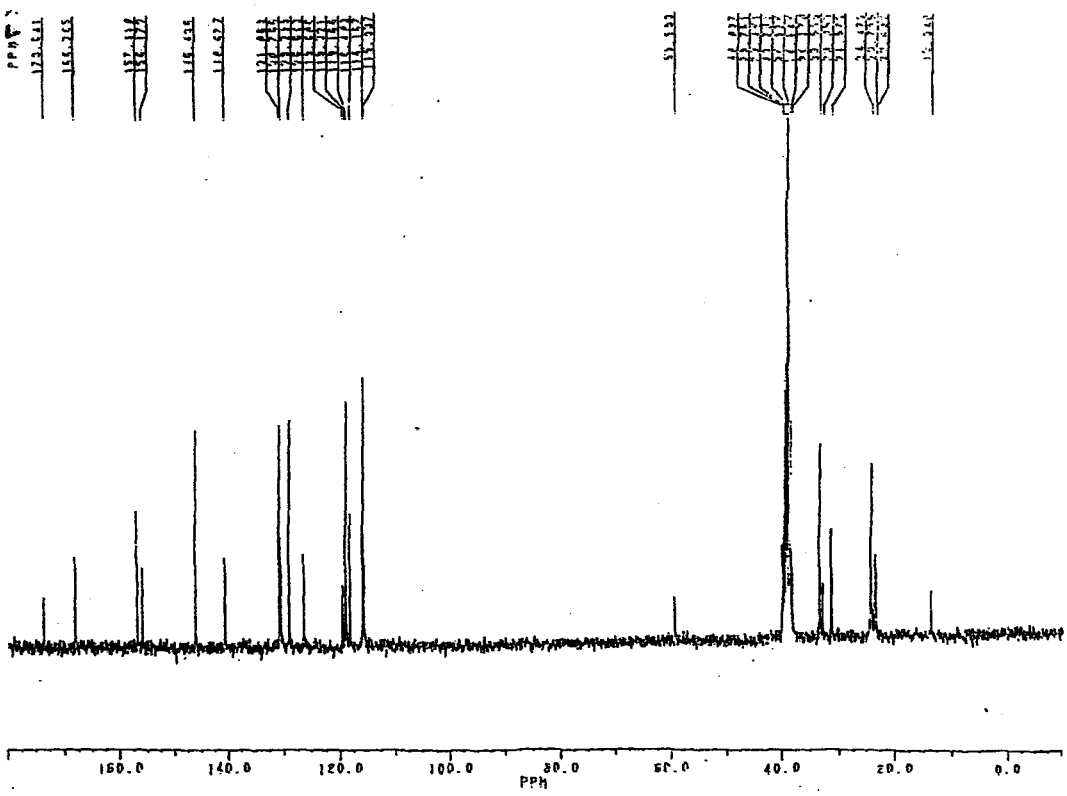

Fig. 5.2.8 ^{13}C NMR spectrum of Ligand Disalicylaldehyde adipoyldihydrazone ($slahH_4$)

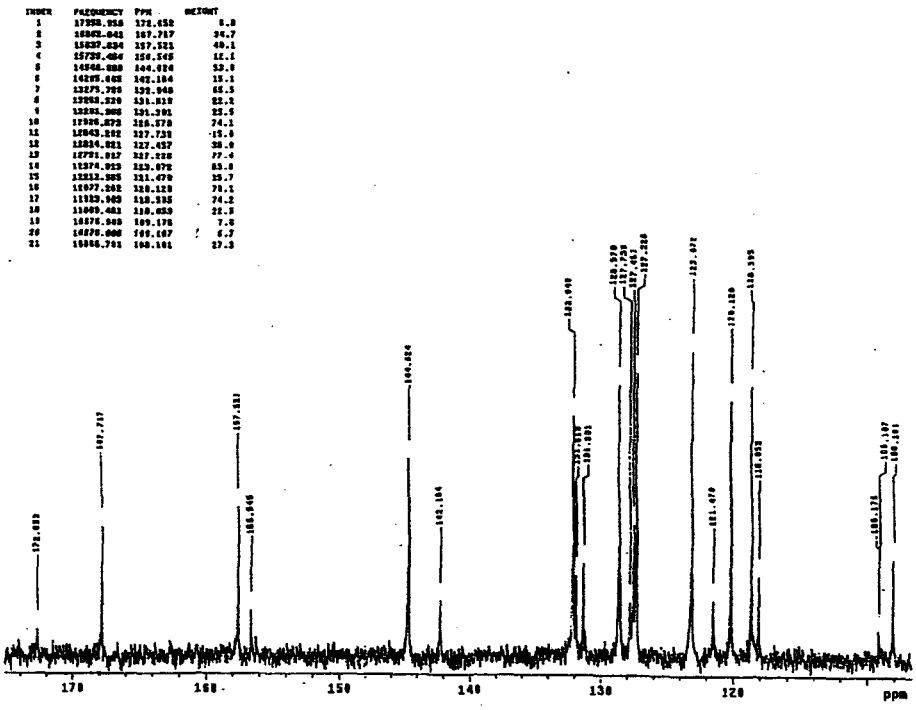

(a)

Fig. 5.2.9 (a) ^{13}C NMR spectrum of Ligand Bis(2-hydroxy-1-naphthaldehyde)adipoyldihydrazone ($npahH_4$)

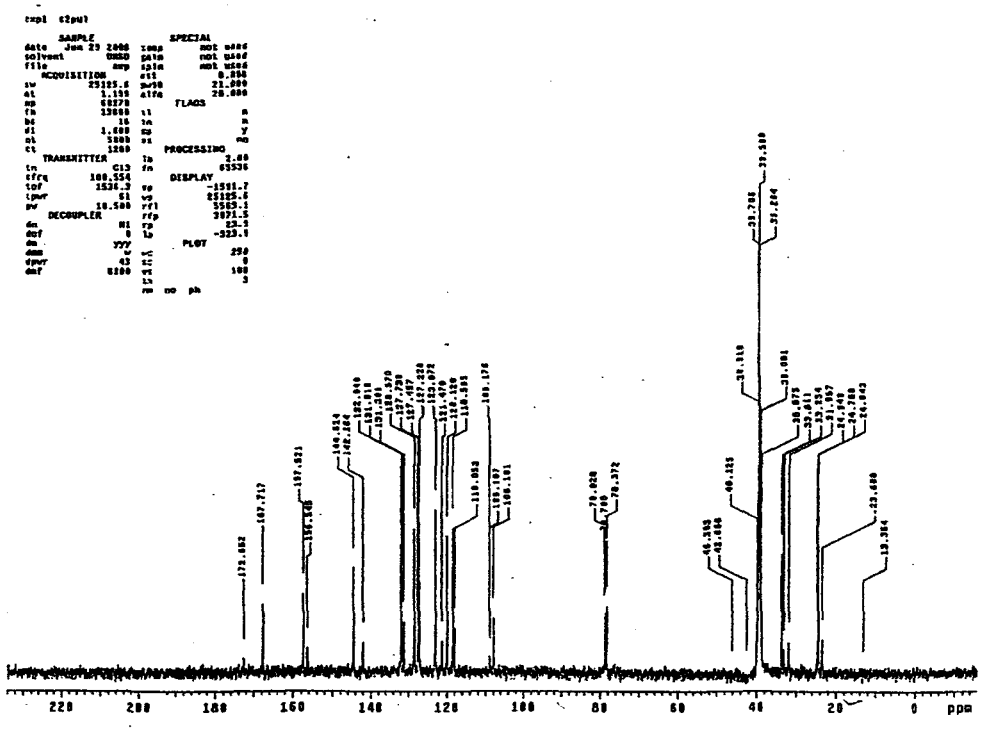

(b)

Fig. 5.2.9 (b) ^{13}C NMR spectrum of Ligand Bis(2-hydroxy-1-naphthaldehyde)-adipoyldihydrazone ($npahH_4$)

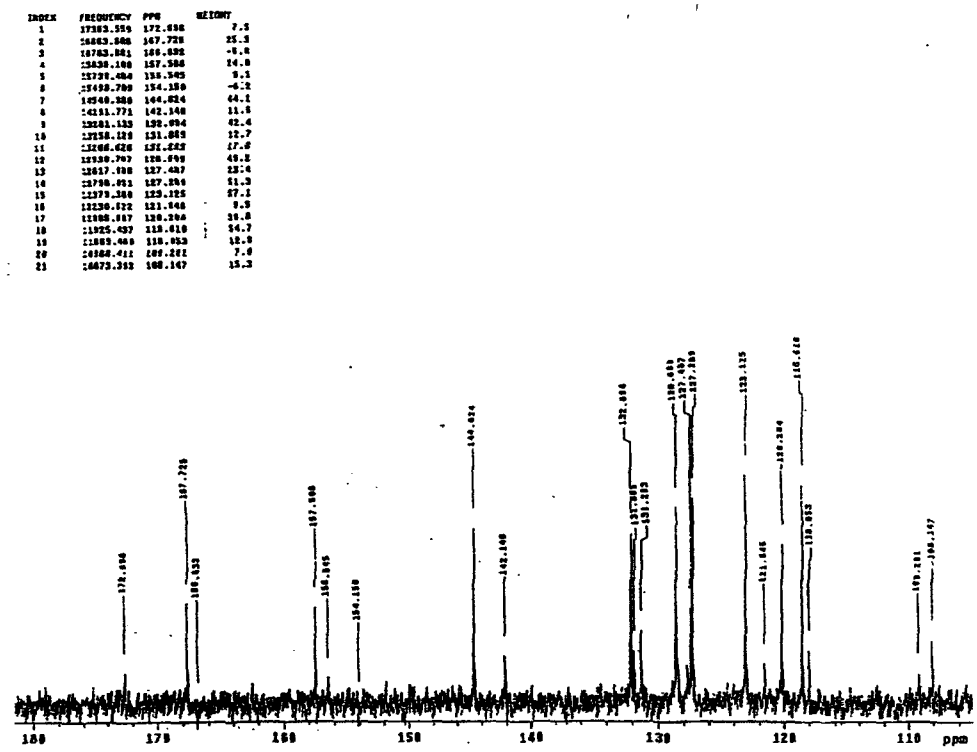

(a)

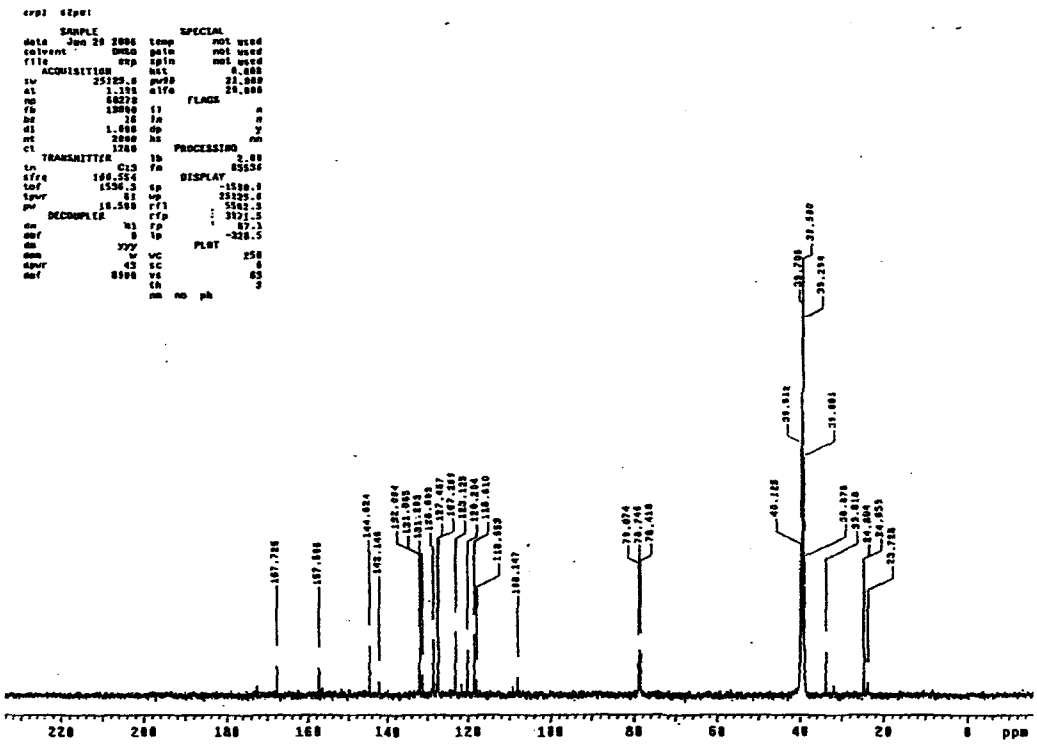

(b)

Fig. 5.2.10 (a) and (b) ^{13}C NMR spectra of $[Ru^{II}(npahH_4)(H_2O)_2]Cl_2$ (29)

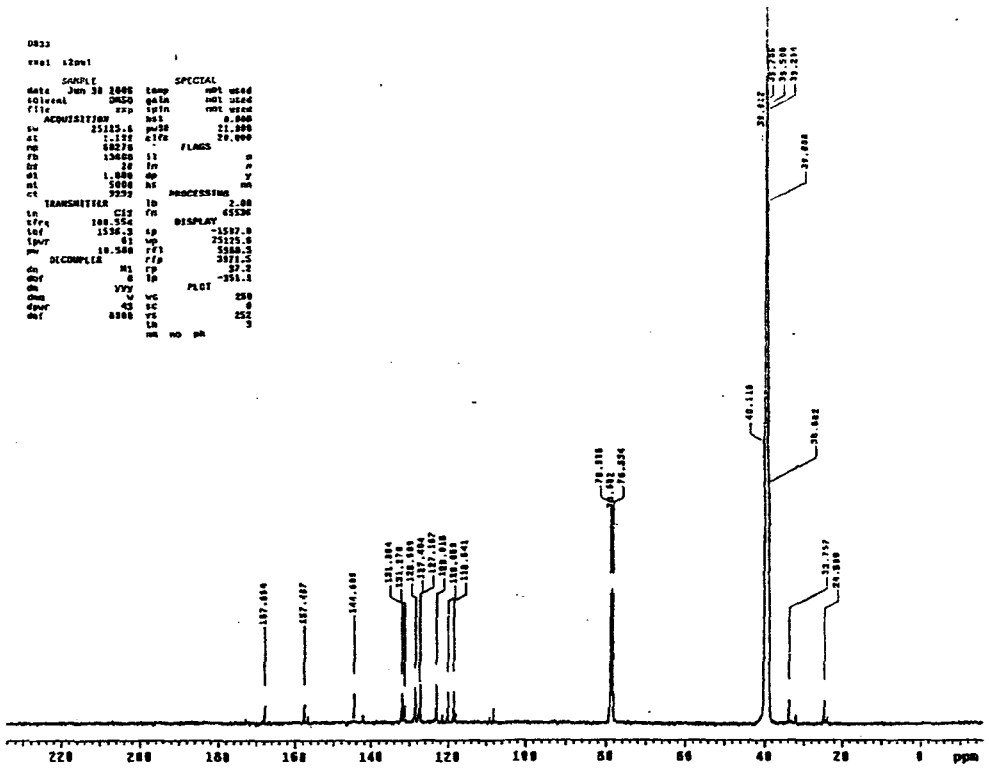

(a)

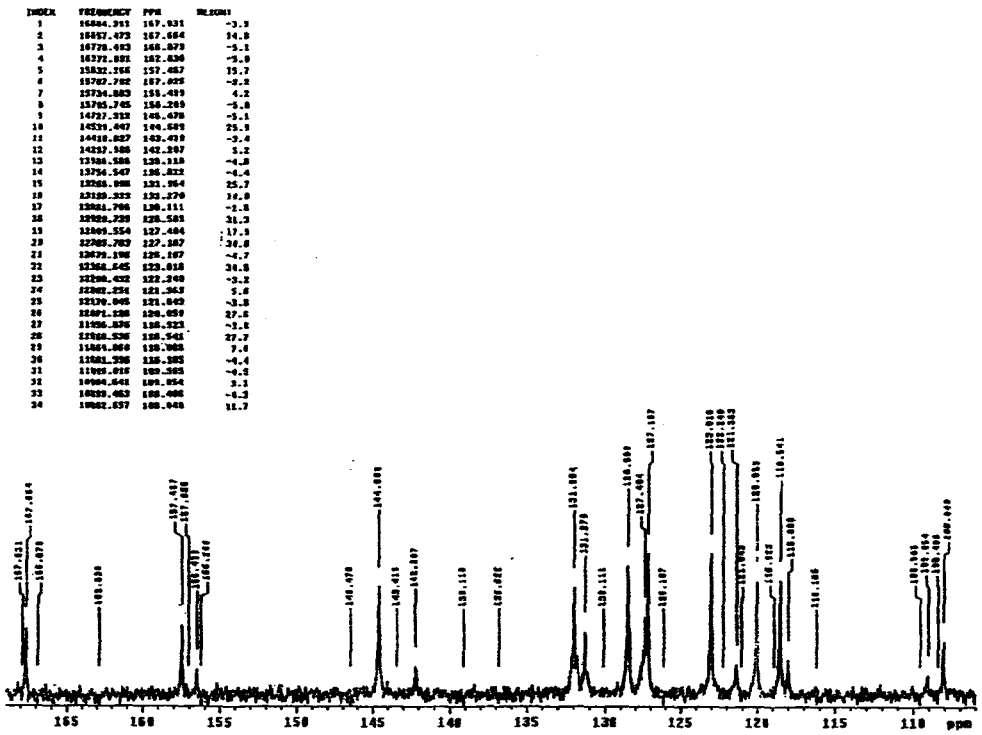

(b)

Fig. 5.2.11 (a) and (b) ^{13}C NMR spectra of $[Ru^{II}(npahH_4)(3\text{-pic})_2]Cl_2$ (32)

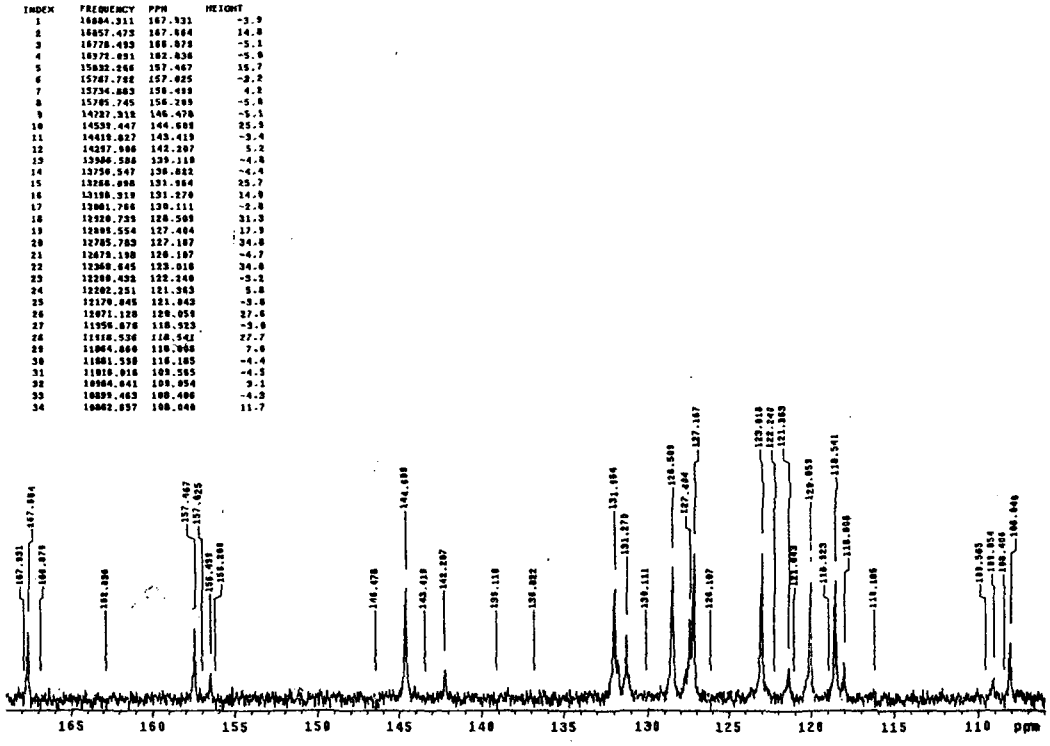

(a)

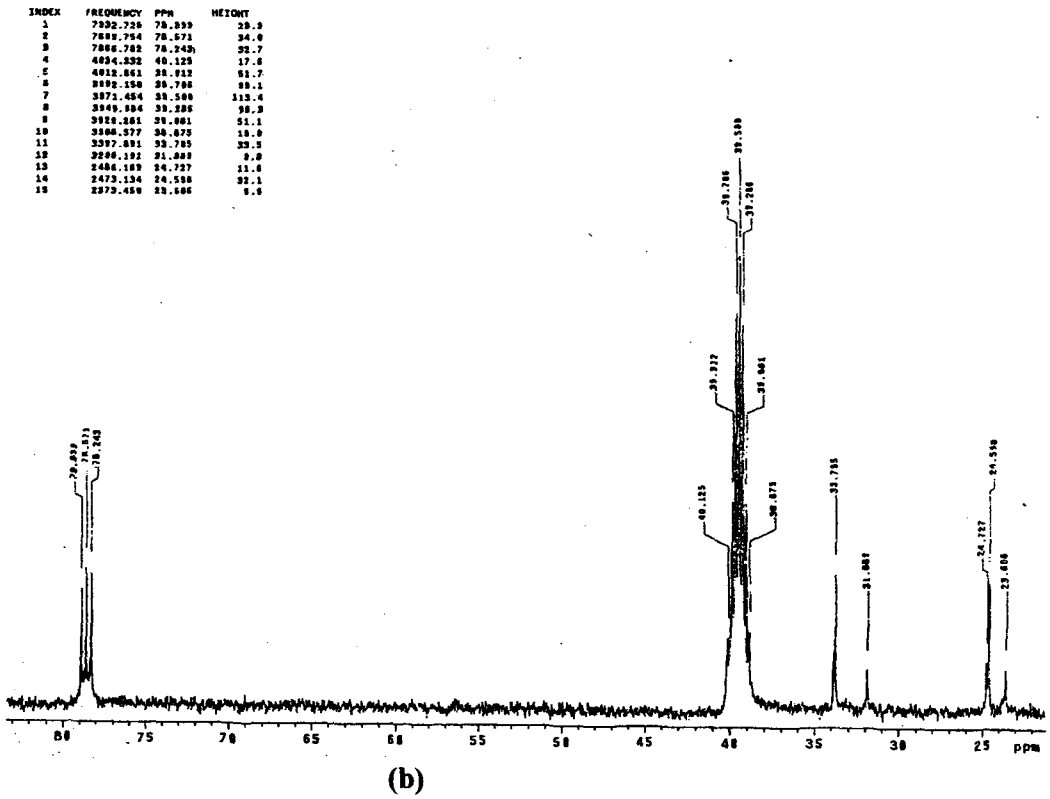

(b)

Fig. 5.2.12 (a) and **(b)** ^{13}C NMR spectra of $[Ru^{II}(npahH_4)(bpy)]Cl_2$ (34)

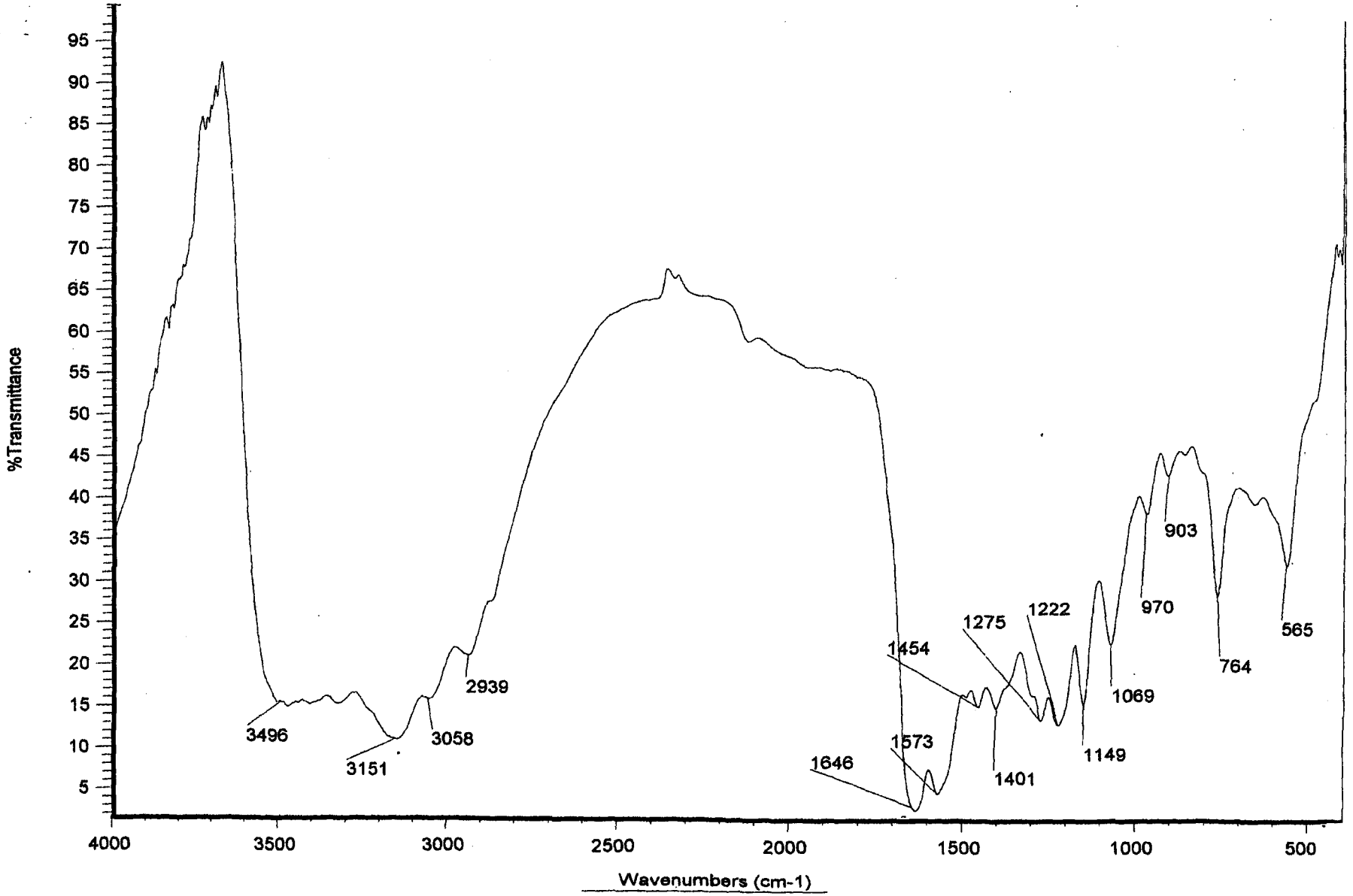

Fig. 5.3.1 IR spectrum of $[Ru^{II}(slahH_4)(H_2O)_2]Cl_2$ **(22)** in KBr

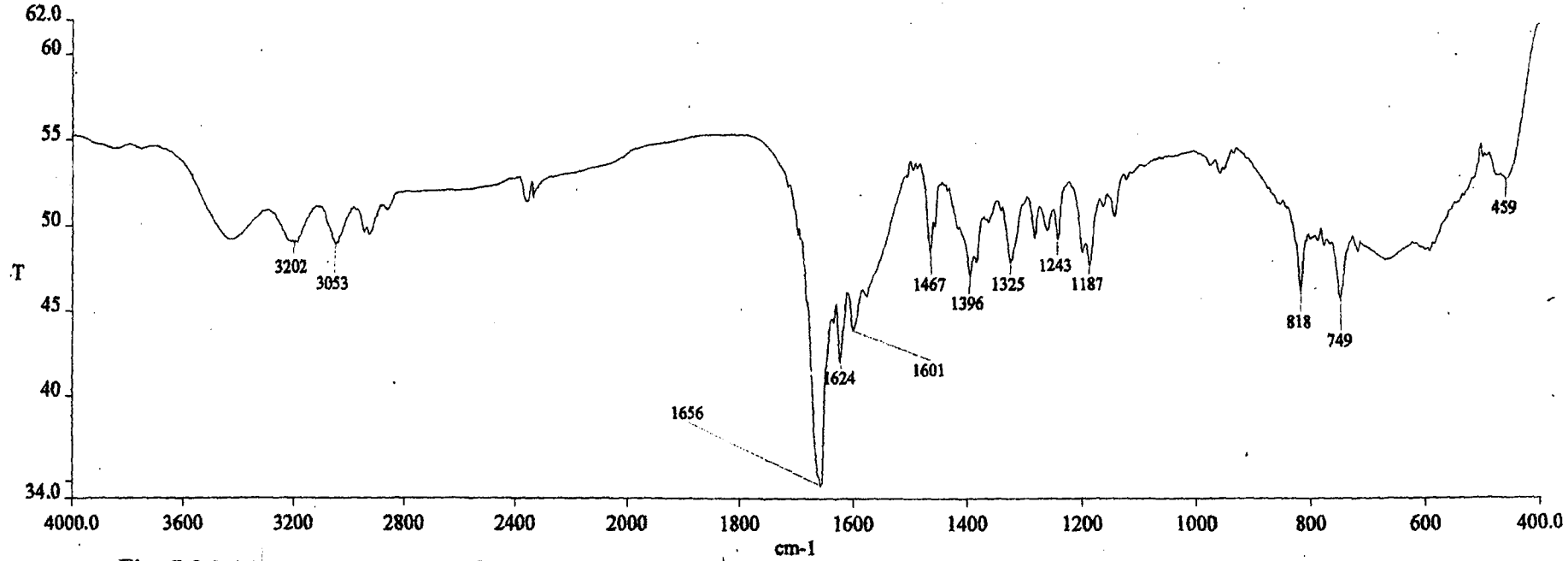

Fig. 5.3.2 (a) IR spectrum of $[Ru^{II}(slahH_4)(py)_2]Cl_2$ **(23)** in KBr

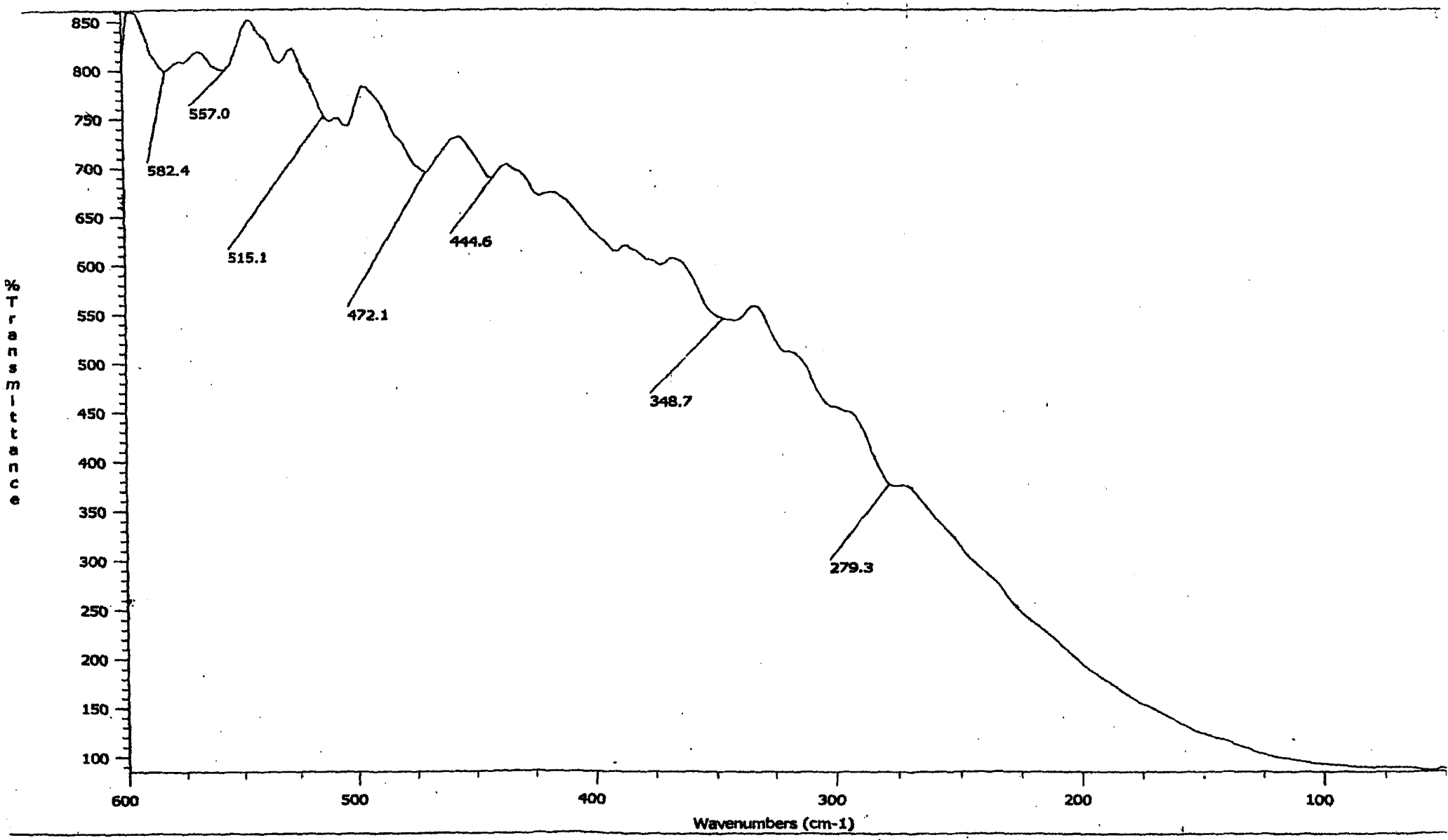

Fig . 5.3.2(b) IR spectrum of complex $[Ru^{II}(siahH_4)(py)_2]Cl_2$ (23) in CsI

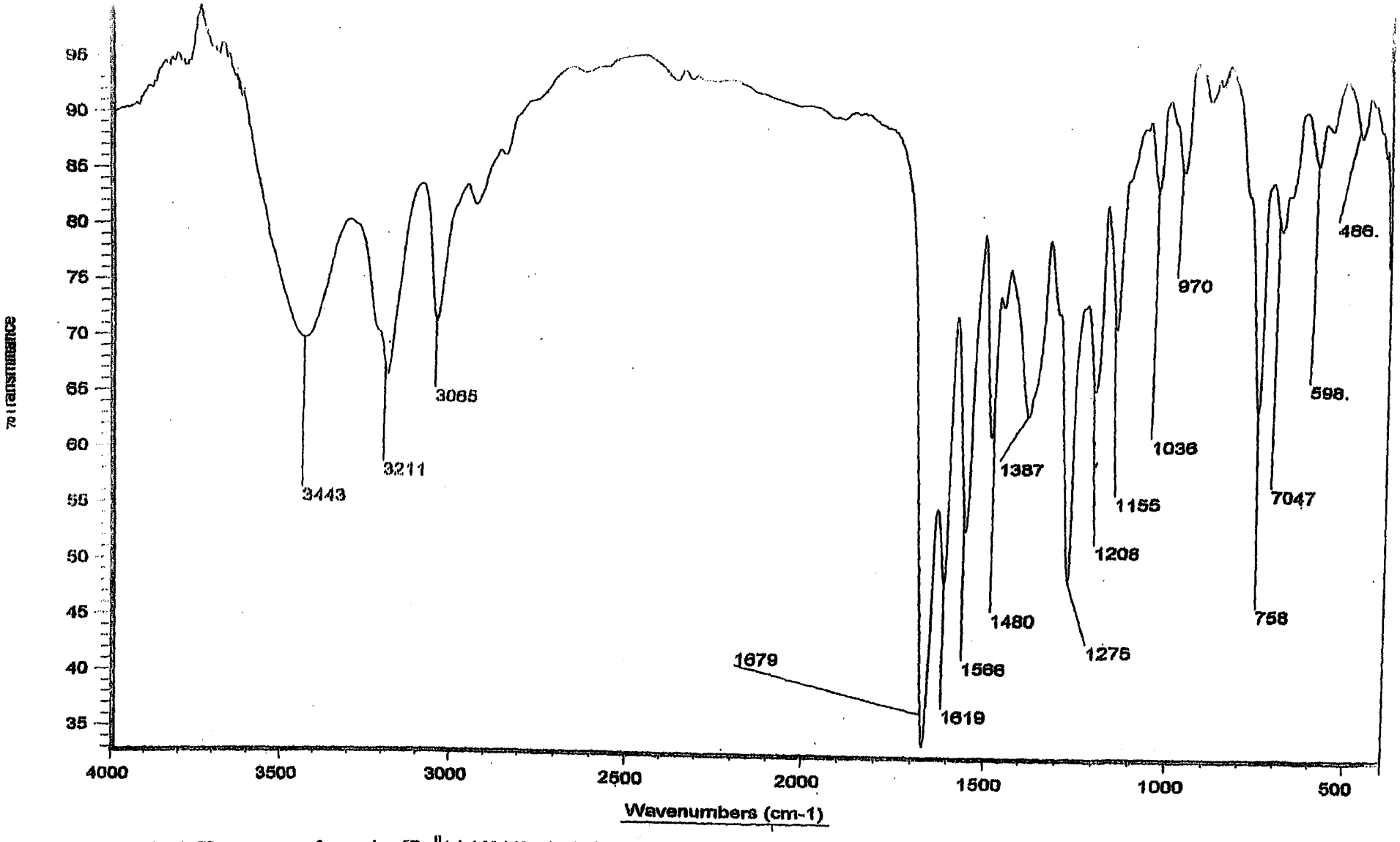

Fig. 5.3.3 IR spectrum of complex $[Ru^{II}(slahH_4)(3\text{-pic})]Cl_2$ (25) in KBr

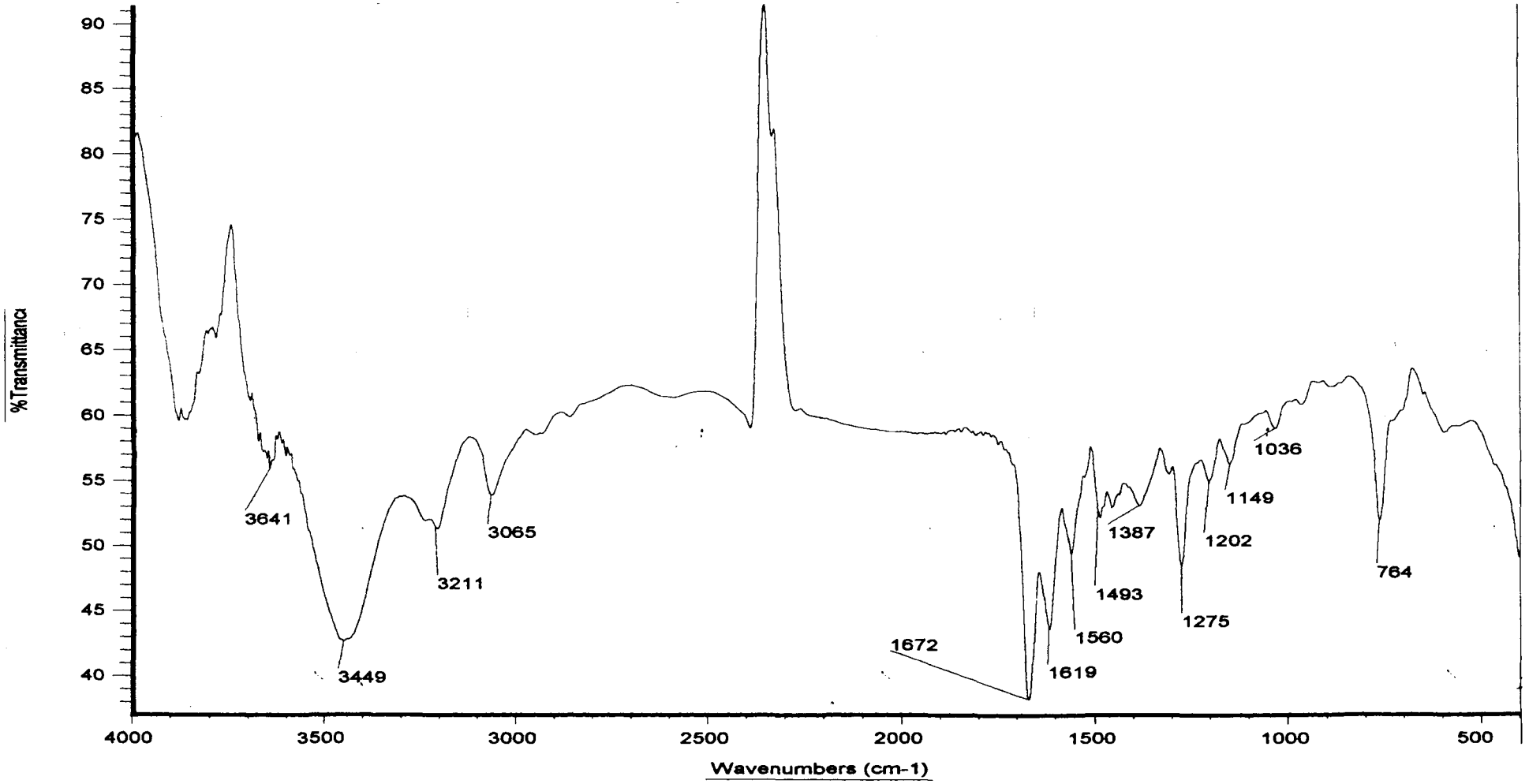

Fig. 5.3.4 IR spectrum of complex $[Ru^{II}(slahH_4)(bpy)]Cl_2$ **(27)**

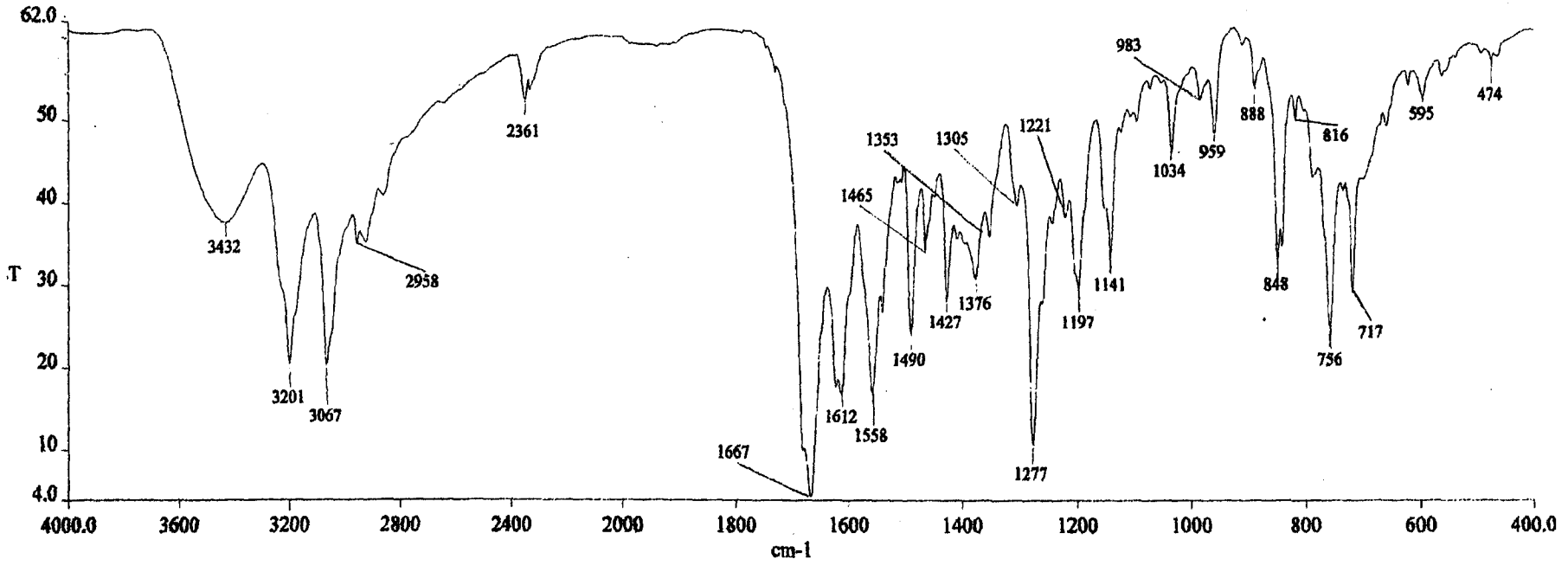

Fig. 5.3.5 IR spectrum of $[Ru^{II}(slahH_4)(phen)]Cl_2$ **(28)** in KBr

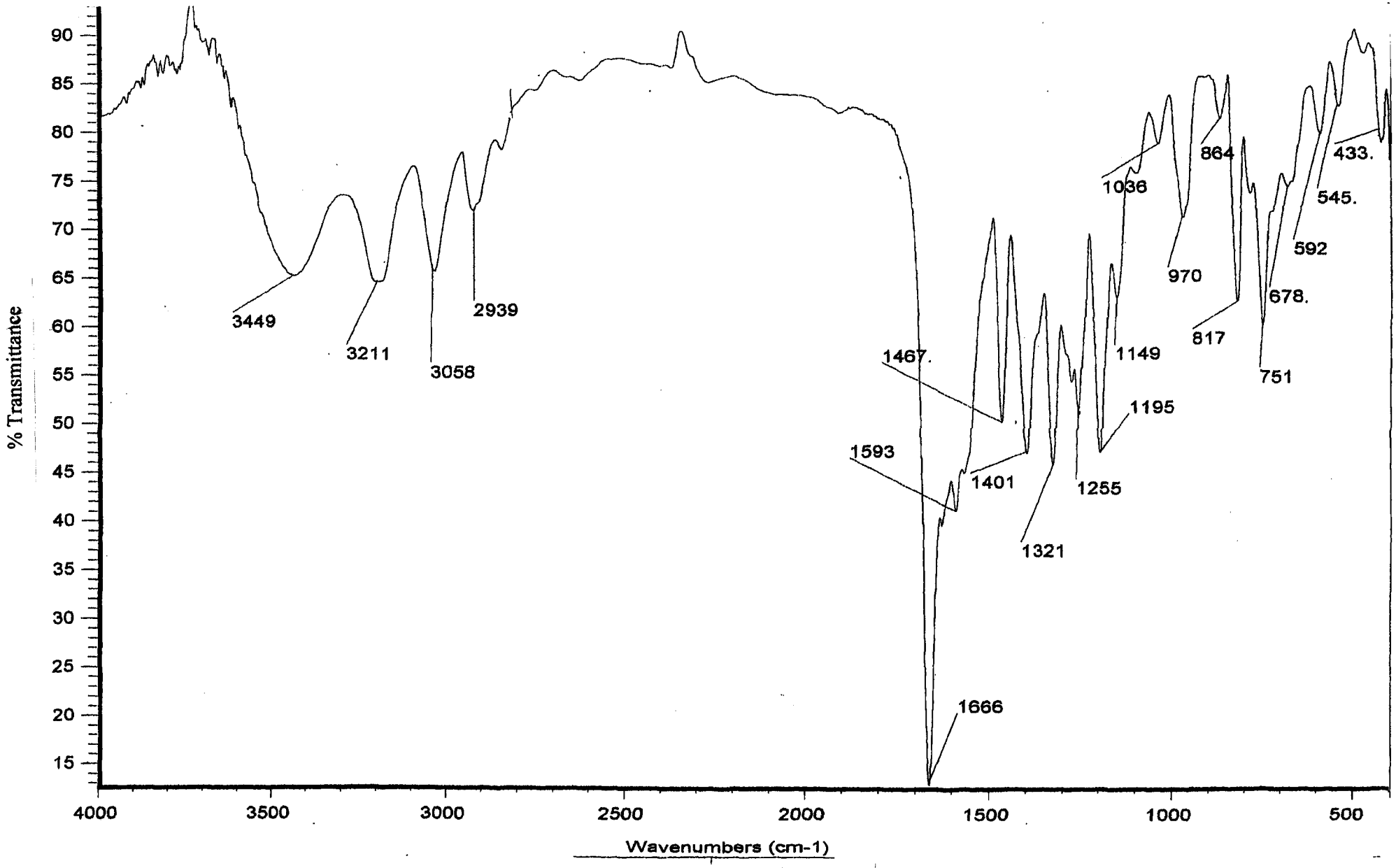

Fig. 5.3.6 (a) IR spectrum of complex $[Ru^{II}(npahH_4)(H_2O)_2]Cl_2$ **(29)** in KBr

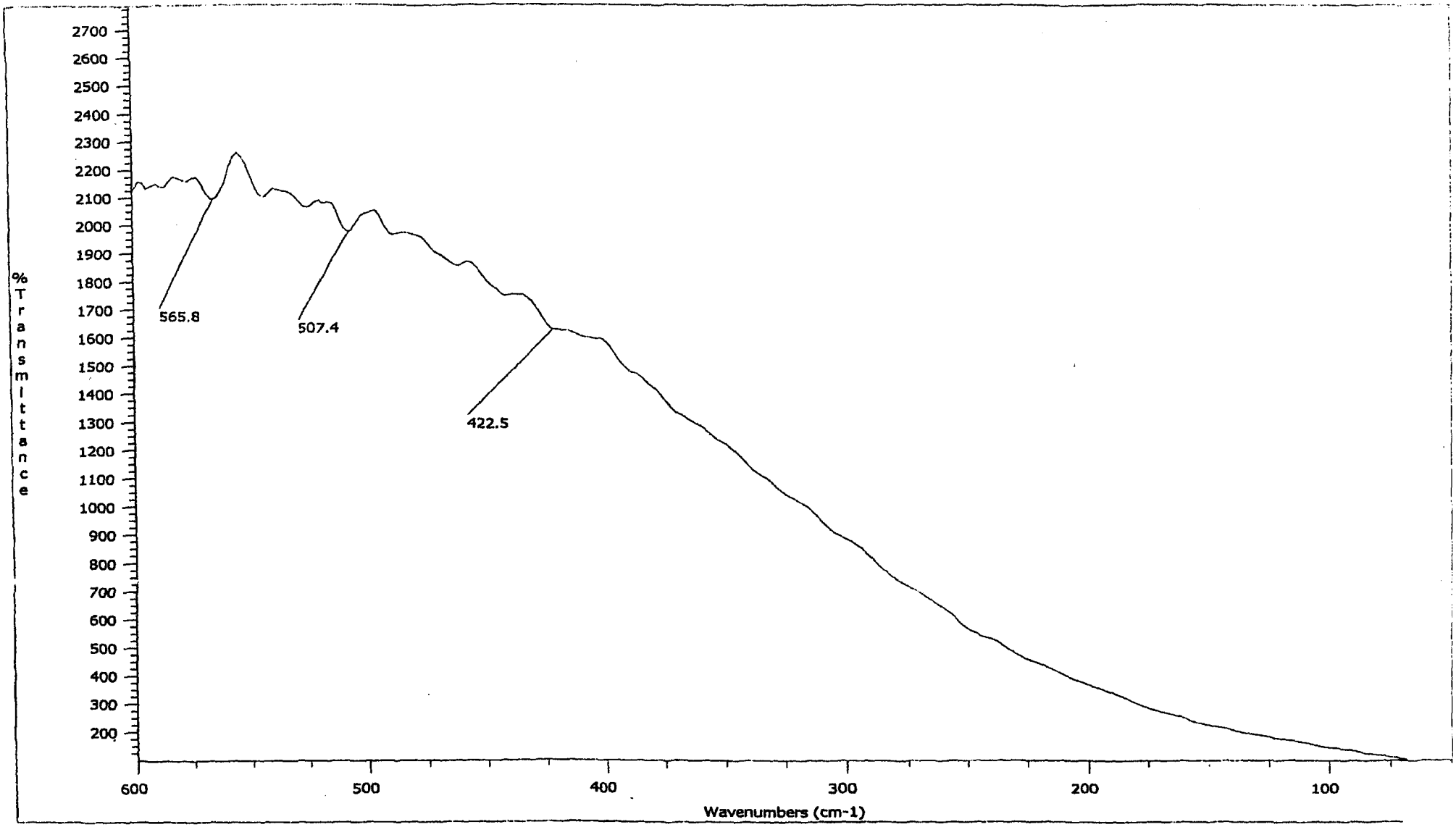

Fig. 5.3.6 (b) IR spectrum of complex $[Ru^{II}(npahH_4)(H_2O)_2]Cl_2$ (29) in CsI

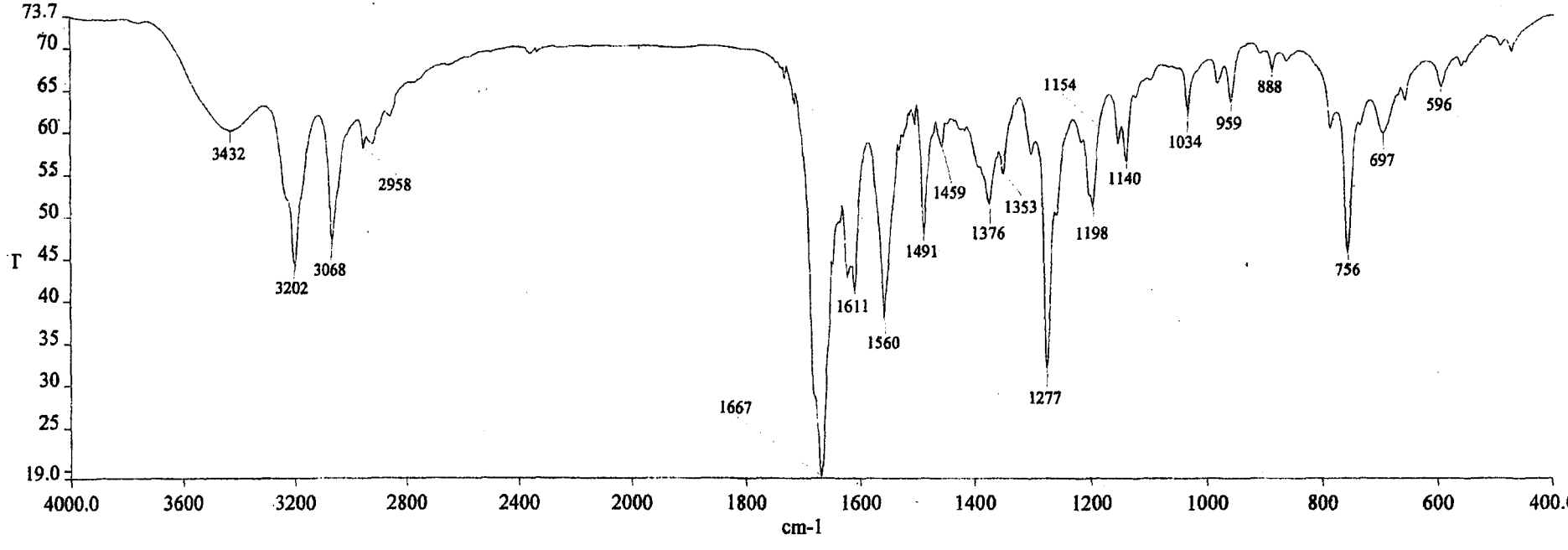

Fig. 5.3.7 IR spectrum of complex $[Ru^{II}(npahH_4)(py)_2]Cl_2$ **(30)** in KBr

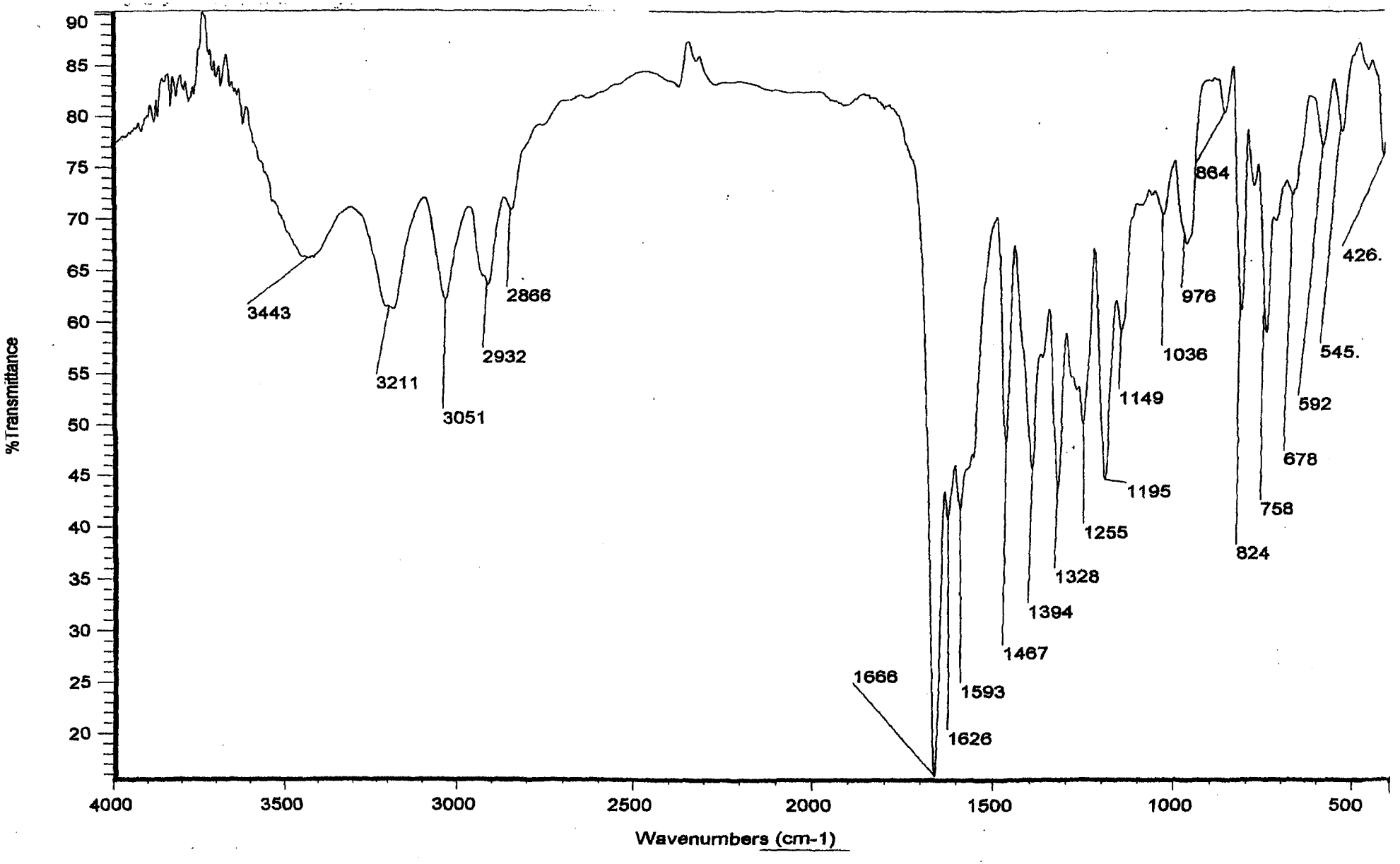

Fig. 5.3.8 IR spectrum of complex $[Ru^{II}(npahH_4)(3\text{-pic})_2]Cl_2$ **(32)** in KBr

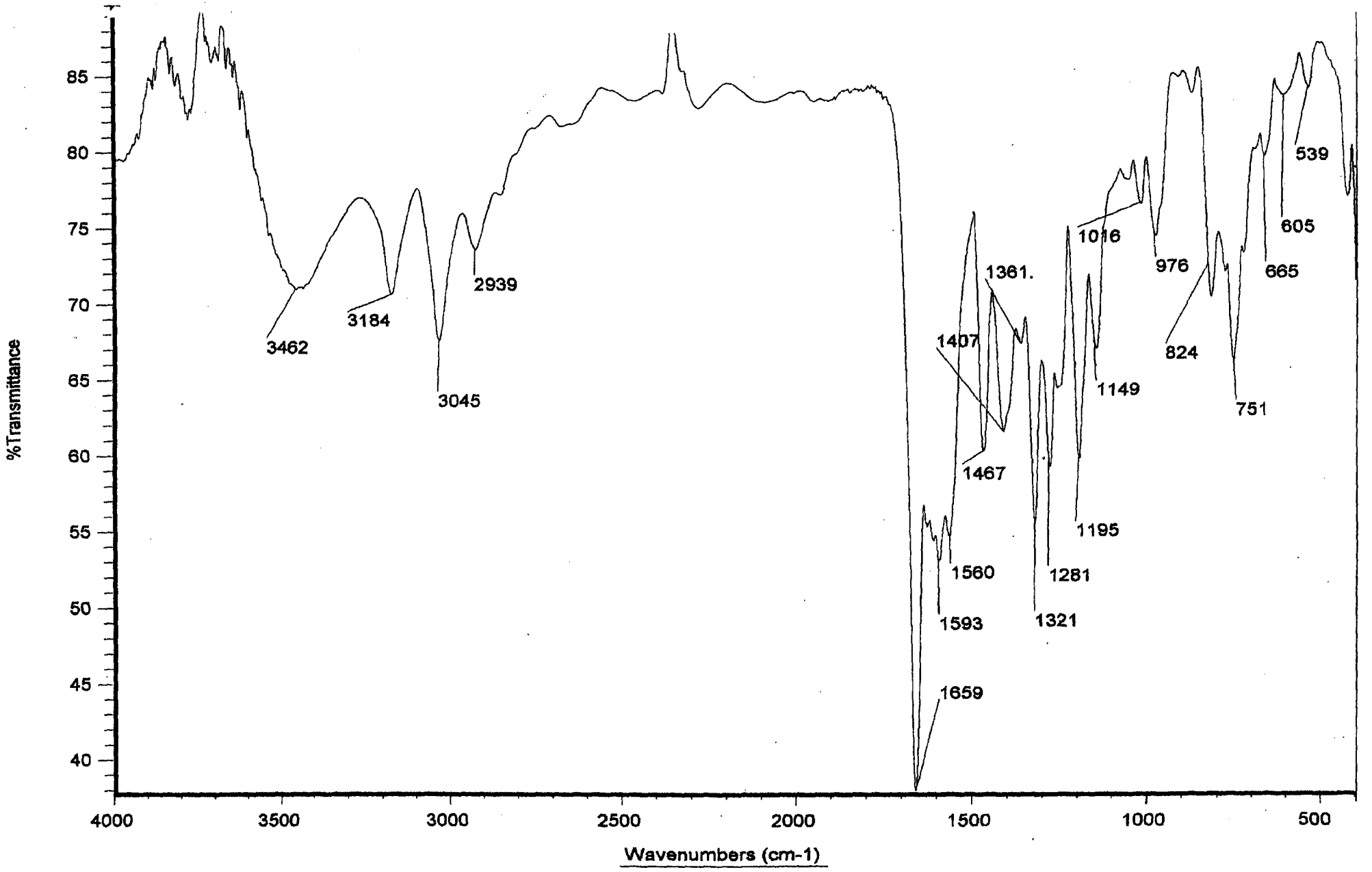

Fig. 5.3.9 (a) IR spectrum of complex $[Ru^{II}(npahH_4)(bpy)]Cl_2$ **(34)** in KBr

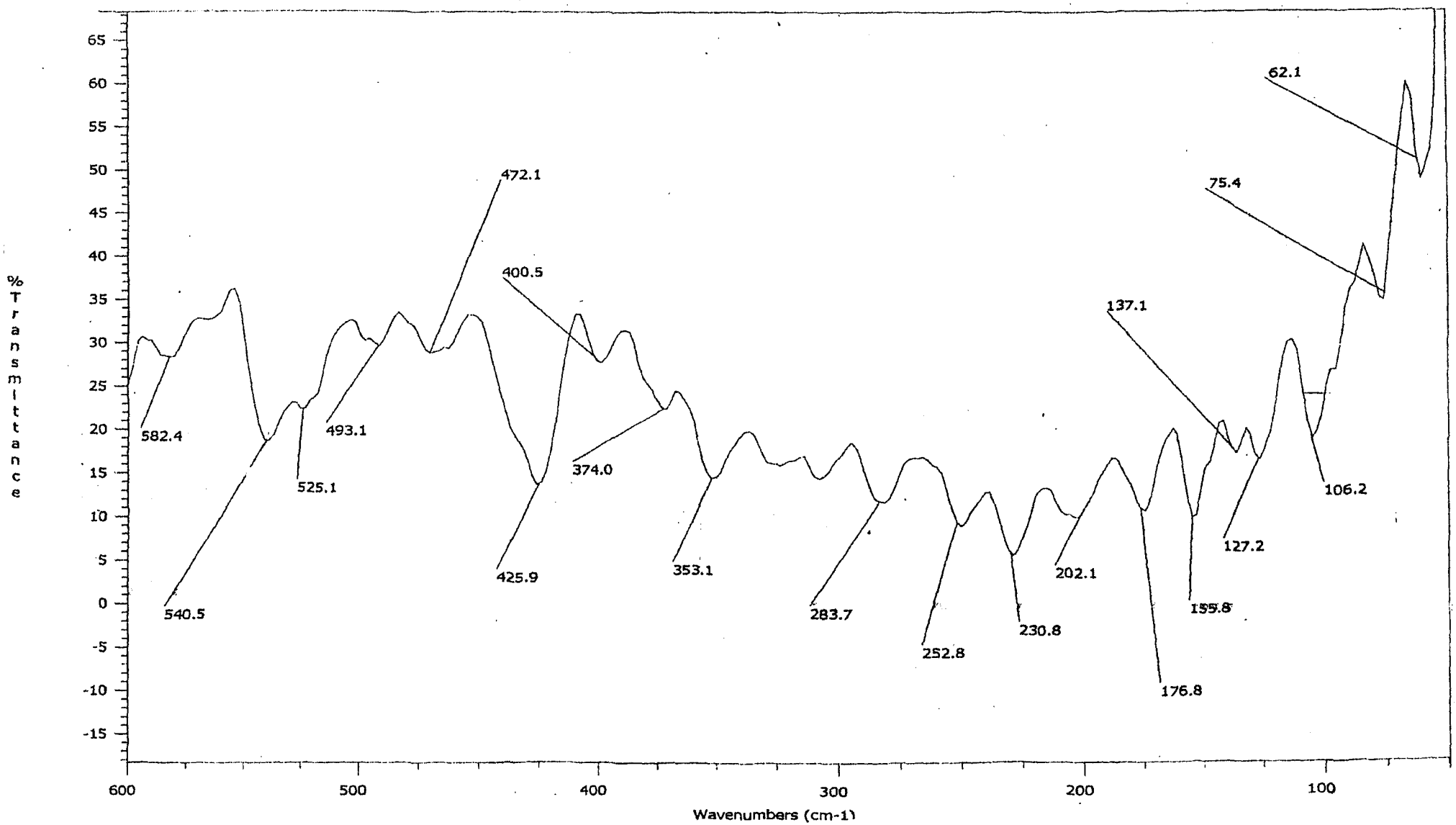

Fig. 5.3.9 (b) IR spectrum of complex $[Ru^{II}(npahH_4)(bpy)]Cl_2$ **(34)** in CsI

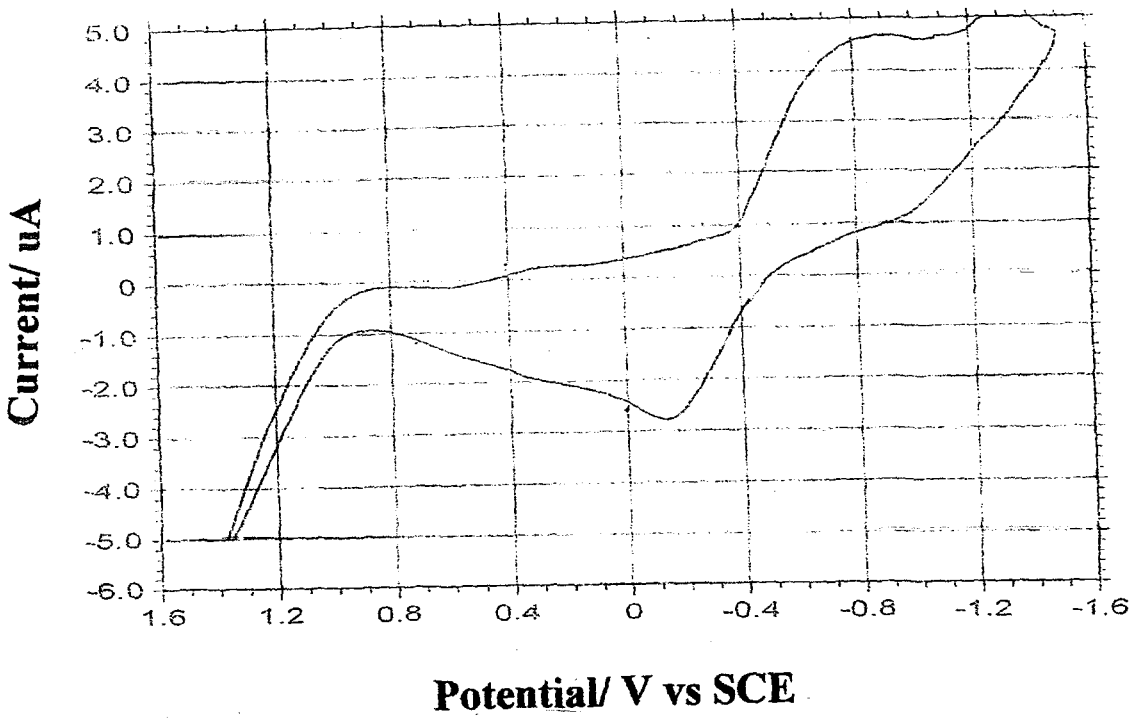

Fig. 5.4.1. Cyclic voltammogram of complex $[Ru^{II}(slahH_4)(2\text{-}pic)_2].Cl_2$ **(24)**

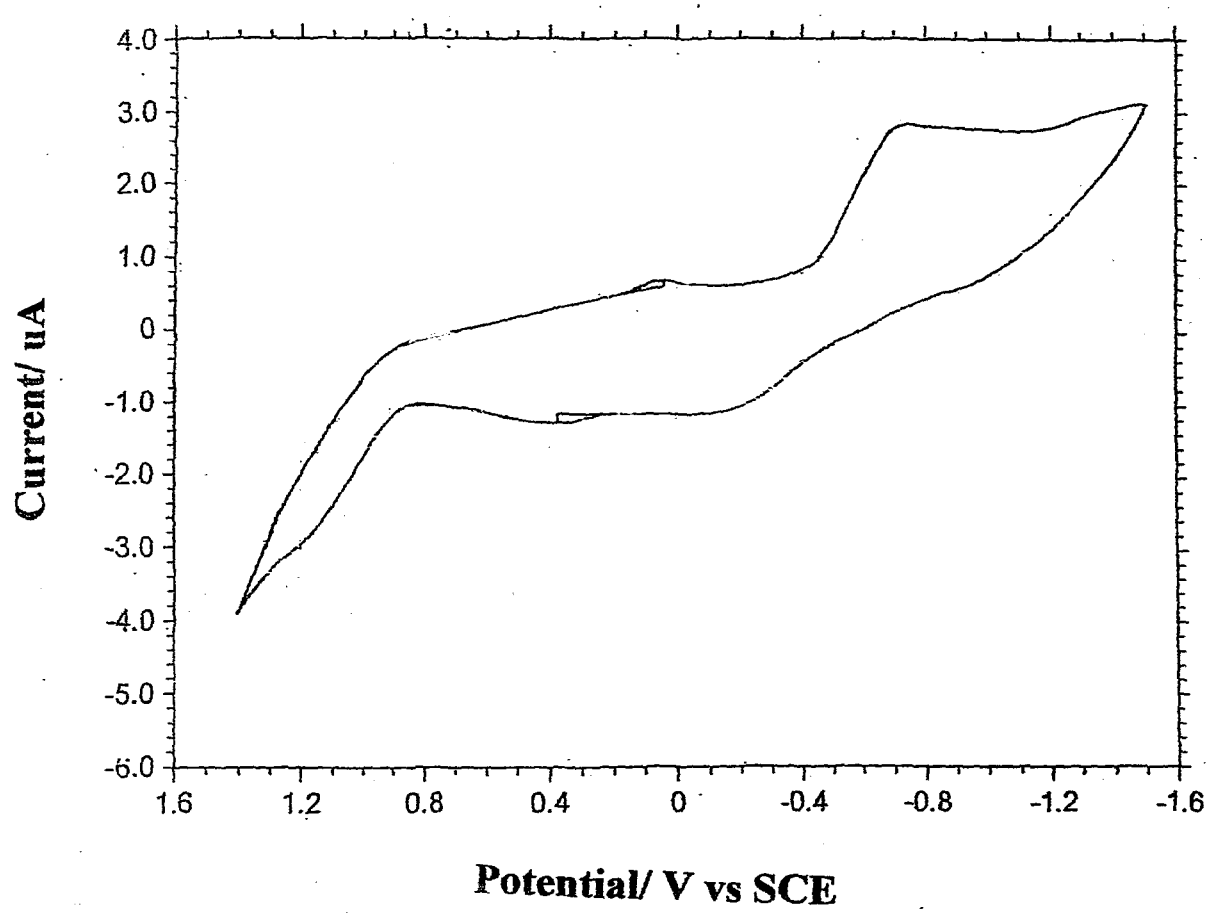

Fig. 5.4.2. Cyclic voltammogram of complex $[Ru^{II}(npahH_4)(H_2O)_2].Cl_2$ **(29)**

Table 5.1: Colour, Decomposition Point and Molar Conductance Data of Monometallic Ruthenium (II) Complexes Derived From Disalicylaldehyde adipoyldihydrazone ($slahH_4$) and Bis(2-hydroxy-1-naphthaldehyde)adipoyldihydrazone ($npahH_4$)

	Complexes	Colour	Decomposition Point (°C)	Molar Conductance (Λ_m) ($ohm^{-1} cm^2 mol^{-1}$)
22.	$[Ru^{II}(slahH_4)(H_2O)_2]Cl_2$	Black	240	1.2
23.	$[Ru^{II}(slahH_4)(py)_2]Cl_2$	Grey	230	1.5
24.	$[Ru^{II}(slahH_4)(2\text{-}pic)_2]Cl_2$	Brownish-black	230	2.9
25.	$[Ru^{II}(slahH_4)(3\text{-}pic)_2]Cl_2$	Grey	230	2.5
26.	$[Ru^{II}(slahH_4)(4\text{-}pic)_2]Cl_2$	Dull-green	230	3.7
27.	$[Ru^{II}(slahH_4)(bpy)]Cl_2$	Dull-brown	238	1.9
28.	$[Ru^{II}(slahH_4)(phen)]Cl_2$	Yellowish-brown	210	1.5

29. $[Ru^{II}(npahH_4)(H_2O)_2]Cl_2$	Dull yellow	220	1.7
30. $[Ru^{II}(npahH_4)(py)_2]Cl_2$	Greyish-Brown	236	2.5
31. $[Ru^{II}(npahH_4)(2\text{-}pic)_2]Cl_2$	Brown	234	3.4
32. $[Ru^{II}(npahH_4)(3\text{-}pic)_2]Cl_2$	Grey	214	2.7
33. $[Ru^{II}(npahH_4)(4\text{-}pic)_2]Cl_2$	Brown	212	2.1
34. $[Ru^{II}(npahH_4)(bpy)]Cl_2$	Grey	240	2.9
35. $[Ru^{II}(npahH_4)(phen)]Cl_2$	Grey	240	4.7

Table 5.2: Analytical and Magnetic Moment Data for Ruthenium (II) Complexes of Disalicylaldehyde adipoyldihydrazone ($slahH_4$) and Bis(2-hydroxy-1-naphthaldehyde)adipoyldihydrazone ($npahH_4$)

Sl. No.	Complex	Analysis: Found (Calcd) %					μ_B (B.M.)
		Ru	C	H	N	Cl	
22.	$[Ru^{II}(slahH_4)(H_2O)_2]Cl_2$	16.785 (16.833)	40.033 (40.001)	4.316 (4.333)	9.284 (9.333)	11.791 (11.833)	diamagnetic
23.	$[Ru^{II}(slahH_4)(py)_2]Cl_2$	14.180 (14.185)	49.741 (50.562)	4.501 (4.494)	12.068 (11.798)	10.201 (9.972)	diamagnetic
24.	$[Ru^{II}(slahH_4)(2\text{-}pic)_2]Cl_2$	13.701 (13.649)	51.921 (51.892)	4.748 (4.865)	11.347 (11.351)	9.591 (9.595)	diamagnetic
25.	$[Ru^{II}(slahH_4)(3\text{-}pic)_2]Cl_2$	13.644 (13.649)	47.011 (51.892)	4.728 (4.865)	11.345 (11.351)	9.570 (9.5912)	diamagnetic
26.	$[Ru^{II}(slahH_4)(4\text{-}pic)_2]Cl_2$	13.644 (13.649)	51.911 (51.892)	4.728 (4.865)	11.35 (11.351)	9.492 (9.501)	diamagnetic
27.	$[Ru^{II}(slahH_4)(bpy)]Cl_2$	14.301 (14.225)	49.011 (50.704)	4.207 (4.225)	11.841 (11.831)	9.831 (10.00)	diamagnetic
28.	$[Ru^{II}(slahH_4)(phen)]Cl_2$	14.106 (13.760)	51.742 (52.316)	4.140 (4.087)	11.364 (11.444)	9.662 (9.673)	diamagnetic

29. $[Ru^{II}(npahH_4)(H_2O)_2]Cl_2$	14.641 (14.553)	48.396 (48.415)	4.861 (4.90)	8.116 (8.069)	10.291 (10.231)	diamagnetic
30. $[Ru^{II}(npahH_4)(py)_2]Cl_2$	12.291 (12.347)	56.290 (55.990)	4.770 (4.890)	10.253 (10.269)	8.691 (8.680)	diamagnetic
31. $[Ru^{II}(npahH_4)(2\text{-}pic)_2]Cl_2$	12.021 (11.967)	55.870 (56.872)	4.760 (4.265)	9.997 (9.953)	8.415 (8.412)	diamagnetic
32. $[Ru^{II}(npahH_4)(3\text{-}pic)_2]Cl_2$	12.102 (11.967)	55.870 (56.872)	4.760 (4.265)	9.997 (9.953)	8.451 (8.412)	diamagnetic
33. $[Ru^{II}(npahH_4)(4\text{-}pic)_2]Cl_2$	12.902 (11.967)	55.870 (56.872)	4.760 (4.265)	9.997 (9.953)	8.451 (8.412)	diamagnetic
34. $[Ru^{II}(npahH_4)(bpy)]Cl_2$	12..415 (12.408)	56.170 (56.020)	3.704 (4.668)	10.370 (10.319)	8.765 (8.722)	diamagnetic
35. $[Ru^{II}(npahH_4)(phen)]Cl_2$	12.131 (12.053)	56.943 (57.280)	4.511 (4.535)	11.213 (10.024)	8.391 (8.473)	diamagnetic

Table 5.3: Important Electronic Spectral Bands of Ligands Disalicylaldehyde adipoyldihydrazone and Bis(2-hydroxy-1-naphthaldehyde)adipoyldihydrazone and their Monometallic Ruthenium(II) complexes

Sl. No	Ligand/Complex	λ_{max}(nm)(ϵ_{max} dm^3 mol^{-1} cm^{-1}) for conc 10^{-2} M soln				
	$slahH_4$	320(2019)				
	$npahH_4$	363(1852)				
22.	$[Ru^{II}(slahH_4)(H_2O)_2]Cl_2$	406(905)	460(2887)	690(100)		
23.	$[Ru^{II}(slahH_4)(py)_2]Cl_2$	355(2354)	387(618)	435(3500)	586(1387)	
24.	$[Ru^{II}(slahH_4)(2\text{-}pic)_2]Cl_2$	422(3313)	614(2561)			
25.	$[Ru^{II}(slahH_4)(3\text{-}pic)_2]Cl_2$	395(880)	419(800)	471(678)	604(252)	679(200)
26.	$[Ru^{II}(slahH_4)(4\text{-}pic)_2]Cl_2$	408(880)	423(2669)	477(2766)	620(100)	
27.	$[Ru^{II}(slahH_4)(bpy)]Cl_2$	406(872)	423(2250)	452(2122)	553(742)	
28.	$[Ru^{II}(slahH_4)(phen)]Cl_2$	406(892)	450(2720)	620(600)		

29. $[Ru^{II}(npahH_4)(H_2O)_2]Cl_2$	352(2335)	399(2244)	436(3500)	540(531)
30. $[Ru^{II}(npahH_4)(py)_2]Cl_2$	383(6248)	420(3169)	635(614)	
31. $[Ru^{II}(npahH_4)(2\text{-pic})_2]Cl_2$	406(880)	423(2558)	437(2539)	654(149)
32. $[Ru^{II}(npahH_4)(3\text{-pic})_2]Cl_2$	405(903)	423(2616)	440(2649)	650(329)
33. $[Ru^{II}(naphH_4)(4\text{-pic})_2]Cl_2$	406(884)	447(2720)	477(2941)	660(654)
34. $[Ru^{II}(npahH_4)(bpy)]Cl_2$	405(886)	449(2764)	554(2753)	620(160)
35. $[Ru^{II}(npahH_4)(phen)]Cl_2$	406(876)	423(2651)	545(755)	620(714)

Table 5.4: ^{1}H NMR spectral data (in δ) for adipoyldihydrazones and some of their Monometallic Ruthenium Complexes

Ligand/ Complex	δ(-CH_2-)	δ(phenyl/ naphthyl)	δ(CH=N)	δ(NH)	δ(OH)
slahH_4	2.11(d, 22.5 Hz) 2.55(d, 22.5 Hz)	6.90-7.35(m)	8.26(s) 8.33(s)	10.18(s)	11.20(s) 11.62(s)
[Ru^{II}(slahH_4)(3-pic)$_2$]Cl_2 (25)	2.20(d, 33.8 Hz) 2.54(d, 33.8 Hz)	6.90-7.60(m)	8.30(s) 8.30(s)	10.20(s)	11.19(s) 11.63(s)
[Ru^{II}(slahH_4)(bpy)]Cl_2 (27)	2.30(s) 2.49(s)	6.80-7.80(m)	8.26(s) 8.36(s)	10.18(s)	11.20(s) 11.63(s)
npahH_4	1.66(d) 2.30(d, 33 Hz) 2.58(d, 33 Hz)	7.10-8.42(m)	8.93(s) 9.15(s)	11.22(s) 11.26(s)	11.69(s) 12.65(s)
[Ru^{II}(npahH_4)(H_2O)$_2$]Cl_2 (29)	1.65(d) 2.20(d, 54 Hz) 2.58(d, 54 Hz)	7.10-8.44(m)	8.94(s) 9.15(s)	11.22(d, 4.8 Hz) 11.26(d, 4.8 Hz)	11.69(s) 12.65(s)
[Ru^{II}(npahH_4)(3-pic)$_2$]Cl_2 (32)	1.668(d) 2.39(d. 41.6 Hz) 2.50(s, intensity high) 2.58(d, 41.6 Hz)	7.10-8.46(m)	8.94(s) 9.15(s)	11.22(s) 11.27(s)	11.71(s) 12.66(s)
[Ru^{II}(npahH_4)(bpy)]Cl_2 (34)	1.72(s) 2.21(d, 61.5 Hz) 2.58(d, 61.5 Hz)	7.08-8.58(m)	8.96(s) 9.15(s)	11.26(d, 4.95 Hz) 11.29(d, 4.95 Hz)	11.67(s) 12.67(s)

Table 5.5: ^{13}C NMR Spectral Data of Bis(2-hydroxy-1-naphthaldehyde)adipoyldihydrazone and some of its Monometallic Ruthenium complexes

Carbon atoms	$npahH_4$ δ^x	$[Ru^{II}(npahH_4)(H_2O)_2]Cl_2$ (29) δ^x	$\Delta\delta^y$	$[Ru^{II}(npahH_4)(3\text{-pic})_2]Cl_2$ (32) δ^x	$\Delta\delta^y$	$[Ru^{II}(npahH_4)(bpy)]Cl$ (34) δ^x	$\Delta\delta^y$
C(3a), C(3b)	172.65	172.99	-0.34	-	-	172.52	+0.13
C(14a), C(14b)	167.72	167.72	0	167.66	+0.06	167.63	+0.09
C(4a), C(4a)	157.52, 156.55	157.51, 156.45	+0.06	157.47, 156.50	+0.55	157.52,156.56	0
C(11a), C(11b)	144.62, 142.18	144.62, 142.15	+0.01	144.61, 142.21	-0.01	144.58, 142.26	-0.02
C(6a), C(6b))	132.04, 131.30	132.09, 131.87, 131.29	-0.08	131.96, 131.27	+0.05	131.91, 131.27	+0.08
C(10a), C(10b)	128.57, 127.74	128.61	-0.55	128.51, 127.40	- 0.02	128.48, 127.64, 127.38	+0.33
C(8a), C(8b)	127.46, 127.23	127.49, 127.29	-0.04	127.17	+0.18	127.10	+0.25
C(9a), C(9b)	123.10, 121.47	123.13	-0.89	123.02, 121.36	+0.76	122.00, 121.13	+0.67
C(7a), C(7b)	120.12	120.20	-0.08	120.06	+0.06	119.93	-0.19
C(5a), C(5b)	118.60, 118.05	118.61, 118.05	0	118.54, 118.01	+0.05	118.54, 118.02	+0.05
C(13a), C(13b)	109.11, 108.101	109.20, 108.15	-0.07	109.05, 108.04	+0.06	109.04, 107.02	+0.09
C(12a), C(12b)	79.03, 78.37	79.07, 78.75, 78.42	-0.05	79.00, 78.66, 78.33	+0.04	78.90, 78.57,78.24	+0.13
C(2a), C(2b)	33.81, 31.96	33.82, 31.71	+0.12	33.76, 31.00	+0.51	33.80, 31.89	+0.04
C(1a), C(1b)	24.95, 24.64	24.80, 24.66	+0.07	24.59, 24.08	+0.46	24.73, 24.60	+0.13

Table 5.6: Structurally Significant Infrared Spectral Bands of Disalicylaldehyde adipoyldihydrazone ($slahH_4$) and Bis(2-hydroxy-1-naphthaldehye)adipoyldihydrazone and their Monometallic Ruthenium(II) Complexes

Sl. No	Ligand/Complex	ν(OH) +ν(NH)	ν(C=O)	ν(C=N)	ν(C-O)	ν (N-N)	ν(M-O) (phenolic/ naphtholic)	ν(M-O) (carbonyl)	ν(M-N) Pyridine base in-plane- ring and out-of –plane ring deformation
	$slahH_4$	3445(m) 3436(m) 3204(s) 3065(sbr)	1679(s)	1620(s)	1275(s)	1036(m)			
	$npahH_4$	3469(s) 3430(sbr) 3224(s) 3051(sbr)	1666(s)	1630(s) 1593(m)	1281(m)	1030(w)			
22.	$[Ru^{II}(slahH_4)(H_2O)_2]Cl_2$	3496 (sbr) 3151(sbr) 3058(sbr)	1646(vs)	1573(s)	1275(s)	-	-	470(m)	-
23.	$[Ru^{II}(slahH_4)(py)_2]Cl_2$	3400(mbr) 3202(mbr) 3053(mbr)	1656(vs)	1624(s) 1601(s)	1280(w)	-	-	472(m)	279(s) 445(m)
24.	$[Ru^{II}(slahH_4)(2\text{-}pic)_2]Cl_2$	3594(sbr) 3418(sbr) 3208(sbr)	1661(vs)	1605(ssh)	1275(s)	1033(m)	-	468(m)	290(w) 435(m) 658(m)
25.	$[Ru^{II}(slahH_4)(3\text{-}pic)_2]Cl_2$	3443(s) 3211(s) 3065(s)	1679(vs)	1619(vs)	1275(m)	1036(w)	-	475(m)	277(s) 435(m) 658(m)
26.	$[Ru^{II}(slahH_4)(4\text{-}pic)_2]Cl_2$	3432(s) 3197(s) 3053(s)	1657(s)	1625(s) 1602(s)	1284(m)	1030(m)	-	480(m)	275(m) 430(m) 650(w)
27.	$[Ru^{II}(slahH_4)(bpy)]Cl_2$	3449 (sbr) 3211(sbr) 3065(sbr)	1672(s)	1619(s)	1275(m)	1036(w)	-	472(m)	270(m) 435(w) 650(w)
28.	$[Ru^{II}(slahH_4)(phen)]Cl_2$	3432(s) 3201(s) 3067(s)	1667(s)	1620(s) 1612(m)	1277(s)	1034(m)	-	468(ssh)	287(m) 430(w) 658(w)

29. $[Ru^{II}(npahH_4)(H_2O)_2]Cl_2$	3449 (mbr) 3211(mbr) 3058(mbr)	1666(vs)	1636(s) 1593(s)	1255(m)	1036(m)	545(m)	-	-
30. $[Ru^{II}(npahH_4)(py)_2]Cl_2$	3442 (mbr) 3202(mbr) 3068(mbr)	1667(vs)	1624(s) 1611(s)	1245(m)	1034(m)	550(w)	-	-
31. $[Ru^{II}(npahH_4)(2\text{-pic})_2]Cl_2$	3431(mbr) 3202(m) 3068(m)	1667(vs)	1620(ssh) 1612(m)	1250(s)	1034(m)	565(s)	-	290(w) 440(m) 665(m)
32. $[Ru^{II}(npahH_4)(3\text{-pic})_2]Cl_2$	3443(mbr) 3221(mbr) 3051(mbr)	1666(vs)	1626(s) 1593(s)	1255(m)	1036(w)	545(m)	-	290(w) 445(w) 660(m)
33. $[Ru^{II}(npahH_4)(4\text{-pic})_2]Cl_2$	3436(sbr) 3211(mbr) 3045(mbr)	1666(s)	1619(s) 1595(ssh)	1255(m)	1036(m)	560(m)	-	291(m) 450(w) 650(w)
34. $[Ru^{II}(npahH_4)(bpy)]Cl_2$	3462 (mbr) 3184(wbr) 3045(mbr)	1669(vs)	1593(s) 1620(s)	1250(m)	1036(w)	539(m)	-	284(m) 426(m) 665(m)
35. $[Ru^{II}(npahH_4)(phen)]Cl_2$	3429 (sbr) 3230(mbr) 3025(mbr)	1666(vs)	1633(s) 1576(ssh)	1248(w)	1050(m)	525(s)	-	288(m) 440(m) 640(m)

Table 5.7: The Electrochemical Parameters for the Dihydrazones and their Monometallic Ruthenium(II) Complexes (Pot vs SCE)

	Ligand/Complex	Epa/V	Epc/V	ΔEp(mV)
	$slahH_4$	+0.35	+0.20	150
	$npahH_4$	0.00 +0.35	-0.15 -	150 -
24.	$[Ru^{II}(slahH_4)(2\text{-}pic)_2]Cl_2$	+0.36 - -0.15	+0.30 -0.30 -0.75	60 - 60
26.	$[Ru^{II}(slahH_4)(4\text{-}pic)_2]Cl_2$	+0.35 +0.12	+0.07 -0.30	280 420
27.	$[Ru^{II}(slahH_4)(bpy)]Cl_2$	+0.01	-0.245	255
28.	$[Ru^{II}(slahH_4)(phen)]Cl_2$	+0.35 -0.12	+0.05 -0.35	300 230
29.	$[Ru^{II}(npahH_4)(H_2O)_2]Cl_2$	+0.38 -0.18	+0.05 -0.71	330 530
30.	$[Ru^{II}(npahH_4)(py)_2]Cl_2$	- -0.20	-0.11 -	- -
31.	$[Ru^{II}(npahH_4)(2\text{-}pic)_2]Cl_2$	+1.00 -1.10	-0.20 -	120 -
32.	$[Ru^{II}(npahH_4)(3\text{-}pic)_2]Cl_2$	+0.48 +0.15	+0.15 -	330 -
33.	$[Ru^{II}(npahH_4)(4\text{-}pic)_2]Cl_2$	+0.80 +0.30	+0.30 -	50 -
34.	$[Ru^{II}(npahH_4)(bpy)]Cl_2$	+0.35 -0.30 -	-0.12 - -0.70	230 - -
35.	$[Ru^{II}(npahH_4)(phen)]Cl_2$	-0.10 +0.50	-0.30 -	200 -

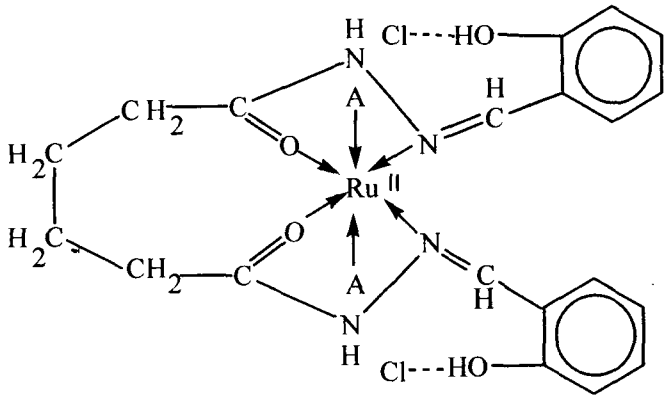

Fig. 5.6.1 Suggested structure of complex $[Ru^{II}(slahH_4)(A)_2]Cl_2$ (where A = H_2O, **(22)**; py, **(23)**; 2-pic, **(24)**; 3-pic, **(25)** and 4-pic, **(26)**)

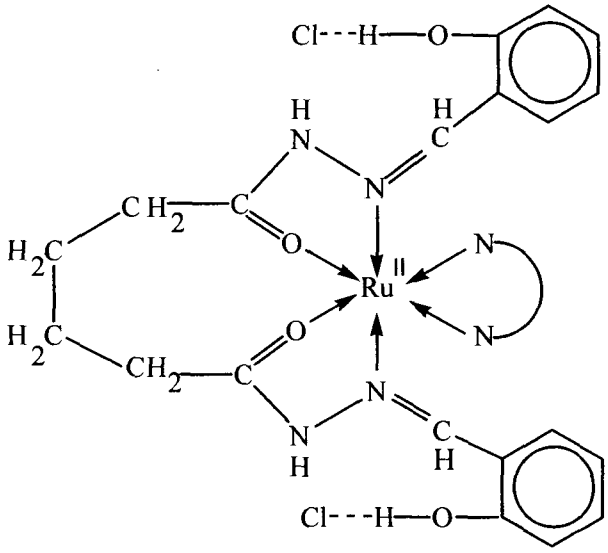

Fig. 5.6.2 Suggested structure of complex $[Ru^{II}(slahH_4)(\overset{\frown}{NN})]Cl_2$ (where $\overset{\frown}{NN}$ = bpy, **(27)** and phen, **(28)**)

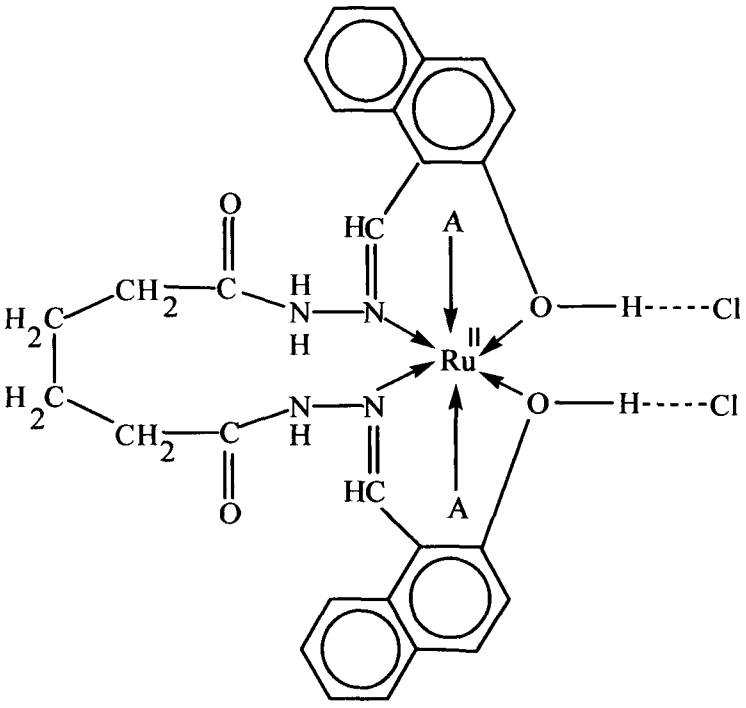

Fig. 5.6.3 Suggested structure of complex $[Ru^{II}(npahH_4)(A)_2]Cl_2$ (where A = H_2O, **(29)**; py, **(30)**; 2-pic, **(31)**; 3-pic, **(32)** and 4-pic, **(33)**)

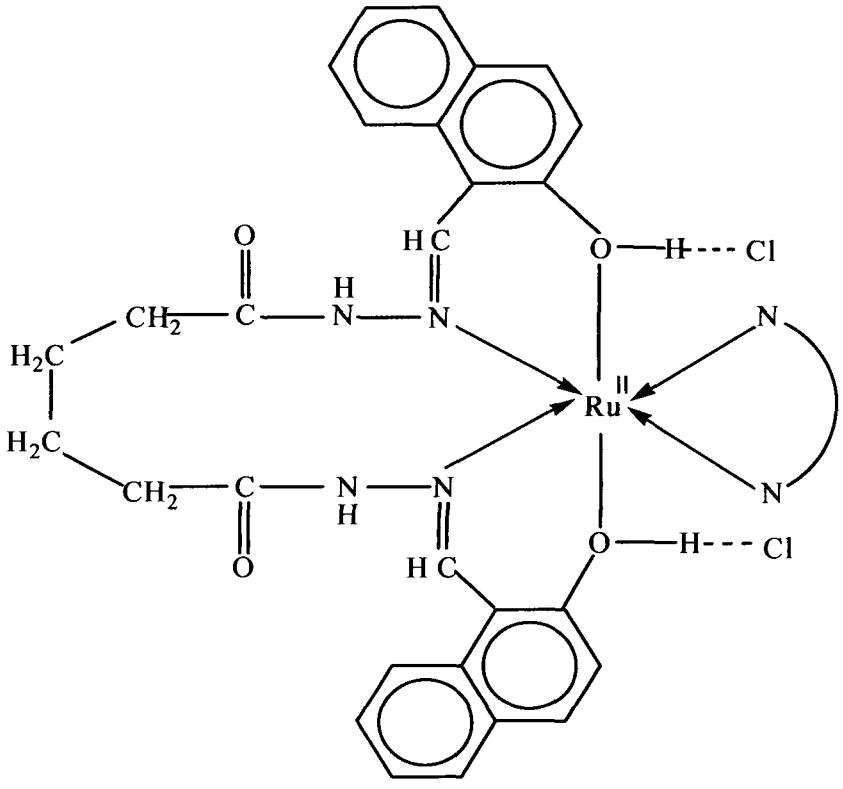

Fig. 5.6.4 Suggested structure of complex $[Ru^{II}(npahH_4)(\overset{\frown}{NN})]Cl_2$ (where $\overset{\frown}{NN}$ = bpy, **(34)** and phen, **(35)**)

CHAPTER-VI

Synthesis And Characterization Of Heterobimetallic Complexes Of Manganese And Ruthenium Derived From Disalicylaldehyde adipoyldihydrazone And Bis(2-hydroxy-1-naphthaldehyde)-adipoyldihydrazone

Introduction

The molecular complexes containing two or more different metal ions are of interest in several areas like multimetallic enzymes [269-271], homogeneous catalysis [267], heterogeneous catalysis [268] and synthesis of solid state phases of industrial and technological importance.

With the exception of scandium and titanium, all first row transition metal ions occur in the biological systems. The metal ions in the enzyme occur either alone or in combination with another atom of their own kind or different kind giving rise to monometallic, homobimetallic and heterobimetallic enzymes, respectively. As an example, Mo, Zn and Ni are present alone in xanthine oxidase, carbonic anhydrase and bacterial hydrogenase and catalase, respectively, giving rise to monometallic enzymes. On the otherhand, copper and manganese present with more atoms of their own kind in haemocyanin and tyrosinase [272] and oxygen evolving complex (OEC) [273] in photosystem II, respectively, giving rise to multimetallic enzymes. Further, Mo is found in the enzyme nitrogenase [274] in combination with iron whereas, Zn and Cu are found together in superoxide dismutase [275] and Ni occurs in combination with iron in jack bean urease [276] and Ni-Fe hydrogenase enzyme [277]. Mn also occurs in superoxide dismutase in combination with copper and iron. Again, Zn also occurs in red kidney bean photophase in combination with iron [278]. Zn also occurs in combination with copper in protein obtained from bovine tissue and

in combination with cadmium in metallothionein protein obtained from rat liver [279].

The heterobimetallic complexes of uranium (VI) and first row transition metal ions exhibit well defined four electron transfer process [280], a process which occurs in the reduction of dioxygen. A cobalt or nickel promoted molybdenum catalyst is important in industrial catalysis, particularly in hydrosulfurization process where organic sulphur compounds in petroleum feed stocks are heterogeneously desulfurized with dihydrogen [281].

Heterobimetallic complexes are also important in the preparation of ceramic materials favouring an intimate mixing of the elements which can enable reactions at lower temperatures rather than for traditional route or the preparation of purer inaccessible solid state phases [282]. The high temperature superconductors may be prepared from soluble precursors owing to their low costs, the possibility to coat large unusually shaped objects and high homogeneity and purity [283]. Thus, the heterobimetallic (heteropolymetallic) complexes may be reduced under ordinary conditions to yield alloys and other materials of industrial and technological importance.

Heterobimetallic complexes derived from combination of Mn and Cu [284] and Mn and Ru [285] might have more potential in the oxidation of H_2O to dioxygen which may find application in the conversion of solar energy into fuel and electricity.

A tetramanganese complex present in photosystem II (PS-II) activates CO_2 and H_2O molecules in such way that light energy is transformed into fuel by reduction of CO_2 and simultaneously water is oxidized to molecular oxygen. Oxygen evolution continues even when some of the manganese atoms are replaced with other divalent metal ions which restore electron transport in PS-II. Thus, metal complexes provide an effective means of the conversion of solar energy into fuel and electricity which emerges as an important part of future sustainable energy systems. An attractive way to

develop efficient system for this conversion is to mimic natural photosystem in green plants. Thus the heterobimetallic complexes of manganese with other metal ions assume much significance in the sense that they might serve as potential candidate for the conversion of solar energy into fuel and electricity [285]. In this connection it is pertinent to mention a dimmer bimetallic Ru(III) complex undergoes oxidation by either chemical or electrochemical means to produce O_2 from two coordinated water molecules [286]. The bipyridyl ruthenium complexes in +3 oxidation state draw particularly more attention because they represent the oxidative portion of the popular $[Ru(bpy)_3]^{2+}$ sensitized photosystem [14]. The significance of ruthenium complexes is that they can form the core of new polymetallic species that may have application in excited state energy and electron–transfer reactions. Heterobimetallic complexes of manganese and ruthenium have potential to develop special characteristics by co-operative interaction which may find applications in the conversion of solar energy into fuel and electricity. Recent work in the field has indicated that homobimetallic systems are more efficient in the activation studies than the corresponding monometallic analogues, the heterobimetallic complexes derived from widely varying transition metal ions have potential to show better promise in this field [288]. Although monometallic and homobimetallic complexes of manganese and ruthenium have been investigated in some details to mimic natural photosynthesis in green plants as well as in oxidation of organic molecules, the studies using manganese and ruthenium in the same complexes are quite meagre [285]. The major problem in this case has been difficult task of synthesizing the pure samples of bimetallic complexes containing two different metal ions. The synthesis of bimetallic products is accessible by the strategies developed by Lintvedt [280] via monometallic complex intermediate by the use of polydentate ligands and Davis et al [282] via transmetallation beginning with complex of discrete molecularity as target and another metal salt or complex as a transmetallator.

Polydentate ligands used to construct discrete heterobimetallic complexes have metal specific sites to prevent their disproportionation into homobimetallic product mixtures. This limits the number of heteromolecules that can be obtained. What is needed is simple and flexible way of making large families of heteromolecules containing manganese and ruthenium. The polyfunctional dihydrazones containing amide, azomethine and phenol functions in duplicate are highly versatile flexible ligands for achieving this.

Manganese and ruthenium have very rich and different co-ordination chemistries but there is evidence that they can coexist in the same molecule. However, the result of having both elements in the same molecule is only beginning to be appreciated because there are so few known examples. It appears pertinent at this stage to survey briefly the recent literature related with heterometal compounds in general and the heterometal compounds of manganese and ruthenium in particular.

Three decades ago Robson initiated a series of studies concerned with a rational synthetic approach to cluster compound [289, 290]. In this work, he introduced the concept of macrocyclic ligand i.e. a ligand capable of securing two metal ions in close proximity. Examples of heterodinuclear complexes started appearing around 1974-75, although an isolated reference appeared in 1963 [291]. However, acyclic ligands having similar properties could also be used for rational synthetic approach to cluster compounds. Since then various types of polynucleating ligands including the end–off type, the side-off type and the macrocyclic type capable of simultaneously binding two or more metal ions in close proximity have been developed [292-294] and their complexation behaviour explored.

Examples of heterodinuclear complexes started appearing around 1974-75 [356-358], although an isolated reference appeared in 1963 [291].

Roberts and Geoffery [357] summarised the synthesis and chemistry of

complexes containing widely divergent transition metal centres.

In 1979, Casellato and coworkers [295] presented a review on homo and hetero-dinuclear complexes of cyclic Schiff bases containing N_2O_2 and O_2O_2 coordination chamber. The heterobimetallic complexes containing first row transition metal ions and UO_2^{2+} ions were described. The characterization of heterobimetallic complexes was carried out by molar conductance, magnetic moment and spectroscopic data. The review also reported crystal structure of some heterodinuclear complexes.

Stephan [296] summarized literature on heterobimetallic complexes of early and late transition metal ions. In this review, the discussion was segregated according to the type of ligands linking the disparate metal centres. The discussion was related with the heterometal complexes in which the ligands such as carbonyl, hydrido, halide, amino and phosphido, selenido and thiolato and chalcogenide-atom linked the heterometal centres. The review dealt with the structural, spectroscopic and theoretical studies of ELHB complexes that described some of the nature and degree of direct electronic interactions between early and late metal centres.

Fenton and coworkers [297] published a review on monometallic, bimetallic and heterobimetallic complexes of first series transition metal ions derived from polyfunctional ligands.

Chetcuti [298] published a review in 1994 on heterobimetallic complexes derived from a variety of ligands. In this review, he summarized the data on structural chemistry of heterobimetallic complexes.

Guerriero and coworkers [299] published a large review which contains a detailed summary of the structures of tetranuclear and other polynuclear complexes formed with acyclic and macrocycles Schiff-base ligands.

Murray [300] presented a review on the magneto-chemistry of homo- and hetero-tetranuclear first–row d-block elements. He reported that except Ti and V, homo- and hetero-tetranuclear complexes of remaining first row transition metal complexes derived from various types of multidentate ligands were investigated in detail.

Okawa and coworkers [301] reviewed literature related with synthesis and structure of various types of heterodinuclear metal complexes derived from symmetrical and unsymmetrical phenol-based compartmental ligands. The heterodinuclear complexes of $N(amine)_4O_2$-type of macrocycles, $N(imine)_4O_2X$- type of macrocycles and $N(amine)_4N(imine)_2O_2$- type macrocycles were described.

Wheatly and Kalck [302] recently published a review on structure and reactivity of early–late heterobimetallic complexes. The review summarizes a large number of early–late heterobimetallic complexes described in the literature. The literature survey indicated that the reactivity of early–late bimetallic complexes are strikingly different from those of their monomeric analogues. In many cases, the metal-metal interactions were found to be weak. The review described the heterometallic complexes with unbridged metal-metal bonds, heterometal compounds containing neutral bridging ligands, monoanionic bridging ligands, bianionic bridging ligands, trianionic bridging ligands and polyanionic bridging ligands and metallomacrocyclic compounds.

Davies and coworkers [303] isolated a family of heteropolymetallic complexes $(\mu_4\text{-}O)L_4Cu_{4-x}MCl_6$ (M = Ni and x = 0 - 4 in I-IV, respectively) where L is N,N'-diethyl nicotinamide. They evaluated these complexes by fast atom bombardment mass spectrometry. They did not observe the formation of molecular ion under the analysis conditions they employed, but they observed the production of characteristic fragments as well as the formation of several metal–ligand complexes. They did not observe formation of heteropolymetallic fragments as a result of fast atom bombardment.

Bosnich and Fraser [304] prepared homobimetallic and heterobimetallic complexes of the type $[M^1(S,S\text{-Cypin})MCl]PF_6$ and $[M^1(S, S\text{-Cypin})M](PF_6)_2$ (where M, M^1 = In, Cu, Ni, Co, Mn) from a chiral macrocyclic binucleating ligand, S, S–Cypin. The macrocyclic framework contains the chiral diamine (1S, 2S)-trans-1, 2-bis(aminomethyl)cyclopentane. The macrocyclic closure with the chiral diamine is achieved in good yield by Schiff base condensation of metaldialdehyde complexes (dialdehyde: 1, 6-bis(2-pyridyl)-2, 5-bis(2-hydroxyl)-3-formyl-5-methyl benzyl)-2, 5-diazahexane). Solution magnetic moments of the bimetallic complexes containing two paramagnetic metals indicate spin-spin coupling at 20 °C. All of the heterobimetallic complexes were reported to be high–spin except that of Co(III). They characterized heterobimetallic copper complexes by EPR spectroscopy. They showed that homobimetallic copper complex exists as a spin–paired singlet, whereas the spectrum of heterobimetallic Ni-Cu complex exhibits the spin–interacting doublet state. They used EPR spectra to monitor both inter and intramolecular metal site scrambling of these complexes and concluded that there was no metal scrambling. The electronic spectral studies indicated that heterobimetallic complexes of the type $(Co^{III}(L)M^{II})$ have distorted trigonal bipyramidal open site metal geometries, whereas the Cu ions in the $[M(L)Cu]^{2+}$ complexes generally have more planar but distorted four or five coordinate structures. Complexes were characterized by cyclic voltammetry as well.

Lundquist et al [305] prepared a heterobimetallic $[(COD)Rh]_2OsH_2P_3CO_2$ from reaction of CO_2 with $(COD)RhH_3OsP_3$ (where COD = 1, 5-cyclooctadiene, P = PMe_2Ph). The complex was characterized by N.M.R and vibrational spectroscopy and the structure of the complex was determined by X-ray crystallographic studies. ^1H NMR and ^{31}P NMR spectroscopic data for complex (1) indicated a material containing two hydrides, one near – OsP_3 unit and two Rh(COD) units, with the two Rh(COD) units being symmetry equivalent. Two of the three phosphine ligands are also symmetry equivalent. The spectroscopic characteristics are consistent with the

molecular structure determined by X-ray diffraction. The compound is stereochemically rigid species with a planar PRh_2OsCO_2 unit. The coordination geometry at osmium is made up of two orthogonal planes. They located the position of hydride hydrogen atoms using molecular mechanics calculations. These hydrogen positions yield a square planar coordination geometry about rhodium. The compound did not show reactivity towards H_2 and external nucleophiles. This was attributed to steric shielding of the $H_2OsRh_2CO_2$ moiety by the phosphine and olefin ligands.

Constable and Harverso [306] synthesized interesting heteroheptanuclear complexes Ru_6Fe and Ru_6Co from bipyridyl based ligands. The formations of the complexes was established by MALDI-TOF mass spectrometry. Based on the molecular modeling, the heptanuclear Ru_6Fe complex was suggested to contain Ru and Fe separated by 19-20 A° with adjacent Ru centres separated by 37 A°. Ru_6Fe complex was characterized by ^1H NMR, U.V-Visible spectra and cyclic voltammetric studies. The heptanuclear Ru_6Co complex was also characterized similarly.

Okawa and coworkers [307] showed that the reaction of N, N^1- dimethyl-N,N^1-ethylene bis(5-bromo-3-formyl-2-hydroxybenzylaminato)copper(II) with ethylene diamine in aqueous DMF with excess perchloric acid resulted in the [2:2] cyclic condensation of the constituents, providing the dinuclear Cu^{II} complex $[Cu_2(H_2R)](ClO_4)_2$. The ligand R^{4-} has two $N(amine)_2O_2$ and two $N(amine)_2O_2$ metal binding sites sharing two phenolic oxygens. $[Cu_2(H_2R)](ClO_4)_2$ has the two Cu^{II} ions in the $N(imine)_2O_2$ and two protons in the $N(amine)_2O_2$ sites. Mixed metal complexes $[Cu_2M_2(R)Cl_4]$ (M = Co^{II}, Ni^{II}, Zn^{II}) were derived by allowing precursor complex $[Cu_2(H_2R)](ClO_4)_2$ to react with appropriate second metal salts (M = Co(II), Ni(II), Zn(II)). The crystal structures of mixed metal Cu_2-Co_2 and Cu_2-Zn_2 complexes were established. The two complexes are isostructural and have a dimmer of dimers structures with two separated $Cu^{II}M^{II}$ units. In each dinuclear unit, the Cu^{II} is bound to the $N(imine)_2O_2$ and M^{II} is bound to a phenolic oxygen and two nitrogens of the

$N(amine)_2O_2$. Cryomagnetic studies for the $Cu_2^{II}Co_2^{II}$ complex indicate an antiferromagnetic spin-exchange interaction within each dinuclear $Cu^{II}Co^{II}$ unit. $Cu_2^{II}Ni_2^{II}$ complex shows a weak antiferromagnetic interaction between the adjacent Cu^{II} and Ni^{II} and a weak ferromagnetic interaction between the Ni^{II} ions.

Reactions of MCl_2-nH_2O with N, N^1-bis(D-glucopyranosyl)-1, 4, 7-triazacyclononane [(D-Glc)$_2$-tacn], which was formed from D-glucose and 1, 4, 7-triazacyclononane (tacn) in situ, afforded a series of mononuclear divalent metal complexes with two β-D glucopyranosyl moieties, [M{(D-Glc)$_2$-tacn}Cl]Cl (M = Zn(I),Cu(2), Ni(3), Co(4)) [308]. Complexes 1- 4 were characterized by analytical and spectroscopic measurements and X-ray crystallography. The complexes were found to have a distorted octahedral M(II) centre ligated by the pentacoordinate N-glycoside ligand, (β-D-glucopyranasyl)$_2$-tacn and a chloride anion. Each D-glucose moiety is tethered to the metal centre through the β-N-glycosidic bond with tacn and additionally coordinated via the C-2 hydroxyl group, resulting in a X-gauche five membered chelate ring. When L-rhamnose (6-deoxy-L-mannose) was used instead of D-glucose, the nickel(II)complex with two β-L-rhamnopyranosyl moieties, [Ni{(D-Man)$_2$-tacn}(MeOH)]Cl_2 (15) was obtained and characterized by an X-ray analysis. Reactions of (1) (M = Zn) with [Zn(XDK)(H_2O)](5) or [Cu(XDK)$(Py)_2$](6) (H_2XDK = m-xylylene diamine bis(kemp's triacid imide) yielded homo and heterotrimetallic complexes formulated as $[Zn_2M^1\{D\text{-}alc)_2\text{-}tacn\}_2(XDK)]Cl_2$ (M^1 = Cu(7), Zn(8)). An X-ray crystallographic study revealed that complex (7) and (8) have either Zn_3^{II} or $Cu^{II}Zn^{II}Cu^{II}$ trimetallic centres bridged by two carboxylate groups of XDK and two D-glucopyranosyl residues. The terminal metal ions are octahedrally coordinated by the (D-Glc)$_2$-tacn ligand through three nitrogen atoms of tacn, two oxygen atoms of the C-2-hydroxyl groups of the carbohydrate and a carboxylate oxygen atom of XDK ligand. The central metal ion site in a distorted octahedral environment ligated by four oxygen atoms of the carbohydrate residues in the (D-Glc)$_2$-tacn ligands and two carboxylate

oxygen atoms of XDK. The deprotonated β-D glucopyranosyl unit at the C-2 hydroxyl group bridges the terminal and central ions with the C-2 μ-alkoxo group, with the C-1N-glycosidic amino and the C-3 hydroxyl groups coordinating to each metal centre. Complexes (7) and (8) are the first examples of metal complexes in which D-glucose units act as bridging ligands. These structures could be very useful substrate binding models of xylose or glucose isomerses, which promote D-glucose = D-fructose isomerization by using divalent dimetallic centres bridged by a glutamate residue.

The heterobimetallic complex $[Ru^{III}(edta)(NC)Fe^{III}(CN)]^{4-}$ (1) [309] was prepared from combination of $[Ru^{III}(edta)(H_2O)]$ (edta = ethylenediamine-N, N, N^1, N^1, tetra aceto) and $[Fe^{III}(CN)_6]^{3-}$ in aqueous solutions by Ward and coworkers [309]. In aqueous solution this complex shows two characteristic absorption maxima in the visible spectral region located at 420 nm and 620 nm. The band at 420 nm is characteristics of the ferricyanide moiety. The band at 620 nm is assigned to a metal to metal charge transfer transition (MMCT). Examination of the same solution after 72 hr shows that a spectral change has occurred forming a new species with a new band at 870 nm and the intensity of the band at 420 and 620 nm decreased. This is indicated the formation of $[Ru^{IV}(edta)(NC)Fe^{II}(CN)_5]^{4-}$ complex (2). The IR spectral features and magnetic susceptibility data of the complex also indicated the formation of complex (2). The complexes were characterized by cyclic voltammetry.

Heterobimetallic complexes of palladium and first row transition metal ions containing uranyl ion as one of the consistuent from polyfunctional Schiff bases $(H_2BAA)_2en$ and $(H_2PAA)_2en$ (where Schiff bases are the condensation products of ethylene diamine with benzoylacetylacetone (1- phenyl-1, 3, 5-hexanetrione) (H_2BAA), pivaloyl acetylacetone(2, 2-dimethyl-3, 5, 7-octanetrione) (H_2PAA) have been described. Some heterobimetallic complexes of dibenzoylacetone (1, 5 diphenyl-1, 3, 5-pentane trione) (H_2DBA) and dipivaloylacetone (2, 2, 8, 8-tetramethyl, 3, 5, 7-nonane-trione) (H_2DPA), are also synthesized and described by Lintvedt and Ahmad [310].

The heterobimetallic complexes of Schiff bases were prepared from reaction of monometallic Schiff base complexes (M = Pd(II), Ni(II) with uranyl acetate in equimolar amount while the heterobimetallic complexes of triketones were prepared by reaction of monouranyl complexes with metal characterized by IR, electronic and magnetic moments. The metal ions were shown to occupy N_2O_2 and O_2O_2 coordination chambers of the ligands H_2BAA and H_2PAA. This work describes the use of preferred isomerism to design specific heterobimetallic complexes containing heavy metal ions.

Wark and Stephan [311] describes heterobimetallic complexes of the type $[(C_2H_5)_2Ti(\mu\text{-}SCH_2CH_3)_2CuL]PF_6$ (where L = $P(C_6H_5)_3$ (4), $P(C_6H_{11})_3$ (5), $P(CH_2CH_3)_3$ (6), $P(CH_2C_6H_5)_3$ (7), NC_5H_5 (8) and $(C_6H_5)_2PCH_2CH_2P(C_6H_5)_2$ (9). Compounds have been characterized by cyclic voltammetry, IR, electronic and X-ray crystallographic studies. The solution studies on these complexes at low temperature indicate the bridging ethanethiolato groups asoid (syn). At higher temperatures a dynamic equilibrium occurs that allows the averaging of the cyclopentadienyl environments. It is suggested that possible mechanisms of this averaging process involve either Cu-S bond cleavage or pyramidal inversion of the bridging S-atom. The crystallographic and spectroscopic data are consistent with $d^{10}\rightarrow d^0$ (Cu→Ti) dative bonds. Such interactions in which Ti(II) acts as a Lewis acid toward an electron rich metal centre have also been proposed for $(C_5H_5)_2Ti(\mu\text{-}SCH_3)_2Mo(CO)_4$ [312]. In the complexes (4) and (5), the TiS_2Cu cores are not planar, rather they are butterfly-shaped.

Kahn and coworkers [313] described two strategies to design heterometal molecular systems with a large spin in the ground state namely, the strategy of irregular spin–state structure. Strategy of strict orthogonality of the magnetic orbitals although leads to ferromagnetic interactions between nearest neighbours is not more efficient than the strategy of irregular spin-structure. They synthesized heterobimetallic trinuclear complexes $\{Mn(Me_6\text{-}[14]ane\text{-}N_4)]_2Cu\text{-}(pba)\}(CF_3SO_3)_2.2H_2O$ (1) and $\{Ni(Me_6\text{-}[14]\ ane\text{-}N_4)]_2Cu(pba)\}(ClO_4)_2$ (2) with (Me_6 - [14] ane $-N_4$) = (±) 5, 7, 7, 12,

14, 14 –hexamethyl-1, 4, 8, 11-tetraazacyclo-tetradecane and pba = propane-1, 3 diylbis(oxamato) by applying the strategy of irregular spin state structure. These complexes have high spin multiplicity in the ground state and ferromagnetic like behaviour in the low temperature range without imposing ferromagnetic interactions between nearest neighbour ions. The magnetic and EPR properties of the complexes were discussed. The CuMn compound (1) in a molecular system is with the largest spin in the ground state. The ground state S = 9/2 is well separated in energy from the first excited state since the energy gap between these two states is found to be -J/2 = 18.2 cm^{-1}.

Balch and coworkers [314] described a heterobimetallic complex $[Ir_2Au(CO)_2Cl_2(\mu\text{-dpma})_2]Cl$ (where dpma = bis(diphenylphosphino)methyphenyl arsine) and SO_2 adduct. The structure of $[IrAu(CO)_2Cl_2(\mu\text{-dpma})_2]Cl$ was established unequivocally by X-ray crystallography [315]. When SO_2 was allowed to react with this complex in dichloromethane, red addition product $[IrAu(SO_2)(CO)_2Cl_2(\mu\text{-dpma})_2].[HSO_4].0.32SO_2.1.23H_2O$ was obtained in crystalline form on prolonged standing in a sulphur dioxide saturated dichloromethane/ether solution. The IR spectrum of the compound shows new bands at 2016 and 1974 cm^{-1}. These are consistent with the formation of an adduct with one sulphur dioxide. In the complex SO_2 is bonded to one of the iridium ions within the complex cation in usual pyramidal fashion. Other iridium atom does not contain any coordinated SO_2. In Ir-Au-Ir unit, the coordination environment of Au is decidedly asymmetric. The authors also tried to prepare SO_2 adduct with $[Ir(SnCl)(CO_2)_2Cl_2(\mu\text{-dpma})_2]BPh_4$ but failed.

Bonomo and coworkers [316] studied EPR frozen solution spectra of copper citrate heterodinuclear species containing Mg(II), ZnII) or Pd(II). From the analysis of the spin Hamiltonian Parameters, they established that copper(II) in heterobimetallic complexes is in coordination environment considerably different from that found in the case of the copper (II) mono-citrate complex which is distinctly octahedral. In

heterodinuclear complexes containing Zn(II) or Mg(II); copper is in a square planar geometry while in that containing Pd(II), copper(II) is in a tetragonally distorted octahedral geometry.

Guerriero and coworkers [317] prepared heterodinuclear lanthanide (III) complexes Ln^1-$Ln^2(L_C)(NO_3)_2.nS$ or Ln^1-$Ln^2(L_D)(NO_3)_2.nS$ (where n = 1 - 3, S = H_2O, CH_3OH), respectively by using the ligands H_4L_C, H_4L_D, which are the Schiff base derived by condensation of 2, 3-dihydroxybenzaldehyde with 1, 5-diamino-3-azo-pentane and 1, 5–diamino-3-thiapentane, respectively. The metal-metal ratio and the homogeneity of the heterodinuclear complexes have been evaluated by electron microscopy together with X-ray fluorescence microprobe [318]. In these complexes, one lanthanide ion occupies inner coordination sphere while the second lanthanide(III) occupies outer coordination sphere. The outer lanthanide (II) reaches its coordination saturation through oiligomerization involving phenolic oxygen bridging. The bridging behaviour of phenolic oxygens was suggested on the basis of similar bridging behaviour of phenolic oxygens in the hetero-dinuclear complexes containing rare earths $[MnLn(LF)NO_3)(dmso)]_2$, where H_4LF is the potentially hexadentate compartmental ligand obtained by condensation of ethylenediamine and 2, 3-dihydroxybenzaldehyde in methanol [319]. Thus, complex $[CuY(LF)(NO_3)(dmso)]$ is a tetranuclear asymmetric unit, two eight coordinate yttrium(III) ions being held together by two phenolic oxygen bridges. One bidentate nitrate group and one oxygen of a dimethyl sulphoxide molecule complete the coordination sphere about each yttrium(III).

Fraser and coworkers [320] synthesized site specific heterobimetallic complexes from two multidentate ligands derived from condensation of 1, 6, bis - bis(2-pyridyl)-2, 5-bis(2-allyloxy)-3 formyl–5-methylbenzyl)-2, 5-diazahexane and 1, 6-bis(2-pyridyl)-2, 5-bis(2-hydroxy-3-formyl-5-methylbenzyl)-2, 5-diazahexane with 1, 3-diamino-propane. The ligands were $(pyral)H_2$ and $(cyclim)H_2$. The ligand $(cyclim)H_2$ has closed six coordinate N_4O_2 and open four–coordinate O_2N_2 site, respectively. The complexes

were prepared by template method by reacting monometallic complexes of dialdehydes with amine and then treating the resulting solution with second metal chelates. The heterobimetallic complexes of the type $[M(cyclim)CoCl]PF_6$ (M = Zn, Co), $[M(cyclim)MnCl]PF_6$ (M = Zn, Mn). $[M(cyclim)ZnCl)PF_6$ and $[M(cyclim)(\mu\text{-}Cl)MnCl]PF_6$ derived from $(cyclim)H_2$ are described. Heterobimetallic complexes containing two magnetically active metal centres indicate weak magnetic coupling. All the metal centres are in high-spin configurations [321]. The electronic spectra of the complex $[Zn(cyclim)CoCl]^+$ show one absorption band at around 760 nm due to open site five–co-ordinate Co atom as characteristic of square–pyramidal spin free Co(II) complexes [322]. The authors studied the reactivity of these complexes with dioxygen and characterized the resulting complexes. Homobimetallic complexes of the title ligands were also studied and structures established by X-ray crystallographic technique.

Escuer and coworkers [323] synthesized three new heterodinuclear Cu^{II}-Ni^{II} complexes of formula $[Ni(cth)Cu(oxpn)](ClO_4)_2$ (1), $[Ni(cth)Cu(OHoxpn)](ClO_4)_2$ (2) and $[Ni(cth)Cu(Meoxpn)](ClO_4)_2$ (3) in which the nickel(II) is octahedrally coordinated. They also synthesized another series of new $Cu^{II}Ni^{II}$ complexes with pentacoordinated Ni^{II}, $[Ni(Me_3[12]N_3)Cu(oxpn)](ClO_4)_2$ (4), $[Ni(Me_3[12]N_3)Cu\text{-}(Me_2oxpn)](ClO_4)_2$ (5), $[Ni(Me_4[12]N_3)Cu(oxpn)](ClO_4)_2$ (6) and $[Ni(Me_4[12]N_3)Cu(oxpn)](ClO_4)_2$ (7) and characterized. The ligand Cth is d, 1-5, 5, 7, 12, 12,14–hexamethyl-1, 4, 8, 11-tetra aza cyclotetradecane; $Me_3[12]N_3$ is 2, 4, 4-trimetyl-1, 5, 9-triazacylododec-1-ene, $Me_3[12]N_3$ is its 9-methyl derivative, OHoxpn and Me_2oxpn are N, N'- bis(3-aminopropyl)oxamide and its 2-hydroxo or 2, 2-dimethyl derivatives respectively. The compounds are characterized by IR, electronic, magnetic moment and EPR data. Bands attributable to the central bridging oxamidato ligands appear at 1600-1630 cm^{-1}. The electronic spectra exhibit three bands (i) an intense band centred at ca. 550 nm interpretated as the envelop of two spin allowed transitions, the

$^3A_2(Ni) \rightarrow {}^3T_1(Ni)$ and the $^2B_2$ (Cu)$\rightarrow {}^2B_1$(Cu) on the basis of O_h and D_{2h} site symmetries for Ni(II) and Cu(II); (ii) a weak and narrow band at ca. 790 nm assigned to the spin–forbidden transition $^3A_2$ (Ni)$\rightarrow {}^1$E(Ni) activated by exchange mechanism [324] (iii) and a weak, broad band in the near, infrared region at 950-980 nm which corresponds to the $^3A_2$ (Ni)$\rightarrow {}^1T_2$(Ni) transition. The magnetic properties of all these compounds have been investigated. The average J value when Ni(II) is octahedral is found to be -95 cm^{-1} while it is ca. -120 cm^{-1} when Ni(II) is penta-coordinated. These results are consistent with the Extended Huckel–MO calculations which suggests that the doublet–quartet gap should be greater when Ni(II) is pentacoordinated. The EPR spectra in powdered state or acetonitrile solution of all the complexes show a very intense signal independent of the temperature at approximately $g \approx 4$. The signal at $g \approx 4$ vanishes when the temperature is lowered. This is interpreted as being due to an axial ZFS in the excited quartet state. The crystal structures of the complexes 1 and 5 have been solved. In complex (1), nickel atom is placed in a distorted octahedral environment while in complex (2), nickel atom is placed in an environment intermediate between a trigonal bipyramid and a square pyramid.

Todokoro and coworkers [325] synthesized copper(II) and lead(II) complexes of two new binucleating macrocycles composed of two molecules of 2, 6-diformyl–4-methy phenol, a diamino(ethylene diamine) or 1, 3– propanediamine), and a diaminophenol (1, 3-diaminopropan–2-ol or 1, 5–diaminopentan–3- ol) as by stepwise template reactions. The macrocycles contain two dissimilar co-ordination sites, a four coordination N_2O_2 donor set and a five coordination N_2O_3 donor set, sharing two bridging phenolic oxygens. The CuPb complex of the macrocycle with ethylenediamine and 1, 3–diaminopropan–2-ol as the amine components has been structurally characterized by single X-ray analysis. The Cu^{II} is bound to the four co-ordination site and has a planar configuration. The Pb^{II} is bound to the five coordination site and assumes a seven co-ordinate geometry with a unidentate perchlorate ion and dimethyl

formamide molecule. In the macrocylcles derived from 1, 3–diaminopropan–2-ol of the alcoholic oxygen can co-ordinate to Pb^{II} in both protonated and deprotonated forms, whereas in the macrocycles derived from 1, 5-diaminopentan–3-ol of the alcoholic oxygen coordinates to Pb^{II} in only the deprotonated forms. The authors also attempted the template synthesis of corresponding $Cu^{II}Ba^{II}$ complex from the macrocycle of 1, 3-propane diamine and 1, 5–diaminopentan-3-ol. However, this process afforded a mononuclear copper(II) complex in which the five co-ordination site of the macrocycle was occupied by a proton instead of Ba^{II}. In their electronic spectra the heterobimetallic complexes showed band in the 530- 600 nm attributed to square planar copper(II). All of the complexes were normal paramagnetic. The frozen DMF solution EPR spectra of the complexes showed axial pattern, a signal at 1600 G was observed with a seven–line hyperfine structure and a coupling constant equal to ca. 85 G. This value is about one half those for monomeric copper(II) complexes [326] and comparable to that of the spin triplet state of binuclear copper(II) complexes [327].

Love and coworkers [328] synthesized two crystalline barium–copper–ethylene glycol complexes. The solution phase complexes were investigated as a molecular precursor for use in sol-gel synthesis of high temperature superconductors. The complexes were characterized structurally by X-ray crystallography. The first compound has the formula $BaCu(C_2H_6O_2)_6(C_2H_4O_2)_2$. In this molecule, copper is co-ordinated to the four oxygen of two ethylene glycolate ligands in a nearly square planar geometry. Barium is co-ordinated by three bidentate ethylene glycol molecules and three monodentate ethylene glycol molecules. The ninefold co-ordination of barium resembles a trigonal prism with each rectangular face capped. The second crystal type has formula $[BaCu(C_2H_6O_2)_3(C_2H_4O_2)_2]$ (2). It was prepared via crystallization of the mixed-metal alkoxide from an ethylene glycol/methylethyl ketone solution. In this compound, copper is co-ordinated to four oxygen atoms of two ethylene glycolate ligands in a nearly square planar arrangement. Barium is 8-co-ordinated in a distorted

cubic geometry. It is co-ordinated to three bidentate ethylene glycol molecules and shares two of the oxygen atoms bound to the copper (one from each co-ordinated ethylene glycol) to form a discrete molecular–barium–copper complex.

Kessissoglou et al [329] synthesized green coloured heterobimetallic complex $[Cu_2Mo_2O_4(5\text{-Cl-saladhp})_2(CH_3O)_2]$ from reaction of $[Mo_2O_5(5\text{-Cl-Hsaladhp})(MeOH)]$ (1), [Hsaladph = 1, 3–dihydroxy-2-methyl-2(salicylideneamino) propane] with $Cu(CH_3COO)_2$ in methanol/CH_3CN. The compound was found to have a $MoCu_2O_4$ cubane like core. When this complex was treated with excess of bpy (bpy = 2, 2'– bipyridine) in acetonitrile solution under reflux for 2 h and the resulting light coloured blue solution was cooled to room temperature and left for evaporation, pale blue/green crystals of the formula $[CuMo_3O_8(5\text{-Cl-Hsaladhp})_2(bpy)]$ (2) were deposited over a period of a week. In the complex, the molybdenum species displays a complex pattern of bands in the 770-920 cm^{-1} range attributed to ν(M=O) modes. The DMSO solution EPR spectrum of the complex shows four copper hyperfine components in the low field region. The magnetic parameters clearly indicate that the unpaired electron is located on the Cu(II) ion, and the oxidation states for copper and molybdenum are +2 and +6, respectively. The X-ray structure of (2) confirms the presence of a trinuclear unit $[Mo_3O_8]^{2-}$ co-ordinatively bound to the $[Cu(bpy)]^{2+}$ ion. The molybdenum part of the structure consists of three oxo-bridged molybdenum centres, alternating one tetraoxomolybdate centre $[MoO_4]^{2-}$ and two six coordinated $[MoO_2(Schiff\text{-}base)]$ moieties. While the octahedron around each molybdenum unit shows a strong cis-distortion, the lack of any elongation or depression along one of the axes of the octahedron is a strong evidence that Mo keeps a d^0 configuration with a Mo(VI) oxidation state. The coordination mode of the Schiff base is also quite interesting. In the starting material, $[MoO_2(5\text{-Cl-Hsaladhp})(MeOH)]$, it acts as tridentate ligand possessing three sites in the equatorial plane of the molybdenum octahedron. In compound (1), the Schiff base is transferred from the molybdenum to

copper ion and acts as tetradentate ligand with two oxygens and one nitrogen bound to Cu^{+2} ion, occupying the three sites in the basal plane of the square pyramid and one oxygen bound to Mo(VI) ion, while in the compound (2), the Schiff base returns to the Mo atom acting again as tridentate ligand and possessing the three sites in the equatorial plane of the molybdenum octahedron.

Fraser and coworkers [330] synthesized a chiral macrocyclic binucleating ligand, S S-cypim, bearing four and six co-ordinate binding sites. The macrocyclic framework contains the chiral diammine (1S, 2S)–trans-1, 2-bis(aminomethyl)-cyclopentane, which induces one topological chirality about the six co-ordinate site. The macrocyclic closure with the chiral diamine is achieved in good yield by Schiff base condensation of metal dialdehyde complexes (dialdehyde = 1, 6-bis(2-pyridyl)-2, 5-bis(2-hydroxy-3-formyl-5-methyl-benzyl)-2, 5-diaxahexane). The method resulted into the monometallic complexes $[M(S, S\text{-cypim})(H^{+})_2]^{2+}$, (M = Zn(II), Cu(II), Ni(II), Co(II) and Mn(II). These complexes contain a metal in the six co-ordination sites and two hydrogen–bonded protons in the four–coordinate site. This has been confirmed by X-ray crystallographic studies of the Mn(II) and Zn(II) complexes. Oxidation of the Co(II) complex gives Co(III) complex $[Co(S, S\text{-cypim})H^{+})_2]^{3+}$ from which the heterobimetallic complexes [Co(S, S-cypim)MCl] (M = Zn(II), Ni(II), Co(II) and Mn(II) and $[Co(S, S\text{-cypim})Cu]^{3+}$ were prepared and isolated. An X-ray crystal structure of the last complex confirms the expected C_2 symmetric geometry. Further, the heterobimetallic complexes $[Mn(S, S\text{-cypim})Cu]^{2+}$ {where M = six-coordinate site metals, Zn(II), Cu(II), Ni(II), Co(II) and Mn(II)} were prepared, isolated and characterized. The homobimetallic complexes [Mn(S, S-cypim)MnCl]$^{+}$ and [Ni(S, S-cypim)NiCl]$^{+}$ were also isolated and characterized. The mixed-valence complex $[Mn^{II}(S, S\text{-cypim})Mn^{III}(Cl)_2]^{+}$, was formed by the aerial oxidation of the dimanganese(III) complex and characterized. The crystal structures of the complexes $[Mn(EtOH)(S, S\text{-cypim})Cu]^{2+}$ and $[Cu(S, S\text{-cypim})Cu(CH_3CN)]^{2+}$

are also reported. In the complex $[Mn(EtOH)(S, S\text{-cypim})Cu]^{2+}$, the Mn(II) atom is seven–coordinate and a highly distorted ligand structure is observed. The dicopper(II) structure is also distorted, but the copper in the potentially six–coordinate site is only five coordinate. The incorporation of the chiral diamine in the ligand enforces the formation of a single diastereomer of the C_2 symmetric complexes. This is confirmed by the ^1H NMR spectra of the diamagnetic complexes $[Zn(S, S\text{-cypim})(H^+)_2]^{2+}$, $[Co(S, S\text{-cypim})Zn]^{3+}$. The topological chirality about the closed site metals in the $[Zn(S, S\text{-cypim})(H^+)^2]^{2+}$ and $[Co(S, S\text{-cypim})Cu(CH_3CN)]^{2+}$ complexes was determined to be Δ by crystallographic methods whereas a Δ absolute configuration was formed for the $[Mn(S, S\text{-cypim})(H^+)_2]^{2+}$ complex. This reversal of diastereo selection is believed to arise from the larger radius of Mn (II) ions, which causes the ligand to adopt a unique twisted conformation which is considerably different from those observed for $[Zn(S, S\text{-cypim})(H^+)_2]^{2+}$ and $[Co(S, S\text{-cypim})Cu(CH_2CN)]^{3+}$. Circular dichroism associated with the azomethine chromphores suggests that all of the C_2 symmetric complexes have the same configuration except the Mn(II) complex.

Breeze and Wang [331] synthesized and characterized three new heterobimetallic copper(II) alkaline-earth metal complexes $[CaCu(bdmap)_2(O_2CCF_3)_2(H_2O)]$(1), $[SrCu_2(bdmap)_4(O_2CCF_3)_4]$ (2) and $[Sr_2Cu_4(bdmap)_6(O_2CCF_3)_4(\mu_3\text{-}OH)_2]$ (3), respectively, where bdmap is 1, 3-bis(dimethyl amino)-2-propanolate. Their structures have been determined by single–crystal X-ray diffraction analyses. Compound (1) is a dinuclear complex and dimerises in the solid state through intermolecular hydrogen bonds. Copper centre is coordinated by two nitrogen atoms and two oxygen atoms in an appropriate square planar fashion with typical Cu-O and Cu-N bond distances. The geometry around copper centre can be described as a square pyramid. The calcium centre is surrounded by two nitrogen and five oxygen atoms in an appropriate pentagonal bipyramidal geometry. The compound (2) is a tetranuclear complex. In the solid state, the

molecule of 2 contains two dinuclear [SrCu(bdmap)$_2$(O_2CCF_3)$_2$] units, related by an inversion centre. The copper(II) ion is coordinated by two oxygen and two nitrogen atoms with normal bond length and an approximate square planar geometry. The fifth position of the copper atom is again occupied by an oxygen atom from the trifluoroacetate ion giving square pyramidal geometry to copper atom. The strontium ion was surrounded by five oxygen and two nitrogen atoms in approximate pentagonal bipyramidal geometry with two oxygen atoms occupying the axial positions. In contrast to the structure of compound 1, where the two dinuclear units are linked together through intermolecular hydrogen bonds, forming a face to face dimmer, the two dinuclear units in 2 are linked together through intermolecular hydrogen bonds, forming a linear chain structure. Compound (3) is a hexanuclear complex, where metal ions are linked together through the bridging ligands. This compound consists of two SrCu units and one Cu_2 unit with a crystallographically imposed inversion centre symmetry. Similar structure has been established for [$BaCu_4$(bdmap)$_4$(PyO)$_4$(O_2CCF_3)$_2$] complex [332]. The common features in all three structures are that the alkaline earth metal ion and the copper ion are linked together through the negatively charged oxygen centre of the bdmap ligand and the carboxylate ligands are coordinated predominantly to alkaline–earth metal ion.

Guilard and coworkers [333] synthesized and characterized a novel family of heterobinuclear cofacial biphenylene–bridged or anthracene–bridged bisporphyrin (DP) CuMnX where DP is either 1, 8 - bis(2, 8, 13, 17 - tetraethyl - 3, 7, 12, 18 - tetramethyl porphyrin-5- yl)biphenylene (DPB) or 1, 8-bis(2, 8, 13,17-tetraethyl-3, 7, 12, 18-tetramethyl porphyrin–5-yl)anthracene (DPA). Each complex has been characterized by mass spectrometry, UV-vis, IR and EPR spectroscopies and magnetic measurements. The electronic spectra of the heterobimetallic complexes [DP)$Cu^{II}Mn^{II}$L] show soret bands in the region 398-443 nm and 535-571 nm respectively. The value of the magnetic moment and the Curie constant in the high

temperature range for [(DPA)$Cu^{II}Mn^{II}Cl$] and [(DPB)$Cu^{II}Mn^{II}Cl$] are consistent with magnetically independent spins of the manganese (S = 2) and the copper (II) (S = 1/2) atoms.

The complexes do not show any EPR spectra at room temperature. At this temperature, the two ions are magnetically independent and relaxation effects are the probable cause of the disappearance of the EPR spectra. The EPR spectrum of [(DPA)CuMnCl] is totally distorted at 100 K. This type of spectra can result from a significant interaction between copper and manganese ions and to a lesser extent to a $\pi \rightarrow \pi$ macrocycle interaction. The EPR experiments demonstrate the presence of a new EPR active state with several transition over a large field domain. The EPR spectrum of [(DPB)CuMnCl] at low temperature comprises of two components :a six- line feature at $g \approx 5.68$ and a multiline pattern at g = 2. The latter should be due to the copper porphyrin core. The splitting of the high–field component takes its origin in the hyperfine coupling with the manganese nuclear spin ($I_{Mn} = 5/2$, a = 59 G).

The structure of the complex [(DPB)CuMnCl] was solved by X-ray crystallographic method. The triclinic P1 unit cell contains two diporphyrin molecule and two ethylbenzene solvates which are related by the inversion centre. The solvent molecules are almost perpendicular to the porphyrin plane.

Cador and coworkers [334] synthesized a tetranuclear compound $[Mn\{Cu)oxpn)\}_3](ClO_4)_2.2H_2O$, where oxpn is N, N'-Bis(3-aminopropyl)oxamide). They characterized the complex with the optical absorption spectroscopy. The central metal ion Mn^{II} is linked to three Cu(oxpn) complex ligands. The spectra, in addition to a d - d transition due to the Cu^{II} in square planar surroundings, exhibit narrow and intense Mn^{II} spin forbidden transitions. These transitions are activated by an exchange by an exchange mechanism.

Basu and coworkers [335] synthesized heterobimetallic complexes {5, 10, 15 – tri–p–tolyl–20-[2, 3-[hydrobis(3, 5-dimethylpyrazolyl}borato)oxomolybdenio) dioxy]phenyl]porphyrinato}bis(2-methylimidazole)iron(III) chloride, [Fe(2, 3-Mo-TPP)(2MeImH)$_2$Cl] (1), {5, 10, 15–tri-p-tolyl-20-3, 4-[hydrotris(3,5-dimethylpyrazolyl)(borato)(oxomolybdenio)dioxy}phenyl]porphyrinato}bis(2-methy-limidazole)iron (III)chloride, [Fe(3, 4-Mo-TTP) (2MeImH)$_2$Cl (2) {5,10,15-tri-p-tolyl-20-[2,3-[(hydrotris(3,5-dimethylpyrazolyl]dioxy]phenyl]porphyrinato}bis-(N-methylimidazole)iron(III)chloride, [Fe(2, 3-Mo-TTP)(NMeImH)$_2$Cl] (3) and [5, 10, 15 tri-p-tolyl-20-[3, 4-hydrotris(3, 5 dimethyl pyrazolyl)(borate)-(oxomolydenio)dioxyl]phenyl{porphyrinato}bis(N-methylimidazole)]iron(III) chloride, [Fe(3, 4-Mo-TPP)(NMeImP)$_2$Cl (4). They studied the complexes in order to make an assessment of the effect of axial ligand plane orientation upon the stability, reduction potential and NMR and EPR spectra of these novel (porphyrinato)iron (III)-Mo(V) systems that possesses two S = 1/2 metal centres. The proton NMR spectra of 1 and 2 are characteristic of perpendicular orientation of the planes of the axial 2-methylimidazole ligands. These results contrast with those previously reported [336] for the analogous compounds with N Melm(N-methylimidazole) as the axial base (3, 4) whose ^{1}H NMR spectra are characteristic of one or both axial ligands in parallel planes. Compounds (1) and (2) were found to have small binding constants than those of (3) and (4), indicative of differences in the steric demands of the axial ligands. The overall EPR spectra of the Mo(V) region of (1) – (4) are independent of the nature of the axial ligand (N Melm vs 2 me ImH), inspite of the fact that EPR spectra of the isolated low-spin Fe(III) porphyrinate centres are dramatically different from one another. This indicates that the nature of the spin-spin coupling between the molybdenum and the heme centre in these molecules is not substantially affected by the ligand plane orientation even

through the magnitudes of the exchange interactions are quite different for (1) and (3). The compounds were characterized by cyclic voltammetry also.

Ramade and coworkers [337] synthesized four heterobimetallic complexes of copper and lanthanides from N, N'- ethylene bis(salicylaldeneaminato)(salen) containing hexafluoroacetylacetonate (hfa) and 1 - methylimidazole (Meim) as co-ligands. The compounds are found to have compositions $[Gd(hfa)_3Cu(salen)]$ (1), $[Y(hfa)_3Cu(salen)]$ (2), $[Gd(hfa)_3Cu(salen)(Meim)]$ (3), and $[(Lahfa)_3(H_2O)Cu(salen)]$ (4). All the compounds were crystallographically characterized. The structures of (1), (2) and (4) consist of dimers of binuclear units in which the metal ions are bridged by the oxygen atoms of the salen ligand, with rather short Cu-Cu intermolecular separations. The Gd^{III} ion in (1) and Y^{III} ion in (2) have a square antiprismatic environment, while the La^{III} ion in (4) is nine–coordinate with a water molecule in the La^{III} coordination polyhedron. In compounds 1, 2 and 4, the Cu^{III} ion has a square planar environment. The structure of (3), consists of perfectly isolated binuclear species, the Meim ligand occupying a peripheral apical position in the copper coordination sphere. The complexes (1) and (3) have revealed Gd^{III} - Cu^{II} ferromagnetic interactions.

Nantakumar and coworkers [338] synthesized hetrobimetallic complexes $[(F8\text{-}TPP)Fe^{III}\text{-}O\text{-}Cu^{II}(TMPA)]^+$ (1), $[(F_8\text{-}TPP)Fe^{III}\text{-}OH\text{-}Cu^{II}(TMPA)]^+$ (2), (where F_8-TPP = tetrakis(2, 6-diflurophenyl)porphryrinate (2); TMPA = tris(2-pyridylmethyl)-amine. The structure of the complexes was established by X-ray crystallography. The complexes were characterized by NMR spectroscopy. The pyrole resonances appear at a position consistent with an S = 2 ground state derived from ferromagnetic coupling of high spin Fe^{III} (S = 5/2) and Cu^{II} (S = 1/2) through the bridging ligand X. The ligand peaks are shifted upfield as compared to those in corresponding monometallic complexes. The observance of these upfield peaks is a consequence of enhancement of the electronic relaxation rate for Cu^{II} due to antiferromagnetic

coupling with the faster relaxing Fe^{III}. This observation represents the prototype of a Fe^{III}-X-Cu^{II}, S = 2 spin state hitherto only theoretically predicted.

Dominangnez-Vera and coworkers [339] synthesized a novel bisimidazolyl tetradentate Schiff base ligand (H_2L) from the condensation of imidazole-2-carbaldehyde and 1, 3–diaminopropane. They prepared its mononuclear copper complex $[Cu(H_2L)(ClO_4)]ClO_4.H_2O$ from reaction with copper(II) perchlorate in neutral medium. The structure of the complex was established by X-ray crystallographic technique. The reaction of this complex with an excess of bis(hexafluoroacetylacetonate)nickel (II), $Ni(hfac)_2$ in basic medium leads to the heterotrinuclear complex $[Cu(L)(H_2O)][Ni(hfac)_2(H_2O)]_2$.This complex was characterized by magnetic and EPR studies. The magnetic properties of this complex agree well with those expected for a $Ni^{II}CuNi^{II}$ trinuclear system with irregular spin state structure and zero-field splitting of the quartet ground state. The X-band powder EPR spectrum of the compound is very complicated with many overlappings resonances. Since the doublet excited states are not far in energy from the quartet ground state, the spectrum should be the result of the superimposition of transitions with in all these states.

Shinoura and coworkers [340] synthesized a di(μ- phenoxo)$Co^{II}Cu^{I}$ complex, $[CoCu(L)]ClO_4.0.5DMF$ $(L)^{2-}$ is a macrocyclic dinucleating compartmental ligand derived from the 2:1:1: condensation of 2, 6–diformyl-4-methyl phenol, ethylenediamine and 3-thia-1, 5– pentanediamine, having a salen–like N_2O_2 metal–binding site (salen = N, N'-ethylenedisalicylideneaminate) and an N_2O_2S site sharing the phenolic oxygen. The Co^{II} resides in the salen–like site and assumes a planar geometry. The Cu^{I} in the N_2O_2S site has a planar four-coordinate geometry with two phenolic oxygens and two amine nitrogens, the thioether sulfur on the lateral chain situated at an axial site of the Cu^{I} but the Cu....S separation is very large. Analogous $Cu^{II}C^{I}$ and $Co^{II}Pb^{II}$ complexes of $(L)^{2-}$ $[Cu^{II}Cu^{I}(L)]ClO_4$ and $[CoPb(L)(ClO_4)_2]$ were

prepared. The dinuclear core of $[Cu^{II}Cu^{I}(L)]ClO_4.0.5DMF$ resembles that of the $Co^{II}Cu^{I}$-complex and shows distortion about the Cu^{I} similar to those found for the $Co^{II}Cu^{I}$-complex. The di-DMF adduct of the $Co^{II}Pb^{II}$ complex $[CoPb(L)(DMF)_2]$-$(ClO_4)_2$ crystallizes in the monoclinic space group. The Co^{II} in the N_2O_2 site has a square pyramidal geometry together with a DMF oxygen at the apical site. The Pb^{II} in the N_2O_2 site has a six – coordinate geometry with the further coordination of a DMF molecule. The reactivilty of the $Co^{II}Cu^{I}$ complex toward dioxygen has been studied in comparison with the $Cu^{II}Cu^{I}$ and $Co^{II}Pb^{II}$ complexes. The $Co^{II}Cu^{I}$ complex in DMF is very sensitive to dioxygen and is oxidized at -50 °C. The $Cu^{II}Cu^{I}$ is inert to dioxygen. The $Co^{II}Pb^{II}$ complex is oxygenated at 0 °C to form a peroxo dimer $[Pb^{II}Co^{III}$-O-O-$Co^{III}Pb^{II}]$. The high sensitivety of the $Co^{II}Cu^{I}$ complex to dioxygen is explained by the irreversible oxidation to a $Co^{III}Cu^{II}$ species through an intramolecular type peroxo complex (Co^{III}-O-O-Cu^{II}).

Fubita and coworkers [341] synthesized trinuclear $Cu^{II}M^{II}Cu^{II}$ complexes $[M\{Cu(HL)(DMF)\}_2(DMF)_2]$ (M^{II} = Mn(1), Co(2), Ni(3) or Zn(4)) from N, N'-bis[2-(hydroxyimino methyl)phenyl]oxamide (H_4L). The structures of all the complexes were established by X-ray crystallography. All attempts by authors to isolate a mononuclear copper(II) precursor complex of H_4L were in vain. Thus the mononuclear copper(II) complex was prepared in solution and treated with a second metal (II) ion to provide the trinuclear complexes. All of the complexes show complicated IR bands in the region 2300-3000 cm^{-1} which are characteristics of the hydrogen bonded –O-H- -O- linkage of the dioximate group. The ν(C=O) band of late group is seen around 1635-1640 cm^{-1} which is low relative to that of H_4L (1691 cm^{-1}) indicating bridging function of the group. An IR band around 1663 cm^{-1} was assigned to the ν(C=O) mode of the coordinated DMF. The reflectance spectrum of compound 1 ($Cu^{II}Mn^{II}Cu^{II}$) shows two visible bands at 525 and 600 nm attributed to the d-d components of $Cu^{II}Mn^{II}$. Compound (4) ($Cu^{II}Zn^{II}Cu^{II}$) also shows two visible

bands at 515 and 600 nm. A similar visible spectrum was obtained for 2, ($Cu^{II}Co^{II}Cu^{II}$). It is considered that the d-d bands of octahedral Co^{II} are weak and are obscured by those of Cu^{II}. In the case of (3) ($Cu^{II}Ni^{II}Cu^{II}$), an additional band is observed at 965 nm that is assigned to a d-d component of Ni^{II}. All of the complexes are isostructural. In compound (1), the asymmetric unit consists of half of the $[Mn\{Cu(HL)(DMF)\}_2(DMF)_2]$, the Mn exists on the mirror plane. The Cu resides in the N_4 cavity of the ligand with two oxamidate nitrogens and two oxime nitrogens. The geometry about the Cu is square pyramidal with DMF molecule occupying apex position. The oxamidato manganese entity forms a good coplane, but the $[Cu(HL)]^-$ molecule is not coplanar. The $[Cu(HL)]^-$ parts in complexes (1 - 4) are essentially similar, some noticeable differences in the structures are seen in the geometry around the M^{II}. The room-temperature magnetic moment of complex (1) is 6.20 μ_B (per molecule) that is slightly smaller than the spin–only value (6.40 μ_B) for two Cu^{II} (S = 1/2) and one Mn^{II} (S = 5/2). The effective magnetic moment decreased with decreasing temperature to a near plateau value of 3.90 μ_B below 20 K. The plateau moment is close to the spin only value for S_T = 3/2 (3.87 μ_B) resulting from anti-ferromagnetic spin coupling in the Cu^{II}-Mn^{II}-Cu^{II} system. The same is applicable for other heterotrinuclear complexes also.

Oseterloh and coworkers [342] synthesized a two cluster compounds $(Et_4N)[(Cl_4cat)_2(Et_3P)_2Mo_2Fe_6S_8(PEt_3)_4]$(2), $[(Ph_3PMe)_5(Cl_4cat)_4(Et_3P)_4Mo_4Fe_{12}S_{20}K_3(DMF)]^{5-}$ (3) from the precursor edge brigdged double cubane cluster $[(Cl_4cat)_2(Et_3P)_2Mo_2Fe_6S_8(PEt_3)_4]$ (1). The precursor complex (1) was characterized by X-ray crystallography and is centrosymmetric [343]. Its structure is viewed as two cuboidal $MoFe_3S_3$ units linked by two μ_4-S atoms. The precursor complex $[(Cl_4cat)_2(Et_3P)_2Mo_2Fe_6S_8(PEt_3)_4]$ (1) reacts with two equivalent of hydrosulfide in acetonitrile and affords high nuclearity cluster $[(Cl_4cat)_6(Et_3P)_6Mo_6Fe_{20}S_{30})]^{8-}$ (4) [344]. Thus cluster is composed of a central $Mo_2Fe_8S_{12}$ and upper and lower

$Mo_2Fe_6S_9$ fragments. The two P-cluster–like $Mo_2Fe_6S_9$ motifs in this cluster is possibly connected to the predominant ferrous character of precursor (1). It is established that the complex (4) is a thermodynamically favoured product in a complex reaction system. On the otherhand, when a suspension of complex (1) in acetonitrile is treated with two equivalents of $(Et_4N)(SH)$, a black solution is formed from which upon slow evaporation of all volatiles, black rhombs of $(Et_4N)[(Cl_4cat)_4(Et_3P)_2Mo_2Fe_6S_8(PEt_3)_4].3CH_3CN$ is formed. When the treatment of 1 with 1 - 4 equivalents of potassium anthracenide in THF is followed by addition of a solution of two equivalents of $(Et_4N)(SH)$ in acetonitrile and the reaction mixture is stirred, the cluster $[(Cl_4cat)_4(Et_3P)_4Mo_4Fe_{12}S_{20}K_3(DMF)]^{5-}$(3) is obtained as the (Et_3N^+) salt. The structure of this cluster is determined as $[Ph_3PMe]^+$ salt. In this cluster, the two $Mo_2F_6S_9$ units are directly linked to each other through two sulphide atoms. Three potassium ions from the reductant are intercarlated into the Mo-Fe-S frame work. All of the complexes were characterized by Mossbauer spectroscopy as well.

Clirac and coworkers [345] synthesized quadruply bonded homobimetallic compound $Mo_2(DPyF)_4$ (1) where $DpyF^-$ is the anion N, N'-di(2-pyridyl)-formamide, by ligand substitution reactions of $Mo_2(OOCCF_3)_4$ either with the neutral ligand, HDpyF, at ambient temperature or with its lithium salt, LiDpyF, under refluxing conditions. An X-ray structural analysis shows that this homobimetallic complex has a paddlewheel structure with a Mo-Mo distance of 2.1108(6) A°. The +FAB mass spectrum of 1 shows a parent ion peak at 981 m/z, consistent with the composition of $Mo_2(DpyF)_4$. The electronic spectrum of (1) exhibits two shoulders at 432 and 516 nm in the visible region, attributed to ligand–to–metal $\pi \rightarrow \delta^*$ charge transfer (LMCT) transition and a $\delta \rightarrow \delta^*$ excitation of the Mo-Mo quadruple bond. The complex was characterized by ^1H NMR spectroscopy and X-ray crystallography. The ^1H NMR spectrum in solution of the complex showed its existence as a mixture

of two isomers. The reaction of this complex with $CoCl_2$ and CuCl in methanol produces paramagnetic heterometal compound $[Mo_2Co(DpyF)_4][CoCl_4].2MeOH$ (2) and diamagnetic heterometal compound $[Mo_2Co_4(DpyF)_4Cl_2][CuCl_2].2MeOH.Et_2O$ (3). The Co(II) atom in the cation $[Mo_2Co(DpyF)_4]^{2+}$ resides on a low-spin hexacoordinate environment (S = 1/2) with a Co....Mo separation of 2.979 (6) A°. This bond distance suggests that there is no direct bonding interaction between the Co and Mo atoms. In the heterometal complex, the ligand underwent rearrangement to change the coordination geometry. The main feature of the electronic spectrum of the compound (2) is a band centred at 545 nm with a molar absorbance at the peak of 4 $\times 10^3$. This band is attributed to the cation. The cobalt atom in the $CoCl_4^{2-}$ ion, which is present in the solid state, becomes a six-coordinate Co(II) ion in solution, possibly $[Co(CH_3OH)_6]^{2+}$. It has an absorption band at about 522 nm but with ϵ equal to only about 20. Axial ligation to the Mo_2^{4+} unit by metal ions has been observed for heteronuclear compounds containing late-transition metal atom. However a heterometal complex $[Mo_2Cu_2(DphIP)_4(CH_3CN)(CuCl_2)_2]$ has been reported [346] in which the Cu(I) ion is not bound directly to the Mo_2 core. Here DPhIP represents 2, 6-di(phenyl imino)biperidine. However, direct axial interaction of metal ions with Mo_2^{4+} core has been observed for the heteronuclear compounds $[Mo_2PtX_2(pyphos)_4](O_2CR)_2]_2$ and $[Mo_2Pd_2(pyphos)_4]$ where pyphos is a tridentate ligand (6-diphenylphosphino)-2-pyridonate) [347]. The μ_{eff} value for the complex is 5.1 μ_B which reflects the presence of two types of uncoupled Co(II) entities, namely, the tetrahedral Co(II) ion in $[Co^{II}Cl_4]^{2-}$ and the Co(II) ion in $[Mo_2Co(DpyF)_4]^{2+}$. When compound $[Mo_2(DpyF)_4]$ (1) reacts with 6 equivalent of of CuCl in methanol, hexanuclear cation $[Mo_2Cu_4(DpyF)_4Cl_2]^{2+}$ and $[CuCl_2]^-$ counter anions are formed. The central molybdenum atoms are bridged by formamidine nitrogen atom similar to that observed in the compound (1). In addition, the pyridyl N-atoms of the ligands are

also bound to four Cu(I) ions. Each Cu atom is bound to a pair of $DpyF^-$ ligands in *cis* positions and to a bridging chloride ion, giving a T-shaped coordination geometry.

Dutta and coworkers [348] synthesized a series of phenoxo-bridged homo- and hetero- dinuclear complexes of 4-methyl-2, 6-bis(5-methylpyrazol-3-yl)phenol (H_3L^1). The IR spectra of all the complexes derived from H_3L^1 exhibit two characteristic bands due to the ligand [δ(NH) and ν(C=N) at about 1600-1620 and 1565-1575 cm^{-1}]. In the case of $[Cu_2(H_2L^1)(\mu\text{-}OH)Cl_2]$ (3), a sharp band observed at 3270 cm^{-1} was attributed to the presence of the bridging hydroxo moiety, while for $[Fe_2(H_2L^1)_4(\mu\text{-}OH)_2].7H_2O$ (7), this band is shifted to a higher energy, 3350 cm^{-1}. By contrast to the hydroxo species, the ν(OH) due to bound/ or lattice water molecules occurs as a broad feature in the range 3400-3500 cm^{-1}. Other prominent bands such as ν(Cu-Cl), ν(C=N), ν(NH) and δ(NH) in other complexes have also been located. The homobimetallic copper complex (1) shows two peaks at 760 and 600 nm while other homo- and heterometallic copper complexes (2), (3) and (5) show bands at 610, 700 and 630 nm. The visible spectrum of the dinickel(II) complex (4) has features typical of octahedral complexes. The lone $PhO^-\rightarrow Fe^{III}$ charge transfer band is exhibited in the visible region of the spectrum of all the three diiron(III) complexes (7) – (9). The authors carried out variable temperature magnetic susceptibility measurements for the homodinuclear complexes $[Cu_2(H_2L^1)_2](ClO_4)$ (1), $[Cu_2(H_2L^1)(acac)_2][ClO_4)_2]$ (2), $[Cu_2(H_2L^1)(\mu\text{-}OH)Cl_2]$ (3), $[Cu_2(H_2L^1)(H_2O)_4][ClO_4)_2]$ (4), $[Fe_2(H_2L^1)_4(\mu\text{-}OH)_2].4H_2O$ (7) and showed that is all the cases, the dinuclear metal centres are antiferromagnetically coupled. The ^1H NMR spectra of the dicopper(II) complexes (1) and (2) are reasonably sharp and the iosotropic shifts of (1) are relatively less compared to those of (2). The EPR spectra of the heterodinuclear complexes $[ZnCu(H_2L^1)_2](ClO)_2.2H_2O$ (5) and $[ZnMn(H_2L^1)_2Cl_2]$ (6), have been examined. The complexes $[Fe_2(H_2L)_4(\mu\text{-}OH)_2].4H_2O$ (7) and $[Cu_2(H_2L^1)(acac)_2][ClO_4)].CHCl_3.2[CHCl_3]$ were characterized

by X-ray crystallography. The structure of complex (7) comprises of two FeO_2N_2 coordination cores linked by two hydroxyl groups, which leads to edge sharing between FeO_4N_2 octahedron. In this complex, the phenolate oxygen atom of the ligand is not involved in bridging the two metal centres. In this case, H_3L^1 acts as a bidentate ligand and utilizes one of the pyrazolyl nitrogen atoms and the phenolate oxygen atoms for binding iron(III). The two metal centres, in turn, are stereochemically non-equivalent, that is the spatial configurations of the two FeO_4N_2 octahedron are different.

Rombaut and coworkers [349] synthesized a 1-D-cyanide-bridged compound $[Mn_2^{II}(L)_2(H_2O)][Mo^{IV}(CN)_8].5H_2O$ from reaction of the complex $[MnL(H_2O)_2]Cl_2.4H_2O$ with $K_4[Mo^{IV}(CN)_8].2H_2O$ in aqueous solution where L is a macrocyclic ligand 2, 13-dimethyl -3, 6, 9, 12, 18-pentaazbicyclo[12.3.1]octadeca-1(18, 2, 12, 14, 16)pentane. The IR spectrum exhibits some bands due to the presence of the macrocycle L (NH stretching vibrations at 3221 cm^{-1} and C=N stretching vibrations at 1648 cm^{-1}) and two broad bands at 2121 and 2103 cm^{-1} which are assigned to CN stretching vibrations of bridging and terminal cyano groups, respectively. The crystal structure of the compound contains three metal sites localized on a general position, one molybdenum site and two manganese sites. The organization is one dimensional and it is made up of chains running in a zigzag fashion along the 6 direction. Each chain consists of alternate Mn1(L) and Mo1$(CN)_8$ units, the Mn2(L) unit being linked to the Mo1 as a pendant arm. The molybdenum atom is surrounded by eight cyano groups with a coordination reminiscent of a square antiprism. All manganese sites are surrounded by the five nitrogen atoms of the macrocycle in the equatorial plane and coordinated by two other atoms along the apical directions, leading to a pentagonal bipyramid geometry. The structure contains six water molecules. One molecule is linked to one Mn atom. Short contacts exist between some non-bridging cyano groups and four oxygen atoms of non-coordinated

water molecules. The compound shows important modifications of its magnetic properties under UV-light irradiation, leading to the formation of ferromagnetic chains. This non-reversible photomagnetic effect is thought to be caused by an internal photo-oxidation of Mo^{IV}(diamagnetic) to Mo^{II} (paramagnetic). The crystallographic data seem to indicate that the formation of hydrogen bonds between water molecules and nitrogen atoms of non-bridging cyano groups is a key factor to observe the molybdenum photo-oxidation.

*Kato and coworkers [350] synthesized mononuclear and dinuclear cis-*dioxomolydenum (VI) complexes containing $[MoO_2(H_2L^{a1})].H_2O(1.H_2O)$, $[(MoO_2)_2(H_2L^{a2})].2CH_3OH(2.2CH_3OH)$, $[MoO_2(L^{b1})].0.5H_2O(3.5H_2O)$, $[(MoO_2)_2(L^{b2})]$(4a) and $[(MoO_2)_2(L^{b3})]$ (4b) where Schiff bases H_3L^{a1} and H_6L^{a2} were derived by condensation of 2-amino-2-methyl-1, 3-propanediol with salicylaldehyde and 2, 5-dihydroxy terephthalaldehyde, respectively H_2L^{b1} and H_2L^{b2} were obtained from condensation of (1R, 2S) norephedrine with salicylaldehyde and 2, 5-dihydroxy terephthalaldehyde and H_4L^{b3} was obtained by mixing 2, 5–dihydroxy terephthaldehyde and (IS, 2R) and (1R, 2S)-norephedrine in a 1:1:1 molar ratio in ethanol. The complexes were prepared by template methods where a solution containing the appropriate ligand was allowed to react with *cis*-$[MoO_2(acac)_2]$ to yield yellow or orange *cis*-dioxomolydenum(VI) complexes. The IR spectra of the complexes (1-4b) exhibited bands in the regions 879-917 and 928-933 cm^{-1} due to ν_{as}(O=Mo=O) and ν_s(O=Mo=O) modes, respectively, of the *cis*-MoO_2 group. No complexes showed a broad IR band in the region 800-850 cm^{-1}, which is diagnostic for the polymeric .....Mo=O.....Mo=O..... structure, indicating that the present complexes do not have a chain structure. The complexes were characterized by variable temperature ^1H NMR spectroscopy. In ^1H NMR spectra of (2) and (4b), two sets of resonances were observed, suggesting the presence of two magnetically nonequivalent species while the ^1H NMR spectra of analogous complexes (1), (3) and

(4a) did not show the presence of such isomers. The electrochemical behaviour of the mono- and dinuclear complexes in DMSO 0.1 M Bu_4NBF_4 was studied by CV at a glassy carbon working electrode. The reduction of dioxomolybdenum (VI) complexes in aprotic solvents is usually irreversible. This indicates that electrochemical reductions are followed by chemical reactions. The UV–Vis spectra of the complexes show a charge transfer band in the region ~450 nm.

Rombaut and coworkers [351] synthesized heterobimetallic complexes $[Cu(bipy)_2]_2[Mo(CN)_8].5H_2O.CH_3OH$ (1) with bipy = bipyridine and $[M_2^{II}Mo^{IV}(CN)_8].xH_2O$ (2 with M = Cu, x = 7.5, 3 with M=Mn, x = 9.5]. The structural information regarding compound (2) was obtained from the wide angle X-ray scattering (WAXS) technique because it crystallized poorly and by comparison with structure of (3). WAXS investigation indicates that 3 has an architecture similar to that of $[Fe_2^{II}(H_2O)_4][Mo^{IV}(CN)_8].4H_2O$ because the experimental reduced intensity and RDF for (3) fit very well those calculated for $[Fe_2^{II}(H_2O)_4][Mo^{IV}(CN)_8].4H_2O$. The case of 2 is more complicated. Indeed, the reduced intensity and RDF of 2 do not properly fit those calculated for $[Fe_2^{II}(H_2O)_4][Mo^{IV}(CN)_8].4H_2O$. Therefore these two compounds do not have the same structure. The magnetic properties have shown that 1 and 2 behave as paramagnet. Under irradiation with light they exhibit important modifications of their magnetic properties, with the appearance at low temperature of magnetic interactions. For 1, the modifications are irreversible whereas they are reversible for 2 after cycling in temperature. These photomagnetic effects are thought to be caused by the conversion of Mo^{IV} (diamagnetic) to Mo^{V} (parmagnetic) through a photo oxidation mechanism for 1 and a photoelectron transfer in 2. These results have been correlated with the structural features.

Burdinski and coworkers [352] described electron transfer reactions of heterometallic tetranuclear complexes of Ru^{II}, Mn^{II} and Mn^{IV} of the type Ru^{II} Mn^{II}_3 (1) and $Ru_3^{II}Mn^{IV}$ (2) derived from bipyridyl type ligands and phenol containing

ligands. The authors have shown that in the heterotetranuclear $Ru^{II}Mn_3^{II}$ complex (1), the source of the electron that reduces the photochemically generated $Ru^{III}\{(tbpy)\}$-moiety is not a phenolate but a Mn^{II}. In contrast, in the complex Ru_3^{II}- Mn^{IV} (2) the electron is extracted from phenolate. The compound Mn_3^{II}-Ru^{II} (1) is the first example of a photochemically induced intramolecular electron transfer from a multinuclear Mn cluster to a covalently attached sensitizer. On the otherhand, the compound is the first example of an electron transfer from a Mn^{IV}-coordinated phenolate to a photochemically produced oxidant (Ru^{III}).

Sun and coworkers [285] synthesized model Mn-Ru heterometal compounds $[Ru(bpy)_2Mebpy\text{-}MebpyMnCl_2.H_2O]Cl_2$ (1) $[Ru(bpy)_2MebpyMn(bpy)Cl_2]Cl_2$ (2) and $[Ru(bpy)_2(4\text{-}CH_3\text{-}4'CN'\text{-}CH_3\text{-}N',N'\text{-}bis(2\text{-}pyridylmethyl)\text{-}1,2\text{-}ethanediammine)\text{-}CH_2\text{-}bpy)Mn(PF6)_2Cl_2$ (3) from 1, 2-bis(4-(4′-methyl)-2, 2′-bipyridyl)]ethane(Mebpy-Mebpy) and N, N′-dimethyl-N, N'-bis(2-pyridylmethyl)-1, 2 - ethanediamine (Me_2bis picen). In compounds (1), (2) and (3), a photosensitizer, ruthenium(II), bis(bipyridyl) complex is covalently bonded to a manganese (II) ion through bridging ligands. The structures of the compounds were characterized by electron paramagnetic resonance measurements and electrospray ionization mass spectrometry. The EPR spectrum of heterobimetallic complex (1) in powder form at low temperature (77K) is characterized as a N_2X_2 ligand donor set with a broad $g \cong 2$ centred resonance without manganese hyperfine structure. The EPR study in solution could not be carried out by authors because of the instability of the complexes in solution. The heterobimetallic complex (2) displays a broad fine structure resonance without any resolved hyperfine patterns. The powder spectrum of heterobimetallic complex (3) was explained considering lignad N_4X_2 donor set. The complex (3) in powder state and in DMSO solution at 77 K gives rise to the rhombic EPR spectra which are similar to that of (2). A comparative study of powder EPR spectra of (3) and the related monometallic manganese complex $[Mn(II)(Me_2bispicen)Cl_2]$($Me_2$bispicen =

N, N′-dimethyl–N, N′-bis(2-pyridyl- methyl)-1, 2-ethanediamine) indicates that ruthenium (II), bis(bipyridyl) in complex (3) has some effect on the structure of Mn(II) centre within the molecule. The interaction between the ruthenium and manganese moieties within the complex was probed by steady–state and time-resolved emission measurements. The authors studied the chemical oxidation of manganese (II) by ruthenium (II) in the binuclear complexes (1), (2) and (3). They observed the oxidation of Mn(II) centre by $[Ru(III)(bpy)_3]$ in acetonitrile. However, when same was carried out with complex (3), the ligand was modified but the Mn(II) centre remained unchanged. These experiments indicate that in acetonitrile solution $[(Ru(bpy)_3]^{+3}$ modifies the ligand of the manganese in complex (3) rather than oxidising Mn(II). The absorption spectra of the compounds (1) to (3) in acetonitrile are quite similar, all with a ruthenium metal to ligand charge transfer [MLCT] band at ca. 452 nm and with similar extinction coefficients. The electron transfer reaction from Mn(II) to photogenerated ruthenium(III) was studied. From their studies, the authors concluded that a coordinated manganese ion can restore the activity of a photooxidized photosensitizer by intramolecular electron transfer which is a crucial event in PSII. When the binuclear complexes are exposed to flash photolysis in the presence of an electron acceptor such as methyl viologen (MV^{2+}) it could be shown that after the initial electron transfer from the excited state of Ru(II) in compound (1), forming Ru(III) and MV^{+}, an intramolecular electron transfer from coordinated Mn(II) to the photogenerated Ru(III) occurred regenerating Ru(II).

Berglund-Baudin and coworkers [288] studied intramolecular electron transfer from manganese(II) to ruthenium(III) with the help of laserflash photolysis experiments at different concentrations of compound $[Ru(bpy)_2MebpyMebpy.MnCl_2.H_2O]Cl_2$ (Mebpy-Mebpy =1, 2-bis[4-(4′-methyl)-2, 2′-bipyridyl}ethane (1). They explained the experimental data on the basis of a kinetic model, taking different parallel reactions into account. Mn(II) was partially

dissociated from (1), giving a fraction of Ru(II) without Mn(II) attached. In the analysis of the data, the fraction of dissociated Mn(II) was determined independently at each concentration of compound (1), utilizing the fact that the bound Mn(II) quenched the excited state by energy transfer.

Georgi and Tocher [354] described a heteronuclear compound of ruthenium and silver containing bridging tris(pyridyl)methanoate ligands. Thus, treatment of $[Ru(\eta^6\text{-}C_6H_6)Cl_2]_2$ with two equivalents of tris(2-pyridyl)methanoate in absolute ethanol results in slow dissolution of the ruthenium compound and the formation of a yellow solution over a period of 3 h. Addition of an ethanolic solution of $[NH_4][PF_6]$ results in the formation of a yellow precipitate of compound $[Ru(\eta^6\text{-}C_6H_6)\{N, N'O(C_5H_4N)_3CO\}][PF_6]$ (1). The cation acts as a metallo ligand towards other transition metal ions. With $AgPF_6$ the hetèro trinuclear complex $[\{Ru(\eta^6\text{-}C_6H_6)(C_5H_4N)_3CO\}_2Ag][PF_6]_3$ (2) is formed, while reaction with $[Pd(PhCN)_2]Cl_2$ gives the bimetallic $[Ru(\eta^6\text{-}C_6H_6)(C_5H_4N)_3(CO)PdCl_2][PF_6]_3$ (3). The ^1H NMR spectrum of (2) resembles that of precursor complex (1) in that there are two sets of pyridyl resonances with relative integrals for the $\eta^6\text{-}C_6H_6$ ligand, δ 6.23 ppm.

The mass spectrum of 2 exhibits a highest mass peak at m/z 1281 with an envelope consistent with the presence of two ruthenium atoms and a single silver atom in the fragment. The compound (2) has been characterized by X-ray crystallography. The structure consists of a central silver ion coordinated by two alkoxide oxygen atoms, which are also bridging to the two ruthenium,and by two pyridyl nitrogens of the rings which were non-metallated in (1). The central Ag atom has highly distorted tetrahedral structure. Compound 1 also reacts with $[Pd(PhCN_2)Cl_2]$ in a similar way with displacement of the benzonitrile ligands leading to the formation of the heterobimetallic compound, $[Ru\{(\eta^6\text{-}C_6H_6)(C_5H_4N)_3CO\}PdCl_2]$ $[PF_6]$ (3). The compound did not yield crystals suitable for X-ray analysis, the mass spectrum clearly displays a peak and associated isotope

distribution pattern for the $[Ru(\eta^{6}\text{-}C_6H_6)(C_5H_4N)_3CO\}PCl_2]^+$ cation. In the ^1H NMR spectrum, there are two sets of pyridyl resonances with those of relative integral two appearing at similar chemical shifts to those for the ruthenated pyridyls of 2. The authors believe that the coordination of the metallo ligand to the palladium occurs through a bridging alkoxide and a non-ruthenated pyridyl groups as found in (2).

A survey of literature reveals that although metal complexes of monoacylhydrazones, aroylhydrazones and pyridoylhydrazones have been studied in some greater details [355] those of acyl, aroyl and pyridoylhydrazones have received attention in recent years only. Further, the reported existence of heterobimetallic complexes of dihydrazones is much less [46, 98, 103, 105]. Moreover, the work on their heterobimetallic complexes derived from polyfunctional dihydrazones containing methylene functions in their molecular skeleton is quite meagre [110].

In view of the above importance of the bi- or polynuclear and heteropolymetallic complexes, quite meagre work on heterobimetallic complexes derived of dihydrazones containing methylene groups in their molecular skeleton and the fact that the chapter III, IV and V described monometallic complexes of Mn and Ru respectively derived from the title ligands, the present chapter aims at synthesizing and characterization of heterobimetallic complexes of the aforesaid metal ions. Further, it also aims at investigating whether, the dihydrazone would coordinate to the metal ions in the resulting heterobimetallic complexes in the anti-cis configurations as in the monometallic complexes or in some other configurations.

The stoichiometry of the complexes has been judged mainly from elemental analyses. The structure of the complexes has been discussed in the light of conductivity, IR, magnetic moment, electronic and EPR spectroscopic data.

Preparation of the complexes

Preparation of $[Mn^{IV}Ru^{II}(slah)(A)_3Cl]Cl.nH_2O$ (where A= H_2O, (36); py, (37); 2-pic, (38); 3-pic, (39); 4-pic, (40); (n=0, 3))

To a solution of salicylaldehyde (sal) (1.60 g, 13.00 mM) in methanol (20 mL), $RuCl_3.3H_2O$ (1.49 g, 5.60 mM) in methanol (20 mL) was added in 2.3: 1 molar ratio and stirred vigorously for 15 mins in warm condition. This brown solution was then set to reflux for 45 mins. Simultaneously another reaction mixture consisting of adipoyldihydrazone (DH_2) (1.00 g, 5.70 mM) in methanol (20 mL) and $Mn(OAc)_2.4H_2O$ (1.40 g, 5.70 mM) in (1:1) molar ratio was vigorously stirred for 15 mins and then allowed to reflux for 45 mins. Both the sets of reaction mixtures were allowed to cool and then followed by addition of $Mn(OAc)_2.4H_2O$-DH_2 mixture at once to $RuCl_3.3H_2O$–sal reaction mixture in warm condition accompanied by stirring vigorously for another 15 mins. The resulting reaction mixture was refluxed for an hour which precipitated a coloured product. The product was isolated in the solid state by filtration and washing several times and finally with ether and then air-dried.

The complexes (37) to (40) were also isolated by essentially following the above method by adding pyridine bases to the reaction mixture containing $RuCl_3.3H_2O$–sal and $Mn(OAc)_2.4H_2O$ maintaining a molar ratio at 1:1:10 and refluxing for 1 h (Yield: 66.2 %, (36); 64 %, (37); 65 %, (38); 63 %, (39); 62.5%, (40)).

Preparation of $[Mn^{IV}Ru^{II}(npah)(A)_3Cl]Cl.nH_2O$ (where A = H_2O, (41); py, (42); 2-pic, (43); 3-pic, (44); 4-pic, (45); (n=0, 3))

The above complexes (41) to (45) were also prepared by following the general method used for the preparation of complexes (36) to (40) except that a solution of 2-hydroxy-1-naphthaldehyde (ohn) (1.55 g, 8.09 mM) in methanol (20 mL) was added to $RuCl_3.3H_2O$ (1.07 g, 4.08 mM) in methanol (20 mL) in the molar ratio 2.3:1 instead of salicylaldehyde (Yield: 62.4 %, (41); 64.3 %, (42); 63 %, (43); 64 %, (44); 66.4 %, (45)).

Results and Discussion

The colour, decomposition point, molar conductance values, analytical and magnetic moment data of the complexes are set out in **Table 6.1**. The electronic spectral data for the complexes have been given in **Table 6.2**. The compositions of the complexes have been deduced based on the data obtained from the elemental analyses.

Here, we have synthesized the heterobimetallic complexes by a method in which the reaction mixture consisting of Mn(II)acetate and adipoyldihydrazone (DH_2) in the molar ratio 1:1 was allowed to react with another reaction mixture containing $RuCl_3.3H_2O$ and salicylaldehyde(sal)/2-hydroxy-1-naphthaldehyde (ohn) in the molar ratio (1: 2.3) in methanol under reflux either as such or in presence of pyridine bases.

Heterobimetallic complexes of the composition $[Mn^{IV}Ru^{II}(slah)(A)_3Cl]Cl.nH_2O$ and $[Mn^{IV}Ru^{II}(npah)(A)_3Cl]Cl.nH_2O$ (where A = H_2O (36), (41); py, (37), (42); 2-pic, (38), (43); 3-pic (39), (44), 4-pic (40), (45); (n = 0, 3)) were isolated.

The formation of the complexes may be represented by the following general scheme.

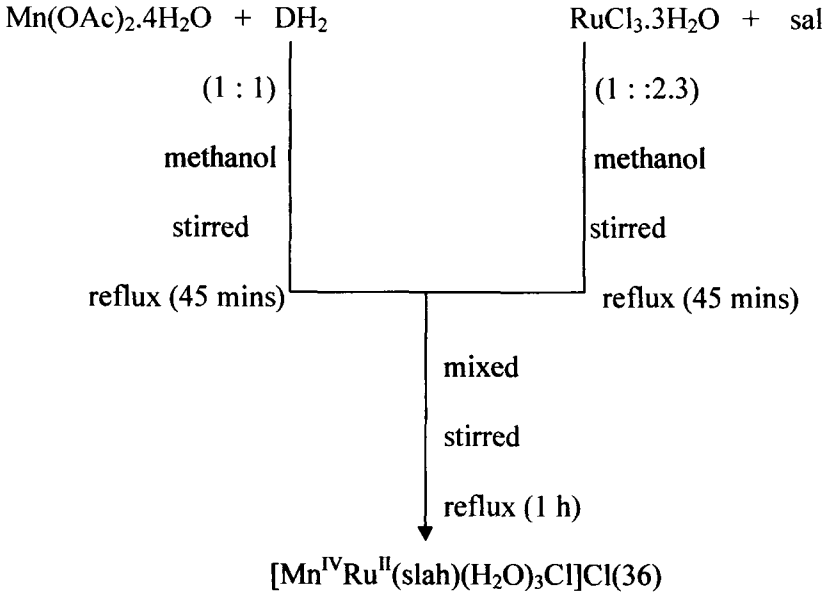

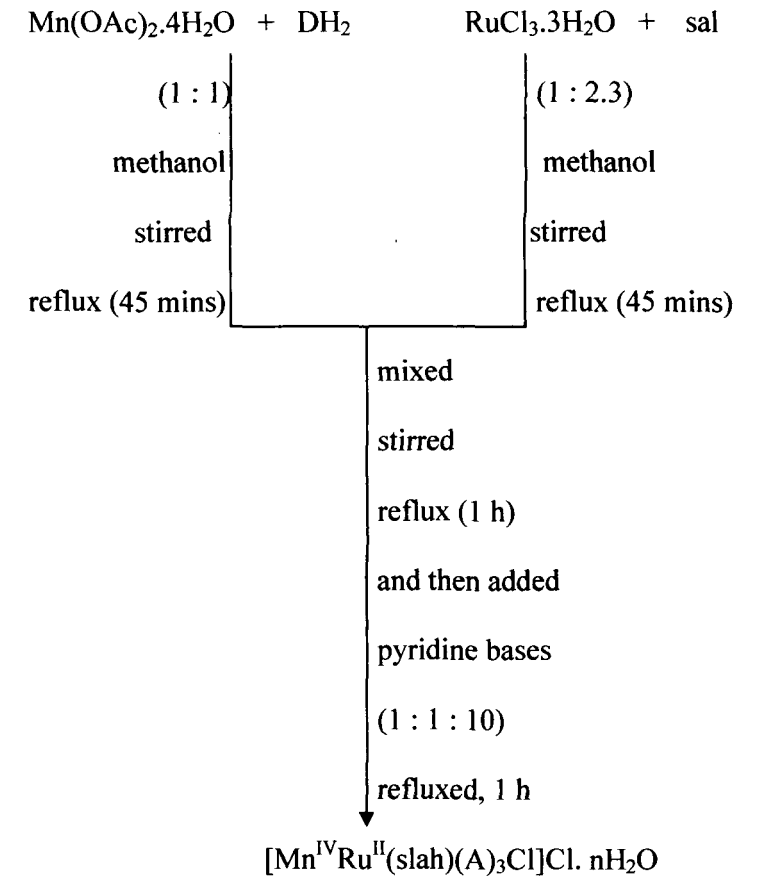
Mn(OAc)2.4H2O + DH2
(1 : 1)
methanol
stirred
reflux (45 mins)
RuCl3.3H2O + sal
(1 : 2.3)
methanol
stirred
reflux (45 mins)
mixed
stirred
reflux (1 h)
and then added
pyridine bases
(1 : 1 : 10)
refluxed, 1 h
[Mn^IV Ru^II (slah)(A)3Cl]Cl. nH2O
(A = py, (37); 2-pic, (38); 3-pic, (39); 4-pic, (40))
(n = 0, 3)

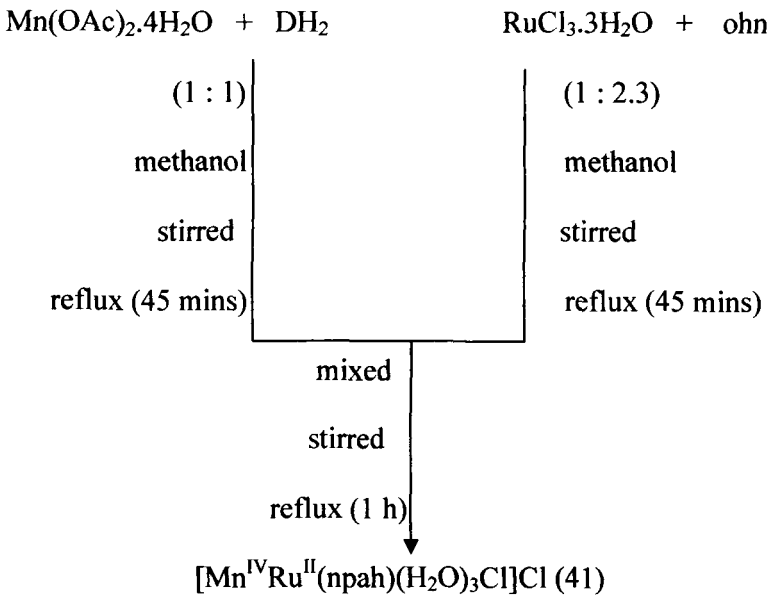
Mn(OAc)2.4H2O + DH2
(1 : 1)
methanol
stirred
reflux (45 mins)
RuCl3.3H2O + ohn
(1 : 2.3)
methanol
stirred
reflux (45 mins)
mixed
stirred
reflux (1 h)
[Mn^IV Ru^II (npah)(H2O)3Cl]Cl (41)

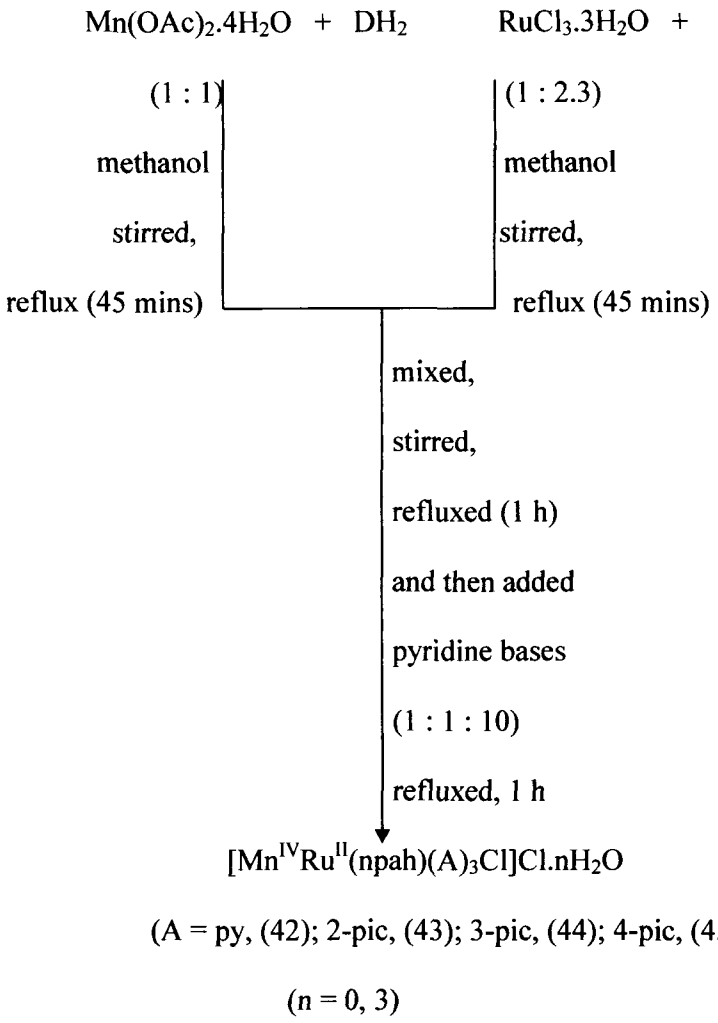

The complexes vary in colour from yellow, brown, dull green, muddy brown, brown green to dark green. The complexes are partially soluble in acetonitrile, CH_2Cl_2 and insoluble in methanol, ethanol, CCl_4, $CHCl_3$, ether, benzene etc. All of them are freely soluble in DMSO and DMF. All of the complexes decompose above 300 °C. The complexes (36) and (41) showed weight loss at 180 °C while the complexes (38), (39), (40) and (44) showed weight loss at 130 °C corresponding to three water molecules. The loss of three water molecules at 180 °C in complexes (36) and (41) indicates that they are coordinated to the metal centre while the loss of three water molecules at 130 °C in the complexes suggests that they are present in the lattice of the complexes in the strongly H-bonded form. However, the remaining complexes showed loss of weight corresponding to three pyridine/2-picoline/3-picoline/4-picoline

molecules at 220 °C. The loss of the donor molecules at such a high temperature indicates their presence in the first coordination sphere around the metal centre.

Molar Conductance

The molar conductance values for all of the complexes have been set out in the **Table 6.1**.

The molar conductance values for the complexes (36) to (45) at 10^{-3} M dilution in DMSO solution lie in the region 35.5–29.7 ohm^{-1} cm^2 mol^{-1}. The molar conductance values for the complexes suggests their 1: 1 electrolytic nature [145].

Magnetic Moment

When two paramagnetic transition metal ions are present in the same molecular entity, the magnetic properties can be totally different from the sum of the magnetic properties of each ion surrounded by its nearest neighbours. This is because the new properties depend on the nature and the magnitude of the interaction between the metal ions through the bridging ligands. In the present study, the two ligands disalicylaldehyde adipoyldihydrazone ($slahH_4$) and bis(2-hydroxy-1-naphthaldehyde)adipoyldihydrazone ($npahH_4$) used are schiff bases with O and N as donor atoms. The phenoxide/naphthoxide oxygen atoms function as bridging atoms by virtue of withdrawing electrons from phenyl/naphthyl ring while nitrogen atoms function as bridging group by virtue of being part of >N–H< grouping. Thus they have the potential to give bridged heteroatoms like 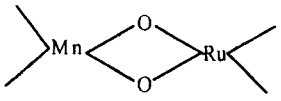

or

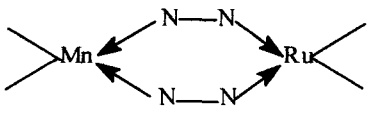

The magnetic moments for all of the complexes in the present study fall in the region 3.02–4.12 B.M. (**Table 6.1**). These values are close to the spin - only value for a d^3 system (Mn(IV)) i.e. it exhibits a magnetic moment for monomanganese (IV) derivatives corresponding to uncoupled S = 3/2.

The EPR spectra of the complexes rule out the possibility of the presence of ruthenium as Ru^{III} as they do not show any signal which could be attributed to Ru^{III}. This suggests that Ru exists in the complexes as Ru^{II}. However, the EPR spectral features of the complexes are consistent with the presence of Mn(IV). The EPR spectra of the complexes suggest that they contain Mn^{IV} and Ru^{II}. Hence experimental values of magnetic moment observed in the present study might be attributed to Mn(IV) d^3 system (S = 3/2). Besides, these values rule out the possibility of the presence of any metal-metal interaction in the complexes i.e. manganese centres is non-interacting with the other metal Ru(II) which is diamagnetic. This is obviously due to the absence of unpaired spin at the second metal centre of the complexes.

Electronic Spectra

All the heterobimetallic complexes (36) to (45) have been characterized by electronic spectroscopy. The complexes are soluble in DMSO in which they give brown or green coloured solution. Hence, their electronic spectra were recorded in this medium in the range 350-800 nm.

The electronic spectral bands for the complexes alongwith their molar extinction coefficients have been given in **Table 6.2**. The electronic spectra for the complexes (36), (38), (40), (41) and (43), (45) are shown in **Figs. 6.1.1- 6.1.6**.

The free ligand $slahH_4$ shows band at 320(2808) while the ligand $npahH_4$ shows band at 363(1852).

In the present study the spectra of the complexes show overlapping bands that stretch well into the visible region. However, the bands can be interpreted as arising from the following types of transitions,

(i) intraligand

(ii) metal to ligand charge transfer

(iii) d-d transition located within the metals

The complexes show bands in the region 350-452 nm which are shifted to longer wavelength as compared to their position in the free ligands. The shift of ligand bands to longer wavelength in the complexes indicates metal-ligand bonding. The prominent bands in the region 350-452 nm in the ultraviolet region in the spectra of the complexes appear to arise due to intraligand bands. The complexes show more number of bands than those present in the free ligands. More number of bands in the region 350-452 nm arise due to splitting of ligand bands which is the result of complexation of the ligand to the metal centre. These bands are attributed to arise due to $n\rightarrow\pi^*$ and $\pi\rightarrow\pi^*$ transitions located in their ligands. The $\pi\rightarrow\pi^*$ transitions occurring in this region is consistent with the stabilization of the π^* orbitals upon complexation of two metal centres [356]. In addition to the ligand bands, the complexes show additional bands in the region 439-732 nm.

For a Mn(IV), d^3 system, the following three types of spin allowed d–d transitions bands are expected. The position of the absorption band for $[MnF_3]^{2-}$ is shown below,

$459\ nm \leftarrow 2180\ cm^{-1}$ $\quad {}^4T_{2g} \leftarrow {}^4A_{2g}$

$356\ nm \leftarrow 28090\ cm^{-1}$ $\quad {}^4T_{1g}(F) \leftarrow {}^4A_{2g}$

$\quad {}^4T_{1g}(P) \leftarrow {}^4A_{2g}$

The third band arising due to ${}^4A_{2g} \rightarrow {}^4T_{1g}(P)$ transition is obscured either by strong charge transfer band or by ligand band.

On the other hand, Ru(II) ion is a d^6 system with a low-spin configuration. It is known to show the ability of π-back donation from its $d\pi$-orbital to the suitable vacant orbital present on the ligand [287, 353].

For a Ru(II) complex four bands corresponding to the following transitions are expected

${}^1A_{1g} \rightarrow {}^3T_{1g}$, ${}^1A_{1g} \rightarrow {}^3T_{2g}$, ${}^1A_{1g} \rightarrow {}^1T_{1g}$ and ${}^1A_{1g} \rightarrow {}^1T_{2g}$

The region between 439–484 nm show an intense band and is assigned to metal-to-ligand charge transfer bands arising due to overlapping of Ru($d\pi^*$)–L(π^*) and Mn($d\pi$)–L(π^*) [356, 360] charge transfer bands.

The band of lowest energy observed in the visible region for the complexes (38), (41) to (43) and (45) between 548 – 732 nm region is assigned to d-d transition mainly localized on Mn(IV) centre. However, they are also expected to have contribution from Ru($d\pi$)–π^*(L) transition as they have appreciably high molar extinction coefficient.

Electron Paramagnetic Resonance Spectra

The complexes (36), (38), (40), (41) and (44) were characterized as representative samples by EPR spectroscopy in polycrystalline state and DMSO solution at LNT. The magnetic parameters have been shown in **Table 6.2** alongwith the electronic spectral data and the spectra of the complexes (36), (38), (40), (41) and (44) have been shown in **Figs. 6.2.1-6.2.5** as representative examples.

The EPR spectral features of the complexes are characteristic of the presence of Mn(IV) and Ru(II). This is evident from the fact that the spectra of the complexes show a strong signal at $g \cong 2$ and another weak signal at $g \cong 4$. The complexes do not show any new signal in the 0– 4000 G range which could be assigned to arise due to Ru(III). Such EPR spectral features of the complexes suggest that the ruthenium is present in +2 oxidation state in them.

The complex (36) shows hyperfine splitting for the signal at $g \cong 2$ in the solid state as well as in the solution state with hyperfine splitting constant equal to 104 G and 96 G, respectively. On the other hand EPR spectra of other complexes do not show hyperfine splitting in the solid but do show hyperfine splitting in the solution state for $g \cong 2$ signal. The hyperfine splitting constant in these complexes varies from 96 to 103 G respectively.

Consistent with the symmetrical electronic configuration of Mn(IV) (t_{2g}^3 half-filled shell) in an octahedral ligand field [162] the observed magnetic hyperfine tensors for these complexes vary from 96 G to 103 G.

Infrared Spectra

Some structurally significant IR bands for uncoordinated dihydrazones, alongwith those of the heterobimetallic complexes have been set out in **Table 6.3** for comparative study. The IR spectra of the complexes (36), (37), (38), (40) to (43) and (45) have been shown in **Figs. 6.3.1-6.3.8.**

A comparative study of the spectra of the complexes with their respective dihydrazones help us in deriving information regarding bonding of the dihydrazone to the metal centre in the complexes.

The IR spectra of the complexes (36) to (45) show a strong broad band in the region 3000-3600 cm^{-1} with their centres lying in the region 3400-3460 cm^{-1}. Further, the complexes (36), (38) to (40) and (44) show an additional strong band in the region 3171–3211 cm^{-1}. The essential features of the bands in the region indicate the involvement of phenolic –OH/naphtholic –OH group in bonding via deprotonation. The absence of band due to secondary NH group indicates destruction of NH group as a result of enolization of the ligands. The strong broad band in the region 3000–3600 cm^{-1} may arise due to lattice and coordinated water molecules. Further, the bands in this region may also have contribution due to water molecules absorbed by KBr pellets which is moisture sensitive.

In order to decide upon whether the bands in this region arise due to H_2O molecules or due to moisture absorbed by KBr during pellet preparation, the compounds were heated at 110 °, 130 ° and 180 °C, respectively. The ensuing vapour was identified by passing through a trap containing anhydrous $CuSO_4$. Thus, none of the complexes showed weight loss at 110 °, 130 ° or 180 °C except the complexes (36), (38), (39), (40) (41) and (44). The absence of loss of weight at 110 °C in these

complexes dismissed the possibility of the presence of water molecules in their lattice structure. This suggests that the strong broad band centred in the region 3423-3462 cm^{-1} in the complexes arise due to moisture absorbed by KBr during pellet preparation. On the other hand, the complexes (36) and (41) showed weight loss at 180 °C corresponding to three water molecules while the complexes (38), (39) (40) and (44) showed weight loss at 130 °C corresponding to three water molecules. The loss of water molecules at 180 °C in the complexes (36) and (41) at such high temperature might suggest their coordination to the metal centre. However, the complexes (38), (39), (40) and (44) show loss of weight at slightly, higher temperature as compared to the lattice water molecules. The classification of solvent molecules on the basis of mass loss alone as being held in the lattice or being coordinated to the metal centre needs utmost caution in view of the fact that loss of solvent molecules at considerably high temperature might occur due to a hydrogen bonded network in the solid state in the complexes that might permeate the lattice. Hence, it is suggested that three water molecules are most probably embedded in the lattice structure of the complexes in the strongly H-bonded form which might permeate the lattice. This is confirmed from the fact that the band corresponding to these water molecules appears in the region 3171-3211 cm^{-1}. In order to decide whether the water molecules in these complexes are coordinated to the metal centre or present in the lattice structure, we scrutinized the IR spectra of the complexes in the region 900–600 cm^{-1} which contain bands due to rocking and wagging vibrations of coordinated water.

A distinct weak band was observed at 795sh and 800 sh in the IR spectra of the complexes (36) and (41) due to rocking mode of coordinated water molecules. On the other hand, the remaining complexes (38), (39), (40) and (44) did not show such IR bands ruling out the possibility of coordination of water molecules to the metal centre. Such a feature of IR spectra of these complexes suggests that the water molecules are not coordinated to the metal centre in the complexes (38), (39), (40) and (44).

The various amide bands arise from the mixed contribution of varying degree of >C=O and >NH group contribution invariably present in amide-I, II, III, and V bands Coordination of monoacylhydrazine [17] through >C=O and $-NH_2$ groups and monoacylhydrazone [163] through >C=O and >C=N group results in lowering of the group stretching frequencies. In the event of enolization, the >C=O and >NH groups are destroyed resulting in –C(OH)=N– group in which νOH, νC-O and νC=N should appear. Reactions with the metal ions in enol form results in –N=C-O and >C=N-N=C< group vibration [41]. In all these complexes (36)–(45), the νC=O mode of the free ligand is absent indicating destruction of >C=O and NH group in enolization followed by deprotonation and complexation to the metal ions.

In all these complexes strong band appears in the region 1600-1613 cm^{-1}. This band is very strong as compared to those in the uncoordinated dihydrazone. Strong band in this region in hydrazone complexes has been attributed to >C=N-N=C< group [157]. The essential features associated with this band suggests that it owes its origin to >C=N-N=C< group. Hence, the band in the region 1606-1613 cm^{-1} is attributed to ν>C=N-N=C< stretching frequency of azomethine group. The origin of this band indicates condensation of $-NH_2$ group of hydrazide and >C=O group of salicylaldehyde/2-hydroxy-1-naphthaldehyde. The position of this band lies in the region where azomethine nitrogen has been suggested to coordinate to the metal centre in hydrazone complexes. In all of the complexes this bands shifts to lower frequency by 5-20 cm^{-1} indicating coordination through >C=N group to the metal centre.

The aromatic ring vibrations occurring at ~1600 cm^{-1} are observed neither in the spectra of ligands nor in the heterobimetallic complexes. Most probably, this band appears to be masked by strong νC=N band in the ligand as well as in the complexes.

A strong to weak intensity band is observed at 1560(s) and 1530(w) in the ligands $slahH_4$ and $npahH_4$ respectively. The band is assigned to [amide II + νC-O(phenolic/naphtholic)]. In complexes (36) to (40), the band shifts to lower frequency

by 20 cm^{-1} while in complexes (41) to (45), the band shifts to higher frequency by 3-10 cm^{-1}. The intensity of this band is considerably increased in the complexes (41) to (45).This indicates that this has contribution from νNCO- vibrations produced as a result of enolization of ligand in addition to νC-O(naphtholate) [41].

The band appearing at 1275 cm^{-1} and 1281 cm^{-1} in the free ligands may be assigned to bending vibration of phenolic/naphtholic (C-O) groups. This band shifts to higher frequency by 14-33 cm^{-1} in the complexes. This indicates strong bonding through phenolate/naphtholate [166] oxygen atom to the metal centre.

All complexes except complexes (36) and (41) show a weak to medium intensity band in the region 1062-1102 cm^{-1}. This band is assigned to the ring breathing mode of coordinated pyridine, 2-picoline, 3-picoline and 4-picoline molecules in the complexes.

All the complexes show a weak to medium intensity non-ligand band in the region 815-857 cm^{-1}. The band is characteristic of tetraatomic species 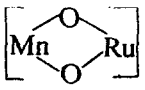

which results from the involvement of phenolate/naphtholate oxygen atom in bridge formation [261].

Low frequency region of IR spectra of the metal complexes provides very useful information regarding the type of metal–ligand bond arising from coordination of the ligand to the metal centre. The νM-O, νM-N, νM-Cl stretching vibration would be expected to depend upon the strength of the bonds which in turn would depend upon the strength of the environment (electrophillic or nucleophillic) in which the donor atoms, oxygen and nitrogen atoms remain present. Due to larger dipole moment change in vibration of M-O bond in comparison to that in the M-N bond, the band due to νM-O occurs at higher frequency. In the present complexes, the oxygen of –OH and nitrogen of >C=N group and pyridine and substituted pyridines are involved in bonding as is evident from results and discussion presented above in the high region of IR spectra.

On examining the spectra of the ligand and metal complexes below 600 cm^{-1}, the non-ligand bands in the range 500-592 cm^{-1} are assigned to νM-O(phenolic/naphtholic) [180, 182] while a new band in the region 430-470 cm^{-1} is assigned to νM-O(carbonyl). The appearance of this band in the complexes suggests the involvement of enolate oxygen atom in bonding to the metal centre.

The complexes show couple of weak to medium intensity bands in the region 241–244, 433-489, 640-671 cm^{-1} . The band in the region 241–244 cm^{-1} is assigned to *νM-N (M = Mn, Ru) stretching frequency due to coordination of pyridyl ring nitrogen* atom to the metal centre [262], while the bands in the region 433-489 and 640-671 cm^{-1} are assigned to arise due to in-plane and out–of–plane ring deformation modes of coordinated pyridine/substituted pyridines.

The metal–halogen vibration occurs in the low-frequency region of infrared spectra. Valuable information regarding the oxidation state and the coordination number of the metal ions as well as the stereochemistry of the complexes can be obtained from the position of metal–halogen vibration in the low frequency region.

The νM-X stretching frequency is dependent upon a number of factors. For example, νM-X is lowered as the structure changes from Td to Oh with the change in coordination number 4 to 6. There may be two types of M-X band viz terminal and bridging. In general bridging M-X modes occur at lower frequencies compared to terminal M-X modes. If other things are equal, M-X stretching frequencies is observed at higher range as the oxidation state of the metals increases. In the present study, the complexes (36) to (40) have also been studied in the range 600-200 cm^{-1}. In these complexes one weak to medium to strong intensity band is observed in the region 302-307 cm^{-1} which is assigned to ν(Ru-Cl) [221].

Cyclic Voltammetry

All of the heterobimetallic complexes have been characterized by cyclic voltammetry except complex (37). The cyclic voltammogram of a 2 mM solution of the

complexes in DMSO with 0.1 M TBAP as a supporting electrolyte were run and the potential values obtained at a scan rate of 100 mV/s are shown in Table 6.4. The voltammograms of the complexes (39), (40), (42) and (44) have been shown in Figs 6.4.1-6.4.4.

All the heterobimetallic complexes have been characterized by CV except the complex (37). In majority of the slahH_4 complexes, the redox processes occur at positive potentials while in those derived from npahH_4, the redox processes occur at positive as well as negative potentials. The complexes show either reversible, quasi-reversible or irreversible electrode processes. In majority of the complexes, the redox processes are either quasi-reversible or irreversible, most probably due to heterogeneous character of the medium.

The complex (36) shows two metal centred redox processes. The first redox process (red. peak: +0.30 V, oxid. peak: +0.60 V) is assigned to be centred on manganese while second redox process (oxid. peak: 0.00 V; red. peak -0.36 V) is attributed to arise from ruthenium. The redox processes are shown below

$$[Mn^{IV}Ru^{II}(slah)(H_2O)_3Cl]^+ + e \rightleftharpoons [Mn^{III}Ru^{II}(slah)(H_2O)_3Cl]$$

$$[Mn^{III}Ru^{II}(slah)(H_2O)_3Cl] + e \rightleftharpoons [Mn^{III}Ru^{I}(slah)(H_2O)Cl]^{-1}$$

This complex shows an additional reductive wave at -1.04 V which is assigned to correspond to ligand based reduction derived from slahH_4.The remaining complexes derived from slahH_4 show only one oxidative wave and one reductive wave.

The oxidative and reductive waves in the complexes (38) to (40) are not related to one another at all. As the complexes (38) to (40) show one oxidative and one reductive wave, it appears that the redox processes observed in the complex (36) are merged into one another in these complexes. However, it appears that in the complexes (38) to (40) the oxidative and reductive waves are concentrated on individual metal centres and there is no cooperative interaction between the metal centres. The oxidative

waves at +0.20 and +0.12 V in the complexes (38) to (40) retain contribution due to oxidative electron transfer process centred on the dihydrazone which is not visible in the complex (36).

The complex (41) shows reductive peak at +0.10 V. The corresponding oxidative wave appears at +0.26 V. This redox process is quasi-reversible and is attributed to arise due to manganese centre. The electrode process corresponding to these redox waves may be represented as

$$[Mn^{IV}Ru^{II}(npah)(H_2O)_3Cl]^+ + e \rightleftharpoons [Mn^{III}Ru^{II}(npah)(H_2O)_3Cl]$$

Another oxidative wave observed at -0.10 V and a reductive wave at -0.70 V are attributed to arise due to ruthenium centre electron transfer process. The electron transfer process is shown below

$$[Mn^{III}Ru^{II}(npah)(H_2O)_3Cl] + e \rightleftharpoons [Mn^{III}Ru^{I}(npah)(H_2O)_3Cl]^{-1}$$

This complex shows an additional oxidative wave at −0.75 V and corresponding reductive wave at −1.20 V which are attributed to ligand centred electron transfer process.

The complex (42) shows a well resolved redox couple (oxid. wave: -0.30 V and red. wave: -0.51 V) which is quasireversible. It appears that in this complex, the redox processes centred on manganese as well ruthenium are merged into one another. Hence, these redox waves may be assigned to redox processes centred on both Mn and Ru.

Alternatively, the essential features of the cyclic voltammogram may be explained by saying that in the complex there is cooperative interaction between two metals. In the electrode process, the single electron is transferred from manganese to ruthenium or from ruthenium to manganese as shown below

$$[Mn^{IV}Ru^{II}(npah)(py)_3Cl]^+ \rightleftharpoons [Mn^{V}Ru^{I}(npah)(py)_3Cl]^+ \quad \text{or}$$

$$[Mn^{IV}Ru^{II}(npah)(py)_3Cl]^+ \rightleftharpoons [Mn^{III}Ru^{III}(npah)(py)_3Cl]^+$$

The remaining complexes (43) to (45) show similar electrochemical behaviour. All the three complexes show two reductive and two oxidative waves. The oxidative waves appear at 0.00 and -0.90 V in complex (43) while the corresponding reductive peaks appear at -0.16 and -0.55 V. Both the redox waves in the complex (43) are quasi-reversible. The first redox waves in complex (44) while the second waves in the complex (45) are almost reversible. The remaining waves in the both the complexes are irreversible. The second wave in the both the complexes are attributed to Ru while first wave is attributed to Mn. The electrode processes in complex (43) are shown below

$$[Mn^{IV}Ru^{II}(npah)(2\text{-}pic)_3Cl]^{+} + e \rightleftharpoons [Mn^{III}Ru^{II}(npah)(2\text{-}pic)_3Cl]$$

$$[Mn^{III}Ru^{II}(npah)(2\text{-}pic)_3Cl]^{+} + e \rightleftharpoons [Mn^{III}Ru^{I}(npah)(2\text{-}pic)_3Cl]^{-1}$$

Conclusion

In the present chapter, the heterobimetallic complexes of manganese and ruthenium have been described. It has been shown that the present polyfunctional dihydrazones can stabilize heterobimetallic complexes. The heterobimetallic complexes have been derived from polynucleating dihydrazones, disalicylaldehyde adipoyldihydrazone ($slahH_4$) and bis(2-hydroxy-1-naphthaldehyde)adipoyldihydrazone ($npahH_4$). In heterobimetallic complexes, the dihydrazones function as tetrabasic hexadentate ligands. The dihydrazones coordinate through phenoxide/naphthoxide oxygen atoms and azomethine nitrogen atoms to ruthenium centre and through the enolate oxygen atoms to the manganese centre. Manganese and ruthenium atoms are held together through oxo-bridging involving phenoxide/naphthoxide oxygen atoms. Thus, the manganese centre occupies O_2O_2 coordination chamber while ruthenium centre occupies N_2O_2 chamber. The metal centres are proposed to have six-coordinated distorted octahedral stereochemistry in all of the complexes. The magnetic moment values of these complexes are consistent with the presence of Mn(IV) and Ru(II) metal centres. This is also supported from EPR spectral studies which are consistent with the presence of Mn(IV) and Ru(II) centres in

the complexes. The complexes show M-L charge transfer bands which arise from superimposition of bands resulted from Ru(dπ)→L(π*) and Mn(dπ)→L(π*) charge transfer bands.

The electron transfer reactions of the complexes have been studied by cyclic voltammetry.

On the basis of results obtained from various physico-chemical and spectral studies, the structures of the complexes have been proposed as shown in **Figs. 6.5.1** and **6.5.2.**

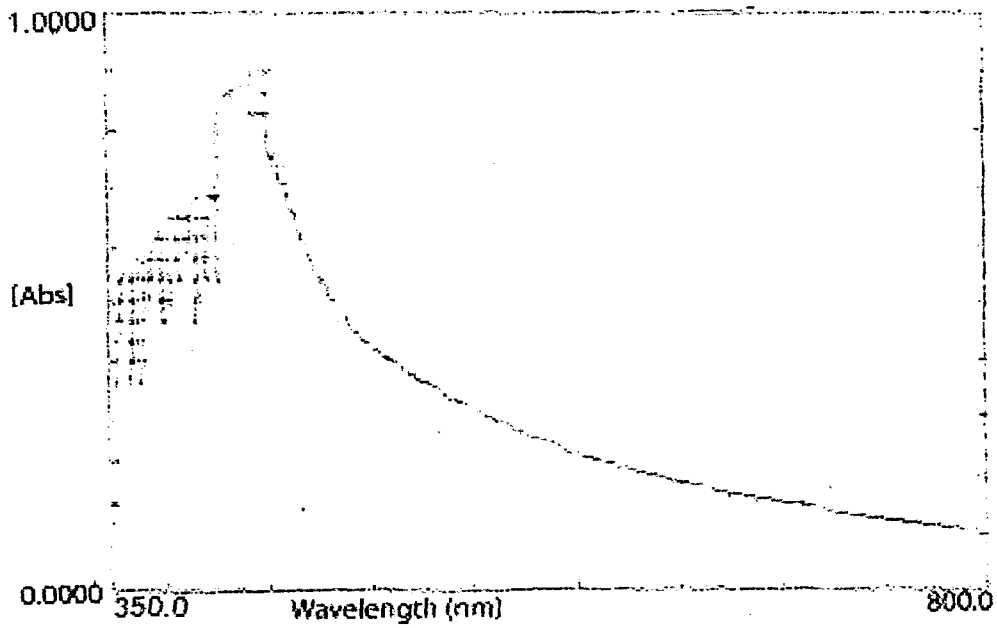

Fig. 6.1.1 Electronic spectrum of complex $[Mn^{IV}Ru^{II}(slah)(H_2O)_3Cl]Cl.3H_2O$ **(36)**

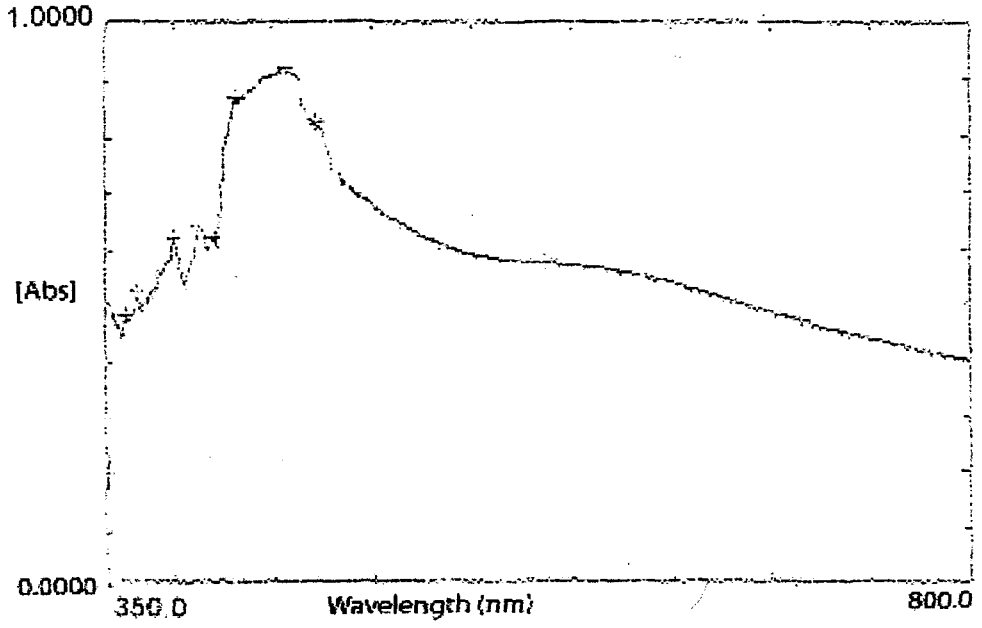

Fig. 6.1.2 Electronic spectrum of complex $[Mn^{IV}Ru^{II}(slah)(2\text{-pic})_3Cl]Cl.3H_2O$ **(38)**

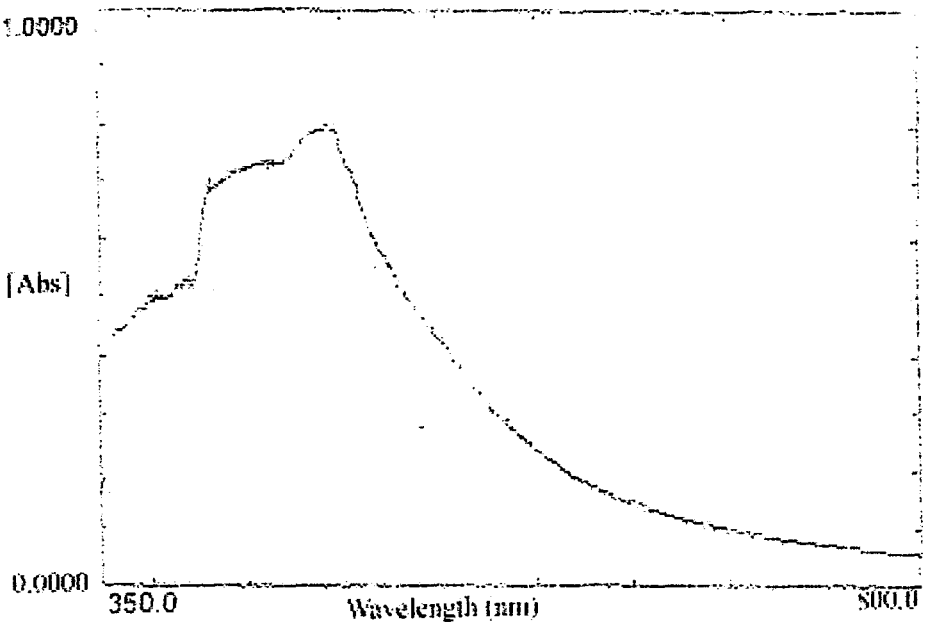

Fig. 6.1.3 Electronic spectrum of complex $[Mn^{IV}Ru^{II}(slah)(4\text{-}pic)_3Cl]Cl$ **(40)**

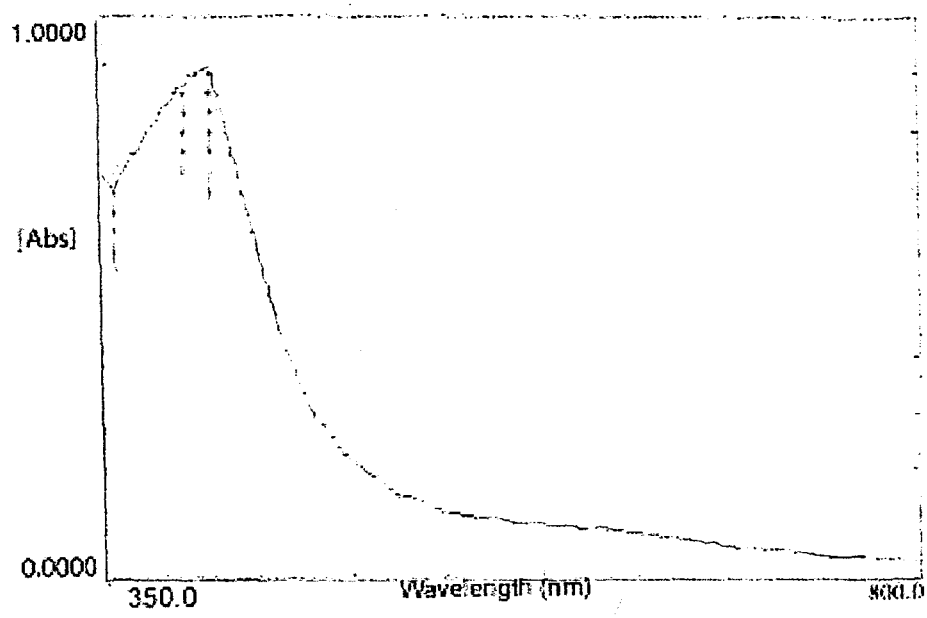

Fig. 6.1.4 Electronic spectrum of complex $[Mn^{IV}Ru^{II}(npah)(H_2O)_3Cl]Cl$ **(41)**

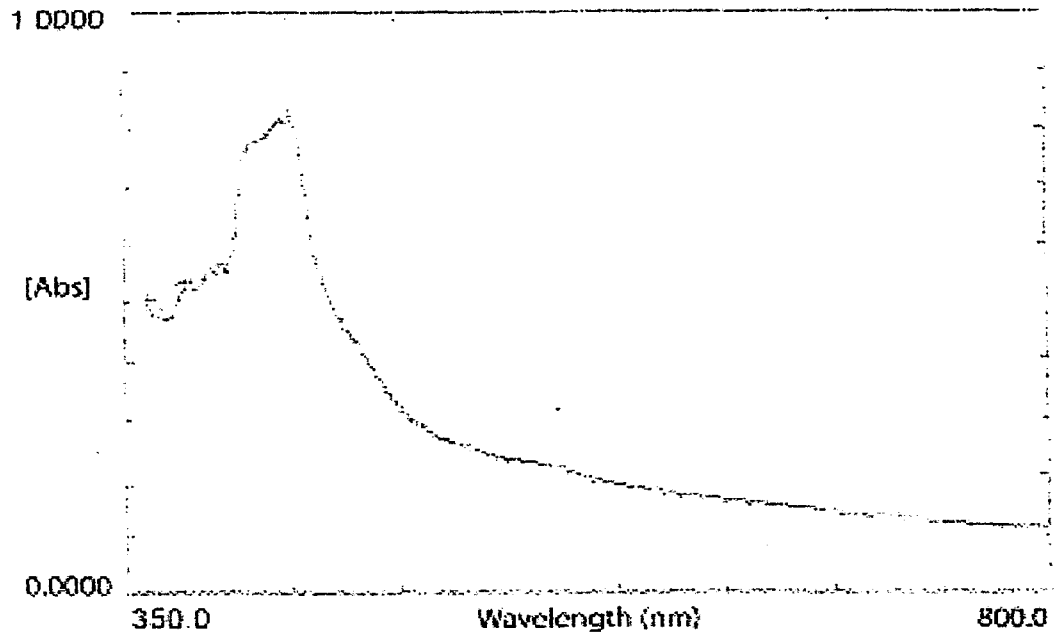

Fig. 6.1.5 Electronic spectrum of complex $[Mn^{IV}Ru^{II}(npah)(2\text{-}pic)_3Cl]Cl$ **(43)**

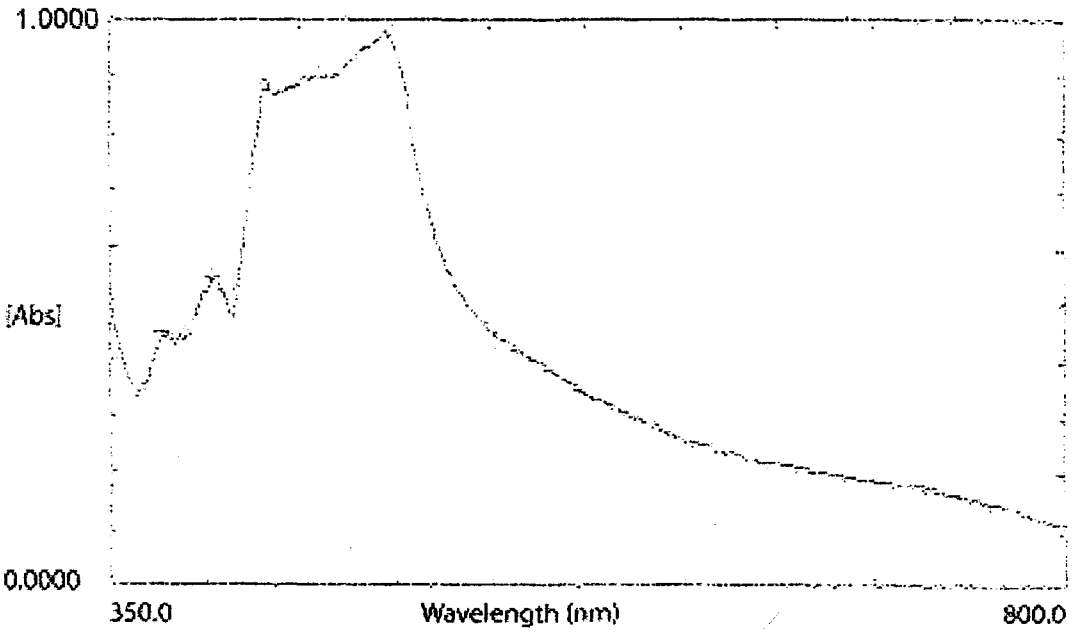

Fig. 6.1.6 Electronic spectrum of complex $[Mn^{IV}Ru^{II}(npah)(4\text{-}pic)_3Cl]Cl$ **(45)**

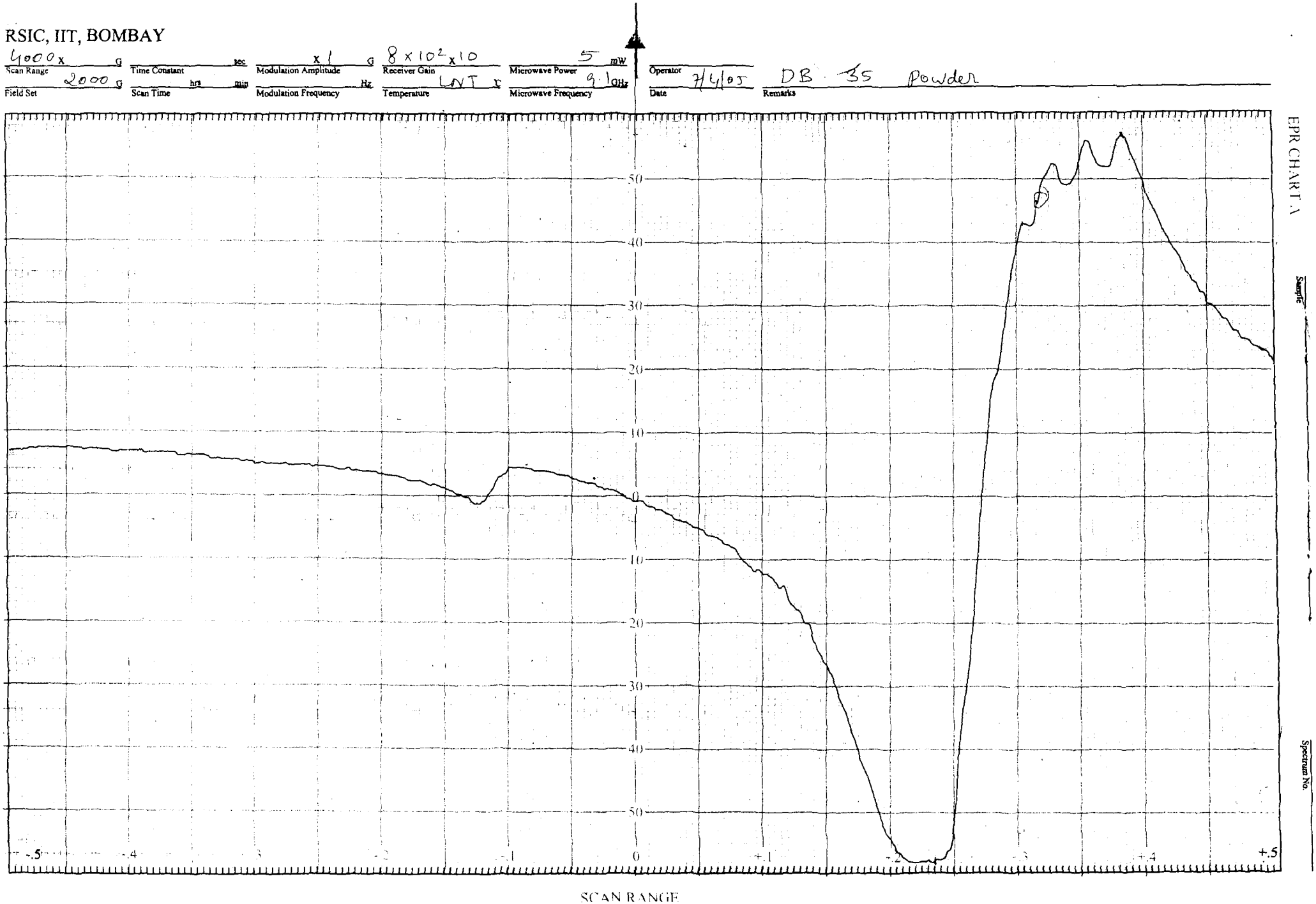

Fig. 6.2.1 (a) EPR powder spectrum of complex $[Mn^{IV}Ru^{II}(slah)(H_2O)_2]$ **(36)** at Temperature: LNT, Frequency: 9.1 GHz, Scan range: 4000 G and Field Set: 2000 G

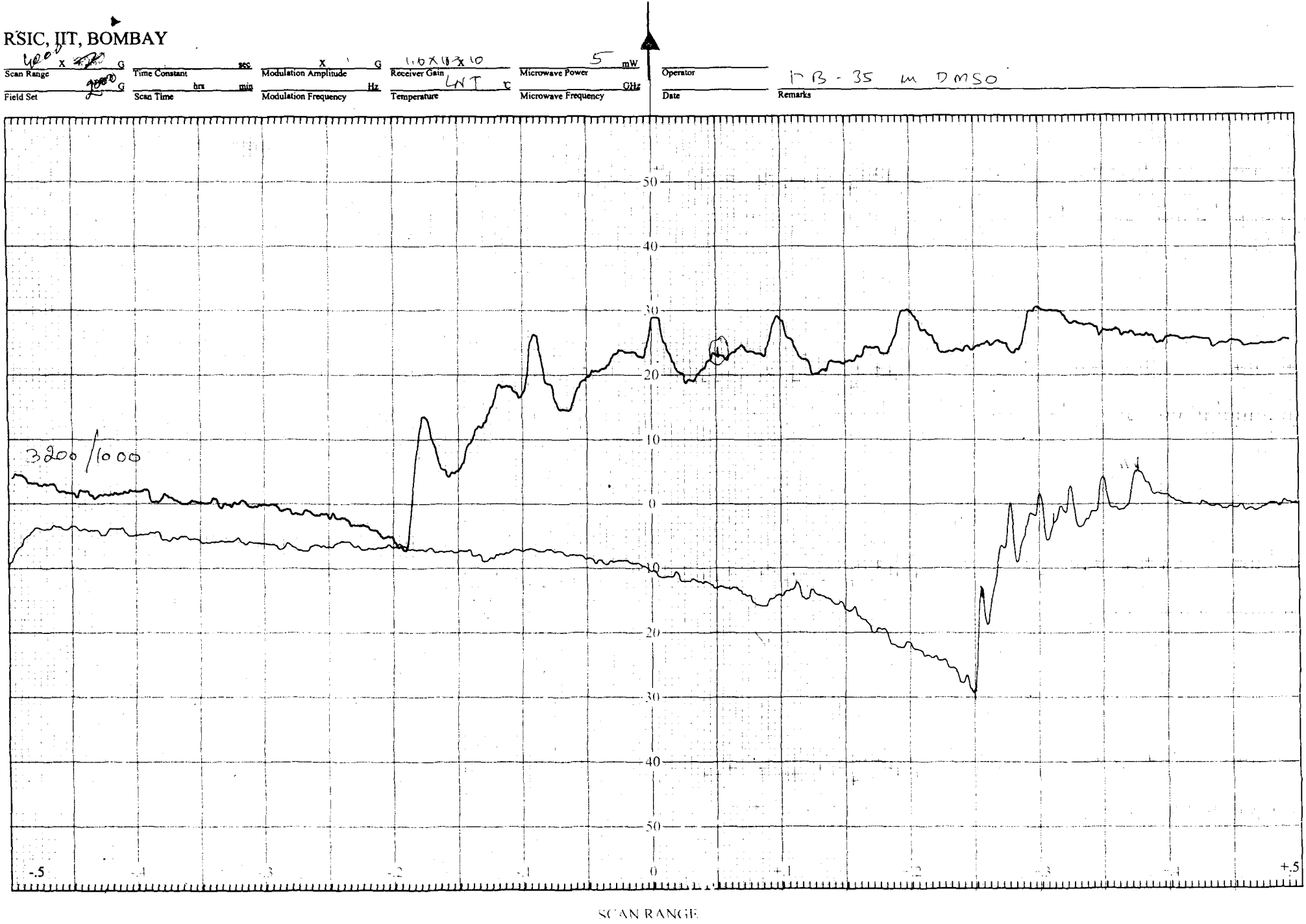

Fig. 6.2.1 (b) EPR spectrum of complex $[Mn^{IV}Ru^{II}(slah)(H_2O)_2]$ **(36)** in DMSO solution at Temperature: LNT, Frequency: 9.1 GHz, Scan range: 4000 G and Field Set: 2000 G

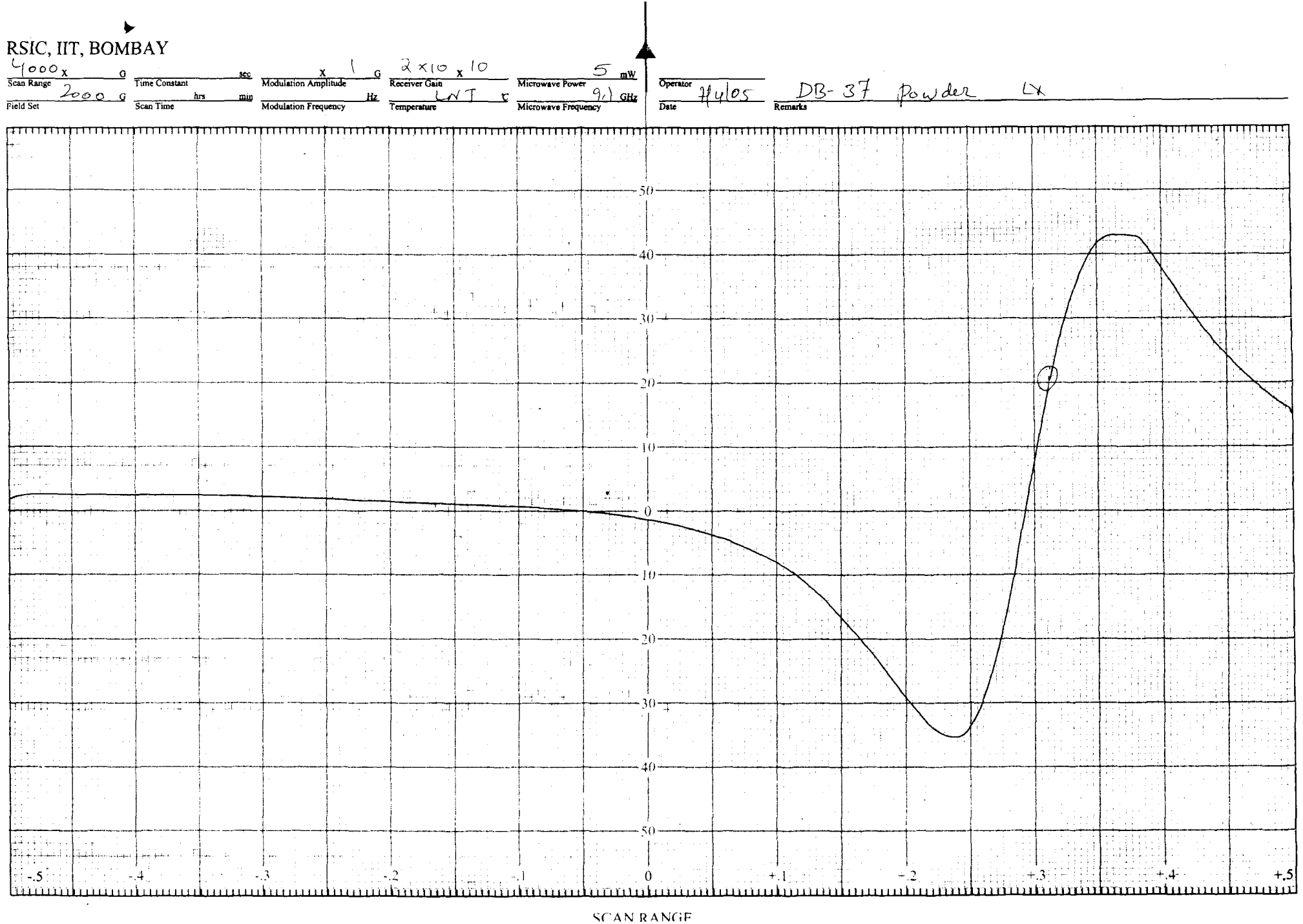

Fig. 6.2.2 (a) EPR powder spectrum of complex $[Mn^{IV}Ru^{II}(slah)(2\text{-}pic)_3Cl]Cl.3H_2O$ **(38)** at Temperature: LNT, Frequency: 9.1 GHz, Scan range: 4000 G and Field Set: 2000 G

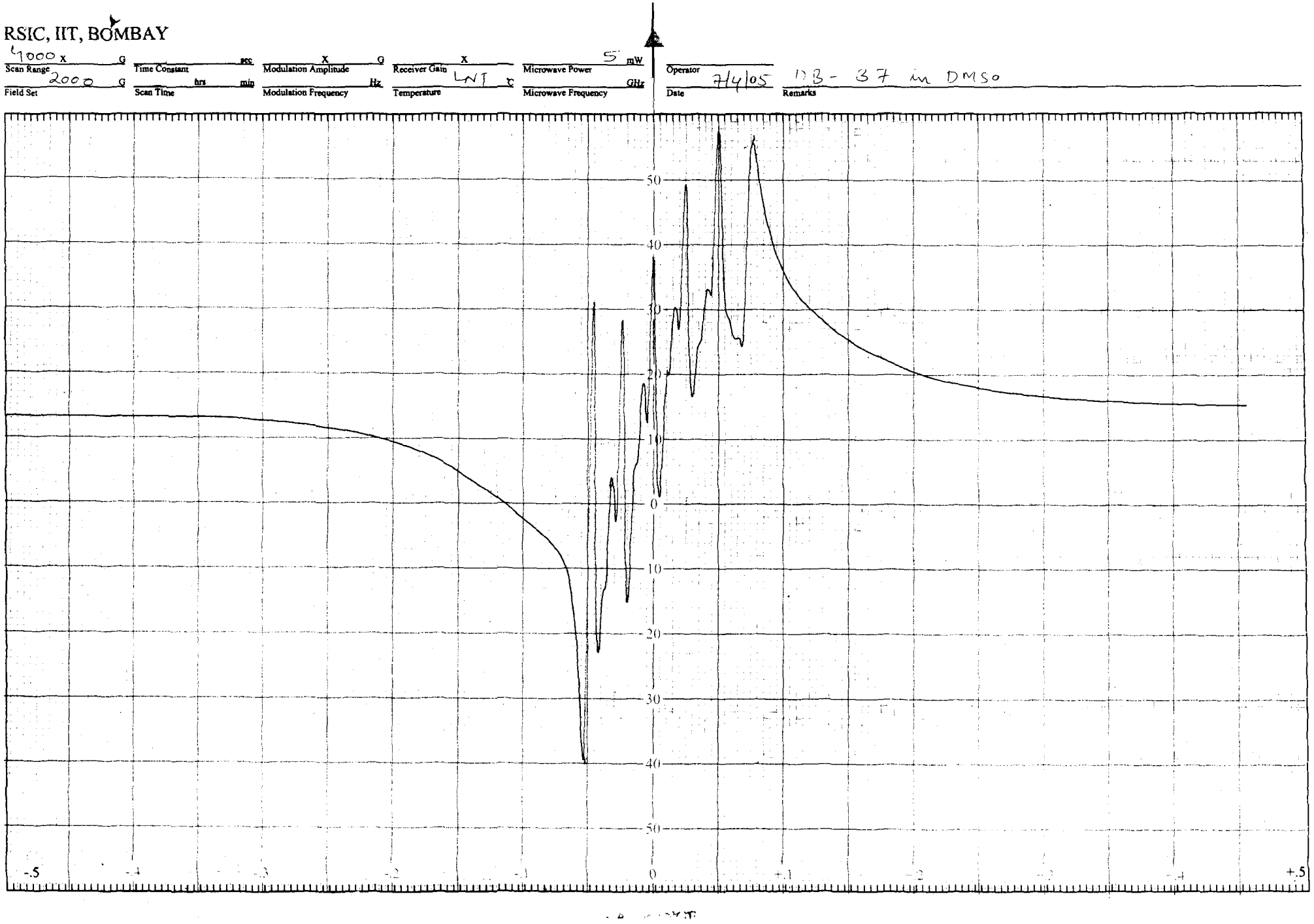

Fig. 6.2.2 (b) EPR spectrum of complex $[Mn^{IV}Ru^{II}(slah)(2\text{-pic})_3Cl]Cl.3H_2O$ **(38)** in DMSO solution at Temperature: LNT, Frequency: 9.1 GHz, Scan range: 4000 G and Field Set: 2000 G

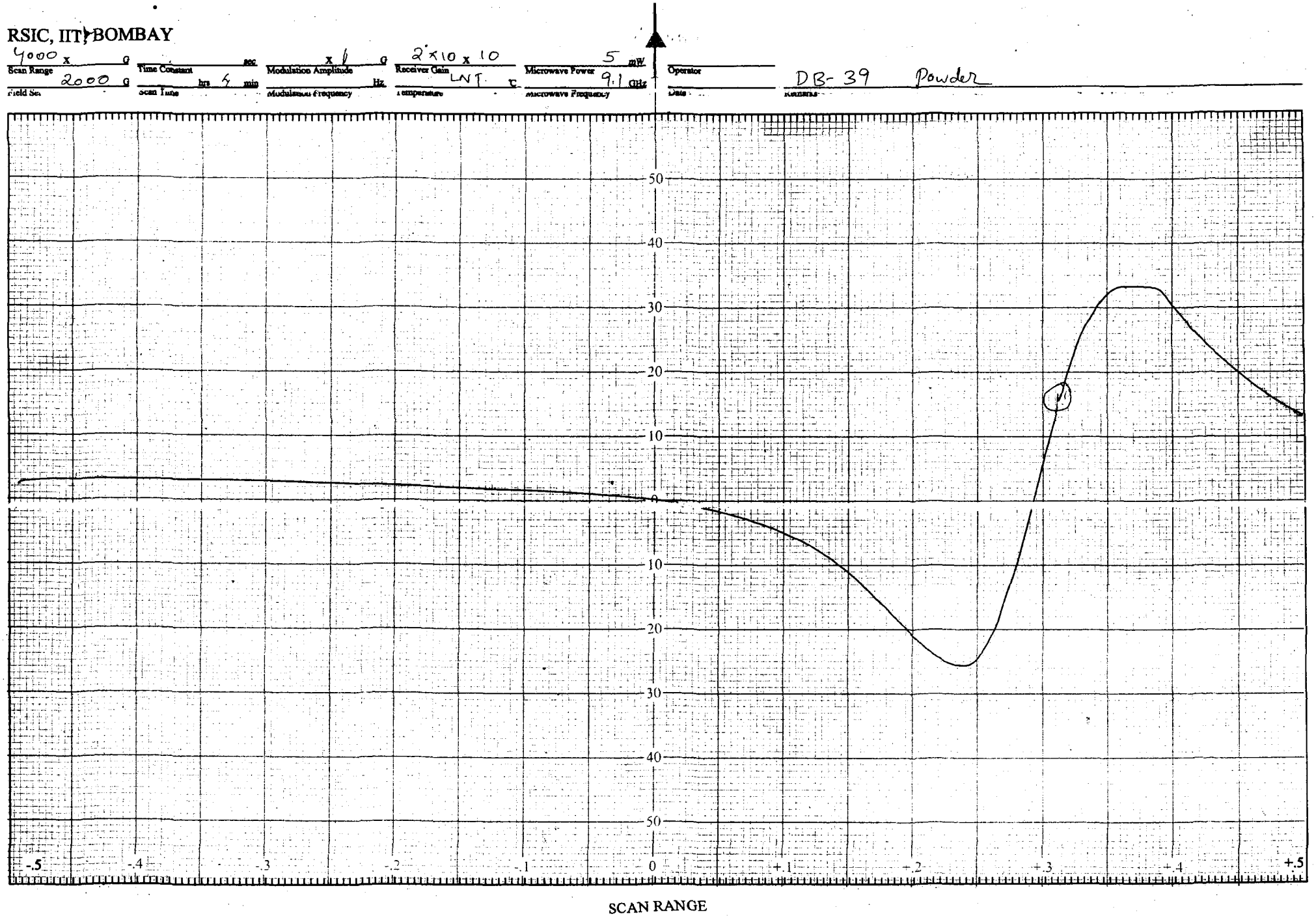

Fig. 6.2.3 (a) EPR powder spectrum of complex: $[Mn^{IV}Ru^{II}(slah)(4\text{-}pic)_3Cl]Cl.3H_2O$ **(40)** at Temperature: LNT, Frequency: 9.1 GHz, Scan range: 4000 G and Field Set: 2000 G

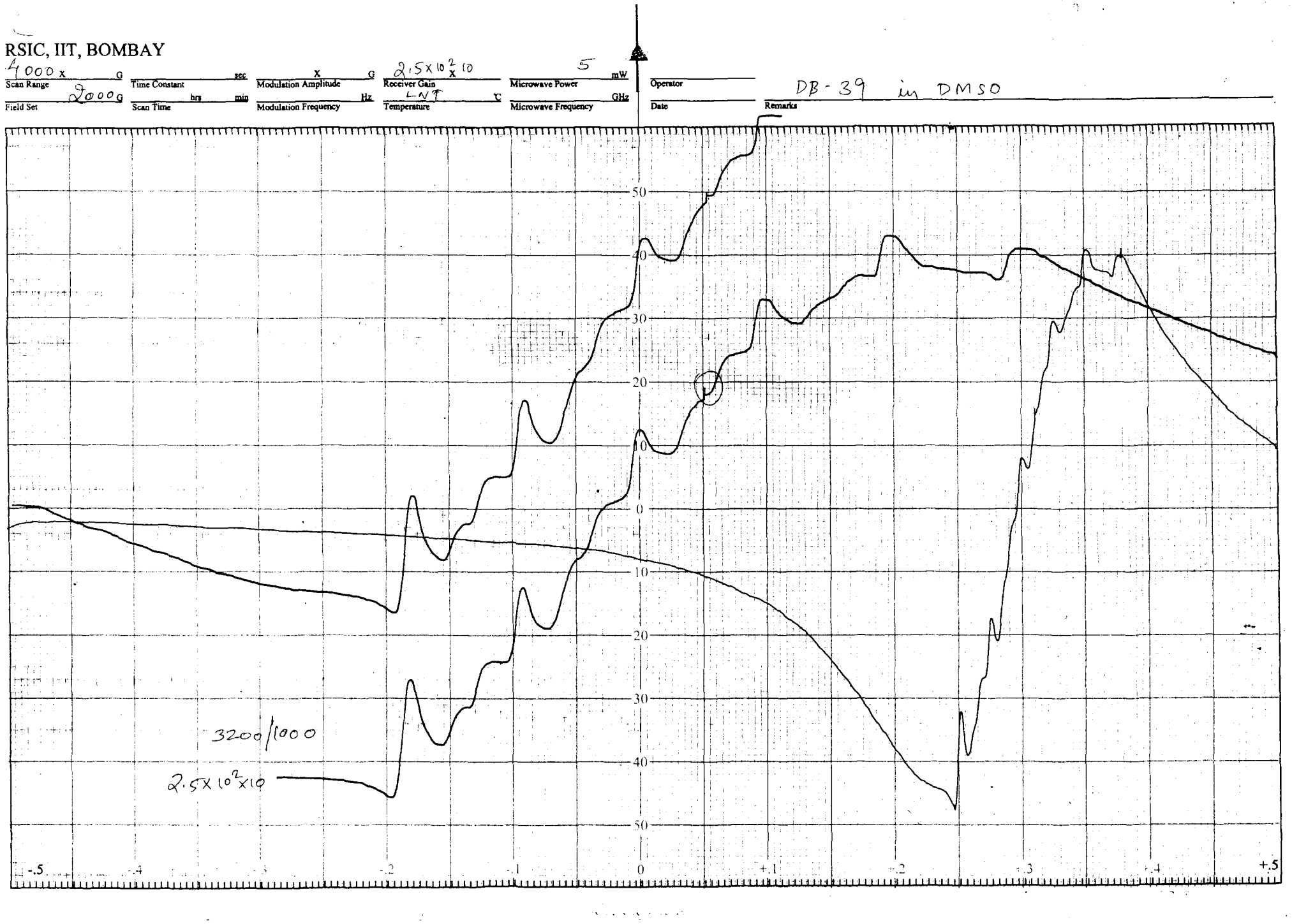

Fig. 6.2.3 (b) EPR spectrum of complex $[Mn^{IV}Ru^{II}(slah)(4\text{-pic})_3Cl]Cl.3H_2O$ **(40)** in DMSO solution at Temperature: LNT, Frequency: 9.1 GHz, Scan range: **4000 G**
Field set : 2000 G

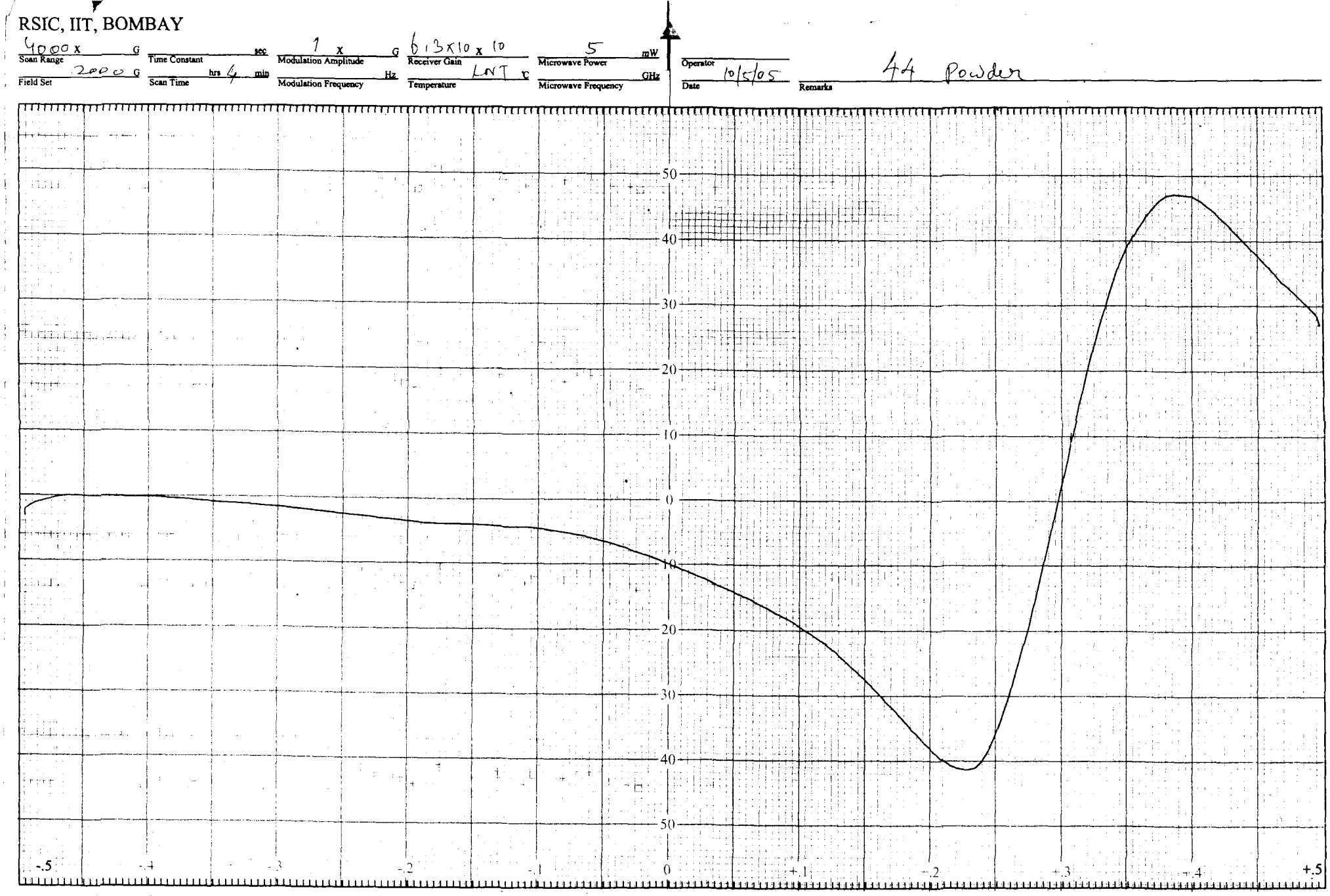

Fig. 6.2.4 EPR powder spectrum of complex $[Mn^{IV}Ru^{II}(npah)(H_2O)_3Cl]Cl$ **(41)** at Temperature: LNT, Frequency: 9.1 GHz, Scan range: 4000 G and Field Set: 2000 G

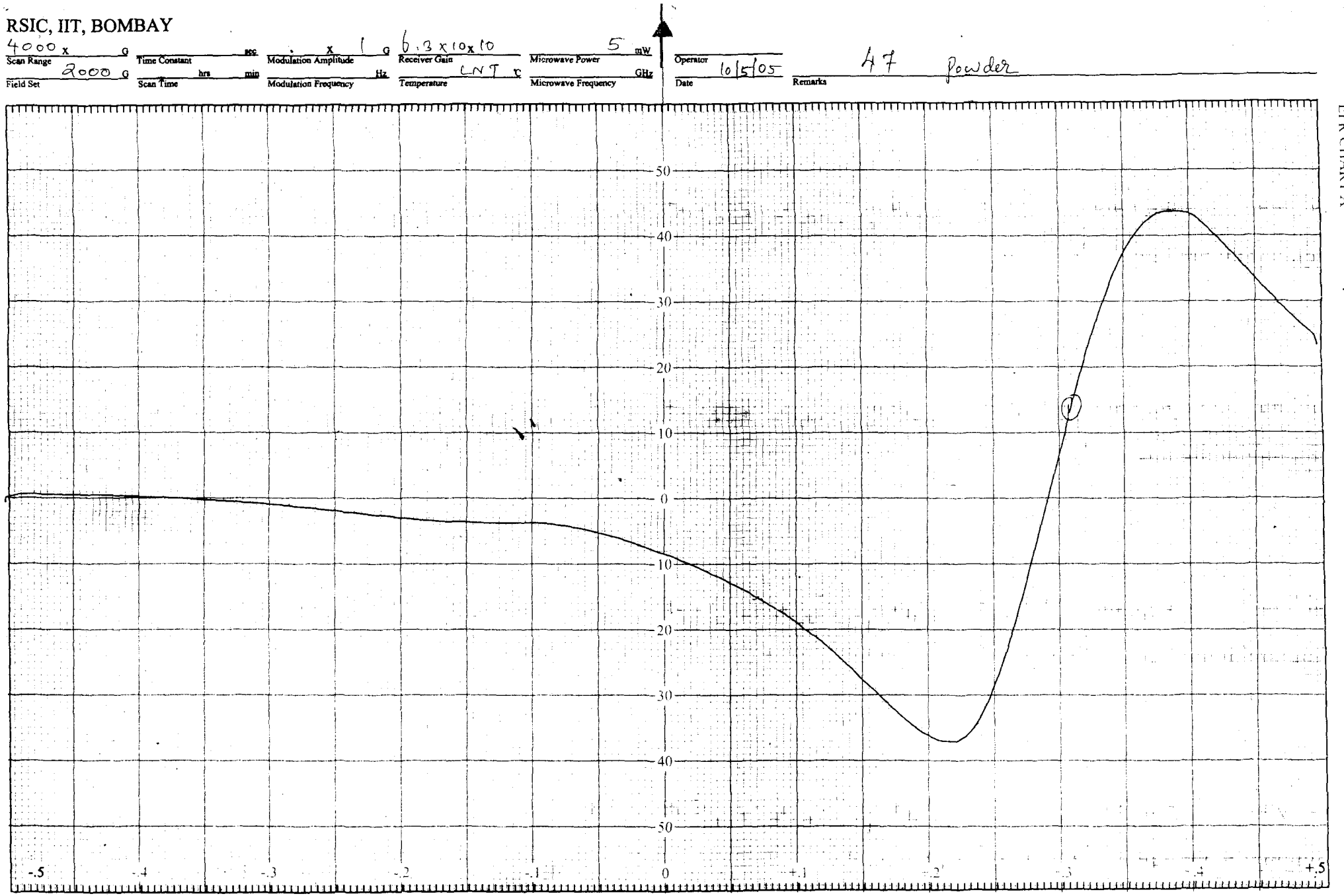

Fig. 6.2.5 EPR powder spectrum of complex $[Mn^{IV}Ru^{II}(npah)(3\text{-pic})_3Cl]Cl.3H_2O$ **(44)** at Temperature: LNT, Frequency: 9.1 GHz, Scan range: 4000 G and Field Set: 2000 G

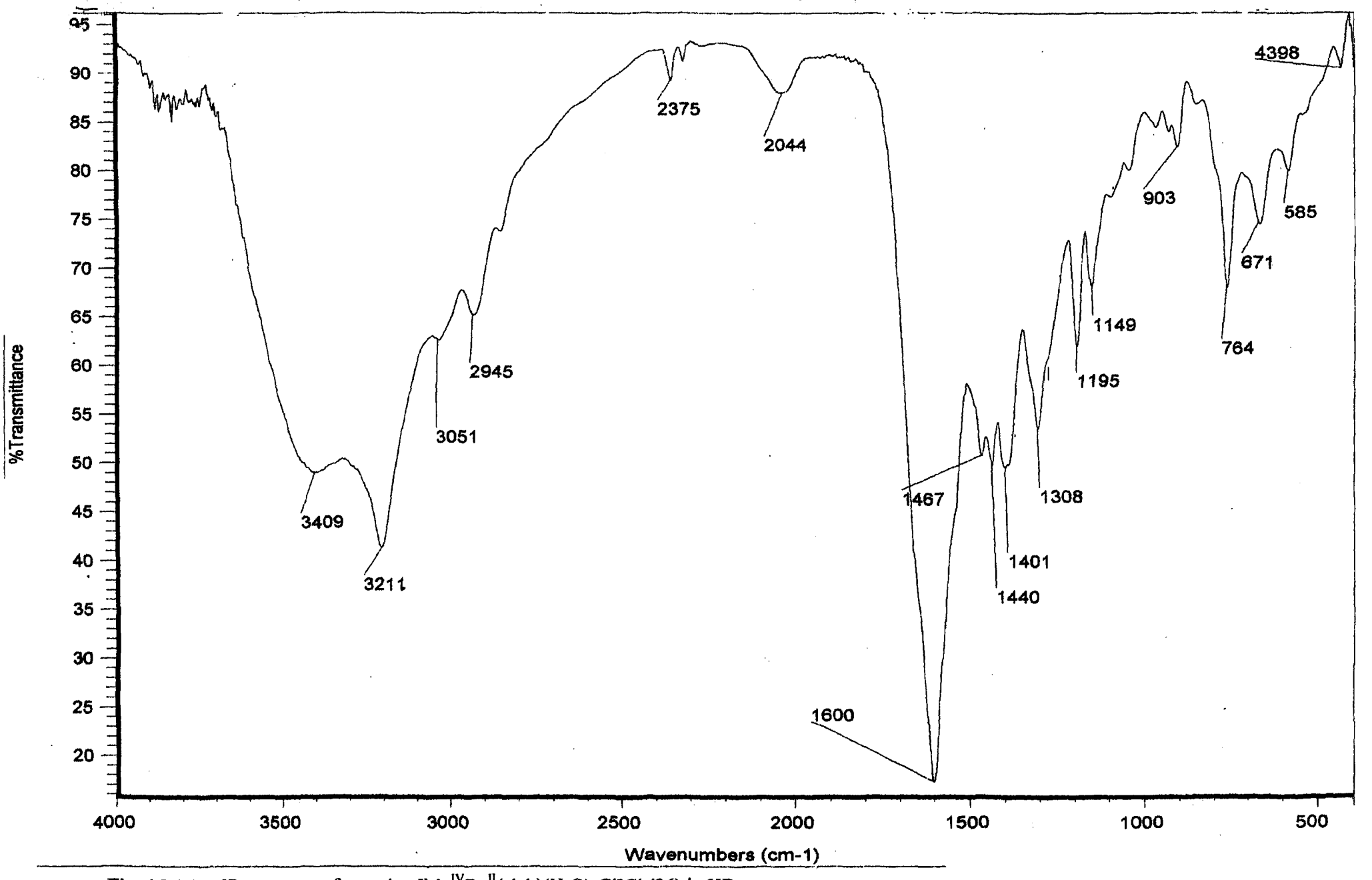

Fig. 6.3.1 (a) IR spectrum of complex $[Mn^{IV}Ru^{II}(slah)(H_2O)_3Cl]Cl$ **(36)** in KBr

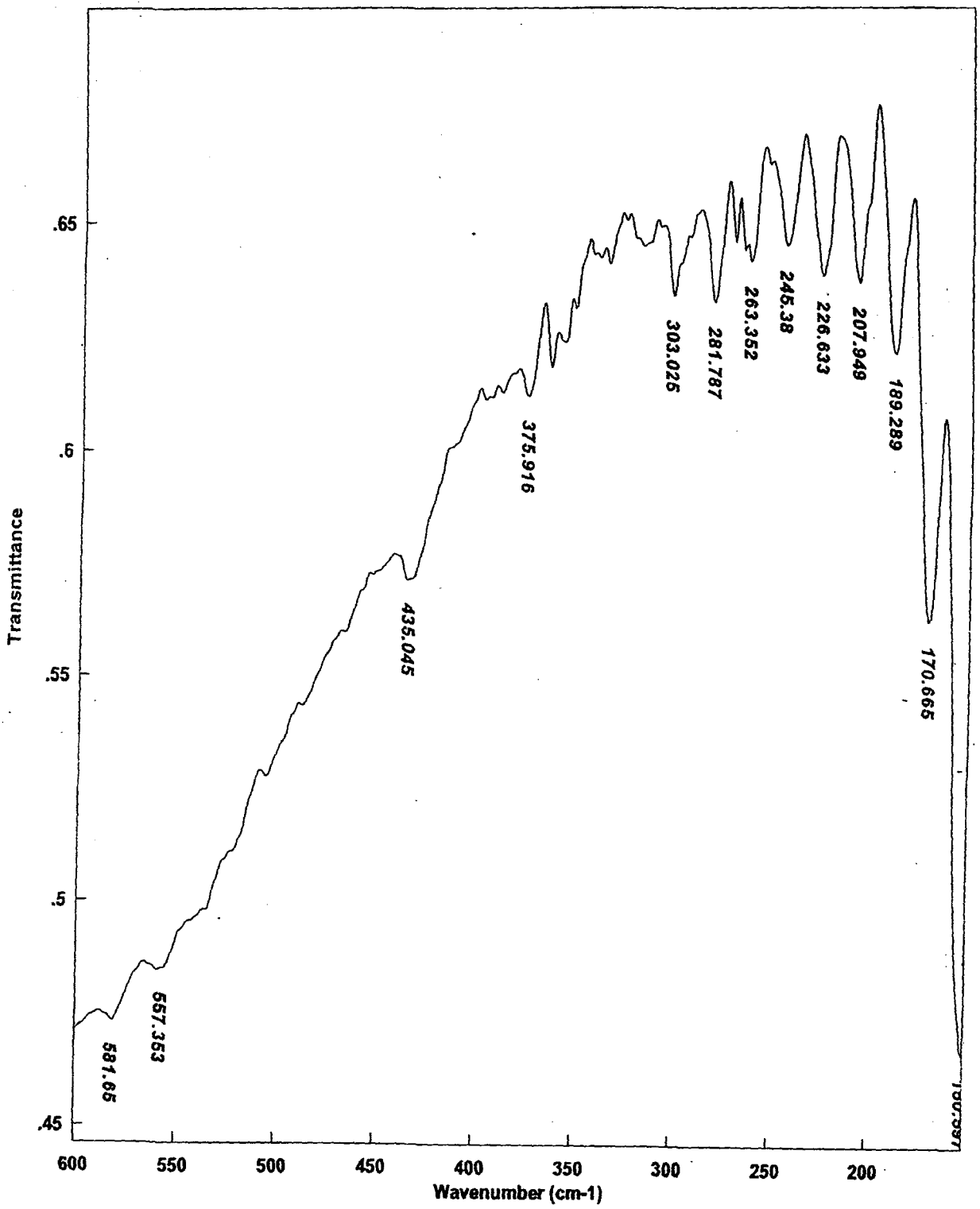

Fig. 6.3.1 (b) IR spectrum of complex $[Mn^{IV}Ru^{II}(slah)(H_2O)_3Cl]Cl$ **(36)** in CsI

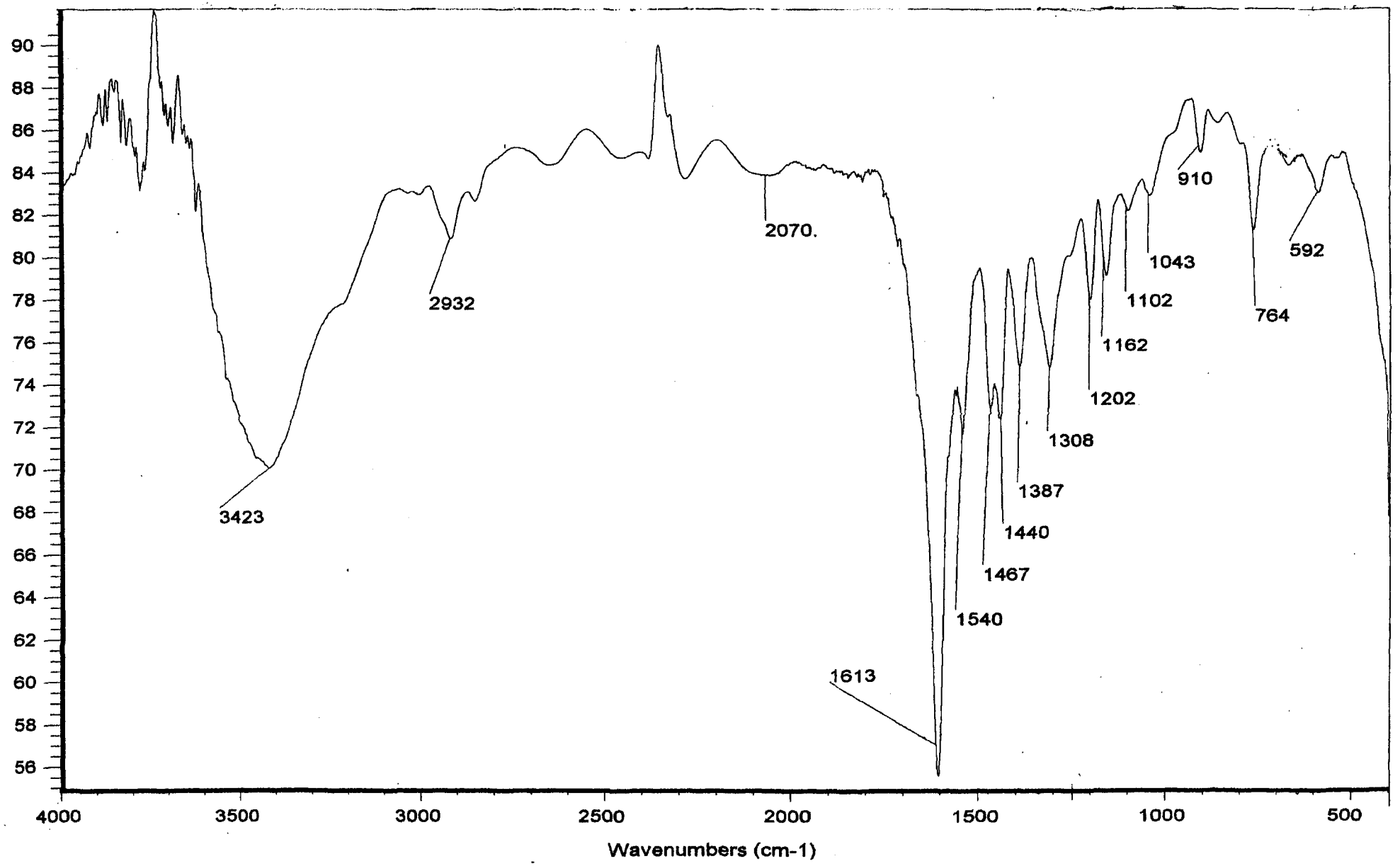

Fig. 6.3.2 (a) IR spectrum of complex $[Mn^{IV}Ru^{II}(slah)(py)_3Cl]Cl$ **(37)** in KBr

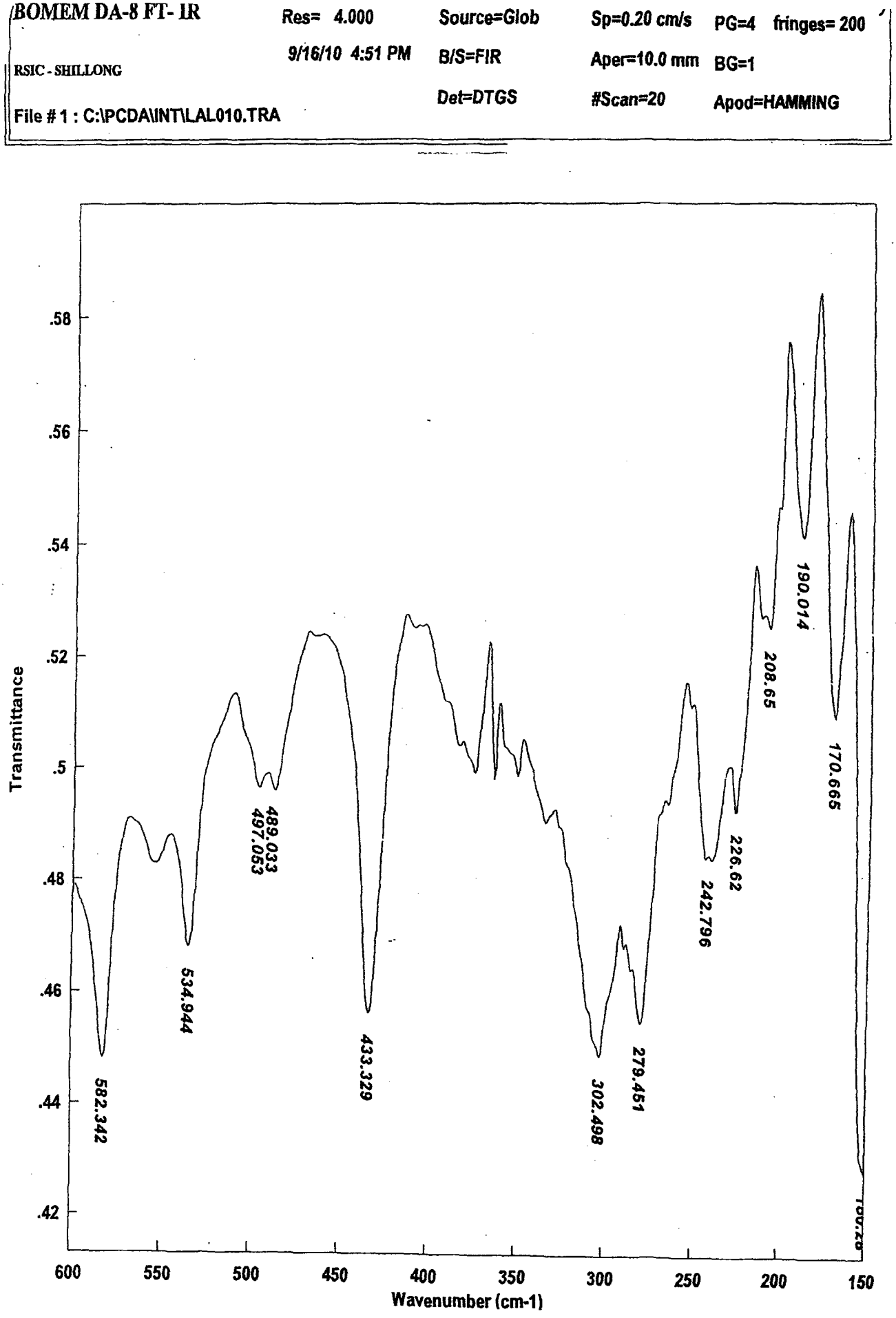

Fig. 6.3.2 (b) IR spectrum of complex $[Mn^{IV}Ru^{II}(slah)(py)_3Cl]Cl$ **(37)** in CsI

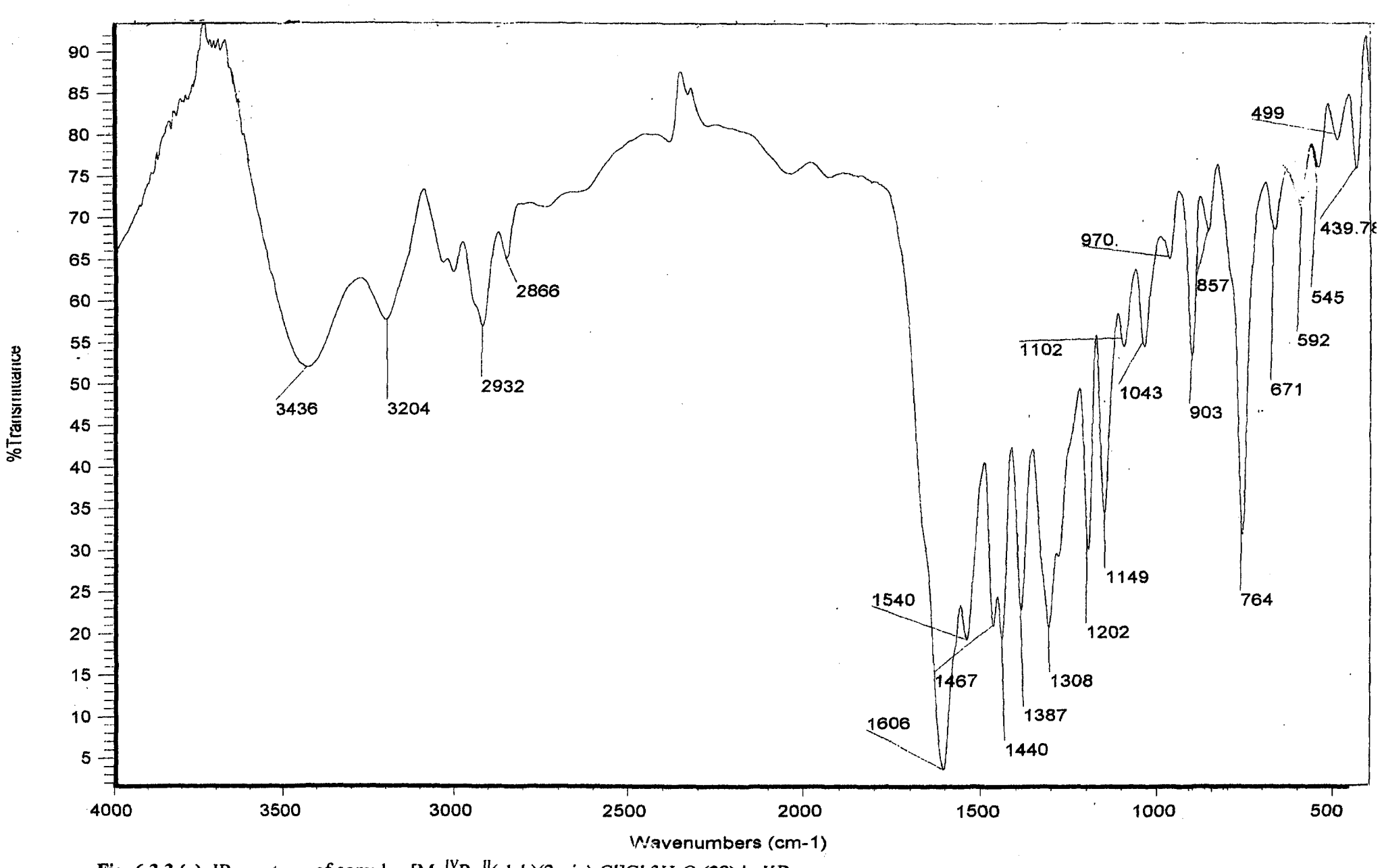

Fig. 6.3.3 (a) IR spectrum of complex $[Mn^{IV}Ru^{II}(slah)(2\text{-pic})_3Cl]Cl.3H_2O$ **(38)** in KBr

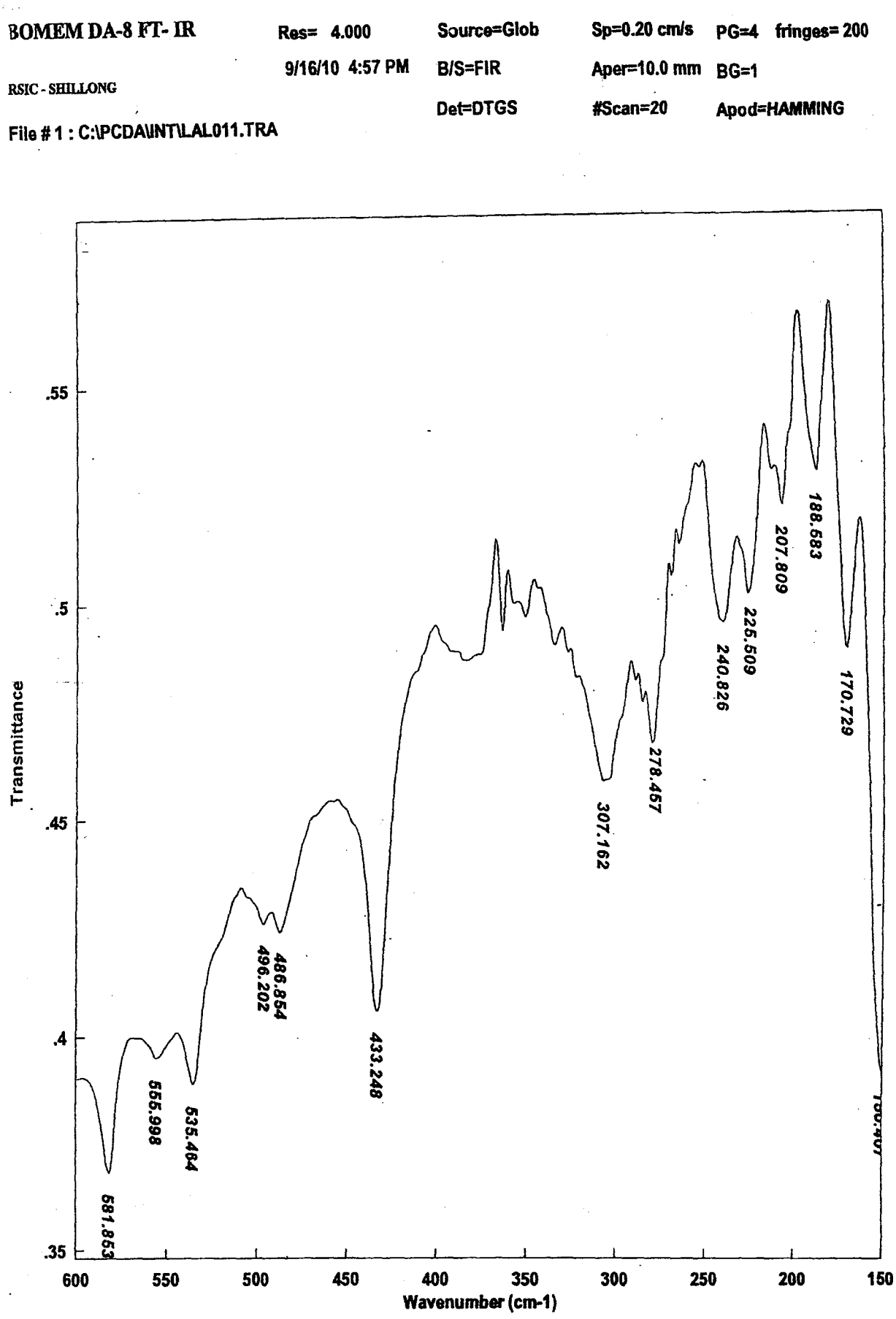

Fig. 6.3.3 (b) IR spectrum of complex $[Mn^{IV}Ru^{II}(slah)(2\text{-pic})_3Cl]Cl.3H_2O$ **(38)** in CsI

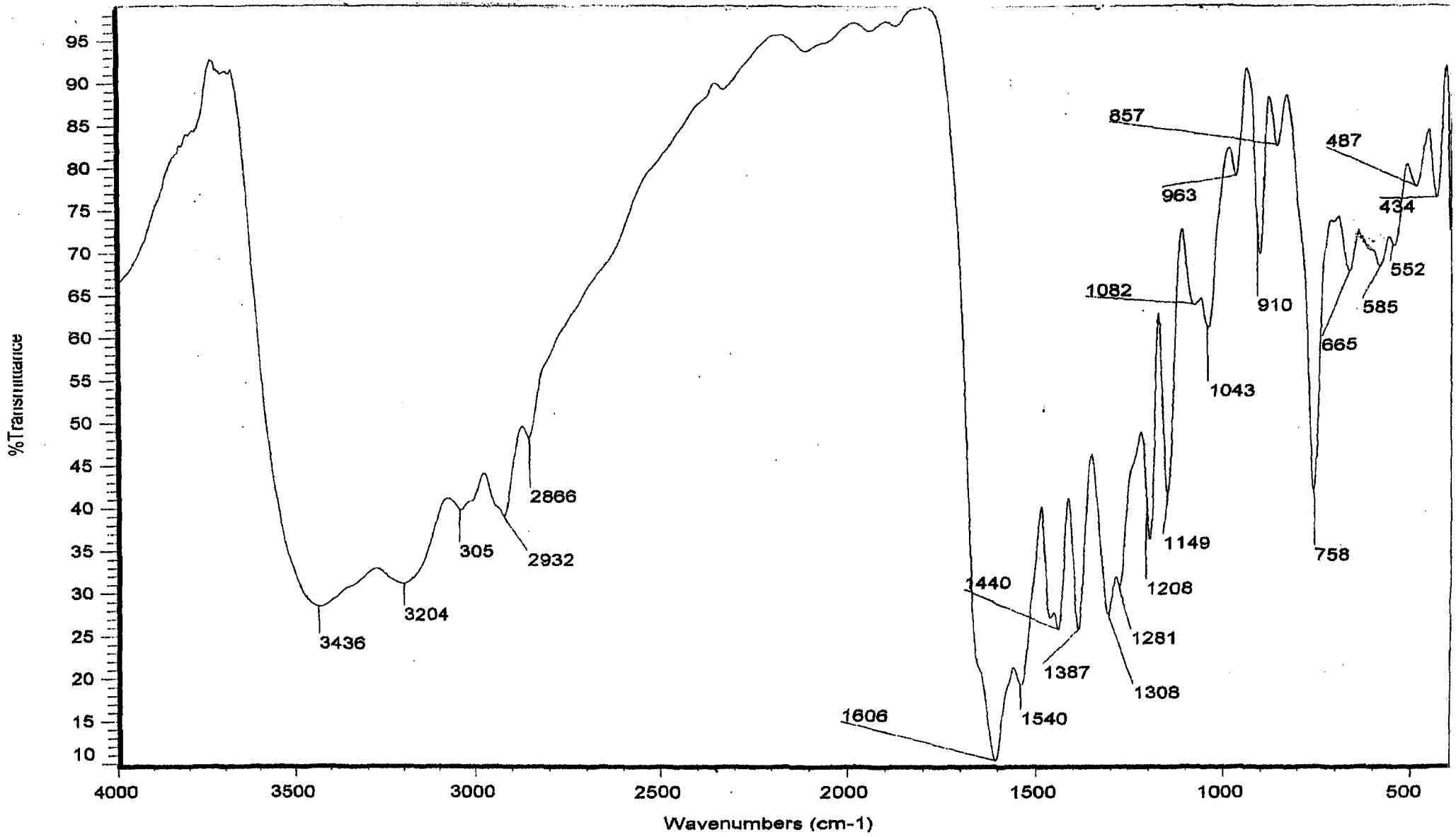

Fig. 6.3.4 (a) IR spectrum of complex $[Mn^{IV}Ru^{II}(slah)(4\text{-pic})_3Cl]Cl.3H_2O$ **(40)** in KBr

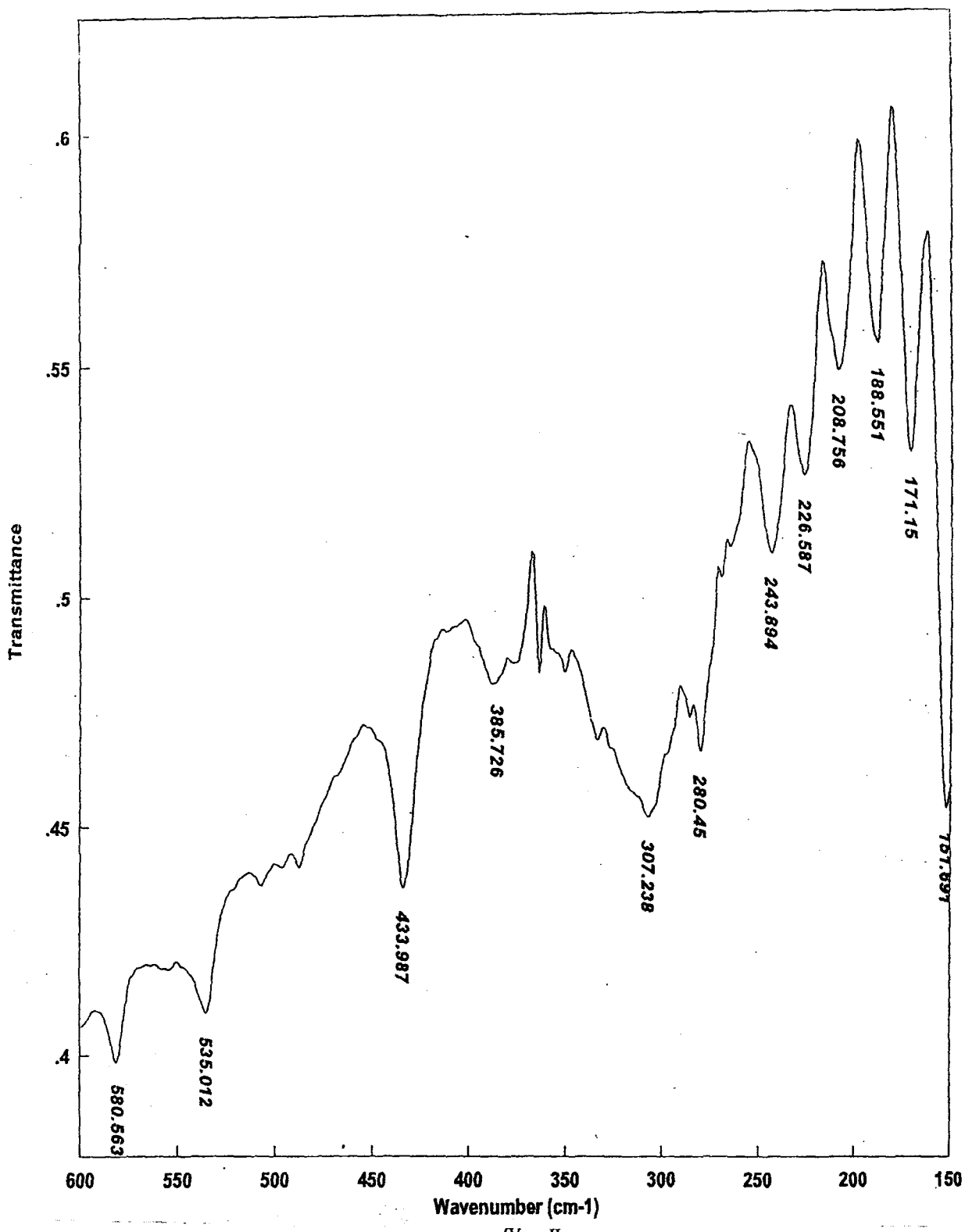

Fig. 6.3.4 (b) IR spectrum of complex $[Mn^{IV}Ru^{II}(slah)(4\text{-pic})_3Cl]Cl.3H_2O$ **(40)** in CsI

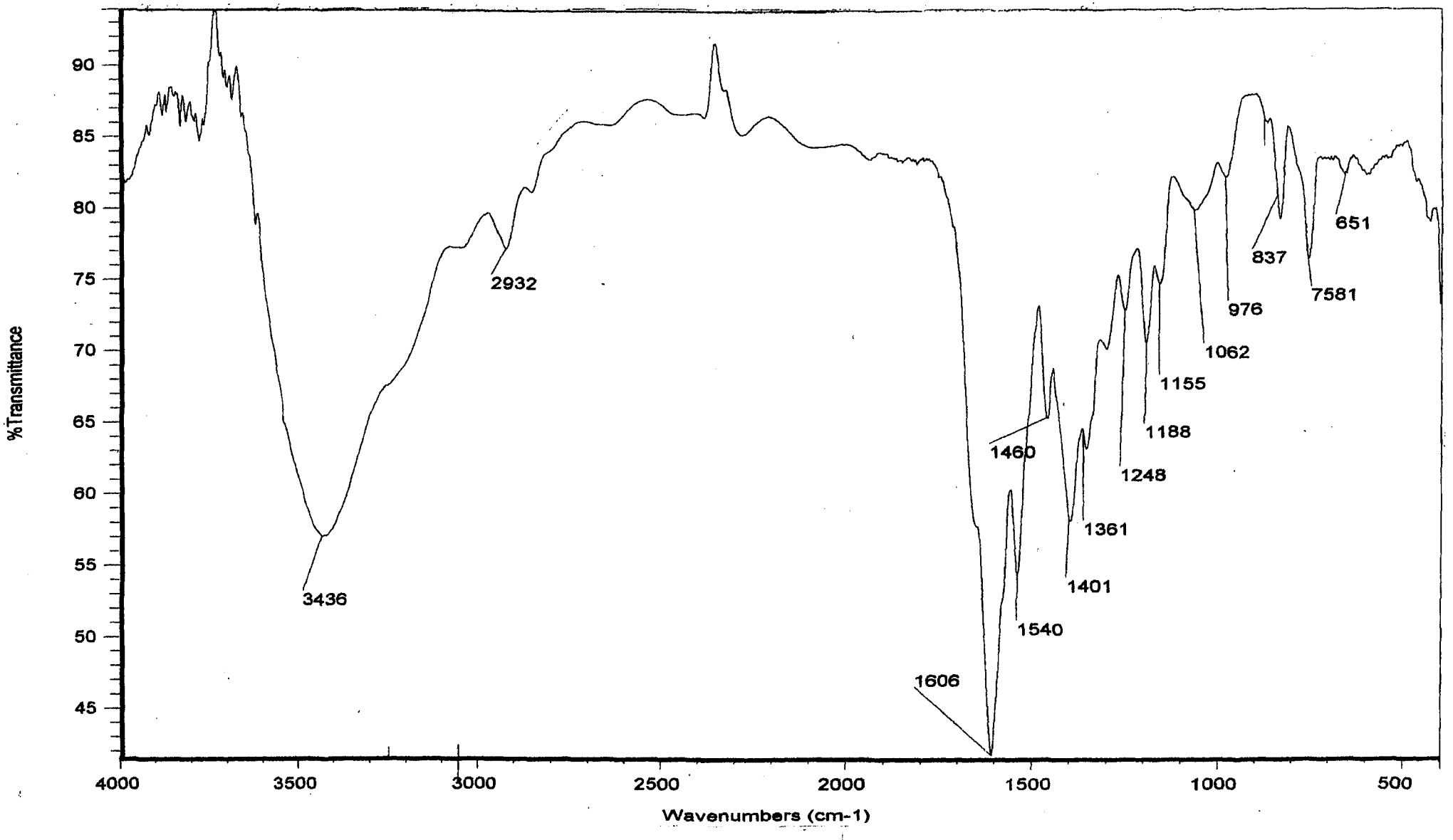

Fig. 6.3.5 IR spectrum of complex $[Mn^{IV}Ru^{II}(npah)(H_2O)_3Cl]Cl$ **(41)** in KBr

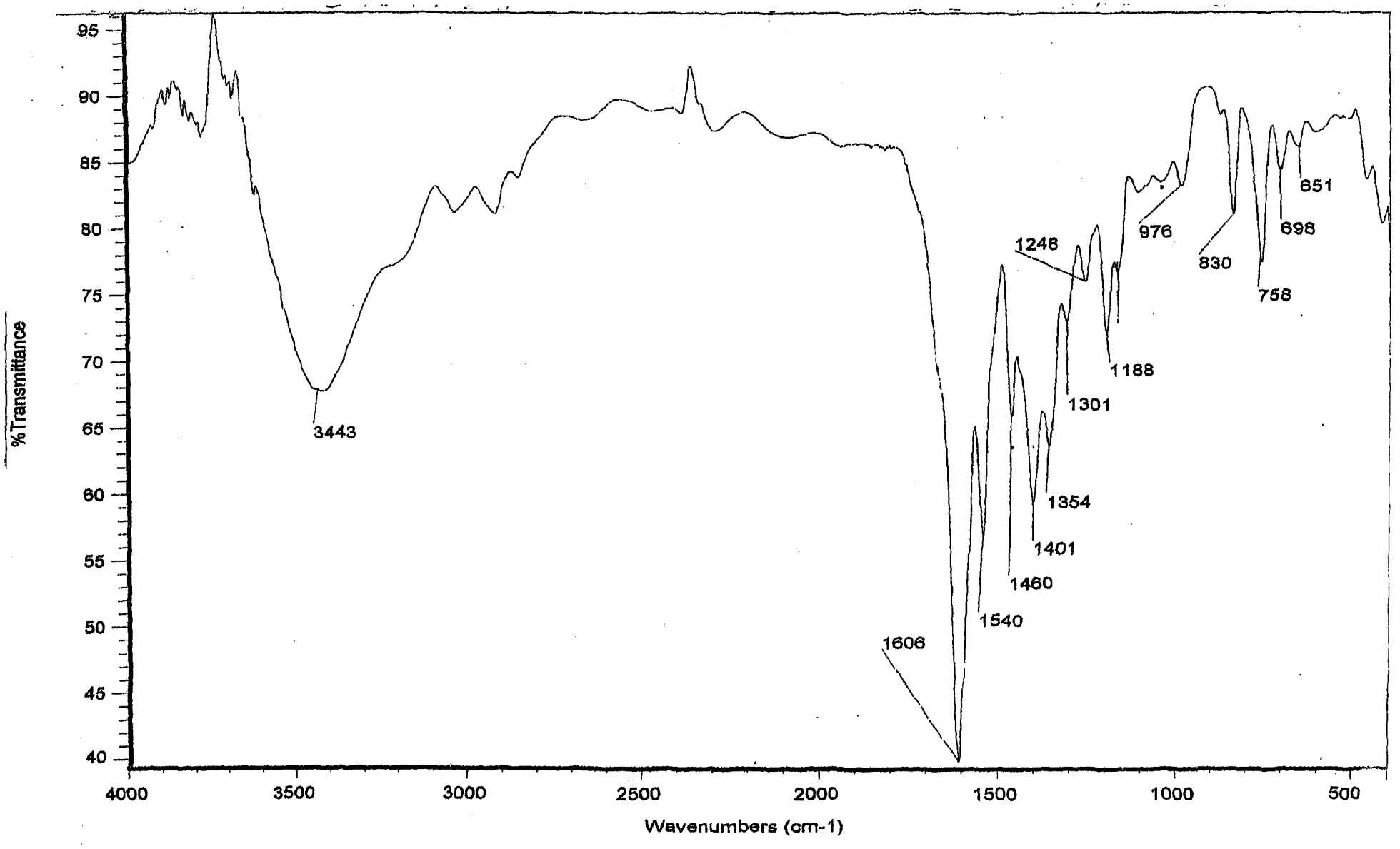

Fig. 6.3.6 IR spectrum of complex $[Mn^{IV}Ru^{II}(npah)(py)_3Cl]Cl$ **(42)**

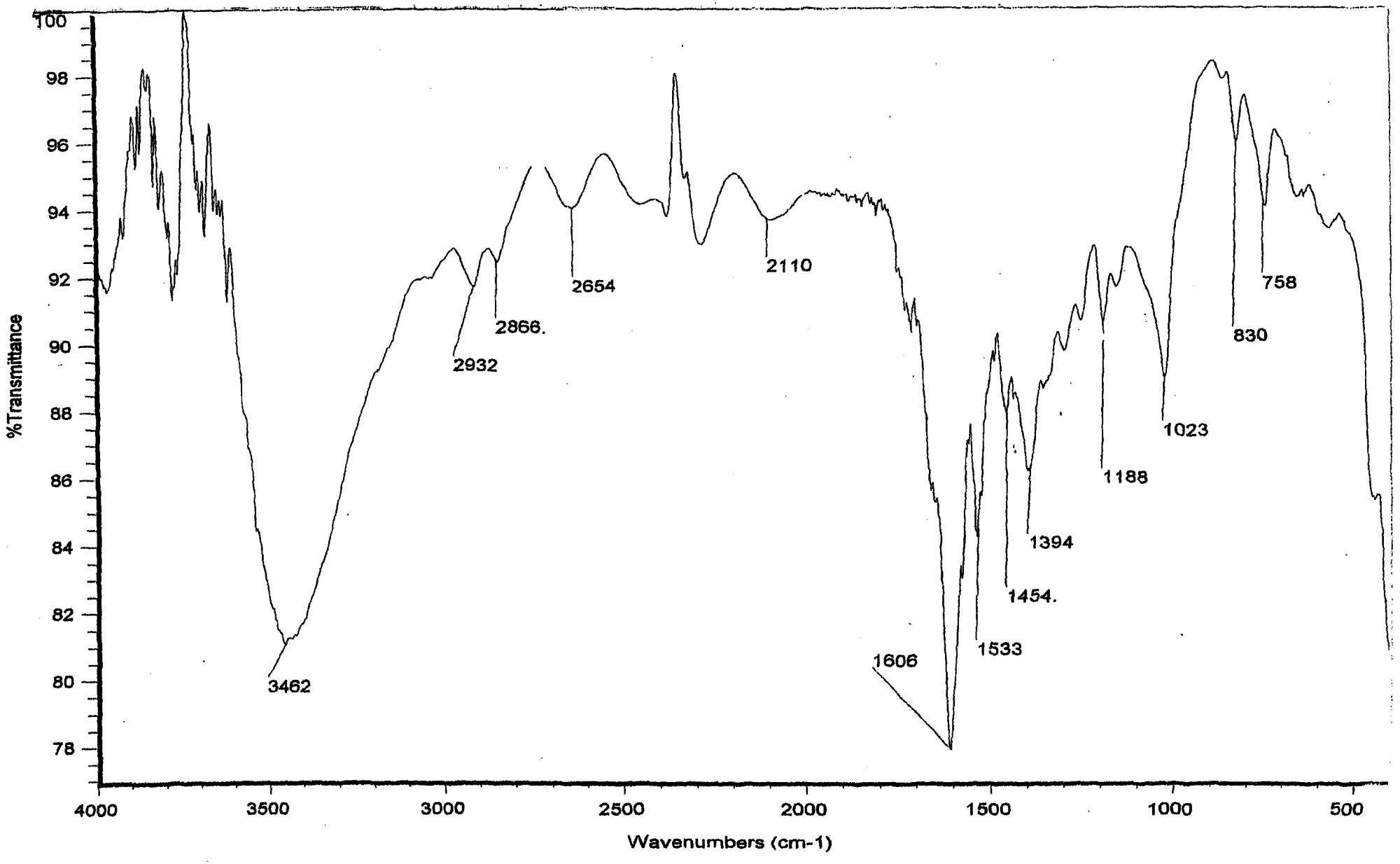

Fig. 6.3.7 IR spectrum of complex $[Mn^{IV}Ru^{II}(npah)(2\text{-}pic)_3Cl]Cl$ **(43)** in KBr

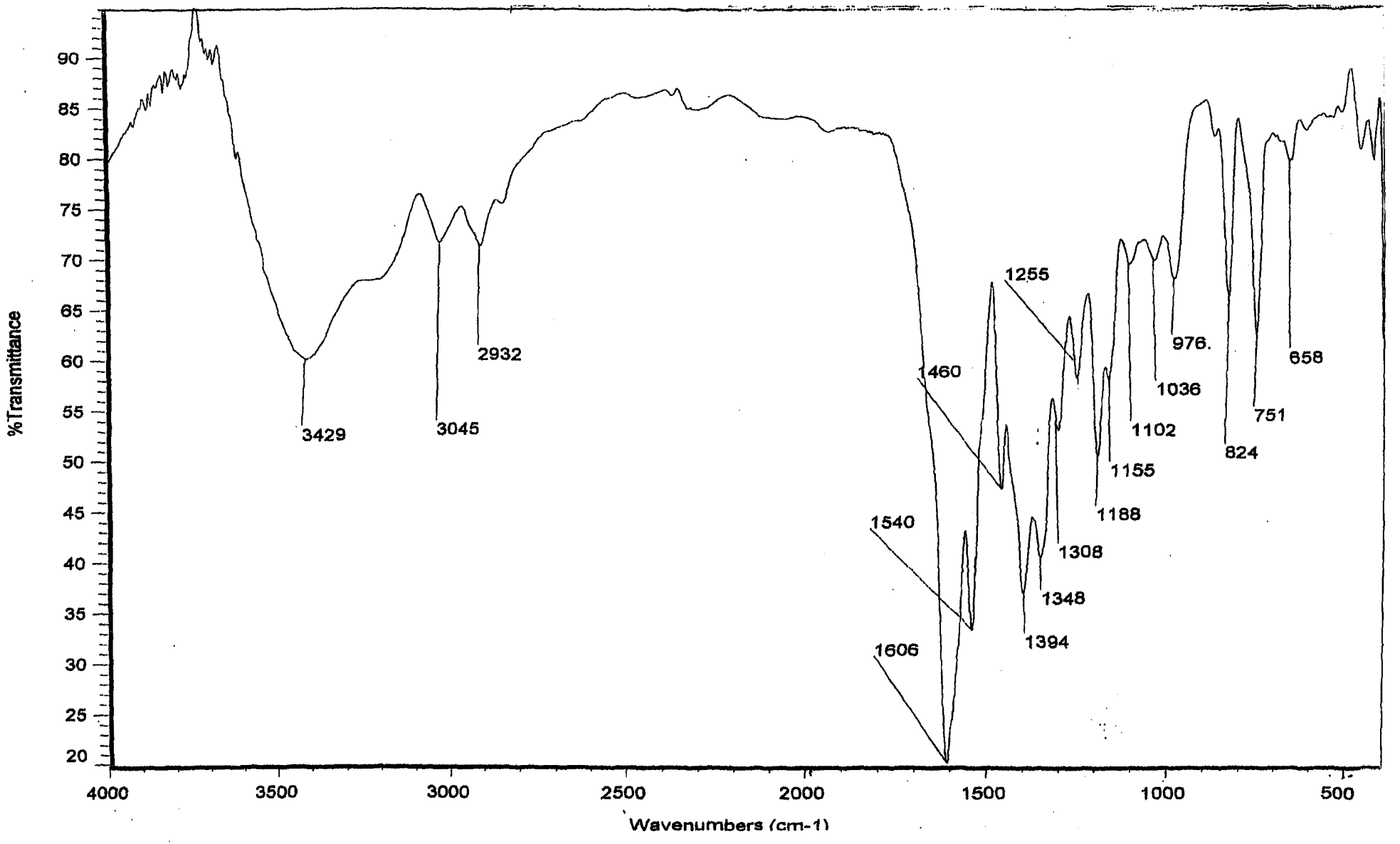

Fig. 6.3.8 IR spectrum of complex $[Mn^{IV}Ru^{II}(npah)(4\text{-pic})_3Cl]Cl$ **(45)** in KBr

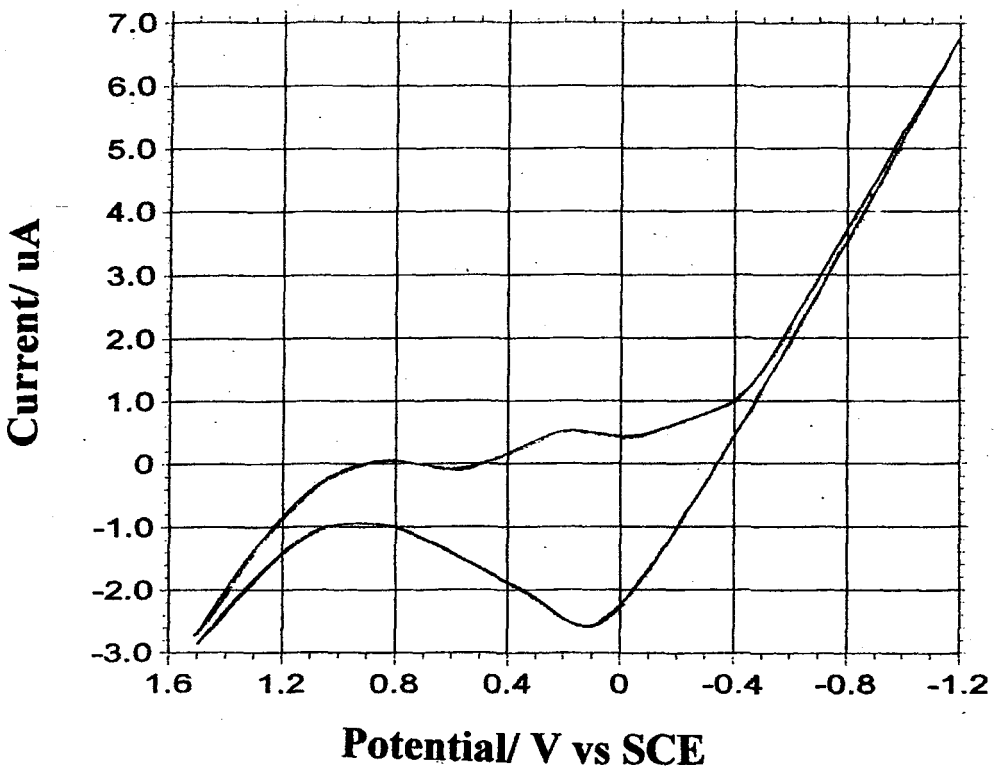

Fig. 6.4.1 Cyclic voltammogram of complex $[Mn^{IV}Ru^{II}(slah)(3\text{-}pic)_3Cl]Cl.3H_2O$ **(39)**

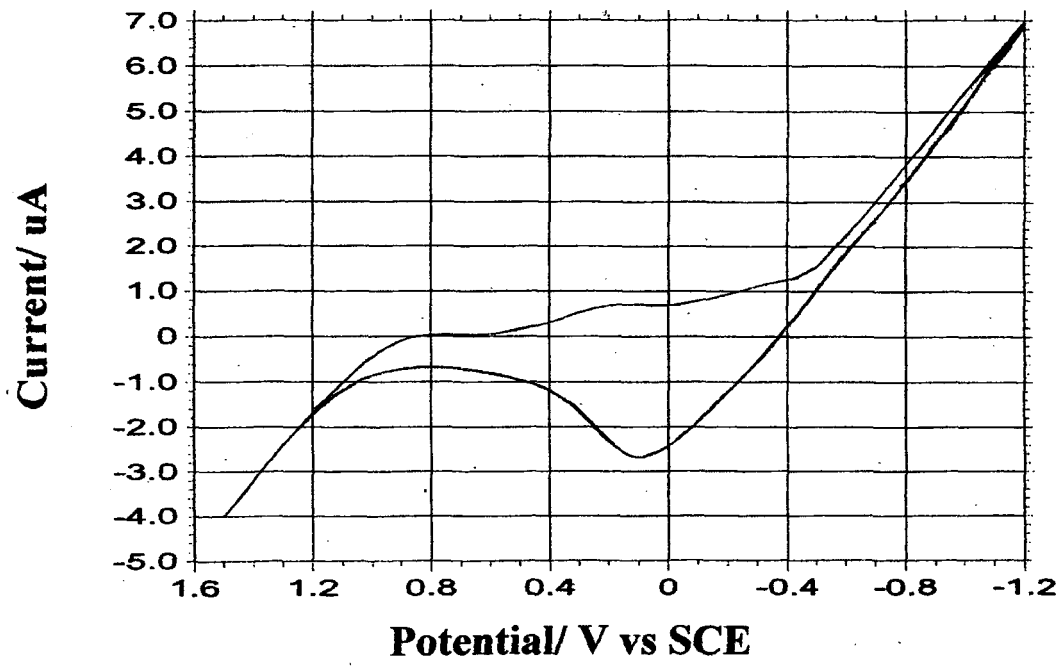

Fig. 6.4.2 Cyclic voltammogram of complex $[Mn^{IV}Ru^{II}(slah)(4\text{-}pic)_3Cl]Cl.3H_2O$ **(40)**

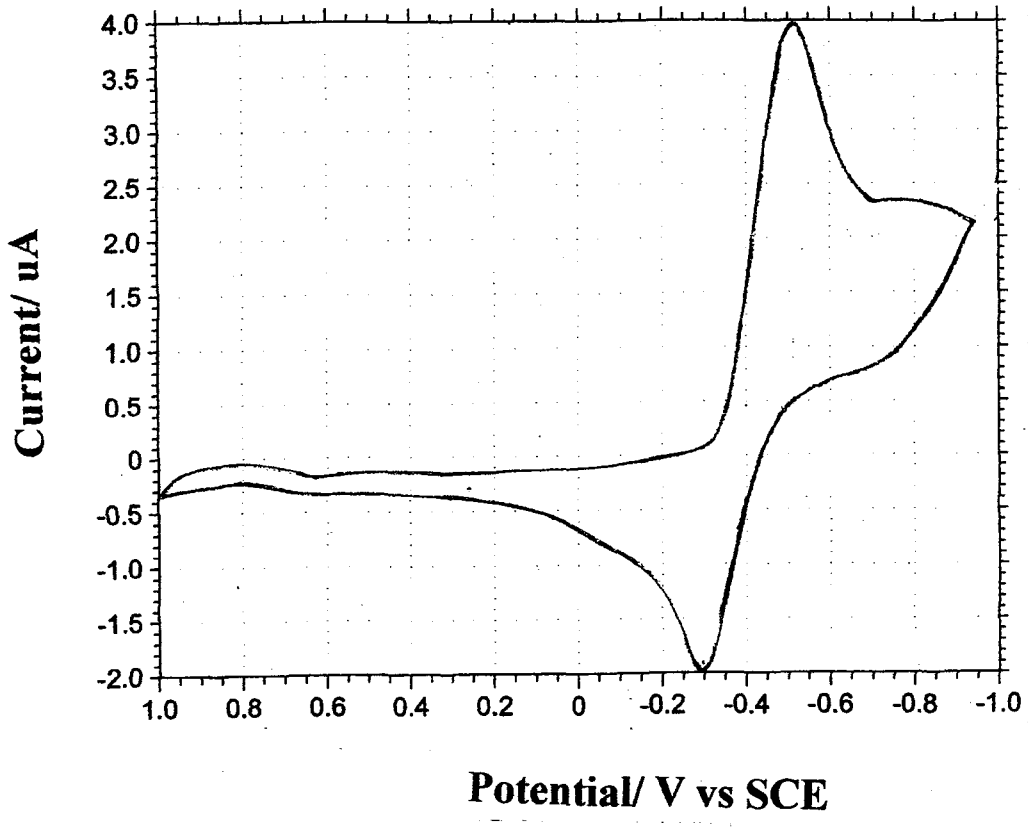

Fig. 6.4.3 Cyclic voltammogram of complex $[Mn^{IV}Ru^{II}(npah)(py)_3Cl]Cl$ **(42)**

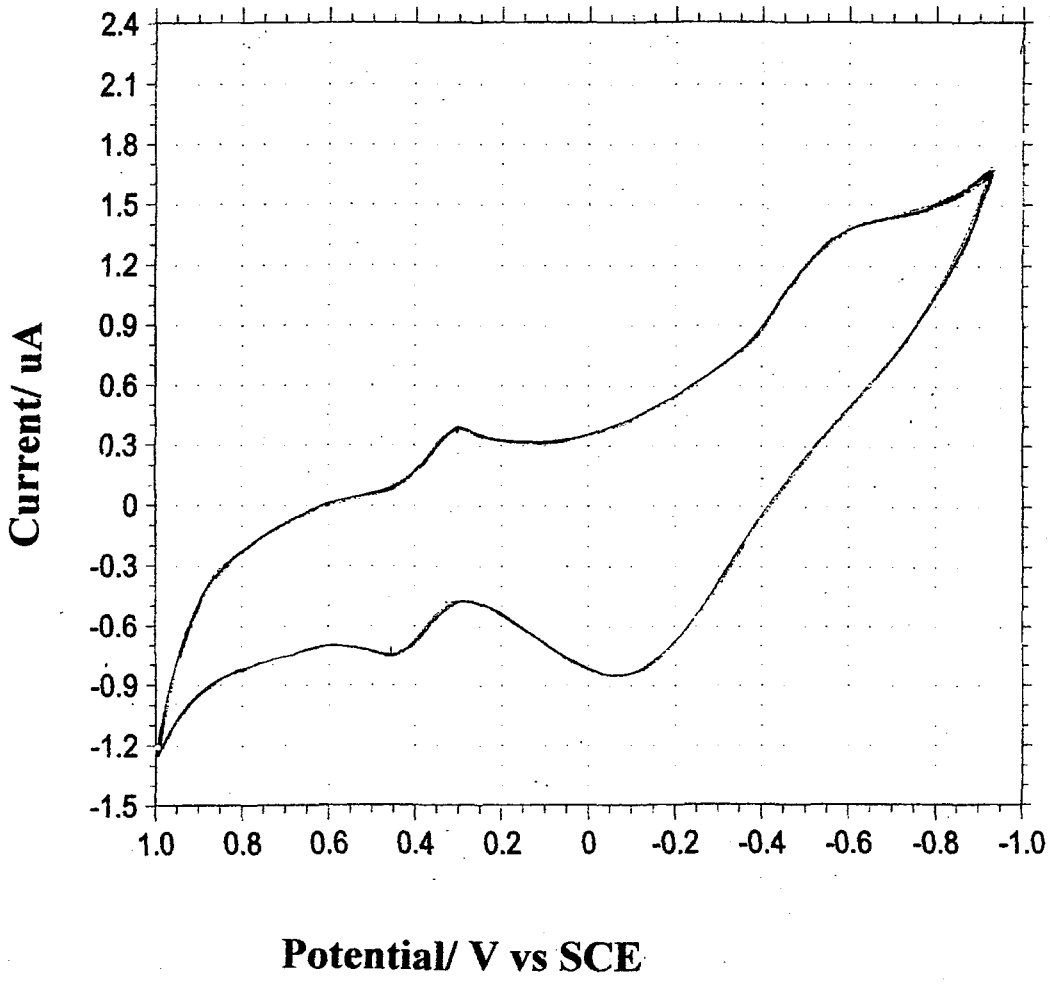

Fig. 6.4.4 Cyclic voltammogram of complex $[Mn^{IV}Ru^{II}(npah)(3\text{-}pic)_3Cl]Cl.3H_2O$ **(44)**

Table 6.1: Colour, Decomposition Point, Analytical, Magnetic Moment and Molar Conductance Data for Heterobimetallic Complexes of Disalicylaldehyde adipoyldihydrazone ($slahH_4$) and Bis(2-hydroxy-1-naphthaldehyde)adipoyldihydrazone ($npahH_4$)

Sl. No	Complex	Colour	D.P (°C)	Analysis:Found(Calcd)%						Molar Conductance Λ_m ($ohm^{-1}\ cm^2\ mol^{-1}$)	μ_B (B.M)
				C	H	N	Mn	Ru	Cl		
36.	$[Mn^{IV}Ru^{II}(slah)(H_2O)_3Cl]Cl$	Brown	> 300	35.915 (36.418)	3.70 (3.642)	8.473 (8.498)	7.959 (8.346)	16.049 (15.320)	11.055 (10.774)	35.5	3.93
37.	$[Mn^{IV}Ru^{II}(slah)(py)_3Cl]Cl$	Dull-green	> 300	50.011 (49.880)	4.011 (3.919)	11.550 (11.639)	6.506 (6.532)	11.897 (11.995)	8.437 (8.432)	30.7	4.12
38.	$[Mn^{IV}Ru^{II}(slah)(2\text{-}pic)_3Cl]Cl.3H_2O$	Muddy-brown	> 300	48.057 (47.303)	4.529 (4.668)	10.150 (10.166)	5.783 (5.705)	10.480 (10.477)	7.355 (7.365)	31.8	3.89
39.	$[Mn^{IV}Ru^{II}(slah)(3\text{-}pic)_3Cl]Cl.3H_2O$	Muddy-brown	> 300	47.980 48.614)	4.340 (4.371)	10.438 (10.448)	5.841 (5.864)	10.710 (10.770)	7.621 (7.569)	29.7	3.02
40.	$[Mn^{IV}Ru^{II}(slah)(4\text{-}pic)_3Cl]Cl.3H_2O$	Dull-brown	> 300	47.513 (48.614)	4.351 (4.371)	10.394 (10.448)	5.821 (5.864)	10.680 (10.770)	7.600 (7.569)	32.5	3.95

41. $[Mn^{IV}Ru^{II}(npah)(H_2O)_3Cl]Cl$	Brownish-green	> 300	44.637 (44.037)	4.600 (4.104)	11.973 (12.844)	7.259 (7.208)	13.120 (13.237)	9.850 (9.305)	34.7	4.02
42. $[Mn^{IV}Ru^{II}(npah)(py)_3Cl]Cl$	Yellowish-green	> 300	54.015 (54.455)	4.011 (4.334)	11.551 (11.359)	5.850 (5.814)	10.187 (10.677)	8.037 (7.505)	30.8	3.92
43. $[Mn^{IV}Ru^{II}(npah)(2\text{-}pic)_3Cl]Cl$	Brownish-green	> 300	55.570 (55.870)	4.729 (4.757)	10.201 (9.919)	5.631 (5.567)	10.401 (10.223)	7.251 (7.186)	33.4	4.12
44. $[Mn^{IV}Ru^{II}(npah)(3\text{-}pic)_3Cl]Cl.3H_2O$	Blackish-green	> 300	56.981 (52.672)	5.401 (5.057)	10.431 (9.351)	5.341 (5.248)	10.110 (9.637)	7.021 (6.775)	32.4	3.95
45. $[Mn^{IV}Ru^{II}(npah)(4\text{-}pic)_3Cl]Cl$	Green	> 300	55.731 (55.870)	4.551 (4.757)	10.391 (9.919)	5.821 (5.567)	10.681 (10.223)	7.101 (7.186)	31.8	3.89

Table 6.2: Important Electronic Spectral Bands and EPR data of Ligands Disalicylaldehyde adipoyldihydrazone and Bis(2-hydroxy-1-naphthaldehyde)adipoyldihydrazone and their heterobimetallic complexes

Sl. No	Ligand/Complex	λ_{max}(nm) (ϵ_{max} dm^3 mol^{-1} cm^{-1}) for conc 10^{-2} M soln				Temp	solid/ soln	Magnetic parameter Mn(IV) g-values	A_{Mn} (G)
	$slahH_4$	320(2808)							
	$npahH_4$	363(1852)							
36.	$[Mn^{IV}Ru^{II}(slah)(H_2O)_3Cl]Cl$	370(1130)	387(1139)	439(1577)		LNT LNT	SOLID DMSO	1.912, 4.330 1.994, 4.335	104 96
37.	$[Mn^{IV}Ru^{II}(slah)(py)_3Cl]Cl$	403(3193)	424(4468)						
38.	$[Mn^{IV}Ru^{II}(slah)(2\text{-}pic)_3Cl]Cl.3H_2O$	409 (2465)	447(3676)	462(3285)	581(2282)	LNT LNT	SOLID DMSO	2.045, 4.664 2.100, 4.644	- 96
39.	$[Mn^{IV}Ru^{II}(slah)(3\text{-}pic)_3Cl]Cl.3H_2O$	376 (2228)	407(1363)	430(1000)	480(900)	LNT LNT	SOLID DMSO	2.0318, 4.664 2.0318, 4.664	- -
40.	$[Mn^{IV}Ru^{II}(slah)(4\text{-}pic)_3Cl]Cl.3H_2O$	391(2519)	452(3670)	484(4025)	548(2000)	LNT LNT	SOLID DMSO	2.018, 4.644 2.045, 4.664	- 103

41. $[Mn^{IV}Ru^{II}(npah)(H_2O)_3Cl]Cl$	356(2247)	412(2731)	610(300)			LNT LNT	SOLID DMSO	2.064, 5.418 2.001	– 96
42. $[Mn^{IV}Ru^{II}(npah)(py)_3Cl]Cl$	372(7725)	588(1627)							
43. $[Mn^{IV}Ru^{II}(npah)(2\text{-}pic)_3Cl]Cl$	365(4799)	408(5116)	439(7797)	568(1922)					
44. $[Mn^{IV}Ru^{II}(npah)(3\text{-}pic)_3Cl]Cl.3H_2O$	423(7648)	452 (7991)	483(8674)			LNT LNT	SOLID DMSO	2.045, 4.746 2.019	– 96
45. $[Mn^{IV}Ru^{II}(npah)(4\text{-}pic)_3Cl]Cl$	375(3851)	399(3840)	450 (4704)	482(6500)	732(1510)				

Table 6.3:- Structurally Significant Infrared Spectral Bands for Disalicylaldehyde adipoyldihydrazone ($slahH_4$), Bis(2-hydroxy-1- naphthaldehyde)adipoyldihydrazone and their Heterobimetallic Manganese and Ruthenium Complexes

Sl. No	Ligand/Complex	νOH + νNH	νC=O	νC=N	Amide II + νC-O(phenolic/ naphtholic)	β(C-O) (phenolic/ naphtholic	νN-N	νM-O (phenolic/ naphtholic)	νM-O()C-O-M)	ν (Mn–O–Ru)	νM-N (pyridine base in-plane and out –of -plane ring deformation)	νM-Cl
	$slahH_4$	3300-3600(sbr) 3445(m) 3436(m) 3204(s) 3065(sbr)	1679(s)	1620(s)	1560(s)	1275(s)	1036(m)					
	$npahH_4$	3300-3600(sbr) 3469(s) 3430(sbr) 3224(s) 3051(sbr)	1666(s)	1630(s) 1593(m)	1530(w)	1281(m)	1030(w)					
36.	$[Mn^{IV}Ru^{II}(slah)(H_2O)_3Cl]Cl$	3000-3550(sbr) 3409(sbr) 3211(s)	-	1600(vs)	1540(wsh)	1308(m)	1078(w)	585(w)	435(m)	830(w)	-	303(w)
37.	$[Mn^{IV}Ru^{II}(slah)(py)_3Cl]Cl$	3000-3500 (sbr) 3423(sbr)	-	1613(vs)	1540(s)	1308(m)	1102(m)	592(w)	433(s)	815(w)	640(w) 489(m) 243(m)	302(s)
38.	$[Mn^{IV}Ru^{II}(slah)(2\text{-}pic)_3Cl]Cl.3H_2O$	3000-3500 (sbr) 3436(mbr) 3204(m)	-	1606(vs)	1540(s)	1308(s)	1102(m)	545(w)	433(s)	857(w)	671(w) 487(m) 241(m)	307(m)
39.	$[Mn^{IV}Ru^{II}(slah)(3\text{-}pic)_3Cl]Cl.3H_2O$	3000-3550(sbr) 3423(sbr) 3197(s)	-	1613(s)	1540(s)	1308(s)	1102(m)	545(w)	433(s)	857(w)	671(m) 488(m) 241(s)	306(m)
40.	$[Mn^{IV}Ru^{II}(slah)(4\text{-}pic)_3Cl]Cl.3H_2O$	3000-3550(s) 3436(sbr) 3204(sbr)	-	1606(s)	1540(s)	1308(m)	1082(m)	552(m)	434(s)	857(w)	665(m) 487(m) 244(m)	307(s)

41. $[Mn^{IV}Ru^{II}(npah)(H_2O)_3Cl]Cl$	3000-3550(sbr) 3436(sbr)	-	1606(vs)	1540(s)	1320(m)	1062(m)	540(w)	430(w)	837(m)	-	-
42. $[Mn^{IV}Ru^{II}(npah)(py)_3Cl]Cl$	3000-3550(sbr) 3443(mbr)	-	1606(vs)	1540(s)	1301(m)	1062(w)	580(w)	440(w)	830(m)	651(w) 475(w)	-
43. $[Mn^{IV}Ru^{II}(npah)(2\text{-}pic)_3Cl]Cl$	3000-3550(sbr) 3462(sbr)	-	1606(vs)	1533(s)	1300(m)	1065(m)	580(w)	-	830(w)	657(w) 470(w)	-
44. $[Mn^{IV}Ru^{II}(npah)(3\text{-}pic)_3Cl]Cl.3H_2O$	3000-3550(sbr) 3429(m) 3177(m)	-	1606(vs)	1540(s)	1295(m)	1102(m)	585(w)	459(w)	824(m)	658(w) 433(w)	-
45. $[Mn^{IV}Ru^{II}(npah)(4\text{-}pic)_3Cl]Cl$	3000-3500 (sbr) 3429(s)	-	1606(vs)	1540(s)	1308(m)	1102(m)	500(w)	430(w)	824(m)	658(w) 465(w)	-

Table 6.4: The Electrochemical Parameters for the Dihydrazones and their Heterobimetallic Mn(IV) and Ru(II) Complexes (Pot vs SCE)

	Ligand/Complex	Epa/V	Epc/V
	$slahH_4$	+0.35	+0.20
	$npahH_4$	0.00 +0.35	-0.15 -
36.	$[Mn^{IV}Ru^{II}(slah)(H_2O)_3Cl]Cl$	+0.60 0.00 -	+0.30 -0.36 -1.04
38.	$[Mn^{IV}Ru^{II}(slah)(2\text{-}pic)_3Cl]Cl.3H_2O$	- +0.20	+0.25 -
39.	$[Mn^{IV}Ru^{II}(slah)(3\text{-}pic)_3Cl]Cl.3H_2O$	- +0.12	+0.20 -
40.	$[Mn^{IV}Ru^{II}(slah)(4\text{-}pic)_3Cl]Cl.3H_2O$	- +0.12	+0.20 -
41	$[Mn^{IV}Ru^{II}(npah)(H_2O)_3Cl]Cl$	+0.26 -0.10 -0.75	+0.10 -0.70 -1.20
42	$[Mn^{IV}Ru^{II}(npah)(py)_3Cl]Cl$	-0.30	-0.51
43.	$[Mn^{IV}Ru^{II}(npah)(2\text{-}pic)_3Cl]Cl$	0.00 -0.75	-0.16 -0.90
44.	$[Mn^{IV}Ru^{II}(npah)(3\text{-}pic)_3Cl]Cl.3H_2O$	+0.46 -0.06	+0.30 -0.55
45.	$[Mn^{IV}Ru^{II}(npah)(4\text{-}pic)_3Cl]Cl$	+0.85 -0.70	+0.30 -0.80

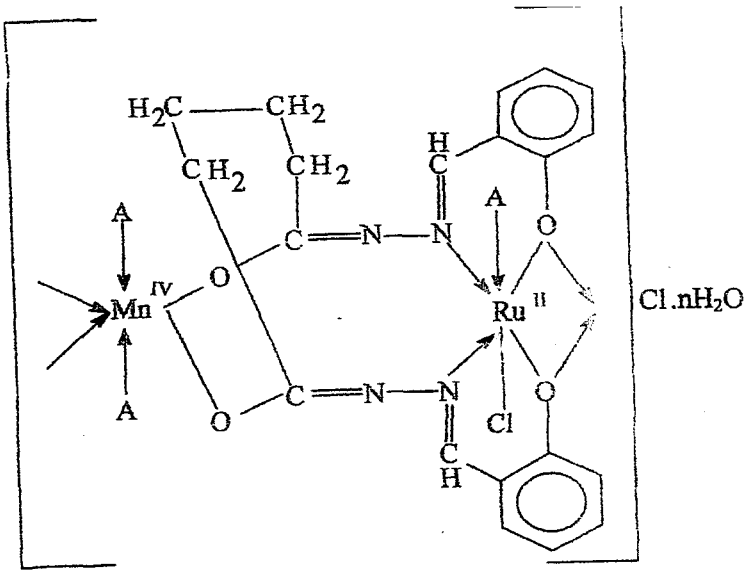

Fig. 6.5.1 Suggested structure of complex $[Mn^{IV}Ru^{II}(slah)(A)_3Cl]Cl.nH_2O$ (where A = H_2O, **(36)**; py, **(37)**; 2-pic, **(38)**; 3-pic, **(39)**; 4-pic, **(40)**; n = 0, 3))

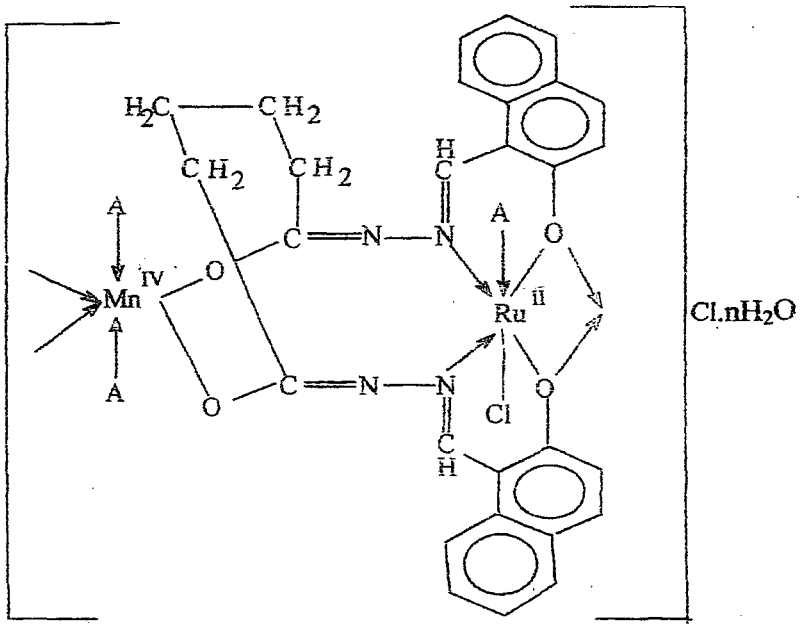

Fig. 6.5.2 Suggested structure of complex $[Mn^{IV}Ru^{II}(npah)(A)_3Cl]Cl.nH_2O$ (where A = H_2O, **(41)**; py, **(42)**; 2-pic, **(43)**; 3-pic, **(44)**; 4-pic, **(45)**; n = 0, 3))

REFERENCES

1. M. L. Ludurig, K. A. Puttrudge and W. C. Stallings, *"In Manganese in Metabolism and Enzyme Functions"*, Eds., V. L. Schramm and F. C. Wedler, Academic Press, New York, ch. 21, 1986, p.405.
2. W. F. Beyer and I. Fridivich, *"In Manganese in Metabolism and Enzymes Function"*, eds. V. L. Schramm and F. C. Wedler, Academic Press, New York, ch. 12, 1986, p.193.
3. G. C. Dismukes, *Chem. Rev.*, **96**, 2909 (1986).
4. M. W. Lynch, D. N. Hendrickson, B. J. Fitzgerald and C. G. Pierpant, *J. Am Chem. Soc.*, **106**, 2041-2049 (1984).
5. S. Mukhopadhyay, H. J. Mok, R. J. Staples and W. H. Armstrong, *J. Am. Chem. Soc.*, **126**, 9202 (2004).
6. J. E. Ritchie and R. W. Murray, *J. Am. Chem. Soc.*, **122**, 2964 (2000).
7. Graitzel, M. Ed, *"Energy Resources, through Photochemistry and Catalysis"*, Academic Press, New York, 1983.
8. K. Kalyanasundaram, *Coord. Chem. Rev.*, **46**, 159 (1982).
9. A. C. Benniston, G. M. Chapman, Anthont Harriman and Sarah A. Roston, *Inorg. Chem.*, **44**, 4029 (2005).
10. W. R. Murphy, Karen J. Brewer, G. Gettlife and John D. Peterson, *Inorg. Chem.* **28**, 81 (1989).
11. Eva Ruba, J. R. Hart and J. K. Barton, *Inorg. Chem.*, **43**, 4570 (2004).
12. K. K-W Lo and T. K-M Lee, *Inorg. Chem.*, **43**, 5275-5282 (2004).
13. B. Gieber and R. Alsfasser, *Dalton Trans.*, 612-618 (2003).
14. M. Ledney and P. K. Dutta, *J. Am. Chem. Soc.*, 80C, **117**, 7687-7695 (1995).
15. J. D. Pererson, W. R. Murphy, R. Sahai, K. J. Brewer and R. R. Rumniki, *Coord. Chem. Rev.*, **64**, 216 (1985).

16. K. Nagano and H. Kinoshita and A. Hirokawa, *Chem. Pharm. Bull. Tokyo*, **12**, 1198 (1964).

17. N. S. Birader and S. D. Angadi, *J. Inorg. Nucl. Chem.*, **38**, 1405 (1976).

18. N. S. Birader, V. B. Mahale and B. R. Hivinale, *Curr. Sci.* (India), **45**, 6 (1976).

19. L. Sacconi, *J. Am. Chem. Soc.*, **74**, 4503 (1952).

20. K. K. Narang and A. Aggarwal, *Indian J. Chem.*, **13**, 1072 (1975).

21. L. Sacconi, *J. Chem. Soc.*, 1326 (1954).

22. R. C. Aggrawal and B. Singh, *Transition Met. Chem.*, **1**, 275 (1976); *Curr. Sci.*, **46**, 836 (1977); *J. Inorg. Nucl. Chem.*, **40**, 1174 (1978).

23. A. El-Toukhy, A. F. M. Henry, L. El-Sayed and M. F. Iskander, M. I. Chan, **113**, 171 (1982); M. F. Iskander, A. F. M. Henfny, L.El-Sayed and S. E. Zayan, *J. Inorg. Nucl. Chem.*, **38**, 2209 (1976).

24. S. Chandra and R. N. Kapoor, *Acta Chim. Hung.*, **112**, 11 (1983).

25. K. K. Narang and R. A. Lal, *Transition Met. Chem.*, **1**, 260 (1977).

26. K. K. Narang and R. A. Lal, *Transition Met. Chem.*, **2**, 100 (1976).

27. K. K. Narang and R. A. Lal, *Transition Met. Chem.*, **3**, 272 (1978).

28. K. K. Narang and R. A. Lal, *Curr. Sci.*, **46**, 401 (1977); **47**, 793 (1978).

29. K. K. Narang and R. A. Lal, *J. Scient. Res.*, BHU, **28**(2), 1 (1978); **31**, 259 (1980-81).

30. S. K. Sahani, S. P. Gupta, V. B. Rana, *J. Indian Chem. Soc.*, **54**, 200 (1977).

31. S. K. Sahani, S. K. Sanyal, S. P. Gupta and V. B. Rana, *J. Inorg. Nucl. Chem.*, **39**, 1098 (1977).

32. R. L. Dutta and A. K. Sarkar, *J. Inorg. Nucl. Chem.*, **43**, 180 (1981).

33. S. Kher, S. K. Sahani and R. N. Kapoor, *Inorg. Chim. Acta*, **37**, 121 (1979).

34. S. Kher, S. K. Sahani, V. Kumari and R. N. Kapoor, *Synth. React. Inorg. Met-Org. Chem.*, **10**, 431 (1980).

35. V. B. Rana and M. P. Teotia, *Indian J. Chem.*, **19A**, 267 (1980).

36. R. Chandra, S. K. Sahani and R. N. Kapoor, *Acta Chim. Hung.*, **112**, 385 (1983); S. Chandra and R. N. Kapoor, *Acta Chim. Hung.*, **112**, 11 (1983).

37. K. K. Narang and U. S. Yadav, *Indian J. Chem.*, **19A**, 697 (1980).

38. K. K. Narang and R. M. Dubey, *Indian J. Chem.*, **21A**, 830 (1982).

39. A. Yacouta Nour, M. M. Mostafa and A. K. T. Maki, *Transition Met. Chem.*, **15**, 34 (1990); *Spectrochim. Acta*, **44A**, 1291 (1988).

40. D. L. Arora, K. Lal, S. P. Gupta and S. K. Sahani, *Polyhedron*, **5**, 1499 (1986), *Indian J. Chem.*, **24A**, 980 (1987).

41. K. K. Narang and M. K. Singh, *Transition Met. Chem.*, **12**, 385 (1987).

42. R. A. Lal, S. Das and R. K. Thapa, *Inorg. Chim. Acta*, **132**, 129 (1987).

43. R. A. Lal and S. Das, *Indian J. Chem.*, **27A**, 225 (1988).

44. R. A. Lal, K. N. Srivastava and S. Das, *Synth. React. Inorg. Met-Org. Chem.*, **18**, 837 (1988).

45. R. A. Lal, *Polyhedron*, **8**, 2527 (1989).

46. M. Hussain, S. S. Bhattacharjee, K. B. Singh and R. A. Lal, *Polyhedron*, **10**, 779 (1991).

47. R. A. Lal, L. M. Mukherjee, A. N. Siva, A. Pal, S. Adhikari, K. K. Narang and M. K. Singh, *Polyhedron*, **12**, 235 (1993).

48. R. A. Lal, A. N. Siva, L. M. Mukherjee, K. K. Narang, M. K. Singh and R. K. Thapa, *Spectrochim. Acta*, **50A**, 1005 (1994).

49. R. A. Lal, A. N. Siva, S. Adhikari and A. Pal, *Indian J. Chem.*, **34A**, 1000 (1995); R. A. Lal, D. Basumatary, A. K. De and A. Kumar, *Transition Met. Chem.*, **32**, 491-493 (2007), R. A. Lal, D. Basumatary, S. Adhikari and A. Kumar, *Spectrochiom. Acta, Part-A*, **69**, 706-714 (2007).

50. S. A. Patil and V. H. Kulkarni, *Inorg. Chim. Acta*, **95**, 195 (1984).

51. T. R. Goudar, S. M. Shindagi and G. S. Nadagouda, *J. Indian Chem. Soc.*, **64**, 636 (1987).

52. V. Kumar, S. K. Sahani, S. Kher and R. N. Kapoor, *Transition Met. Chem.*, **5**, 85 (1980).

53. B. Sahoo and A. K. Rout, *Indian J. Chem.*, **25A**, 609 (1986); B. Sahoo and B. K. Mohapatra, *Indian J. Chem.*, **22A**, 494 (1983); **23A**, 844 (1984); **24A**, 653 (1985).

54. O. P. Pandey, *Polyhedron*, **6**, 1021 (1987).

55. G. H. Havanur and V. B. Mahale, *Indian J. Chem.*, **26A**, 1063 (1987).

56. A. K. Panda, S. Rout and H. Mohanty, *Indian J. Chem.*, **33A**, 788 (1994).

57. S. Gopinathan, S. S. Tavale, V. G. Puranik and M. P. Degaonkar, *Bull. Chem. Soc.*, Japan. **41**, 1797 (1994).

58. L. Sacconi, *Z. Anorg. Allg. Chem.*, **275**, 249 (1954).

59. L. Sacconi, G. Lombardo and P. Paoletti, *J. Chem. Soc.*, 848 (1960).

60. L. Sacconi, G. Lombardo and R. Ciofalo, *J. Am. Chem. Soc.*, **82**, 4182 (1960).

61. R. Cefalu, F. Maggio, L. Pellerito and V. Romano, *Inorg. Nucl. Chem. Lett.*, **10**, 529 (1974).

62. A. Mangia, C. Pellizi, G. Pellizi, *Acta Crystallogr.*, **30B**, 2146 (1974).

63. C. Pellizi, G. Pellizi, G. Predieri and S. Resola, *J. Chem. Soc, Dalton Trans.*, 1349 (1982).

64. M. Nardelli, C. Pellizi, G. Pellizi, *Transition Met. Chem.*, **2**, 35 (1977).

65. J. W. J. Martin, J. H. Johnston and N. F. Curtis, *J. Chem. Soc., Dalton Trans.*, 68 (1978)

66. L. Sacconi and I. Bertini, *J. Am. Chem. Soc.*, **88**, 5180 (1966).

67. T. J. Giordano, G. J. Palenik, R. C. Palenik and D. A. Sullivan, *Inorg. Chem.*, **18**, 2445 (1979).

68. J. E. Thomas, R. C. Palenik and G. J. Palenik, *Inorg. Chim. Acta*, **37**, 2459 (1979).

69. G. Paolucci, G. Marangoni, G. Bandoli and D. D. Clemente, *J. Chem. Soc., Dalton Trans.*, 1304 (1980).

70. C. Pellizi and G. Pellizi, *J. Chem. Soc., Dalton Trans.*, 1970 (1980).

71. M. P. Teotia, I. Singh and V. B. Rana, *Transition Met. Chem.*, **6**, 60 (1981).

72. V. B. Rana, I. Singh and M. P. Teotia, *Crot. Chim. Acta*, **54**, 267 (1981).

73. G. Paolucci, P. A. Vigato, G. Rosseto, V. Casselto, *Inorg. Chim. Acta*, **65**, 171 (1982).

74. R. L. Dutta and Md. M. Hossain, *Indian J. Chem.*, **21A**, 746 (1982).

75. R. L. Dutta nd A. K. Sarkar, *Indian J. Chem.*, **19A**, 1188 (1980); *J. Indian Chem. Soc.*, **57**, 332 (1980).

76. R. L. Duta and A. Bhattacharya, *J. Indian Chem. Soc.*, **54**, 239 (1977).

77. A. A. D. Mathis, M. R. Snow and J. A. Vanzo, *Chem. Commun.*, 7, 264 (1976).

78. R. L. Dutta and A. K. Pal, *Indian J. Chem.*, **21A**, 1130 (1982).

79. V. B. Singh, D. P. Singh, P. Singh and M. P. Teotia, *Indian J. Chem.*, **21A**, 528 (1982).

80. C. Lorenzini, C. Pellizi, G. Pellizi and G. Predieri, *J. Chem. Soc., Dalton Trans.*, 1304 (1980).

81. R. L. Dutta and A. K. Pal, *Indian J. Chem.*, **22A**, 871 (1983).

82. V. B. Rana, V. K. Chauhan, D. P. Singh and M. P. Teotia, *Orient. J. Chem.*, **1**, 24 (1985).

83. K. Dey, A. K. Sinha Roy, K. K. Bhasin and R. D. Verma, *Indian J. Chem.*, **26A**, 230 (1987).

84. G. Marangoni, G. Chessa, B. Pitteri, V. Bertolasi, V. Ferroti and G. Gilli, *J. Chem. Soc., Dalton Trans.*, 1479 (1988).

85. S. Ianelli, G. Minardi, C. Pellizi, G. Pellizi, R. Reverbari, C. Solinas and P.

Tarasconi, *J. Chem. Soc., Dalton Trans.*, 2213 (1991); D. Belletti, M. Carcelli, C. Pellizi and G. Pellizi, *J. Crystallogr. Spectross. Res.*, **22**, 185 (1992).

86. A. Bonardi, S. Ianelli, C. Pellizi and G. Pellizi, *Inorg. Chim. Acta*, **187**, 1617 (1991).

87. M. T. H. Tarafder and A. R. Khan, *Polyhedron*, **10**, 973 (1991).

88. M. T. Toshev, V. G. Yusupov, M. M. Karimov and R. N. Shehelokov, *Koord. Khim.*, **18**, 202 (1992).

89. A. Bacchi, L. P. Bhattaghia, M. Carcelli, C. Pelizzi, G. Pellizi, C. Solinas and M. A. Zorodu, *J. Chem. Soc., Dalton Trans.*, 773 (1993).

90. P. K. Singh, H. Jimerez, K. V. Katti, W. A. Vokert and C. Barnes, *Inorg. Chem.*, **33**, 736 (1994).

91. N. G. Lukyanenko, N. Y. Nazarova, V. I. Vetrogen, H. J. Holdt. J. Aurich and G. Kurntoch, *Inorg. Chim. Acta*, **155**, 36 (1989).

92. B. Ji, Q. Du, K. Ding, Y. Li and Z. Zhou, *Polyhedron*, **15**, 403 (1996).

93. L. Xiaozeng, W. Genglin, L. Zaizheng, Y. Shiping, J. Zonghui, W. Honggen and Y. Xinkan, *Polyhedron*, **14**, 511 (1995).

94. A. Bonardi, S. Ianelli, C. Pellizi, G. Pellizi and C. Solinas, *Inorg.Chim. Acta*, **232**, 211 (1995).

95. D. P. Singh, M. N. Ansari and V. B. Rana, *J. Indian Chem. Soc.*, **74**, 448 (1997).

96. G. Paolucci, S. Sitran, D. Aju, F. Benetollo, A. Polo and G. Bombieri, *Inorg. Chim. Acta*, **193**, 57 (1992).

97. M. R. Maurya, D. C. Antony, S. Gopinathan and C. Gopinathan, *Indian J. Chem.*, **34A**, 967 (1995).

98. R. A. Lal, S. Adhikari, A. Kumar and M. L. Pal, *J. Indian Chem. Soc.*, **75**, 345 (1998).

99. R. A. Lal and S. Adhikari, *Indian J. Chem.*, **35A**, 607 (1996).

100. R. A. Lal, S. Adhikari, A. Pal, A. N. Siva and A. Kumar, *J. Chem. Res.* (S), 122 (1997); *J. Chem. Res.* (M), 749 (1997).

101. R. A. Lal, S. Adhikari and A. Kumar, *Indian J. Chem.*, **36A**, 1063 (1997).

102. R. A. Lal and A. Kumar, *Indian J. Chem.*, **37A**, 921 (1998).

103. R. A. Lal, A. Kumar and M. L. Pal, *J. Indian Chem. Soc.*, **76**, 71 (1999).

104. R. A. Lal, A. N. Siva, S. Adhikari and A. Pal, *Indian J. Chem.*, **34A**, 1000 (1995).

105. R. A. Lal and A. Kumar, *Indian J. Chem.*, **38A**, 839 (1999).

106. H. Adams, D. E. Fenton, G. Minardi, A. M. Pistudi and C. Solinas, *Inorg. Chem. Comm.*, **3**, 24 (2000).

107. R. A. Lal, S.Adhikari, A. Kumar, J. Chakroborty, *Synth. React. Met. Org. Chem.*, **31** (1), 65-83 (2001).

108. R. A. Lal, A. Kumar and J. Chakraborty, *Indian J. Chem.*, **40A**, 422-425 (2001).

109. R. A. Lal, S. Adhikari, Arvind Kumar, J. Chakraborty and S. Bhaumik, *Synth. React. Inorg. Met. Org. Chem.*, **32**, 81 (2002).

110. R. A. Lal, J. Chakroborty and S. Bhaumik, *Indian J. Chem.*, **41A**, 1157, (2002).

111. F. A. Cotton, G. Wilkinson, C. A. Murillo, M. Bochmann "*Advanced Inorganic Chemistry*", John Wiley and sons, Inc, New York, 6th Ed, 1999, p. 757.

112. R. A. Lal, J. Chakraborty, A. Kumar, S. Bhaumik, R. K. Nath, D. Ghosh, **43,** 3, 516 (2004).

113. R. A. Lal, D. Basumatary, J. Chakroborty, S. Bhaumik and A. Kumar, *Indian J. Chem.*, **45A**, 619 (2006).

114. L. Yongmen, H. Guosency, M. Yongxiang and Z. Gang, *Polyhedron*, **12**, 1043-1046 (1990).

115. A. Bolger, G. Ferguson, J. P. James, C. Long, P. Ma. Ardle and J. G. Vos, *J. Chem. Soc., Dalton Trans.*, 1577-1583 (1993).

116. A. Khan, S. S. Hasan, S. P. Varkey, M. A. Rather, N. Jahan and M. Shakir, *Transition Met. Chem.*, **22**, 4-8 (1997).

117. L. Labib, L. A. Mohamed and M. F. Iskander, K. Griesar and W. Haase, *Transition Met. Chem.*, **25**, 700-705 (2005).

118. G. M. Larin, V. E. Shugin, A. N. Gusev and A. N. Charmega, *Russ. Chem. Bull.*, **53**, 775-779 (2004); **52**, 1301-1304 (2003).

119. K. Andelkovic, G. Jakovkjevic, M. Zlatovic, Z. Tesic, D. Sladic, J. Howing and R. Tellgren, *J. Sarb. Chem. Soc.*, **69**, 651-660 (2004).

120. A. Para, S. Karolczyk-Kostuch and M. Fietorowicz, *Carbohydrate Polymer*, **56**, 187-193 (2004).

121. L. Zhao, V. Niel, L. K. Thompson, Z. Yu, V. A. Milway, R. G. Harvey, D. O. Miller, Wilson, M. Leech, J. A. K. Howard and S. L. Heath, *J. Chem. Soc., Dalton Trans.*, 1446-1455 (2004).

122. E. Tirosh, R. Maman and I. Goldberg, *Acta Cryst.*, **E61**, 541-542 (2005).

123. M. Carcelli, S. Ianelli, P. Pelagatti, G. Pelizzi, D. Rogolina, C. Solinas and M. Tegam, *Inorg. Chim. Acta*, **358**, 903-911 (2005).

124. N. M. H. Salem, *Synth. React. Inorg. Met-Org and Nano-Met. Chem.*, **35**, 369-377 (2005).

125. H. Elengoz, R. Shoshvik and I. Goldberg, *Acta Cryst.*, **E61**, 538-540 (2005).

126. C. R. Hamar, G. S. King, E. L. McCool, W. B. Euler, J. D. Ferrara and W. J. Youngs, *J. Am. Chem. Soc.*, **109**, 5760-5765 (1987).

127. F. Fiegel, V. Anger and R. F. Oesper, "*Spot test in Organic Analysis*", Elsevier Scientific Publishing Co., New York, 7th Ed, 1975, p. 172.

128. A. I. Vogel, "*A Textbook of Quantitative Inorganic Analysis Including Elementary Instrumentation Analysis*", (ELBS and Longman), 4th Ed, 1978.

129. F. D. Snell and C. T. Snell, *"Calorimetric Methods of Analysis"*, vol-**II** A, D. Van, Nostrand Co. Inc, Princeton, New Jersey, 1959.

130. B. N. Figis and J. Lewis, *"Modern Coordination Chemistry"*, Eds, J. Lewis and R. G. Wilkins, Interscience, New York, 1960, p. 403.

131. A. Earnshaw, *"Introduction to Magnetochemistry"*, Academic Press, London, 1968, p.35.

132. J. R. Dilworth, *Coord. Chem. Rev.*, **21**, 29 (1976).

133. R. M. Issa, M. F. Iskander and M. F. Elshazty, *Z. Inorg. Allg. Chem.*, 90, 354 (1967).

134. R. A. Lal, *Indian J. Chem.*, **25A**, 976 (1986).

135. A. Sengupta and N. K. Dutta, *J. Inorg. Nucl. Chem.*, **37**, 270 (1975).

136. H. Ohta, *Bull. Chem.Soc.*, Japan, **31**, 1056 (1958); ibid, **33**, 2 (1960).

137. M. F. Iskander, A. M. Al-Aggan, L. S. Refaat and L. El-Sayed, *Inorg. Chim. Acta,* **14**, 167 (1975).

138. N. K. Dutta and A. Sengupta, *J. Inorg. Nucl. Chem.*, **33**, 418 (1971).

139. S. Kher, S. K. Sahani and R. N. Kapoor, *Inorg. Chim. Acta,* **37**, 121 (1979).

140. S. K. Sahani, S. K. Sanyal, S. P. Gupta and V. B. Rana, *J. Inorg. Nucl. Chem.*, **39**, 1098 (1977).

141. A. Yacouta-Nour, A. K. T. Maki and M. M. Mostafa, *J. Indian Chem. Soc.*, **72**, 447 (1995).

142. R. C. Aggarwal and B. Singh, *Transition Met. Chem.*, **1**, 275 (1976); Curr. Sci, **46**, 832 (1977); *J. Inorg. Nucl. Chem.*, **40**, 1174 (1978).

143. E. Sinm and C. M. Harries, *Coord. Chem. Rev.*, **4**, 391 (1969).

144. S. Yamanda, E. Ohno, Y. Kuge, A. Takeuchi, K. Vamanouchi and K. Iwasaki, *Coord. Chem. Rev.*, **3**, 247 (1968).

145. W. J. Geary, *Coord. Chem. Rev.*, 7, 81 (1971).

146. P. Chakraborty, S. Karmakar, S. K. Chandra and A. Chakraborty, *Inorg. Chem.*, **33**, 816 (1994); P. Chakraborty, S. K. Chandra and A. Chakraborty, *Inorg. Chem.*, **33**, 4959 (1994).

147. P. T. Manoharan and H. B. Gray, *Chem. Commun.*, 324 (1965); W. Jakob and T. Senkowski, *Rocz. Chem.*, **38**, 1751 (1964).

148. N. G. Connelly, K. A. Hassard, B. J. Dunne, A. G. Orpen, S. J. Raven, G. A. Carriedo and V. Riera, *J. Chem. Soc., Dalton Trans.*, 1623 (1988).

149. S. Chattopadhyay, P. Basu, S. Pal and A. Chakraborty, *Inorg. Chem.*, **29**, 3829 (1990); P. Basu, S. Pal and A. Chakraborty, *Inorg. Chem.*, 31, 4980 (1992); P. Couzerh, Y. Jeannin, C. Rocchicioli Deltcheff and F. Valentini, *J. Coord. Chem.*, **6**, 221 (1979).

150. P. Basu and A. Chakraborty, *Inorg. Chem.*, **31**, 4980 (1992); P. Couzerh, Y. Jeannin, C. Rocchiciolli Deltcheff and F. Valentini, *J. Coord. Chem.*, **6**, 221 (1979).

151. B. N. Figgis, *Trans. Faraday Soc.*, **57**, 204 (1961); R. R. Manchamp, R. J. M. Henry and R. C. Young, *J. Inorg. Nucl. Chem.*, **10**, 28 (1959).

152. S. Chattopadhyay, P. Basu, S. Pal and A. Chakraborty, *Inorg. Chem.*, **29**, 3829 (1990); P. Basu, S. Pal and A. Chakravarty, *Inorg. Chem.*, **27**, 1848 (1988).

153. R. A. Lal, "Zinc"(II), Copper(II), Nickel(II) and Cobalt(II) Complexes of some Schiff bases derived from Organic Acid Hydrazide" Ph.D thesis, B.H.U., 1978.

154. T. N. Sorrell, *Tetrahedron*, 145 (1989).

155. A. B. P. Lever, *"Inorganic Electronic Spectroscopy"*, Elsevier, New York, 2nd Ed, 1984, p. 448.

156. G. R. Karteweg and L. L. Van Reijen, *J. Mag. Resonance*, **44**, 159 (1981); El-Baradie K. Y., R. M. Issa and M. Gaddar, *Indian J. Chem.*, **43A**, 1126 (2004).

157. P. Vishwanathan, R. Karvembu, V. Tharaneeswaran and K. Natarajan, *J. Chem. Sci*, **117**(3), 235-238 (2005).

158. R. P. Bonomo, E. Rizzarelli, M. Bressan and A. Morvillon, *Inorg. Chem. Acta*, **188**, 21 (1991).

159. P. Mathur, M. Crowder and G. C. Dismukes, *J. Am. Chem. Soc.*, **109**, 5227 (1987).

160. F. F. Bently and E. F. Wolforth, *Spectrochim. Acta*, **15**, 165 (1959).

161. C. S. Marvell, S. Aspey Alan and E. A. Dodley, *J. Am. Chem. Soc.*, **82**, 6064 (1960).

162. M. Zheng, S. V. Khangulov, G. C. Dimukes and V. V. Barynin, *Inorg. Chem.*, **33**(2), 382-387 (1994).

163. R. L. Dutta, M. M.Hussain. *J. Sci. Ind. Res.*, **44**(12), 635 (1985).

164. H. Yamada, *Bull. Chem. Chem. Soc.*, Japan., **32**, 1051 (1959).

165. G. C. Percy, *Spectrochim. Acta*, **32A**(6), 1287-1290 (1976).

166. K. R. Barnard, M. Bruch, H. Susan, J. H. Enemark, R. W. Gable and A. G. Wedd, *Inorg. Chem.*, **36**, 637 (1997).

167. K. Broderson, *Z. Anorg. Allg. Chem.*, **290**, 4 (1959).

168. J. C. Decius and D. P. Pearson, *J. Am. Chem. Soc.*, **75**, 2436 (1953).

169. V. J. Goubean and V. Kull, *Z. Anor. Allg.Chem.*, **316**, 182 (1962).

170. W. G. Peterson and M. Onyszchuk, *Can. J. Chem.*, **39**, 968 (1961).

171. L. Sacconi and A. Sabatini, *J. Inorg. Nucl. Chem.*, **35**, 1389 (1963).

172. A. Braibanti, F. Dallarealle, M. A. Pellinghelli and E. Leporati, *Inorg. Chem.*, **7**, 1430 (1968).

173. R. C. Aggarwal and K. K. Narang, *Inorg. Chim. Acta*, **7**, 651 (1973); *Indian J. Chem.*, **14A**, 64 (1967); **9**, 1413 (1971).

174. A. C. Fabretti, C. G. Frenchini, C. P. Preti and G. Tosi, *Can. J. Chem.*, **19A**, 137 (1980); J. Fijita, K. Nakamoto and M. Kobayashi, *J. Am. Chem. Soc.*, **78**, 3936 (1956).

175. A. V. Nikolov, V. A. Logvineenko and L. I. Myachina, "*Thermal Analysis*", vol. **2**, Academic Press, New York , 1969.

176. G. Sartori, C. Furlani and A. Damiani, *J. Inorg. Nucl. Chem.*, **8**, 119 (1958).

177. K. Nakamoto, *"Infrared and Raman Spectra of Inorganic and Coordination Compounds"*, 4th Ed, John Wiley and Sons, New York, 1986.

178. B. Meunier, *Chem. Rev.*, **92**, 1411 (1992); G. Pratviel, J. Bernadou, B. Meunier, *Angew. Chem.*, Int. Ed., Engl, **34**, 746 (1995).

179. J. Lecomte, M. L. Josien and J. Lascombe, *Bull. Soc. Chem., France*, **63** (1956).

180. G. C. Percy, *J.Inorg. Nucl. Chem.*, **37**, 2071 (1975).

181. M. Mikami, I. Nakagawa and T. Shimanonchi, *Spectrochim. Acta*, **23A**, 1037 (1967).

182. G. C. Percy and D. A. Thornton, *J. Inorg. Nucl. Chem.*, **34**, 3369 (1972).

183. A. E. Martell, K. Nakamoto, P. J. Mccarthy, *Nature*, **183**, 459 (1959); K. Nakamoto and A. E. Martell, *J. Chem. Phys.*, **32**, 588 (1960).

184. J. Fujiter, A. E. Martell and K. Nakamoto, *J. Chem. Phys.*, **36**, 324-331 (1962).

185. L. Sacconi, A. Sabatini and P. Gans, *Inorg. Chem.*, **3**, 772 (1964).

186. D. M. Adams, "*Metal-Ligand and Related Vibration*", Edward Ernold Press, London, 1967.

187. W. J. Eilbeak, H. F. Holmes, A. E. Underhill and C. E. Taylor, *J. Chem. Soc.*, A, 128 (1968).

188. C. W. Frank and L. B. Rogers, *Inorg. Chem.*, **5**, 615 (1966).

189. A. B. P. Lever and E. Mantovani, *Can. J. Chem*, **51**, 1567 (1973).

190. K. K. Narang and A. Aggarwal, *Trans. Met. Chem.*, **2**, 29 (1977).

191. A. Zoumi, H. T. Witt, J. Keru, P. Fromme, N. Kraub, W. Saenger and P. Orth, *Nature*, **409**, 739 (2001).

192. W. Rutinger and G. C. Dismukes, *Chem. Rev.*, **97**, 1 (1997).

193. V. J. Leeveque, M. E. Stroupe, J. R. Lipock, D. E. Cabelli, J. A. Taimer, H. S.

Nick and D. N. Silverman, *Biochemistry*, **39**, 7131 (2000).

194. V. V. Bargnin, M. M. Whittaker, S. V. Antonyuk, V. S. Lanzin, P. M. Harrison, P. J. Artywink and J. W. Whittarker, *Structure*, 725 (2001).

195. M. Hogbson, M. E. Andersson and P. Nordlund, *J. Biol. Inorg. Chem*, 315 (2001).

196. Y. Gultneh, B. Ahvazi, A. R. Khan, R. J. Butcher and J. P. Tuchagues, *Inorg. Chem.*, **34**, 3633-3645 (1995).

197. Y. Gultneh, T. B. Visgedu, T. Tesema and R. J. Butcher, *Inorg. Chem*, **42**, 1857 (2003).

198. Y. J. Hamada, *IEEE Trans–Electron Devices*, **44**, 1208 (1997).

199. S. Mukhopadhyay, S. K. Mandal, S. Bhadhuri and W. H. Armstrong, *Chem. Rev.*, **104**, 3981 (2004).

200. M. Koikawa and H. Okawa, *J. Chem. Soc., Dalton Trans.*, 641- 645 (1988).

201. L. Helmholtz and M. E. Russousso, *J. Chem. Phys.*, **59**, 5455 (1973).

202. M. E. Bodini, L. A. Willis, T. H. Richel and D. T. Sawyer, *Inorg. Chem.*, **15**, 1538 (1976).

203. D. P. Kessissoglou, X. Li, W. M. Butler and V. L. Percoraro, *Inorg. Chem.*, **26**(15), 2487-2492 (1987).

204. J. R. Hartman., B. M. Foxman and S. R. Cooper, *Inorg. Chem.*, **23**(10), 1381-1387 (1984).

205. H. Okawa, M. Nakamura, S. Kida., *Bull. Chem. Soc., Japan*, **55**(2), 466-470 (1982).

206. S. L. Chodas, A. M. Black and C. D. Flint, *J. Chem. Phys.*, **65**, 4816 (1976).

207. P. G. Rasmussen, K. M. Beem and E. J. Hornyak, *J. Chem. Phys.*, **50**, 3647 (1969); M. Nakadu, K. Awazu, S. Ibuki, I. Miyako and D. M. Date, *J. Phys. Soc.*, Japan, **19**, 781 (1964).

208. S. K. Chandra, P. Basu, D. Ray, S. Pal and A. Chakravarty, *Inorg. Chem.*, **29**, 2423 (1990).

209. P. Bukavee and R. Hoppe, *J. Fluorine Chem.*, **23**, 579 (1983)

210. P. Moews, *Inorg. Chem.*, **5**, 5 (1966); B. R. McGarvey in: R. L. Karlin (Ed.), *Transition Met. Chem.*, vol. **3**, Marcel Dekker, New York, 1966, p. 89.

211. E. Peduson and H. Toftlund, *Inorg. Chem.*, **13** 1603 (1974); D. C. Bradley, R. Coopewhite, S. A. Cotton, K. D. Sales and J. E. Gibson, *J. Chem. Soc. Dalton Trans.*, 191 (1973).

212. J. C. Hempd, L. O. Morgen and W. B. Lewis, *Inorg. Chem.*, **9**, 2064 (1970); L. S. Singer, *J. Chem. Phys.*, **23**, 379 (1955).

213. A. Abraham and M. H. L. Pryce, *Proc. Roy. Soc. London*, A, **230**, 206 (1951).

214. R. S. Drago, "*Physical Methods in Inorganic Chemistry*," Affiliated East-West Press, New Delhi, 1971, p. 355.

215. S. Pal, P. Ghosh and A. Chakraborty, *Inorg. Chem.*, **24**, 3704 (1985).

216. K. L. Brown, R. M. Golding, P. C. Healy, K. J. Jessop and W. C. Ten, *Aust. J. Chem.*, **27**, 275 (1974).

217. T. M. Aminbhami, N. S. Birader, G. V. Karajagi and W. E. Rudzinski, *Inorg. Chimica Acta*, **91**, 49-52 (1984).

218. E. L. Eliel, "*Stereochemistry of Carbon Compounds*", Mc Craw Hill, T. M. H. Edition, New Delhi, 1975, p-217.

219. A. Syamal and K. S. Kale, *Inorg. Chem.*, **18**, 992 (1979); S. Purohit, A.P. Koley, I. S. Prasad, P. T. Manoharan and S. Ghosh, *Inorg. Chem.*, **28**, 3735 (1987); J. M. Beng and R. H. Holm, *Inorg. Chem.*, **22**, 1768 (1983); E. I. Stifel, *Prog. Inorg. Chem.*, **31**, 511 (1992).

220. H. W. Nurnberg "*Electroanalytical Chemistry*", Interscience Publication, John Wiley and sons, vol. **10**, 1974, p. 498.

221. P. K.Santra, C. Sinha, Wen-Jyh.Sheen, Fen-Ling Liao, Tian-Huey Lu., *Polyhedron.*, **20**, 599-606 (2001).

222. P. Mark "*Fundamentals of Electroanalytical Chemistry*", Manchester Metropolitan University, Manchester, UK, John Wiley and sons Ltd., 2001, p. 36.

223. H. Okawa, M. Koikawa, S. Kida, *J. Chem.Soc., Dalton Trans.*, 641-645 (1988).

224. M. J. Clarke, M. Stubbs, *Metal Ions in Biological Systems*, **33**, 727 (1996).

225. E. D. A. Stemp, J. K. Barton, *Metal Ions in Biological Systems*, **33**, 325 (1996).

226. K. Nakamoto, C. Udovich and J. Takemoto, *J. Am. Chem. Soc.*, **92**, 3973 (1970).

227.U. Casellato, M. Vidali and P. A. Vigato, *Inorg. Nucl. Chem.*, Letters, **10**, 437 (1974).

228. U. Casellato, M. Vidali and P. A. Vigato, *J. Inorg. Nucl. Chem.*, **37**, 1715 (1975).

229. M. K. Chen, W. H. Armstrong, *Inorg. Chem.*, **28**, 3777-3779 (1989).

230. A. Chakravarty and S. K. Chandra, *Inorg. Chem.*, **31**, 760-765 (1992).

231. Bon-Kweon, Koo and U. K. Lee, *Bull. Korean Chem. Soc.*, **23**(4), 613-616 (2002).

232. S. Hotchandani, U. Ozdemir, C. Nasr, S. I. Allakhverdiev, V. V. Klimov, P. V. Kamat, R. Carpentier, *Bioelectroch. Bioener.*, **48** (1), 53-59 (1999).

233. J. A. Kirby, A. S. Robertson, J. P. Smith, A. C. Thompson, S. R. Cooper, M. P. Klein, *J. Am. Chem.*, **103**, 5529-5537 (1981).

234. C. S. G. Phillips, R.T. P. Williams, "*Inorganic Chemistry*", Claredon Press, Oxford, vol **2**, 1966, p. 313.

235. T. Matsubura, P. C. Ford, *Inorg. Chem.*, **15**, 1107 (1976).

236. M. T. Indelli, F. Scandola, J. P. Collin, J. P. Sauvage and A. Sour, *Inorg. Chem.*, **35**, 303 (1996).

237. K. Kalyanasundaram, M. Gratzel (Eds), "*Photosensitization and Photocatalysis using Inorganic and Organometallic Compounds*" Kluwer Academic Publishers, Dordrecht, 1993.

238. K. Kalyanasundaram, "*Photochemistry of Polypyridine and Porphyrin Complexes*", Academic, London, 1992.

239. E. Muller, M. K. Nazeeruddin, M. Gratzel, K. Kalyanasundaram, J. C. Prome, *New J. Chem.*, **20**, 759 (1996).

240. X. Zhang, M. A. J. Rodgers, *J. Phys. Chem.*, **99**, 12797 (1995).

241. M. E. Garcia Posse, N. E. Katz, L. M. Baraldo, D. D. Polonuer, C. G. Colombano, J. A. Olabe, *Inorg. Chem.*, **34**, 1830 (1995).

242. M. –L. Collomb-Dunand-Suthier, A. Deronzier and R. Ziessel, *Inorg. Chem.*, **33**, 2961 (1994).

243. M. –L. Collomb-Dunand-Suthier, A. Deronzier, R. Ziessel, *J. Chem. Soc. Chem. Commun.*, 189 (1994).

244. H. Okawa, M. Tanake and S. Kida, *Chem. Letters*, 987 (1974).

245. P. Frediani, M. Bianchi, A. Salvini, R. Guarducci, L. C. Carluccio, F. Piancenti, *J. Organometal. Chem.*, **498**, 187 (1995).

246. P. Frediani, M. Bianchi, A. Salvini, R. Guarducci, L. C. Carluccio, F. Piacenti, *J. Organometal. Chem.*, **476**, 7 (1994).

247. N. Gupta, N. Grover, G. A. Neyhart, P. Singh and H. H. Thorp, *Inorg. Chem.*, **32**, 310 (1993).

248. N. Grover, S. A. Ciftan, P. Singh, H. H. Thapa, *Inorg. Chim. Acta*, **240**, 335 (1995).

249. A. Hagfeldt, M. Gratzel, *Chem. Rev.*, **95**, 49 (1995); I. Ortmans, C. Moucheron, A. Kirschde Mesmaeker, *Coord. Chem. Rev.*, **168**, 233 (1998).

250. S. Silgel, "*Encyclopedia of Reagents for organic synthesis*", Paquette, L. A. Ed, John Wiley and Sons, Chicheter, vol. **6**., 1996, p. 4415.

251. (a) M. A. Bennet, T. W. Matheson, "*In Comprehensive Organometallic Chemistry*", G. Wilkinson, F. G. A. Stone, E. W. Abel, Eds, Pergamon Press, Oxford, vol. **4**, 1982, p. 931 (b) B. R. James, "*Homogeneous Hydrogenation*",

Wiley New York, 1973 (c) M. Freifelder, "*Practical Catalytic Hydrogenetions*", Wiley-Inter Science, New York, 1971.

252. T. Naota, H. Takaya and S. Murahashi, *Chem. Rev.*, **98**, 2599-2660 (1998).

253. (a) S. M. Zakeeruddin, M. D. K. Nazeeruddin, R. Humphry-R. Baker, M. Gratzel, *Inorg. Chem.*, **37**, 5251 (1998) (b) J. Bolger, A. Gourdon, E. Ishow, J. P. Launay, *Inorg. Chem.*, **35**, 2937 (1996) (c) V. Balzani, F. Barigelleti, P. Belser, S. Bernhad, L. De cola, L. Flamingni, *J. Phys. Chem.*, **100**, 16786 (1996) (d) A. Gourdon, J. P. Launay, *Inorg. Chem.*, **37**, 5336 (1998) (e) T. Kajita, R. M. Leasure, M. Devenney, D. Friesen, T. J. Meyer, *Inorg. Chem.*, **37**, 782 (1998) (f) C. Mouscheron, A. K. D. Mesmarker, S. Chouha, *Inorg. Chem.*, **36**, 584 (1997) (g) M. T. Indelli, C. A. Beganozza, F. Scandola, J. P. Collin, *Inorg. Chem.*, **37**, 6084 (1998) (h) R. M. Hartshorn, J. K. Barton, *J. Am. Chem. Soc.*, **114**, 5919 (1992) (i) J. P. Collin, P. Govina, V. Heitz; J. P. Suavage, *Eur. J. Inorg. Chem.*, 1 (1998).

254. (a) F. Basalo and R. G. Pearson, "*Mechanism of Inorganic Reactions*", 2nd Ed John Wiley and Sons, Inc., New York, 1967 (b) H. Taube, *Pure Appld. Chem.*, **51**, 901 (1997); **63**, 651 (1991).

255. N. Dharmraj and K. Natarajan, *Indian J. Chem.* **33A**, 785 (1994); N. Jayakumar, T. Banumathy, M. V. Chandini Devi and K. Natarajan, *Indian J. Chem.*, **23A**, 885 (1990).

256. L. M. Jackmann and S. Sternhill, "*Applications of nuclear magnetic resonance spectroscopy in organic chemistry*", Pergamen press, New York, vol **10**, 1978, p. 282, 334.

257. J. L. Sumider and C. N. Reilley, *Anal. Chem.*, **36**, 1689 (1964); **36**, 1707 (1964); Y. F. Ujiwara and C. N. Reilley, *Anal. Chem.*, **40**, 890 (1968).

258. J. C. N. Ma and E. W. Warhoff, *Canada. J. Chem.*, **43**, 1849 (1965).

259. T. K. Wu and B. P. Dailey, *J. Chem. Phys*, **41**, 3307 (1964).

260. C. Piguel, G. Bernardinellic, G. Hoptgarter, *Chem. Rev.*, **97**, 2005 (1997); R. Cotton, A. O. Agostion, J. C. Traeger., *Mass Spectros. Rev.*, 1479 (1995).

261. W. P. Griffith, C. A. Pumphrey and T. A. Rainey, *J. Chem. Soc.,Dalton Trans.*, 1125 (1986); A. M. Hendawy, W. P. Griffith and C. A. Pumphrey, *J. Chem. Soc., Dalton Trans.*, 1817 (1988).

262. A. B. P. Lever and B. S. Ramaswamy, *Can. J. Chem.*, **51**, 1582 (1973).

263. K. N. Kumar and R. R. Ramesh, *Polyhedron*, **14**, 1885-1892 (2005).

264. M. D. Godbole, E. Grigiotti, P. Zanello, A. M. Mills, A. L. Spek and E. Bouwwmann, *Inorg. Chim. Acta*, **358**, 233-238 (2005).

265. G. C. Percy and D. A. Thorton, *J. Inorg. Nucl. Chem.*, **35**, 2719 (1973).

267. C. P. Casey, *J. Organomet. Chem.*, **205**, 400 (1992).

268. R. T. K. Baker, S. J. Transter and J. A. Dumesic, "*Strong Metal Support Interactions*", Eds, American Chemical Society, Washington, D.C., 1986.

269. C. Frieden, *J. Chem. Educ.*, **62**, 917 (1985).

270. P. A. Vigato, S. Tamburini and D. E. Fenton, *Coord. Chem. Rev.*, **106**, 25 (1990).

271. R. G. Wilkins, *Chem. Soc. Rev.*, 171 (1992); E. I. Solomon, M. J. Baldwin and M. D. Lowery, *Chem. Rev.*, **521**, 92 (1992).

272. K. D. Karlin and J. Zubieta, "*Copper Coordination Chemistry*", vol. **1** and **2**, Adernine press, Guilderland, New York, 1984.

273. P. J. Riggs, R. Mei, C. F. Yocum and J. E. Penner-Holm, *J. Am. Chem. Soc.*, **114**, 10650 (1992).

274. C. G. Young and A. Wedd, "*In Molybdenum Enzymes, Cofactors and Model System*", Eds. E. I. Stiefel, D. Coucouvanis and W. E. Newton, A. C. S. Symposium Series 535, American Chemical Society; Washington, DC, 1993, p

275. W. P. G. Gaykema, A. Volbeda and W. G. J. Hol, *J. Mol. Biol.*, **187**, 255 (1985).

276. R. K. Andrews, R. L. Blakely and B. Zenner, "*Advances in Inorganic Biochemistry*" , G. L. Eichhorn and L. G. Marzilli, Eds., Elsevier, New York, vol. **5**, 1984, p. 245.

277. S. Mondal, R. N. Bose, J. W. Reed and E. S. Gould, *Inorg. Chem.*, **36**, 3159 (1996).

278. J. L. Beck, J. deJersey, B. Zerner, M. P. Hendrich and P. G. Debrunner, *J. Am. Chem. Soc.*, **110**, 3317 (1988).

279. D. C. Dalgarno and I. M. Armitage, *Adv. Inorg. Biochem.*, **6**, 113 (1984).

280. R. L. Lintvedt, W. E. Lynch and J. K. Zehetmair, *Inorg. Chem.*, **29**, 3009 (1990).

281. C. G. Young and A. G. Wedd, "*In Encyclopaedia of Inorganic Chemistry*", Ed.,

282. G. Davies, M. A. Ei-Sayed and A. El-Toukhy, *Chem. Soc. Rev.*, **21**,101 (1992); J. B. Carlson, G. Davies and P. Vorous, *Inorg. Chem.*, **33**, 2334 (1994).

283. U. Casellato, P. Guerriero, S. Tamburini, S. Sitran and P. A. Vigato, *J. Chem. Soc., Dalton Trans.*, 2145 (1991); D. G. McCollum, C. Fraser, R. Ostrander, A. L. Reingold and B. Bosnich, *Inorg. Chem.*, **33**, 2383 (1994).

284. D. Burdinskl, K. Weighardt and S. Stephan, *J. Am. Chem. Soc*, **121**, 10781 (1999).

285. L. Sun, H. Berglund-Baudin, R. Davydov, T. Norrby, L. Hammarstrom, P. Korall, A. Borje, C. Philouze, K. Berg, A. Tran, M. Andersson, G. Stenhagem, J. Martensson, M. Almgren, S. Styring and B. Akermark, *J. Am. Chem. Soc*, **119**, 6996 (1997).

286. S. W. Gersten, G. T. Samuels and T. J. Mayer, *J. Am. Chem. Soc.*, **104**, 4029-4030 (1982).

287. H. Taube, Comments, *Inorg. Chem.*, **1**, 17 (1981).

288. H. Berglund-Baudin, L. Sun, R. Davydov, M. Sundahl, S. Styring, B. Akermarck, M. Almgren and L. Hammarsteom, *J. Phys, Chem.*, **102**, 2512, (1998).

289. R. Robson, *Aust. J. Chem.*, **23**, 2217 (1970).

290. N. N. Pilkington and R. Robson, *Aust. J. Chem.*, **23**, 2225 (1970).

291. S. N. Podder, *Z. Anorg. Chem.*, **322**, 326 (1963).

292. U. Casellato, P. A. Vigato and M. Vidali, *Coord. Chem. Rev.*, **23**, 31 (1977).

293. D. E. Fenton, U. Casellato, P. A. Vigato and M. Vidali, *Inorg. Chim. Acta*, **82**, 57 (1982).

294. P. Zanello, S. Tamburini, P. A. Vigato and G. A. Mazzochin, *Coord. Chem. Rev.*, 77, 165 (1987).

295. U. Casellato, P. A. Vigato and M. Vidali, *Chem. Soc. Rev.*, **8**, 199 (1979).

296. D. W. Stephan, *Coord. Chem. Rev*, **95**, 41 (1989).

297. D. E. Fenton, S. Tamburini and P. A. Vigato, *Coord. Chem. Rev.*, **106**, 25 (1990).

298. M. J. Chetcuti, "*In Comprehensive Coordination Chcmistiy II*", E. W. Abel, F. G. A. Stone and G. W. Wilkinson (Eds), Pergaman, New York, vol. **10**, 1994, p. 23-84.

299. P. Guerriero, S. Tamburini and P. A. Vigato, *Coord. Chem. Rev.*, **139**, 17 (1995).

300. K. S. Murray, *Adv. Inorg. Chem.*, **43**, 261 (1995).

301. H. Okawa, H. Furutachi and E. Fenton, *Coord. Chem. Rev.*, **174**, 51-75 (1998).

302. N. Wheatly and P. Kalck, *Chem. Rev.*, **99**, 3379 (1999).

303. B. Carlson, G. Davies and P. Vorous, *Inorg. Chem.*, **23**, 2334 (1994).

304. C. Fraser and B. Bosnich, *Inorg. Chem.*, **33**, 338 (1994).

305. E. G. Lundquist, J. C. Hoffman, K. Folting, B. E. Maun, and K. G. Canltor, *Inorg. Chem.*, **29**, 128 (1990).

306. E. C. Constable and P. Harverso, *Polyhedron*, 1891 (1999).

307. Y. Nakamura, M. Yonmura. K. Arimura. N. Usuki. M. Ohba and H. Okawa, *Inorg. Chem.*, **40**, 3739 (2001).

308. T. Tanase, H. Inukai, T. Onaka, M. Kato, S. Yano and S. J. Lippard, *Inorg. Chem.*, **40**, 3943-3953 (2001).

309. R. M. D. Ward, D. Chatterjee and R. E. Shopherd, *Polyhedron*, **19**, 1339-1346 (2000).

310. R. L. Lintvedt and N. Ahmad, *Inorg. Chem.*, **21**, 2356 (1982).

311. T. A. Wark and D. W Stephan, *Inorg. Chem*, **26**, 363 (1987)

312. G. R. Davies, B. T. Kilbourn, *J. Chem. Soc*, 87 (1971).

313. Y. Pei., Y. Journaue and O. Kahn, *Inorg. Chem*, **27**, 399 (1988).

314. A. L. Balch, B. J. Davis and M. M. Olmstead, *Inorg. Chem.*, **28**, 3148-3153 (1989).

315. A. L. Balch, J. K. Nagle, D. P. Oram and P. E. Ready, *J. Am. Chem. Soc*, **110**, 454 (1988).

316. R. P. Bonomo, A. J. D. Bilio and G. Areana, *Inorg. Chim. Acta.*, **161**, 125 (1989).

317. P. Guerriero, S. Tamburini, P. A. Vigato and C. Benelli, *Inorg. Chim. Acta.*, **189**, 19-27 (1991).

318. P. Guerriero, P. A. Vigato and B. Burtet-Fabris, *Inorg. Chim. Acta*, **164**, 155 (1989).

319. U. Casellato, P. Guerriero, S. Tamburini, S. Sitran and P. A. Vigato, *J. Chem. Soc, Dalton. Trans.*, 2145 (1991).

320. C. Fraser, L. Johnston, A. L. Rheingold, B. S. Haggerty, G. K.Williams, J. Wholan and B. Bosnich, *Inorg. Chem.*, **31**, 1835-1844 (1992).

321. B. Chiswell, E. D. Mckenzie and L. F. Lindey, "*In Comprehensive Coordination Chemistry*", G. William son. Ed, Pergaman Press, New York. vol. **4**, ch. 41, 1987.

322. F. Lions, I. G. Dance and J. Lewis, *J. Chem. Soc., A*, 565 (1967).

323. A. Escuer, R. Vicente, J. Ribas, R. Costa and X-Solans, *Inorg. Chem.*, **31**, 2627-2633 (1992).

324. D. Gatteschi and A. Bensim, "*EPR spectra of oligonuclear Complexes, In Magneto Structural Correlations in Exchange Coupled systems*", R. D. Willet, D. Gatteschi and O. Kahn, Eds., NATO series, Reidel, Dordrecht, The Netherlands,1985.

325. M. Todokoro, H. Sabiyama, N. Matsumoto, M. Kodera, H. Okawa and S. Kida, *J. Chem. Soc., Dalton Trans.*, 313 (1992).

326. Y. Nonake, T. Tokii, and S. Kida. *Bull. Chem. Soc., Japan*, **47**, 312 (1974).

327. G. F. Kokoszka, M. J. Linzer, and G. Gordon, *Inorg. Chem.*, **1**, 1730 (1968); T. Kamiusubi, H. Okawa, E. Kitaura, M. Koikawa, H. Matsumoto, H. Oshio and S. Kida, *J. Chem. Soc., Dalton Trans.*, 2077 (1989).

328. C. P. Love, C. C. Torardi and C. J. Page, *Inorg. Chem.*, **31**, 1784 (1992)

329. D. P. Kessissoglou, C. P. Raptopoulou, E. G. Bakalbasis, A. Terzis, and J. Mrozinski, *Inorg.Chem.*, **31**(21), 4339-4345 (1992).

330. C. Fraser, R. Ostrander, A. L. Rheingold, C. White and B. Bosnich, *Inorg. Chem.*, **33**, 324 (1994); **31**, 4339 (1992).

331. S. R Breeze and S. Wang, *Inorg. Chem.*, **33**, 5113 (1994).

332. S.Wang, S. J. Trepanier and M. Wagrer, *Inorg. Chem.*, **32**, 833 (1993).

333. R. Guilard, S. Brandes, A. Tabard, N. Bouhmaida, C. Lecomte, P. Richard, and J. M. Latour, *J. Am. Chem. Soc*, **116**, 10202 (1994).

334. O. Cador, C. Mathoniere and O. Kahn, *Inorg. Chem.*, **36**, 1923 (1997).

335. P. Basu, A. M. Raitsiming, J. H. Enemark and F. A. Walker, *Inorg. Chem.*, **36**, 1088 (1997).

336. P. Basu, N. V. Shokircr, J. H. Enemark, and F. A. Walker, *J. Am. Chem. Soc*, **117**, 9042-9055 (1995).

337. I. Ramade, O. Kahn, Y. Jeanin and F. Robert, *Inorg. Chem*, **36**, 930 (1997).

338. A. Nantakumar, S. Fox, N. K. Murthy and K. D. Karlin, *J. Am. Chem. Soc.*, **119**, 3898 (1997), Z. Tyeklar, R. R. Jacobson, N. Wei, N. N. Murthy, J. J. Zubieta and K. D. Karlin, *J. Am. Chem.*, **115**, 2677 (1993).

339. J. M. Dominangnez-Vera, F. Camara, J. M. Morena, E. Colacio and H. Stoeckli-Evans, *Inorg. Chem.*, **37**, 3046 (1998).

340. M. Shinoura, S. Kida, M. Ohba, H. Okawa, H. Furutachi and M. Suzuki, *Inorg. Chem.*, **39**, 4520 (2000).

341. N. Fubita, M. Ogha, T. Shiga, H. Okawa and Y. Ajiro, *J. Chem.* Soc., *Dalton Trans.*, 64 (2001).

342. F. Osterloh, C. Achim and R. H. Holm, *Inorg. Chem.*, **40**, 224 (2001).

343. F. Osterloh, B. M. Segal, C. Achim and R. H. Holm, *Inorg. Chem.*, **39**, 980 (2000).

344. F. Osterloh, Y. Sanakis, R. J. Staples, E. Munch and R. H. Holm, *Angew Chem.*, Int. Ed. Engl., **38**, 2066 (1999).

345. R. Clirac, F. A. Cotton, K. R. Dunbar, C. A. Murillo and X. Wang, *Inorg. Chem.*, **40**, 420 (2001).

346. F. A. Cotton, C. A. Murillo, L. E. Roy and H. C. Zohn, *Inorg. Chem.*, **39**, 1743 (2001).

347. H. Nakano, A. Nakamura and K. Mashima, *Inorg. Chem.*, **35**, 4007 (1996).

348. S. R. Dutta, K. K. Nanda, U. Florke, M. Bhadhbade and K. Nag, *J. Chem. Soc, Dalton Trans.*, 2371 (1996).

349. G. Rombaut, S. Golhen, L. Ouahab, C. Mathoniere and O. Kahn, *J. Chem. Soc, Dalton Trans.*, 3609 (2000).

350. M. Kato, K. Nakajima., Y. Yoshikawa, M. Hirotsu, M. Kojima, *Inorg. Chim. Acta*, **311**, 69 (2000).

351. G. Rombaut, M. Verelst, S. Golhen, L. Ouahab, C. Mathoniene and O.Kahn, *Inorg. Chem.*, **40**, 1151 (2001).

352. D. Burdinski, K. Weighardt and S. Stephan, *J. Am. Chem. Soc.*, **121**, 10781 (1999).

353. H. Taube, *Pure Appl. Chem.*, **51**, 901(1979); 63, 651 (1991).

354.Georgi and Tocher, *Polyhedron*, **18**, 2981 (1999).

355. R. L. Lintvedt, B. A. Schoenfelner, C. Ceccarelli and M. D. Glick, *Inorg. Chem.*, **23**, 2867 (1984); R. L. Lintvedt and Z. K. Zehetmair, *Inorg. Chem.*, **29**, 220 (1990).

356. L. M. Vogler, Brian Scott and K. J. Brewer, *Inorg. Chem.*, **32** (6), 898-903 (1993).

357. D. A. Roberts and G. L. Geoffroy, G. Wilkinson and F.G.A. Stone (Eds), "*Comprehensive Organometallic Chemistry*", Pergamon, Oxford, vol **6**, ch. 40, 1982.

358. D. E. Fenton and S. E. Gayda, *Inorg. Chim. Acta*, **14L**,111 (1975).

359. B. Tomlonovic, R. L. Hough, M. D. Glick and R. L. Lindvedt, *J. Am. Chem. Soc.*, **97**, 2925 (1975).

360. Mark M. Richter and Karen J. Brewer, *Inorg. Chem.*, **31**, 1594-1598 (1992).

ABSTRACT

Chapter-I

Introduction and Literature Survey

This chapter presents a brief account of the importance of the monometallic complexes of the metal ions manganese and ruthenium selected in the present study in various fields such as biological, homogeneous catalysis and synthesis of solid state phases of industrial and technological importance.

This is followed by description of various characteristic coordination modes of the dihydrazones.

At the end, it also deals with the relevant literature on transition and non-transition metal complexes of dihydrazones derived from condensation of aryl, aroyl, pyridoyl dihydrazones and thiocarbohydrazides with variety of aldehydes and ketones as well as on dihydrazones derived from condensation of dialdehydes and diketones with monoacylhydrazines, pyridoylhydrazines, thiosemicarbozide and related ligands. An effort has been made to survey literature on all these ligands up-to date.

Chapter-II

Experimental

In this chapter the experimental details regarding the preparation of adipoyldihydrazine, disalicylaldehyde adipoyldihydrazone and bis(2-hydroxy-1-naphthaldehyde)adipoyldihydrazone have been described. Procedure for elemental analysis, physico-chemical techniques and instruments used are also described.

Chapter-III

Synthesis, Characterization and Structural Assessment of Monometallic Manganese(II) Complexes derived from Polyfunctional Adipoyldihydrazones

This chapter deals with the preparation, characterization and structural assessment of fourteen monometallic manganese(II) complexes derived from polyfunctional disalicylaldehyde adipoyldihydrazone ($slahH_4$) and bis(2-hydroxy-1-naphthaldehyde)adipoyldihydrazone ($npahH_4$) ligands.

In the beginning, a brief account of literature in respect of coordination behaviour of ligands related to adipoyldihydrazone such as monoacylhydrazines, monoaroyldihydrazines and their hydrazones, acyldihydrazines, aroyldihydrazines, pyridoyldihydrazines, simple dihydrazones and dihydrazones containing hydroxy groups, is discussed.

The monometallic manganese(II) complexes of the compositions $[Mn^{II}(slahH_2)(H_2O)_2]$ (1), $[Mn^{II}(npahH_2)]$ (8), $[Mn^{II}(slahH_2)(A)_2].nH_2O$ (where A = py(pyridine, 2); 2-pic(2-picoline, 3); 3-pic(3-picoline 4); 4-pic(4-picoline, 5), (n = 0, 1)), $[Mn^{II}(npahH_2)(A)_2]$ (where A = py(pyridine, 9); 2-pic(2-picoline, 10); 3-pic(3-picoline, 11); 4-pic(4-picoline, 12), (n = 0, 1)),$[Mn^{II}(slahH_2)(NN)]$ (where NN = bpy(2, 2' bipyridine, 6), phen(1, 10-phenanthroline, 7)) and $[Mn^{II}(npahH_2)(NN)]$ (where NN = bpy(2, 2' bipyridine, 13) and phen(1, 10-phenanthroline, 14)) were isolated.

The complexes (1) to (7) are dull or light brown in colour while complexes (8) to (14) are yellowish brown in colour. All of the complexes are air-stable and decompose above 300 °C without melting.

The mass spectral signal at m/z value equal to 536 of the complex (8) indicates its monomeric nature.

The molar conductance values in the range 1.5-3.7 ohm^{-1} cm^2 $mole^{-1}$ for these complexes are attributed to their non-electrolytic nature in DMSO solution.

The μ_{eff} value for the complex (8) is 1.12 B.M which indicates that the complex is in the low-spin state. This value is much less than the values reported for the Mn(II) complexes in the low-spin state. This indicates considerable interaction between metal ions in the structural unit of the complex in the solid state.

On the other hand, the μ_{eff} values for remaining complexes fall in the range 5.79-6.02 B.M. These values lie well within the range reported for Mn(II) complexes in the high-spin state ($t_{2g}^3 e_g^2$, S = 5/2).

The essential features of the ligand bands in the electronic spectra of the complexes suggest that the ligands are bonded to the metal centre in the same conformation as in the uncoordinated state.

In addition to the intra-ligand bands, the complexes of $npahH_4$ possess one additional absorption bands in the region 448-600 nm, respectively in their electronic spectra. These bands can be assigned to the charge transfer transitions from phenolate/naphtholate oxygen atom to the metal centre.

The EPR spectrum of the complex (8) in the polycrystalline state shows an isotropic spectrum with g = 2.019. The width of the signal at g = 2.019 is about 330 G which indicates spin-exchange between manganese(II) centres in the solid state which is consistent with very low μ_{eff} value of the complex. The width of the signal in the g = 2.019 region is increased to about 500 G in DMSO solution. This rules out the possibility of the presence of any exchange interaction between the metal centres in DMSO solution.

The central resonance in this complex shows splitting into five components with average nitrogen superhyperfine splitting constant A_N equal to 12 G indicating coordination of two nitrogen atoms to the manganese metal centre.

The remaining complexes show EPR spectral features characteristic of Mn(II) in high spin state. The isotropic g-values lie in the region 1.994-2.050.

The uncoordinated ligands show a strong band at 1679 and 1666 cm^{-1} which are assigned to νC=O stretching vibration. The band at 1679 cm^{-1} in free $slahH_4$ disappears in the IR spectra of the complexes (1) to (5) indicating that the ligand $slahH_4$ coordinate to the metal centre in enol form. On the other hand, these bands appear in the region 1640-1680 cm^{-1} in the remaining complexes. This indicates coordination of the ligands to the metal centre in keto form. However, the νC=O band is shifted either to lower frequency by about 10-26 cm^{-1} as in the complexes (6) to (10) and (13), (14) or remains almost unshifted in position as in the complexes (11) and (12). Such a feature associated with νC=O band in the IR spectra of the complexes rule out the possibility of coordination of >C=O group to the metal centre because the >C=O group absorbs almost in the same region in these complexes in which uncoordinated >C=O groups have been reported to absorb in dihydrazone metal complexes as has been confirmed by X-ray crystallography. The lower shift of νC=O band has been attributed to involvement of >C=O groups in the strong intermolecular H-bonding with secondary NH group in the complexes. The bands observed at 1620 and 1630, 1573 cm^{-1} in free dihydrazones are attributed to νC=N stretching vibrations. These bands, on an average, shift to lower frequency by 2-15 cm^{-1} in the complexes indicating coordination of >C=N group to the metal centre.

In the dihydrazones, a strong band appears at 1275 cm^{-1} in $slahH_4$ and a medium intensity band at 1281 cm^{-1} in $npahH_4$, respectively. These bands are assigned to β(C-O)(phenolic/naphtholic). In the complexes (1) to (7) derived from $slahH_4$, this band,

on an average, undergoes shift to lower position by 5 to12 cm^{-1} while in the complexes (8) to (14) derived from $npahH_4$, this bands shifts to higher frequency by 2 to 20 cm^{-1}. Such a feature associated with β(C-O) band in these complexes suggests involvement of phenolic/naphtholic C-O group in coordination. The shift of β(C-O)(phenolic) to lower position in the complexes (1) to (7) may be related to flow of π-electron density of aromatic ring to metal centre through azomethine group while the shift of β(C-O)(naphtholic) band to higher frequency in the complexes (8) to (14) suggest that the π-electron density of aromatic ring in these complexes flow to metal centre through naphtholate oxygen atom. The complex (1) shows a distinct band at 635 cm^{-1} which is attributed to arise from rocking mode of coordinated water molecules to the metal centre. The free pyridine bases absorb at around ~604 cm^{-1} due to in-plane ring deformation mode. In the complexes (2), (4) to (7) and (9) to (14), a new medium to weak band is observed in the region 657-696 cm^{-1}. This band has been assigned to arise due to in-plane ring deformation mode of coordinated pyridine bases.

The complexes have been characterized by cyclic voltammetry also.

At the end, the tentative structures for the complexes have been proposed.

Chapter-IV

Synthesis and Characterization of Monometallic Manganese(IV) complexes of Bis(2-hydroxy-1-naphthaldehyde)adipoyldihydrazone

The present chapter describes the synthesis and characterization of Mn(IV) complexes derived from bis(2-hydroxy-1-naphthaldehyde)adipoyldihydrazone ($npahH_4$).

The complexes of the compositions $[Mn^{IV}(npah)(A)_2].nH_2O$ and $[Mn^{IV}(npah)(NN)]$ (where A = H_2O. (15); py. (16); 2-pic. (17); 3-pic. (18); 4-pic.

(19); NN = bpy, (20); phen, (21), (n = 0, 1)) were isolated.

All of the complexes are shining black. They are air stable. All of the complexes decompose above 300 °C without melting. The complexes are insoluble in water and common organic solvents such as ether and benzene. The complexes are sparingly soluble in methanol, acetonitrile and dichloromethane. They are completely soluble in DMSO and DMF.

The complex (17) was characterized by FAB mass spectra as representative sample to assess the molecular complexity of the complexes. The mass spectrum of the complex (17) shows a signal at m/z value 536, which most probably, results from the formation of $[Mn(npah)]^+$ species. Such a feature of the mass spectrum of the complex shows its monomeric nature.

The molar conductance values for the complexes in DMSO indicate that they are all non-electrolytic in nature.

The magnetic moment values for the complexes lie in the range 3.83-4.39 B.M. The μ_{eff} values suggest the presence of Mn(IV) centres in the complexes.

The electronic spectra of all the complexes recorded in DMSO show red shift of ligand bands that gives a good evidence of chelation of dihydrazone to the metal centre. The magnitude of shift of ligand bands indicates strong bonding between the ligand and the metal. The ligand bands show almost similar feature in the complexes as in case of manganese(II) complexes in Chapter III and in the uncoordinated ligand indicating that the conformation of the ligand in the complexes remains almost the same as that in the uncoordinated state. In addition to the ligand bands, the complexes show a cluster of three bands in the region 400-470 nm. A band in this region is assigned to $^4T_{2g} \leftarrow {}^4A_{2g}$ transition. One band in this region is assigned to ligand band at 363 nm. But it is difficult to pin point which of the bands arises from ligand band

The complexes (16) and (18) showed featureless EPR spectra in the solid state as

the solid state and in the solution state. The former resonance is of greater intensity in the solid state but for glassy state, the resonances are almost of the same intensity. For the complexes (20) and (21), $g_{\perp} \sim 5.0$ and $g_{\parallel} \sim 2.0$ with the signal at former g-value being of low intensity is observed in both crystalline and glassy state. The EPR signal at $g \cong 2$ shows ^{55}Mn hyperfine splitting constant is equal to 80 G in complexes (20) and (21) which is closer to the values observed for Mn(IV) than that for Mn(II).

The complexes (16) — (18) showed featureless EPR spectra in the solid state as well as in the solution state at R.T and liquid nitrogen temperature. Hence, the complexes (15) and (19) to (21) only have been analyzed by EPR spectroscopy. All of these complexes exhibit highly anisotropic EPR spectra in polycrystalline state as well as in the glassy state.

The EPR spectra reveals that the ligand provides effective electronic environment for the metal that is highly distorted in the ground state in the complexes (15) and (19) but only slightly distorted in the ground state in the complexes (20) and (21). The distortion is sensitive to geometrical orientation of the donor atoms. The effective environment of Mn(IV) lie close to ideally pseudo-octahedral environment.

The essentially contrasting EPR spectra of the complexes (15) and (19) as compared to those of the complexes (20) and (21) has been related to coordination of the nitrogen donor atoms from co-ligands bipyridine and 1, 10-phenanthroline in the complexes (20) and (21) which occupy *cis*-position around the metal atoms by virtue of their geometry while the donor atoms from co-ligands in the complexes (15) and (19) occupy *trans*-positions.

The dihydrazone is coordinated to the metal centre in enol form in all of the complexes. The νC=N bands observed at 1630 and 1593 cm^{-1} in free dihydrazone shift to lower frequency, on an average by 3-11 cm^{-1}. This indicates coordination of azomethine nitrogen atoms to the metal centre. The νC=N bands appear as a couple

of bands in metal complexes. The existences of two bands of almost same intensity similar to that in the uncoordinated dihydrazone suggest that the ligand retains same conformation in the complexes as in the uncoordinated state. The free dihydrazone shows a medium intensity band at 1281 cm^{-1} attributed to β(C-O) vibrations. This band shifts to higher frequency by 1-18 cm^{-1} in all of the complexes indicating coordination of naphtholic C-O group to the metal centre in the complexes. The complexes (17) to (19) and (21) also show a weak band in the region 650-660 cm^{-1} which is assigned to arise due to in-plane ring deformation modes of pyridine bases indicating their coordination to the metal ion.

The bands observed in the region 265 to 280 cm^{-1} as weak bands in the complexes (16) to (19) and (21) are assigned to ν(M-N) band from coordinated pyridine or substituted pyridine bases. The non-ligand band appearing in the region 510-526 cm^{-1} is tentatively assigned to νM-O(naphtholate).

These complexes have also been characterized by cyclic voltammetry.

The tentative structures for the complexes have been proposed at the end.

Chapter-V

Synthesis and Characterization of Monometallic Ruthenium(II) Complexes of Disalicylaldehyde adipoyldihydrazone and Bis(2-hydroxy-1-naphthaldehyde) adipoyldihydrazone

The introductory part dwells briefly on the rationality for selecting ruthenium in the present study. Subsequently, it describes the importance of ruthenium complexes in various fields like photochemistry, photocatalyis, biology and electrochemistry. The chapter describes following complexes

(1) $[Ru^{II}(slahH_4)(H_2O)_2]Cl_2$ (22)

(2) $[Ru^{II}(slahH_4)(A)_2]Cl_2$ [A = py, (23); 2-pic, (24); 3-pic, (25); 4-pic, (26)]

(3) $[Ru^{II}(slahH_4)(bpy)]Cl_2$ (27)

(4) $[Ru^{II}(slahH_4)(phen)]Cl_2$ (28)

(5) $[Ru^{II}(npahH_4)(A)_2]Cl_2$ [A = H_2O, (29); py, (30); 2-pic, (31); 3-pic, (32); 4-pic, (33)]

(6) $[Ru^{II}(npahH_4)(bpy)]Cl_2$ (34)

(7) $[Ru^{II}(npahH_4)(phen)]Cl_2$ (35)

The complexes have been prepared by four general methods.

All of the complexes are amorphous in nature. Their colour ranges from brown, grey to dull green. All of these complexes melt in the temperature range 210-240 °C and are stable for some period of time. They then decompose and change their colours and become brown. When the complexes are dissolved in DMF, they yield a mixture of colours. All of these complexes are insoluble in water and other common organic solvents such as ethanol, methanol, acetone, CCl_4, $CHCl_3$, ether and benzene. However, they are partially soluble in acetonitrile and completely so in DMSO and DMF.

The molar conductance values for the complexes suggest that they are non-electrolyte in DMSO. All of the complexes are diamagnetic indicating presence of ruthenium in the +2 oxidation state consistent with low spin d^6 configuration of the metal centre.

In addition to ligand bands the complexes show either one or two moderate –to-strong bands in the 540-690 nm region. The band in the region 614 -690 nm has been assigned to the spin–allowed $^1A_{1g} \rightarrow {}^1T_{1g}$ transition while the band in the region 545-604 nm to $^1A_{1g} \rightarrow {}^1T_{2g}$ transition. Further, the complexes show a strong band in the region 429-470 nm. The molar extinction

coefficient for this band lies in the region 678-3500 $dm^3mol^{-1}cm^{-1}$. Such a high intensity of this band indicates that it owes its origin to the charge transfer, most probably from metal-to-ligand.

The complexes (25), (27), (29), (32) and (34) were characterized by ^1H NMR spectroscopy. Two proton doublet observed in the regions δ 11.20-12.665 ppm and δ 10.18-11.26 ppm downfield of TMS have been assigned to δOH and δNH protons while those in the region δ 8.20-9.15 ppm to δ-CH=N protons, respectively. The multiplets appearing in the region δ 6.90-8.42 ppm have been assigned to phenyl/naphthyl protons. The dihydrazones show doublets in the region δ 2.11-2.58 ppm which are assigned to methylene protons $(-CH_2-)_4$.

δOH proton signals remain almost unshifted on complexation. This indicates that the phenolic/naphtholic –OH groups are not deprotonated even on complexation.

Signals observed in the region δ10.18-11.26 ppm and δ 8.26-9.15 ppm also retain essentially similar position in the complexes which rules out the possibility of coordination of secondary NH nitrogen atom or azomethine group to the metal centre. It appears that the effect of coordination on downfield shifting of the δ-CH=N proton signal is almost the same as that of H-bonding i.e. the non-shift of δ-CH=N-signals may be related to the difference of bonded species to the azomethine group i.e. >CH=N....H to >CH=N→M. It is worth mentioning that δOH and δ-CH=N- signals appear in the form of two signals in all of the complexes. This may be related to coordination of dihydrazone to the metal centre in anti-cis configuration.

The complexes (25) and (32) show an intense signal at δ 2.54 and 2.50 ppm due to methyl protons of 3-picoline molecules. Features associated with 2-pyridyl protons of pyridine, 3-picoline, and 4-picoline confirm flow of electron density from ring nitrogen atoms of these donor molecules. The naphthyl protons multiplet appears

in the region δ 7.11-8.42 ppm. The complexes (29), (32) and (34) have been characterized by ^{13}C NMR spectroscopy as well which confirm the findings of ^{1}H NMR spectroscopy.

IR spectral evidences confirm the findings obtained from ^{1}H NMR and ^{13}C NMR spectra.

Electron transfer reaction some of the complexes have been studied by cyclic voltammetry.

Chapter-VI

Synthesis and Characterization of Heterobimetallic Complexes of Manganese and Ruthenium Derived From Disalicylaldehyde adipoyldihydrazone and Bis(2-hydroxy-1-naphthaldehyde)-adipoyldihydrazone

The introductory part of the chapter dwells briefly on the importance of monometallic and heterobimetallic complexes in various fields like metalloenzymes, homogeneous catalysis and synthesis of solid state phase of industrial and technological importance followed by brief literature on heterobimetallic complexes in general and on manganese and ruthenium complexes in particular.

Heterobimetallic complexes of the compositions $[Mn^{IV}Ru^{II}(slah)(A)_3Cl]Cl.nH_2O$ (where A = H_2O, (36); py, (37); 2-pic, (38); 3-pic, (39); 4-pic, (40), (n = 0, 3)) and $[Mn^{IV}Ru^{II}(npah)(A)_3Cl]Cl.nH_2O$ (where A = H_2O, (41); py, (42); 2-pic, (43); 3-pic, (44); 4-pic, (45), n = 0, 3)) were isolated.

The complexes vary in colour from yellow, brown, dull green, muddy brown, brownish green to dark green. The complexes are partially soluble in acetonitrile, CH_2Cl_2 and insoluble in methanol, ethanol, CCl_4, $CHCl_3$, ether, benzene etc. All of them are freely soluble in DMSO and DMF. All of the complexes decompose above

300 °C. The molar conductance values for the complexes (36) to (45) at 10^{-3} M dilution in DMSO solution lie in the region 35.5–29.7 ohm^{-1} cm^2 mol^{-1}. The molar conductance values for the complexes suggest their 1:1 electrolytic nature.

The magnetic moments for all of the complexes in the present study fall in the region 3.02–4.12 B.M. These values are close to the spin–only value for a d^3 Mn(IV) system i.e. it exhibits a magnetic moment for monomanganese(IV) derivatives corresponding to uncoupled S = 3/2 system. Such a magnetic behaviour of these complexes suggest the presence of Mn(IV) and Ru(II) in these complexes.

The complexes (36) to (40) and (43) show more number of bands than those present in the free ligands due to splitting of ligand bands which is the result of heterobimetallic complex formation. These bands have been attributed to arise due to $n\rightarrow\pi^*$ and $\pi\rightarrow\pi^*$ transitions located on the ligands. In addition to the ligand bands, the complexes show additional bands in the region 439-732 nm. The band of lowest energy observed in the visible region for the complexes (38) and (40) to (45) between 548-732 nm region is assigned to d-d transition mainly localized on Mn(IV) centre but it is also expected to have contribution from Ru($d\pi$)–π^*(L) transition as these bands have appreciably high molar extinction coefficient values.

The EPR spectral features of the complexes are characteristic of the presence of Mn(IV) and Ru(II) in the complexes. This is evident from the fact that the spectra of the complexes show a strong signal at $g \cong 2$ and another weak signal at $g \cong 4$. The complexes do not show any new signal in the 0–4000 G range which could be assigned to arise due to Ru(III).

The essential features of the IR bands in the region 3000-3600 cm^{-1} indicate the involvement of phenolic –OH/naphtholic –OH group in bonding via deprotonation. The ligand is coordinated to the metal centre in the enol form. The IR structural features of these complexes suggest that the water molecules are not coordinated to

the metal centre in the complexes (38) to (40) and (44). In all these complexes a strong band appears in the region 1600-1613 cm^{-1} attributed to >C=N-N=C< group that indicates condensation of $-NH_2$ group of hydrazide and >C=O group of salicylaldehyde/2-hydroxy-1-naphthaldehyde. The position of this band lies in the region where azomethine nitrogen has been suggested to coordinate to the metal centre in hydrazone complexes. The higher shift of ν(C-O) band in the complexes suggests bonding through phenolate/naphtholate oxygen to the metal centre and reflects strength of (M-O) phenolate/naphtholate band.

All the complexes show a weak to medium intensity non-ligand band in the region 815-857 cm^{-1} which is characteristic of tetraatomic species 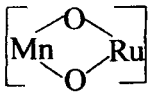

which results from the involvement of phenolate/naphtholate oxygen atom in bridge formation. The band in the region 241–244 cm^{-1} is assigned to νM-N (M = Mn, Ru) stretching frequency due to coordination of pyridyl ring nitrogen atom to the metal centre.

Weak to medium intensity band is observed in the region at 302-307 cm^{-1} in the complexes which is assigned to ν(Ru-Cl).

The electron-transfer reactions of the complexes have been studied with the help of cyclic voltammetry.

List of Figures

Chapter-III

Cyclic voltammograms

3.5.1 Cyclic voltammogram of Ligand Disalicylaldehyde adipoyldihydrazone ($slahH_4$)

3.5.2 Cyclic voltammogram of Ligand Bis(2-hydroxy-1-naphthaldehyde)adipoyldihydrazone ($npahH_4$)

3.5.3 **(a), (b)** and **(c)** Cyclic voltammograms of complex $[Mn^{II}(slahH_2)(H_2O)_2]$ **(1)** at scan rates **(a)** 100 mV/s **(b)** 300 mV/s **(c)** 500 mV/s

3.5.4 Cyclic voltammogram of complex $[Mn^{II}(slahH_2)(py)_2].H_2O$ **(2)** at scan rate 100mV/s

3.5.5 **(a), (b), (c), (d)** and **(e)** Cyclic voltammograms of complex $[Mn^{II}(slahH_2)(2\text{-pic})_2].H_2O$ **(3)** at scan rates **(a)** 100 mV/s **(b)** 200 mV/s **(c)** 300 mV/s **(d)** 400 mV/s **(e)** 500 mV/s

3.5.6 **(a)** and **(b)** Cyclic voltammograms of complex $[Mn^{II}(slahH_2)(3\text{-pic})_2].H_2O$ **(4)** at scan rates **(a)** 100 mV/s **(b)** 200 mV/s

3.5.7 **(a)** and **(b)** Cyclic voltammograms of complex $[Mn^{II}(slahH_2)(4\text{-pic})_2].H_2O$ **(5)** at scan rates **(a)** 100 mV/s **(b)** 200 mV/s

3.5.8 Cyclic voltammogram of complex $[Mn^{II}(slahH_2)(phen)]$ **(7)** at scan rate 100 mV/s

3.5.9 **(a)** and **(b)** Cyclic voltammograms of complex $[Mn^{II}(npahH_2)(py)_2]$ **(9)** at scan rates **(a)** 5 mV/s **(b)** 100 mV/s

3.5.10 Cyclic voltammogram of complex $[Mn^{II}(npahH_2)(4\text{-pic})_2]$ **(12)**

3.5.11 **(a)** and **(b)** Cyclic voltammograms of complex $[Mn^{II}(npahH_2)(bpy)]$ **(13)** at scan rates **(a)** 5 mV/s **(b)** 100 mV/s

Suggested structures for complexes

3.6.1 Suggested structure for complex $[Mn^{II}(slahH_2)(A_2)].nH_2O$ (A= H_2O, **(1)**; py, **(2)**; 2-pic, **(3)**; 3-pic, **(4)** and 4-pic, **(5)**; (n = 0, 1))

3.6.2 Suggested structure for complex $[Mn^{II}(slahH_2)(\overset{\frown}{NN})]$ ($\overset{\frown}{NN}$ = bpy, **(6)** and phen, **(7)**)

3.6.3 Suggested structure for complex $[Mn^{II}(npahH_2)]$ **(8)**

3.6.4 Suggested structure for complex $[Mn^{II}(npahH_2)(A_2)]$ (A= py, **(9)**; 2- pic, **(10)**; 3-pic, **(11)** and 4-pic, **(12)**) .

3.6.5 Suggested structure for complex $[Mn^{II}(npahH_2)(\overset{\frown}{NN})]$ ($\overset{\frown}{NN}$ = bpy, **(13)** and phen, **(14)**)

Chapter-IV

Mass spectrum

4.1.1 Mass spectrum of complex $[Mn^{IV}(npah)(2\text{-pic})_2]$ **(17)**

Suggested structures

5.6.1 Suggested structure for complex $[Ru^{II}(slahH_4)(A)_2]Cl_2$ (where A = H_2O, **(22)**; py, **(23)**; 2-pic, **(24)**; 3-pic, **(25)** and 4-pic, **(26)**)

5.6.2 Suggested structure for complex $[Ru^{II}(slahH_4)(\overset{\frown}{NN})]Cl_2$ ($\overset{\frown}{NN}$ = bpy, **(27)** and phen, **(28)**)

5.6.3 Suggested structure for complex $[Ru^{II}(npahH_4)(A)_2]Cl_2$ (A = H_2O, **(29)**; py, **(30)**; 2-pic, **(31)**; 3-pic, **(32)** and 4-pic, **(33)**)

5.6.4 Suggested structure for complex $[Ru^{II}(npahH_4)(\overset{\frown}{NN})]Cl_2$ (where $\overset{\frown}{NN}$ = bpy, **(34)** and phen, **(35)**)

Chapter-VI

Electronic spectra

6.1.1 Electronic spectrum of complex $[Mn^{IV}Ru^{II}(slah)(H_2O)_3Cl]Cl.3H_2O$ **(36)**

6.1.2 Electronic spectrum of complex $[Mn^{IV}Ru^{II}(slah)(2\text{-}pic)_3Cl]Cl.3H_2O$ **(38)**

6.1.3 Electronic spectrum of complex $[Mn^{IV}Ru^{II}(slah)(4\text{-}pic)_3Cl]Cl$ **(40)**

6.1.4 Electronic spectrum of complex $[Mn^{IV}Ru^{II}(npah)(H_2O)_3Cl]Cl$ **(41)**

6.1.5 Electronic spectrum of complex $[Mn^{IV}Ru^{II}(npah)(2\text{-}pic)_3Cl]Cl$ **(43)**

6.1.6 Electronic spectrum of complex $[Mn^{IV}Ru^{II}(npah)(4\text{-}pic)_3Cl]Cl$ **(45)**

EPR spectra

6.2.1 (a) EPR powder spectrum of complex $[Mn^{IV}Ru^{II}(slah)(H_2O)_2]$ **(36)** at LNT

(b) EPR spectrum of complex $[Mn^{IV}Ru^{II}(slah)(H_2O)_2]$ **(36)** in DMSO solution at LNT

6.2.2 (a) EPR powder spectrum of complex $[Mn^{IV}Ru^{II}(slah)(2\text{-}pic)_3Cl]Cl.3H_2O$ **(38)** at LNT

(b) EPR spectrum of complex $[Mn^{IV}Ru^{II}(slah)(2\text{-}pic)_3Cl]Cl.3H_2O$ **(38)** in DMSO solution at LNT

6.2.3 (a) EPR powder spectrum of complex $[Mn^{IV}Ru^{II}(slah)(4\text{-}pic)_3Cl]Cl.3H_2O$ **(40)** at LNT

(b) EPR spectrum of complex $[Mn^{IV}Ru^{II}(slah)(4\text{-}pic)_3Cl]Cl.3H_2O$ **(40)** in DMSO solution at LNT

6.2.4 EPR powder spectrum of complex $[Mn^{IV}Ru^{II}(npah)(H_2O)_3Cl]Cl$ **(41)** at LNT

6.2.5 EPR powder spectrum of complex $[Mn^{IV}Ru^{II}(npah)(3\text{-}pic)_3Cl]Cl.3H_2O$ **(44)** at LNT

IR spectra

6.3.1 (a) and **(b)** IR spectrum of complex $[Mn^{IV}Ru^{II}(slah)(H_2O)_3Cl]Cl.3H_2O$ **(36)**

6.3.2 (a) and **(b)** IR spectrum of complex $[Mn^{IV}Ru^{II}(slah)(py)_3Cl]Cl$ **(37**

ANNEXURE-I

Bis(2-hydroxy-1-naphthaldehyde)azine has been isolated from a complex reaction mixture of $RuCl_3.3H_2O$, bis(2-hydroxy-1-naphthaldehyde)adipoyldihydrazone ($npahH_4$) in the presence of 3-picoline in methanol. The structure of the compound is established with the help of X-ray crystallographic study and is reported in the Annexure-I. The results have been published in International Journal of Synthesis and Characterization, 2008.

Isolation of Bis(2-hydroxy-1-naphthaldehyde)azine from a complex reaction mixture and its X-ray crystallographic characterization

---

R. A. Lal*, D. **Basumatary** and A. Kumar, International Journal of Synthesis and Characterization, **1**, 1-4, 2008.

International Journal of Syntheses and Characterization 1(1), *(January-June 2008) pp. 1-4*

Isolation of Bis (2-hydroxy-1-naphthaldehyde) Azine from a Complex Reaction Mixture and its X-ray Crystallographic Characterization

Ram A. Lal[1]*, Debajani Basumatary[1], Arjun K. De[2] & Arvind Kumar[3]

[1]*Department of Chemistry, North-Eastern Hill University, Shillong-793022, Meghalaya, India.*

[2]*Department of Chemistry, Tripura University, Suryamaninagar-799130, Tripura, India.*

[3]*Institute of Chemistry, Academia Sinica 128, Academia Road, Sec.2, Nankag, Taipei 115, ROC.*

Abstract: Bis(2-hydroxy-1-naphthaldehyde) azine has been isolated from a complex reaction mixture of $RuCl_3.H_2O$ and bis (2 hydroxy-1-naphthaldehyde)adipoyldihydrazone in methanol. The structure of the compound is unequivocally established with the help of X-ray crystallographic study. The structure consists of two naphthalidene groups connected by –N-N– moiety arranged in trans-forms about the –N=N– bond with a –C(10)-C(11)-N(1)-N(1A) torsional angle 179.3 °. The molecule is essentially a planar structure giving rise to an extended conjugation. The bond between N(1)-N(1A) is comparable to other reported structures of related compounds. The crystal structure is stabilized by the two intermolecular hydrogen bonds between O atoms and the π-π interactions between the naphthyl rings.

Key words: Bis(2-hydroxy-1-naphthaldehyde)azine, isolation, X-ray crystallography.

PACS: 61.10Nz

Introduction

Hydrazones continue to be a field of interests as it constitutes one of the best derivatives with the potential application in medicine [1-3], analytical chemistry [4] and other scientific and technological fields [5, 6]. Hydrazones are very good chelating agents as well and have been widely studied as chelating ligands for the spectroscopic and flurometric determination of trace metal ions [7]. The metal complexes derived from polyfunctional dihydrazone continue to attract attention of workers in this field because they can yield monometallic, homobimetallic, heterobimetallic, homotrimetallic and heterotrimetallic complexes which find diverse applications in many fields such as metalloenzymes, homogeneous, heterogeneous catalysis and synthesis of solid state phases of industrial importance. Because of this, we [7, 8] and others [9, 10] have been interested in synthesis, characterization and structural characterization of metal complexes derived from dihydrazones containing azomethine, phenol and amide functions in duplicate and pyridyl nitrogen. While synthesizing monometallic ruthenium complexes of bis(2-hydroxy-1-naphthaldehyde) adipoyldihydrazone (Fig. 1) from reaction of $RuCl_3.3H_2O$ with the title ligands in methanol in the presence of 3-picoline and purifying by column chromatography, we came with a hitherto crystalline yellow azine which was devoid of metal complexation. This compound was characterized crystallographically. Accordingly, the crystal structure of the compound is reported in this communication (Fig. II).

Experimental

$RuCl_3.3H_2O$, diethyladipate, hydrazine hydrate and 2-hydroxy-1-naphthaldehyde were of E-Merck grade. Adipoylhydrazine was prepared by reacting diethyl adipate (1 mol) with hydrazine hydrate (2 mols) and recrystallizing from methanol. Bis(2-hydroxy-1-naphthaldehyde) adipoyldihydrazone ($naphH_4$) was prepared by reacting a solution of adipoyldihydrazone (1 mol) in ethanol with 2-hydroxy-1-naphthaldehyde under hot condition. The yellow precipitate obtained on cooling the solution, was washed thoroughly with ethanol and air dried (m.p. = 305 °C).

Isolation of bis (2-hydroxy-1-naphthaldehyde)azine

In order to isolate a ruthenium complex of the title ligand, $RuCl_3.3H_2O$ (1 g, 3.78 mM) in methanol was allowed to react with $naphH_4$ (1.8 g, 3.75 mM) in 1:1 molar ratio followed by addition of 3-picoline (3.492g, 30.74 mM) accompanied by vigorous stirring for half an hour at room temperature maintaining the molar ratio at 1:1:10 ($RuCl_3.3H_2O$: $naphH_4$: 3-pic) in methanol. The reaction mixture was refluxed for 1hr. A brownish

green precipitate was obtained which was filtered and washed with methanol. In order to purify the above compound by column chromatography the column was loaded with a solution of the complex. On eluting the column with pure acetonitrile, a yellow solution was obtained as the first fraction. This fraction on evaporation gave us yellow crystal suitable for X-ray analysis (m. p. 280 °C).

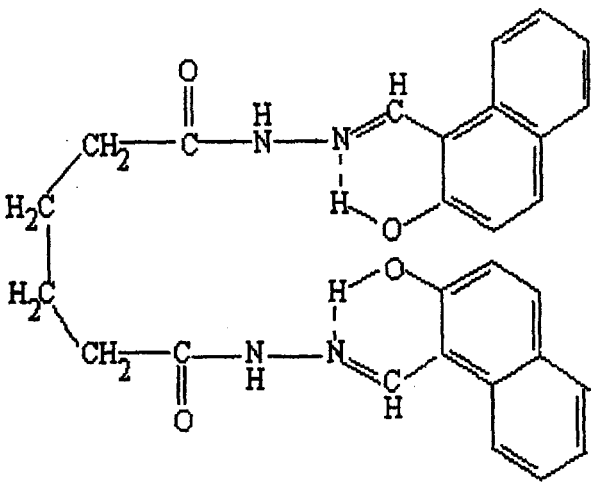

Figure I: Bis(2-hydroxy-1-naphthaldehyde)-adipoyldihydrazone ($naphH_4$)

Crystal Structure Determination

Suitable X-ray quality crystals of the compound were grown by solvent at room temperature for about seven days and X-ray diffraction study was undertaken. Relevant crystallographic data and details of measurements are given in Table 1. X-ray crystallographic data were collected from single crystal samples (0.35× 0.30× 0.30 mm^3). Unit cell dimensions were obtained using 25 centered reflections in range 5.4600-11.44000 mounted on a Nonius MACH 3 diffractometer equipped with graphite monochromated Mo Kα radiation (0.71073 Å). The intensity data were collected by scan mode, and corrected by Lorentz Polarization and absorption effects using Psi-Scan (ψ-scan). The Standard reflection monitored every 200 and 3 Intensity control reflection monitored every hour, and showed no significant changes (< 3 %). The structure was solved by direct methods shelxl 97 and refined by full-matrix lest squares against F^2 using shelxl 97 software. Non-hydrogen atoms were refined with anisotropic thermal parameters. All hydrogen atoms were geometrically fixed and allowed to refine using a riding model.

Results and Discussion

Because of importance of multimetallic complexes in fields like homogenous catalysis, multimetallic enzymes and synthesis of solid state phases of industrial importance, we were interested in synthesis of monometallic, homobimetallic and heterobimetallic complexes of polyfunctional ligand bis(2-hydroxy-1-naphthaldehyde)adipoyldihydrazone and their characterization. Accordingly, when the reaction of $RuCl_3.3H_2O$ with title ligand in the presence of 3-picoline in methanol was carried out under reflux for 1 hr, a greenish coloured compound precipitated which was filtered, purified by repeated washings and air dried. For further purification, the complex dissolved in acetonitrile was subjected to column chromatography over silica gel which on elution with acetonitrile gave a deep yellow solution as the first fraction. This solution on evaporation at ambient temperature yielded a needle shaped crystal devoid of metal. The crystal so obtained was characterized by X-ray crystallography as described below. A single unit cell with atomic numbering scheme and atom connectivity is shown in fig. II.

The X-ray crystallographic data are listed in Table I. Selected bond distances and angles are listed in Table II. The molecule of the title compound adapts an E-configuration about N-N bond an -N(1A) -N(1)-C(11)-C(10) torsion angle of 179.3° (Fig. II).

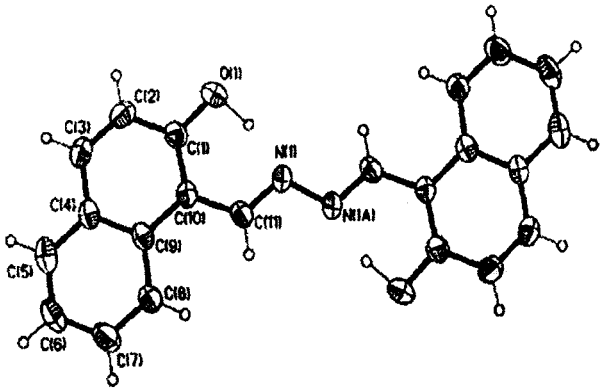

Figure II: Molecular structure of the title compound with atom numbering scheme. The thermal ellipsoids are drawn at the 50% probability level.

The N(1)-C(11) bond length is 1.290(3). This bond length is shorter than the mean reported bond length for a single C-N bond (1.437 Å) and is very close to the mean bond length reported for a C=N double bond (1.289 Å). These data clearly reveal complete localization of the electron lone pair of N(1) atoms [11].

The two parts of the molecule has a centre of symmetry. The dihedral angle between the planes containing naphthyl ring and the plane containing atoms C(10)-C(11)-N(1) is 2.64 °. This non-planarity is essentially small to conserve the extended conjugated system of the organic compound. Accordingly, the hydrazine N(1) and N(1A) atoms are almost co-planar with the C(10) atom.

Table I
Crystal Data and Structure Refinement of Bis (2-hydroxy-1-naphthaldehyde)-Azine

Empirical formula	C11 H8 N O
Formula weight	170.18
Temperature	293(2) K
Wavelength	0.71073 A
Crystal system, space group	Monoclinic, P 21/n
Unit cell dimensions	a = 8.5536(13) A alpha = 90deg.
	b = 6.100(3) A beta = 1.18(4)deg.
	c = 15.993(9) A gamma = 90 deg.
Volume	834.3(6) A^3
Z, Calculated density	4, 1.355 Mg/m^3
Absorption coefficient	0.088 mm^-1
F(000)	356
Crystal size	0.35 x 0.30 x 0.25 mm
Theta range for data collection	2.55 to 24.95 deg.
Index ranges	0<=h<=10, 0<=k<=7, -18<=l<=18
Reflections collected/unique	1558 / 1454 [R(int) = 0.0357]
Completeness to 2theta	= 24.95 90.0%
Absorption correction	Psi-scan
Max. and min. transmission	0.9783 and 0.9698
Refinement method	Full-matrix least-squares on F^2
Data/restraints/parameters	1454 / 0 / 119
Goodness-of-fit on F^2	0.970
Final R indices [I>2sigma(I)]	R1 = 0.0499, wR2 = 0.1100
R indices (all data)	R1 = 0.1507, wR2 = 0.1386
Largest diff. peak and hole	0.157 and -0.224 e.A^-3

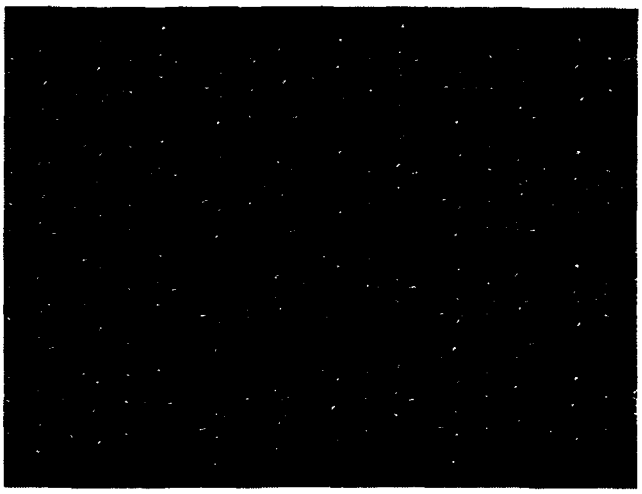

Figure III: Packing along b-axis showing intramolecular bonding between O1 and N1 to form 5 membered ring between O1N1C1C10C11.

Table II
Bond Lengths [A] and Angles [deg]

Bond lengths [A]	*angles [deg]*
N(1)-C(11)	1.290(3)
N(1)-N(1)#1	1.392(4)
O(1)-C(1)	1.351(3)
O(1)-H(101)	1.1033
C(1)-C(10)	1.385(4)
C(1)-C(2)	1.406(4)
C(2)-C(3)	1.345(4)
C(2)-H(2)	0.9300
C(3)-C(4)	1.406(4)
C(3)-H(3)	0.9300
C(4)-C(5)	1.411(4)
C(4)-C(9)	1.416(4)
C(5)-C(6)	1.363(4)
C(5)-H(5)	0.9300
C(6)-C(7)	1.403(4)
C(6)-H(6)	0.9300
C(7)-C(8)	1.362(4)
C(7)-H(7)	0.9300
C(8)-C(9)	1.413(4)
C(8)-H(8)	0.9300
C(9)-C(10)	1.442(4)
C(10)-C(11)	1.436(3)
C(11)-H(11)	0.9300
C(11)-N(1)-N(1)#1	114.0(3)
C(1)-O(1)-H(101)	98.7
O(1)-C(1)-C(10)	122.8(3)
O(1)-C(1)-C(2)	116.6(3)
C(10)-C(1)-C(2)	120.6(3)
C(3)-C(2)-C(1)	120.4(3)
C(3)-C(2)-H(2)	119.8
C(1)-C(2)-H(2)	119.8
C(2)-C(3)-C(4)	121.9(3)
C(2)-C(3)-H(3)	119.1
C(4)-C(3)-H(3)	119.1
C(3)-C(4)-C(5)	121.6(3)
C(3)-C(4)-C(9)	119.0(2)
C(5)-C(4)-C(9)	119.4(3)
C(6)-C(5)-C(4)	121.4(3)
C(6)-C(5)-H(5)	119.3
C(4)-C(5)-H(5)	119.3
C(5)-C(6)-C(7)	119.2(3)
C(5)-C(6)-H(6)	120.4
C(7)-C(6)-H(6)	120.4
C(8)-C(7)-C(6)	120.8(3)
C(8)-C(7)-H(7)	119.6
C(6)-C(7)-H(7)	119.6
C(7)-C(8)-C(9)	121.4(3)
C(7)-C(8)-H(8)	119.3
C(9)-C(8)-H(8)	119.3
C(8)-C(9)-C(4)	117.7(2)
C(8)-C(9)-C(10)	123.4(3)
C(4)-C(9)-C(10)	118.9(3)
C(1)-C(10)-C(11)	120.0(2)
C(1)-C(10)-C(9)	119.1(3)
C(11)-C(10)-C(9)	120.9(3)
N(1)-C(11)-C(10)	122.3(3)
N(1)-C(11)-H(11)	118.9
C(10)-C(11)-H(11)	118.9

There is an intramolecular bonding between O(1) and N(1) with bond length 2.70 Å to form 5-membered ring involving atoms O(1)-N(1)-C(10)-C(11). The molecule contains -N-N- bond (N(1)-N(1A)) which connects the two naphthaldimine fractions. The N(1)-N(1A) bond length is 1.3923 Å which is very close to the N-N value in N-benzidene-N′-(2-caboxyphenyl)hydrazine [12]. The slightly longer N(1)-N(1A) value may be attributed to withdrawal of electron density from N(1) and N(1A) atoms by naphthyl rings.

The geometric isomerization about this bond affords the possibility of E and Z isomers. In the E-isomer, the N(1)-C(11) and N(1)-C(11′) bonds are in trans-position with respect to N(1)-N(1A) bond. The N(1)-N(1A) bond has an essentially planar atomic arrangement. The r.m.s deviation from the best plane passing through atoms C(1)-C(2)-C(3)-C(4)-C(9)-C(10) is 0.0098 ˚. The slight deviations from ideal geometry are observed in the bond angle around atoms C(11), C(10) and (C9) while the angle around these atoms are 122.3(3), 118.9, 118.9, 120.0(2), 119.1(3), 120.93(3) and 117.7(2), 123.4(3), 118.9(3), respectively.

The mode of packing of the compound in stereoprojection along b-direction is illustrated in Fig. III. In addition to Vander Waals forces, intermolecular hydrogen bonding contributes to the stabilization of the crystal structure. Weak intermolecular π-π^* interaction is observed in the molecule.

ACKNOWLEDGEMENT

We are thankful to Prof. P. Mathur, incharge of Crystallographic centre, IIT, Bombay, India for carrying out X-ray crystallographic study.

REFERENCES

[1] Siemann S., Evanoff D. P., Marrone L., Clarke A. J., Viswanatha T. and Dmitrienko G. I., *Antimicrob. Agents Chemother.*, *N*-Arylsulfonyl Hydrazones as Inhibitors of IMP-1 Metallo-β-Lactamase, 46(8), 2002.

[2] Agarwal R. K., Sharma D., Singh L. and Agarwal H., *Bioinorg Chem. Appl.*, Synthesis, Biological, Spectral, and Thermal Investigations of Cobalt(II) and Nickel(II) Complexes of N-Isonicotinamido -22, 42-Dichlorobenzalaldimine, 2006.

[3] Gudasi K., Patil, M., Vadavi R., Shenoy R., Patil, S., N-(salicylidene)-nitrosophenylglycine Schiff base as NOOO-donor towards transition metal ions, *Transition Met. Chem.*, 31(8), 2006, 986-991.

[4] Harris T. D., Sworin M., Williams N., Rajopadhye M., Damphousse P. R., Glowacka D., Poirier M. J. and Yu K., Synthesis of Stable Hydrazones of a Hydrazinonicotinyl-Modified Peptide for the Preparation of ^{99m}Tc-Labeled Radiopharmaceuticals, *J. Am. Chem. Soc.*, 10(5), 1999, 808-814.

[5] Corondo E., Delhaes P., Gatteschi D. and Miller J. S., In Molecular Magnetism From Molecular Assemlies to the Devices; Kluwer Academic Publishers Dordrecht, The Netherlands, 1996; Verdguer M., Bleuzen A., Marvand V., Vaissevmann J., Seuleiman M., Desplanches C., Schiller A., Train C., Garde R., Gelley G., Lomenech C., Rosemana I., Veillet P., Cartier C. and Villain F., *Coord. Chem. Rev.*, 190-192, 1999, 1023.

[6] Kashiwagi T., Ohkoshi S. I., Seino H., Mizobe Y. and Hashimoto K., Manganese(II) Octacyanotungstate(V)-Based Magnet Containing a Noncoordinated Aromatic Molecule, *J. Am. Chem. Soc.*, 126, 2004, 5024-5025; Song Y., S.-I; Ohkosh, Arimoto Y., Seino H., Mizobe and Hashimoto K., *Inorg. Chem.*, 42, 1848, 2003.

[7] Lal R. A., Basumatary D., Chakravarty J., Bhaumik S. and Kumar A., Binuclear and tetranuclear dioxouranium(VI), Zinc(II) and Copper(II) Complexes Derived from Bis(2-hydroxy-1-naphthldehyde) malonoyl-adipoyldihydrazone, *Indian J. Chem.*, 45A, 2006, 619-628.

[8] Lal R. A., Siva A. N., Mukherjee L. M., Narang K. K., Singh M. K. and Thapa R. K., ^{1}H NMR spectral evidence for the chair conformation in mono- and bis (dioxouranium (VI) complexes of bis (o-hydroxynaphthaldehyde) oxaloyldihydrazone, *Spectrochim. Acta*, 50A, 1994, 1005.

[9] Gopinath S., Tavale S. S., Puranik V. G. and Deaonkar M. P., *Bull. Chem. Soc. Japan*, 41, 1797, 1994; Singh P. K., Jaimerez H., Katti K. V., Wokert W. A. and Barnes C., *Inorg.Chem*, 33, 736, 1994.

[10] Ianelli S., Minardi G., Pellizi C., Pellizi G., Reverbari R., Solinas C. and Tarasconi P., *J. Chem. Soc. Dalton Trans*, 2213, 1991; Belletti D., Carelli M., Pellizi C., Pellizi G., *J. Crystallogr. Spectross. Les.*, 22, 185, 1992.

[11] Orpen A. G., Brammer L., Allen F. H., Kennard D., Watson D. G. and Taylor R. T., *J. Chem. Soc, Dalton Trans*, 51, 1989; Figueroa W., Fuentella M., Manzur C., Canvillo D., Mata J. A. and Hamon J. R., *J. Chilean. Chem. Soc.*, 11, 2005.

[12] Tezcan H., Tunc T., Sahin E. and Yagbasan R., Crystal Structure of N-Benzlidene-N′-(2-caroxyphenyl) hydrazine, *Anal. Sci.*, 20, 2004.

LIST OF PUBLICATIONS

1) Synthesis and Crystal Structure of $[Mn_2(H_2sal)_2(H_2O)_4]$. First Example Of the Reductive Synthesis Of Binuclear Manganese(I) Salicylate Complex, R. A. Lal, **D. Basumatary**, A. Lemtur, S. Choudhury, M. Chakravarty, M. K. Singh, S. Bhaumik, A. De and A. Kumar, *Transition Metal Chemistry,* **31**, 423-428, 2006.

2) Synthesis, Characterization And Crystal Structure Of Manganese(IV) Complex Derived From Salicylic Acid, R. A. Lal, S. Bhaumik, A. Lemtur, M. K. Singh, **D. Basumatary**, S. Choudhury, A. De and A. Kumar, *Inorganica Chimica Acta,* **359**, 3105-3110, 2006.

3) Binuclear And Tetranuclear Dioxouranium(VI), Zinc(II) And Copper(II) Complexes Derived From Bis(2-Hydroxy-1-Naphthaldehyde)Malonoyl-dihydrazone, R. A. Lal, **D. Basumatary**, J. Chakravarty, S. Bhaumik and A. Kumar, *Indian Journal of Chemistry*, **45A**, 619-628, 2006.

4) Alkali Metal, Ammonium And Pyridinium Oxo-Peroxovanadium Complexes Derived From Salicylaldehyde Isonicotinoylhydrazone, R. A. Lal, **D. Basumatary,** Arjun De and A. Kumar *Transition Metal Chemistry*, **32**, 491-493, 2007.

5) Synthesis And Proper Of Mononuclear And Binuclear Molybdenum Complexes Derived From Bis(2-hydroxy-1-naphthaldehyde)oxaloyldihydrazone, R. A. Lal, **D. Basumatary**, S. Adhikari and A. Kumar, *Spectrochimica Acta, Part-A*, **69**, 706-714, 2007.

6) Isolation Of Bis(2-Hydroxy-1-Naphthaldehyde)Azine From A Complex Reaction Mixture And Its X-Ray Crystallographic Characterization, R. A. Lal, **D. Basumatary** and A. Kumar, *International Journal of Synthesis and Characterization*, **1**, 1-4, 2008.

7) Synthesis, Characterization And Structural Assessment Of Monometallic Manganese(II) Complexes Derived From Polyfunctional Adipoyldihydrazones, R. A. Lal, **D. Basumatary** and A. Kumar, *Transition Metal Chemistry* (Communicated).

8) Synthesis And Characterization Of Monometallic Manganese(IV) Complexes Of Bis(2-hydroxy-1-naphthaldehyde)adipoyldihydrazone, R. A. Lal, **D. Basumatary** and A. Kumar, *Inorganic Chemistry* (Communicated).